JSC -07759
Revision A

PROJECT/SPACE SHUTTLE

DIGITAL FLIGHT CONTROL SOFTWARE DESIGN REQUIREMENTS

GUIDANCE AND CONTROL SYSTEMS BRANCH
AVIONICS SYSTEMS ENGINEERING DIVISION

National Aeronautics and Space Administration
LYNDON B. JOHNSON SPACE CENTER
Houston, Texas

Revised July 6, 1973

JSC - 07759
REVISION A

NASA SPACE SHUTTLE PROGRAM WORKING PAPER

DIGITAL FLIGHT CONTROL SOFTWARE DESIGN REQUIREMENTS

Revised
July 6, 1973

NATIONAL AERONAUTICS AND SPACE ADMINISTRATION
LYNDON B. JOHNSON SPACE CENTER
HOUSTON, TEXAS

Prepared by
Guidance and Control Systems Branch
Avionics Systems Engineering Division

Kenneth J. Cox

Kenneth J. Cox, Chief
Guidance and Control Systems Branch

Authorized for Distribution Robert A. [illegible]

Maxime A. Faget
Director of Engineering and Development

8-6-73

FOREWORD

This document updates the Shuttle digital flight control design developed by the JSC Guidance and Control Systems Branch and the Draper Laboratory Control and Flight Dynamics Division. The flight control algorithms of the Space Shuttle from launch through touchdown, and for powered horizontal flight are presented. It is anticipated that this document will be utilized in establishing an initial baseline for the digital flight control software design. This report supports the generation (by Rockwell) of the Level I "Orbiter Avionics Functional Subsystem Software Requirements" documentation series.

Revision A of the Digital Flight Control Software Design document incorporates updates from the design activities performed over the past six months. In addition, Honeywell has completed an extensive review of the original version and many changes in Revision A resulted from the constructive review comments to NASA. Additionally, treatment of control modes in this revision reflect technical design exchanges with Rockwell and the Flight Crew personnel.

There are several important design areas which have not been covered in the revision. It is anticipated that they will be addressed as baseline additions in the future. These areas include the treatment of redundant sensors and redundant actuators, interface with pilot type displays, and roll-out control. All design to date has assumed rigid body models; however, the filter structure has been specified to facilitate the handling of bending and slosh dynamics.

In this document, a number of design elements have been addressed in detail. The following paragraphs summarize the scope of the document.

The unified structure which is presented for the DFCS (digital flight control system) is a flexible framework for the evolving Space Shuttle control system.

Two designs for jet selection are included. The first, which is based upon linear programming, is considered flexible. The second, which is based upon a table look-up scheme, is more restricted. The latter is recommended for the baseline design until the Shuttle requirements are found to go beyond its capabilities.

The design for the cruise phase addresses the requirement for a variety of manual, semi-automatic and automatic control modes during the developmental horizontal flight tests as well as during the final stages of operational vertical flights and during ferry flights. The control gains have been calculated for the Rockwell 0089B vehicle, but only for a single flight condition; the scheduling of gains for a full range of conditions is currently in progress.

A number of features have been added to the design for the entry phase. The applicable flight regime has been extended to subsonic, thus eliminating the separate transition phase, and a state estimator has been introduced. Rudder augmentation has been added to the control during the early part of entry. The gains have been calculated for the Rockwell 0089B vehicle. A capability for higher maneuver rates in response to large bank commands has been added. The elevator-trim algorithm during early entry has been changed from open-loop to closed-loop.

The design for control using the reaction control jets during the on-orbit mission phase has been developed and implemented, as has been the design for the attitude maneuver routine during the phase. Attitude control design presented herein does not reflect the availability of vernier jets or the unavailability of a clock for on-off commands other than once per minor cycle; these factors must be considered in designing firing policies. The design for control during major maneuvers in orbit (including insertion) is in development; only a functional outline is presented in this document for that segment of the DFCS.

There are areas where the various design efforts have not yet been fully integrated. As an example, the phase plane developed for on-orbit ACPS control may well be usable in the entry phase.

A version of the DFCS which incorporates the designs for the cruise, entry, and boost phases has been implemented in FORTRAN for testing on the SSFS (Space Shuttle functional simulator). A second version has been programmed in HAL using structured programming techniques. It incorporates the designs for the on-orbit phase, and runs on the functional simulator at the Charles Stark Draper Laboratory.

ABSTRACT

The objective of the integrated Digital Flight Control System is to provide rotational and translational control of the Space Shuttle orbiter in all phases of flight: from launch ascent through orbit to entry and touchdown, and during powered horizontal flights. The program provides a versatile control system structure while maintaining uniform communications with other programs, sensors, and control effectors by using an executive routine/functional subroutine format. The program reads all external variables at a single point, copies them into its dedicated storage, and then calls the required subroutines in the proper sequence. As a result, the flight control program is largely independent of other programs in the GN&C computer complex and is equally insensitive to the characteristics of the processor configuration.

Section 1 of Part I describes the integrated structure of the control system and the DFCS executive routine which embodies that structure. Section 2 deals with the input and output. The succeeding sections show the specific estimation and control algorithms used in the various mission phases.

Part II describes attitude maneuver routines that interface with the DFCS.

TABLE OF CONTENTS

PART 1

TABLE OF CONTENTS (Cont)

PART 1 (Cont)

DIGITAL FLIGHT CONTROL SYSTEM

SECTION 1

INTEGRATED STRUCTURE; EXECUTIVE ROUTINE

1.1 Integrated Structure

The DFCS program consists of an executive routine, several major (functional) subroutines, and a number of utility subroutines. The executive routine performs "housekeeping" which is required regardless of the mission phase and calls the major subroutines in the appropriate order. There is a major subroutine for each of the following functions: Backup Control System (BCS) implementation, "pad load" manipulation, input manipulation, filter and parameter initialization, filter update (or measurement incorporation), control logic, command transmission, filter pushdown, (or state extrapolation), and parameter estimation. Most of these routines are divided, at least in part, into separate segments for the various mission phases.

This structure of executive routine and functional subroutines gives modularity to the program; it allows complete flexibility in designing the state estimation and control algorithms for each of the mission phases, designating new sensors or control effectors, and indeed, redefining the mission phases themselves. At the same time, however, the unified structure which groups together the coding for similar functions encourages economy both in computer storage, and in engineering design and programming effort because it is so easy for different mission phases to use common coding whenever it is appropriate to do so. Another advantage to this structure is that the calls to the functional subroutines indicate the completion of one set of calculations and the beginning of another; hence, they are suitable break points for external interrupts, and they facilitate the testing of new coding. For example, if modification to the orbit thrust vector control law is contemplated while other segments of this phase's computations are unchanged, the new coding can be added as a totally separate subroutine, leaving the old coding intact. During testing, it is then possible to switch between old and new control laws following completion of the first segment of state filtering. This feature also could be of utmost importance for emergency or backup coding that is required to be functionally separated from the primary coding.

The unified DFCS structure has additional, managerial advantages that are valuable in an enterprise as complex as the Space Shuttle program. The use in different mission phases of the same assumptions about input/output, timing and other interfaces is encouraged if not enforced. Furthermore, commonality in conventions, nomenclature and formats is encouraged, which simplifies and clarifies both testing and documentation.

Not all operations of a control system need to be performed with the same frequency. The current version makes allowance for 3 sampling intervals, the longer intervals being multiples of the shortest interval. In the current cruising flight phase, for example, the "fast" rate (10 sps) is used for angular control, the "medium" rate (2 sps) is used for velocity control, and the "slow" rate (1/2 sps) is used for altitude control and parameter updating. The medium and slow computations are offset, in order to prevent them from occurring on the same control cycle. Allowance is made for different sets of sampling intervals in different mission phases.

1.2 DFCS Executive Routine

An overview of the logic flow through the DFCS Executive Routine is shown in Fig. 1-1; Fig. 1-2 illustrates the implementation of this logic. The major subroutines of the DFCS are denoted in these figures by the hexagonal blocks. Although the executive serves all the mission phases, many of the algorithms within the subroutines are specifically designed for a single phase. Table 1-1 defines the mission phases for which the DFCS makes provision. The inputs to the Executive Routine are listed in Table 1-2; the outputs are listed in Table 1-3. The operations performed by the Executive Routine are discussed in the following paragraphs.

The phase indication is changed from "entry" to "cruise" when the Mach number drops below 0.9. All other determination of phase is currently assumed to be done outside the DFCS.

When the Backup Control System (BCS) is requested, almost all the control system functions are performed using algorithms in a special subroutine that is separate from the rest of the DFCS. The executive transfers control to this subroutine if the appropriate flags have been set. The BCS mode has been designed only for the cruise phase at this time.

If there is an external restart request, or the phase or mode has changed since the previous pass, the executive sets flags to

1) call for a DFCS initialization pass
2) call for initialization of parameters for any modes that are new
3) cause the computations that are done at the slower sample rates to be performed this pass.

If the reason for initialization was an external restart request or a phase change, the Executive Routine establishes the counters and timers that reflect the desired

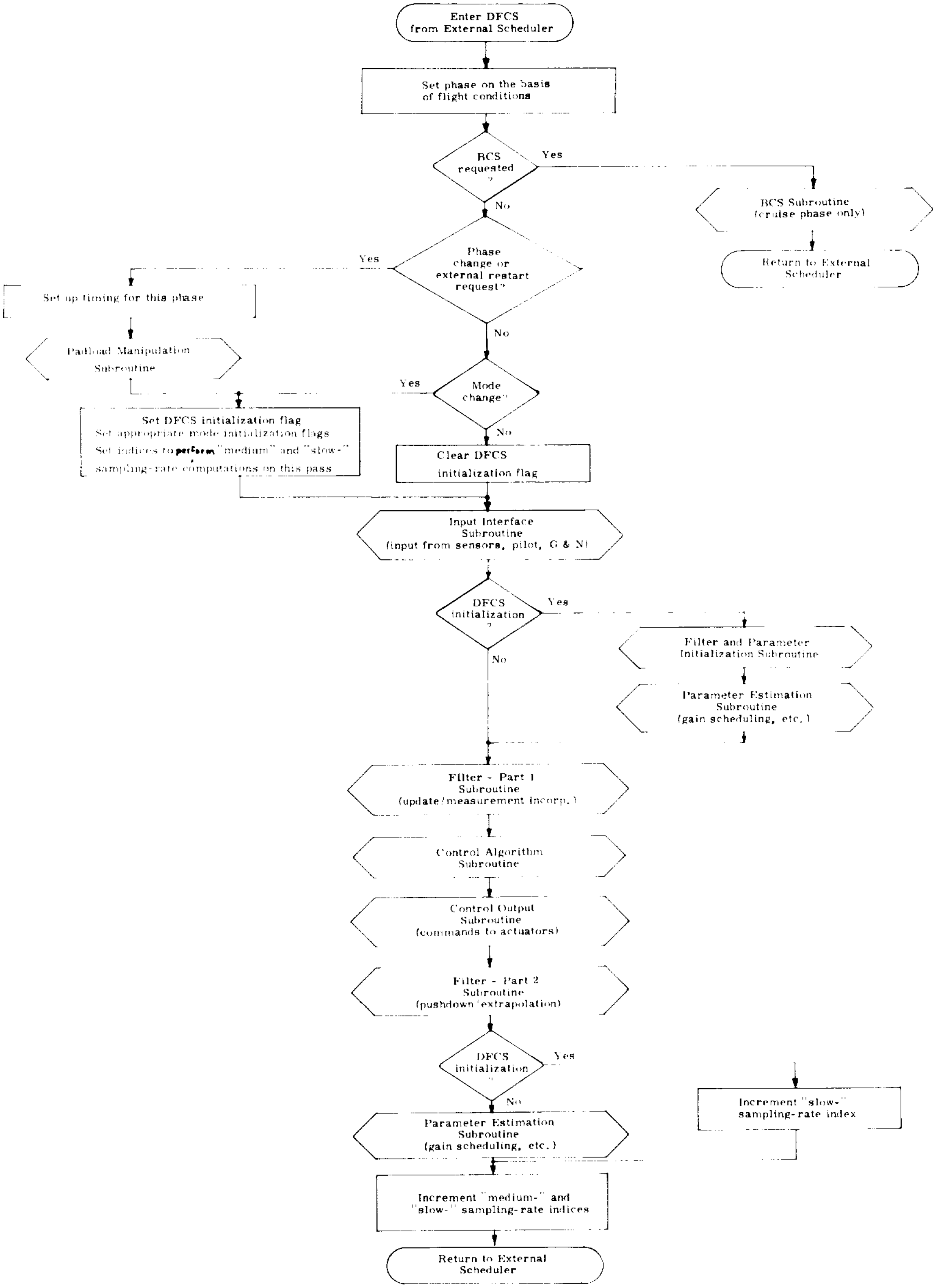

Enter DFCS from External Scheduler
Set phase on the basis of flight conditions
BCS requested ?
Yes
No
BCS Subroutine (cruise phase only)
Return to External Scheduler
Phase change or external restart request?
Yes
No
Set up timing for this phase
Payload Manipulation Subroutine
Set DFCS initialization flag
Set appropriate mode initialization flags
Set indices to perform "medium" and "slow-" sampling-rate computations on this pass
Mode change?
Yes
No
Clear DFCS initialization flag
Input Interface Subroutine (input from sensors, pilot, G & N)
DFCS initialization ?
Yes
No
Filter and Parameter Initialization Subroutine
Parameter Estimation Subroutine (gain scheduling, etc.)
Filter - Part 1 Subroutine (update/measurement incorp.)
Control Algorithm Subroutine
Control Output Subroutine (commands to actuators)
Filter - Part 2 Subroutine (pushdown/extrapolation)
DFCS initialization ?
Yes
No
Increment "slow-" sampling-rate index
Parameter Estimation Subroutine (gain scheduling, etc.)
Increment "medium-" and "slow-" sampling-rate indices
Return to External Scheduler

Fig. 1-1 Logic Flow of DFCS Executive

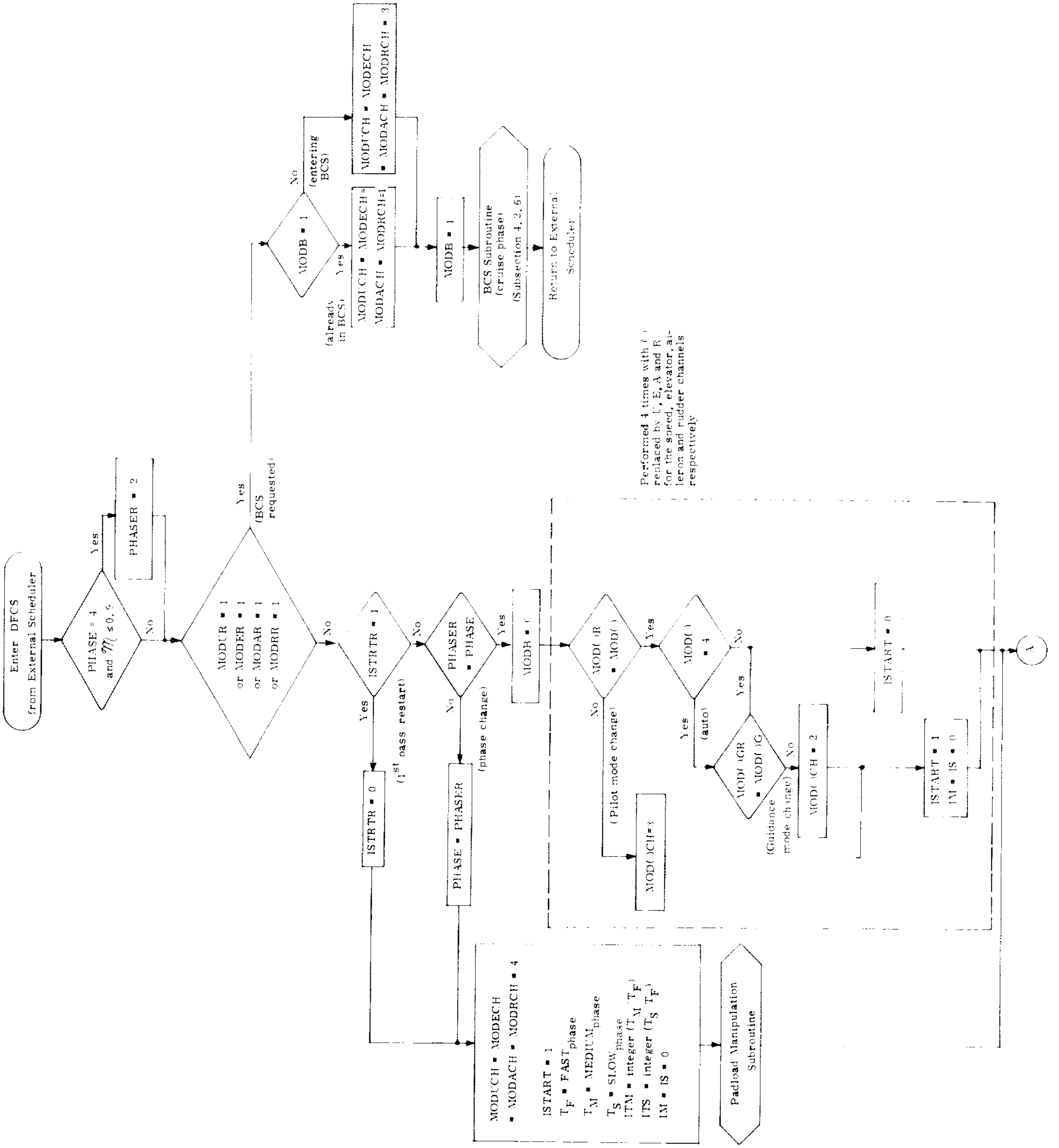
Enter DFCS from External Scheduler
PHASE = 4 and $\eta_l \le 0.9$
Yes
PHASER = 2
No
MODUR = 1 or MODER = 1 or MODAR = 1 or MODRR = 1
Yes (BCS requested)
MODB = 1
(already in BCS)
Yes
MODUCH = MODECH = MODACH = MODRCH=1
No (entering BCS)
MODUCH = MODECH = MODACH = MODRCH = 3
MODB = 1
BCS Subroutine (cruise phase) (Subsection 4.2.6)
Return to External Scheduler
No
ISTRTR = 1
Yes (1st pass restart)
ISTRTR = 0
No
PHASER = PHASE
No (phase change)
PHASE = PHASER
Yes
MODB = 0
MOD( )R = MOD( )
No (Pilot mode change)
MOD( )CH=3
Yes
MOD( ) = 4
Yes (auto)
MOD( )GR = MOD( )G
No (Guidance mode change)
MOD( )CH = 2
No
Yes
ISTART = 0
ISTART = 1
IM = IS = 0
A
Performed 4 times with ( ) replaced by U, E, A and R for the speed, elevator, aileron and rudder channels respectively
MODUCH = MODECH = MODACH = MODRCH = 4
ISTART = 1
$T_F = FAST_{phase}$
$T_M = MEDIUM_{phase}$
$T_S = SLOW_{phase}$
ITM = integer (T_M / T_F)
ITS = integer (T_S / T_F)
IM = IS = 0
Padload Manipulation Subroutine

Fig. 1-2 Detailed Logic Flow of DFCS Executive

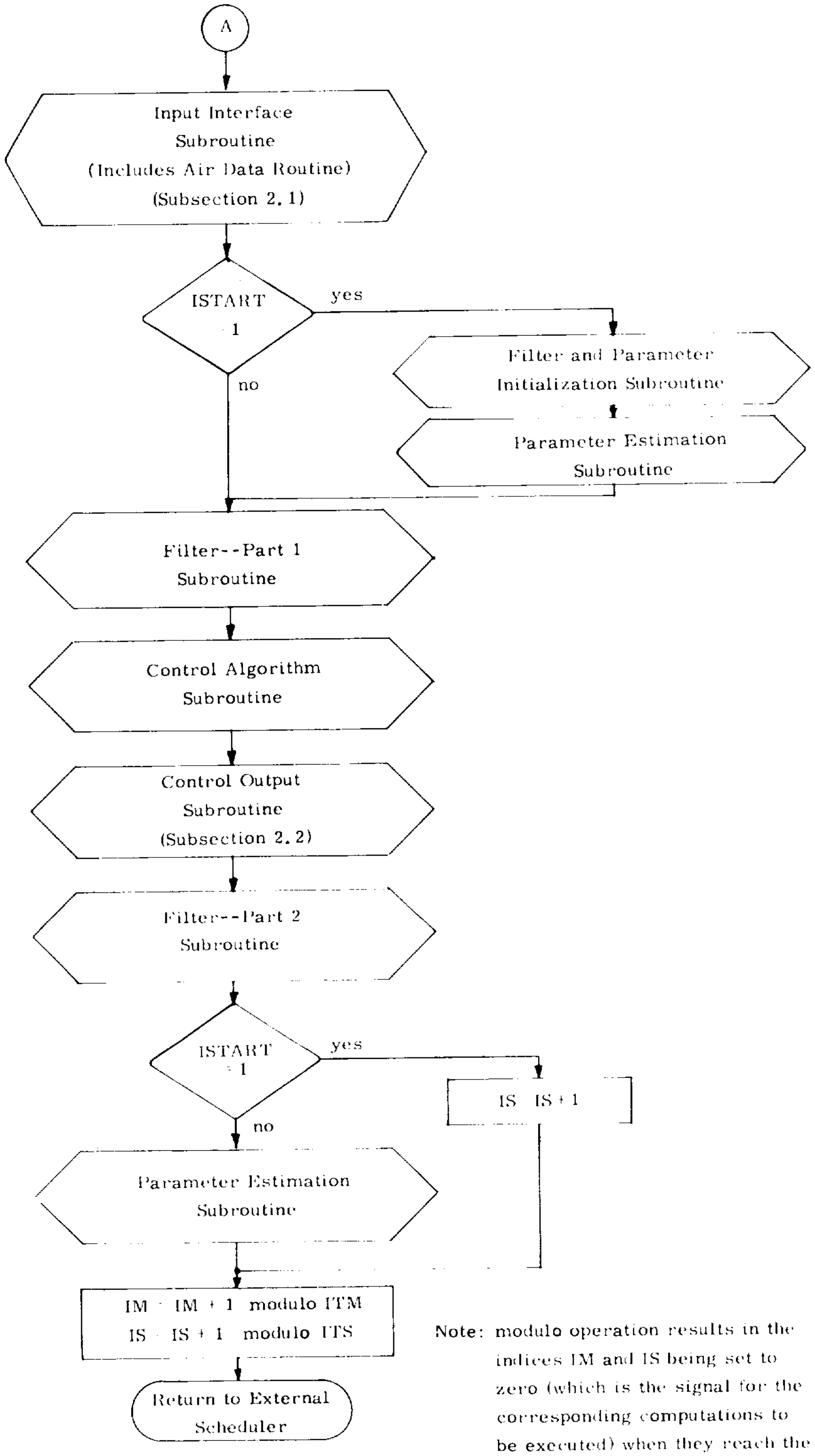
A
Input Interface Subroutine (Includes Air Data Routine) (Subsection 2.1)
ISTART = 1
yes
no
Filter and Parameter Initialization Subroutine
Parameter Estimation Subroutine
Filter--Part 1 Subroutine
Control Algorithm Subroutine
Control Output Subroutine (Subsection 2.2)
Filter--Part 2 Subroutine
ISTART = 1
yes
no
IS = IS + 1
Parameter Estimation Subroutine
IM = IM + 1 modulo ITM
IS = IS + 1 modulo ITS
Return to External Scheduler

Note: modulo operation results in the indices IM and IS being set to zero (which is the signal for the corresponding computations to be executed) when they reach the values ITM and ITS respectively.

Fig. 1-2 Detailed Logic Flow of DFCS Executive (Cont)

Table 1-1 DFCS Mission Phases

1	Rollout	Transition from aerodynamic control to steering and braking with landing gear; after touchdown; not currently implemented.
2	Cruise	Approach and landing following entry phase (currently below Mach 0.9) and horizontal powered flight (take-off through landing).
3	——	
4	Entry	From after the deorbit maneuver to cruise phase; from total reliance on jets (ACPS), high angle of attack and hypersonic to primary control with the aerodynamic surfaces (ACS), low angle of attack and subsonic.
5	On-orbit, TVC	Thrust vector control during maneuvers with the Orbital Maneuvering System.
6	On-orbit, ACPS	Control with the jets during coasting flight.
7	Insertion	Insertion into orbit following the Boost phase; not currently implemented, probably identical to On-orbit TVC.
8	Boost	Flight with Solid Rocket Motors and/or Main Propulsion System.

Table 1-2 Inputs to DFCS Executive Routine

ISTRTR	External request for DFCS initialization (1); none (0); cleared in Executive Routine
$\mathcal{M}$	Mach number
MODA, MODE, MODR, MODU	Current control mode - aileron, elevator, rudder, speed loops
MODAG, MODEG, MODRG, MODUG	Current guidance mode - aileron, elevator, rudder, speed loops
MODAGR, MODEGR, MODRGR, MODUGR	Requested guidance mode - aileron, elevator, rudder, speed loops
MODAR, MODER, MODRR, MODUR	Requested control mode - aileron, elevator, rudder, speed loops
PHASER	Flight phase flag (external)

Table 1-3 Outputs of DFCS Executive Routine

IM, IS	Medium- and slow- sampling-rate indices: 0 = perform calculations this pass
ISTART	Initialization pass (1), not initialization (0)
ITM, ITS	Number of fast passes per medium (slow) pass
MODB	BCS mode (1), not BCS mode (0)
MODACH, MODECH, MODRCH, MODUCH	Indicate mode change - aileron, elevator, rudder, speed loops : 1 = no change; 2 = guidance mode change; 3 = control mode change; 4 = phase initialization
PHASE	Flight phase flag (internal copy of PHASER)
T_F, T_M, T_S	Fast-, medium- and slow- sampling-rate sample periods for current phase

sampling rates for the current phase, and calls the major subroutine which transfers the set of pad-loaded constants required for the current phase from the pad-load locations into working storage. The "pad-load" denotes those parameter values that are determined prior to a flight and are loaded into the flight computer on the launch "pad".

Regardless of whether or not it is an initialization pass, the Executive Routine calls the Input Interface Routine, which reads all the dynamic input required by the current phase and mode: sensor measurements, navigation estimates, guidance commands, and manual commands. All the dynamic data is read at the same point to ensure that all the values are registered with respect to the other values. The parameters are differenced, rotated into other coordinate systems and otherwise manipulated so as to be in the proper form for use in the other routines. During the appropriate phases, an Air Data Routine is called which manipulates some aerodynamic parameters. These two routines are described in Section 2.

At this point, the logic flow is detoured in an initialization pass to go through the Filter and Parameter Initialization Routine and the Parameter Estimation Routine. The former assigns values to those variables that need to be initialized when the phase (or mode) is entered. The latter determines the current values of parameters that will be regularly updated in the course of this phase (or mode).

The flow then returns to the normal path. The subroutines entitled Filter - Part 1, Control Algorithms, Control Output and Filter - Part 2 are called in sequence. These subroutines comprise the core of the control system. After they are executed, the Parameter Estimation Routine is called; it is not called at this point in an initialization pass because it was executed earlier in the pass. The state filters are divided into two parts in order to minimize the amount of computation between data input and control command. The first part is limited to updating the filter estimate according to the most current measurement. The second part, which occurs after the control is exercised, is used to pushdown data (in the case of classical digital filters) or to propagate the state (in the case of discrete-time modern control estimation). The Control Algorithm Routine scales and combines the error signals from the filter routine to form control commands for the aerodynamic surfaces, reaction control thrusters, etc. The Control Output Routine, which is described in Subsection 2.2, prepares the control commands for the DFCS interface with the control actuators. The Parameter Estimation Routine updates the gains required for estimation and control. The functions performed in this routine may include scheduled or adaptive gain adjustment. Much of the Parameter Estimation Routine is executed only at the slow sampling rate.

After these routines have been executed, the Executive Routine increments the indices that indicate the "medium-" and "slow-sampling-rate" DFCS passes. If it is the end of an initialization pass, the "slow-sampling-rate" index is given an extra increment. This extra increment will smooth the load on the computer by offsetting future "slow" passes from "medium" passes, provided that one sampling rate is an integer multiple of the other. The Executive Routine then returns control to the external executive.

The algorithms incorporated in the routines pertaining to input and output are presented in the following section of this document. The contents of the other routines are presented phase by phase in the succeeding sections.

SECTION 2

DFCS INPUT AND OUTPUT

This section describes the interface between the DFCS and other components of the Space Shuttle avionics. Subsection 2.1 discusses the DFCS inputs. It lists all the inputs; i.e., state measurements, guidance commands, and pilot commands. It includes a description of a routine which processes some of these quantities prior to their use in the filtering and control algorithms. It also describes a routine that fills the function of an air data computer.

Subsection 2.2 lists all the outputs from the DFCS to the control actuators and describes the limiting performed on these commands. Finally, Subsections 2.3 and 2.4 present two candidate jet selection schemes; the first is powerful and flexible, but the second may suffice for the Space Shuttle requirements.

Much of what is presented in this section depends heavily on many features of the Shuttle avionics that have not yet been specified, much less modelled in a simulator. Therefore, in many cases convenient assumptions have been made for the sake of proceeding with the DFCS design. These assumptions include the following:

1) The inputs indicated in Subsection 2.1 are, in fact, available to the DFCS.

2) The actuators indicated in Subsection 2.2 are, in fact, available to the DFCS.

3) The DFCS does not deal with redundancy management of sensors or actuators.

4) The DFCS does not create outputs for pilot displays or telemetry.

5) The DFCS can schedule software tasks to turn ACPS jets off and a sufficiently fine clock granularity is available for such scheduling.

It is expected that each of these assumptions will, in time, be replaced by more realistic specifications, at which time these designs will have to be revised.

2.1 Inputs Required by the DFCS

Table 2-1 lists all inputs currently required by the DFCS in the various mission phases. They are presumed to be available from sensors (or sensor-interface modules), the guidance and navigation module, and the pilot (or command-interface modules). In this interface, and throughout the DFCS, English units (viz feet, pounds, and seconds) and radians are used.

Table 2-1 Inputs to the DFCS

Phase	Mnemonic	Symbol in Text	Definition
2,4	ACCBOD	$\tilde{\underline{a}}^b$	Linear accel measurement (body coord)
2,4	AG	α_G	Angle-of-attack guidance command
8,6	AIV(1)	ϕ	Platform outer gimbal angle
8,6	AIV(2)	θ	Platform inner gimbal angle
8,6	AIV(3)	ψ	Platform middle gimbal angle
8	AIVC(1)	ϕ_C	Platform outer gimbal angle command
8	AIVC(2)	ψ_C	Platform inner gimbal angle command
8	AIVC(3)	ψ_C	Platform middle gimbal angle command
2	AYM	$\tilde{a}y$	Measured lateral acceleration
2	AZM	$\tilde{a}z$	Measured normal acceleration (+zbody)
4	BANKG	ϕ_{VG}	Bank guidance command
2	BG	β_G	Sideslip guidance command
2	CG	c_G	CAS guidance command (QG or CSTARG)
2,4	CRTB	C_r^b	Reference-to-body direction cosine matrix
2	DAG	δa_G	Aileron guidance command
2	DDG	$\dot{\delta}_G$	TAEM guidance interface variable
2	DEG	δe_G	Elevator guidance command
8	DELORB	δ_{ORB}	Prestored orbiter engine deflection command
8	DELSRM	δ_{SRM}	Prestored SRM engine deflection command
2	DRG	δr_G	Rudder guidance command
2	DSG	δs_G	Speed brake guidance command
2	DTG	δt_G	Throttle guidance command
2,4	DYNP	$\tilde{\bar{q}}$	Dynamic pressure estimate
2	HG	H_G	Altitude guidance command
2	HM	$\tilde{H}$	Measured altitude
2	IAGAIN		AGAIN switch position (1 thru 4)
2	IATRIM		Roll stick trim activity: 0,+1(rgt),-1(left)

Table 2-1 Input to the DFCS (Cont)

Phase	Mnemonic	Symbol in Text	Definition
2	IEGAIN		EGAIN switch position (1 thru 4)
2	IPTRIM		Pitch stick trim activity: 0,+1(fwd),-1(aft)
2	IGEARY		Extend gear (1), retract gear (0)
-	INGUID	INGUID	Flag specifies guidance command set
2	IPHM		PHM valid (1), invalid (0)
2	IRCHAI		Request change IAINT state (1), no request(0)
2	IRCHEI		Request change IEINT state (1), no request(0)
2	IRGAIN		RGAIN switch position (1 thru 4)
2	IRTRIM		Pedal trim activity: 0,+1(lft),-1(rgt)
-	ISTRTR	ISTRTR	Request initialization(1), no request(0)
2	MODAGR		Requested values for MODAG
2	MODAR		Requested values for MODA
2	MODBR		Requested values for MODB
2	MODEGR		Requested values for MODEG
2	MODER		Requested values for MODE
2	MODRGR		Requested values for MODRG
2	MODRR		Requested values for MODR
2	MODUGR		Requested values for MODUG
2	MODUR		Requested values for MODU
2	PG	p_G	Roll rate guidance command
-	PHASER	PHASER	Flight phase flag (external):1=rollout phase 2=cruising phase 4=entry phase 5=orbit TVC phase 6=orbit RCS phase 7=insertion TVC phase 8=booster TVC phase
2	PHSEL	ϕ_{SEL}	Pilot-selected values for PHREF
2,4	PM	$\tilde{p}$	Measured roll rate

Table 2-1 Input to the DFCS (Cont)

Phase	Mnemonic	Symbol in Text	Definition
2	PSG	ψ_G	Heading guidance command
2	PSM	$\tilde{\psi}$	Measured heading
2	PSSEL	ψ_{SEL}	Pilot-selected values for PSREF
2	QG	q_G	Pitch rate guidance command
2,4	QM	$\tilde{q}$	Measured pitch rate
2,4	RM	$\tilde{r}$	Measured yaw rate
2,4	ROLL	$\tilde{\phi}_b$	Computed roll angle
2	ROLLG	ϕ_{bG}	Guidance commanded roll angle
4	RP	$\underline{R}_{rel}$	Position vector in reference coordinates
2,4	TEMPRK	TK_A	Input air temperature in deg. Kelvin
2	THG	θ_G	Theta guidance command
2	THM	$\tilde{\theta}$	Measured theta
2	THSEL	θ_{SEL}	Pilot-selected values for THREF
6,8	TNOW	t_n	Present time
2	UG	U_G	Velocity guidance command
2	USEL	u_{SEL}	Pilot-selected values for UREF
2,4	UXV,UYV,UZV	$\underline{UV}_x, \underline{UV}_y, \underline{UV}_z$	Unit vectors along the velocity coordinate system, in reference coordinates
4	VBODY		Air-relative velocity in body coordinates
4	VMACH1		Lateral switch parameter
4	VB	$\underline{V}_{rel}$	Air-relative velocity in reference coordinates
8	WB(1,I)	$RRATE_i$	Individual roll rate gyro signal
8	WB(2,I)	$PRATE_i$	Individual pitch rate gyro signal
8	WB(3,I)	$YRATE_i$	Individual yaw rate gyro signal
2	XAM	$\widetilde{xa}$	Measured roll stick deflection
2	XEM	$\widetilde{xe}$	Measured pitch stick deflection
2	XFM	$\widetilde{xf}$	Measured flap controller deflection
2	XRM	$\widetilde{xr}$	Measured pedal deflection

Table 2-1 Input to the DFCS (Cont)

Phase	Mnemonic	Symbol in Text	Definition
2	XSM	$\tilde{xs}$	Measured speed brake controller deflection
2	XTM	$\tilde{xt}$	Measured throttle controller deflection
8	YACIN(I)	$\ddot{Y}_i$	Individual y accelerometer signal
8	ZACIN(I)	$\ddot{Z}_i$	Individual z accelerometer signal

Table 2-2 Inputs to the Input Interface Routine

Phase	Mnemonic	Symbol in Text	Definition
2,4	ACCBOD	$\tilde{\underline{a}}^b$	Linear accel measurement (body coord)
2,4	AG	α_G	Angle-of-attack guidance command
4	BANKDO(2)	$\Delta\hat{\dot{\phi}}'_V$	Bank rate filter extrapolated value
4	BANKG	ϕ_{VG}	Bank guidance command
4	CAT	$\cos\alpha_T$	Cos (AMEAN)
2,4	CRTB	C_r^b	Reference-to-body direction cosine matrix
2,4	DYNP	$\bar{q}$	Dynamic pressure estimate
2	HM	$\tilde{H}$	Measured altitude
2,4	PM	$\tilde{p}$	Measured roll rate
2	QG	q_G	Pitch rate guidance command
2,4	QM	$\tilde{q}$	Measured pitch rate
4	RDOTC	$\dot{\phi}_C$	Bank rate command
2,4	RM	$\tilde{r}$	Measured yaw rate
2,4	ROLL	$\tilde{\phi}_b$	Computed roll angle
2	ROLLG	ϕ_{bG}	Guidance commanded roll angle
4	RR	$\underline{R}_{rel}$	Position vector in reference coordinates
4	SAT	$\sin\alpha_T$	Sin (AMEAN)
4	VR	$\underline{V}_{rel}$	Air-relative velocity in reference coordinates

2.1.1 Input Interface Routine

The purpose of the Input Interface Routine is to preprocess measurements and compute state-estimator inputs. Inputs to the routine are listed in Table 2-2. Outputs are listed in Table 2-3. Interface-routine operations are governed by the discretes INGUID, ISTART, PHASE, and MODA in the manner summarized in Table 2-4. The remainder of this subsection is a description of the logic flow of the Input Interface Routine, which is illustrated in Fig. 2-1.

The routine is called by the DFCS executive. If the phase is not either entry or cruise, it returns immediately. If it is a DFCS initialization pass, some variables internal to this routine are set to nominal values.

The section of the routine for preprocessing of measurements is then entered. The angle of attack, the sideslip angle, and the air speed are computed using the air-relative velocity and the direction-cosine matrix. The Air Data Routine is called if the phase is in the aerodynamic regime. Some aerodynamic "measurements" are generated in the Air Data Routine, which is described in the next subsection. The computation of bank angle (under the indicated conditions) concludes the measurement preprocessing segment of the interface routine.

The next section of the routine computes some nominal state values. Nominal values are computed for those state components of the entry phase state estimator (Section 3) for which nominal values are not specified by guidance. Nominal body rates are computed to provide turn coordination in the entry phase. A nominal (commanded) bank rate is also computed for use in the entry phase control logic in the specified flight regime ($I_{LAT} = 0, \bar{q} \geq \bar{q}_3^*$) when the bank error is sufficiently large.

The filter input computation section is now entered. When in cruise phase, either the current roll angle or the bank angle measurement is put into the cell PHI for processing by the cruise phase filters. When in entry phase, the state estimator inputs (namely, errors in the angles of attack, sideslip and bank, and errors in the body rates) are computed. Additionally, estimator extrapolated values are adjusted for changes in the state-variable nominal values.

Finally, a check is made to ensure that INGUID is negative. This avoids reprocessing non-updated G&N inputs in subsequent DFCS passes. Control is then returned to the DFCS executive routine.

2.1.2 Air Data Routine

The Air Data Routine is called by the Input Interface Routine during the atmospheric flight phases. It computes several parameters required for aerodynamic control, serving the purpose of an air data computer.

Table 2-3: Outputs from Input Interface Routine

Phase	Mnemonic	Symbol in Text	Definition
4	AI(1)	$\Delta\tilde{\alpha}$	Angle-of-attack filter input
2	AM	$\tilde{\alpha}$	Measured angle-of-attack
4	AO(2)	$\Delta\hat{\alpha}'$	Angle-of-attack filter extrapolated value
4	BANKI(1)	$\Delta\tilde{\phi}_V$	Bank filter input
4	BI(1)	$\Delta\tilde{\beta}$	Sideslip angle filter input
2	BM	$\tilde{\beta}$	Measured sideslip
2	HM	$\tilde{H}$	Measured altitude
2	PHG	ϕ_G	Bank angle guidance command
2	PHM	$\tilde{\phi}$	Measured bank angle
4	PI(1)	$\Delta\tilde{p}$	Roll rate filter input
4	QI(1)	$\Delta\tilde{q}$	Pitch rate filter input
4	RI(1)	$\Delta\tilde{r}$	Yaw rate filter input
2	VM	$\tilde{V}$	Measured velocity

Table 2-4 Discretes Governing Logic Flow in Input Interface Routine

ISTART	DFCS initialization pass flag. = 1: initialize variables this pass. = 0: do not initialize this pass.
PHASE	Mission phase. = 2: cruise phase. = 4: entry phase. (Routine not entered in other phases.)
INGUID	Flag from guidance. = ±2: guidance commands are pitch rate and roll (about body x-axis); terminal part of cruise phase. = ±1: guidance commands are angle-of-attack and bank (about velocity vector); entry and early cruise. < 0: as above, but no new guidance commands to process this pass (set negative internally).
MODA	Mode flag for cruise phase aileron channels. = 4: automatic mode; compute roll (or bank) filter inputs. ≠ 4: not automatic mode.
I_{LAT}	Mode flag for entry phase lateral control. = 0: early entry, compute desired bank rate. = 1: late entry

Note: The parameters $\bar{q}_3^*$, $r_{\phi 1}$, $r_{\phi 2}$, $r_{\phi 3}$ are used in the Input Interface Routine as limits. They are introduced in the discussion of the entry phase control logic in Section 5.

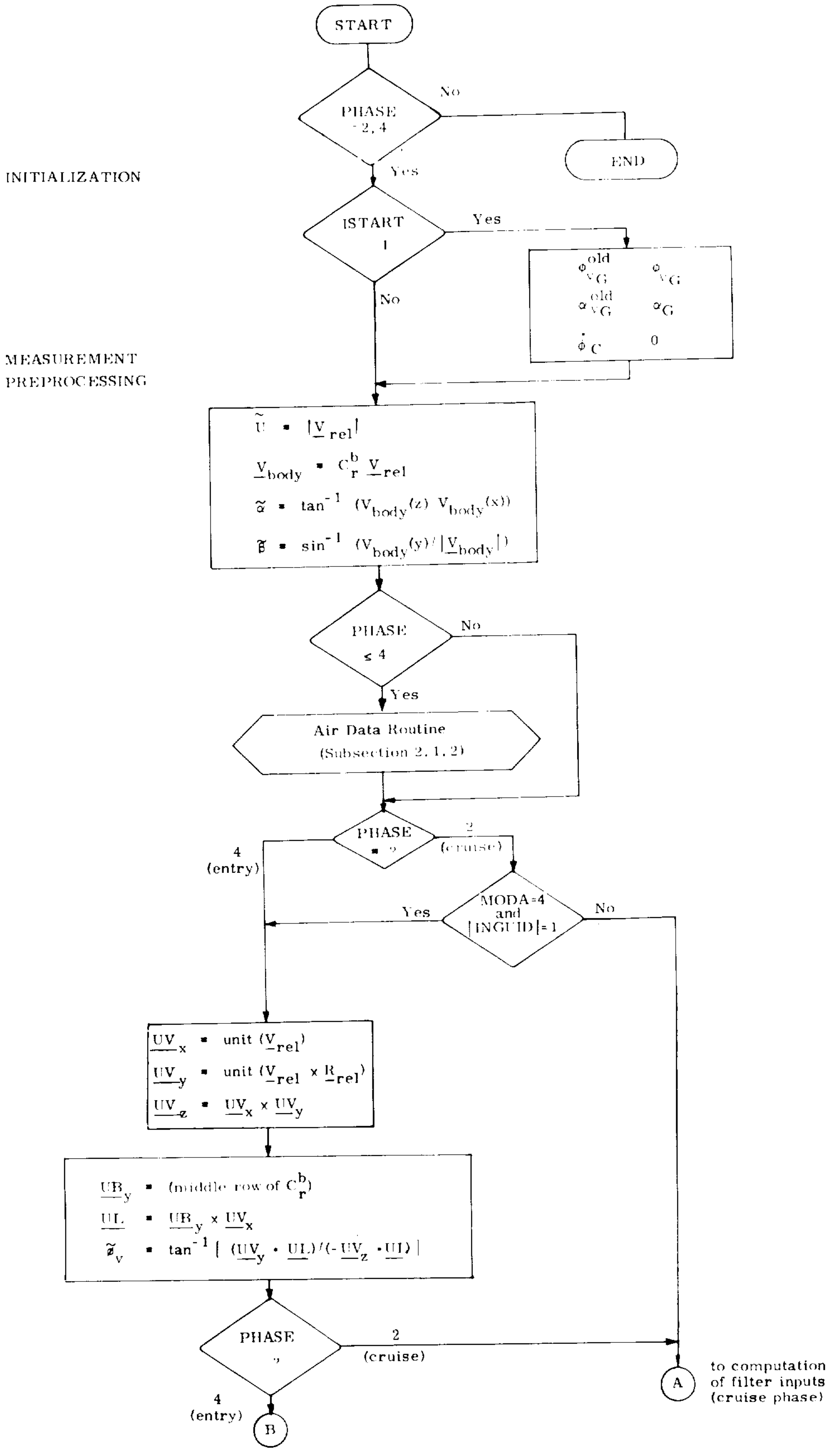
START
PHASE
= 2, 4
No
END
Yes
INITIALIZATION
ISTART
1
Yes
ϕ^{old}_{vG} ϕ_{vG}
α^{old}_{vG} α_G
$\dot{\phi}_C$ 0
No
MEASUREMENT
PREPROCESSING
$\tilde{U} = |\underline{V}_{rel}|$
$\underline{V}_{body} = C^b_r \underline{V}_{rel}$
$\tilde{\alpha} = \tan^{-1} (V_{body}(z) V_{body}(x))$
$\tilde{\beta} = \sin^{-1} (V_{body}(y)/|\underline{V}_{body}|)$
PHASE
≤ 4
No
Yes
Air Data Routine
(Subsection 2. 1. 2)
PHASE
= 2
4
(entry)
2
(cruise)
MODA=4
and
|INGUID|=1
Yes
No
$\underline{UV}_x = \text{unit} (\underline{V}_{rel})$
$\underline{UV}_y = \text{unit} (\underline{V}_{rel} \times \underline{R}_{rel})$
$\underline{UV}_z = \underline{UV}_x \times \underline{UV}_y$
$\underline{UB}_y = (\text{middle row of } C^b_r)$
$\underline{UL} = \underline{UB}_y \times \underline{UV}_x$
$\tilde{\phi}_v = \tan^{-1} [(\underline{UV}_y \cdot \underline{UL})/(-\underline{UV}_z \cdot \underline{UL})]$
PHASE
2
2
(cruise)
4
(entry)
B
A
to computation
of filter inputs
(cruise phase)

Fig. 2-1 Input Interface Routine Logic Flow

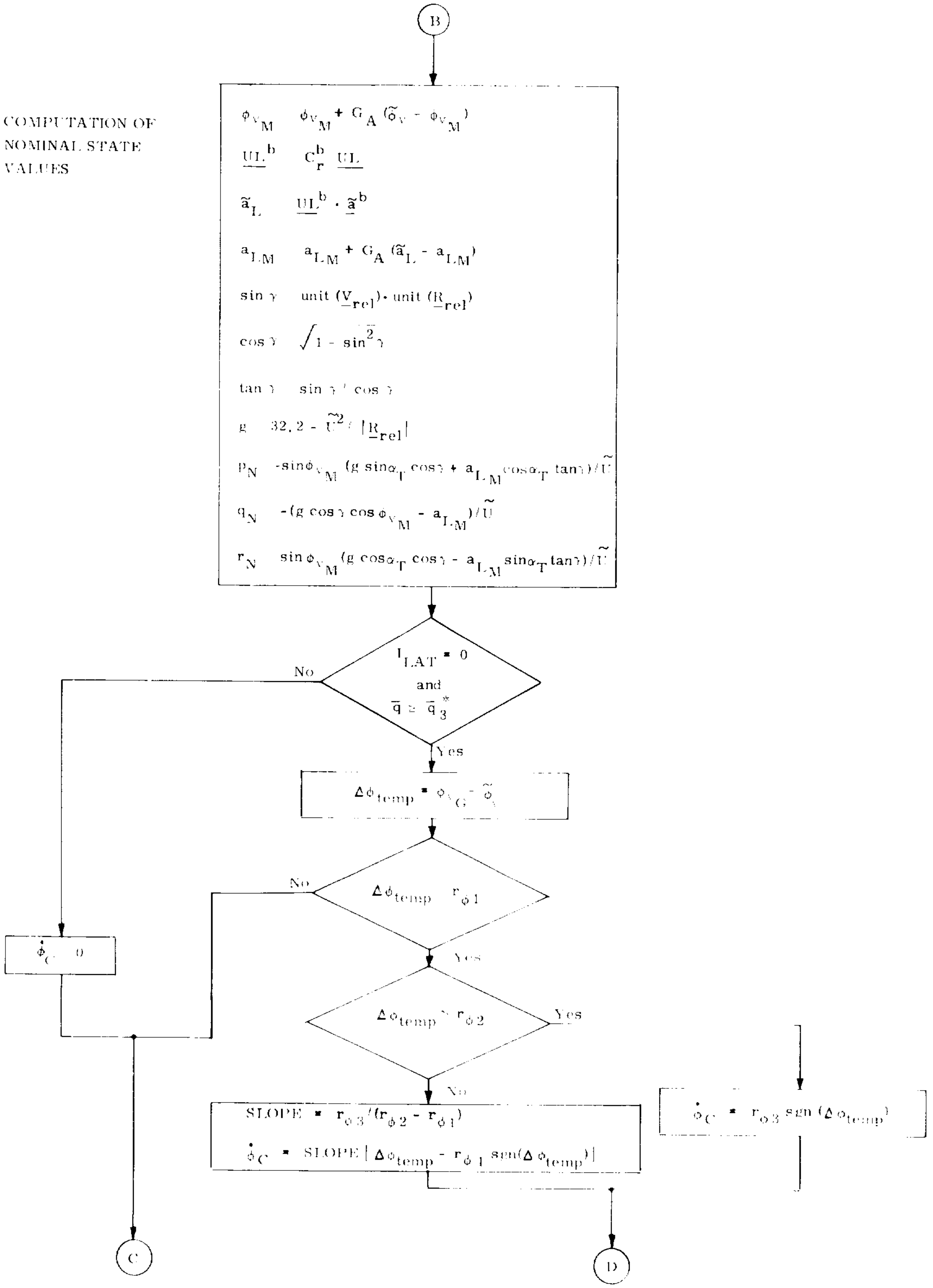
B
COMPUTATION OF NOMINAL STATE VALUES
ϕ_{v_M} $\phi_{v_M} + G_A (\tilde{\phi}_v - \phi_{v_M})$
$\underline{UL}^b$ $C_r^b \underline{UL}$
$\tilde{a}_L$ $\underline{UL}^b \cdot \underline{\tilde{a}}^b$
a_{LM} $a_{LM} + G_A (\tilde{a}_L - a_{LM})$
$\sin\gamma$ unit $(\underline{V}_{rel})$ · unit $(\underline{R}_{rel})$
$\cos\gamma$ $\sqrt{1 - \sin^2\gamma}$
$\tan\gamma$ $\sin\gamma / \cos\gamma$
g $32.2 - \tilde{U}^2 / |\underline{R}_{rel}|$
p_N $-\sin\phi_{v_M} (g \sin\alpha_T \cos\gamma + a_{LM} \cos\alpha_T \tan\gamma)/\tilde{U}$
q_N $-(g \cos\gamma \cos\phi_{v_M} - a_{LM})/\tilde{U}$
r_N $\sin\phi_{v_M} (g \cos\alpha_T \cos\gamma - a_{LM} \sin\alpha_T \tan\gamma)/\tilde{U}$
$I_{LAT} = 0$ and $\bar{q} \geq \bar{q}_3^*$
No
Yes
$\Delta\phi_{temp} = \phi_{v_G} - \tilde{\phi}_v$
$\Delta\phi_{temp}$ $r_{\phi 1}$
No
Yes
$\dot{\phi}_C$ 0
$\Delta\phi_{temp} > r_{\phi 2}$
Yes
No
SLOPE $= r_{\phi 3}/(r_{\phi 2} - r_{\phi 1})$
$\dot{\phi}_C$ = SLOPE $| \Delta\phi_{temp} - r_{\phi 1} \text{sgn}(\Delta\phi_{temp})|$
$\dot{\phi}_C = r_{\phi 3} \text{sgn}(\Delta\phi_{temp})$
C
D

Fig. 2-1 Input Interface Routine Logic Flow (Cont)

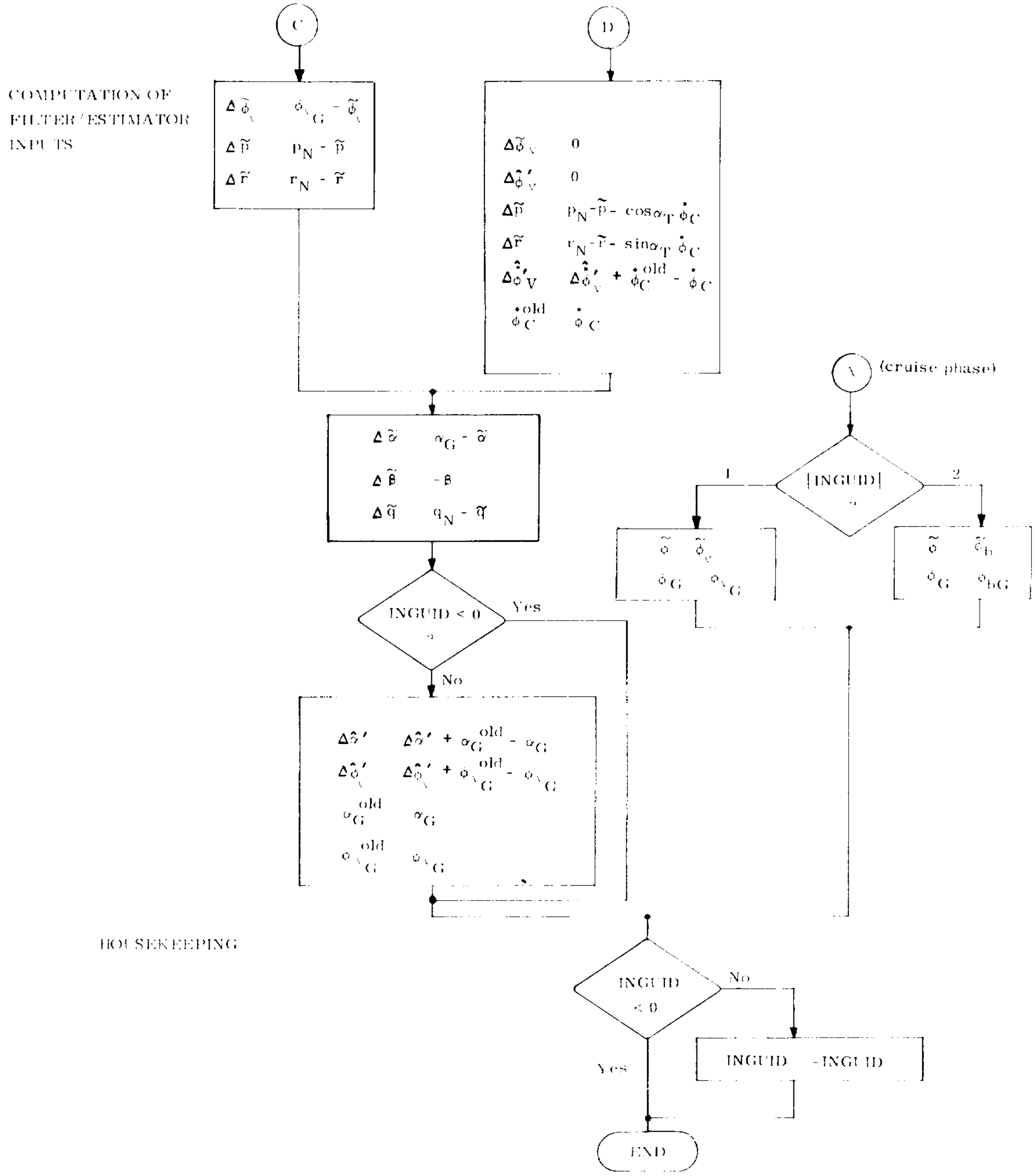
C
D
COMPUTATION OF FILTER/ESTIMATOR INPUTS
$\Delta\tilde{\phi}_V$ $\phi_{VG} - \tilde{\phi}_V$
$\Delta\tilde{p}$ $p_N - \tilde{p}$
$\Delta\tilde{r}$ $r_N - \tilde{r}$
$\Delta\tilde{\phi}_V$ 0
$\Delta\hat{\phi}'_V$ 0
$\Delta\tilde{p}$ $p_N - \tilde{p} - \cos\alpha_T \dot{\phi}_C$
$\Delta\tilde{r}$ $r_N - \tilde{r} - \sin\alpha_T \dot{\phi}_C$
$\Delta\hat{\phi}'_V$ $\Delta\hat{\phi}'_V + \dot{\phi}_C^{old} - \dot{\phi}_C$
$\dot{\phi}_C^{old}$ $\dot{\phi}_C$
A (cruise phase)
|INGUID|
1
2
$\tilde{\phi}$ $\tilde{\phi}_V$
ϕ_G ϕ_{VG}
$\tilde{\phi}$ $\tilde{\phi}_b$
ϕ_G ϕ_{bG}
$\Delta\tilde{\alpha}$ $\alpha_G - \tilde{\alpha}$
$\Delta\tilde{\beta}$ $-\beta$
$\Delta\tilde{q}$ $q_N - \tilde{q}$
INGUID < 0
Yes
No
$\Delta\hat{\alpha}'$ $\Delta\hat{\alpha}' + \alpha_G^{old} - \alpha_G$
$\Delta\hat{\phi}'_V$ $\Delta\hat{\phi}'_V + \phi_{VG}^{old} - \phi_{VG}$
α_G^{old} α_G
ϕ_{VG}^{old} ϕ_{VG}
HOUSEKEEPING
INGUID < 0
No
Yes
INGUID -INGUID
END

Fig. 2-1 Input Interface Routine Logic Flow (Cont)

The inputs to this routine are the following measurements which are obtained from outside the DFCS or are computed by the Input Interface Routine:

TK_A	-	temperature in degrees Kelvin
$\tilde{\alpha}$	-	angle-of-attack (radians)
$\tilde{H}$	-	barometric altitude (ft)
$\tilde{U}$	-	air-relative velocity (ft/sec)

The outputs are:

α_T	-	mean (trim) angle-of-attack (radians)
$\left.\begin{matrix}\sin\alpha_T \\ \cos\alpha_T\end{matrix}\right\}$		sine (cosine) of α_T
U_M	-	mean airspeed (ft/sec)
$\mathcal{M}$	-	Mach number

The means (which are the outputs of first-order filters with time constants equal to the slow sampling period) and the sine and cosine are updated every pass. The means are set equal to the values of their respective measured inputs in an initialization pass.

The other outputs are only computed on slow-sample-rate passes. The computations are shown in Fig. 2-2.

It is expected that, in the future, when more realistic models of the sensors are available, this routine will compute the dynamic pressure and perform other computations.

2.2 Outputs to Control Effectors

The DFCS computes commands for the control effectors listed in Table 2-5. The question of how the commands are transmitted to these effectors is considered to be outside the scope of this document; the following simple implementation is currently assumed:

1) Commands are transmitted by the DFCS to the actuators (or a software module that interacts with the actuators) at the end of each execution of the control routine.
2) The DFCS limits the magnitude of each output, but not its rate of change.
3) Timing of jet firings is obtained by means of a computer clock that can be set to call a DFCS routine which will turn jets off after the required time.

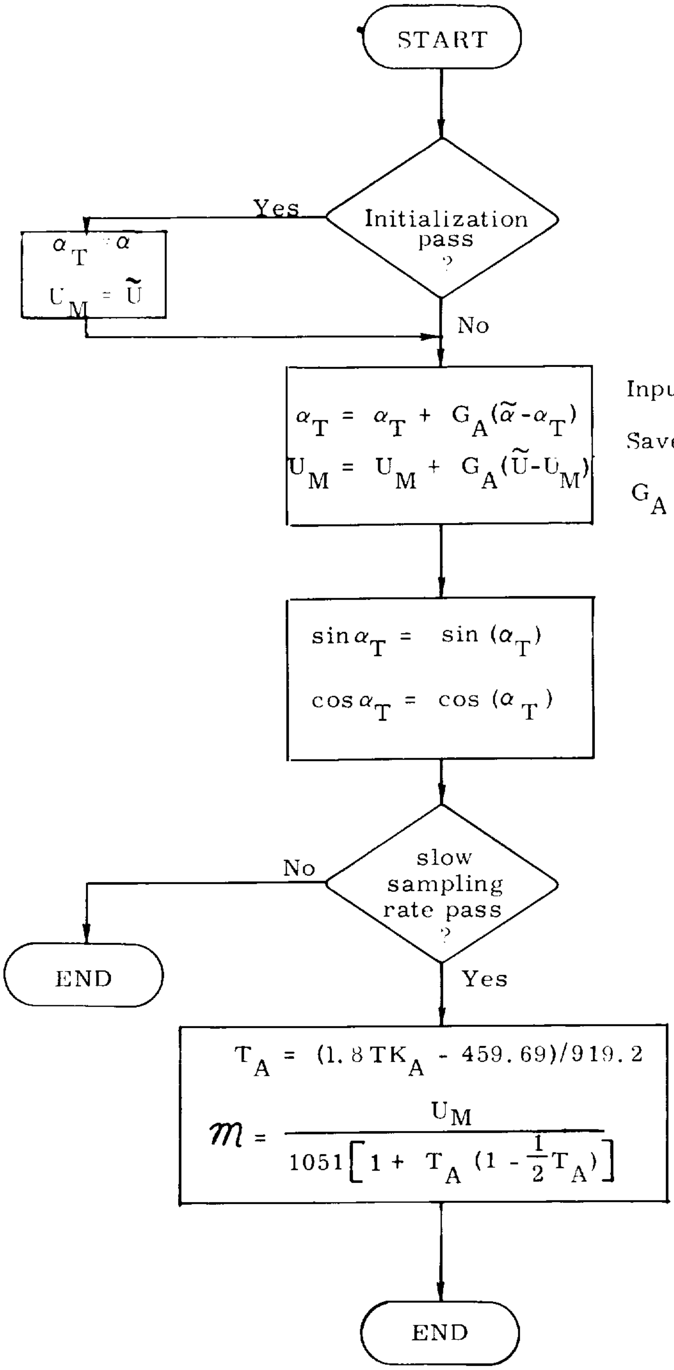
START
Initialization pass ?
Yes
$\alpha_T = \alpha$
$U_M = \tilde{U}$
No
$\alpha_T = \alpha_T + G_A(\tilde{\alpha} - \alpha_T)$
$U_M = U_M + G_A(\tilde{U} - U_M)$
$\sin\alpha_T = \sin(\alpha_T)$
$\cos\alpha_T = \cos(\alpha_T)$
slow sampling rate pass ?
No
END
Yes
$T_A = (1.8 TK_A - 459.69)/919.2$
$\mathcal{m} = \frac{U_M}{1051\left[1 + T_A(1 - \frac{1}{2}T_A)\right]}$
END

Inputs: $\tilde{\alpha}$, $\tilde{H}$, $\tilde{U}$, TK_A

Saved from past: α_T, U_M

$G_A = T_F/T_S$

Fig. 2-2 Computations in Air Data Routine

Table 2-5 Control Effectors Used by the DFCS

		Phases in Which Used*
Aerodynamic Control System (ACS)	elevons, rudder, speed brake, flaps	1, 2, 4, , 8
Attitude Control Propulsion System (ACPS)	40 jet thrusters	4, 5, 6, 7
Air Breathing Engine System (ABES)	throttle	1, 2 (horizontal flight only)
Solid Rocket Motors (SRM)	2 engines; gimballed at 45° from body axes	8
Main Propulsion System (MPS)	3 engines; gimballed	7, 8
Orbital Maneuvering System (OMS)	2 engines; gimballed	5, 7

* Phase designations defined in Table 1-1.

Table 2-6: DFCS Limits for Commands to Control Effectors

Effector	Limit (deg)
aileron (differential elevon)	$\delta a^{max} = \pm 15.0$
elevator (tandem elevon)	$\delta e^{max} = +15.0$ $\delta e^{min} = -40.0$
rudder	$\delta r^{max} = \pm 15.0$
speed brake	$\delta s^{max} = +70.0$ $\delta s^{min} = -17.6$
flap	$\delta f^{max} = +10.0$ $\delta f^{min} = -12.0$
throttle	δt^{max} = 18,000 lb δt^{min} = 500 lb
SRM and MPS gimbals	$\delta g^{max} = \pm 8.0$

The assumed sign conventions for the aerodynamic control surfaces and the associated pilot controller motions are illustrated in Fig. 2-3.

All the commands are limited within the DFCS prior to being issued. The limits magnitudes are shown in Table 2-6. The aileron and elevator commands are treated separately even though they apply to the same pair of actuators, the elevons, and are, therefore, interrelated; this question will be dealt with in the future.

The limiting and blending (for the elevons and MPS gimbals) of the actuator commands is performed in the Command Output Routine, which is called by the DFCS executive after the Control Routine. The Command Output Routine serves as the single point from which the actuators (or the software modules that interact with the actuators) are addressed by the DFCS.

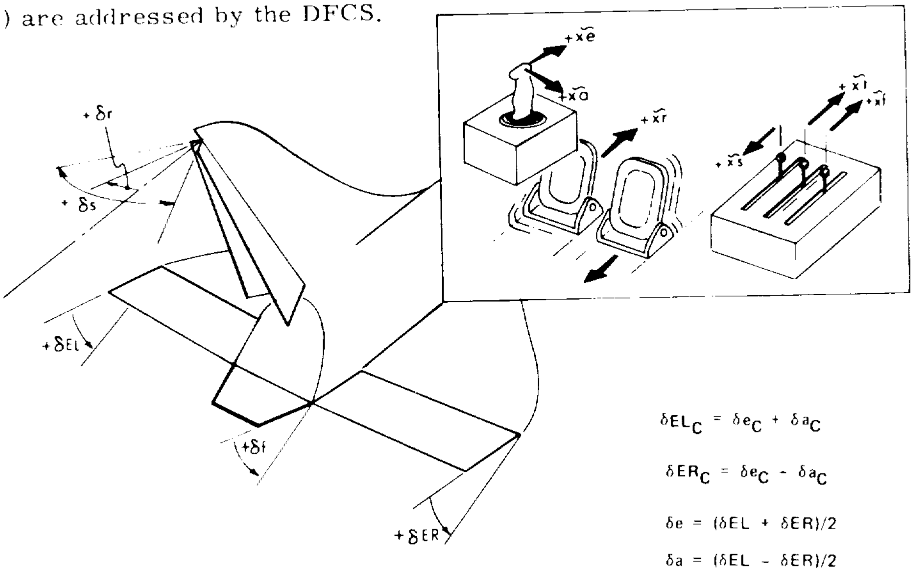

$\delta EL_C = \delta e_C + \delta a_C$

$\delta ER_C = \delta e_C - \delta a_C$

$\delta e = (\delta EL + \delta ER)/2$

$\delta a = (\delta EL - \delta ER)/2$

POSITIVE DEFLECTION OF	PRIMARY VEHICLE RESPONSE	PRIMARY FORCES AND MOMENTS	PILOT CONTROLLER MOTION
δe	$-\theta, -\alpha$	$-C_m$	+xe
δr	$+\beta, -\psi$	$+C_y, -C_n$	+xr
δa	$+\phi$	$+C_\ell$	+xa
δER	$-\phi$	$-C_\ell$	
δEL	$+\phi$	$+C_\ell$	
δs	(- U)	$+C_D$	+ xs
δf	$-\theta, -\alpha$	$-C_M$	+xf

Fig. 2-3 Sign Conventions for Aerodynamic Control Surfaces and Manual Controllers

2.3 ACPS Jet Selection Subroutine

This section describes a scheme for converting angular-rate-change and translation requests into timed jet firing policies for the ACPS (Attitude Control Propulsion System). This routine has been tested with the DFCS program.

2.3.1 Thruster Geometry

The thruster configuration currently incorporated in the jet selection routine is the North American Rockwell ATP design.

As shown in Fig. 2-4, the thrusters for the ATP configuration are grouped in 16 locations. There are 40 thrusters in all, and these are distributed among the 16 locations as shown in Tables 2-7 and 2-8. There are 16 thrusters in the nose of the fuselage and 24 in the "tail".

2.3.2 Jet Selection Logic

The DFCS Control Routine determines a commanded velocity change and calls the jet selection subroutine, which handles angular velocity components and translational velocity components simultaneously with a single algorithm. A flag can be set instructing the jet selection subroutine to ignore translation, simplifying and speeding up the jet selection procedure. Furthermore, the jet selection logic can be instructed to deal with jet clusters or with the individual thrusters.

Figure 2-5 is a functional flow diagram of the jet selection logic. A discussion of this logic follows.

The ACPS jet control authority subroutine is only fully executed when the jet selection routine is called for the first time in a mission phase. The control authority subroutine calculates the ACPS control authorities on the basis of total vehicle mass, the vehicle inertia matrix, and the center of mass location. The control authorities are calculated for the jet clusters and for the individual thrusters. The control authority is the angular and translational acceleration in vehicle coordinates generated by firing a jet or cluster of jets. In addition, a cost per unit firing time is assigned to each jet. Currently, all these costs are equal. When a jet is disabled (or restored) and the jet-selection logic is operating on clusters, the jet control authority subroutine is partially executed, appropriately altering the corresponding acceleration vector and cost element.

The jet selection subroutine next checks its inputs to see whether or not there is a new velocity change request. If not, the jet selection subroutine call must be for the purpose of turning off jets which have completed their firing intervals. If the velocity change request is a new one, the linear programming subroutine is called, which expresses the velocity change vector as a linear combination of jet acceleration vectors, the linear coefficients being the firing times.

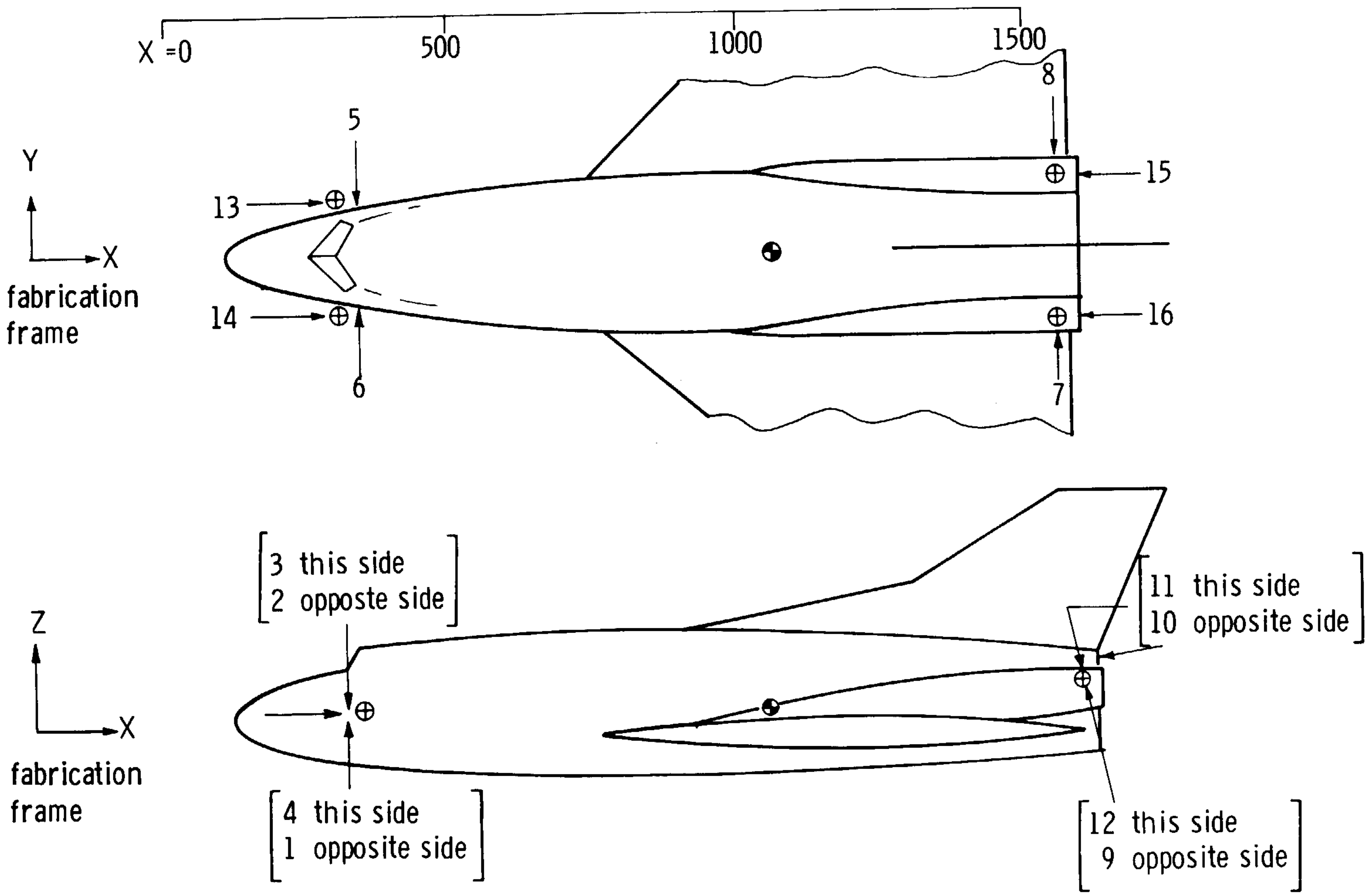

Fig. 2-4 Thruster Locations - NR ATP Baseline Orbiter

Table 2-7 Distribution of ACPS Thrusters

NR ATP Baseline Orbiter

Thruster Location	Number of Thrusters	Thruster ID
1	2	10, 12
2	2	14, 16
3	2	13, 15
4	2	9, 11
5	2	6, 8
6	2	5, 7
7	4	17, 19, 21, 23
8	4	18, 20, 22, 24
9	3	32, 34, 36
10	3	26, 28, 30
11	3	25, 27, 29
12	3	31, 33, 35
13	2	2, 4
14	2	1, 3
15	2	38, 40
16	2	37, 39
	40 total	

Table 2-8 Parameters of Individual Jets

ID	Jet Location — Body Station (inches)			Thrust Components		
	Fabrication	Frame			Vehicle	Frame
1	318.0	- 96.0	374.0	-1.0	0.0	0.0
2	318.0	96.0	374.0	-1.0	0.0	0.0
3	318.0	- 96.0	349.0	-1.0	0.0	0.0
4	318.0	96.0	349.0	-1.0	0.0	0.0
5	318.0	-109.0	368.0	0.0	1.0	0.0
6	318.0	109.0	368.0	0.0	-1.0	0.0
7	318.0	-109.0	355.0	0.0	1.0	0.0
8	318.0	109.0	355.0	0.0	-1.0	0.0
9	318.0	-109.0	346.0	0.0	0.0	-1.0
10	318.0	109.0	346.0	0.0	0.0	-1.0
11	330.0	-109.0	346.0	0.0	0.0	-1.0
12	330.0	109.0	346.0	0.0	0.0	-1.0
13	318.0	- 80.0	367.0	0.0	0.0	1.0
14	318.0	80.0	367.0	0.0	0.0	1.0
15	330.0	- 80.0	367.0	0.0	0.0	1.0
16	330.0	80.0	367.0	0.0	0.0	1.0
17	1536.5	-158.0	425.0	0.0	1.0	0.0
18	1536.5	158.0	425.0	0.0	-1.0	0.0
19	1532.5	-158.0	438.0	0.0	1.0	0.0
20	1532.5	158.0	438.0	0.0	-1.0	0.0
21	1528.5	-158.0	450.0	0.0	1.0	0.0
22	1528.5	158.0	450.0	0.0	-1.0	0.0
23	1525.5	-158.0	464.0	0.0	1.0	0.0
24	1525.5	158.0	464.0	0.0	-1.0	0.0
25	1541.5	-130.0	480.0	-0.234	0.0	0.980
26	1541.5	130.0	480.0	-0.234	0.0	0.980
27	1555.5	-130.0	484.0	-0.234	0.0	0.980
28	1555.5	130.0	484.0	-0.234	0.0	0.980
29	1567.5	-130.0	487.0	-0.234	0.0	0.980
30	1567.5	130.0	487.0	-0.234	0.0	0.980
31	1546.5	-130.0	416.0	0.407	0.0	-0.915
32	1546.5	130.0	416.0	0.407	0.0	-0.915
33	1559.5	-130.0	420.0	0.407	0.0	-0.915
34	1559.5	130.0	420.0	0.407	0.0	-0.915
35	1572.5	-130.0	428.0	0.407	0.0	-0.915
36	1572.5	130.0	428.0	0.407	0.0	-0.915
37	1579.5	-149.9	468.0	0.980	0.0	0.234
38	1579.5	149.0	468.0	0.980	0.0	0.234
39	1579.5	-149.0	455.0	0.980	0.0	0.234
40	1579.5	149.0	455.0	0.980	0.0	0.234
c.g.	1096.5	0.1	367.9			

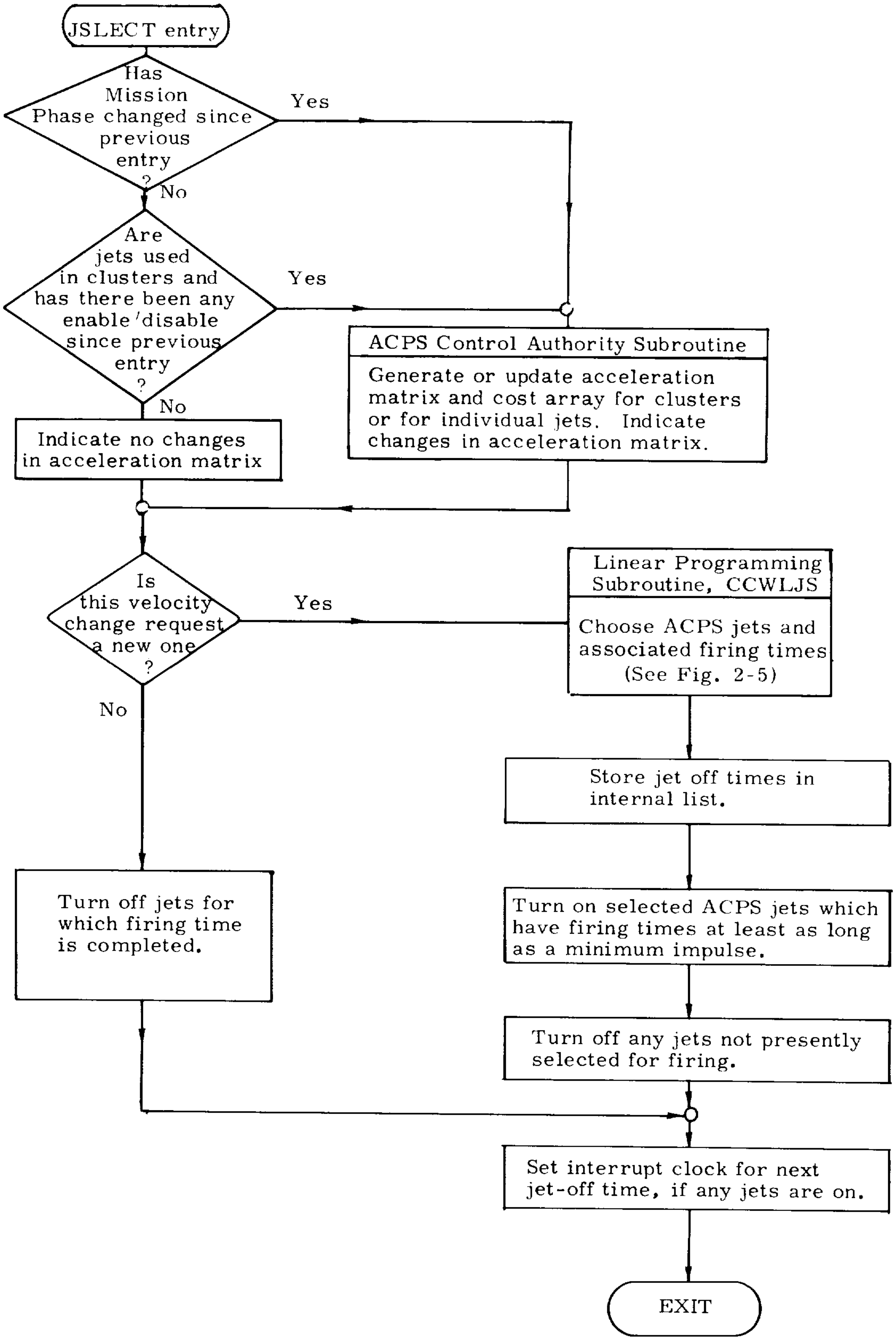
JSLECT entry
Has Mission Phase changed since previous entry ?
Yes
No
Are jets used in clusters and has there been any enable/disable since previous entry ?
Yes
No
ACPS Control Authority Subroutine
Generate or update acceleration matrix and cost array for clusters or for individual jets. Indicate changes in acceleration matrix.
Indicate no changes in acceleration matrix
Is this velocity change request a new one ?
Yes
No
Linear Programming Subroutine, CCWLJS
Choose ACPS jets and associated firing times (See Fig. 2-5)
Store jet off times in internal list.
Turn off jets for which firing time is completed.
Turn on selected ACPS jets which have firing times at least as long as a minimum impulse.
Turn off any jets not presently selected for firing.
Set interrupt clock for next jet-off time, if any jets are on.
EXIT

Fig. 2-5 ACPS Jet Selection Functional Flow Diagram

Generally, many different jet combinations could satisfy a given velocity change request; if there is more than one such combination, the total cost is minimized in the selection process. Any jet which is flagged because of failure or mission-related constraints is omitted from consideration.

The selected jets are turned on (if they are not already firing), and all others are turned off and removed from the internal jet-off list. The interrupt clock is set to return control to the jet selection subroutine when the next jet-off is due, and the "new velocity request" flag is zeroed.

The interface parameters for the jet selection package are:

INPUT:

a) Velocity change command vector.
b) Flag for new velocity vector.
c) ACPS jet exclusion list.
d) Translation inclusion flag.
e) Phase flag.

OUTPUT:

a) Jet-on/off commands.
b) Interrupt clock settings.
c) Zeroed flag for new request.

Figure 2-6a presents features of the linear programming subroutine, CCWLJS, and Fig. 2-6b describes its logic flow.

Linear Programming Subroutine

PURPOSE: Represents input vector W as a linear combination of linearly independent columns from matrix B, choosing columns from B to minimize cost of solution.

INPUTS: LROW - Number of components in W. (Dimension of requests)

LCOL - Number of columns in B matrix. (Number of jets or clusters)

W - Vector (size LROW) to be analyzed as a linear combination of columns from B.

COST - Array (size LCOL) of strictly positive cost coefficients, one associated with each B column.

B - Matrix (LROW by LCOL). Each column represents the acceleration associated with a one-second firing of the corresponding jet in vehicle coordinates. Components may include rotational or translational acceleration elements, or both.

LALARM - Non-zero indicates that previous jet selection may not be taken as a starting basis, for one of the following reasons:

1) Jet exclusion list has been changed
2) $\overset{*}{B}$, LROW, or LCOL have been altered since the preceding pass
3) Preceding delta-V request was not successfully resolved into jet firings. Initialized to 1 on first pass.

JFAIL - Array (size LCOL) of flags, J^{th} element non-zero to indicate J^{th} jet failed.

$\overset{*}{B}I$, $\overline{CF}$, $L\overline{Q}$ - Can be inputs as well as outputs. See definitions below under OUTPUTS.

PARAMETERS - SAVING, MAXPAS, MAXITR, TOLRNC, URGNCY can be chosen to match the precision of the computation and the accuracy of the data.

Fig. 2-6a Features of Linear Programming Subroutine, CCWLJS

Linear Programming Subroutine (Cont)

OUTPUTS:

BI - Transformation matrix (LROW by LROW) going from vehicle coordinates to coordinates based on selected columns of B.

V - Solution vector (size LROW) of coefficients for selected columns of B matrix, satisfying: $\overset{*}{BI}\ \bar{W} = \bar{V}$

CF - Vector (size LROW) of cost coefficients selected from COST array, corresponding to chosen columns from B matrix.

Z - Cost of solution, satisfying: $Z = \bar{CF} \cdot \bar{V}$.

LQ - Array (size LROW) giving the indices and sequence of selected B columns.

MCOUNT - Number of basis element substitutions performed in current execution.

LALARM - Non-zero if $\bar{W}$ was not successfully resolved into jet firings before MCOUNT exceeded MAXITR.

ASSUMPTIONS:

1) Cost array entries are all strictly positive, i.e., greater than zero.

2) Negative LQLIST outputs and negative V components are to be excluded from any implementation of the solution.

3) COST array entries are small compared to URGNCY.

4) BI matrix is never altered by any other program.

5) LALARM will be input as non-zero whenever changes occur in LROW, LCOL, B, or the jet exclusion list.

ENTRY: Call CCWLJS (B, W)

EXIT: RETURN to caller.

Fig. 2-6a Features of Linear Programming Subroutine, CCWLJS (Cont)

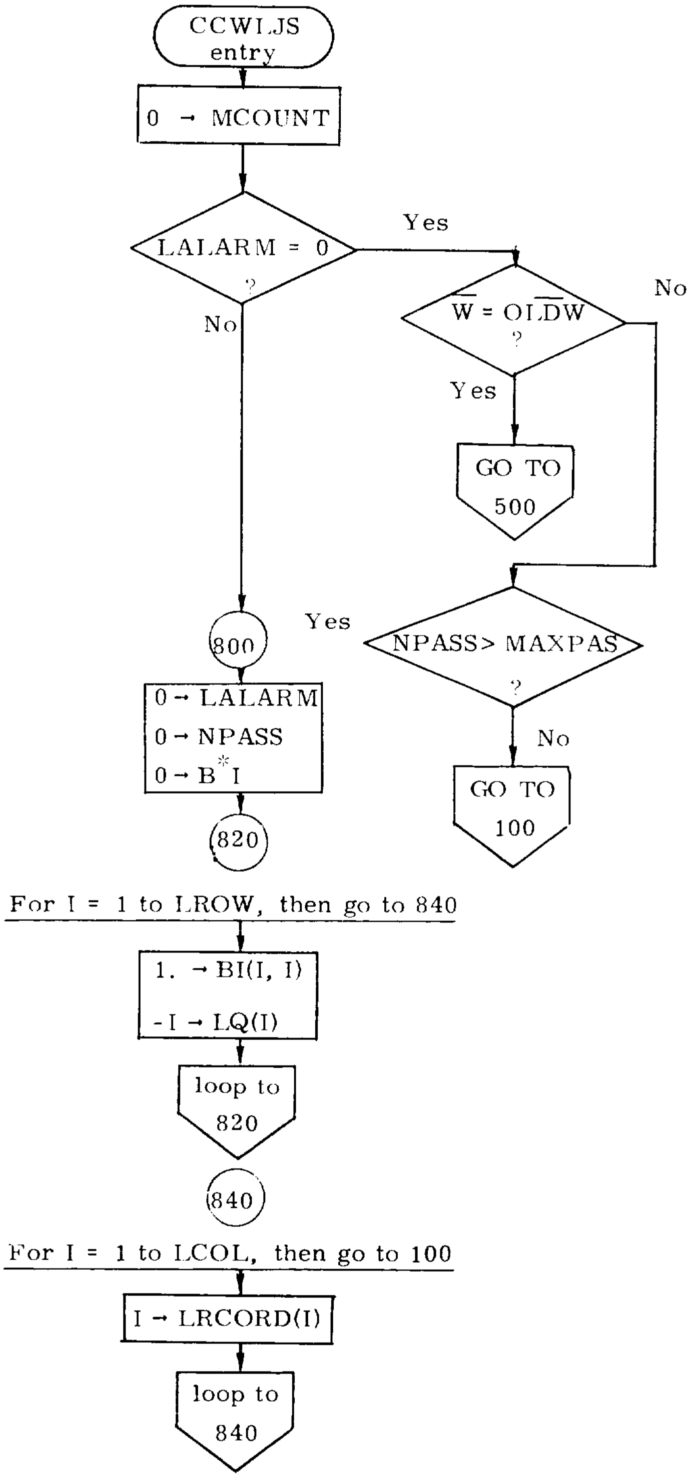

MCOUNT counts iterations on this pass

If $\overset{*}{\overline{B}}I$ cumulative roundoff is not bad, if previous solution was valid, and if $\overset{*}{\underline{B}}$, LROW, LCOL are unchanged, then start with solution from previous pass. Otherwise initialize completely.

If $\overline{W}$ is unchanged from previous pass, use same solution.

NPASS counts iterations since last complete initialization.

Negative LQ values identify vehicle frame coordinates, which are non-jets.

Positive LRCORD values correspond to non-selected jets.

Fig. 2-6b Flow Chart of Linear Programming Subroutine, CCWLJS

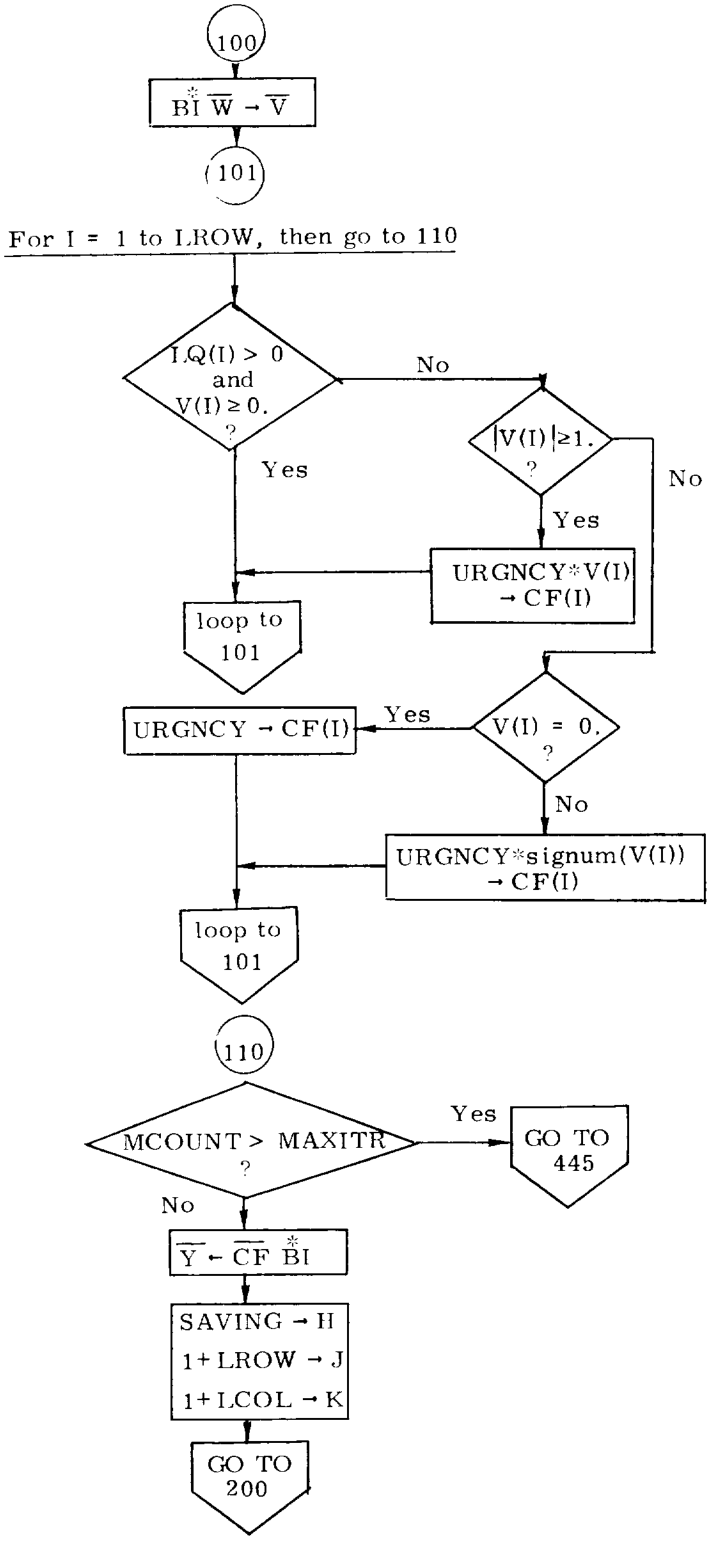

$\overline{V}$ contains latest version of solution in terms of current basis.

Cost target vector is initially a weighted version of $\overline{V}$ (or a signum ($\overline{V}$) vector).

URGNCY factor places premium on jets which approximate $\overline{W}$ or which fire in directions represented so far by non-jets.

Y(I) is weighted cost of generating the Ith original (vehicle) basis vector as a linear combination of current basis vectors.

Initialize the search for the next jet to be included in basis.

Fig. 2-6b Flow Chart of Linear Programming Subroutine, CCWLJS (Cont)

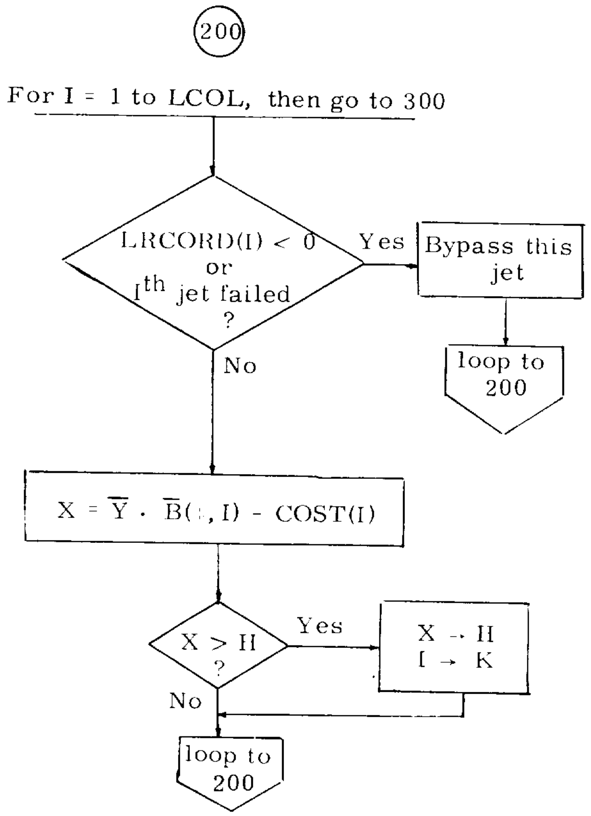
200
For I = 1 to LCOL, then go to 300
LRCORD(I) < 0 or Ith jet failed ?
Yes
Bypass this jet
loop to 200
No
X = Ȳ · B̄(:,I) - COST(I)
X > H ?
Yes
X → H
I → K
No
loop to 200

Search for next jet to be introduced to basis, bypassing any which are failed or already in basis.

X is the weighted price penalty for simulating a one-sec firing of I^{th} jet, using the basis rather than the jet itself.

Greatest saving per second is H; corresponding jet is K.

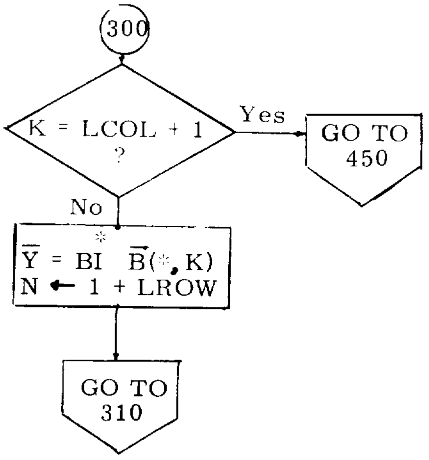

If no jet was selected for inclusion, then exit.

K^{th} jet is to be included. Y is K^{th} jet acceleration vector described in current basis.

Fig. 2-6b Flow Chart of Linear Programming Subroutine, CCWLJS (Cont)

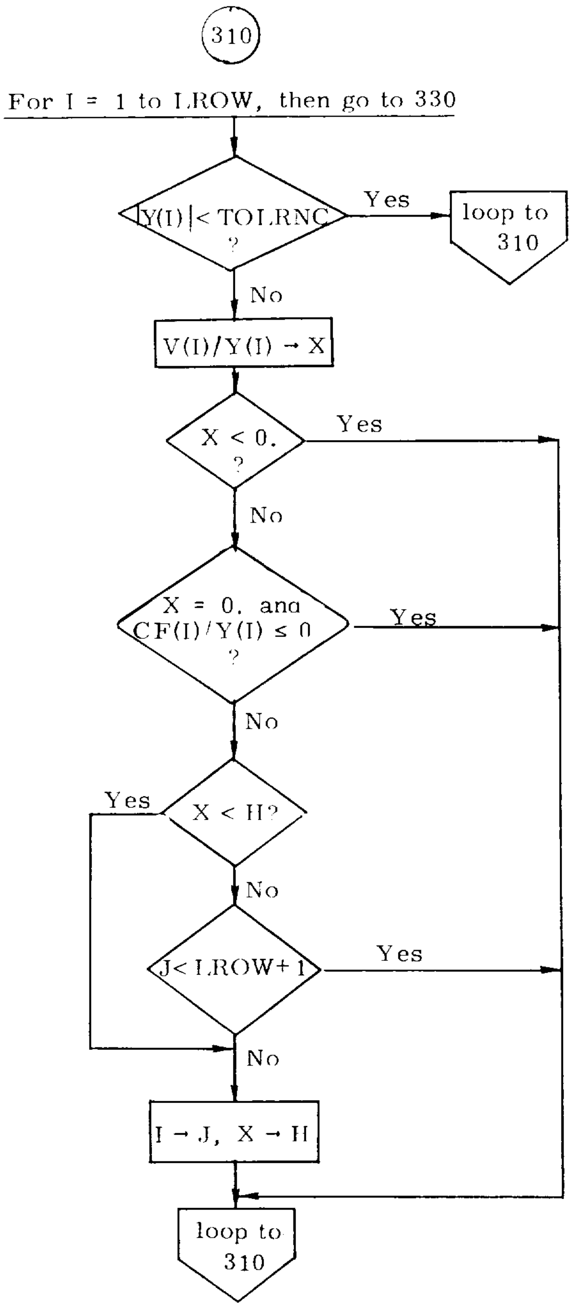

Choose Jth basis member for replacement so that the new V(J) is ≥ 0., and no other V component changes sign.

Fig. 2-6b Flow Chart of Linear Programming Subroutine, CCWLJS (Cont)

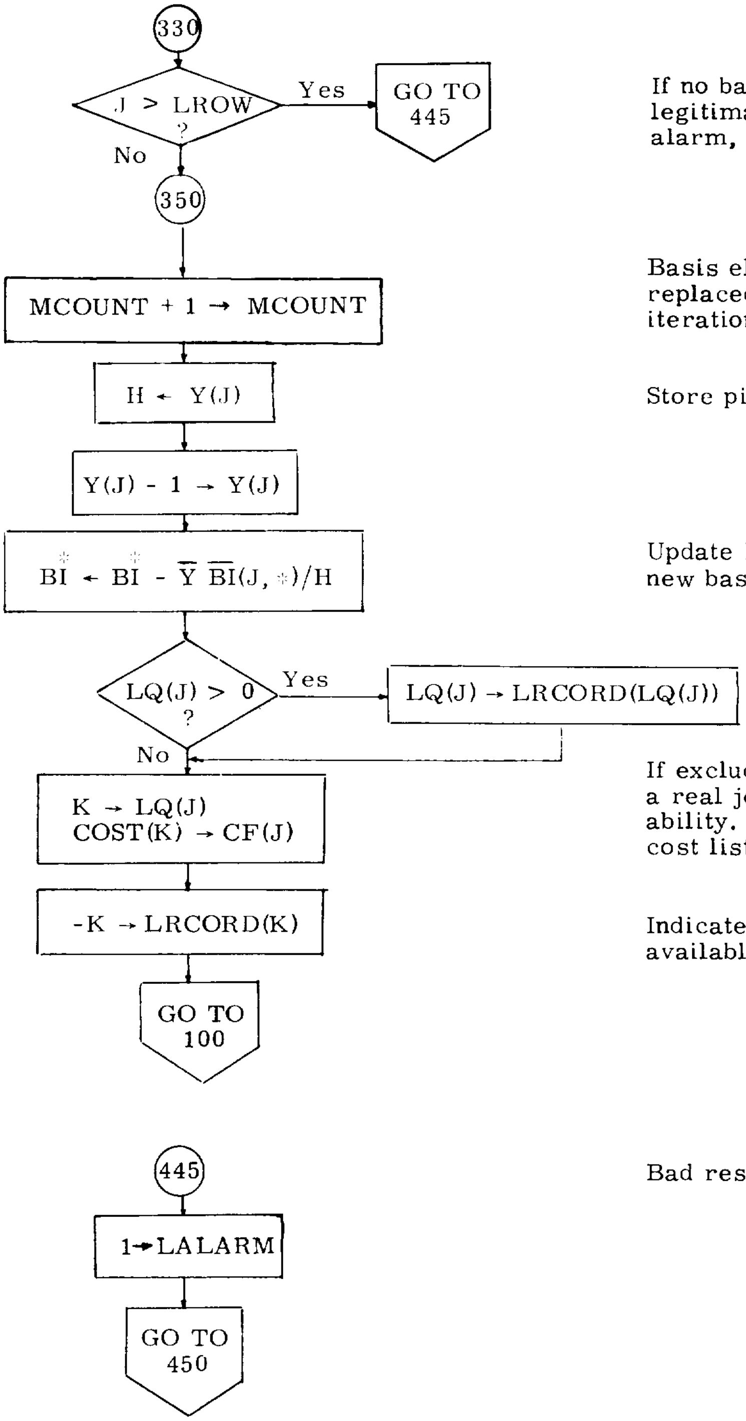

If no basis element can be legitimately replaced, set alarm, and exit.

Basis element J is to be replaced by jet K. Step the iteration counter.

Store pivot element.

Update BI* matrix to reflect new basis composition.

If excluded basis element was a real jet, indicate its availability. Update basis list, cost list.

Indicate K^{th} jet no longer available. Repeat iteration.

Bad result.

Fig. 2-6b Flow Chart of Linear Programming Subroutine, CCWLJS (Cont)

EXIT

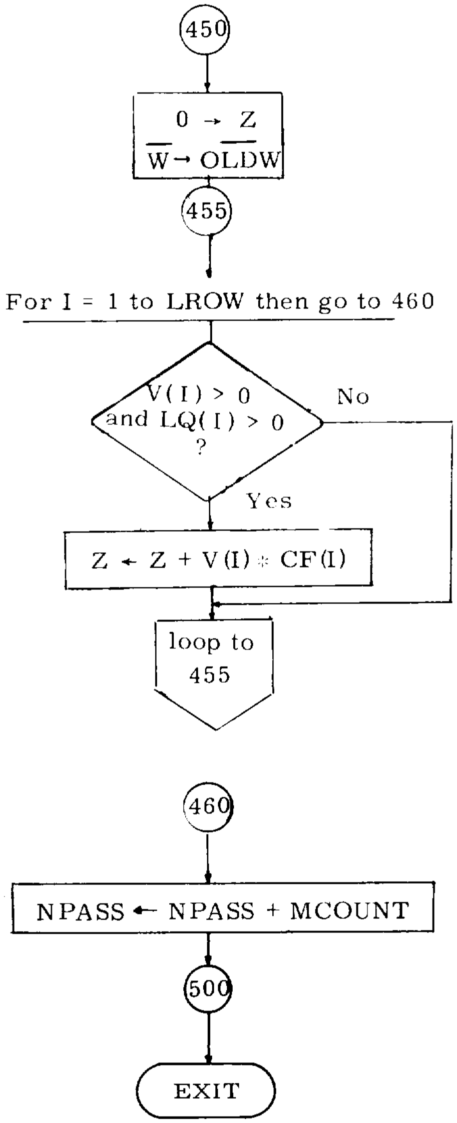

Calculate cost of solution:
$Z = \overline{CF} \cdot \overline{V}$

Save $\overline{W}$ for comparison in next pass.

Negative firing times represent requests which cannot be met with currently non-failed jets.

NPASS reflects quality of BI matrix.

Return to caller.

Fig. 2-6b Flow Chart of Linear Programming Subroutine, CCWLJS (Cont)

2.4 ACPS Jet Selection Logic for the ATP Configuration

A jet selection routine is presented in this section that is more restricted than the design of the preceding section. It is essentially a table look-up; the firing policy for each possible command, as well as the individual jets and the control authority corresponding to each jet cluster are pre-determined and stored for access by this on-line routine. The North American Rockwell ATP design for the ACPS, which has been presented in Fig. 2-4 and Tables 2-7 and 2-8 was assumed in the off-line computations.

The flow chart of Fig. 2-7a describes in detail the jet selection logic for the ATP configuration. Figure 2-7b defines the flowchart symbols. A discussion of some of the features of the logic follows.

General - To provide attitude control with no translational disturbances, jet couples must be used. However, pure jet couples exist in only one axis, the roll axis. Jet couples to be used for pitch control (e. g. 3 & 12) and yaw control (e. g. 5 & 7), also effect roll. To achieve pure pitch or yaw two thruster couples must be fired to null the roll disturbance; for example, 3 and 1 12 with 2 and 10 for pitch and 5 and 7 with 3 and 1 for yaw. Hence, couple control can require as many as four thrusters to fire whereas non-couple control may require only one thruster firing (e. g. yaw control). Additionally, the multiple thruster firings required for couple control produces large minimum impulse rate changes and these cause fast limit cycles and inefficient propellent usage. This logic has the option of attitude control with either coupled or non-coupled jets.

Nose versus Tail Thrusters - for Non-coupled Jet Operation - The logic allows the crew to select either nose or tail thrusters for control of each axis. This serves two purposes:

1) Comparing nose thrusters to tail thrusters, the nose thrusters have shorter roll moment arms, but longer pitch and yaw moment arms. Hence, the crew can select the preferable moment arm length for each axis.

2) This is a simple means of accounting for thruster failures. Should all the thrusters in any single location fail, control can still be maintained (Note: Individual failures in any jet location are accounted for by placing another jet of the same location in "common" with the location, see page 16 of the flowcharts).

Phase Plane Jet Selection Logic Interaction - (Non-coupled Operation) - Thrusters in locations 1 through 4, and 9 through 12, produce both pitch and roll torques. Hence, it takes two thrusters to provide either pure roll or pure pitch. However, smaller minimum impulse rate changes are possible by firing only one thruster. Therefore, even if there is a phase plane command from only one axis (roll or pitch), the logic will attempt to do the latter (fire only one thruster) if the resulting disturbance in the "non-command" axis reduces the rate error (called RR_X or RR_Y in the logic).

Use of the tail thrusters for yaw control causes a roll disturbance; should the roll disturbance exceed a rate limit, the logic will consider the disturbance part of the phase plane command and cause corrective roll thrusters to fire.

Translations - No combination of thrusters will produce Y or Z translations with negligible rotational disturbances. Thrusters must be modulated to null rotational disturbances. This modulation could be performed either open loop in the jet selection logic, or closed loop through the phase plane logic (the crossing of a switching line) and jet selection logic. The latter method was chosen because it will not produce unnecessary modulation (thruster firings) during small Y or Z translations (i. e., when rotational disturbance is not long enough to cause switching line crossing).

During +X-translations, it is possible to control yaw by modulating the +X-thrusters; this option is available in the logic.

Jet Coupling and Logic Flow - With respect to thruster control actions, there are two basic types of thrusters:

1) Those that produce Y translation and yaw.

2) Those that produce Z translation and roll and pitch.

Sequentially, the logic first calculates commands for Y translation and yaw and then issues commands for Z translation, roll, and pitch control.

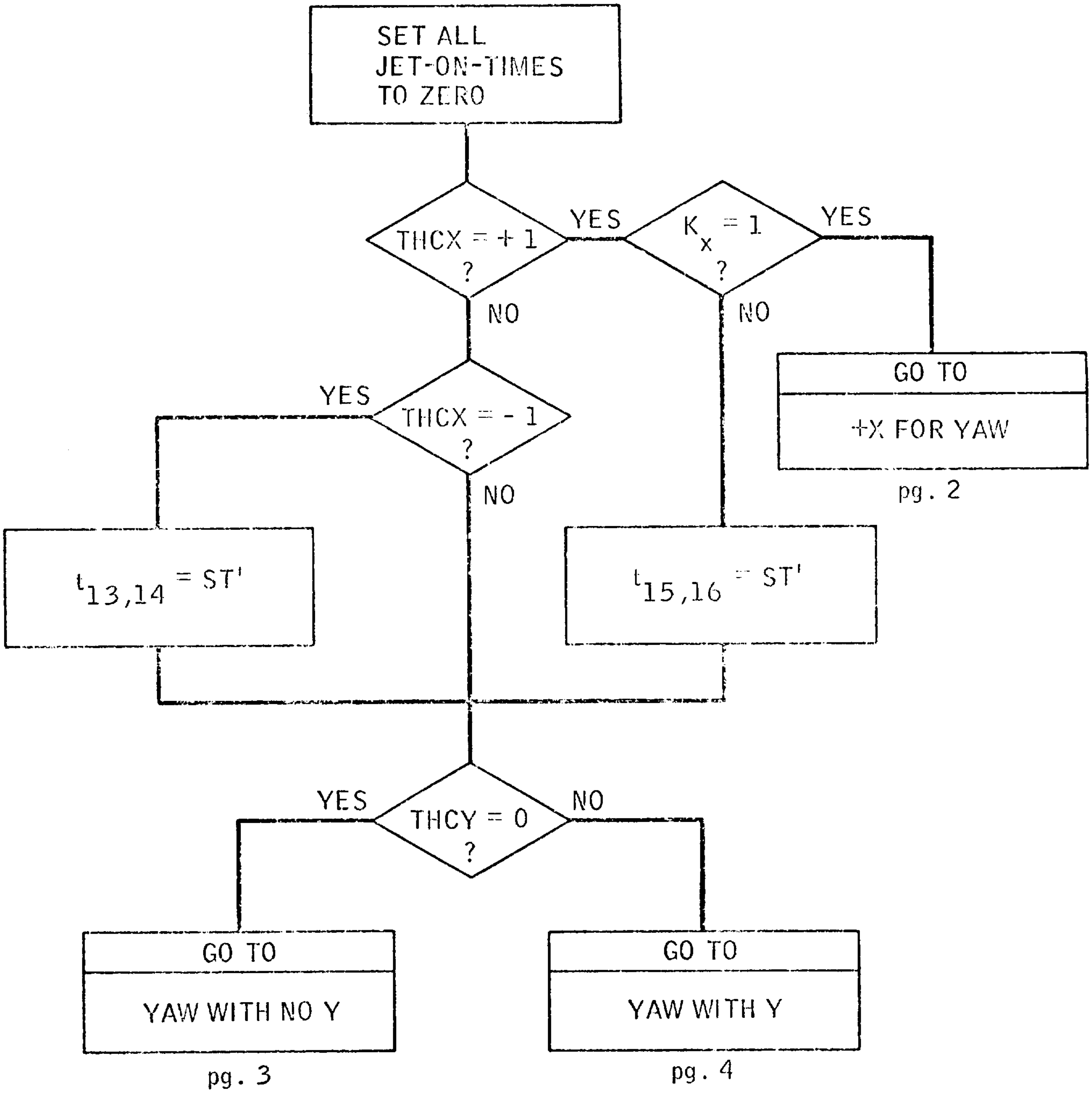

Fig. 2-7a Flow Chart Jet Selection Logic for ATP Configuration
(Flow Chart continues for 22 pages)

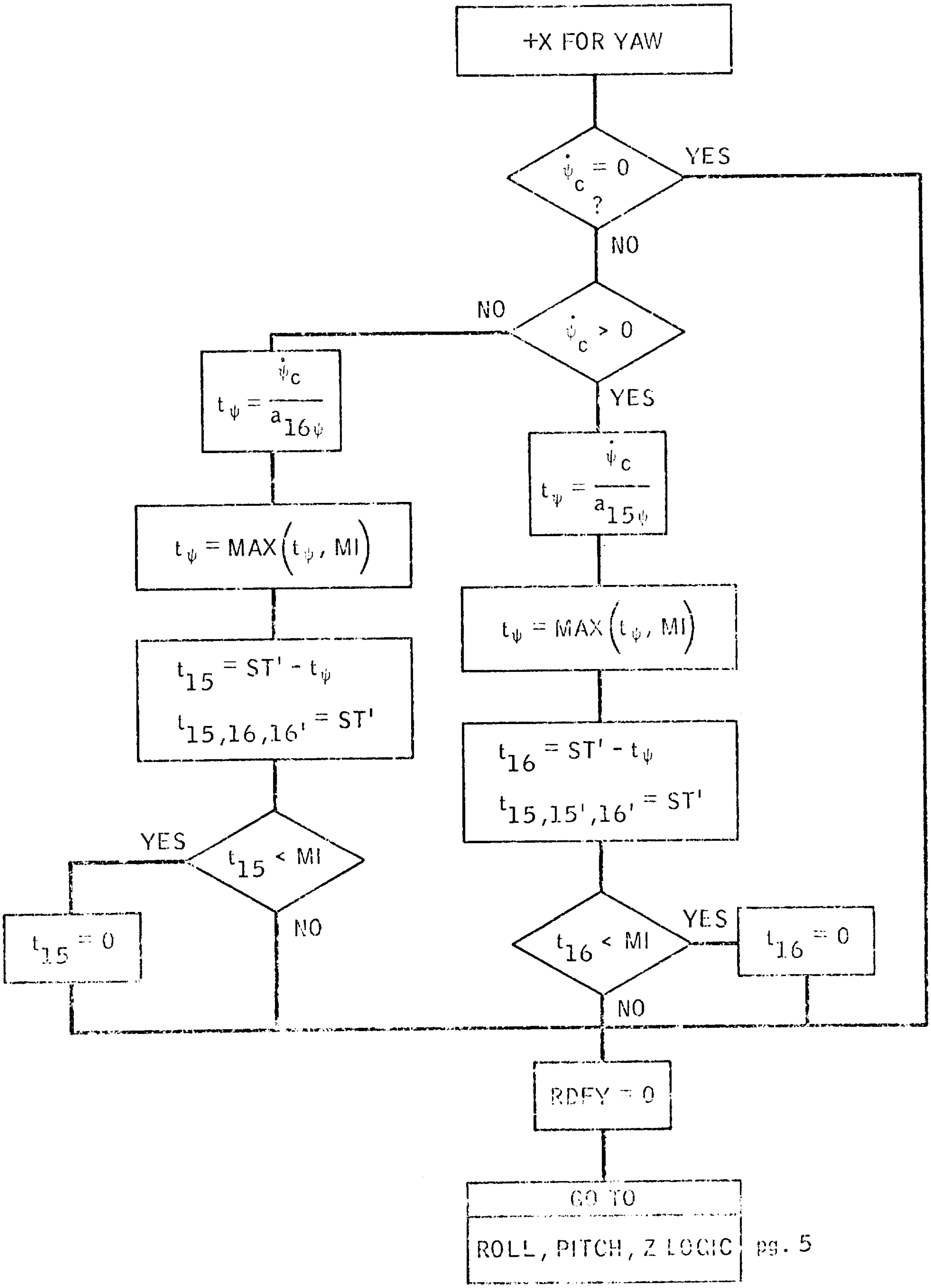
+X FOR YAW
$\dot{\psi}_c = 0$?
YES
NO
$\dot{\psi}_c > 0$
NO
YES
$t_\psi = \frac{\dot{\psi}_c}{a_{16\psi}}$
$t_\psi = \frac{\dot{\psi}_c}{a_{15\psi}}$
$t_\psi = MAX(t_\psi, MI)$
$t_\psi = MAX(t_\psi, MI)$
$t_{15} = ST' - t_\psi$
$t_{15,16,16'} = ST'$
$t_{16} = ST' - t_\psi$
$t_{15,15',16'} = ST'$
$t_{15} < MI$
YES
NO
$t_{15} = 0$
$t_{16} < MI$
YES
NO
$t_{16} = 0$
RDFY = 0
GO TO
ROLL, PITCH, Z LOGIC
pg. 5

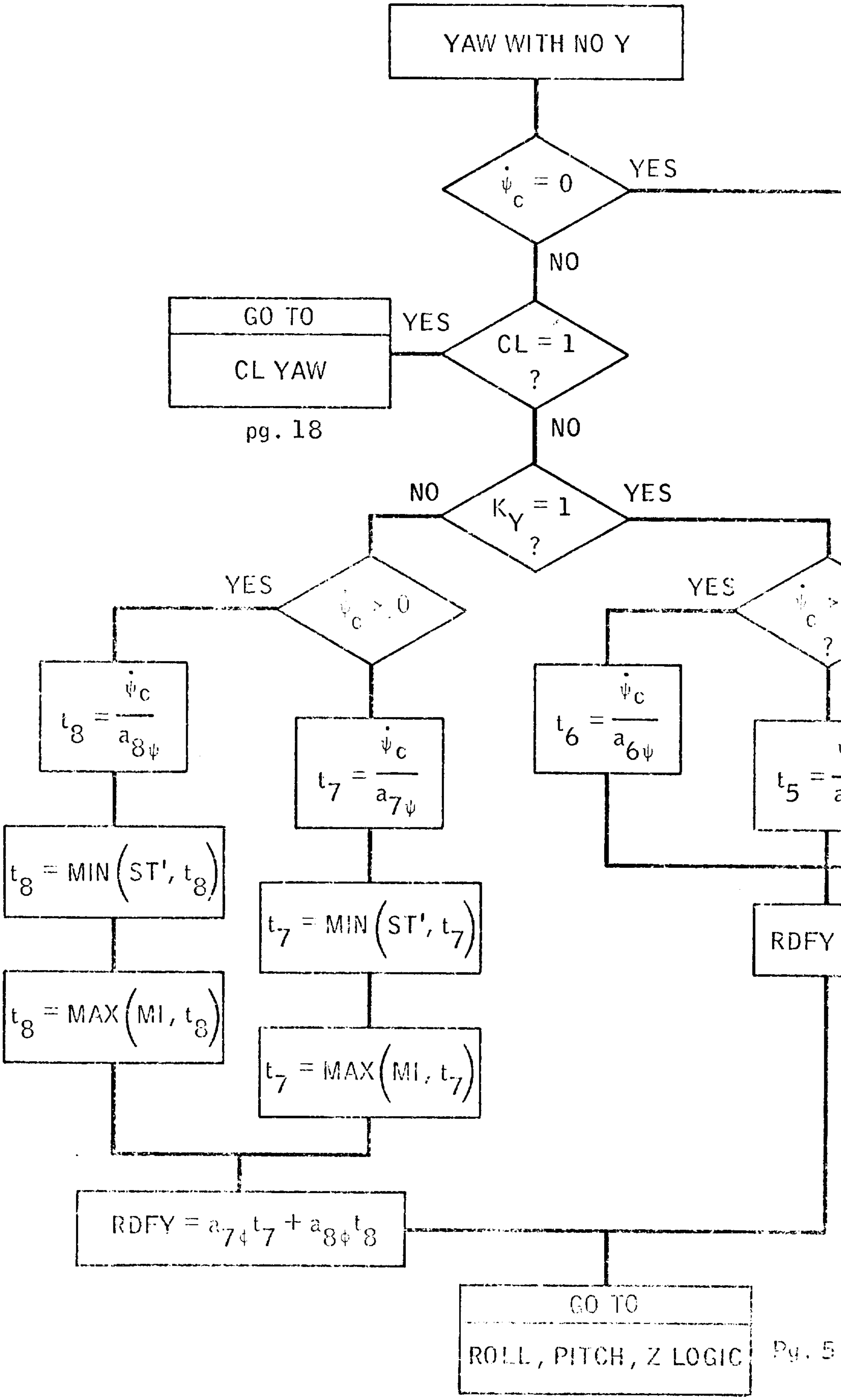
YAW WITH NO Y
$\dot{\psi}_c = 0$
YES
NO
GO TO
CL YAW
pg. 18
YES
CL = 1
?
NO
NO
$K_Y = 1$
?
YES
YES
$\dot{\psi}_c > 0$
$t_8 = \frac{\dot{\psi}_c}{a_{8\psi}}$
$t_8 = MIN(ST', t_8)$
$t_8 = MAX(MI, t_8)$
$t_7 = \frac{\dot{\psi}_c}{a_{7\psi}}$
$t_7 = MIN(ST', t_7)$
$t_7 = MAX(MI, t_7)$
YES
$\dot{\psi}_c > 0$
?
NO
$t_6 = \frac{\dot{\psi}_c}{a_{6\psi}}$
$t_5 = \frac{\dot{\psi}_c}{a_{5\psi}}$
RDFY = 0
$RDFY = a_{7\psi}t_7 + a_{8\psi}t_8$
GO TO
ROLL, PITCH, Z LOGIC
Pg. 5

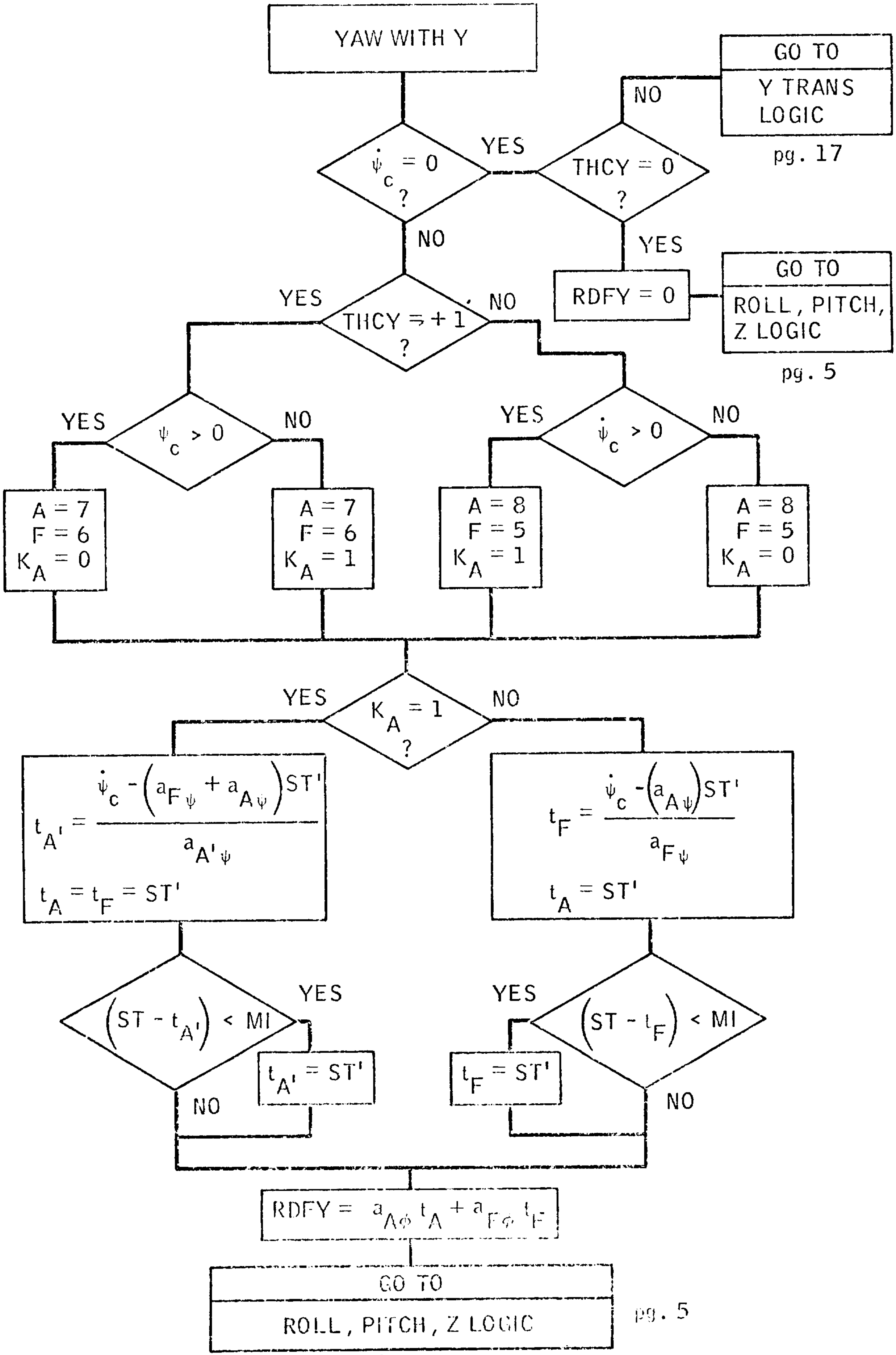
YAW WITH Y
$\dot{\psi}_c = 0$?
YES
THCY = 0 ?
NO
GO TO
Y TRANS LOGIC
pg. 17
YES
RDFY = 0
GO TO
ROLL, PITCH, Z LOGIC
pg. 5
NO
YES
THCY = + 1 ?
NO
YES
$\psi_c > 0$
NO
YES
$\dot{\psi}_c > 0$
NO
$A = 7$ $F = 6$ $K_A = 0$
$A = 7$ $F = 6$ $K_A = 1$
$A = 8$ $F = 5$ $K_A = 1$
$A = 8$ $F = 5$ $K_A = 0$
YES
$K_A = 1$?
NO
$t_{A'} = \dfrac{\dot{\psi}_c - \left(a_{F_\psi} + a_{A_\psi}\right)ST'}{a_{A'_\psi}}$
$t_A = t_F = ST'$
$t_F = \dfrac{\dot{\psi}_c - \left(a_{A_\psi}\right)ST'}{a_{F_\psi}}$
$t_A = ST'$
$\left(ST - t_{A'}\right) < MI$
YES
$t_{A'} = ST'$
NO
YES
$\left(ST - t_F\right) < MI$
$t_F = ST'$
NO
$RDFY = a_{A\phi} t_A + a_{F\phi} t_F$
GO TO
ROLL, PITCH, Z LOGIC
pg. 5

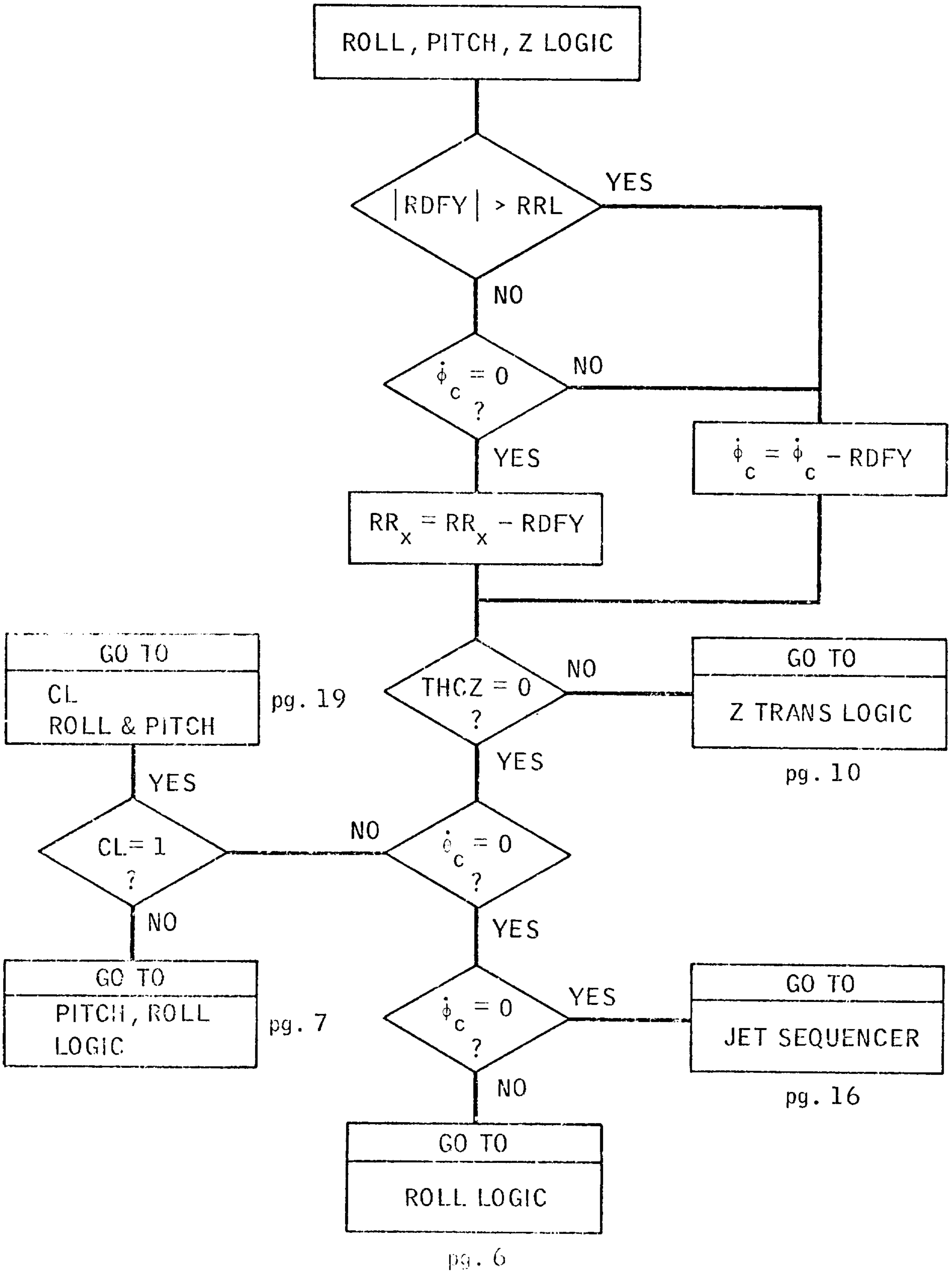
ROLL, PITCH, Z LOGIC
|RDFY| > RRL
YES
NO
$\dot{\phi}_c = 0$?
NO
YES
$\dot{\phi}_c = \dot{\phi}_c$ − RDFY
$RR_x = RR_x$ − RDFY
THCZ = 0 ?
NO
GO TO
Z TRANS LOGIC
pg. 10
YES
GO TO
CL
ROLL & PITCH
pg. 19
YES
CL = 1 ?
NO
$\dot{\theta}_c = 0$?
NO
GO TO
PITCH, ROLL LOGIC
pg. 7
YES
$\dot{\psi}_c = 0$?
YES
GO TO
JET SEQUENCER
pg. 16
NO
GO TO
ROLL LOGIC
pg. 6

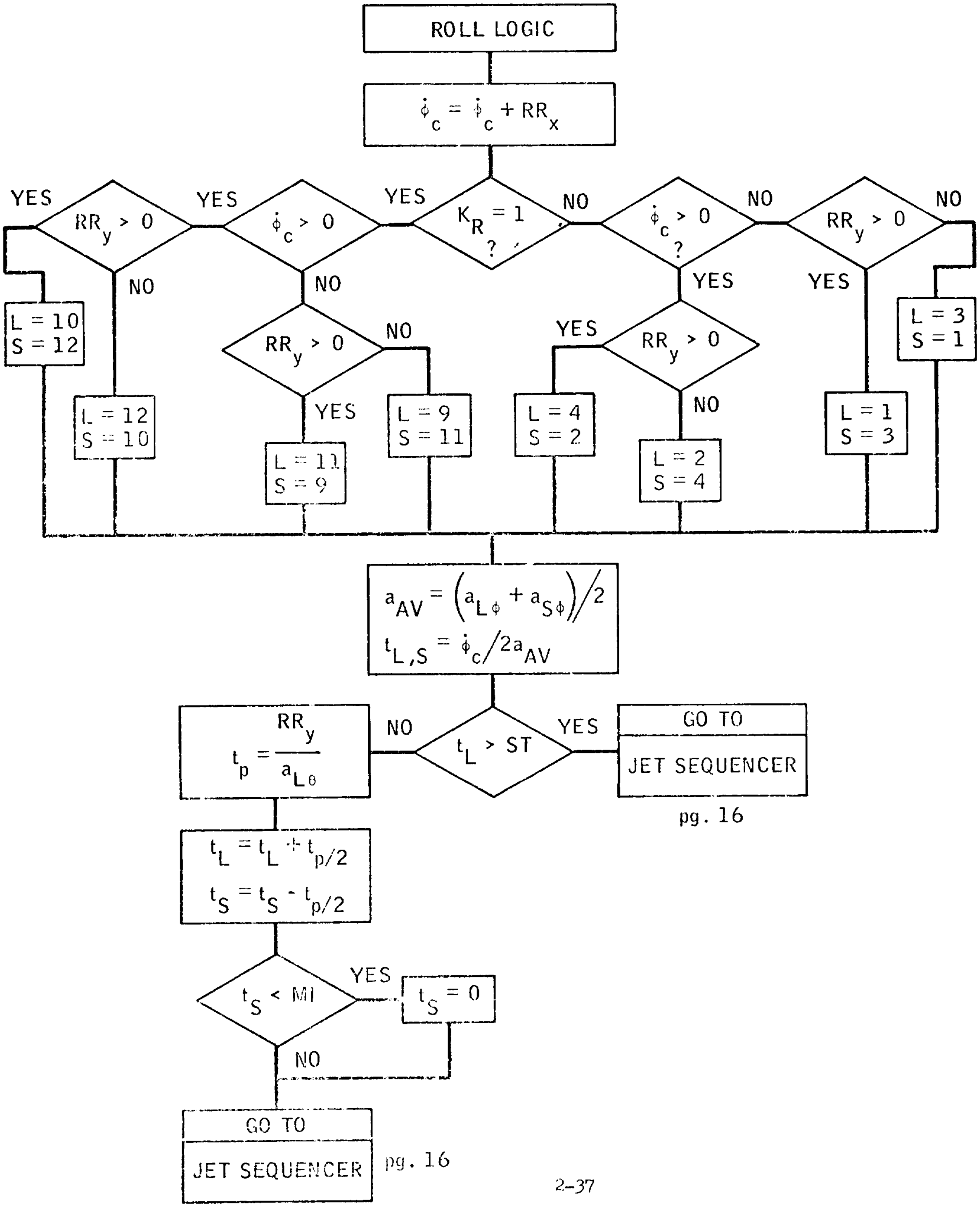
ROLL LOGIC
$\dot{\phi}_c = \dot{\phi}_c + RR_x$
$K_R = 1$?
YES
NO
$\dot{\phi}_c > 0$
YES
NO
$RR_y > 0$
YES
NO
$L = 10$ $S = 12$
$L = 12$ $S = 10$
$RR_y > 0$
YES
NO
$L = 11$ $S = 9$
$L = 9$ $S = 11$
$\dot{\phi}_c > 0$?
NO
YES
$RR_y > 0$
YES
NO
$L = 3$ $S = 1$
$L = 1$ $S = 3$
$RR_y > 0$
YES
NO
$L = 4$ $S = 2$
$L = 2$ $S = 4$
$a_{AV} = \left(a_{L\phi} + a_{S\phi}\right)/2$
$t_{L,S} = \dot{\phi}_c/2a_{AV}$
$t_L > ST$
YES
GO TO
JET SEQUENCER
pg. 16
NO
$t_p = \frac{RR_y}{a_{L\theta}}$
$t_L = t_L + t_{p/2}$
$t_S = t_S - t_{p/2}$
$t_S < MI$
YES
$t_S = 0$
NO
GO TO
JET SEQUENCER
pg. 16

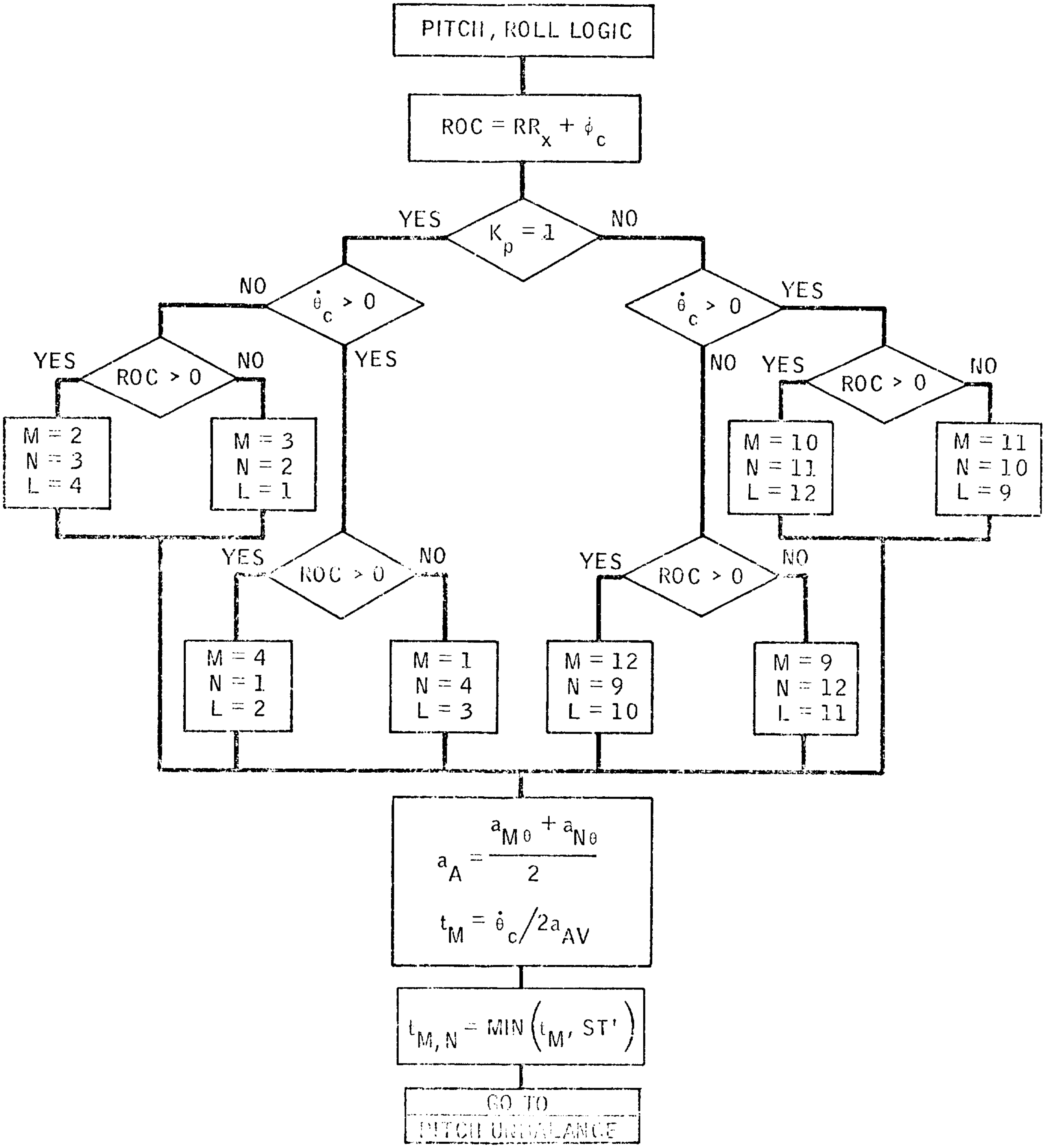

PITCH, ROLL LOGIC
$ROC = RR_x + \dot{\phi}_c$
$K_p = 1$
YES
NO
$\dot{\theta}_c > 0$
NO
YES
$\dot{\theta}_c > 0$
YES
NO
ROC > 0
YES
NO
$M = 2$ $N = 3$ $L = 4$
$M = 3$ $N = 2$ $L = 1$
ROC > 0
YES
NO
$M = 10$ $N = 11$ $L = 12$
$M = 11$ $N = 10$ $L = 9$
ROC > 0
YES
NO
$M = 4$ $N = 1$ $L = 2$
$M = 1$ $N = 4$ $L = 3$
ROC > 0
YES
NO
$M = 12$ $N = 9$ $L = 10$
$M = 9$ $N = 12$ $L = 11$
$a_A = \frac{a_{M\theta} + a_{N\theta}}{2}$
$t_M = \dot{\theta}_c / 2a_{AV}$
$t_{M,N} = MIN\left(t_M, ST'\right)$
GO TO
PITCH UNBALANCE

pg. 8

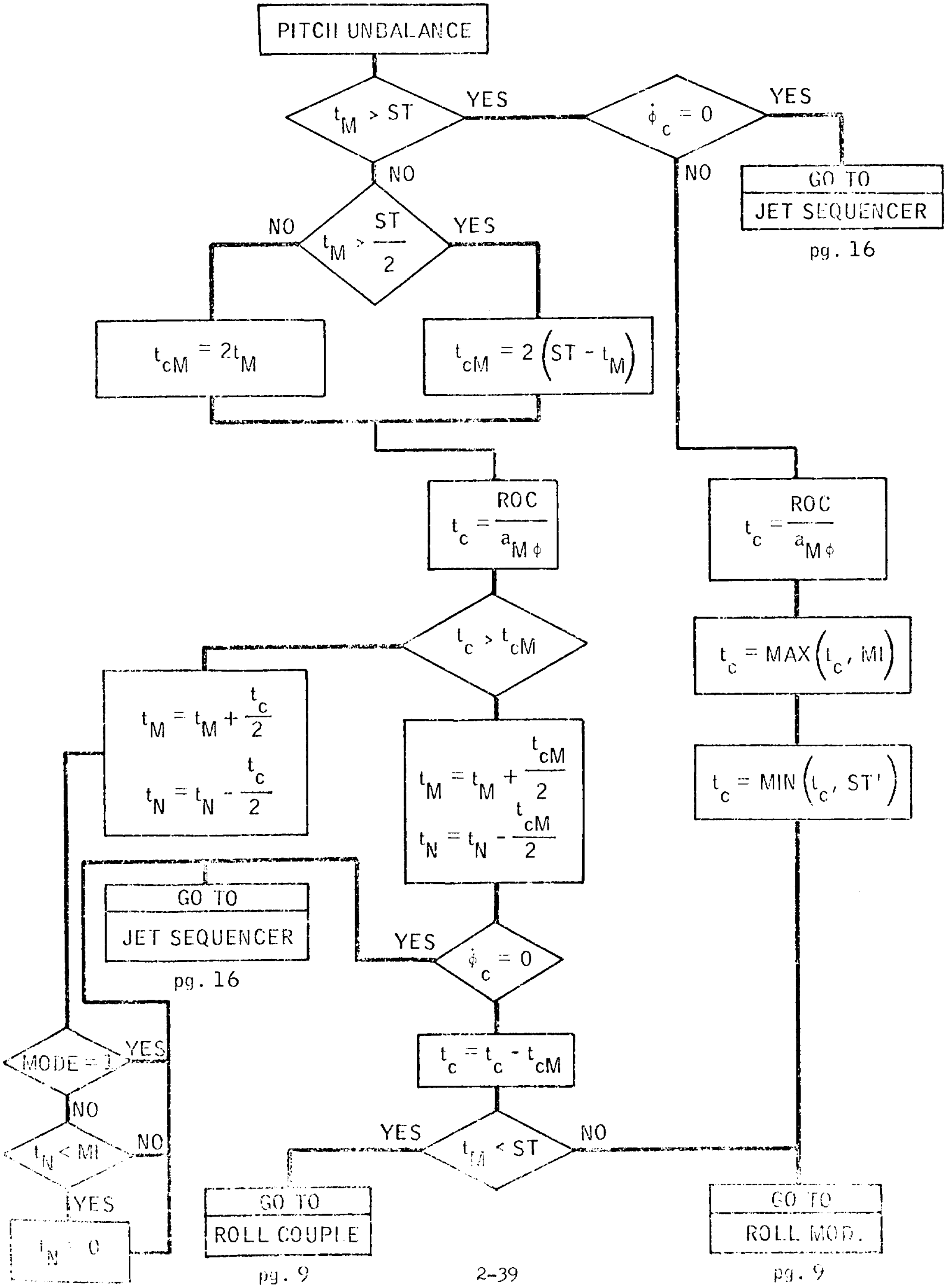
PITCH UNBALANCE
$t_M > ST$
YES
$\dot{\phi}_c = 0$
YES
GO TO
JET SEQUENCER
pg. 16
NO
NO
NO
$t_M > \frac{ST}{2}$
YES
$t_{cM} = 2t_M$
$t_{cM} = 2\left(ST - t_M\right)$
$t_c = \frac{ROC}{a_{M\phi}}$
$t_c = \frac{ROC}{a_{M\phi}}$
$t_c > t_{cM}$
$t_c = MAX\left(t_c, MI\right)$
$t_M = t_M + \frac{t_c}{2}$
$t_N = t_N - \frac{t_c}{2}$
$t_M = t_M + \frac{t_{cM}}{2}$
$t_N = t_N - \frac{t_{cM}}{2}$
$t_c = MIN\left(t_c, ST'\right)$
GO TO
JET SEQUENCER
pg. 16
YES
$\dot{\phi}_c = 0$
MODE = 1
YES
$t_c = t_c - t_{cM}$
NO
YES
$t_M < ST$
NO
$t_N < MI$
NO
YES
GO TO
ROLL COUPLE
pg. 9
GO TO
ROLL MOD.
pg. 9
$t_N = 0$

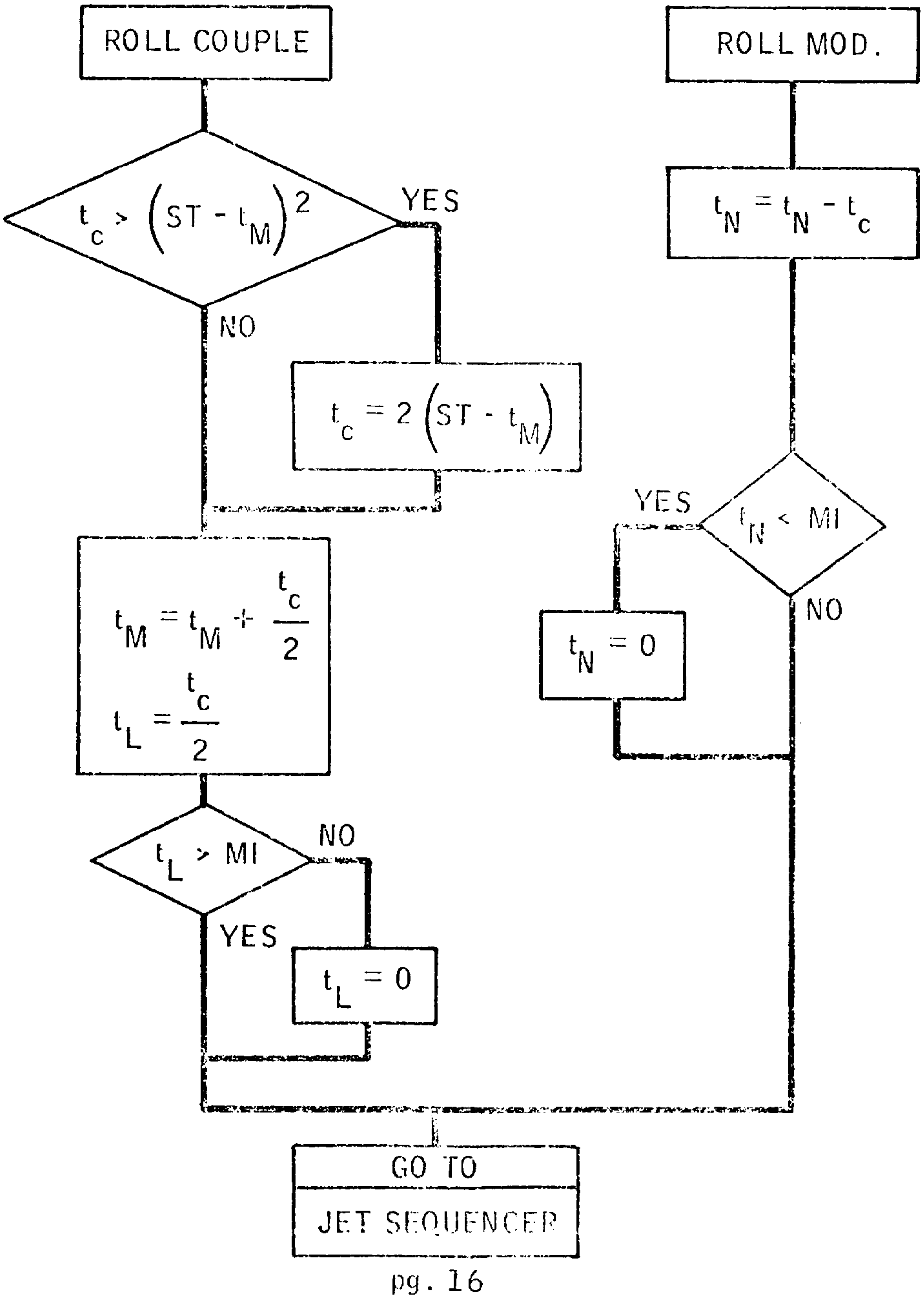
ROLL COUPLE
$t_c > (ST - t_M)^2$
YES
NO
$t_c = 2\left(ST - t_M\right)$
$t_M = t_M + \frac{t_c}{2}$
$t_L = \frac{t_c}{2}$
$t_L > MI$
NO
YES
$t_L = 0$
ROLL MOD.
$t_N = t_N - t_c$
$t_N < MI$
YES
NO
$t_N = 0$
GO TO
JET SEQUENCER
pg. 16

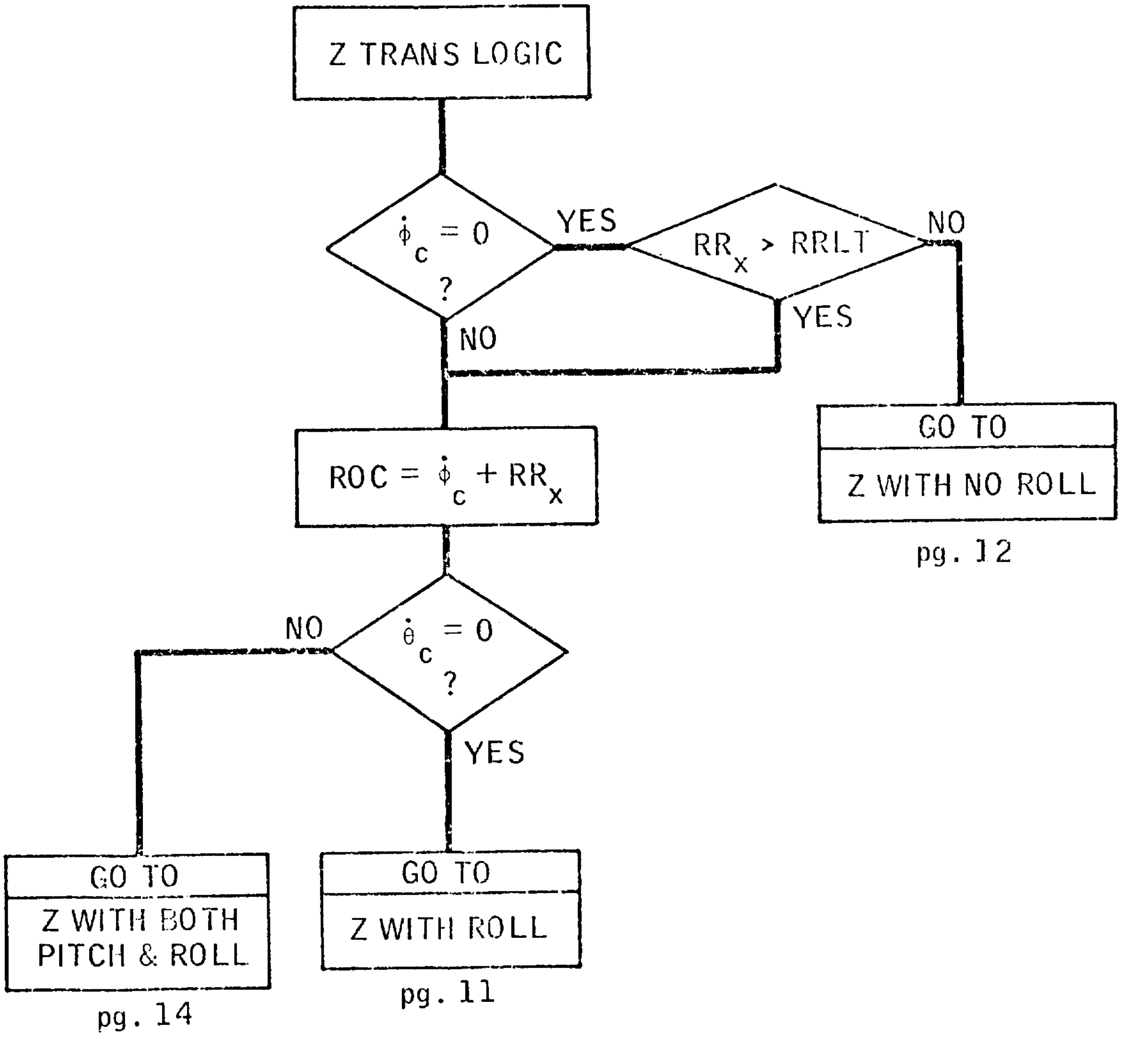
Z TRANS LOGIC
$\dot{\phi}_c = 0$?
YES
NO
$RR_x > RRLT$
NO
YES
$ROC = \dot{\phi}_c + RR_x$
GO TO
Z WITH NO ROLL
pg. 12
$\dot{\theta}_c = 0$?
NO
YES
GO TO
Z WITH BOTH PITCH & ROLL
pg. 14
GO TO
Z WITH ROLL
pg. 11

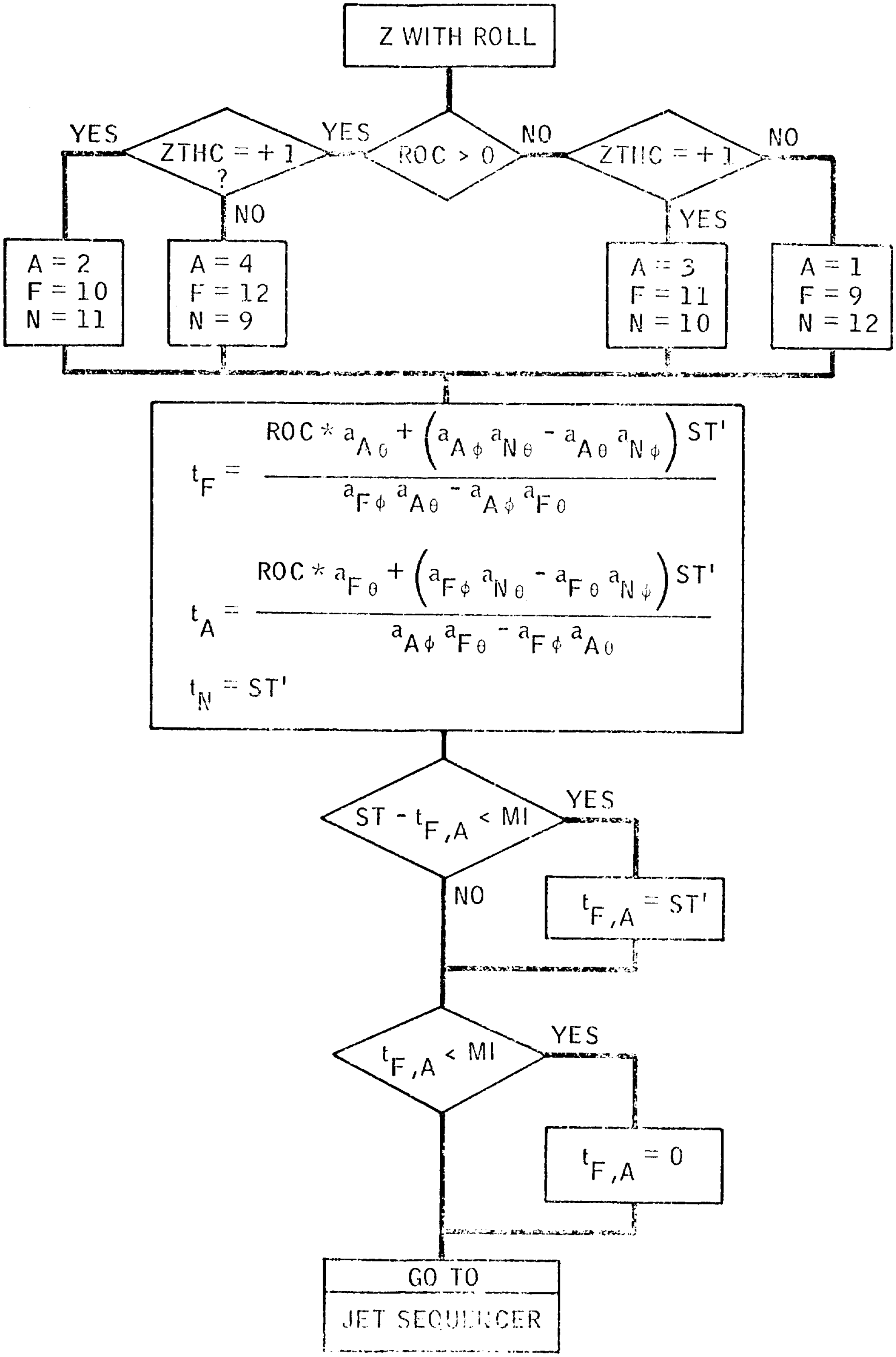
Z WITH ROLL
ROC > 0
YES
NO
ZTHC = + 1 ?
YES
NO
ZTHC = + 1
NO
YES
A = 2 F = 10 N = 11
A = 4 F = 12 N = 9
A = 3 F = 11 N = 10
A = 1 F = 9 N = 12
$t_F = \frac{ROC * a_{A\theta} + \left(a_{A\phi} a_{N\theta} - a_{A\theta} a_{N\phi}\right) ST'}{a_{F\phi} a_{A\theta} - a_{A\phi} a_{F\theta}}$
$t_A = \frac{ROC * a_{F\theta} + \left(a_{F\phi} a_{N\theta} - a_{F\theta} a_{N\phi}\right) ST'}{a_{A\phi} a_{F\theta} - a_{F\phi} a_{A\theta}}$
$t_N = ST'$
$ST - t_{F,A} < MI$
YES
NO
$t_{F,A} = ST'$
$t_{F,A} < MI$
YES
$t_{F,A} = 0$
GO TO
JET SEQUENCER

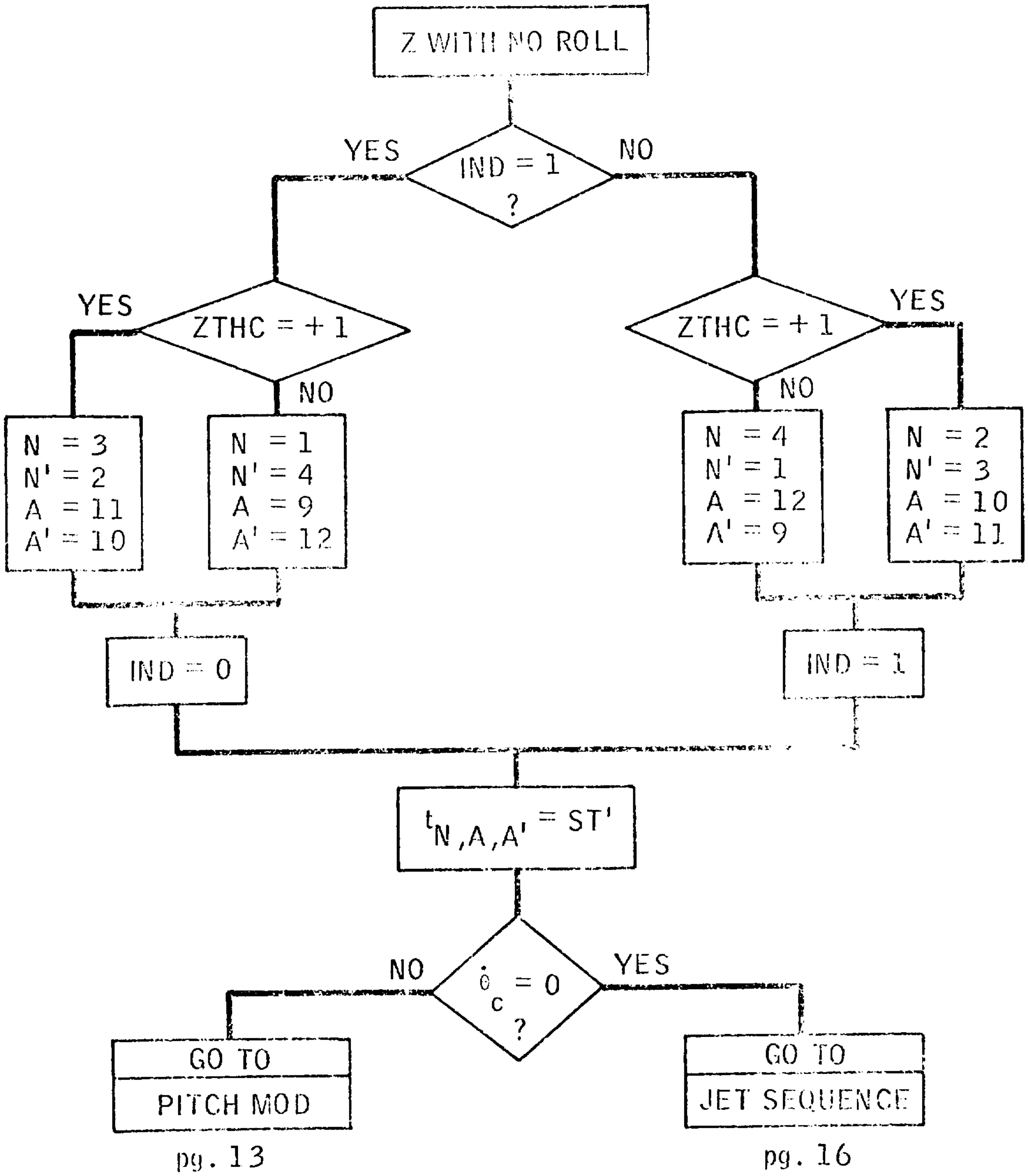

Z WITH NO ROLL
IND = 1 ?
YES
NO
ZTHC = +1
YES
NO
ZTHC = +1
YES
NO
N = 3
N' = 2
A = 11
A' = 10
N = 1
N' = 4
A = 9
A' = 12
N = 4
N' = 1
A = 12
A' = 9
N = 2
N' = 3
A = 10
A' = 11
IND = 0
IND = 1
$t_{N,A,A'}$ = ST'
$\dot{\theta}_c = 0$?
NO
YES
GO TO
PITCH MOD
pg. 13
GO TO
JET SEQUENCE
pg. 16

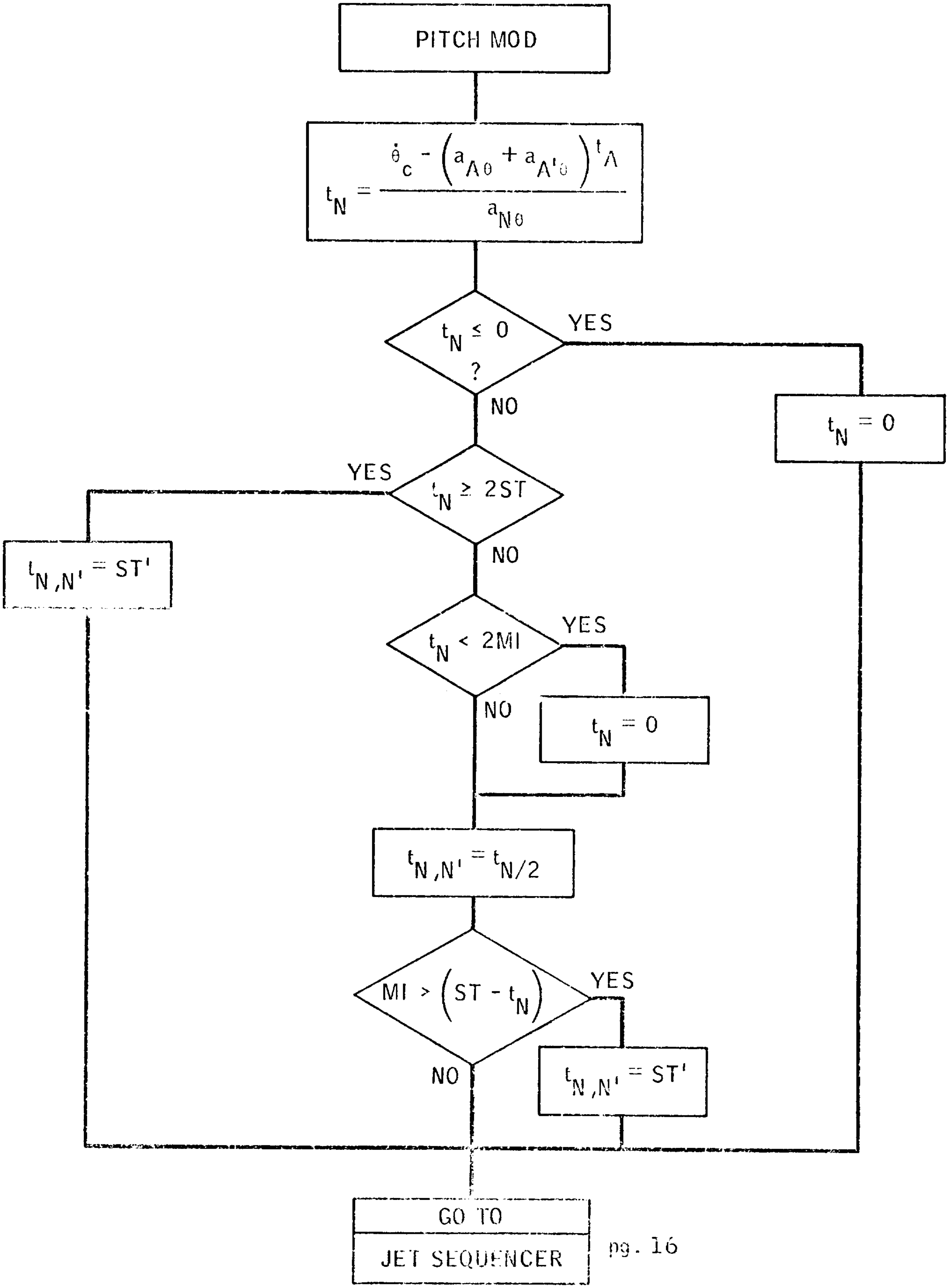
PITCH MOD
$t_N = \frac{\dot{\theta}_c - \left(a_{A\theta} + a_{A'\theta}\right) t_A}{a_{N\theta}}$
$t_N \leq 0$?
YES
NO
$t_N = 0$
$t_N \geq 2ST$
YES
NO
$t_{N,N'} = ST'$
$t_N < 2MI$
YES
NO
$t_N = 0$
$t_{N,N'} = t_{N/2}$
$MI > \left(ST - t_N\right)$
YES
NO
$t_{N,N'} = ST'$
GO TO
JET SEQUENCER

pg. 16

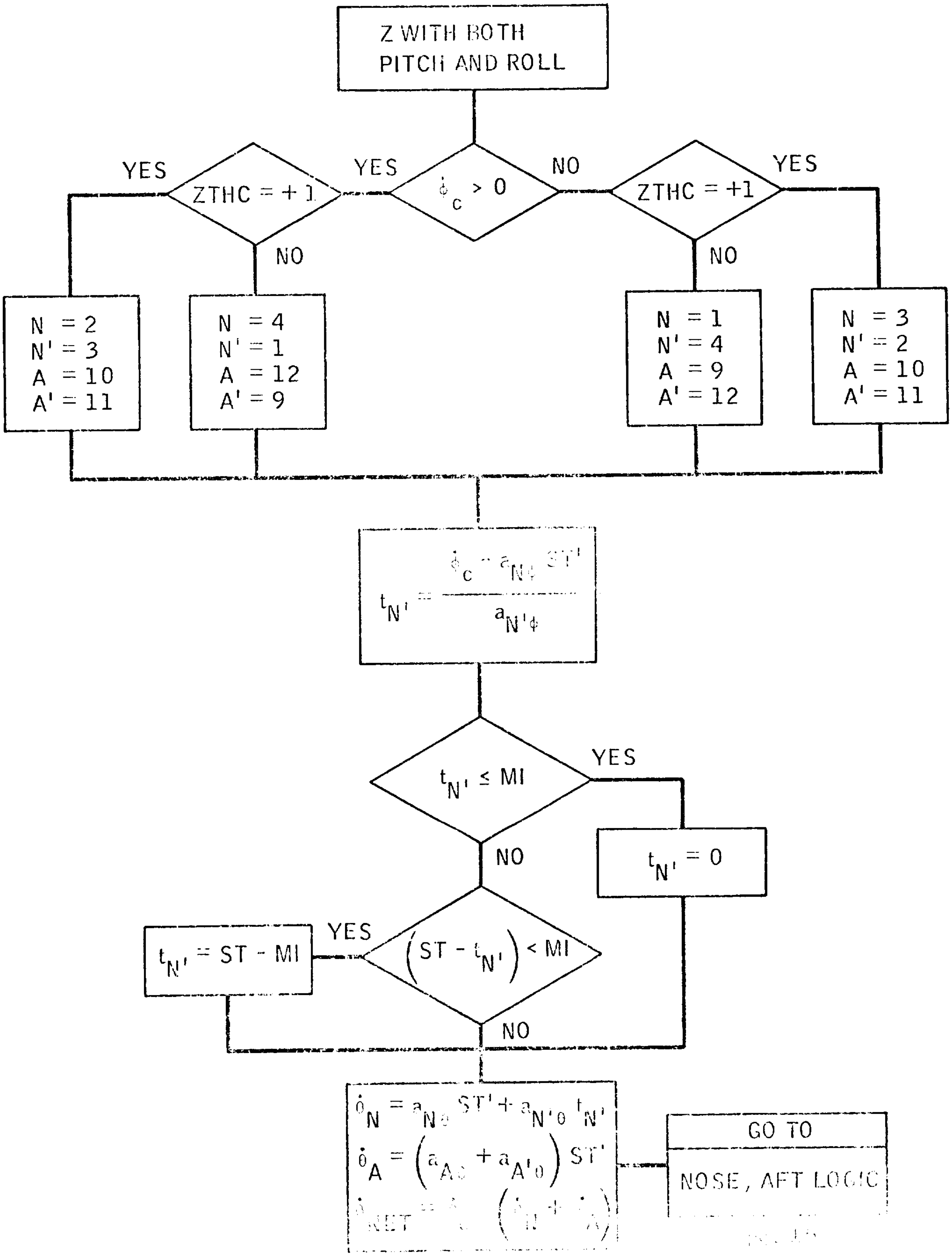
Z WITH BOTH PITCH AND ROLL
$\dot{\phi}_c > 0$
YES
NO
ZTHC = +1
YES
NO
ZTHC = +1
YES
NO
N = 2
N' = 3
A = 10
A' = 11
N = 4
N' = 1
A = 12
A' = 9
N = 1
N' = 4
A = 9
A' = 12
N = 3
N' = 2
A = 10
A' = 11
$t_{N'} = \frac{\dot{\phi}_c - a_{N\phi} ST'}{a_{N'\phi}}$
$t_{N'} \leq MI$
YES
NO
$t_{N'} = 0$
$(ST - t_{N'}) < MI$
YES
NO
$t_{N'} = ST - MI$
$\dot{\theta}_N = a_{N\theta} ST' + a_{N'\theta} t_{N'}$
$\dot{\theta}_A = (a_{A\theta} + a_{A'\theta}) ST'$
$\dot{\theta}_{NET} = (\dot{\theta}_N + \dot{\theta}_A)$
GO TO
NOSE, AFT LOGIC

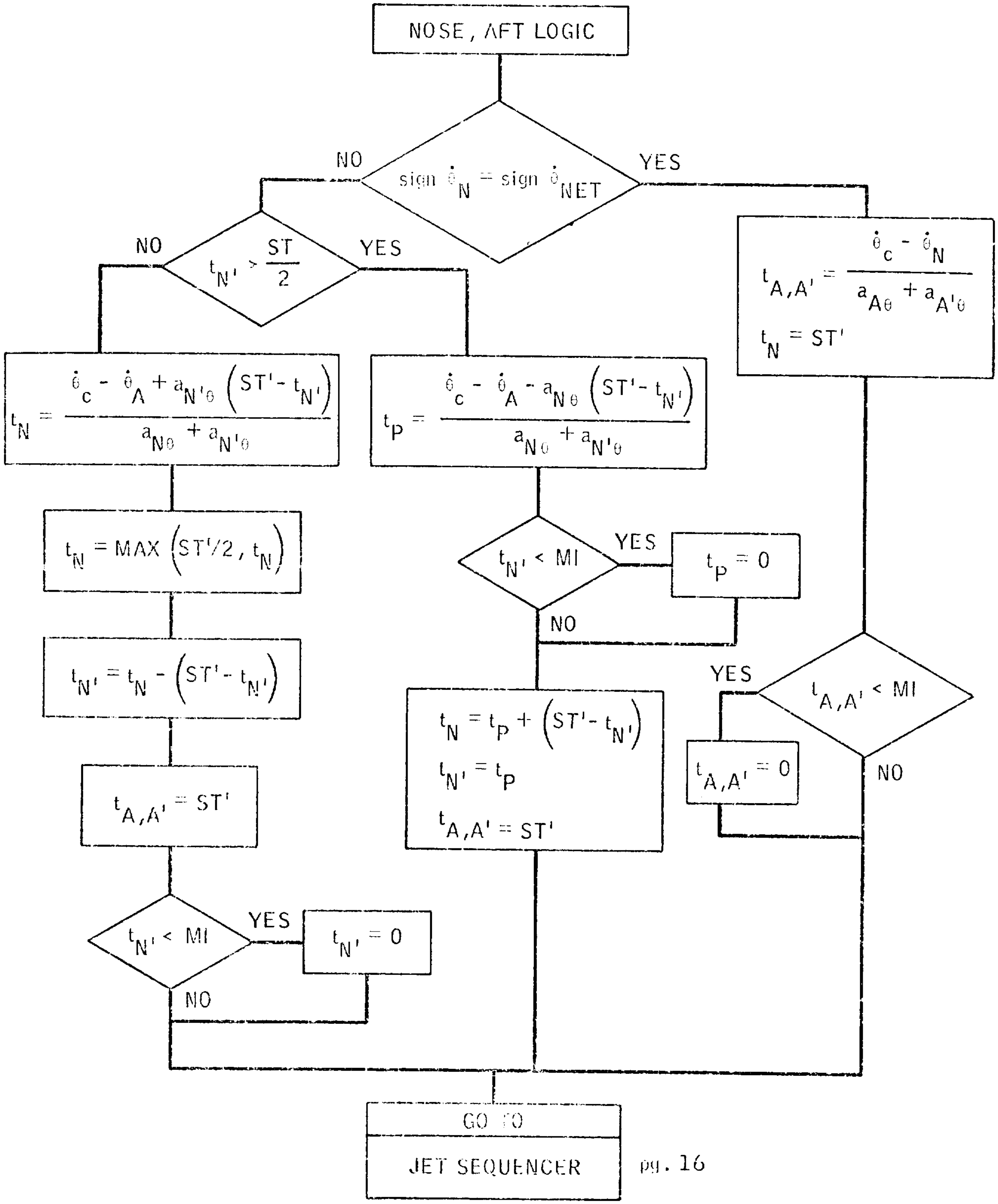
NOSE, AFT LOGIC
sign $\dot{\theta}_N$ = sign $\dot{\theta}_{NET}$
NO
YES
$t_{N'} > \frac{ST}{2}$
NO
YES
$t_{A,A'} = \frac{\dot{\theta}_c - \dot{\theta}_N}{a_{A\theta} + a_{A'\theta}}$
$t_N = ST'$
$t_N = \frac{\dot{\theta}_c - \dot{\theta}_A + a_{N'\theta}\left(ST' - t_{N'}\right)}{a_{N\theta} + a_{N'\theta}}$
$t_P = \frac{\dot{\theta}_c - \dot{\theta}_A - a_{N\theta}\left(ST' - t_{N'}\right)}{a_{N\theta} + a_{N'\theta}}$
$t_N = MAX\left(ST'/2, t_N\right)$
$t_{N'} < MI$
YES
$t_P = 0$
NO
$t_{N'} = t_N - \left(ST' - t_{N'}\right)$
YES
$t_{A,A'} < MI$
$t_N = t_P + \left(ST' - t_{N'}\right)$
$t_{N'} = t_P$
$t_{A,A'} = ST'$
$t_{A,A'} = 0$
NO
$t_{A,A'} = ST'$
$t_{N'} < MI$
YES
$t_{N'} = 0$
NO
GO TO
JET SEQUENCER
pg. 16

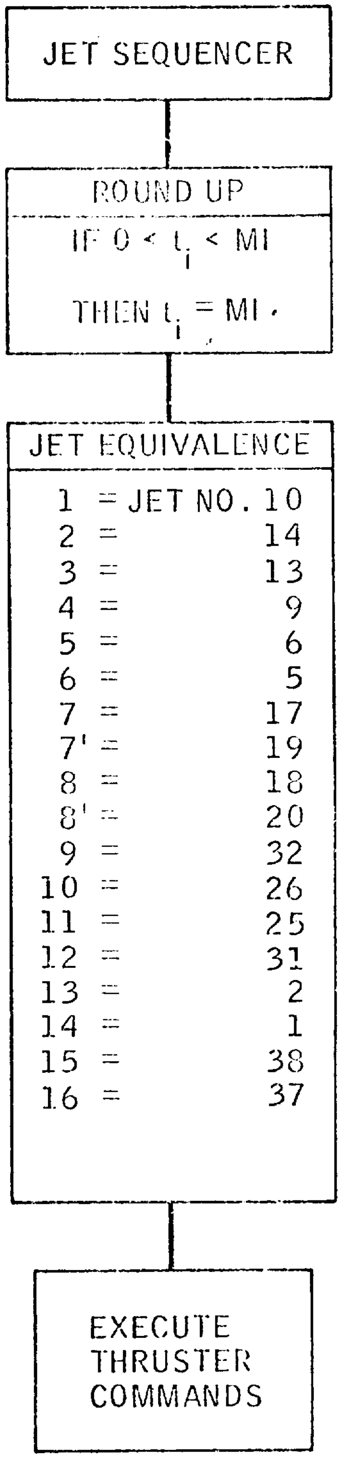

JET SEQUENCER

ROUND UP

IF $0 < t_i < MI$

THEN $t_i = MI$

JET EQUIVALENCE

1	= JET NO.	10
2	=	14
3	=	13
4	=	9
5	=	6
6	=	5
7	=	17
7'	=	19
8	=	18
8'	=	20
9	=	32
10	=	26
11	=	25
12	=	31
13	=	2
14	=	1
15	=	38
16	=	37

EXECUTE THRUSTER COMMANDS

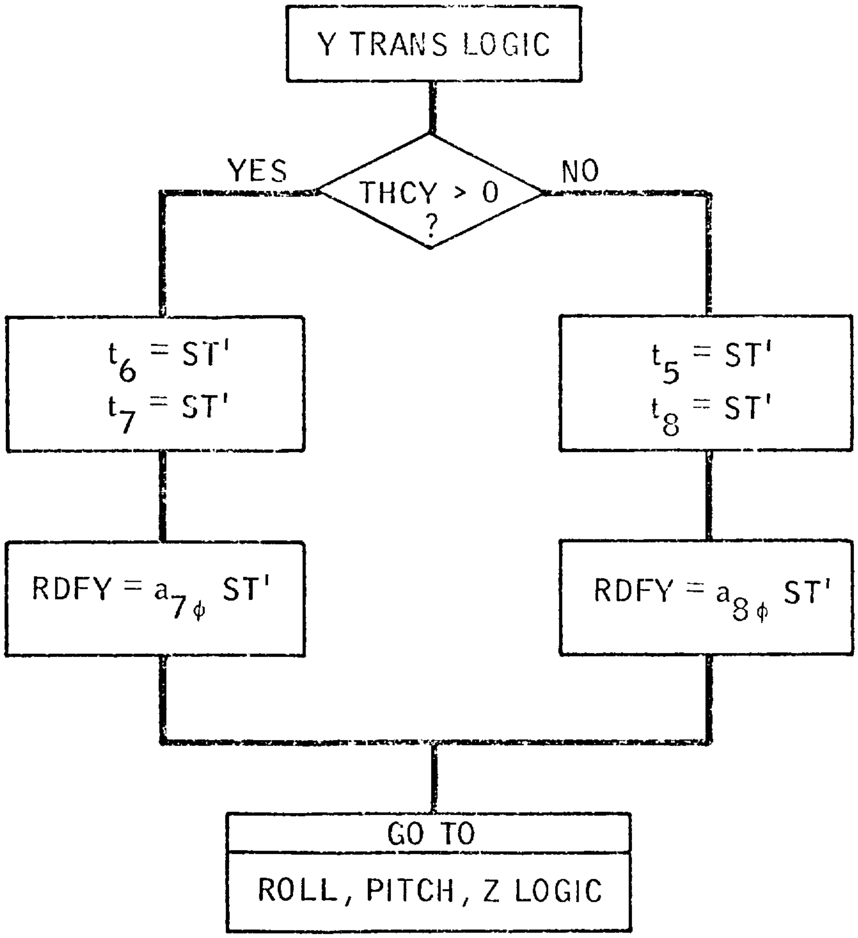
Y TRANS LOGIC
THCY > 0 ?
YES
NO
$t_6 = ST'$
$t_7 = ST'$
$t_5 = ST'$
$t_8 = ST'$
$RDFY = a_{7\phi} ST'$
$RDFY = a_{8\phi} ST'$
GO TO
ROLL, PITCH, Z LOGIC

pg. 5

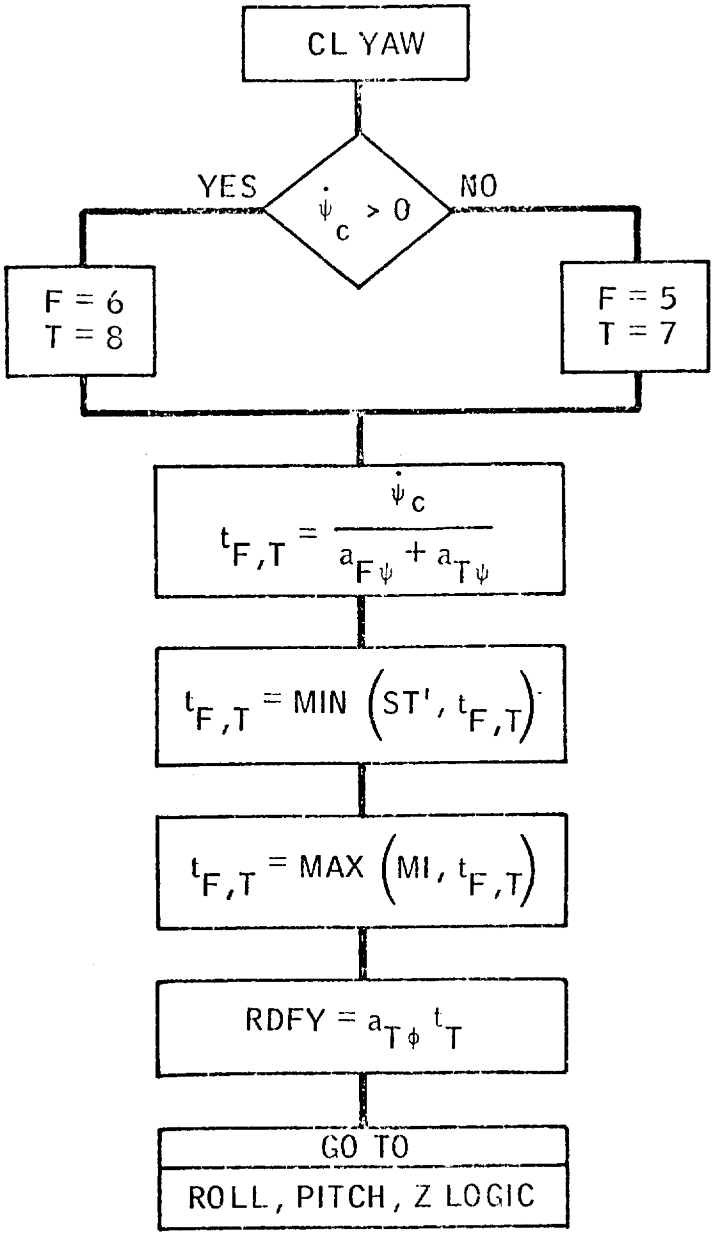
CL YAW
YES
$\dot{\psi}_c > 0$
NO
F = 6
T = 8
F = 5
T = 7
$t_{F,T} = \frac{\dot{\psi}_c}{a_{F\psi} + a_{T\psi}}$
$t_{F,T} = \text{MIN}\left(ST', t_{F,T}\right)$
$t_{F,T} = \text{MAX}\left(MI, t_{F,T}\right)$
$RDFY = a_{T\phi}\, t_T$
GO TO
ROLL, PITCH, Z LOGIC

pg. 5

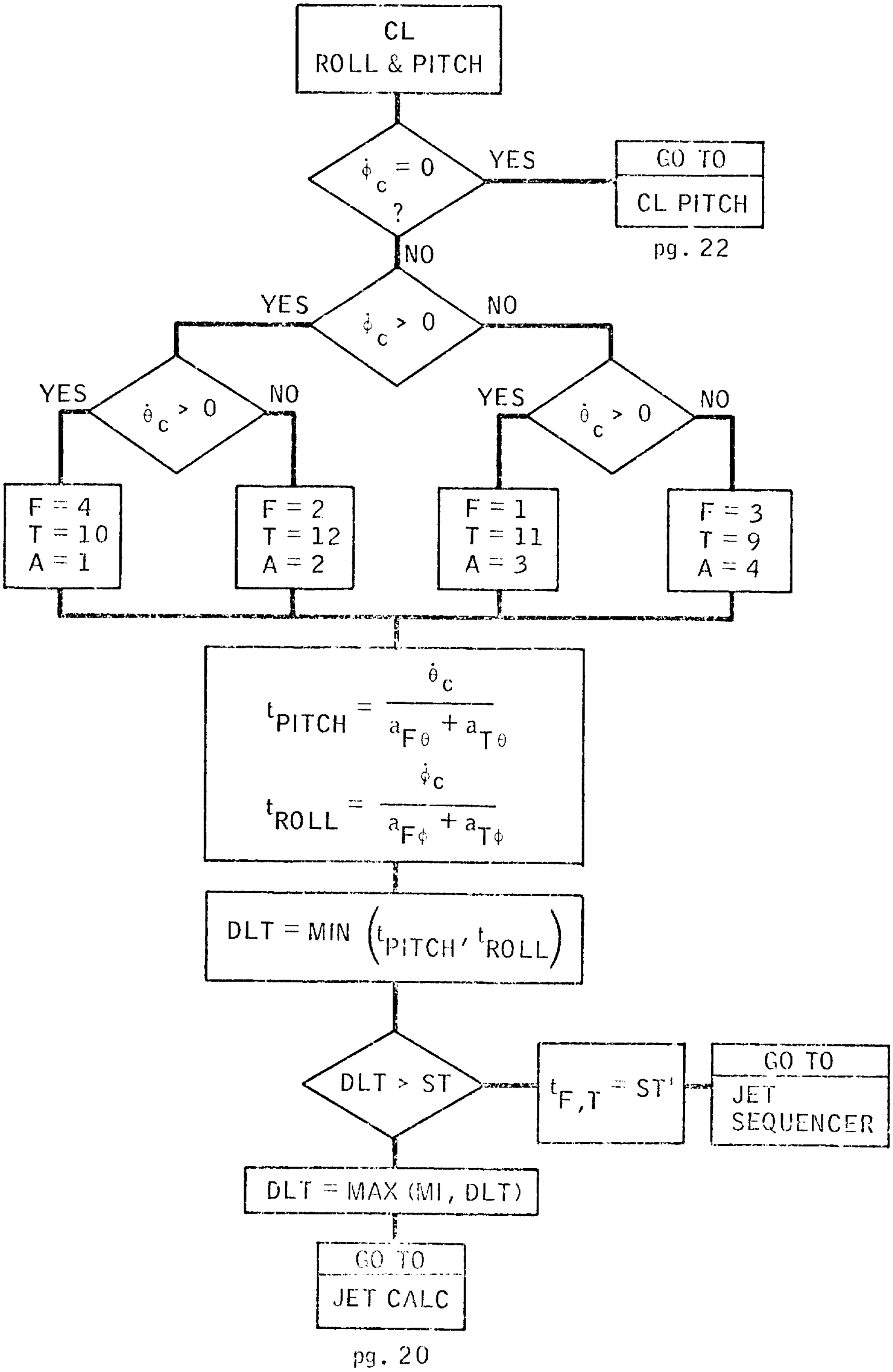
CL
ROLL & PITCH
$\dot{\phi}_c = 0$?
YES
GO TO
CL PITCH
pg. 22
NO
$\dot{\phi}_c > 0$
YES
NO
$\dot{\theta}_c > 0$
YES
NO
$\dot{\theta}_c > 0$
YES
NO
F = 4
T = 10
A = 1
F = 2
T = 12
A = 2
F = 1
T = 11
A = 3
F = 3
T = 9
A = 4
$t_{PITCH} = \frac{\dot{\theta}_c}{a_{F\theta} + a_{T\theta}}$
$t_{ROLL} = \frac{\dot{\phi}_c}{a_{F\phi} + a_{T\phi}}$
$DLT = MIN \left(t_{PITCH}, t_{ROLL}\right)$
DLT > ST
$t_{F,T} = ST'$
GO TO
JET
SEQUENCER
DLT = MAX (MI, DLT)
GO TO
JET CALC
pg. 20

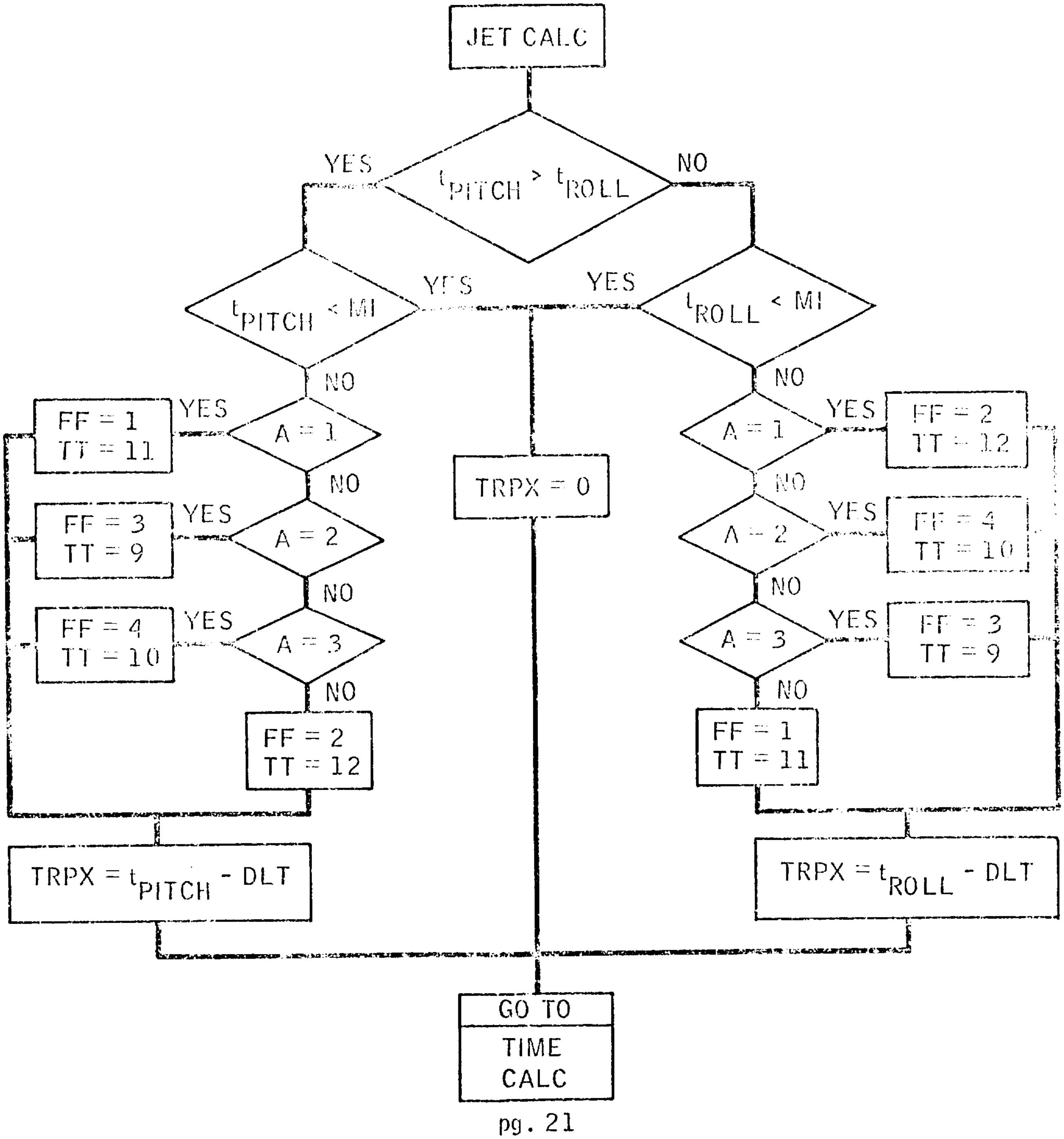
JET CALC
$t_{PITCH} > t_{ROLL}$
YES
NO
$t_{PITCH} < MI$
YES
NO
$t_{ROLL} < MI$
YES
NO
A = 1
FF = 1
TT = 11
A = 2
FF = 3
TT = 9
A = 3
FF = 4
TT = 10
FF = 2
TT = 12
TRPX = 0
A = 1
FF = 2
TT = 12
A = 2
FF = 4
TT = 10
A = 3
FF = 3
TT = 9
FF = 1
TT = 11
TRPX = t_{PITCH} - DLT
TRPX = t_{ROLL} - DLT
GO TO
TIME
CALC
pg. 21

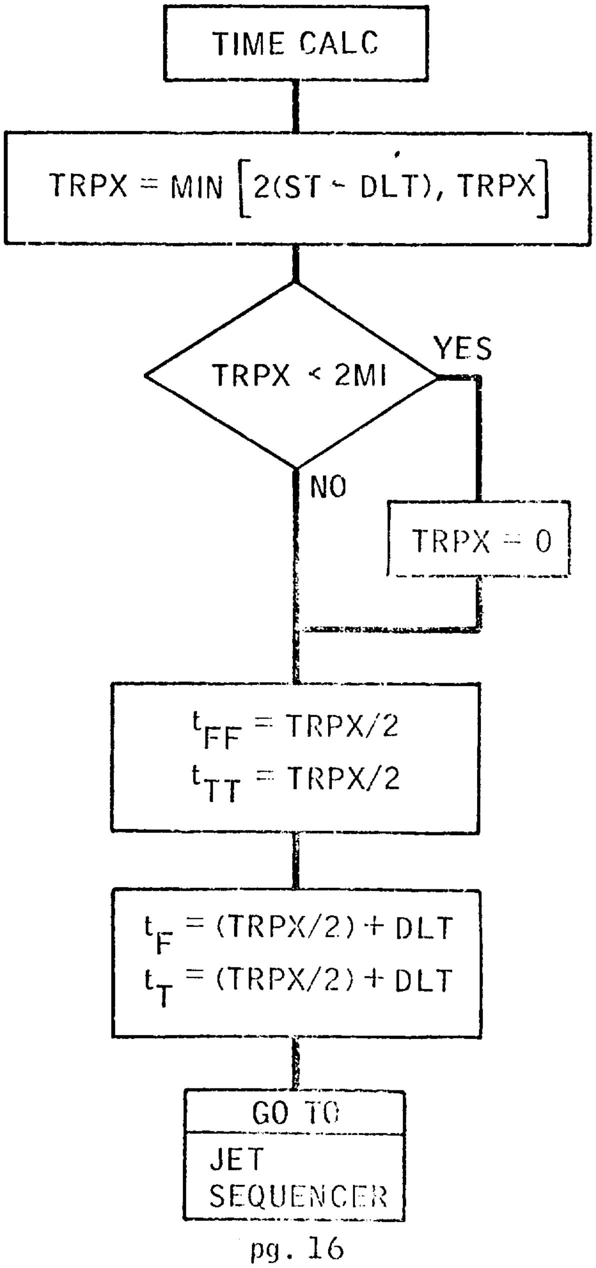
TIME CALC
TRPX = MIN [2(ST - DLT), TRPX]
TRPX < 2MI
YES
NO
TRPX = 0
t_{FF} = TRPX/2
t_{TT} = TRPX/2
t_F = (TRPX/2) + DLT
t_T = (TRPX/2) + DLT
GO TO
JET SEQUENCER
pg. 16

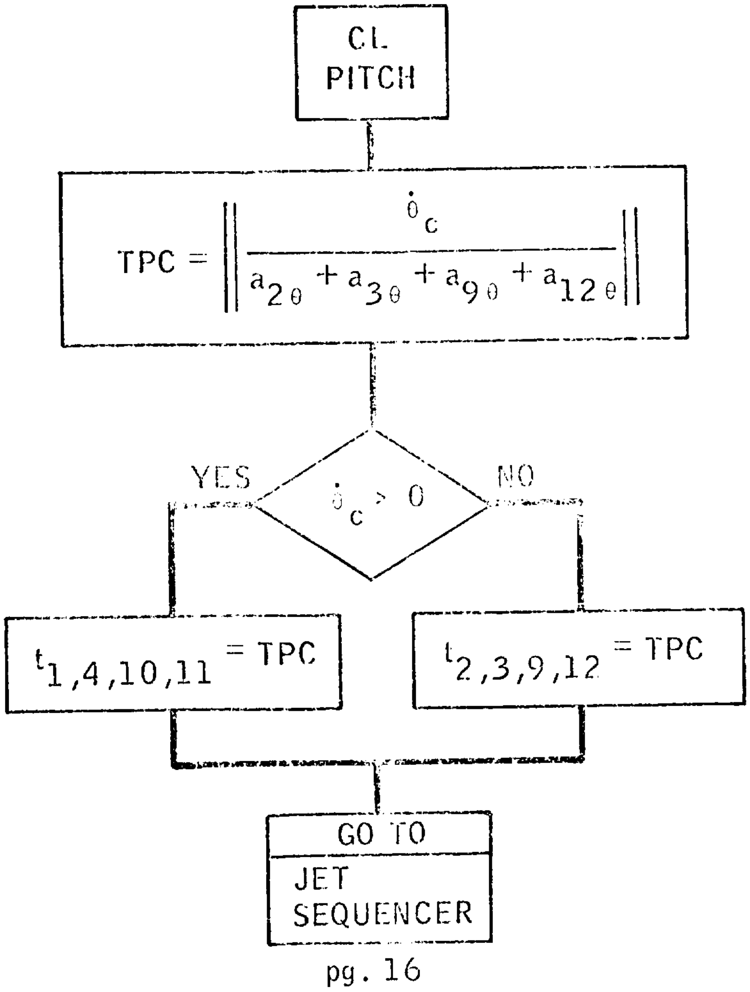
CL PITCH
TPC = $\left\| \frac{\dot{\theta}_c}{a_{2\theta} + a_{3\theta} + a_{9\theta} + a_{12\theta}} \right\|$
$\dot{\theta}_c > 0$
YES
NO
$t_{1,4,10,11} = TPC$
$t_{2,3,9,12} = TPC$
GO TO
JET SEQUENCER
pg. 16

THCX,Y,Z	Commands for translation, either positive, none, or negative,depending on +1, 0 , or -1
$\dot{\Phi}_C, \dot{\Theta}_C, \dot{\psi}_C$	Commanded rate changes from switching logic.
$a_{i,\ \phi,\Theta,\text{ or }\psi}$	Angular Acceleration for i^{TH} jet for either roll, pitch, or yaw.
K_R, K_P, K_Y	Value of 1 (not 0) signifies request for long moment arm thrusters
J,K	Indices for jets
MI	Minimum impulse time
RDFY	Roll rate disturbance for yaw and/or Y translation firings
RRL	Roll rate limit before RDFY is added directly to $\dot{\phi}_C$
RR_X	Roll rate error from phase plane logic when $\dot{\phi}_C$ is zero
PI	Index indicating presence (1) or absence (0) of roll command
ST	Sample time
M,N	Jet indices
t_{CM}	Maximum roll compensation time available by unbalancing pitch firing times
E	Small number to account for round off in comparisions (say 10^{-4})
t_C	One jet roll correction time
ROC	Net roll command, i.e., RR + $\dot{\phi}_C$
RRLT	Roll rate limit before RR_X is added to $\dot{\phi}_C$ during translation
ST^1	Sample time plus E
RR_Y	Pitch rate error from phase plane logic when $\dot{\Theta}_C$ is zero
CL	Couple option

Fig. 2-7b Definition of Symbols for Jet Selection Logic

SECTION 3

STATE ESTIMATOR (ENTRY PHASE)

3.1 Introduction

The function of the state estimator is to obtain estimates of controller state variables in an uncertain environment. This uncertainty arises from noise in the measurement process and noise driving the states directly, e.g., due to wind gusts.

The state estimator design must meet certain prescribed requirements in the face of externally-imposed constraints. These requirements, many of which are not yet specified quantitatively, pertain to the degree of accuracy and smoothness in the estimated state variables, the time delay between reading the sensors and issuing computed control commands, and the effective phase lag associated with filter dynamics. External constraints are imposed by fixed sensor hardware and configuration characteristics and computer timing and sizing limitations.

Meeting all requirements while satisfying all constraints may necessitate design compromises. The design should be comprehensive to ensure prescribed accuracy by making best use of available information, but design sophistication is limited by computer constraints. Noisy inputs may require heavy attenuation to ensure prescribed smoothness, but the low gains associated with heavy attenuation must not cause excessive phase lag or excessive sensitivity to modeling errors. These compromises are central in the development of the design presented below.

The current state estimator is designed specifically for the entry flight phase (and some of the parameters used by the estimator are defined in the entry control description, Section 5). The structure used, however, is applicable to any flight phase. Extension of the state estimator to other flight phases is under study.

3.2 General Description

The design presented for the state estimator is linear and therefore implies approximation, namely linearization of the state dynamics about a set of operating points and linear modeling of control effector and sensor operation. The linear assumptions facilitate both design and analysis. Nonlinear effects will be noted as development continues and possibly included.

The design is cast in the state-space formulation and uses more than one measurement to produce each state-variable estimate (multi-input, multi-output). It is comprehensive in the sense that it uses all pertinent information. However, approximations are made to decrease computer requirements; namely, only a reduced number of state-variables are estimated, and decoupling of longitudinal and lateral dynamics is assumed. An important feature of the design is that control effects are fed into the estimator's state-extrapolation step, keeping the estimator response fast even while noisy inputs are being heavily attenuated.

Time delay between reading sensors and issuing control commands is minimized in the sense that it provides for incorporating the current measurements and extrapolating the state[†] in two separate steps with the latter performed after the commands are generated. Furthermore, the slow-varying filter parameters are updated separately at a slower repetition rate. Details of these computer timing considerations are given in Implementation, Subsection 3.3.

The estimator gains are constant with respect to time at any particular flight condition; however, their on-board computation is dependent on the current estimates of dynamic pressure and Mach number. When the dynamic pressure is below a prescribed level,[††] the estimator gains are set equal to predetermined fixed values. When dynamic pressure is above this level, the gains are interpolated from predetermined tabulated values with Mach number as the sole independent variable.

The fixed gain values used at very low dynamic pressure were determined classically on the basis of desired filter bandwidth and damping ratio.[†††] The scheduled gain values used for high (above $\bar{q}_1^*$ or $\bar{q}_2^*$) dynamic pressure were found by analogy to the steady-state Kalman (Wiener) filter for the reduced, decoupled, linearized state assuming locally stationary noise statistics at each operating point. Measurement noise strengths were chosen to reflect relative sensor quality; driving noise strengths were chosen to keep the gains at a selected level, sufficiently low to achieve desired smoothness but sufficiently high to exclude extreme sensitivity to modeling errors.

[†] Analogous to "filter update" and "filter pushdown" in classical filters.

[††] The prescribed dynamic pressure level is $\bar{q}_1^*$ for the longitudinal channel and $\bar{q}_2^*$ for the lateral channel. Current values for $\bar{q}_1^*$ and $\bar{q}_2^*$ are 20 and 30 lb/ft^2, respectively.

[†††] Currently, the low-dynamic-pressure estimator bandwidth is 5 rps and the damping ratio is 0.7 sec^{-1}.

3.3 Implementation

3.3.1 Input-Output

Estimator state variables (outputs) are linearized variations about nominal or commanded states. These state variables are the error angle-of-attack $\Delta\hat{\alpha}$ and its time derivative $\Delta\hat{\dot{\alpha}}$, the error sideslip angle $\Delta\hat{\beta}$ and its time derivative $\Delta\hat{\dot{\beta}}$, and the error bank angle $\Delta\hat{\phi}_V$ and its time derivative $\Delta\hat{\dot{\phi}}_V$. (The symbol [^] signifies an estimated quantity.)

To obtain variational outputs, the measurements must be differenced with their respective desired values to form variational inputs. These variational inputs are the measured errors in angle-of-attack $\Delta\tilde{\alpha}$, body pitch rate $\Delta\tilde{q}$, sideslip angle $\Delta\tilde{\beta}$, bank angle $\Delta\tilde{\phi}_V$, body roll rate $\Delta\tilde{p}$, and body yaw rate $\Delta\tilde{r}$. (The tilda [~] symbolizes a measured quantity.) The measurements are either read directly from sensors or computed (preprocessed) from the sensor data. The body rate measurements are assumed to be directly accessible from body-mounted rate gyros, but the angle measurements are derived from IMU (Inertial Measurement Unit) and body-mounted accelerometer information. Commanded values corresponding to each of the measurements are either received from the guidance subsystem or computed internally. A detailed description of estimator input computation is presented in Subsection 2.1.

3.3.2 Measurement Incorporation

Current measurements are incorporated into the state estimate immediately after they are obtained and preprocessed. This is immediately before the control subroutine is called, in order that control commands computed using the most recent information may be issued as soon as possible after the DFCS is called. Subsequently, the state estimate is extrapolated in preparation for the next DFCS pass, as shown in Subsection 3.3.3 below.

Measurements are incorporated according to the equations

$$\begin{Bmatrix} \Delta\hat{\alpha} \\ \Delta\hat{\dot{\alpha}} \end{Bmatrix}_k = \begin{Bmatrix} \Delta\hat{\alpha}' \\ \Delta\hat{\dot{\alpha}}' \end{Bmatrix}_k + K_{lon} \begin{Bmatrix} (\Delta\tilde{\alpha} - \Delta\hat{\alpha}') \\ (\Delta\tilde{q} - \Delta\hat{\dot{\alpha}}') \end{Bmatrix}_k \qquad (3\text{-}1)$$

$$\begin{Bmatrix} \Delta\hat{\beta} \\ \Delta\hat{\dot{\beta}} \\ \Delta\hat{\phi}_V \\ \Delta\hat{\dot{\phi}}_V \end{Bmatrix}_k = \begin{Bmatrix} \Delta\hat{\beta}' \\ \Delta\hat{\dot{\beta}}' \\ \Delta\hat{\phi}'_V \\ \Delta\hat{\dot{\phi}}'_V \end{Bmatrix}_k + K_{lat} \begin{Bmatrix} (\Delta\tilde{\beta} - \Delta\hat{\beta}') \\ (\Delta\tilde{\phi}_V = \Delta\hat{\phi}'_V) \\ (\Delta\tilde{p} - \Delta\hat{\dot{\beta}}' \sin\alpha_T - \Delta\hat{\dot{\phi}}'_V \cos\alpha_T) \\ (\Delta\tilde{r} + \Delta\hat{\dot{\beta}}' \cos\alpha_T - \Delta\hat{\dot{\phi}}'_V \sin\alpha_T) \end{Bmatrix}_k \qquad (3\text{-}2)$$

where the prime (′) indicates a state variable propagated from the previous sample instant, K_{lon} is the 2x2 longitudinal gain matrix, and K_{lat} is the 4x4 lateral gain matrix. The gain matrices are updated at the slow repetition rate in the parameter estimation routine, which is performed after the state extrapolation step in the normal DFCS cycle.

The flow charts in Fig. 3-1 and 3-2 show the implementation in the DFCS program of the measurement incorporation equations and the computation of the estimator gain matrices. When dynamic pressure is below $\bar{q}_1^*$ for the longitudinal channel and $\bar{q}_2^*$ for the lateral channel, the constant values KC1 and KC2 are loaded into the estimator gain matrices as shown; the current values for these parameters are 0.45 and 2.5 respectively. For dynamic pressure greater than $\bar{q}_1^*$ and $\bar{q}_2^*$ for longitudinal and lateral channels respectively, the estimator gain matrices are found by linear interpolation on Mach number; the values are given in Tables 3-1 and 3-2.

3.3.3 State Extrapolation

After control commands are computed using the current state estimate (from Eq (3-1) and (3-2)) and issued, the estimator state is extrapolated to the next sample according to the equations:

$$\begin{Bmatrix} \Delta\hat{\alpha}' \\ \\ \Delta\hat{\dot{\alpha}}' \end{Bmatrix}_{k+1} = \Phi^{CL}_{lon} \begin{Bmatrix} \Delta\hat{\alpha} \\ \\ \Delta\hat{\dot{\alpha}} \end{Bmatrix}_{k} + \begin{Bmatrix} 0 \\ \\ \Delta q^{j} \end{Bmatrix}_{k} \qquad (3\text{-}3)$$

$$\begin{Bmatrix} \Delta\hat{\beta}' \\ \\ \Delta\hat{\dot{\beta}}' \\ \\ \Delta\hat{\phi}_v' \\ \\ \Delta\hat{\dot{\phi}}_v' \end{Bmatrix}_{k+1} = \Phi^{CL}_{lat} \begin{Bmatrix} \Delta\hat{\beta} \\ \\ \Delta\hat{\dot{\beta}} \\ \\ \Delta\hat{\phi}_v \\ \\ \Delta\hat{\dot{\phi}}_v \end{Bmatrix}_{k} + \begin{bmatrix} 0 & 0 \\ \\ (\sin\alpha_T) & (-\cos\alpha_T) \\ \\ 0 & 0 \\ \\ (\cos\alpha_T) & (\sin\alpha_T) \end{bmatrix} \begin{Bmatrix} \Delta p^{j} \\ \\ \Delta r^{j} \end{Bmatrix}_{k} \qquad (3\text{-}4)$$

where Φ^{CL}_{lon} and Φ^{CL}_{lat} are the longitudinal (2x2) and lateral (4x4) state transition matrices[†]; Δp^j, Δq^j, Δr^j are the average changes in body angular rates about the x, y and z axes due to ACPS jet activity over the previous sample interval, and α_T is the mean angle-of-attack.

[†] The transition matrices are designated Φ^{CL} (i.e., Φ closed-loop) to indicate that closure of the aerodynamic control loop is taken into account in their derivation:

$$\Phi^{CL} = \Phi^{OL} + \Gamma^{aero} C^{aero}$$

where Φ^{OL} is the open-loop state transition matrix, Γ^{aero} is the aerodynamic-control-to-state matrix, and C^{aero} are the linear-feedback aerodynamic control gains.

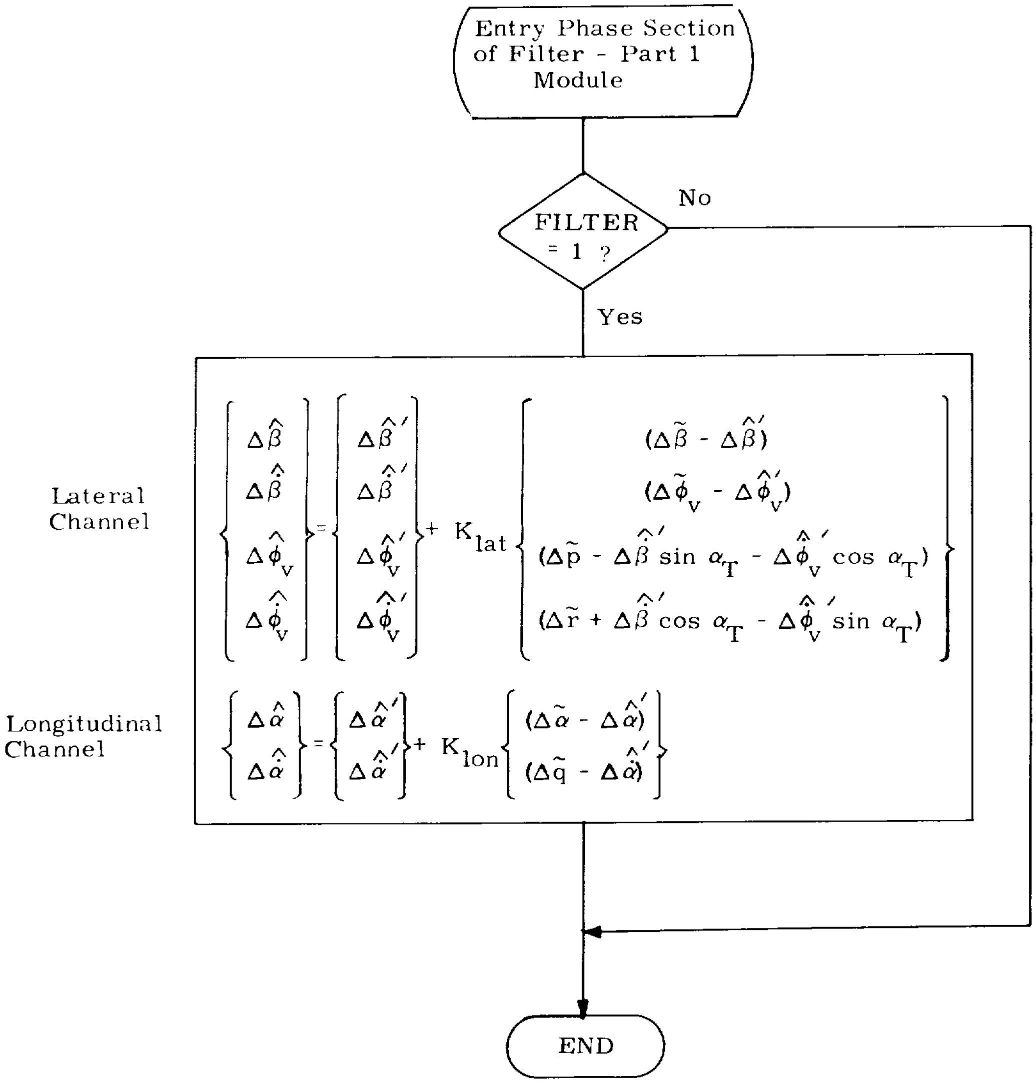
Entry Phase Section of Filter - Part 1 Module
FILTER = 1 ?
No
Yes
Lateral Channel
$\begin{Bmatrix} \Delta\hat{\beta} \\ \Delta\dot{\hat{\beta}} \\ \Delta\hat{\phi}_v \\ \Delta\dot{\hat{\phi}}_v \end{Bmatrix} = \begin{Bmatrix} \Delta\hat{\beta}' \\ \Delta\dot{\hat{\beta}}' \\ \Delta\hat{\phi}_v' \\ \Delta\dot{\hat{\phi}}_v' \end{Bmatrix} + K_{lat} \begin{Bmatrix} (\Delta\tilde{\beta} - \Delta\hat{\beta}') \\ (\Delta\tilde{\phi}_v - \Delta\hat{\phi}_v') \\ (\Delta\tilde{p} - \Delta\dot{\hat{\beta}}' \sin \alpha_T - \Delta\dot{\hat{\phi}}_v' \cos \alpha_T) \\ (\Delta\tilde{r} + \Delta\dot{\hat{\beta}}' \cos \alpha_T - \Delta\dot{\hat{\phi}}_v' \sin \alpha_T) \end{Bmatrix}$
Longitudinal Channel
$\begin{Bmatrix} \Delta\hat{\alpha} \\ \Delta\dot{\hat{\alpha}} \end{Bmatrix} = \begin{Bmatrix} \Delta\hat{\alpha}' \\ \Delta\dot{\hat{\alpha}}' \end{Bmatrix} + K_{lon} \begin{Bmatrix} (\Delta\tilde{\alpha} - \Delta\hat{\alpha}') \\ (\Delta\tilde{q} - \Delta\dot{\hat{\alpha}}') \end{Bmatrix}$
END

Fig. 3-1 Measurement Incorporation for State Estimation

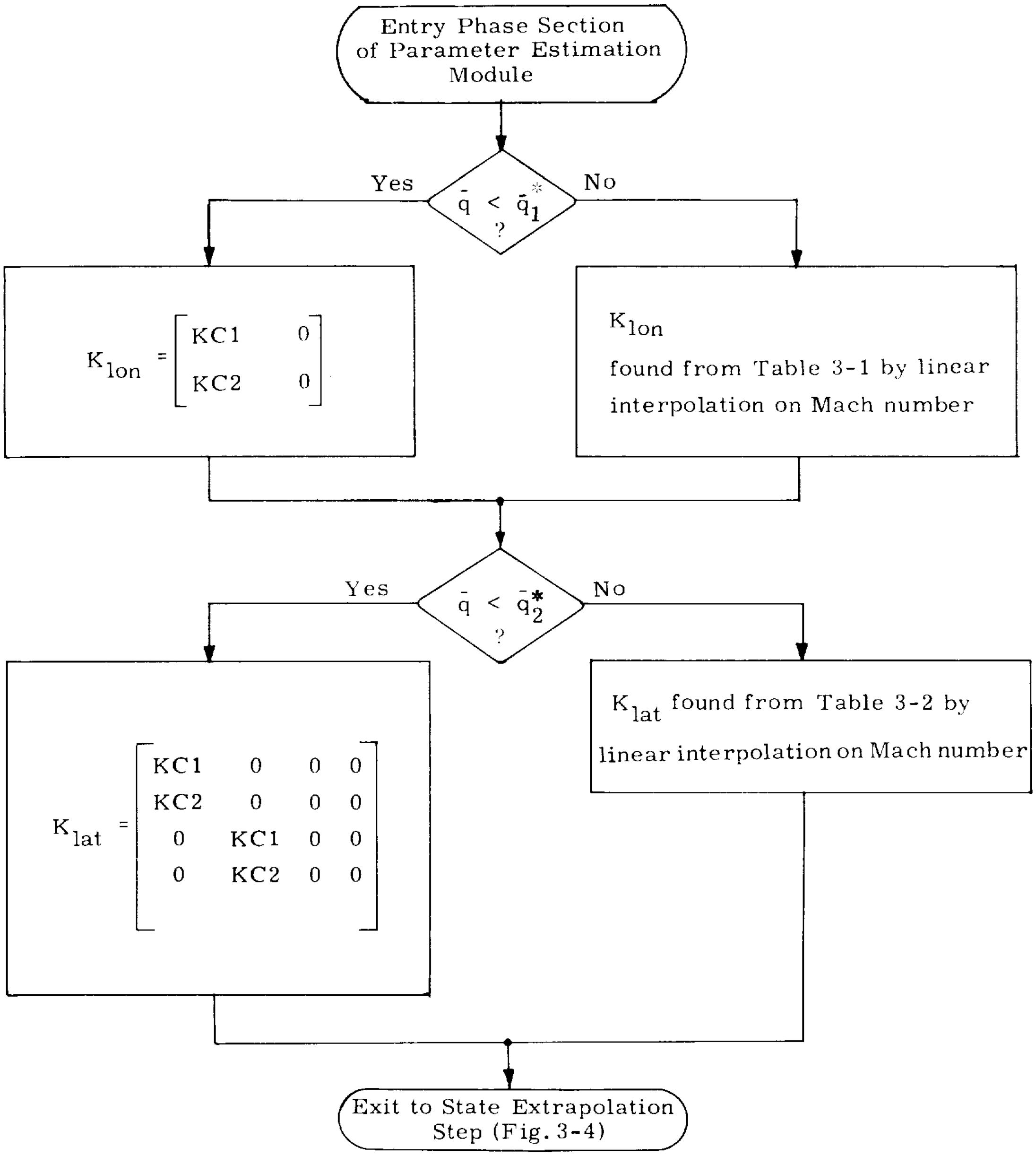
Entry Phase Section of Parameter Estimation Module
$\bar{q} < \bar{q}_1^*$?
Yes
No
$K_{lon} = \begin{bmatrix} KC1 & 0 \\ KC2 & 0 \end{bmatrix}$
K_{lon} found from Table 3-1 by linear interpolation on Mach number
$\bar{q} < \bar{q}_2^*$?
Yes
No
$K_{lat} = \begin{bmatrix} KC1 & 0 & 0 & 0 \\ KC2 & 0 & 0 & 0 \\ 0 & KC1 & 0 & 0 \\ 0 & KC2 & 0 & 0 \end{bmatrix}$
K_{lat} found from Table 3-2 by linear interpolation on Mach number
Exit to State Extrapolation Step (Fig. 3-4)

Fig. 3-2 Computation of Estimator Gain Matrices

Table 3-1 Longitudinal Estimator Gains Scheduled vs Mach Number

		Mach = 0.9	Mach = 2	Mach = 5	Mach = 10	Mach = 20
K_{lon}	(1, 1)	0.0731	0.0769	0.0680	0.0568	0.0401
	(1, 2)	0.0408	0.0411	0.0554	0.0523	0.0586
	(2, 1)	0.0538	0.0353	0.0329	0.0207	0.0116
	(2, 2)	0.4320	0.4289	0.2351	0.2616	0.1909

Table 3-2 Lateral Estimator Gains Scheduled vs Mach Number

		Mach = 0.9	Mach = 2	Mach = 5	Mach = 10	Mach = 20
K_{lat}	(1, 1)	0.2119	0.0578	0.0427	0.0314	0.0222
	(1, 2)	-0.0297	-0.0794	-0.1495	-0.1098	-0.0942
	(1, 3)	-0.0115	-0.0282	-0.0234	-0.0210	-0.0203
	(1, 4)	-0.0337	-0.0456	-0.0637	-0.0605	-0.0659
	(2, 1)	0.2410	0.0238	0.0214	0.0115	0.0065
	(2, 2)	0.0257	0.0155	0.0016	0.0177	0.0075
	(2, 3)	0.0298	0.0696	0.0701	0.1256	0.0900
	(2, 4)	-0.4127	-0.4213	-0.2223	-0.2261	-0.1650
	(3, 1)	-0.0027	-0.0008	-0.0015	-0.0011	-0.0009
	(3, 2)	0.4924	0.4372	0.3569	0.3213	0.2440
	(3, 3)	0.0148	0.0187	0.0198	0.0224	0.0256
	(3, 4)	0.0010	0.0030	0.0072	0.0122	0.0142
	(4, 1)	-0.1164	-0.0212	-0.0181	-0.0133	-0.0070
	(4, 2)	1.355	1.130	0.8698	0.6984	0.4032
	(4, 3)	0.3703	0.3846	0.1853	0.2043	0.1473
	(4, 4)	0.0387	0.0725	0.0783	0.1229	0.0903

The state transition matrices are computed to be the discrete versions of the respective matrices which describe the desired continuous closed-loop aerodynamics:

$$\Phi^{CL} \approx I + F^{CL} \Delta T \qquad (3\text{-}5)$$

where I is the identity matrix, ΔT is the sample interval, and F^{CL} is the system dynamics matrix; i.e.,

$$\Delta \dot{\underline{x}} = F^{CL} \Delta \underline{x} \qquad (3\text{-}6)$$

where $\Delta \underline{x}$ is the variational state. Equation (3-5) is the first order power series expansion to the solution of Eq (3-6). A more accurate representation of Φ^{CL} would probably be necessary only if ΔT were not small with respect to the natural time constants of F^{CL}.

The longitudinal state transition matrix is found by Eq (3-5) from F_{lon}^{CL}, which takes on either of two forms:

$$F_{lon}^{CL} = \begin{bmatrix} 0 & 1 \\ 0 & 0 \end{bmatrix} \qquad (3\text{-}7)$$

or

$$F_{lon}^{CL} = \begin{bmatrix} 0 & 1 \\ -\omega_d^2 & -2\zeta_d \omega_d \end{bmatrix} \qquad (3\text{-}8)$$

where the parameters ω_d and ζ_d specify the desired longitudinal response. (See Subsection 5.3.1.1). Equation (3-7) is used for dynamic pressure below $\bar{q}_1^*$, when the elevator is essentially used only for trim. Equation (3-8) is used for dynamic pressure above $\bar{q}_1^*$.

The lateral state transition matrix is found by Eq (3-5) from F_{lat}^{CL}, which takes on either of two forms:

$$F_{lat}^{CL} = \begin{bmatrix} 0 & 1 & 0 & 0 \\ 0 & 0 & 0 & 0 \\ 0 & 0 & 0 & 1 \\ 0 & 0 & 0 & 0 \end{bmatrix} \qquad (3\text{-}9)$$

or

$$F_{lat}^{CL} = \begin{bmatrix} 0 & 1 & 0 & 0 \\ -b_{11} & -a_{11} & -b_{12} & -a_{12} \\ 0 & 0 & 0 & 1 \\ -b_{21} & -a_{21} & -b_{22} & -a_{22} \end{bmatrix} \qquad (3\text{-}10)$$

where the parameters a_{11} through b_{22} specify the desired lateral response (see Subsection 5.3.2.1.2). Equation (3-9) is used for dynamic pressure below $\bar{q}_2^*$, when the aileron is essentially not used. Equation (3-10) is used for dynamic pressure above $\bar{q}_2^*$.

The flow charts in Figs. 3-3 and 3-4 show the implementation in the DFCS program of the state extrapolation equations and the computation of the state transition matrices. The numerical values of the parameters used in the state extrapolation are indicated in Table 3-3. The control gains $C'_{\ell_{\delta a}}$, $C'_{n_{\delta a}}$, C'_{ℓ_β}, C'_{n_β} will be obtained from the entry control module in the future. Currently, however, they are independently scheduled as functions of Mach number, as shown in Fig. 3-5.

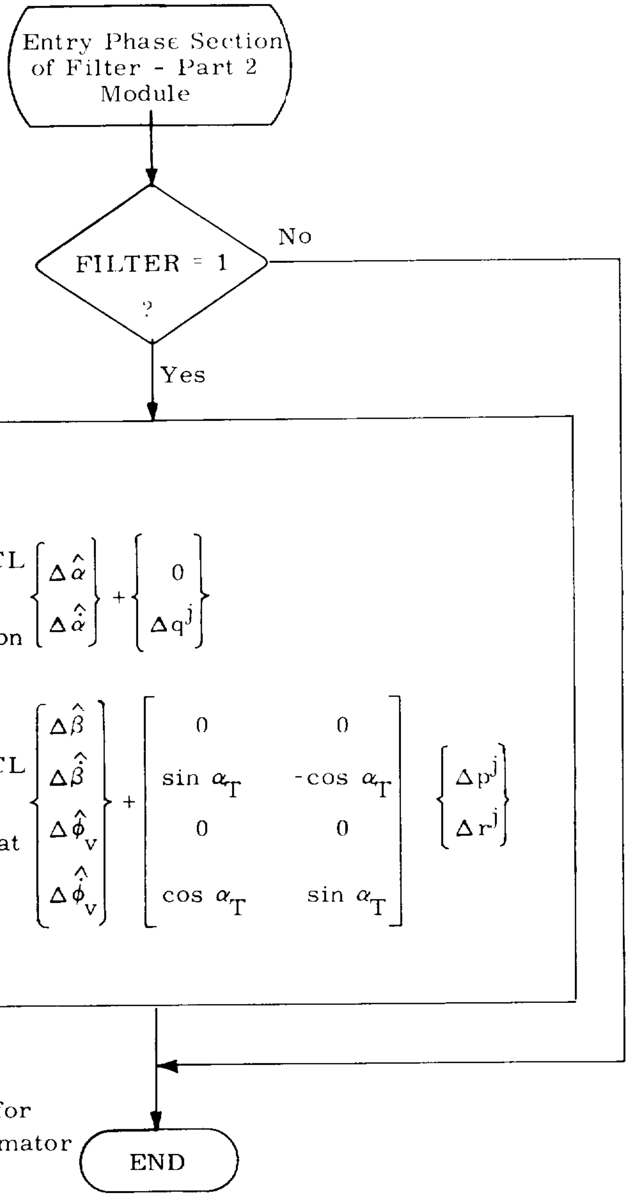

$$\begin{Bmatrix} \Delta\hat{\alpha}' \\ \Delta\hat{\dot{\alpha}}' \end{Bmatrix} = \Phi^{CL}_{lon} \begin{Bmatrix} \Delta\hat{\alpha} \\ \Delta\hat{\dot{\alpha}} \end{Bmatrix} + \begin{Bmatrix} 0 \\ \Delta q^j \end{Bmatrix}$$

$$\begin{Bmatrix} \Delta\hat{\beta}' \\ \Delta\hat{\dot{\beta}}' \\ \Delta\hat{\phi}_v' \\ \Delta\hat{\dot{\phi}}_v' \end{Bmatrix} = \Phi^{CL}_{lat} \begin{Bmatrix} \Delta\hat{\beta} \\ \Delta\hat{\dot{\beta}} \\ \Delta\hat{\phi}_v \\ \Delta\hat{\dot{\phi}}_v \end{Bmatrix} + \begin{bmatrix} 0 & 0 \\ \sin\alpha_T & -\cos\alpha_T \\ 0 & 0 \\ \cos\alpha_T & \sin\alpha_T \end{bmatrix} \begin{Bmatrix} \Delta p^j \\ \Delta r^j \end{Bmatrix}$$

Fig. 3-3 State Extrapolation for the Entry State Estimator

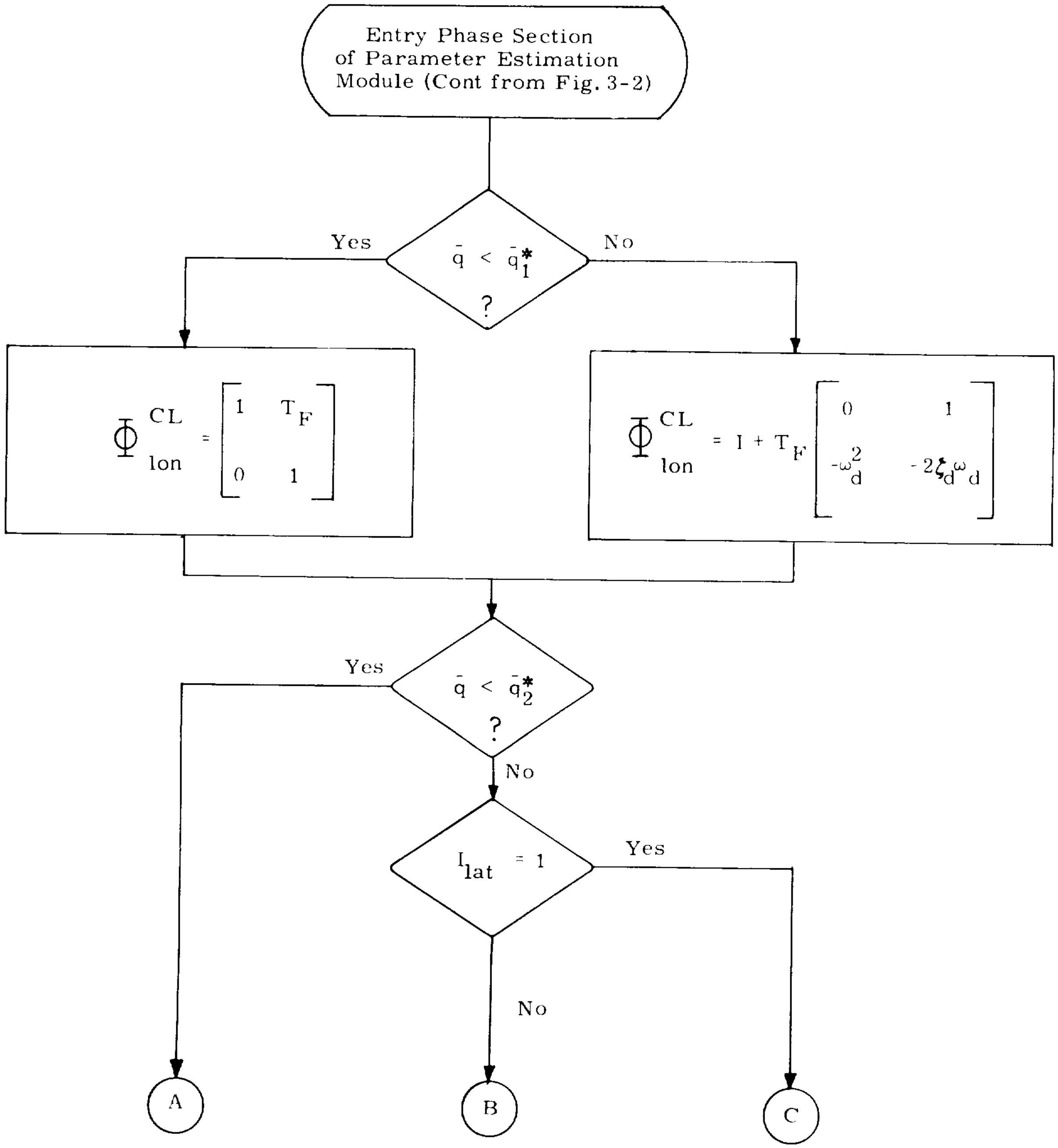
Entry Phase Section of Parameter Estimation Module (Cont from Fig. 3-2)
$\bar{q} < \bar{q}_1^*$?
Yes
No
$\Phi_{lon}^{CL} = \begin{bmatrix} 1 & T_F \\ 0 & 1 \end{bmatrix}$
$\Phi_{lon}^{CL} = I + T_F \begin{bmatrix} 0 & 1 \\ -\omega_d^2 & -2\zeta_d\omega_d \end{bmatrix}$
$\bar{q} < \bar{q}_2^*$?
Yes
No
$I_{lat} = 1$
Yes
No
A
B
C

Fig. 3-4 Computation of Estimator State Transition Matrices

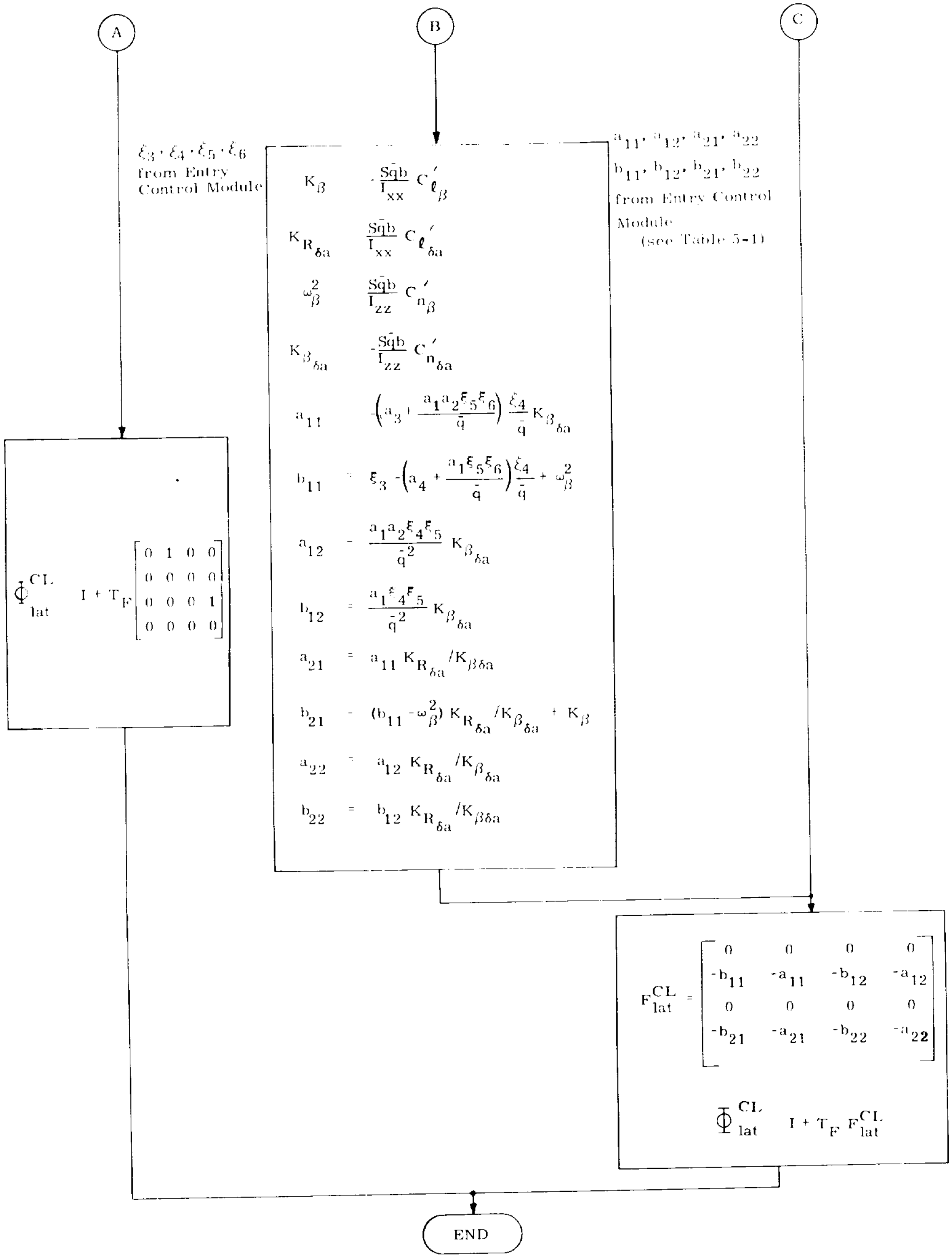

A
B
C
$\xi_3, \xi_4, \xi_5, \xi_6$ from Entry Control Module
$a_{11}, a_{12}, a_{21}, a_{22}$
$b_{11}, b_{12}, b_{21}, b_{22}$
from Entry Control Module (see Table 5-1)
$K_\beta \quad -\frac{S\bar{q}b}{I_{xx}} C'_{\ell_\beta}$
$K_{R_{\delta a}} \quad \frac{S\bar{q}b}{I_{xx}} C'_{\ell_{\delta a}}$
$\omega_\beta^2 \quad \frac{S\bar{q}b}{I_{zz}} C'_{n_\beta}$
$K_{\beta_{\delta a}} \quad -\frac{S\bar{q}b}{I_{zz}} C'_{n_{\delta a}}$
$a_{11} \quad -\left(a_3 + \frac{a_1 a_2 \xi_5 \xi_6}{\bar{q}}\right) \frac{\xi_4}{\bar{q}} K_{\beta_{\delta a}}$
$b_{11} = \xi_3 - \left(a_4 + \frac{a_1 \xi_5 \xi_6}{\bar{q}}\right) \frac{\xi_4}{\bar{q}} + \omega_\beta^2$
$a_{12} = \frac{a_1 a_2 \xi_4 \xi_5}{\bar{q}^2} K_{\beta_{\delta a}}$
$b_{12} = \frac{a_1 \xi_4 \xi_5}{\bar{q}^2} K_{\beta_{\delta a}}$
$a_{21} = a_{11} K_{R_{\delta a}} / K_{\beta \delta a}$
$b_{21} = (b_{11} - \omega_\beta^2) K_{R_{\delta a}} / K_{\beta_{\delta a}} + K_\beta$
$a_{22} = a_{12} K_{R_{\delta a}} / K_{\beta_{\delta a}}$
$b_{22} = b_{12} K_{R_{\delta a}} / K_{\beta \delta a}$
$\Phi_{lat}^{CL} \quad I + T_F \begin{bmatrix} 0 & 1 & 0 & 0 \\ 0 & 0 & 0 & 0 \\ 0 & 0 & 0 & 1 \\ 0 & 0 & 0 & 0 \end{bmatrix}$
$F_{lat}^{CL} = \begin{bmatrix} 0 & 0 & 0 & 0 \\ -b_{11} & -a_{11} & -b_{12} & -a_{12} \\ 0 & 0 & 0 & 0 \\ -b_{21} & -a_{21} & -b_{22} & -a_{22} \end{bmatrix}$
$\Phi_{lat}^{CL} \quad I + T_F F_{lat}^{CL}$
END

Fig. 3-4 Computation of Estimator State Transition Matrices (Cont)

Table 3-3: Parameter Values for State Extrapolation

Aerodynamic and Inertial Parameters

S	2690.
b	78.056
I_{xx}	805000
I_{zz}	6067000

Fixed Control Gains

a_1	0.2401
a_2	6.0
a_3	2.94
a_4	2.9008
a_{11}	See Table 5-1
a_{12}	
a_{21}	
a_{22}	
b_{11}	
b_{12}	
b_{21}	
b_{22}	

Scheduled Control Gains

ξ_1	See Figs. 5-16 through 5-21	$C'_{\ell_{\delta a}}$	See Fig. 3-5
ξ_2		$C'_{n_{\delta a}}$	
ξ_3		$C'_{\ell_{\beta}}$	
ξ_4		$C'_{n_{\beta}}$	
ξ_5			
ξ_6			

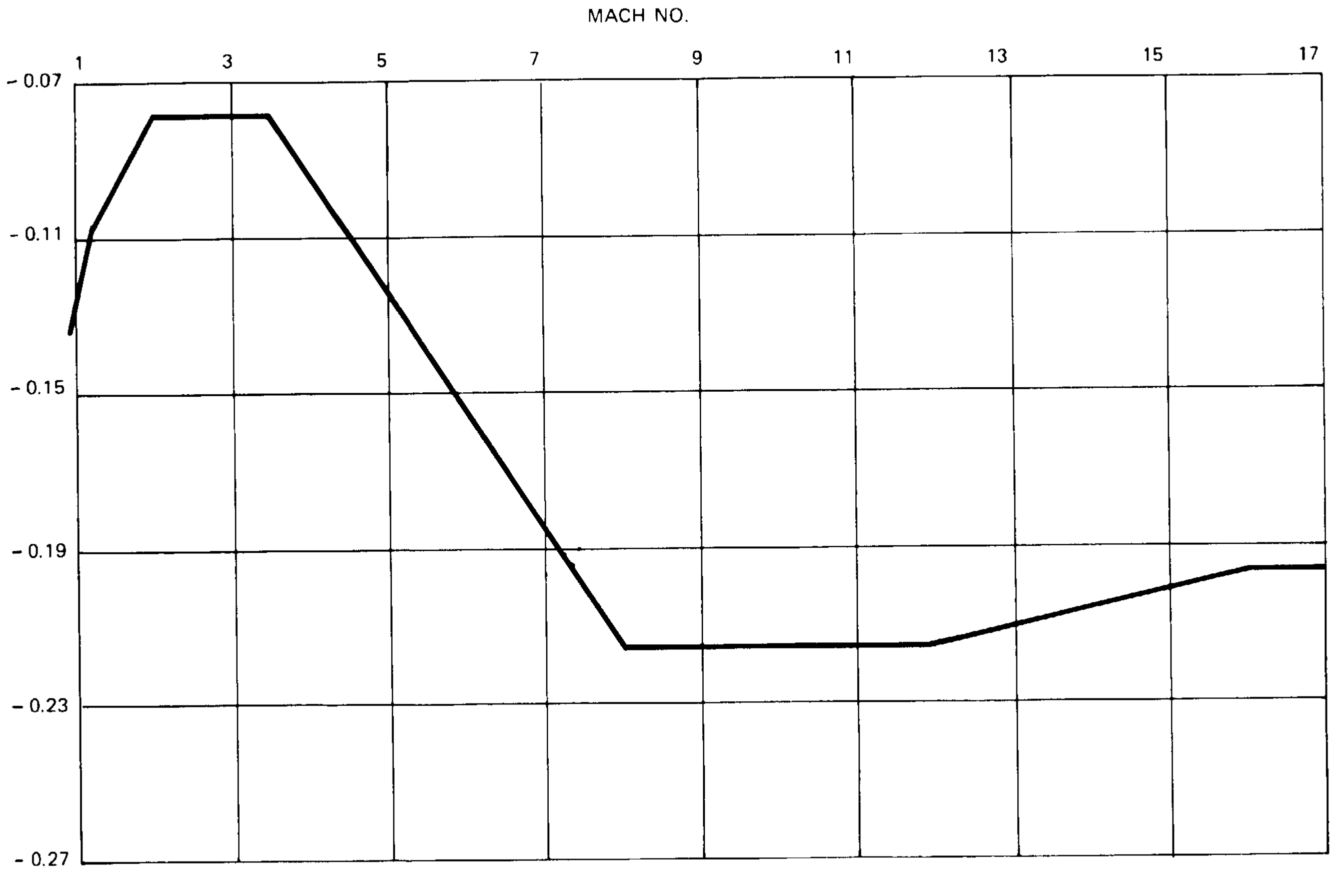

Fig. 3-5a $C_{\ell_{\delta a}}'$ vs Mach Number

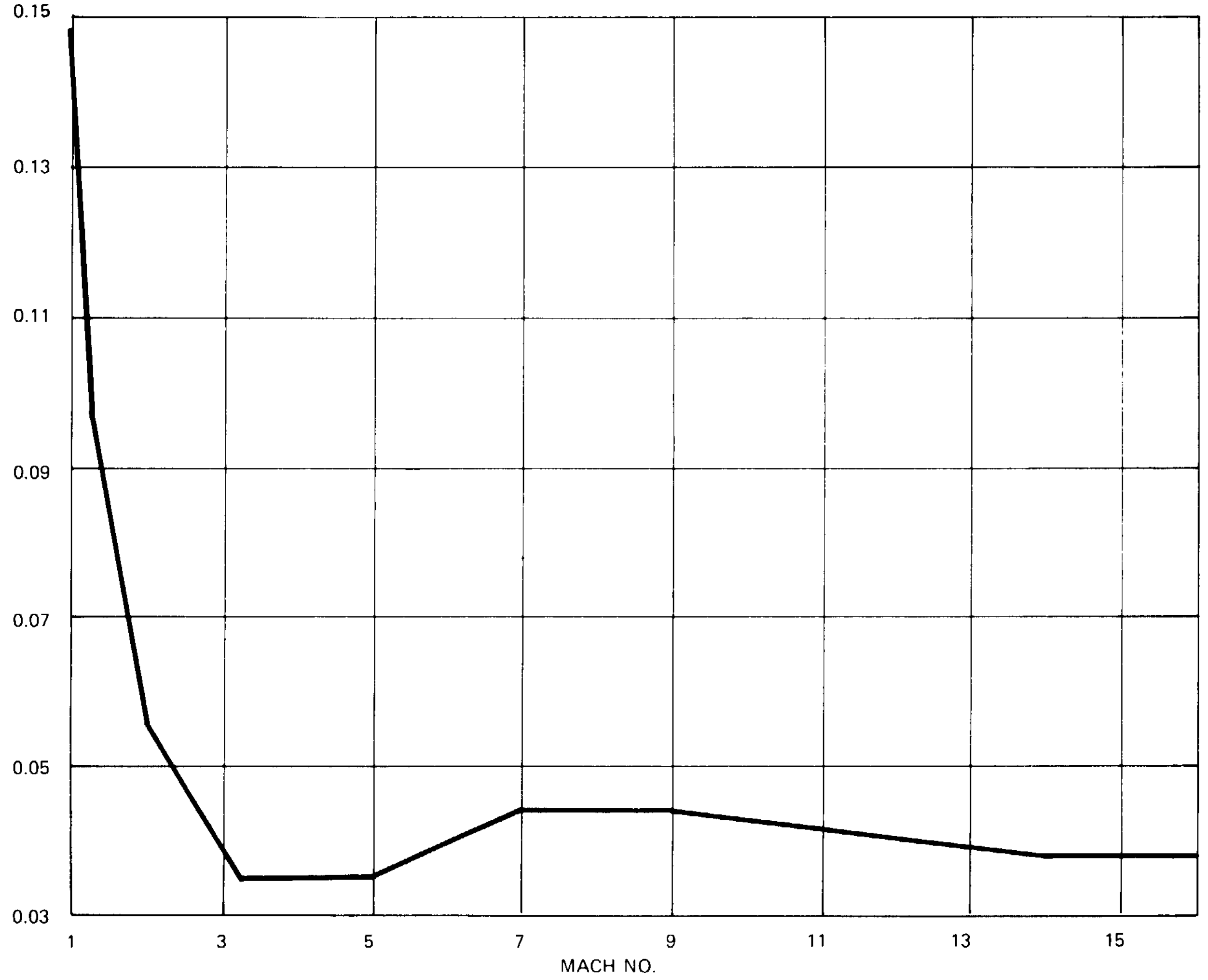

Fig. 3-5b $C_{n_{\delta a}}'$ vs Mach Number

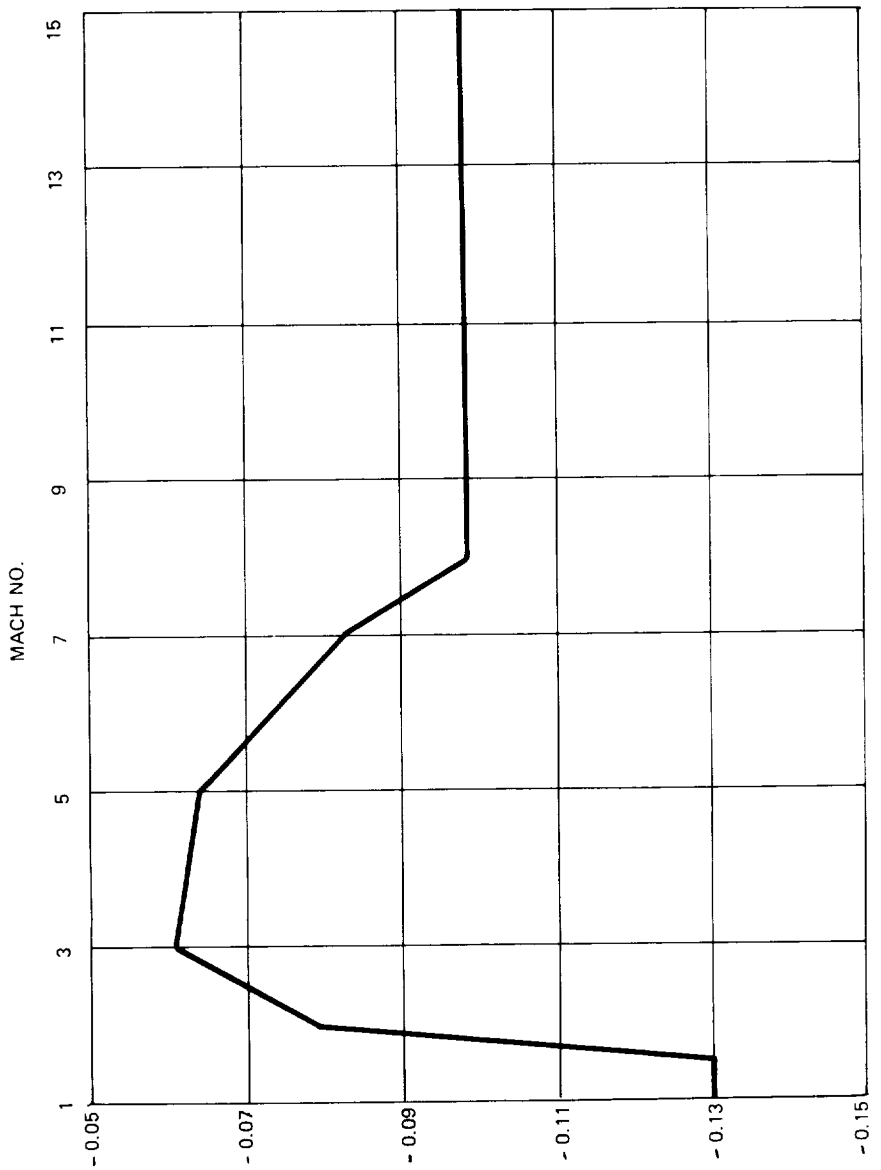

Fig. 3-5c C'_{ℓ_β} vs Mach Number

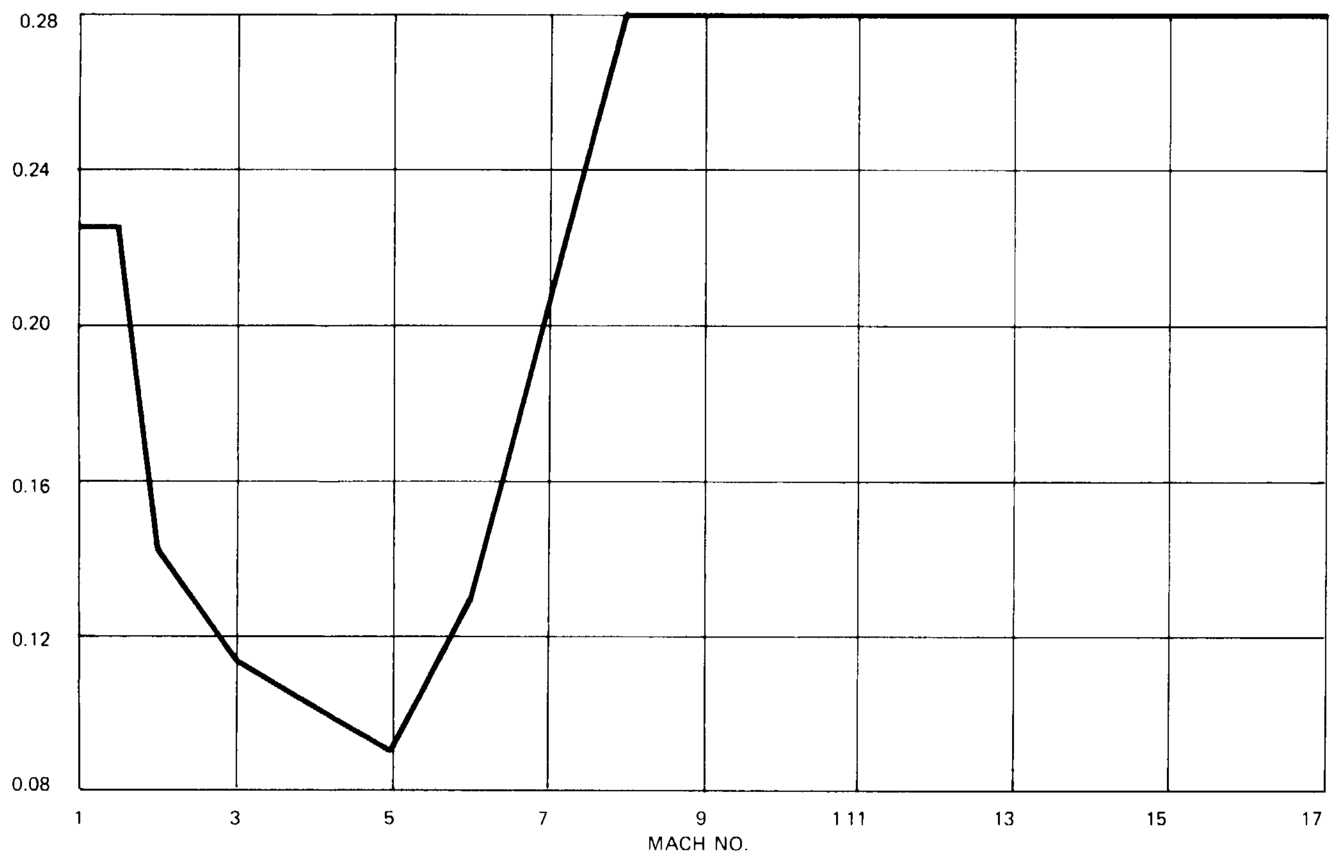

Fig. 3-5d C_{n_β}' vs Mach Number

3.4 Preliminary Performance Summary

Simulated maneuvers have been performed on the Space Shuttle Functional Simulator using the state estimator in conjunction with the entry DFCS and the NR00089B (February version) vehicle. Both large and small step changes in angle of attack and bank were commanded under a wide range of flight conditions (Mach = 2, $\overline{q}$ = 150 lbs/ft^2 to Mach = 25, $\overline{q}$ = 0.25 lbs/ft^2).

Comparisons were made between simulations in which the DFCS controller operated on state estimator outputs (FILTER = 1) and corresponding simulations in which the DFCS controller operated directly on measured data (FILTER = 0). When random noise sources were not simulated (perfect measurements), comparisons between corresponding simulations were very good in every case. When random noise sources were simulated, corresponding simulations exhibited similar mean behavior, but aerodynamic surface commands were smoother for those cases which used the estimator. Figure 3-6, for example, shows actual angle of attack, roll angle, and aerodynamic surface position time histories for corresponding cases at Mach 14 and a dynamic pressure of 108 lbs/ft^2.

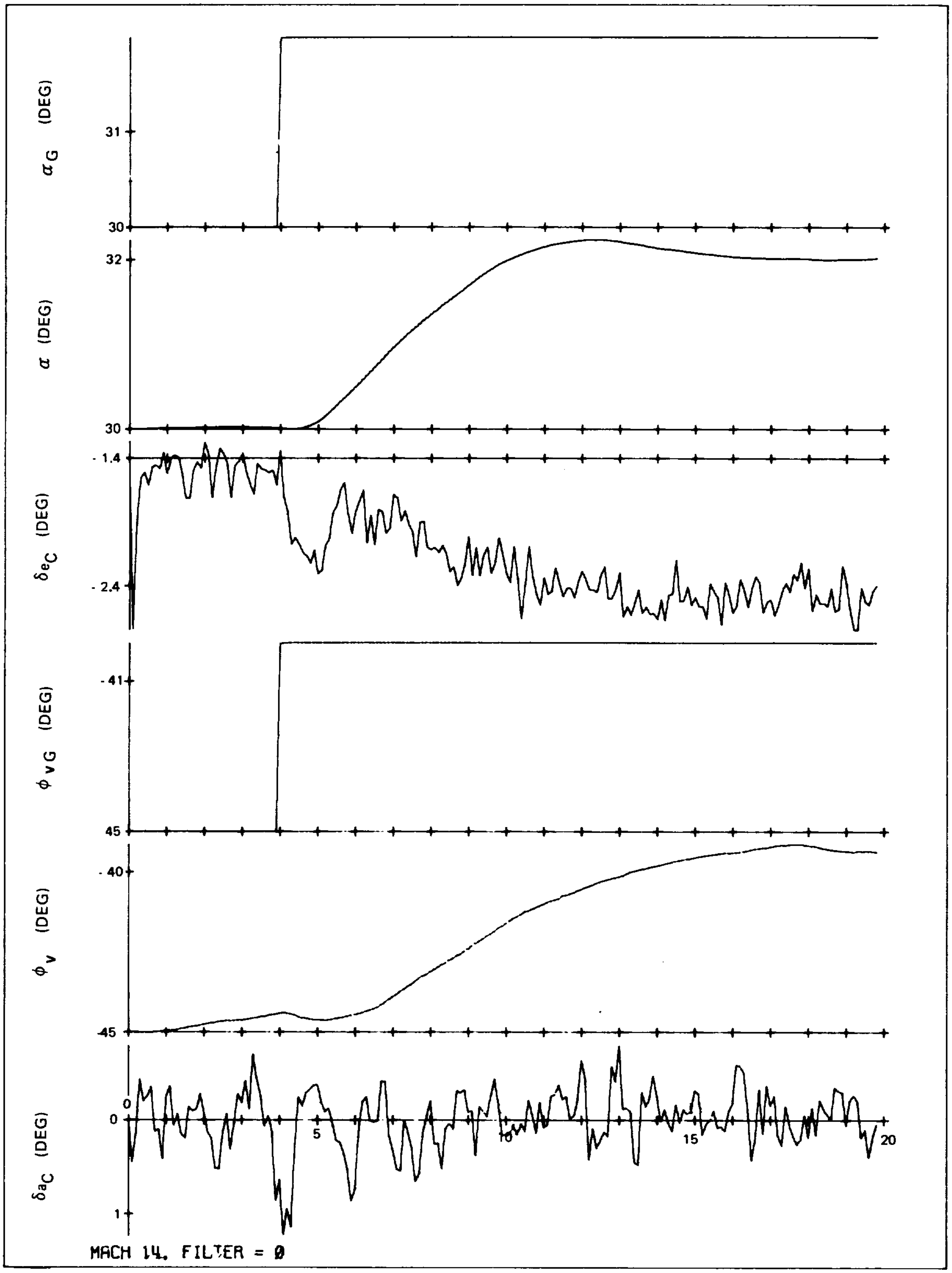

Fig. 3-6a Longitudinal and Lateral Responses with Noise Sources Simulated and FILTER = 0 (no estimator in loop)

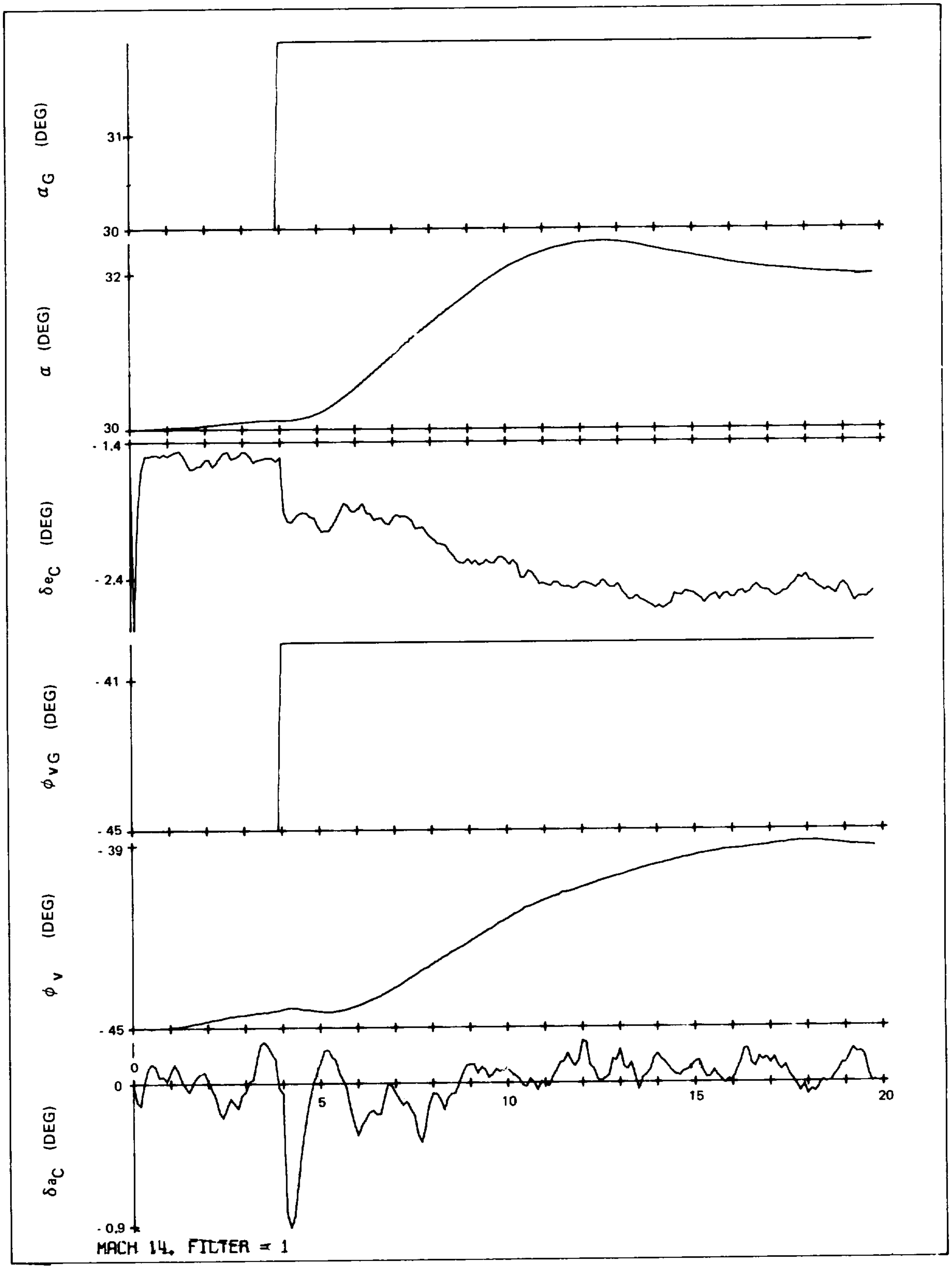

Fig. 3-6b Longitudinal and Lateral Responses with Noise Sources Simulated and FILTER = 1 (estimator in loop)

SECTION 4

DFCS - CRUISE PHASE

4.1 Introduction

The cruising flight phase of an orbital space shuttle flight begins at about Mach 0.9, ends at touchdown, and follows the high-angle-of-attack/high-Mach-number entry phase. During the cruise phase the control is accomplished by moving the aerodynamic control surfaces: elevons, rudder, rudder flare (speed brake), and body flap. In addition, the cruise phase DFCS has been extended to deal with shuttle powered horizontal flight, which encompasses developmental testing and ferry missions. During powered flights, thrust is an additional control variable.

For the cruise phase the DFCS contains three primary modes of operation: manual, semiautomatic and automatic. Manual mode consists of two types of control systems: Stability Augmentation System (SAS) and Command Augmentation System (CAS). By means of a side arm controller and rudder pedals, the pilot uses either of these two systems to manually control the orbiter. The pilot can reduce his workload while controlling the orbiter by selecting certain automatic functions provided by outer loops. This is the semiautomatic mode of operation. In the automatic mode of operation guidance algorithms provide the commands to the digital flight control system, and the pilot's control role is reduced to monitoring the overall performance. One further system available is the Backup Control System (BCS) which is nearly identical to the SAS. This system is completely manual, and following its initial flight test, is intended to remain unchanged throughout the Space Shuttle Program.

Speed control is accomplished by using either speed brake or throttle. The settings can be controlled in an open loop fashion either by the pilot in the manual mode or by the guidance algorithms in the automatic mode. Alternatively the settings can be obtained from closed loop speed control loops. In this case, depending on the mode of operation, the speed commands come either from the pilot (select/hold mode) or from the guidance. For the purpose of pitch trimming, the body flap's setting is scheduled as a function of Mach number, which can be supplemented by a manual flap command.

Stabilization of the vehicle in the cruise phase is accomplished with compensation filters which appear in forward loop, feedback, and crossfeed paths. It was found that for control of the rigid body many of these filters are not needed and good control performance can be obtained with simpler compensations than allowed for. However, these filters will become necessary and may, in fact, become insufficient in size as control of the flexible vehicle is considered. A table of gains suitable for control of the rigid body 89B vehicle at a particular flight condition (Mach No. 0.6, dynamic pressure 300 psf, altitude 6000 ft) is provided (Table 4-1). The gains which must be varied as a function of some flight parameter (such as dynamic pressure), are marked by an asterisk.

The description of the cruise phase autopilot is presented in the order of increasing detail, starting with a discussion of simplified block diagrams, proceeding to detailed functional block diagrams, and then finally to detailed flow charts. Subsection 4.2 describes manual, semiautomatic, and automatic control modes as well as speed and body flap controls. The description of the BCS is followed by that of mode selection and mode change trim initialization. Filter implementation is discussed in Subsection 4.3 where a generalized n^{th}-order digital filter implementation is detailed along with low-pass and washout filters, and integration functions. Subsection 4.4 describes preflight initialization of gains and filter coefficients, as well as limits, deadbands and other items. Subsection 4.5 presents summaries of input/output quantities for various channels such as elevator, aileron, etc. The detailed functional block diagrams in Subsection 4.6 are preceded by a list of conventions in order to facilitate their presentation. Subsection 4.7 contains functional flow charts for initialization subroutine of the cruise DFCS, and then detailed flow charts are presented in the Appendix, Subsection 4A.

4.2 Control Modes

4.2.1 Manual Modes of Operation

For manual operation the two types of control systems are a command augmentation system (CAS) for normal operation, and a stability augmentation system (SAS) for lower performance downmode operation. The pitch rate and roll rate feedback loops, with simple gain compensations in the feedback paths, are employed in SAS (Fig. 4-1). The manual commands to the elevator and aileron are summed with these feedback signals and sent out to the control surfaces. The manual rudder command is summed with two feedbacks and one crossfeed signal from the aileron before it is sent to the rudder. Washed-out yaw rate feedback augments the dutch-roll stability. The turn coordination in SAS is achieved by either a combination of aileron to rudder crossfeed and lateral acceleration, or sideslip feedback. For selecting the best control response, pitch rate, roll rate, and yaw rate gains can be scaled by the pilot from his control panel.

A simplified block diagram of CAS is shown in Fig. 4-2. The longitudinal and lateral control systems are pitch rate (or C^*)loop and roll rate loop closures having similar forward path compensation filters followed by a proportional path and an integral

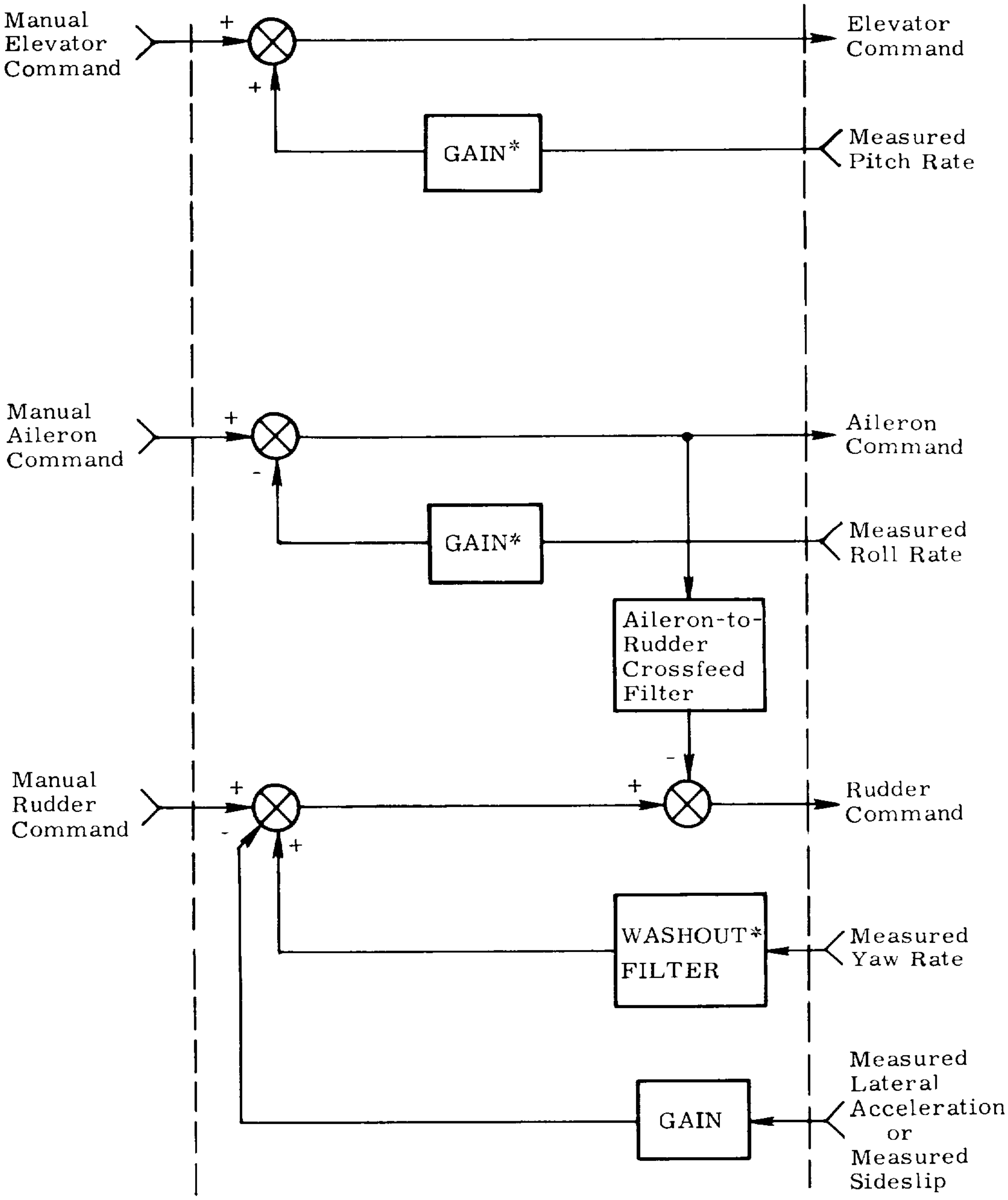

* Gain-switch-sensitive gains

Fig. 4-1 Simplified Functional Block Diagram of The Stability Augmentation System (also Backup Control System) Mode

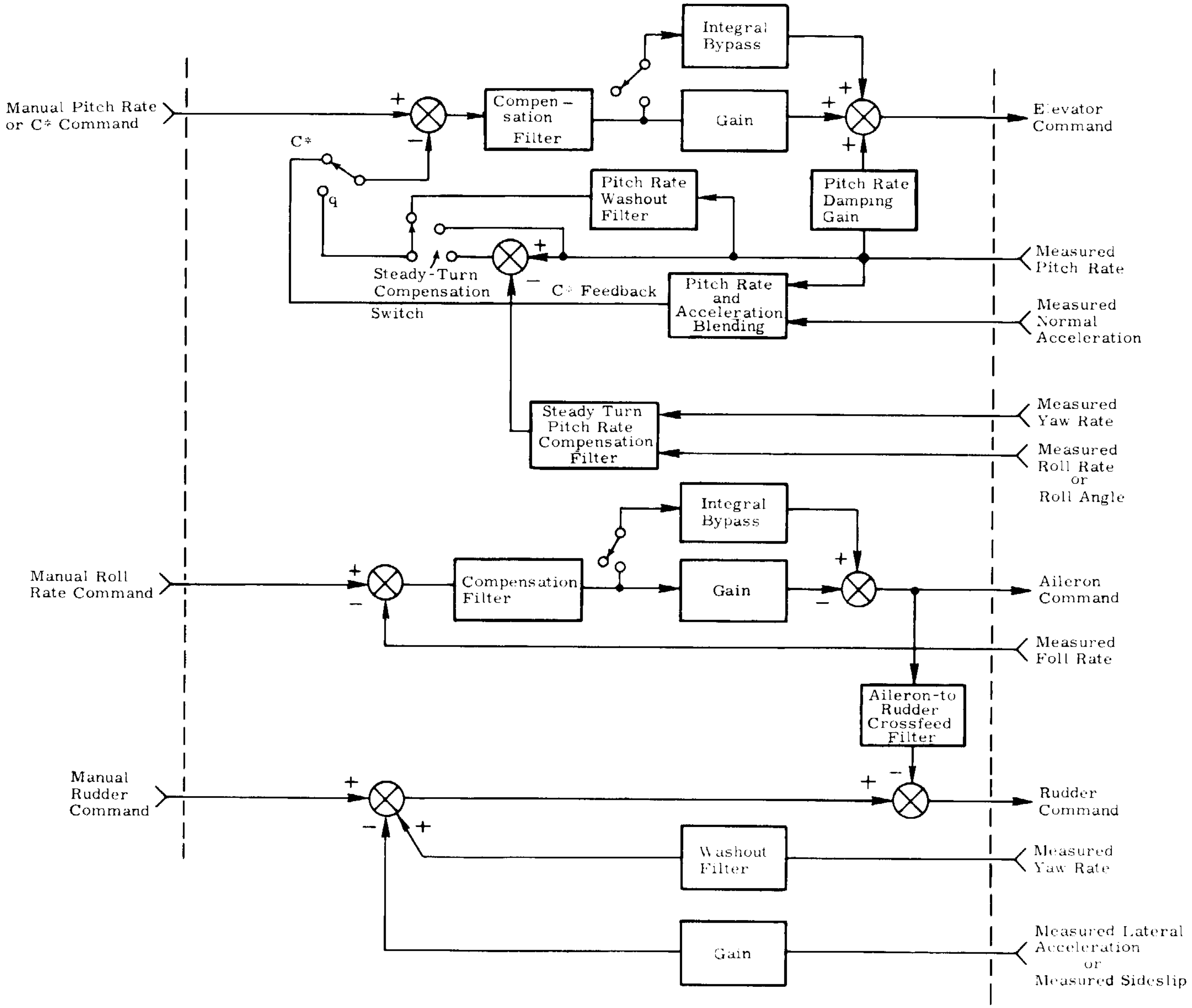
Manual Pitch Rate or C* Command
Manual Roll Rate Command
Manual Rudder Command
C*
q
+
−
Compen – sation Filter
Integral Bypass
Gain
Pitch Rate Washout Filter
Pitch Rate Damping Gain
Steady-Turn Compensation Switch
C* Feedback
Pitch Rate and Acceleration Blending
Steady Turn Pitch Rate Compensation Filter
Compensation Filter
Integral Bypass
Gain
Aileron-to Rudder Crossfeed Filter
Washout Filter
Gain
Elevator Command
Measured Pitch Rate
Measured Normal Acceleration
Measured Yaw Rate
Measured Roll Rate or Roll Angle
Aileron Command
Measured Foll Rate
Rudder Command
Measured Yaw Rate
Measured Lateral Acceleration or Measured Sideslip

Fig. 4-2 Simplified Functional Block Diagram of the Command Augmentation System Mode

bypass. The integral bypass provides automatic trimming and assures unit-gain rate tracking. This function can be switched in or out from the control panel, and the pitch rate/C^* loop has an inner damping loop and an outer feedback loop enabling a selection of either C^* or pitch rate. C^* is a blend of pitch rate and normal acceleration. The pitch rate feedback can be fed back directly, passed first through a washout filter, or fed back with an added steady turn compensating component. This component is proportional to the yaw rate and tangent of the roll angle which is measured or derived from the measured roll rate. Depending on the type of feedback (C^* or pitch rate), the manual command is scaled according to either C^* or q for the control variable. The roll rate loop does not have an inner damping loop and thus uses roll rate feedback. The rudder channel is the same as in the SAS.

4.2.2 Semiautomatic Modes of Operation

Certain selectable outer loop closures provide semiautomatic modes of operation, the construction of which is shown in Fig. 4-3. For longitudinal control the inputs are either pitch attitude or altitude references with the controlled variables being pitch attitude and altitude. For lateral control the references and the controlled quantities are the bank angle and heading. In both cases, engaging the control stick opens these outer loops and enables the control stick steering function. Therefore, returning the stick to null reengages the selected semiautomatic mode once the body rates fall below a threshold value.

4.2.3 Automatic Modes of Operation

For one particular cruise phase guidance scheme the automatic mode is subdivided into two regions of operation according to the following table:

Name of guidance phase	Approximate altitude range	Guidance commands
Approach	40000 to 7000 feet	α_G, ϕ_{v_G}
Terminal	7000 feet to touchdown	q_G, ϕ_{b_G}

During the approach phase the longitudinal control is of the angle-of-attack. In the terminal phase, longitudinal control is accomplished by the pitch rate loop which is identical to the CAS loop described in Subsection 4.2.1 (including pitch rate compensation during steady turns). In both cases the lateral control is of the roll attitude. However, the roll angle commands are different in the two guidance cases: roll angle is taken about the velocity vector in the approach phase, and about the body (vehicle x-axis) in the terminal phase. For both cases the form of the lateral control system and the gains are the same.

As illustrated in Fig. 4-4, guidance commands other than those shown above can also be accommodated. Thus the longitudinal control system can be configured

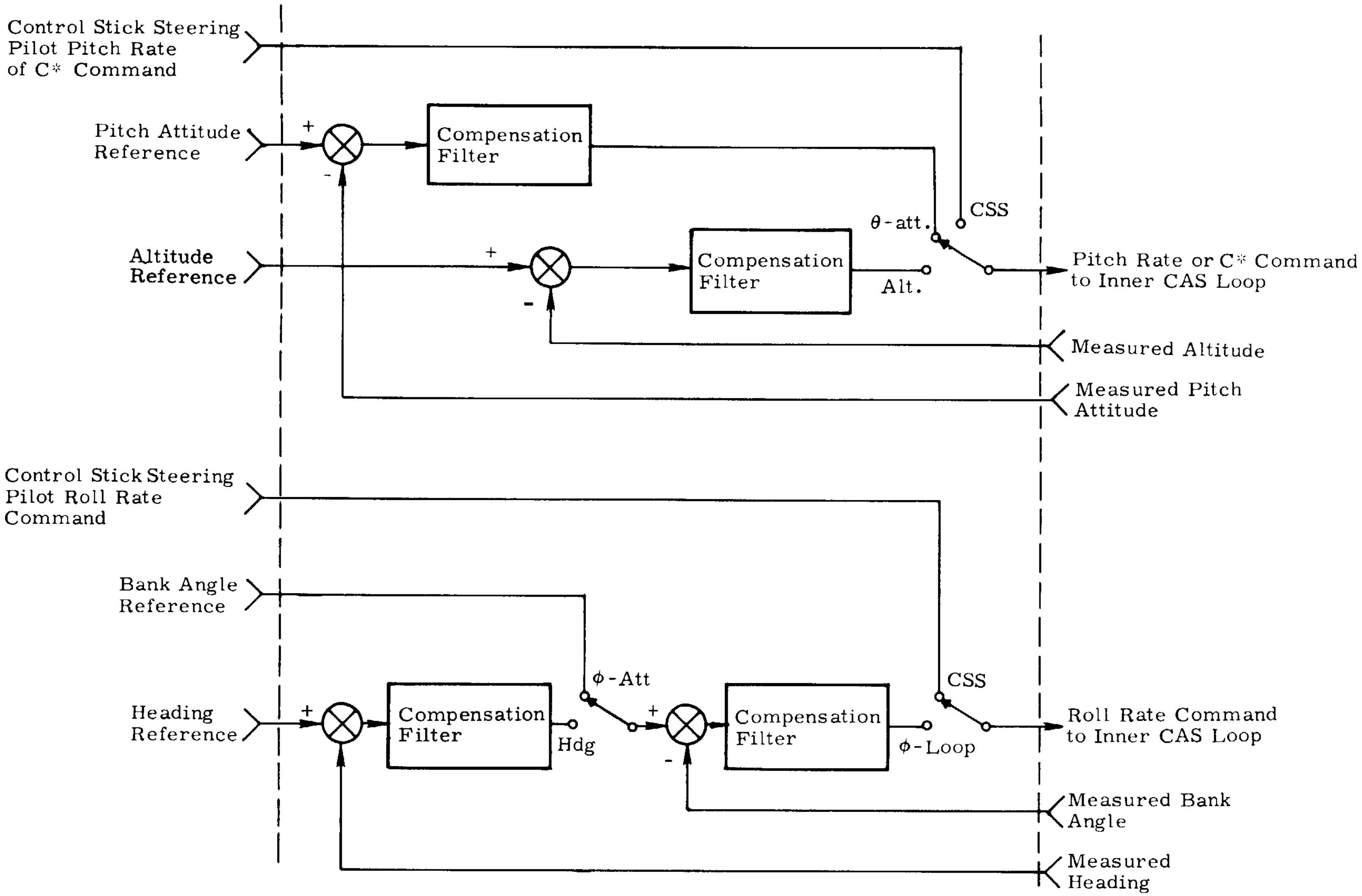

Fig. 4-3 Simplified Functional Block Diagram of Outer Loops for Semiautomatic Modes of Operation

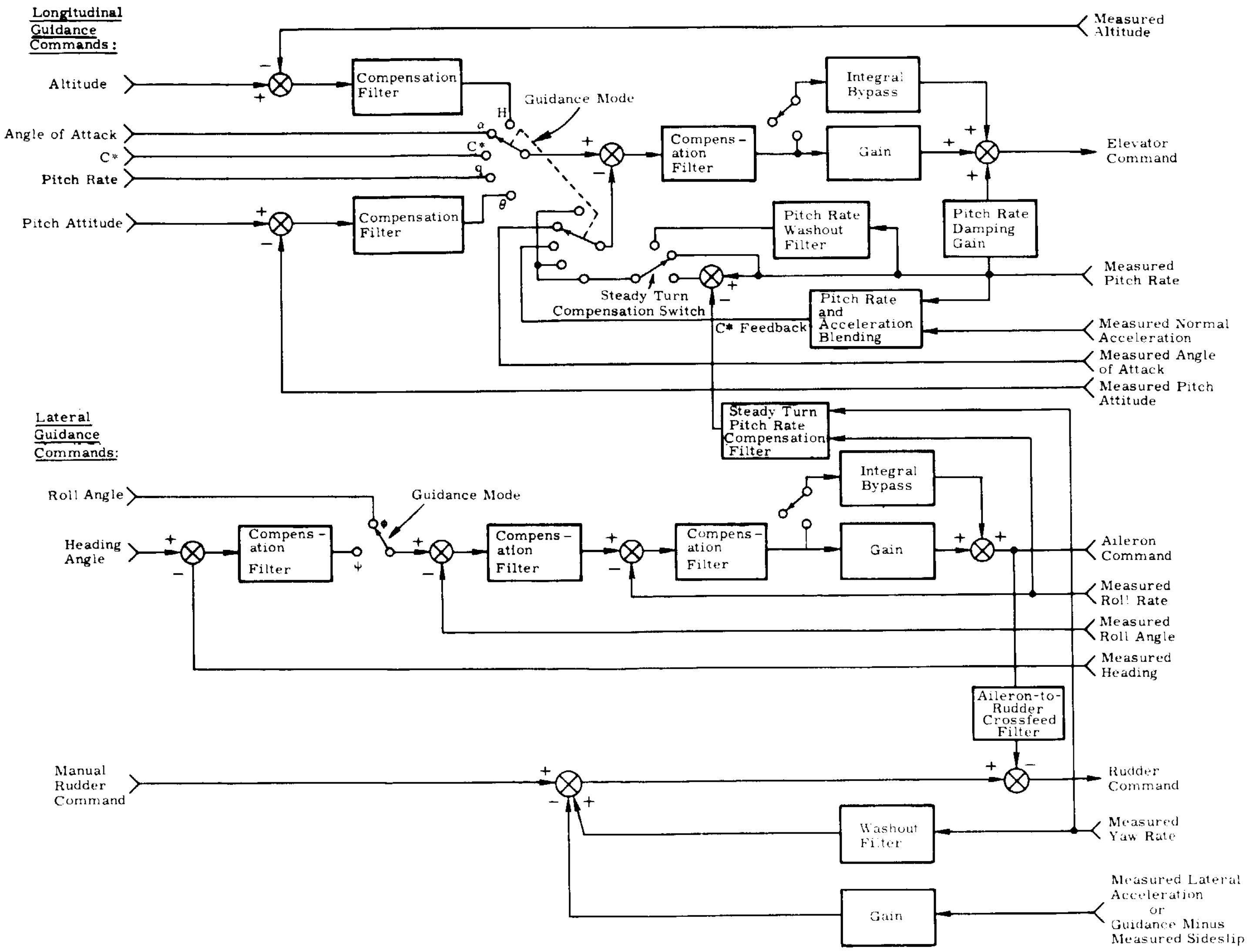

Fig. 4-4 Simplified Functional Block Diagram of the Automatic Mode

as either an altitude loop or a pitch attitude loop, both of which are outer loops closed around the inner CAS loops. Similar to the CAS, an additional longitudinal control mode has C^* feedback. As well as the roll angle loop already discussed, the lateral control system is provided with a heading loop closed around the roll attitude loop.

The rudder loop is implemented similar to the SAS or CAS mode, except that a provision is made to accept sideslip guidance commands and direct or washed-out yaw rate feedback for automatic decrab maneuver. Rudder pedal commands enable this maneuver to be made manually.

It should be mentioned that, although not shown on the simplified block diagram, additional guidance commands can be applied in the automatic mode. These are elevator, aileron, and rudder commands applied directly to the appropriate summing junctions, and roll rate guidance command to the roll rate summing junction.

4.2.4 Speed Control

Control of indicated airspeed for the cruise phase is accomplished by two control effectors, the speed brake (also commonly known as "rudder flare"), and the air breathing engine system (ABES). Use of the ABES is anticipated only for purposes of powered horizontal flight operations, but the appropriate control algorithms resulting in throttle command are instituted in the current comprehensive cruise DFCS. Simplified functional block diagrams of the speed control modes are presented in Fig. 4-5.

In BCS and manual modes, which are functionally identical, the pilot's manual commands are passed directly to the control actuators. Although not indicated in Fig. 4-5, speed brake and throttle commands in BCS and manual modes, as in all speed modes, are crossfed to the elevator for the purpose of trimming out resulting pitching moment. Note that BCS and manual control may employ speed brake or throttle or both.

The IAS-hold mode is functionally similar to the automatic guidance mode which provides IAS commands, and is a velocity loop closure with forward loop compensation. Currently, the speed brake loop is implemented with proportional plus-integral compensation, and the throttle loop has lead-integral lag compensation. In this mode either speed brake or throttle is utilized and the nominal elevator mode selection is CAS.

The automatic (direct guidance) mode issues commands to the speed brake and throttle based directly on guidance issued speed brake and throttle commands. This may occur for either speed brake or throttle or both.

Finally, the automatic Terminal Area Energy Management (TAEM) guidance mode receives the TAEM guidance rate command and first passes through switching logic to decide whether the command is to be issued to speed brake or throttle. If

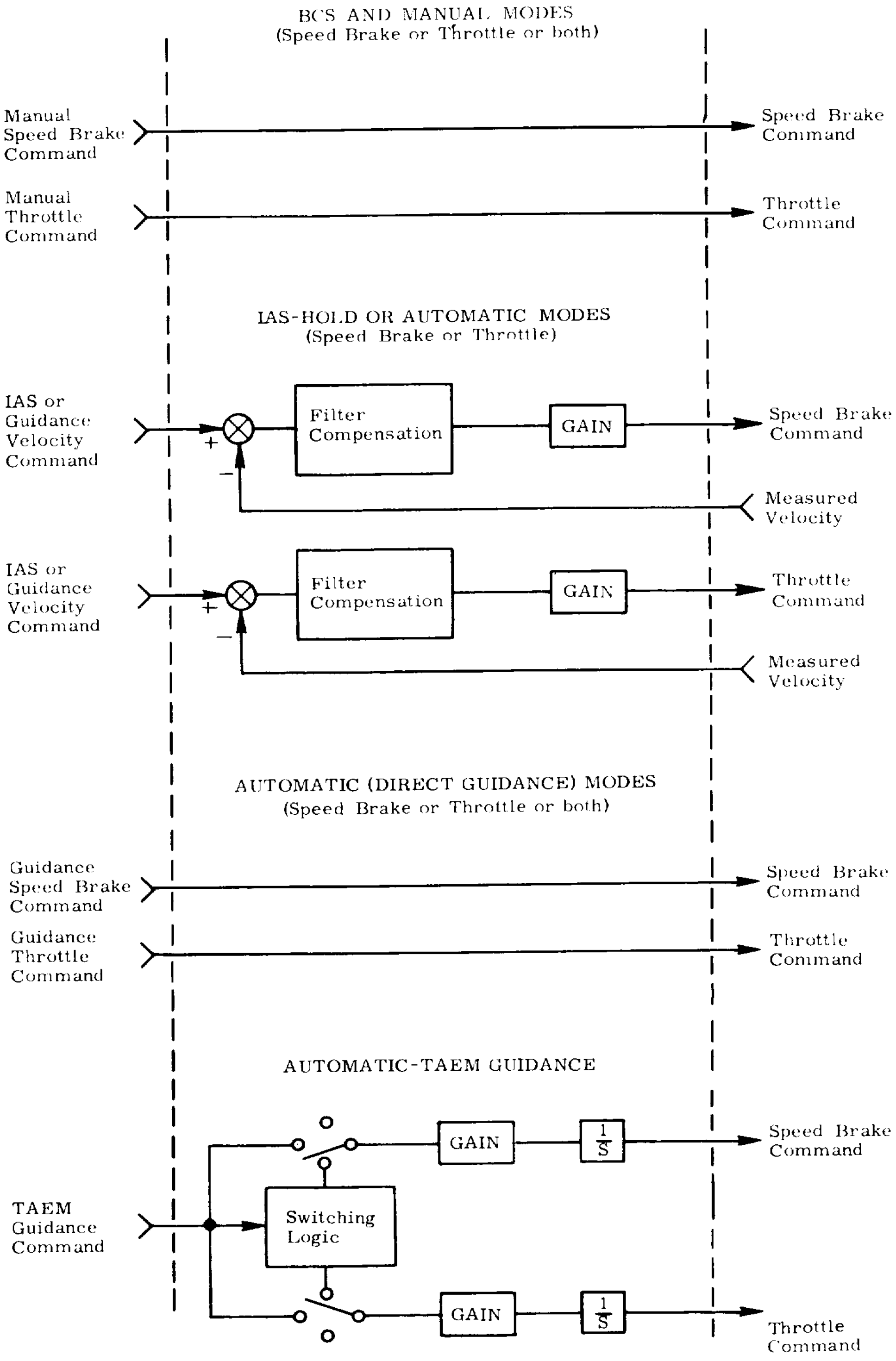

Fig. 4-5 Simplified Functional Block Diagrams - Speed Control

an indicated airspeed decrease is called for and the throttle is presently opened above its minimum, the command is issued to decrease throttle, or otherwise, the speed brake is opened. On the other hand, if an indicated airspeed increase is called for and the speed brake is presently opened above minimum, the command is issued to close the speed brake, or otherwise, the throttle is opened. These commands are scaled appropriately, integrated, and issued to the controller.

4.2.5 Body Flap

Control of the body flap, an aft pitching moment generator, is achieved via commands issued according to a piecewise linear body flap versus Mach number profile, biased with a direct pilot manual command (see Fig. 4-6). In addition, appropriate command biases are instituted to provide for full control surface deflection range.

4.2.6 Backup Control System (BCS)

The BCS mode is an autonomous, digitally implemented, multi-axis manual control capability which serves as pilot requested backup in the event of primary DFCS failure. Although the design presented here is only of a preliminary nature, it is intended to demonstrate the capabilities currently envisioned for BCS mode plus techniques for their implementation.

Whereas the primary DFCS is likely to be subject to modifications throughout the flight testing and orbital flight operations, the intent for BCS is to obtain an acceptable design prior to the first flight and to leave it unmodified thereafter. As the only BCS coding which is integrated into the primary DFCS structure is the BCS call flag from the executive routine, possibility of subsequent faulty modifications is virtually eliminated, thus providing the pilot with a continuously reliable alternative.

BCS mode is functionally similar to primary manual mode and shares the same simplified functional block diagrams (Figs. 4-1, 4-5, and 4-6). However, there are several fundamental differences which are not indicated: The axis-by-axis, multi-routine format of the primary DFCS is replaced by a single routine which processes all axes in succession; and the filter update, control and filter pushdown (wrap-up) functions are imbedded in the proper sequence. Whereas the primary system will have some gains scheduled as a function of dynamic pressure, a single set of fixed gains which provides suitable performance over as large a cruise flight spectrum as possible will be utilized for BCS. Finally, pilot signal preprocessing is not included for elevator,. aileron, and rudder, and there is no Mach number profile for body flap.

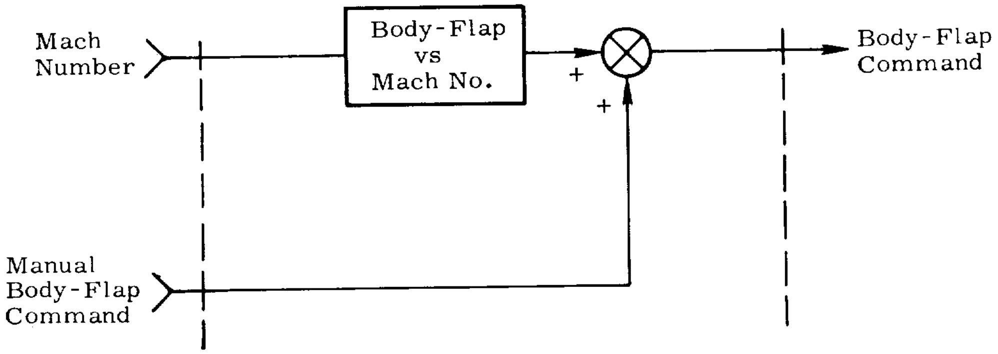

Fig. 4-6 Functional Block Diagram of Body Flap

4.2.7 Mode Selection

Mode select/indicate interfaces with the pilot are helpful in understanding the capabilities of the cruise phase DFCS, especially where manual control and a multiplicity of modes complicate the picture. Figure 4-7a is compatible with simultaneous multi-axis mode selection in contrast to axis-by-axis mode selection. Thus it is compatible with earlier versions of the cruise phase DFCS wherein axis-by-axis mode changes were not considered. Multi-axis mode selection is not unlikely for the ultimate cruise phase DFCS version, considering such things as control loop design failure modes, pilot training, and computer input/output simplifications. The gain-select switches and integrator moding select/indicators are on a separate panel. This panel might be associated with the ABES console since these capabilities are intended primarily for the flight test phases of development.

Figure 4-7b, on the other hand, suggests an axis-by-axis mode selection capability compatible with the present cruise phase DFCS design, including all peripheral moding capability. All indicated functions are implemented, except for the pilot selectable pitch turn-coordination-override capability. Gain-select switches are active only in the SAS mode. Pilot-selectable integrator-moding-override capability is provided only in the CAS mode (pitch and/or roll).

4.3 Digital Filters and Their Implementation

4.3.1 Generalized n^{th}-Order Filters

Control filters for the cruising mode are classical, recursive, n^{th}-order digital filters, whose Z transform is D(Z):

$$D(Z) = \frac{a_1 + a_2 Z^{-1} + \ldots + a_{2n} Z^{-n}}{1 + a_3 Z^{-1} + \ldots + a_{2n+1} Z^{-n}}$$

The general form of their implementation is presented in block diagram format in Fig. 4-8. The symbol x represents the controlled variable and the a's are either fixed or scheduled gains (currently fixed) which correspond to the gains of form "Gx" which appear in the flow charts and block diagrams presented later in this section.

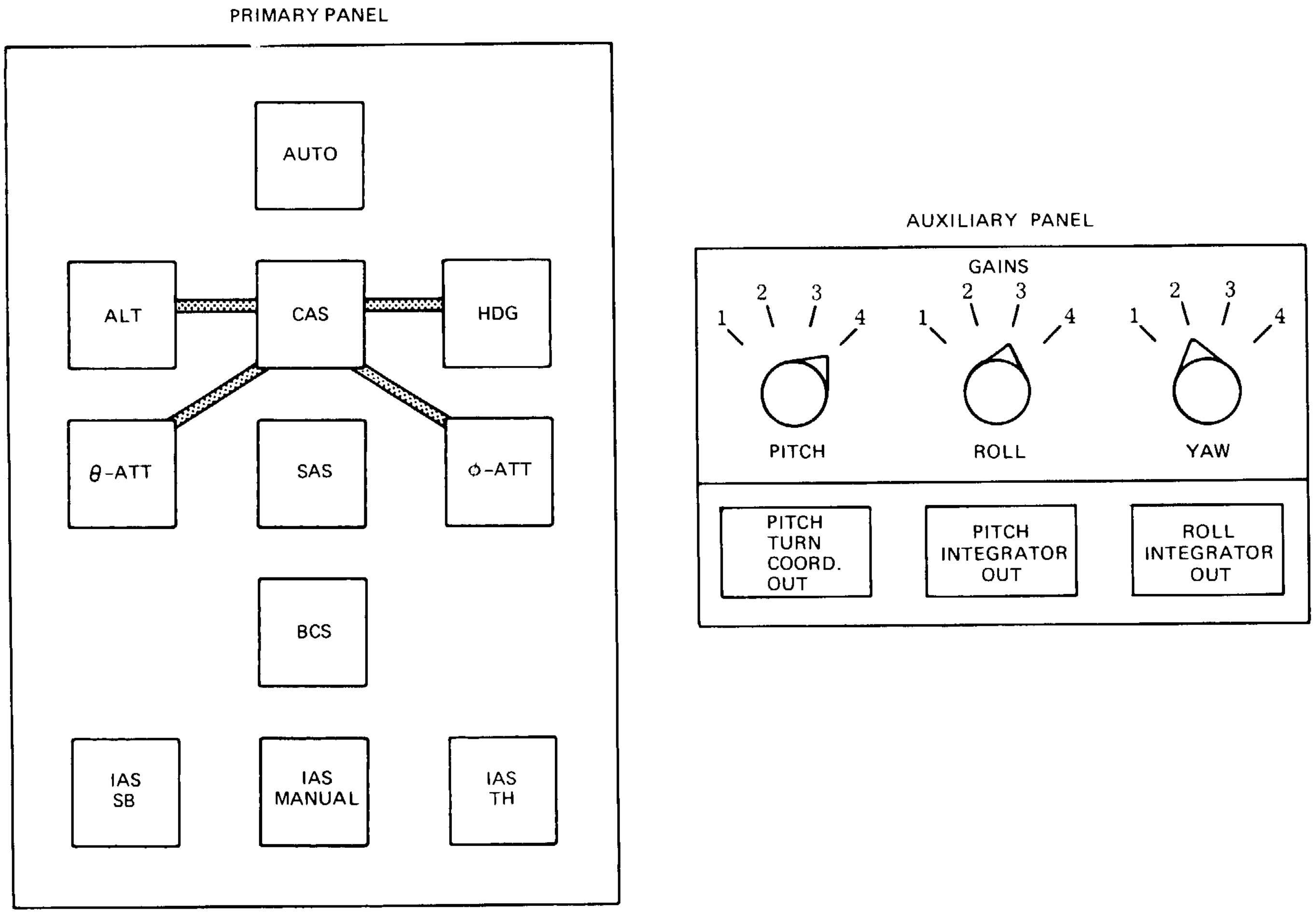

Fig. 4-7a Mode Select/Indicate Panels, Type 1, Cruise Phase DFCS

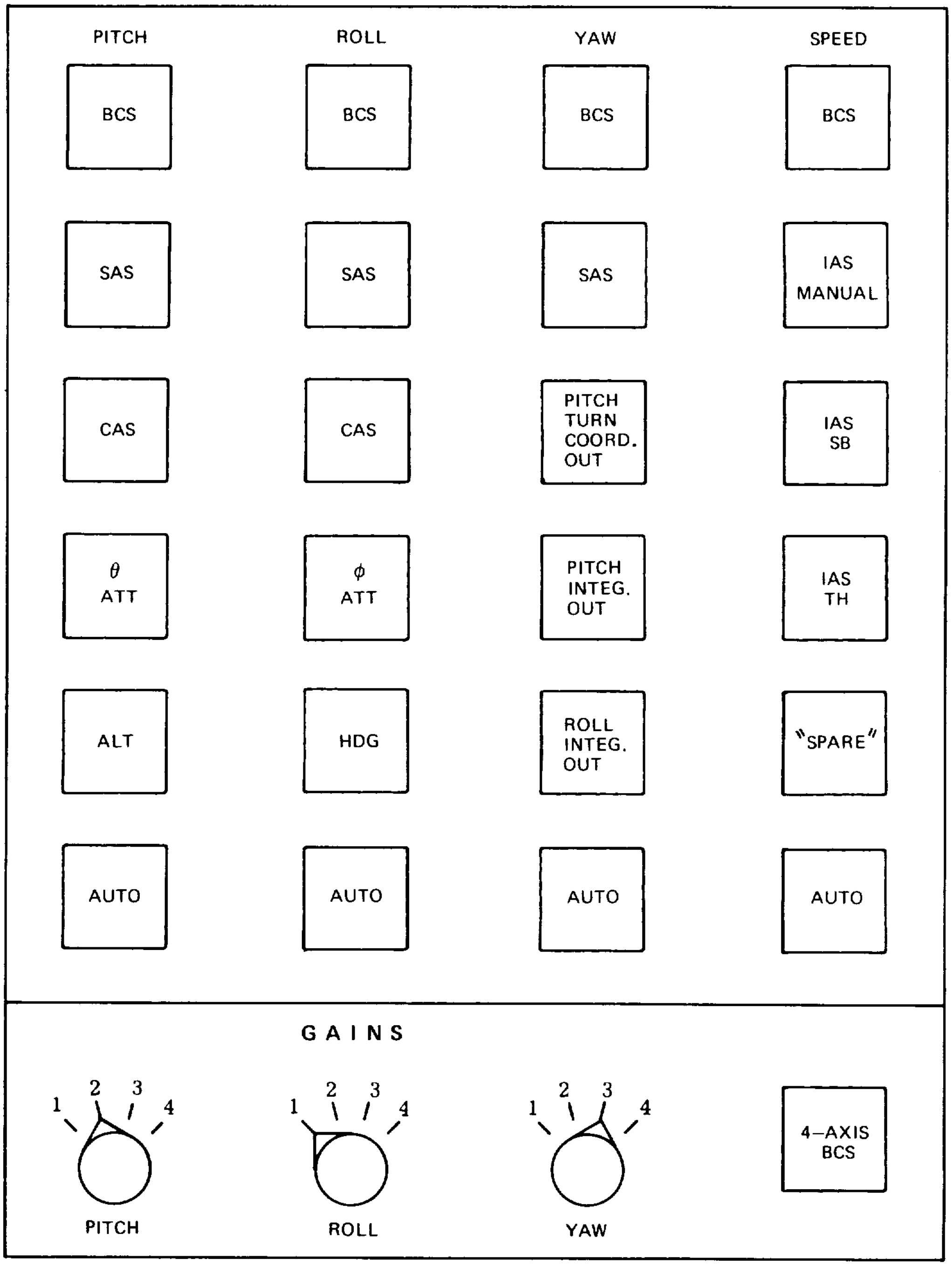

Fig. 4-7b Mode Select/Indicate Panels, Type 2 (Axis-by-Axis) Cruise Phase DFCS

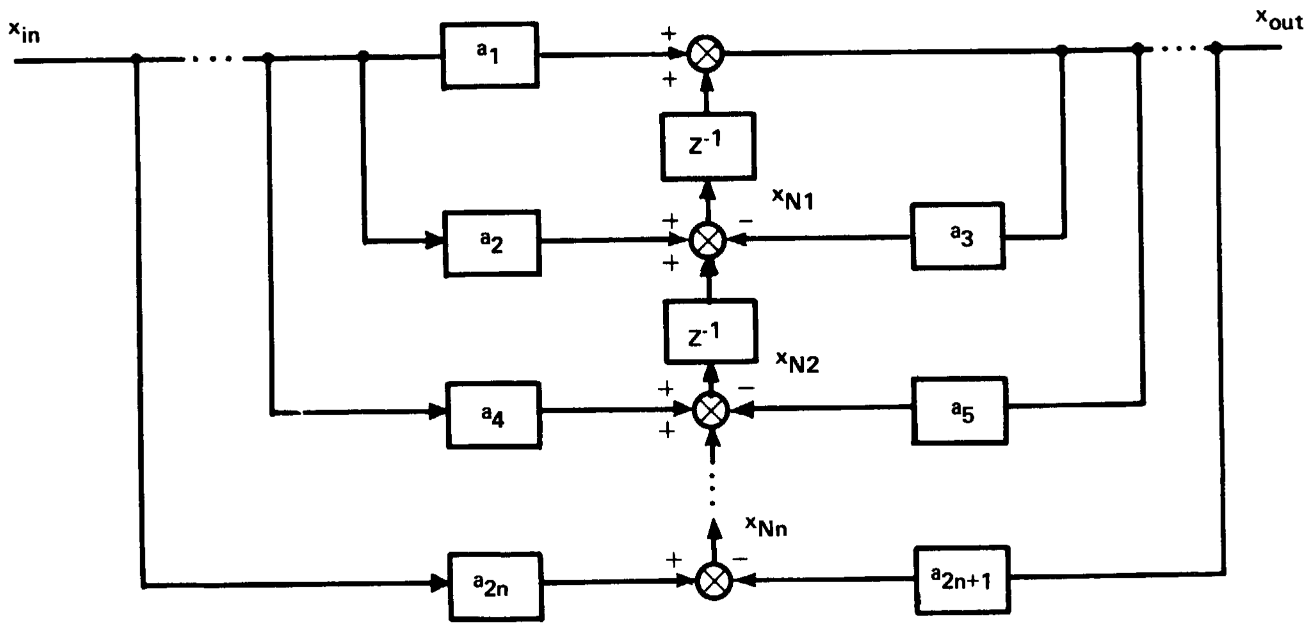

Fig. 4-8 N^{th} -Order Digital Filter

The current filter implementation provides for no greater than 2^{nd}-order filter capability, but extension to higher order filters (if needed) is straightforward. The Z^{-1} calculation blocks are achieved in the DFCS programming by the relative sequence of instructions, which permits the DFCS cycle time lag to occur at the point so designated. In the coding, each 2^{nd}-order state filter is divided into two parts in order to minimize the computational transport lag between data input and control command. The first part, which occurs in the Filter Update Routine is limited to updating the filter estimate according to the most current measurement:

$$x_{out} = a_1 x_{in} + x_{N1}$$

Where x_{Nn} represents the n^{th}-node, or summing junction, of the filter. Note that exactly n nodes are reauired to implement an n^{th}-order filter.

The Filter Update Routine is sequentially followed by the Control Routine which issues control commands based upon the most current filter output value x_{out}. Filter data "pushdown", which is actually the tabulation of the current value associated with each node, is then accomplished in the Filter Pushdown Routine by the following two equations for a 2nd-order filter:

$$x_{N1} = a_2 x_{in} - a_3 x_{out} + x_{N2}$$

$$x_{N2} = a_4 x_{in} - a_5 x_{out}$$

This sequence of instructions results in the following equivalent difference equation for the filter output:

$$x_{out} = a_1 x_{in} + a_2 x_{in_{-1}} + a_4 x_{in_{-2}} - a_3 x_{out_{-1}} - a_5 x_{out_{-2}}$$

Where subscripts -1 and -2 denote past values, one and two samples previous.

Control loops which utilize 2^{nd}-order filter capability are available for control of the following quantities:

BCS	Manual Modes	Automatic and Semi-Automatic Modes	Feedback Quantities	Others
roll rate	roll rate	roll angle	measured pitch rate	turn coordination
pitch rate	pitch rate	pitch angle	measured yaw rate	rudder crossfeed
yaw rate	yaw rate	yaw angle	measured lateral acceleration;	
		angle-of-attack	normal acceleration (with gravity)	
		sideslip angle		
		indicated air-speed		
		altitude		

4.3.2 Specialized 1^{st}-Order Filters

Recursive, 1^{st}-order washout filters are utilized in the pitch rate and yaw rate feedback paths of the primary system and in the yaw rate feedback path of BCS. The Z transform of the filter is:

$$D(Z) = \frac{1 - Z^{-1}}{1 + G_{xW} Z^{-1}}$$

A block diagram and the update and pushdown equations for the washout filter are presented below

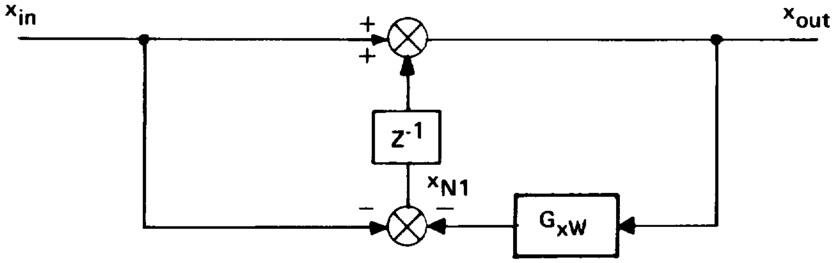

Fig. 4-9 Digital Washout Filter

Filter Update: $x_{out} = x_{in} + x_{N1}$

Filter Pushdown: $x_{N1} = -x_{in} - G_{xW} x_{out}$

Recursive, 1^{st}-order low pass filters are utilized for the filtering of the following quantities:

1) pilot stick inputs
2) crossfeeds to elevator (from speed brake, throttle, and body flap)
3) elevator trim tracker
4) yaw rate for pitch turn coordination

The Z transform of the low pass filter is

$$D(Z) = \frac{1 + G_x}{1 + G_x Z^{-1}}$$

and the block diagram and update and pushdown equations are presented below

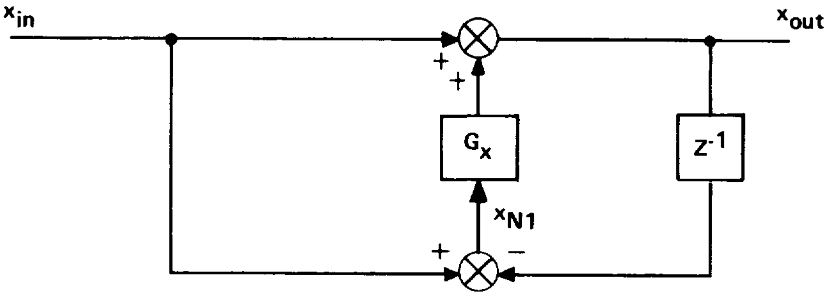

Fig. 4-10 Digital Low Pass Filter

Filter Update: $x_{out} = x_{in} + G_x \, x_{N1}$

Filter Pushdown: $x_{N1} = -x_{out} + x_{in}$

4.3.3 Integrators

Integration is achieved by both trapezoidal and rectangular integrators. Trapezoidal integrators are employed for the integral bypass functions in the elevator and aileron loops, while rectangular integrators are utilized for functions in which trapezoidal integration proves to be of no additional advantage. Thus, rectangular integrators are utilized for the integration of pilot trim discretes (elevator, aileron, and rudder in primary system and BCS) and for the integration of TAEM guidance rate commands (speed brake and throttle). The Z transforms of these integrators are

Rectangular: $D(Z) = \dfrac{T_F}{1-Z^{-1}}$ Trapezoidal: $D(Z) = \dfrac{T_F}{2} \; \dfrac{1+Z^{-1}}{1-Z^{-1}}$

and the block diagrams and update and pushdown equations are as follows:

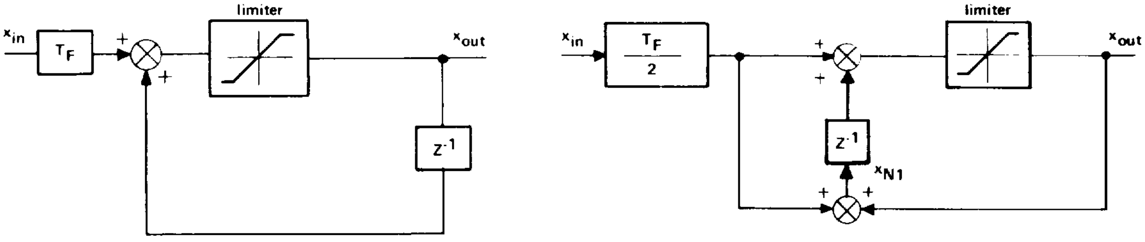

Rectangular Integrator Trapezoidal Integrator

Fig. 4-11 Digital Integrator Filters
Rectangular Integrator Trapezoidal Integrator

	Rectangular	Trapezoidal
Filter Update:	$x_{out} = x_{out} + T_F \, x_{in}$	$x_{out} = \frac{T_F}{2} x_{in} + x_{N1}$
Filter Pushdown:	none	$x_{N1} = \frac{T_F}{2} x_{in} + x_{out}$

Note from the block diagrams that the output of the integrators is limited; in practice this occurs in the filter update routine. Also notice that rectangular integration requires no pushdown equation, thus substantiating its use whenever possible.

4.4 Preflight Parameter Specifications

Basic parameters for the cruise phase DFCS include filter coefficients, gains, limits, deadbands, logic-control flags, etc. Each of these basic parameters must be numerically specified prior to the cruise phase initialization pass. A representative preflight parameter specification is presented alphabetically: Table 4-1a for non-subscripted parameters and Table 4-1b for subscripted parameters. All numerical data is based upon a single-point design at Mach 0.6 and 300 psf (about 6000 feet) utilizing aerodynamic data for the February 1973 AERO16 version of the 89B orbiter. The RCAH version of the CAS elevator mode is indicated (ICSTAR = 0); the rudder sideslip feedback option is chosen (IBFDBK = 1); pitch turn coordination is bypassed (IQTRN = 1).

Most of the basic parameters are utilized directly, but a number of "working" quantities are employed, such as sample-interval-multiplied trim rates or α-guidance values of CAS filter coefficients, limits and loop gains. These are computed on the initialization first pass (Fig. 4-24) or upon mode initialization as required (Fig. 4-25 through 4-28).

Earlier orbiter cruise phase DFCS designs have utilized scheduled gains and coefficients to provide desirable response characteristics over the cruise phase flight envelope (including Powered Horizontal Flight). The scheduling parameter has been dynamic pressure. The scheduling operations (when enabled) are carried out every slow pass by the Parameter Estimation Routine (Fig. 4-12), which operates on preflight-specified tables of parameter value vs dynamic pressure. Typically seven data points are used: 100, 150, 225, 300, 425, 525, and 650 psf. The thirteen parameters corresponding to the scheduled quantities of earlier designs are identified by asterisks in Table 4-1. Tabular specifications for these gains and coefficients will be added to the preflight parameter specification tables, as they become available.

4.5 Input/Output Summaries

Figures 4-13a through 4-13e detail those quantities which are input to and output by the five basic control channels (speed, elevator and body flap, aileron, rudder and BCS). Input includes information transferred across the various interface boundaries – executive, guidance, and pilot, as well as miscellaneous moding information, crossfeeds from other loops, and sensor measurements. Output contains control effector commands, pertinent mode status for display, and crossfeeds to other loops.

Table 4-1a Preflight Parameter Specifications for the Cruise Phase

(Non-subscripted Parameters)

AINTMX	.2400	ETMN	-.1745	GESB	0.
CCAMN	-.0873	ETMX	.0654	GET	0.
CCAMX	.3491	* GAINT	.707	GETB	0.
CCCMN	-.0873	* GAP	.288	GETF	-.9900
CCCMX	.3491	GAPMB	.288	GEX	.2327
DACMX	.4800	GAX	.2400	GEXB	.2327
DECMN	-.6981	GAXB	.2400	GFX	.7679
DECMX	.2618	GCFOM	12.422	GFXB	.7679
DECMN	-.3840	GCH	.3	* GPHPS	4.
DECMNB	-.3840	* GCTH	1.4	* GPPH	1.19
DRCMX	.2618	GCX	-.1163	GPX	.1745
DSCMN	-.3072	GDEC	-.9048	GOW	-.9802
DSCMNB	-.3072	GDSC	-.3679	GRAY	0.
DSCMX	1.2217	GDTC	-.9753	* GRB	.314
DSDMX	.1257	* GECA	-.5	GRCPH	0.
DTCMN	500	* GECC	-1.	GRDAC	0.
DTCMNB	500	GEE	0.	GRDACB	0.
DTCMX	18000.	GEEB	0.	GRM	-.9802
DTDMX	8750.	* GEINTA	.4	GRRF	0.
DTDMXB	8750.	* GEINTC	.707	* GRRWA	1.19
EINTMN	-.3491	* GEOMA	.2	GRRWB	1.19
EINTMX	.1309	GEOMB	1.	GRW	-.9802
ETDB	.0087	* GEOMC	0.	GRWB	-.9802
ETDMX	.0174	GES	0.	GRXAD1	.2096

*Scheduled Gains

Table 4-1a Preflight Parameter specifications for the Cruise Phase (Cont)

(Non-subscripted Parameters)

GRXB	.2094	ICSTAR	0	XEMX	.5406
GRXSAS	.2094	IPHRC	1	XETMN	-0.75
GSDDG	1.	IOTRM	1	XETMNB	-0.75
GSU	1.	IRWP	1	XETMX	0.75
GSX	2.0385	PCMX	.3491	XETMXB	0.75
GSXB	2.0385	PHCMX	.5236	XETR	0.075
GTDDG	152.25	PMDIS	.0873	XETRB	0.3
GTU	8.3X10000	QCTMX	.0367	XFMMN	0.
GTX	35000	TFB	.1	XFMMNB	0.
GTXB	35000	XAB	0.	XRB	0.
GXA	-.6065	XADB	.02	XRDB	.02
GXAX	1.	XADMX	.5	XRDMX	.25
GXE	-.6065	XAMDIS	.05	XRMX	1.
GXEX	2.	XAMX	1.	XRTMX	.3125
GXR	-.6065	XATMX	.5	XRTMXB	.3125
GXRX	.25	XATMXB	.5	XRTR	.0156
GXSX	.25	XATR	.05	XRTRB	.0625
GXSXB	.25	XATRB	.2	XSMDIS	.1
GXTX	.5	XEB	0.	XSEMT	0.
GXTXB	.5	XEDB	.02	XTMDIS	.1
IAHFS	1	XEDMX	.3	XT[illegible]	0.
IANGRV	3	XEMDIS	.05		
IBFDBK	1	XEMN	-1		

*Scheduled Gains

Table 4-1b Preflight Parameter Specifications for the Cruise Phase (Cont)

(Subscripted Parameters)

```
DFCMCH(I,J) (-.2094, .1), (-.2094, .2), (-.2094, .5),
              (-.0873, .52), (-.0873, 6), (.1745, 8), (.1745, 9)
GAN(I)    1., 0., 0., 0., 0.
GAPMS(I) .144,.2304,.288,.3456
GAYM(I)   1., 0., 0., 0., 0.
GBF(I)    1., 0., 0., 0., 0.
GCEA(I)   1., 0., 0., 0., 0.
GCEC(I)   1., 0., 0., 0., 0.
GDAC(I)   1., 0., 0., 0., 0.
GEOMS(I) .5, .8, 1., 1.2
GHF(I)    1., -.9905, .01, 0., 0.
GPF(I)    1., 0., 0., 0., 0.
GPHF(I)   1., 0., 0., 0., 0.
GPHT(I)  .1, 0., -.999, 0., 0.
GPM(I)    1., 0., 0., 0., 0.
GPMB(I)   1., 0., 0., 0., 0.
GPSF(I)   1., 0., 0., 0., 0.
GQM(I)    1., 0., 0., 0., 0.
GQMB(I)   1., 0., 0., 0., 0.
GRF(I)    1., 0., 0., 0., 0.
GRFB(I)   1., 0., 0., 0., 0.
GRRWS(I) .595, .952, 1.19, 1.428
GSUF(I)   1., -.92, -1., 0., 0.
GTHF(I)   1., 0., 0., 0., 0.
GTUF(I)   1., -1.9713, -1.905, .9716, .9048
```

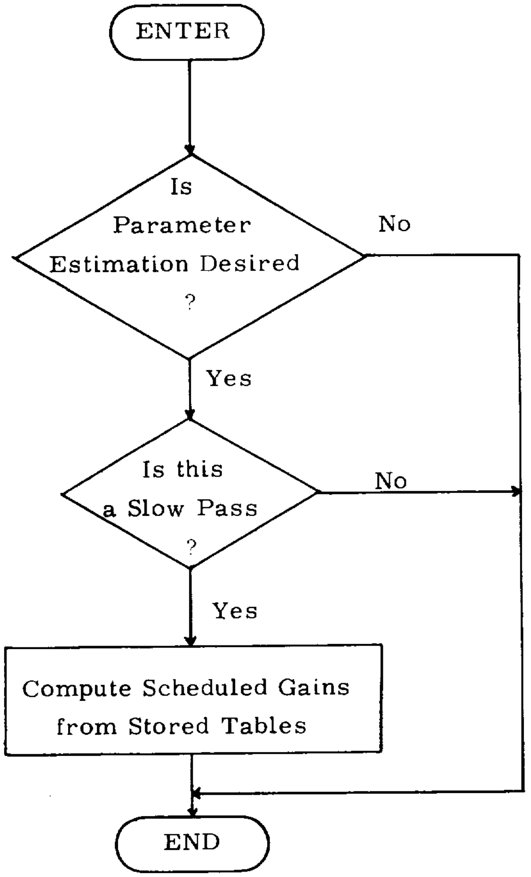
ENTER
Is Parameter Estimation Desired ?
No
Yes
Is this a Slow Pass ?
No
Yes
Compute Scheduled Gains from Stored Tables
END

Fig. 4-12 Parameter Estimation Routine for Cruise Phase

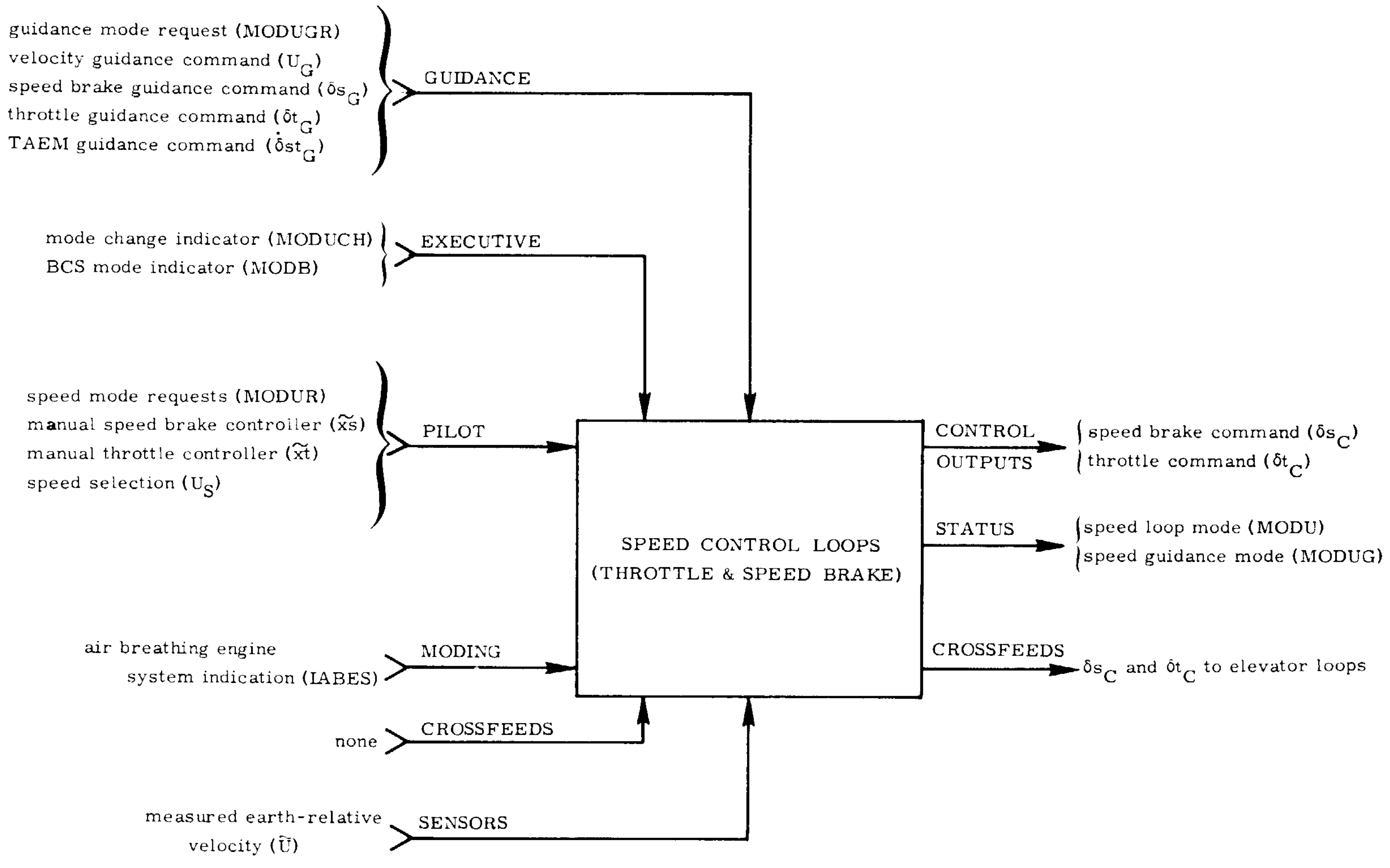
guidance mode request (MODUGR)
velocity guidance command (U_G)
speed brake guidance command (δs_G)
throttle guidance command (δt_G)
TAEM guidance command ($\dot{\delta} st_G$)
GUIDANCE
mode change indicator (MODUCH)
BCS mode indicator (MODB)
EXECUTIVE
speed mode requests (MODUR)
manual speed brake controller ($\widetilde{xs}$)
manual throttle controller ($\widetilde{xt}$)
speed selection (U_S)
PILOT
air breathing engine system indication (IABES)
MODING
none
CROSSFEEDS
measured earth-relative velocity ($\tilde{U}$)
SENSORS
SPEED CONTROL LOOPS (THROTTLE & SPEED BRAKE)
CONTROL OUTPUTS
speed brake command (δs_C)
throttle command (δt_C)
STATUS
speed loop mode (MODU)
speed guidance mode (MODUG)
CROSSFEEDS
δs_C and δt_C to elevator loops

Fig. 4-13a Speed Control Input/Output Interface Variables

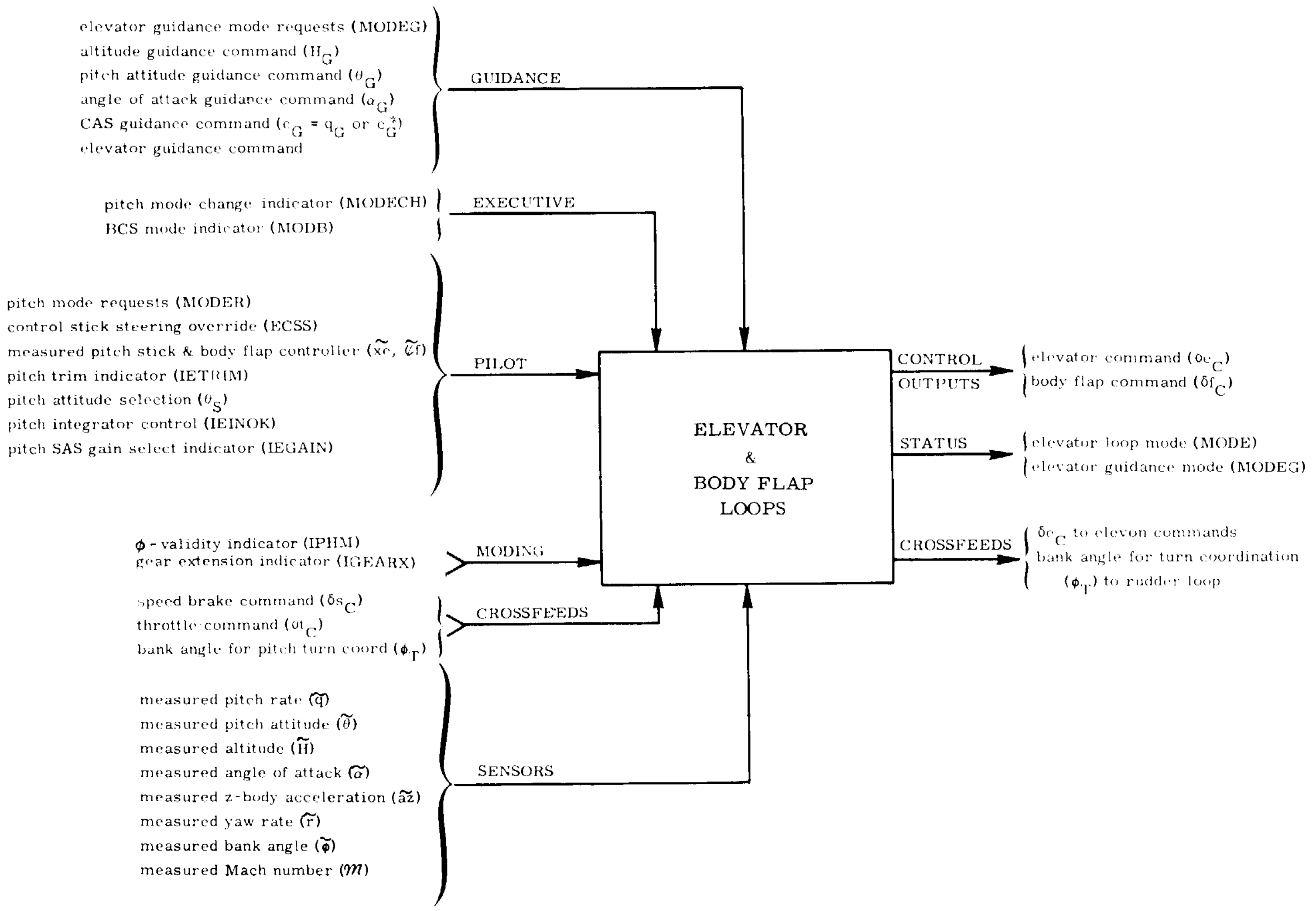
elevator guidance mode requests (MODEG)
altitude guidance command (H_G)
pitch attitude guidance command (θ_G)
angle of attack guidance command (α_G)
CAS guidance command ($c_G = q_G$ or c_G^*)
elevator guidance command
GUIDANCE
pitch mode change indicator (MODECH)
BCS mode indicator (MODB)
EXECUTIVE
pitch mode requests (MODER)
control stick steering override (ECSS)
measured pitch stick & body flap controller ($\tilde{xe}$, $\tilde{\mathcal{C}f}$)
pitch trim indicator (IETRIM)
pitch attitude selection (θ_S)
pitch integrator control (IEINOK)
pitch SAS gain select indicator (IEGAIN)
PILOT
ϕ - validity indicator (IPHM)
gear extension indicator (IGEARX)
MODING
speed brake command (δs_C)
throttle command (υt_C)
bank angle for pitch turn coord (ϕ_T)
CROSSFEEDS
measured pitch rate ($\tilde{q}$)
measured pitch attitude ($\tilde{\theta}$)
measured altitude ($\tilde{H}$)
measured angle of attack ($\tilde{\alpha}$)
measured z-body acceleration ($\tilde{az}$)
measured yaw rate ($\tilde{r}$)
measured bank angle ($\tilde{\phi}$)
measured Mach number ($\mathcal{M}$)
SENSORS
ELEVATOR & BODY FLAP LOOPS
CONTROL OUTPUTS
elevator command (δe_C)
body flap command (δf_C)
STATUS
elevator loop mode (MODE)
elevator guidance mode (MODEG)
CROSSFEEDS
δe_C to elevon commands
bank angle for turn coordination (ϕ_T) to rudder loop

Fig. 4-13b Elevator and Flap Input/Output Interface Variables

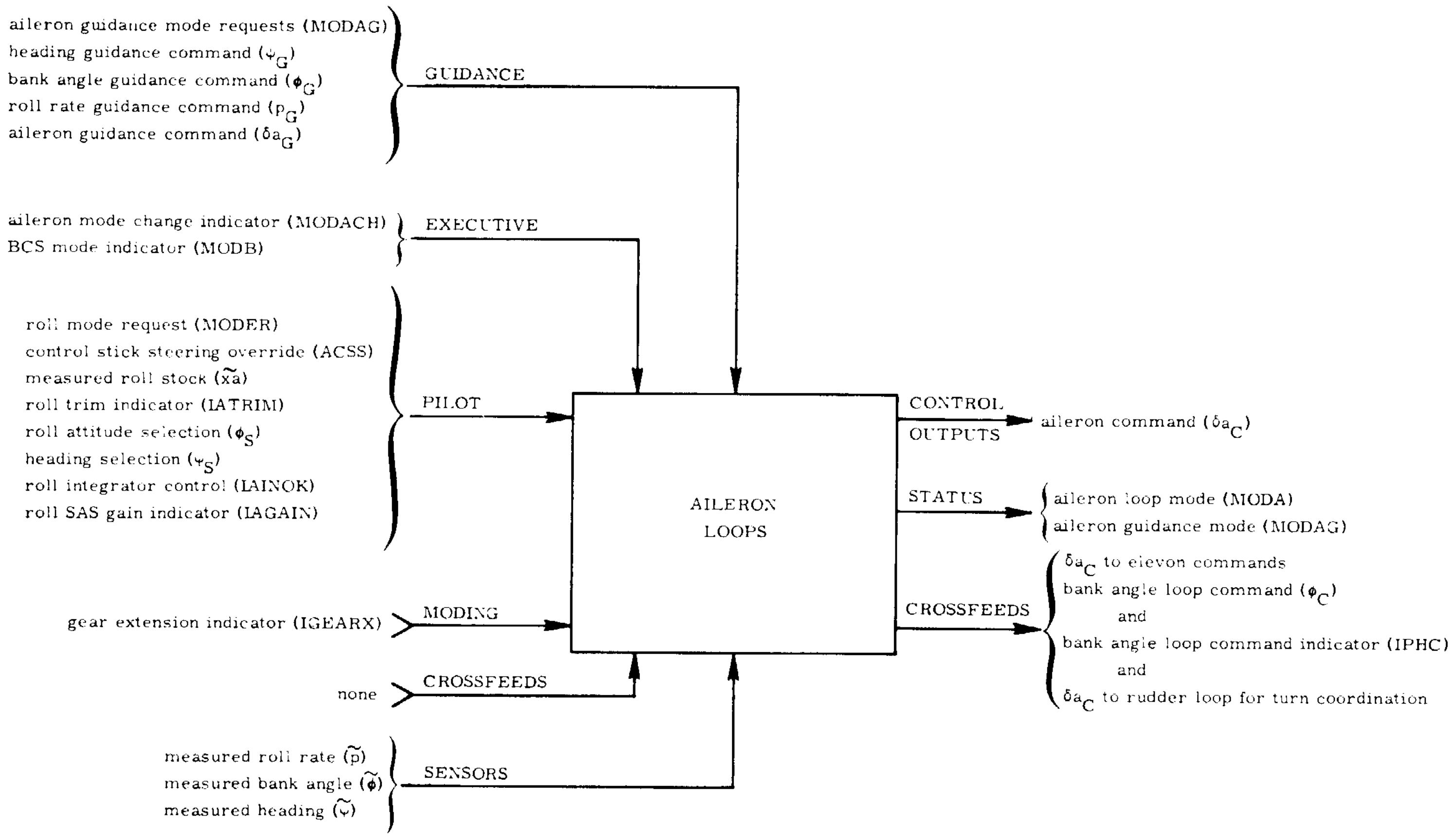
aileron guidance mode requests (MODAG)
heading guidance command (ψ_G)
bank angle guidance command (ϕ_G)
roll rate guidance command (p_G)
aileron guidance command (δa_G)
GUIDANCE
aileron mode change indicator (MODACH)
BCS mode indicator (MODB)
EXECUTIVE
roll mode request (MODER)
control stick steering override (ACSS)
measured roll stock ($\tilde{xa}$)
roll trim indicator (IATRIM)
roll attitude selection (ϕ_S)
heading selection (ψ_S)
roll integrator control (IAINOK)
roll SAS gain indicator (IAGAIN)
PILOT
gear extension indicator (IGEARX)
MODING
none
CROSSFEEDS
measured roll rate ($\tilde{p}$)
measured bank angle ($\tilde{\phi}$)
measured heading ($\tilde{\psi}$)
SENSORS
AILERON LOOPS
CONTROL OUTPUTS
aileron command (δa_C)
STATUS
aileron loop mode (MODA)
aileron guidance mode (MODAG)
CROSSFEEDS
δa_C to elevon commands
bank angle loop command (ϕ_C)
and
bank angle loop command indicator (IPHC)
and
δa_C to rudder loop for turn coordination

Fig. 4-13c Aileron Input/Output Interface Variables

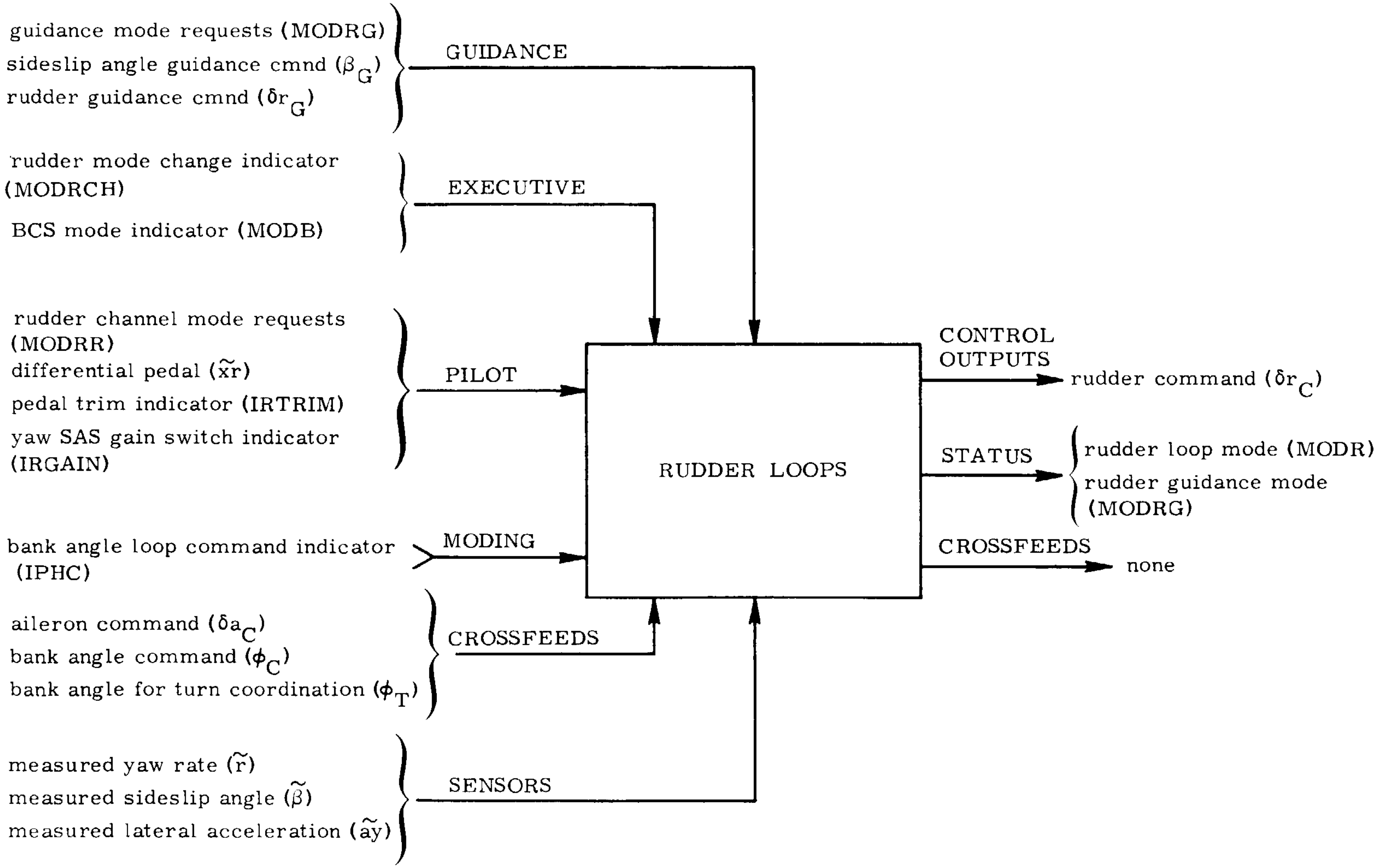
guidance mode requests (MODRG)
sideslip angle guidance cmnd (β_G)
rudder guidance cmnd (δr_G)
GUIDANCE
rudder mode change indicator (MODRCH)
BCS mode indicator (MODB)
EXECUTIVE
rudder channel mode requests (MODRR)
differential pedal ($\tilde{xr}$)
pedal trim indicator (IRTRIM)
yaw SAS gain switch indicator (IRGAIN)
PILOT
bank angle loop command indicator (IPHC)
MODING
aileron command (δa_C)
bank angle command (ϕ_C)
bank angle for turn coordination (ϕ_T)
CROSSFEEDS
measured yaw rate ($\tilde{r}$)
measured sideslip angle ($\tilde{\beta}$)
measured lateral acceleration ($\tilde{ay}$)
SENSORS
RUDDER LOOPS
CONTROL OUTPUTS
rudder command (δr_C)
STATUS
rudder loop mode (MODR)
rudder guidance mode (MODRG)
CROSSFEEDS
none

Fig. 4-13d Rudder Input/Output Interface Variables

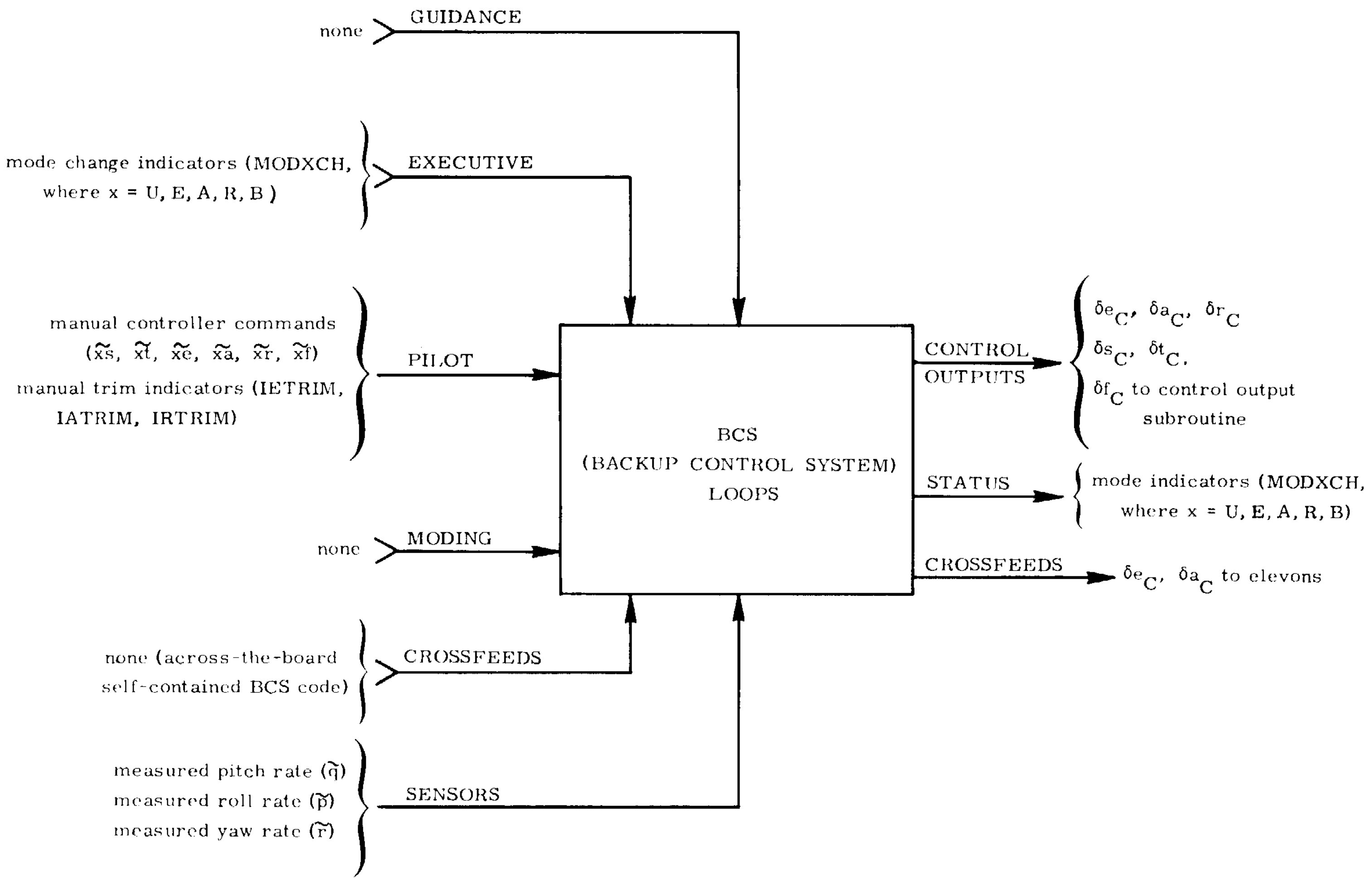
none
GUIDANCE
mode change indicators (MODXCH, where x = U, E, A, R, B)
EXECUTIVE
manual controller commands ($\tilde{\tilde{x}}s$, $\tilde{\tilde{x}}t$, $\tilde{\tilde{x}}e$, $\tilde{\tilde{x}}a$, $\tilde{\tilde{x}}r$, $\tilde{\tilde{x}}f$)
manual trim indicators (IETRIM, IATRIM, IRTRIM)
PILOT
none
MODING
none (across-the-board self-contained BCS code)
CROSSFEEDS
measured pitch rate ($\tilde{q}$)
measured roll rate ($\tilde{p}$)
measured yaw rate ($\tilde{r}$)
SENSORS
BCS
(BACKUP CONTROL SYSTEM)
LOOPS
CONTROL OUTPUTS
δe_C, δa_C, δr_C
δs_C, δt_C,
δf_C to control output subroutine
STATUS
mode indicators (MODXCH, where x = U, E, A, R, B)
CROSSFEEDS
δe_C, δa_C to elevons

Fig. 4-13e Backup Control System Input/Output Interface Variables

4.6 Functional Block Diagrams for Cruise Phase DFCS

This section presents a detailed control-engineer's description of the cruise phase DFCS, using functional block diagrams. These include all the feedbacks, crossfeeds, limiters, switches, and compensation filters currently available with preflight parameter specification options.

A number of simplifying conventions have been employed, particularly in the areas of filter and limiter descriptions. These conventions are summarized in Fig. 4-14.

Tables 4-2 through 4-4 indicate the realizable cruise phase DFCS modes of operation, and the corresponding settings of all flags. Note for example, that while MODS = 3 (speed brake using ρ u-filter for IAS-hold) and MODT = 3 (throttle using u-filter for IAS-hold) are both valid modes of operation, they must not occur simultaneously. The mode change Initialization Subroutine (Fig. 4-25 through 4-28) handles all the setting of all derived flags, according to the logic indicated in these tables.

Pilot input signal processing for speed brake throttle and flap controllers, for pitch and roll sidearm stick, and for pedals, is shown in Fig. 4-15. Pitch, roll and yaw manual trim circuits are shown in Fig. 4-16. Outer loop (semi-automatic or automatic) error signal generation is shown in Fig. 4-17. Note that the pilot "Select" option is implied (except for altitude) simply by "writing" into the appropriate storage location, e.g., H_{REF}.

Speed control, including throttle and speed brake options, is shown in Fig. 4-18a, which indicates an input from TAEM-guidance interface signal processing as shown in Fig. 4-18b. Elevator control loops are shown in Fig. 4-19. Also shown in Fig. 4-19 are the generation of ϕ_{TF} for turn coordination (pitch and yaw rate command circuits), the generation of body flap commands (manual override of a Mach profile), and an elevator trim-tracker network akin to conventional stabilizer trim-tracking. (This trim indication is being studied for trim-initialization on emergency downmodes.)

Figure 4-20 presents the aileron control loops, and Fig. 4-21 presents the rudder control loops, including provision for both β feedback and "$\dot{\beta}$" feedback (a combination of yaw rate command, yaw rate feedback without washout filtering, lateral acceleration, and aileron). Note that pedal and trim are available even in auto mode (through the gain GRXAUT) for manual decrab maneuvers.

Figure 4-22 indicates the override capability of the BCS mode, indicated by MODB = 1. Details of BCS loops (essentially the corresponding MANUAL or SAS loops with independently specified gains, coefficients, and nonlinearities) are given in Fig. 4-23.

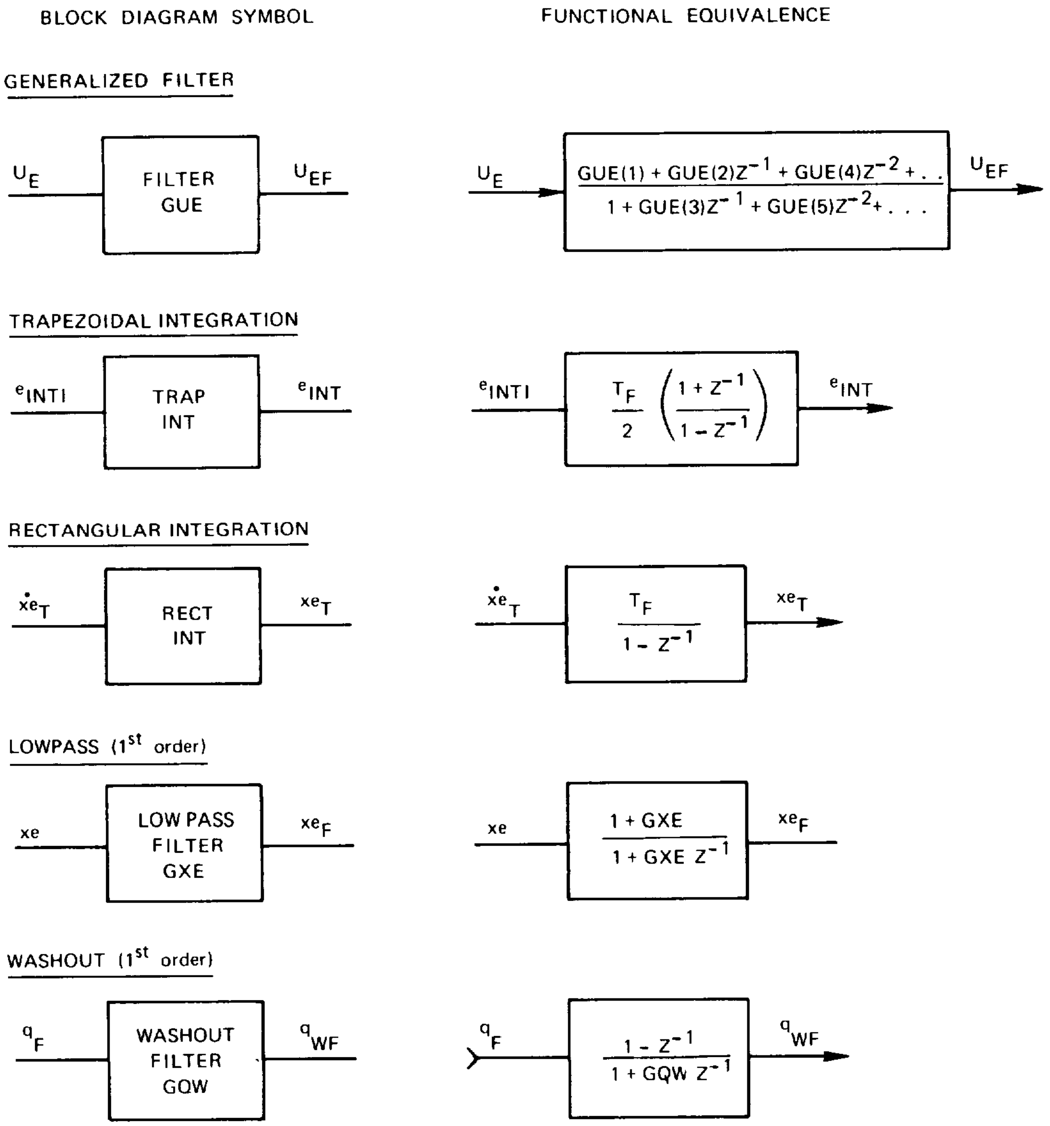

Fig. 4-14 Simplifying Conventions for Block Diagrams

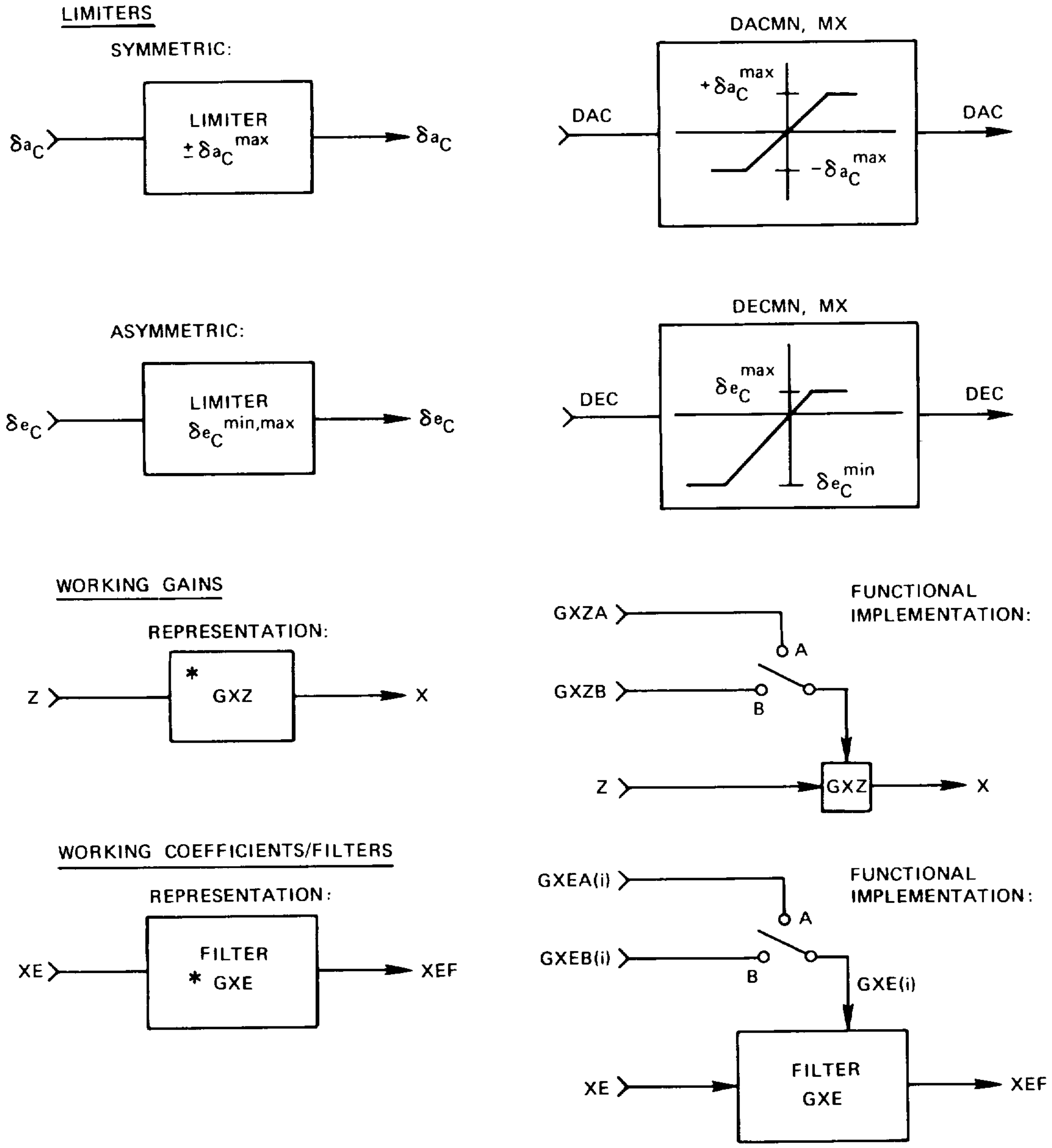

Fig. 4-14 Simplifying Conventions for Block Diagrams (Cont)

Table 4-2 Logic for Speed Control Flag Settings

	Input Flags		Derived Flags			
	MODU	MODUG	MODS	MODT	MODUFT	MODUFP
BCS, UBCS	1	X	1	0	X	X
	1	X	1	1	X	X
UMAN	2	X	2	0	0	1
(IAS - MAN)	2	X	2	2	0	1
UASB	3	X	3	0	1	2
(IAS - SB)	3	X	3	2	1	2
AUTO, UAUT	4	1	5	0	0	1
		1	5	5	0	1
		2	4	0	1	3
		2	4	2	1	3
		3	4	5	1	3
		4	2	4	2	3
		5	5	4	2	3
		6	6	0	0	4
		6	6	2	0	4
		7	6	5	0	4
		8	2	6	0	4
		9	5	6	0	4
	↓	10	6	6	0	4
UATH	5	X	2	3	2	2
(IAS - TH)						

Table 4-3: Logic for Elevator Control Flag Settings

	Input Flags		Derived Flags				
	MODE	MODEG	ICC1	ICC2	ITHC	IHC	ICF
BCS, EBCS	1	X	X	X	X	X	X
SAS, ESAS	2	X	X	X	X	X	X
CAS, ECAS	3	X	1	X	X	X	1, 2
AUTO, EAUT	4	1	4	X	X	X	1, 2
	4	2	3	1	2	X	1, 2
	4	3	5	X	X	X	3
	4	4	3	2	X	2	1, 2
EATT	5	X	2	1	1	X	1, 2
EALT	6	X	2	2	X	1	1, 2

Table 4-4 : Logic for Aileron Control Flag Settings

	Input Flags		Derived Flags		
	MODA	MODAG	IPC	IPHC	IPSC
ABCS	1	X	X	X	X
ASAS	2	X	X	X	X
ACAS	3	X	1	X	X
AUTO	4	1	4	0	X
	4	2	3	4	X
	4	3	3	3	2
AATT	5	X	2	1	X
AHDG	6	X	2	2	1

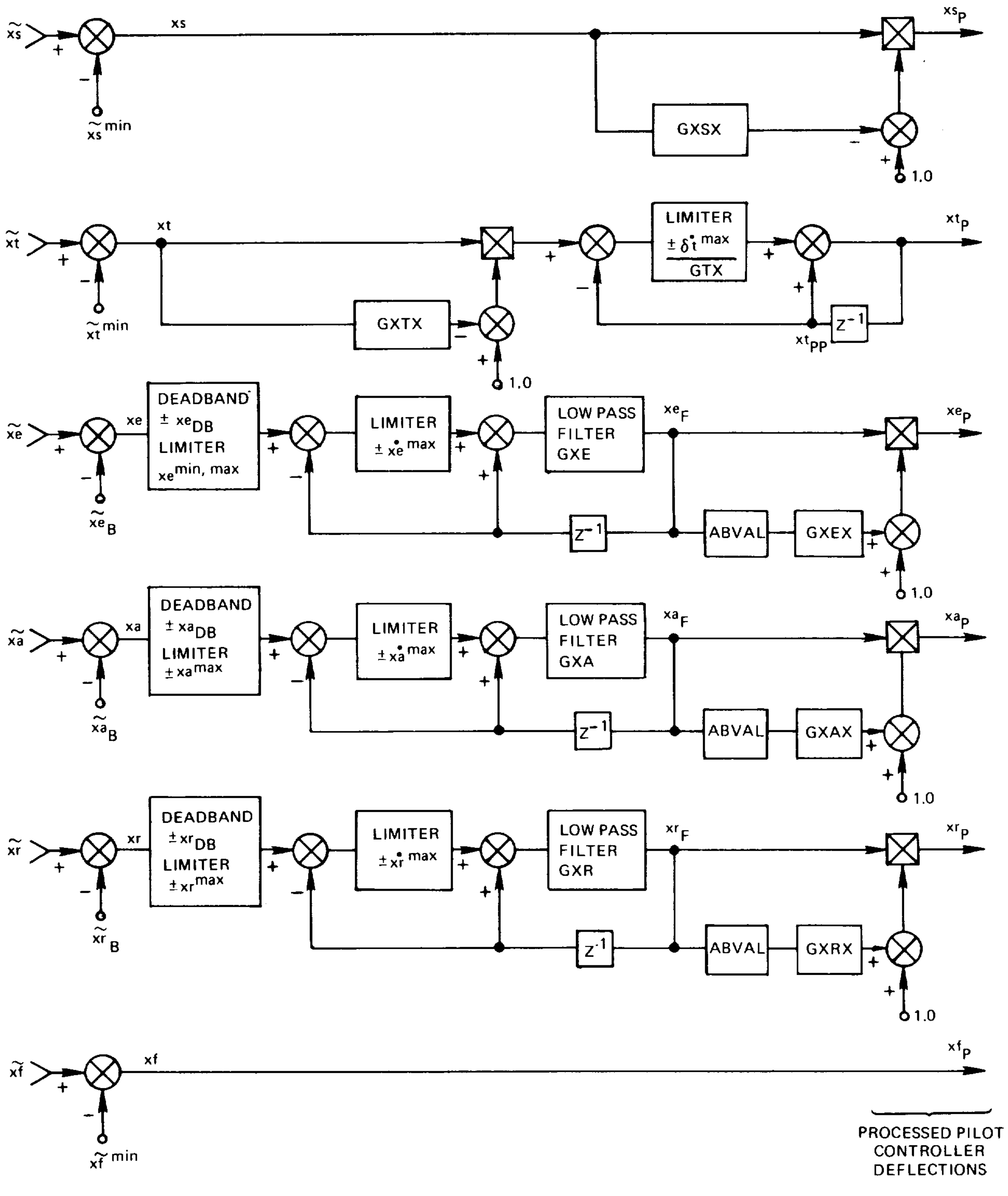

Fig. 4-15 Block Diagram, Pilot Input Signal Processing

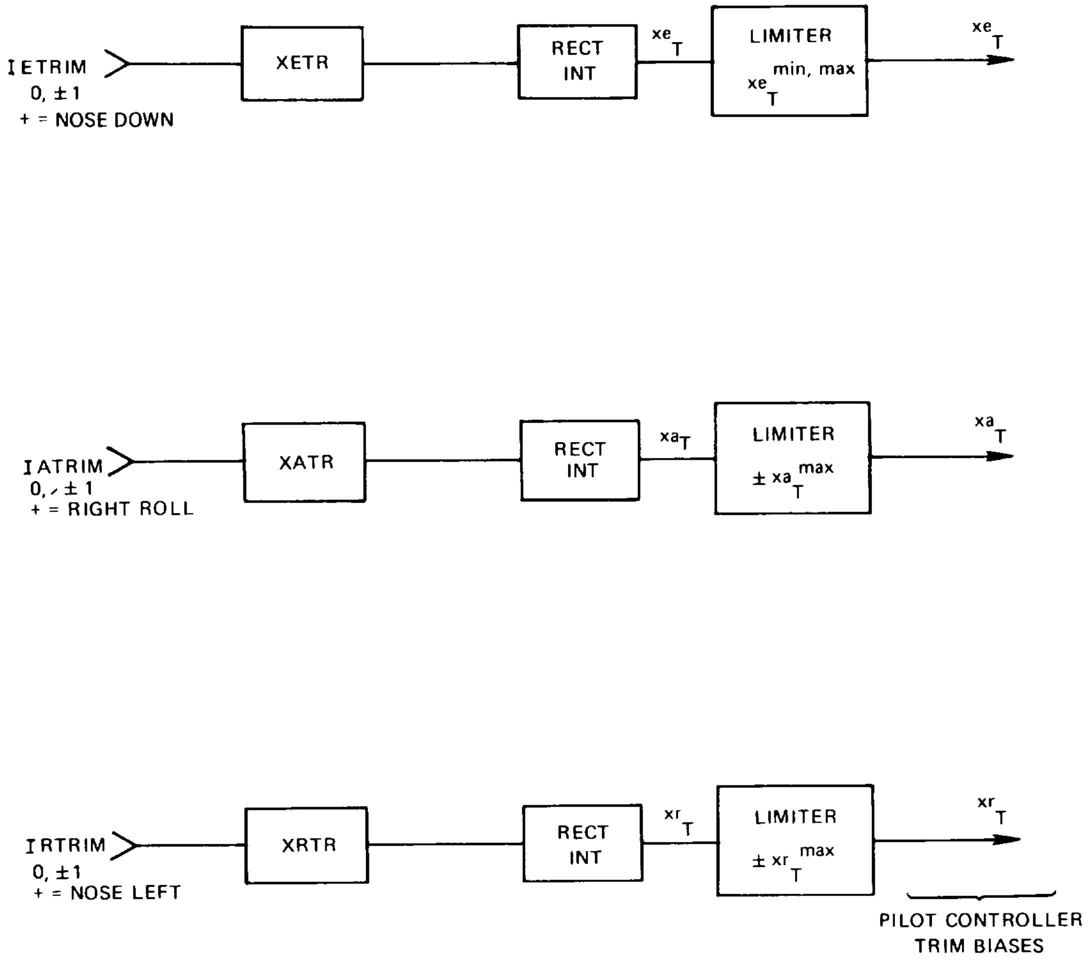

Fig. 4-16 Block Diagram, Pilot Manual Trim Circuits

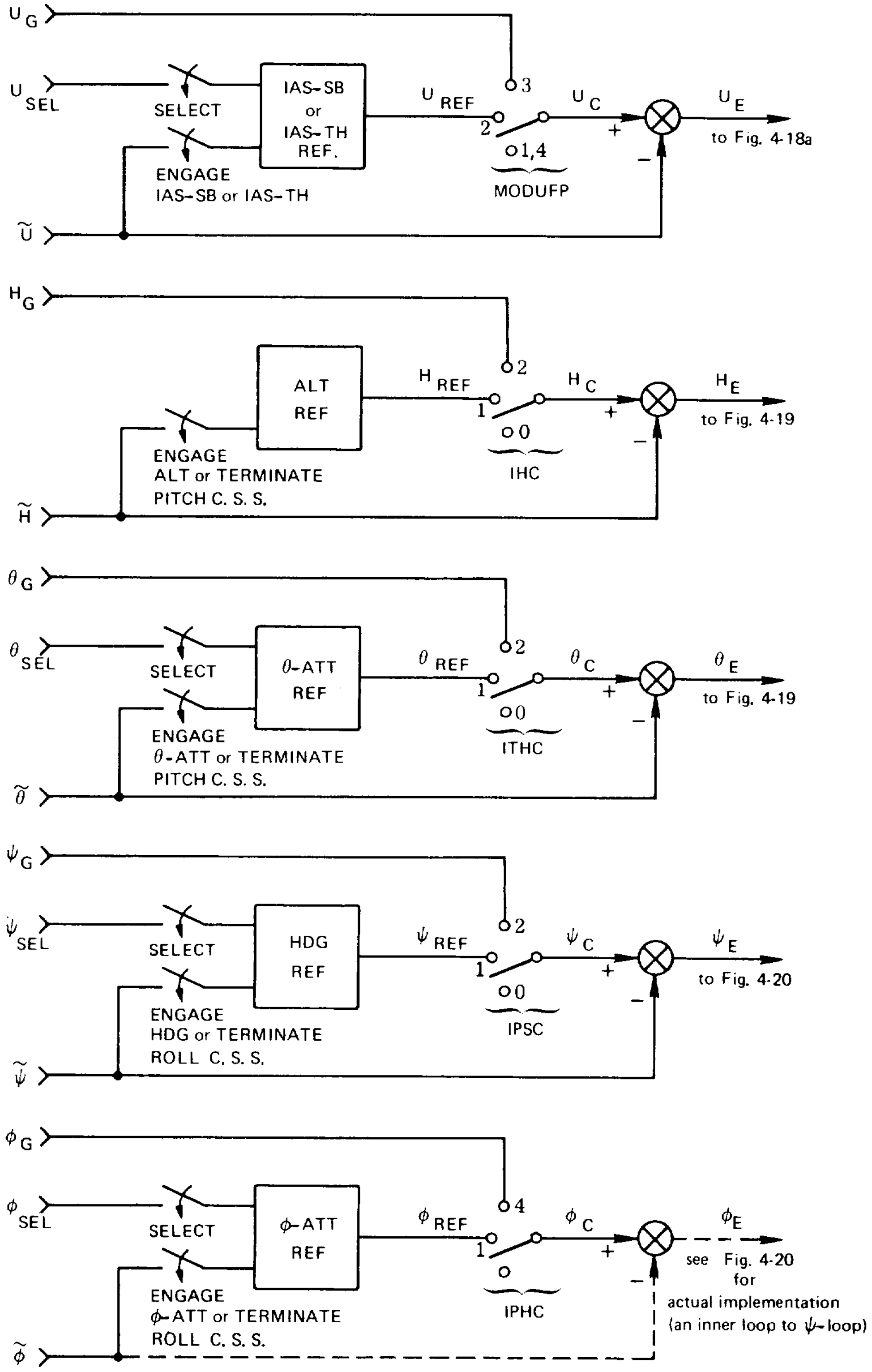

Fig. 4-17 Block Diagram, Outer Loop Error Signal Generation

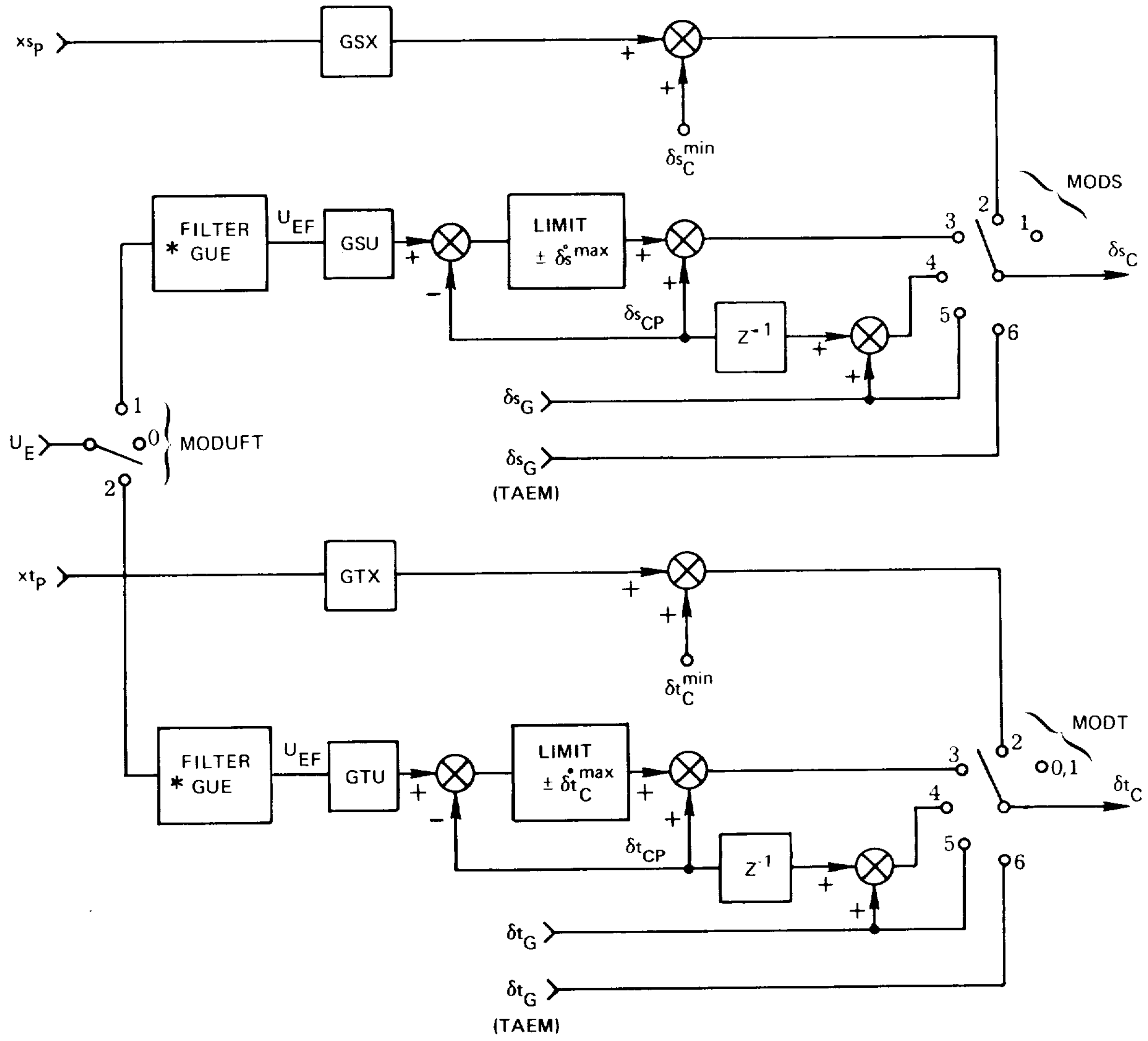

Fig. 4-18a Speed Control Loops

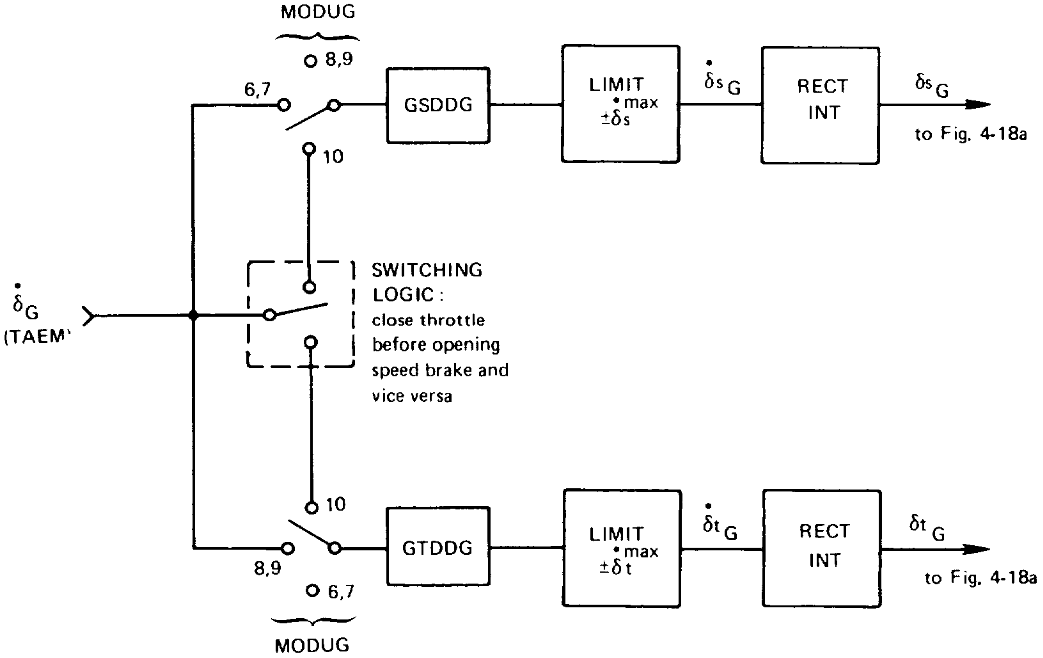

Fig. 4-18b TAEM Guidance Processing for Speed Control

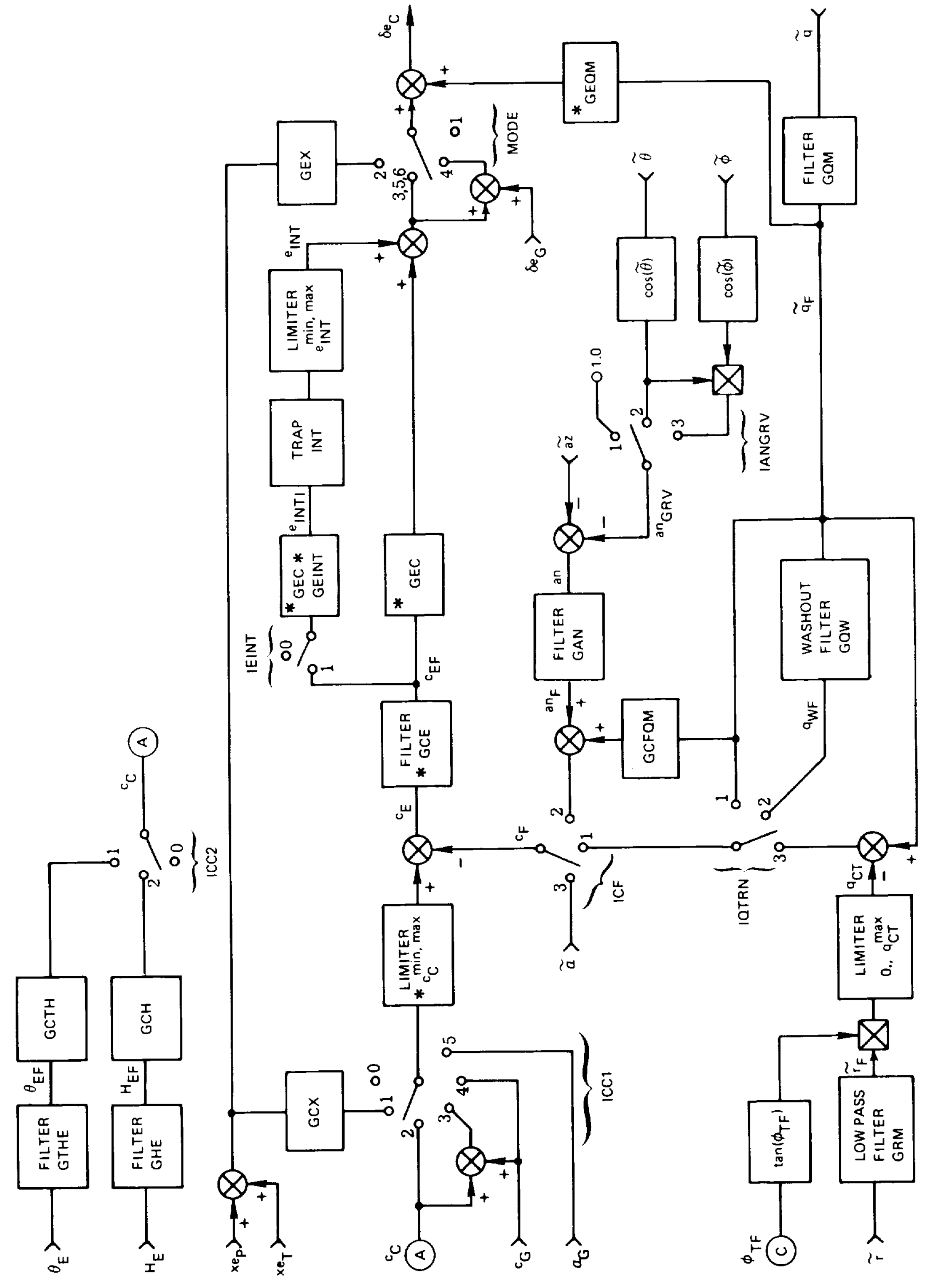

Fig. 4-19 Elevator Control Loops

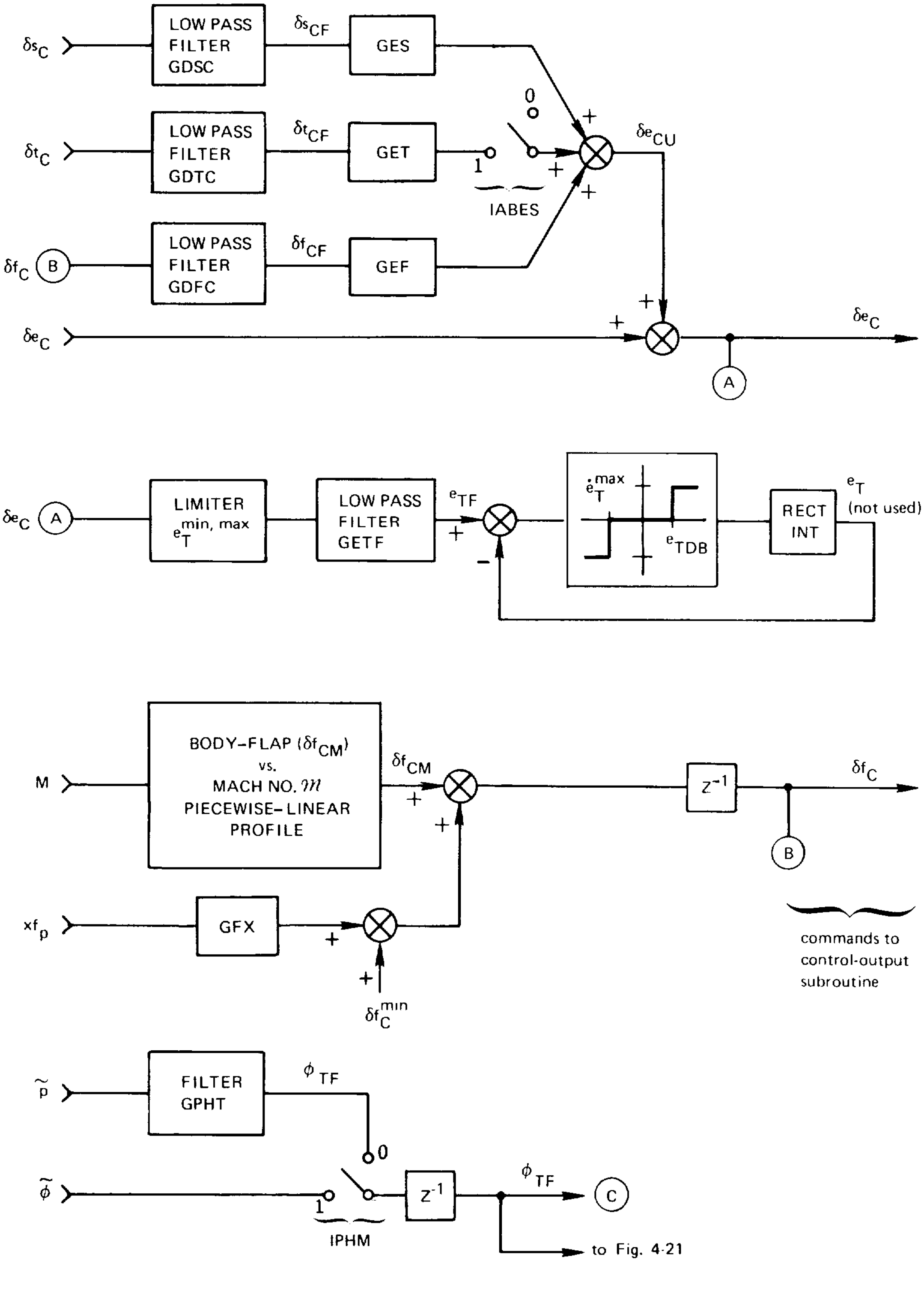

Fig. 4-19 Elevator Control Loops (Cont)

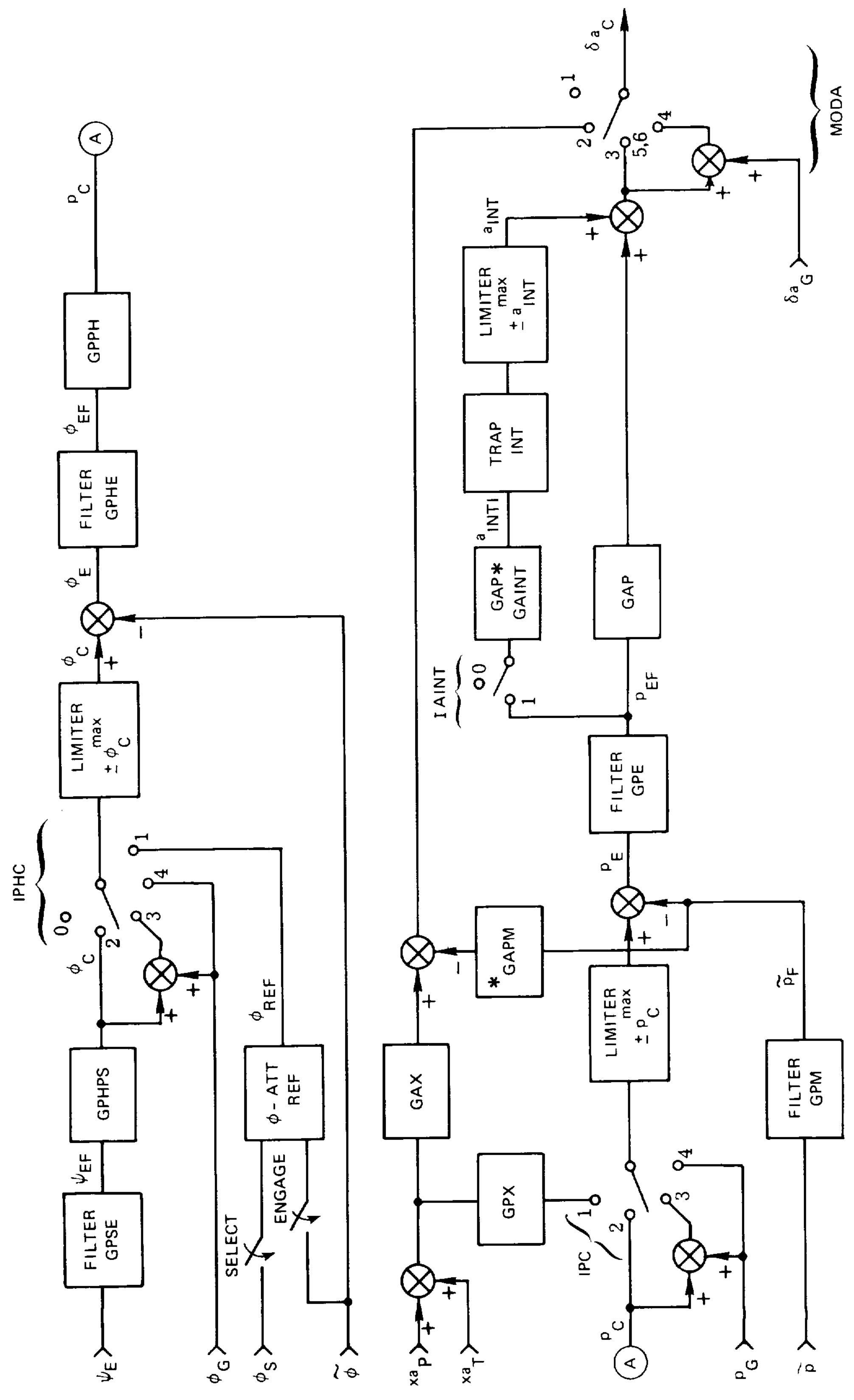

Fig. 4-20 Aileron Control Loops

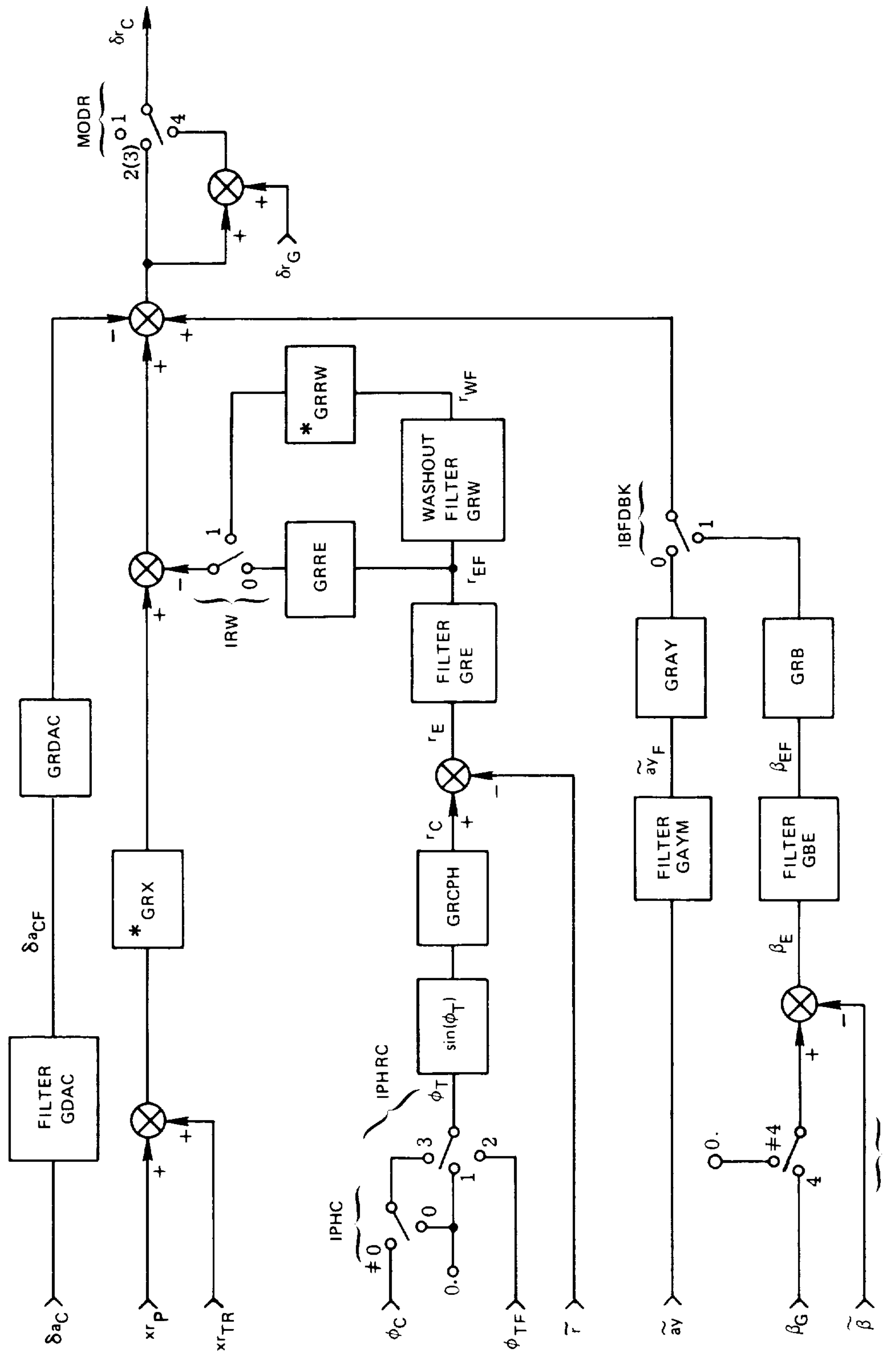

Fig. 4-21 Rudder Control Loops

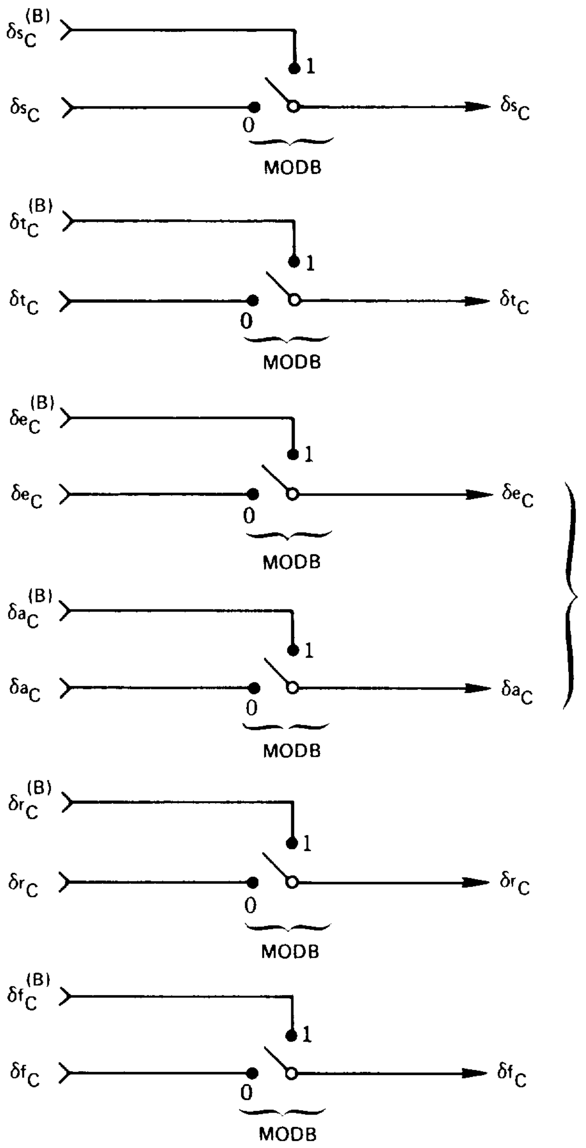

NOTE:

BCS mode selection is "across-the-board" (MODB = 1: MODX = 1 where X = U, E, A, and R) rather than axis-by-axis. BCS is activated by selecting the BCS mode in any one axis (MODXR = 1, where X = U or E or A or R) or by selecting 4-axis BCS (MODUBR = 1).

combined to generate elevon commands δEL_C and δER_C in the control output subroutine

Fig. 4-22 Control Output Signals

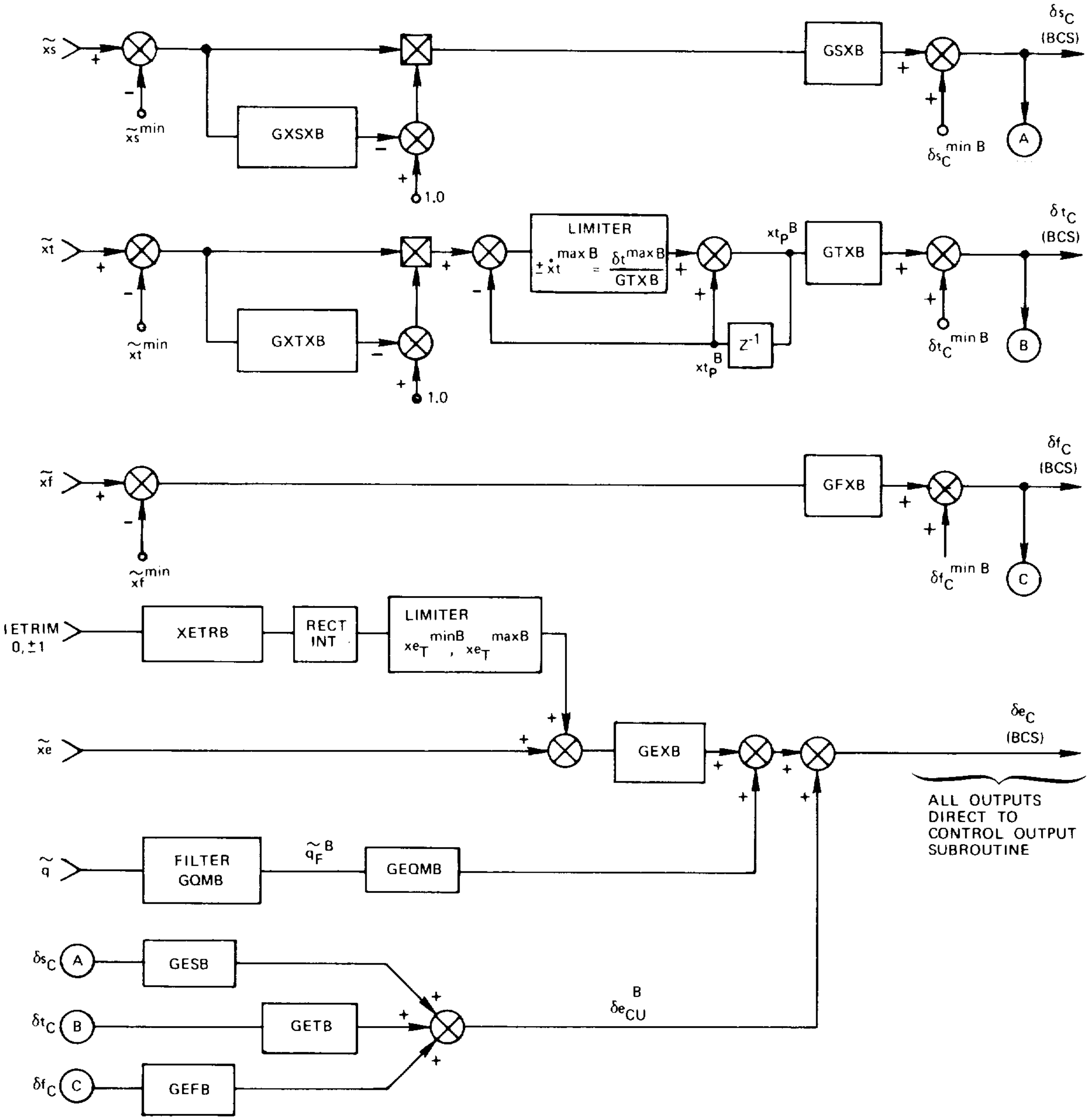

Fig. 4-23 Backup Control System

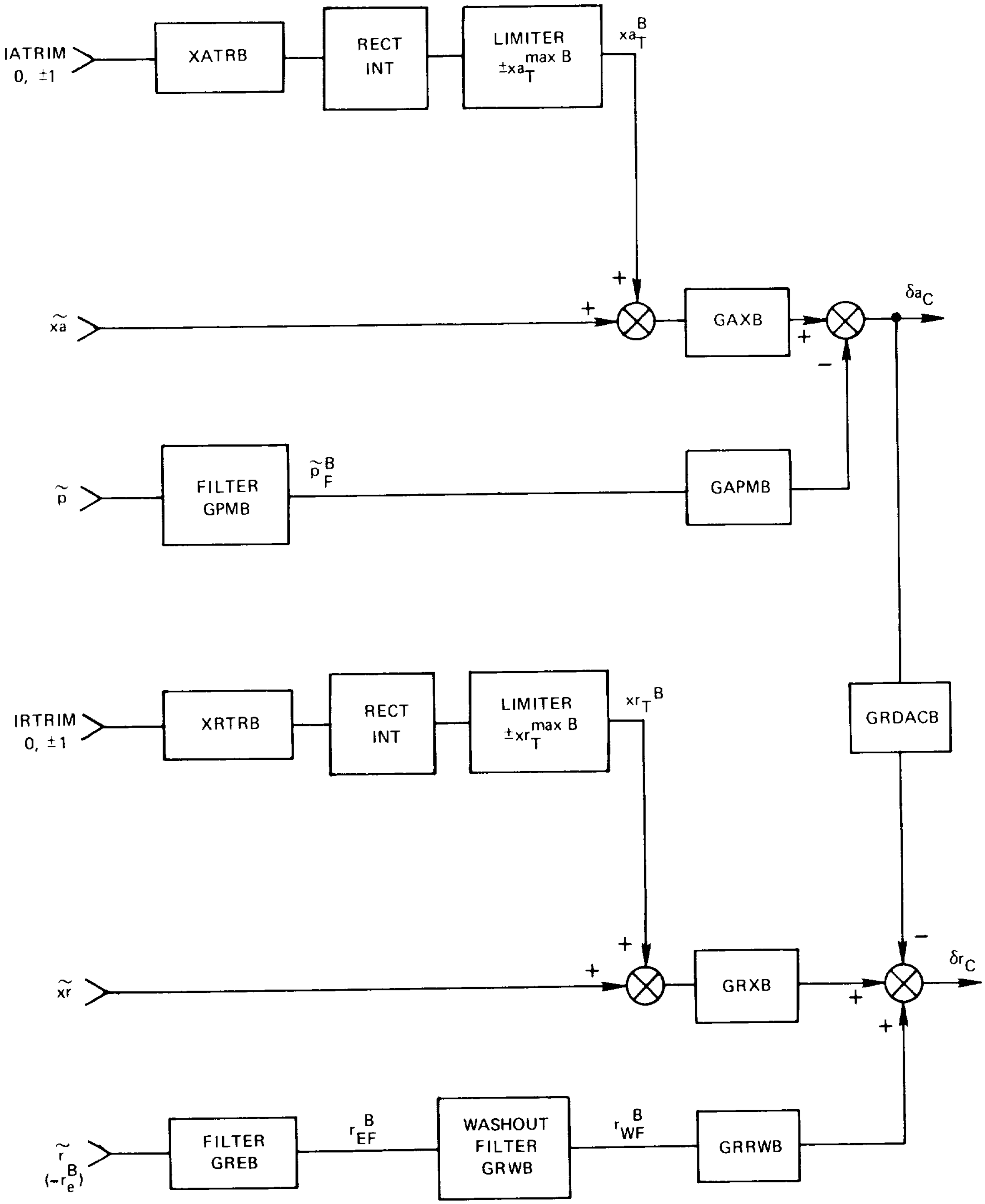

Fig. 4-23 Backup Control System (Cont)

4.7 Functional Flow Charts - Cruise Phase Initialization

Figures 4-24 through 4-28 represent preliminary attempts to specify the details of the cruise phase DFCS at the engineering/functional level rather than at the coded software level presented in Appendix 4A. Implementational freedom (especially with respect to programming language syntax) should not be restricted by software over-specification. Hence, the flow charts of this section will be augmented, until such time as a total engineering/functional specification is achieved. Figures 4-25 through 4-28 interface with the skeletal structure shown in Fig. 4a-2.

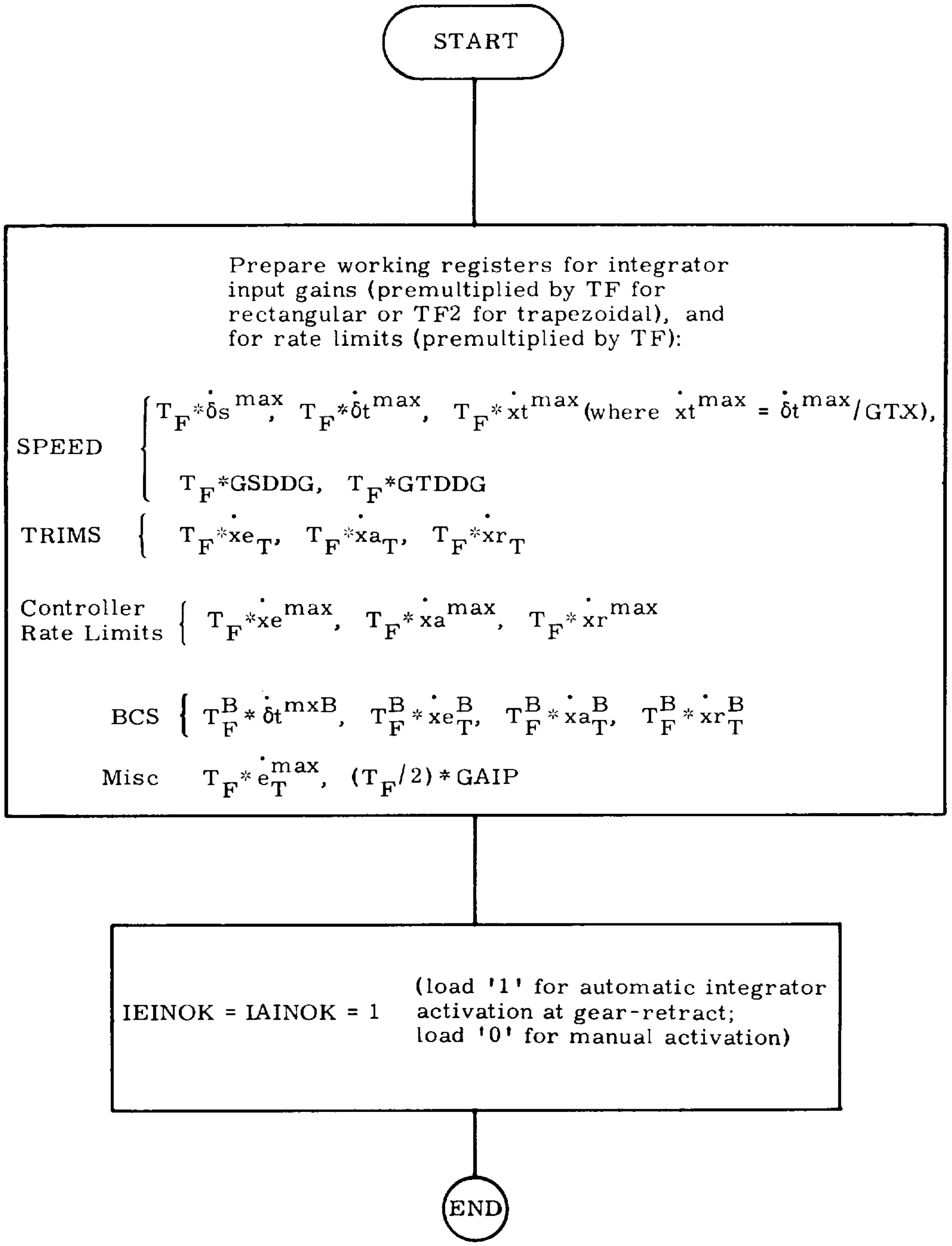
START
Prepare working registers for integrator input gains (premultiplied by TF for rectangular or TF2 for trapezoidal), and for rate limits (premultiplied by TF):
SPEED
$T_F*\dot{\delta}s^{max}$, $T_F*\dot{\delta}t^{max}$, $T_F*\dot{x}t^{max}$ (where $\dot{x}t^{max} = \dot{\delta}t^{max}/GTX$),
$T_F*GSDDG$, $T_F*GTDDG$
TRIMS
$T_F*\dot{x}e_T$, $T_F*\dot{x}a_T$, $T_F*\dot{x}r_T$
Controller Rate Limits
$T_F*\dot{x}e^{max}$, $T_F*\dot{x}a^{max}$, $T_F*\dot{x}r^{max}$
BCS
$T_F^B*\dot{\delta}t^{mxB}$, $T_F^B*\dot{x}e_T^B$, $T_F^B*\dot{x}a_T^B$, $T_F^B*\dot{x}r_T^B$
Misc
$T_F*\dot{e}_T^{max}$, $(T_F/2)*GAIP$
IEINOK = IAINOK = 1
(load '1' for automatic integrator activation at gear-retract; load '0' for manual activation)
END

Fig. 4-24 Functional Flow Diagram, Load Manipulation Routine

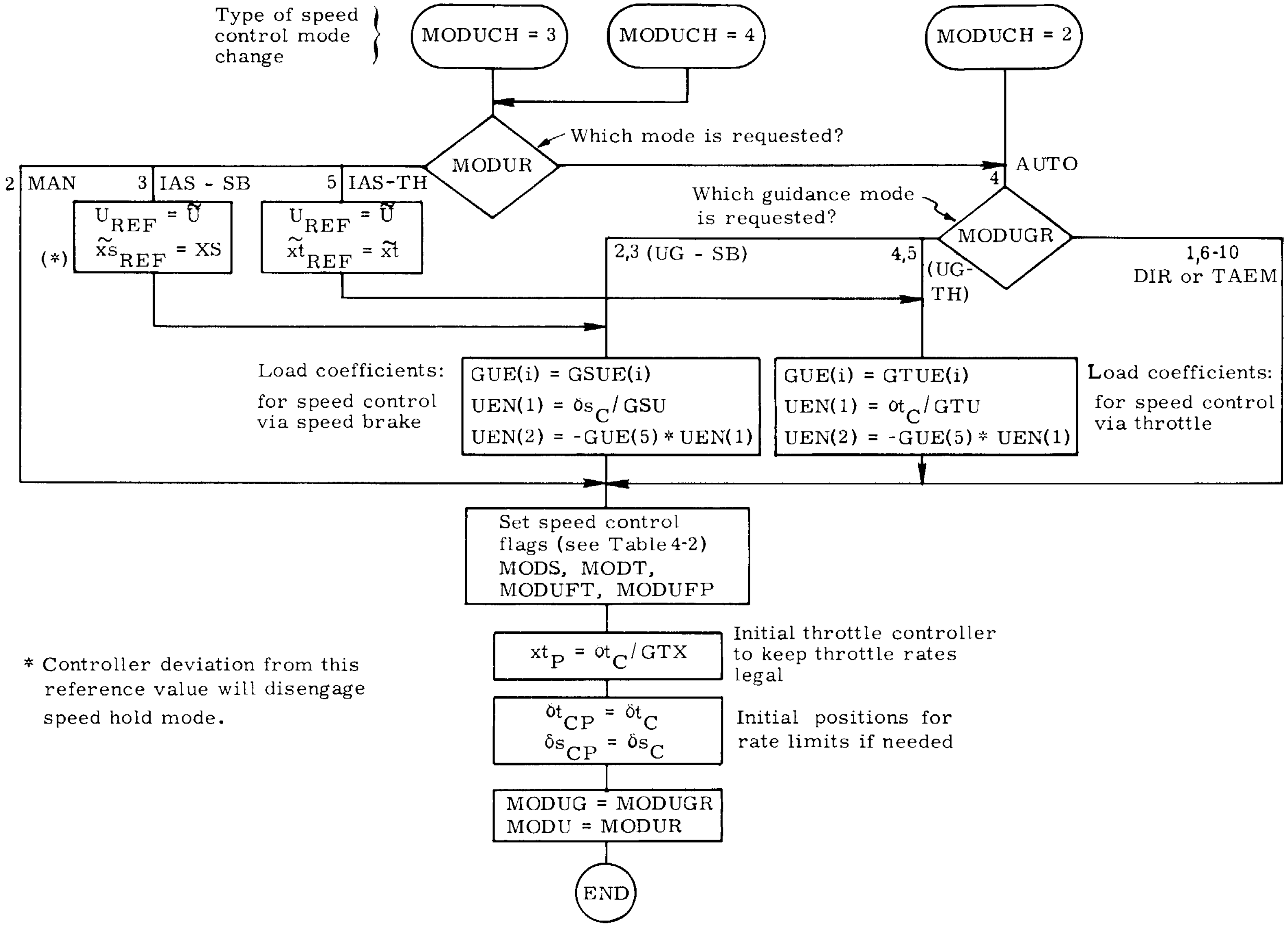
Type of speed control mode change
MODUCH = 3
MODUCH = 4
MODUCH = 2
MODUR
Which mode is requested?
2 MAN
3 IAS - SB
5 IAS-TH
4 AUTO
(*)
$U_{REF} = \tilde{U}$
$\tilde{xs}_{REF} = XS$
$U_{REF} = \tilde{U}$
$\tilde{xt}_{REF} = \tilde{xt}$
Which guidance mode is requested?
MODUGR
2,3 (UG - SB)
4,5 (UG-TH)
1,6-10 DIR or TAEM
Load coefficients: for speed control via speed brake
GUE(i) = GSUE(i)
UEN(1) = δs_C/GSU
UEN(2) = -GUE(5) * UEN(1)
GUE(i) = GTUE(i)
UEN(1) = δt_C/GTU
UEN(2) = -GUE(5) * UEN(1)
Load coefficients: for speed control via throttle
Set speed control flags (see Table 4-2) MODS, MODT, MODUFT, MODUFP
$xt_P = \delta t_C$/GTX
Initial throttle controller to keep throttle rates legal
$\delta t_{CP} = \delta t_C$
$\delta s_{CP} = \delta s_C$
Initial positions for rate limits if needed
MODUG = MODUGR
MODU = MODUR
END

* Controller deviation from this reference value will disengage speed hold mode.

Fig. 4-25 Functional Flow Diagram, Speed Initialization Routine

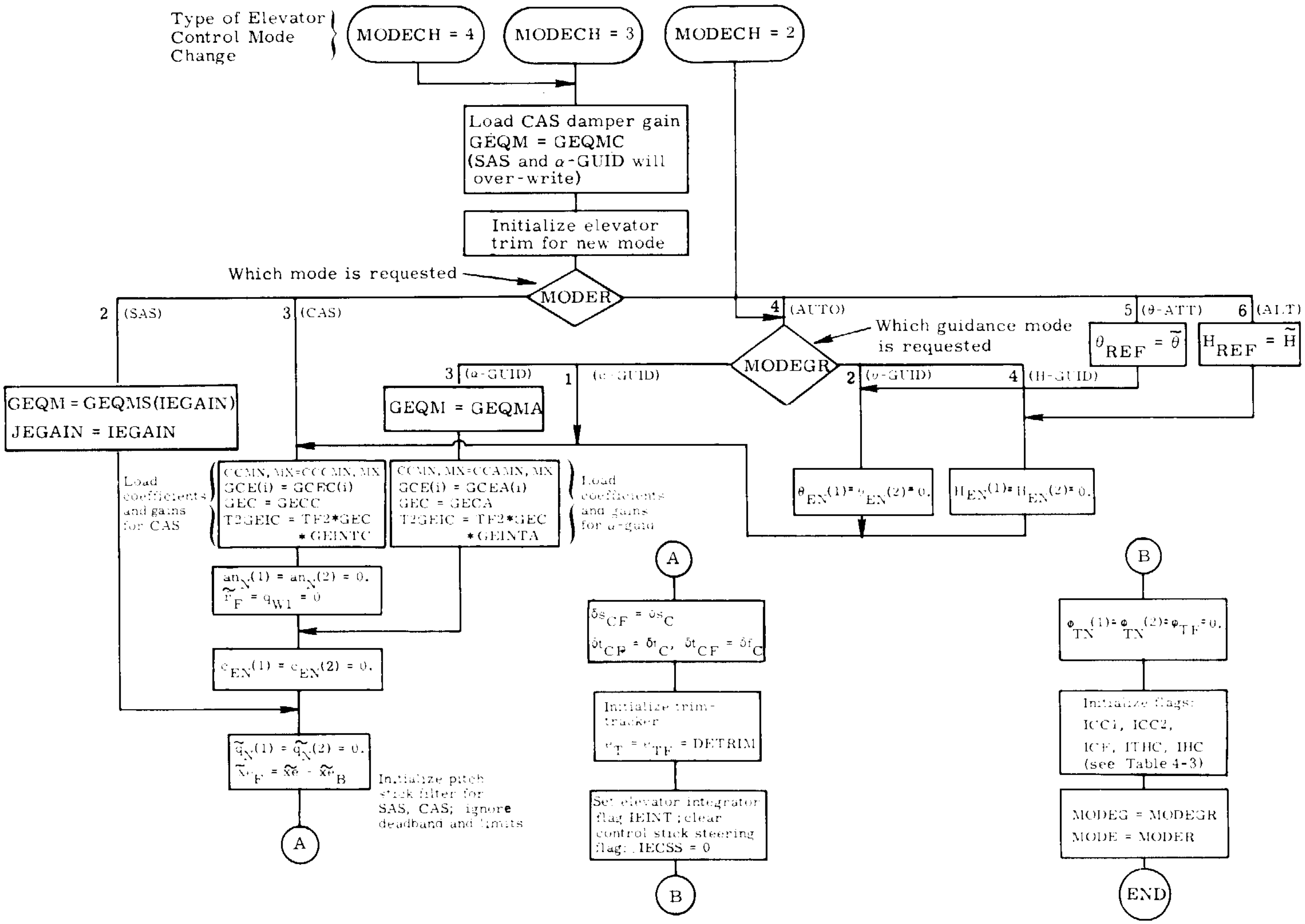
Type of Elevator Control Mode Change
MODECH = 4
MODECH = 3
MODECH = 2
Load CAS damper gain GEQM = GEQMC (SAS and α-GUID will over-write)
Initialize elevator trim for new mode
Which mode is requested
MODER
2 (SAS)
3 (CAS)
4 (AUTO)
5 (θ-ATT)
6 (ALT)
Which guidance mode is requested
MODEGR
$\theta_{REF} = \tilde{\theta}$
$H_{REF} = \tilde{H}$
3 (α-GUID)
1 (ε-GUID)
2 (θ-GUID)
4 (H-GUID)
GEQM = GEQMS(IEGAIN)
JEGAIN = IEGAIN
GEQM = GEQMA
Load coefficients and gains for CAS
CCMN, MX=CCCMN, MX
GCE(i) = GCEC(i)
GEC = GECC
T2GEIC = TF2*GEC *GEINTC
CCMN, MX=CCAMN, MX
GCE(i) = GCEA(i)
GEC = GECA
T2GEIC = TF2*GEC *GEINTA
Load coefficients and gains for α-guid
$\theta_{EN}(1)=\theta_{EN}(2)=0.$
$H_{EN}(1)=H_{EN}(2)=0.$
$an_N(1) = an_N(2) = 0.$
$\tilde{r}_F = q_{W1} = 0$
$\epsilon_{EN}(1) = \epsilon_{EN}(2) = 0.$
$\tilde{q}_N(1) = \tilde{q}_N(2) = 0.$
$\tilde{x}_F = \tilde{x}e - \tilde{x}e_B$
Initialize pitch stick filter for SAS, CAS; ignore deadband and limits
A
$\delta s_{CF} = \delta s_C$
$\delta t_{CF} = \delta t_C,\ \delta t_{CF} = \delta f_C$
Initialize trim-tracker
$\epsilon_T = \epsilon_{TF}$ = DETRIM
Set elevator integrator flag IEINT ; clear control stick steering flag: IECSS = 0
B
$\varphi_{TN}(1)=\varphi_{TN}(2)=\varphi_{TF}=0.$
Initialize flags: ICC1, ICC2, ICF, ITHC, IHC (see Table 4-3)
MODEG = MODEGR
MODE = MODER
END

Fig. 4-26 Functional Flow Diagram, Elevator Initialization Routine

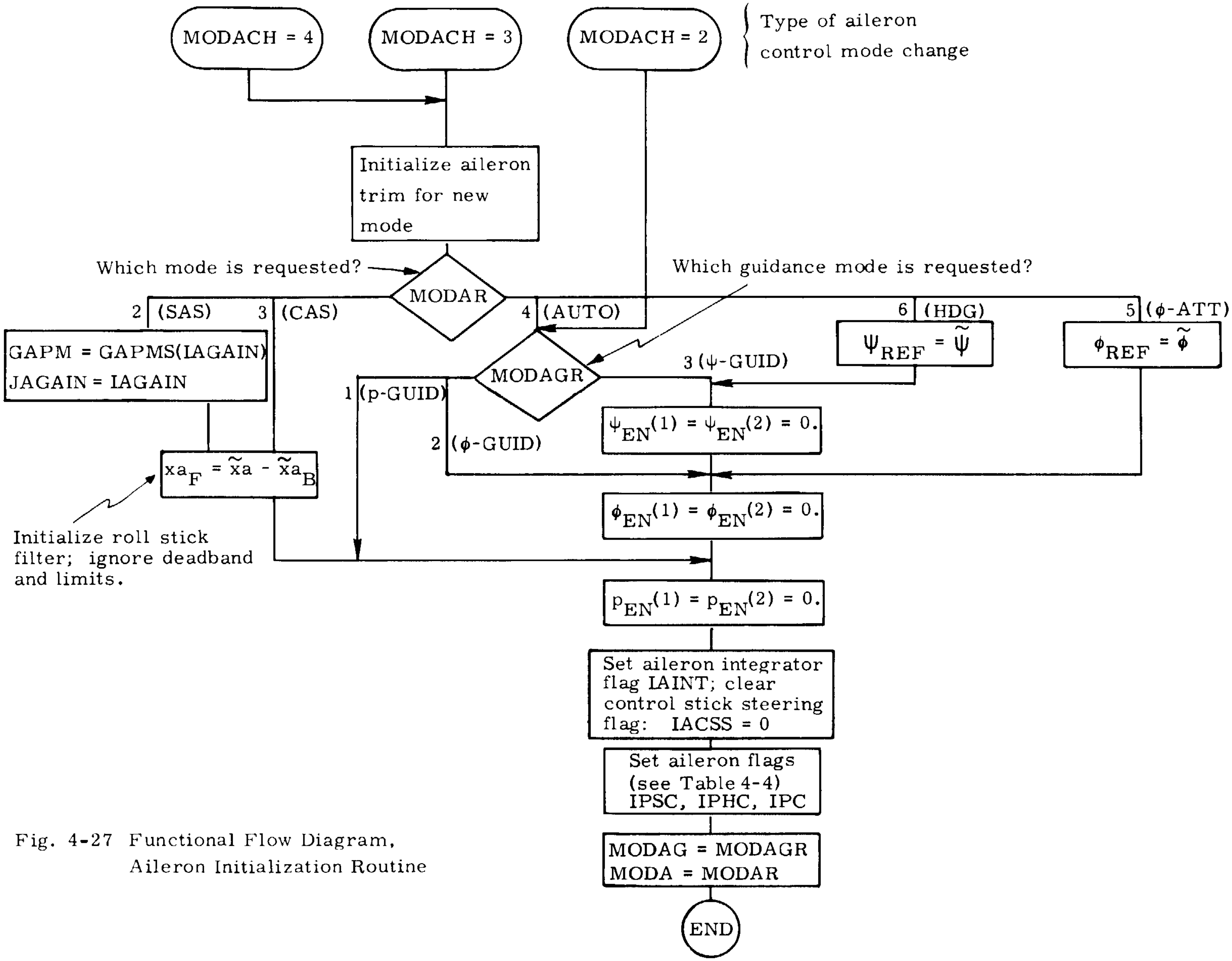
MODACH = 4
MODACH = 3
MODACH = 2
Type of aileron control mode change
Initialize aileron trim for new mode
Which mode is requested?
MODAR
2 (SAS)
3 (CAS)
4 (AUTO)
6 (HDG)
5 (φ-ATT)
Which guidance mode is requested?
GAPM = GAPMS(IAGAIN)
JAGAIN = IAGAIN
$\Psi_{REF} = \tilde{\Psi}$
$\phi_{REF} = \tilde{\phi}$
MODAGR
3 (ψ-GUID)
1 (p-GUID)
2 (φ-GUID)
$xa_F = \tilde{x}a - \tilde{x}a_B$
Initialize roll stick filter; ignore deadband and limits.
$\psi_{EN}(1) = \psi_{EN}(2) = 0.$
$\phi_{EN}(1) = \phi_{EN}(2) = 0.$
$p_{EN}(1) = p_{EN}(2) = 0.$
Set aileron integrator flag IAINT; clear control stick steering flag: IACSS = 0
Set aileron flags (see Table 4-4) IPSC, IPHC, IPC
MODAG = MODAGR
MODA = MODAR
END

Fig. 4-27 Functional Flow Diagram, Aileron Initialization Routine

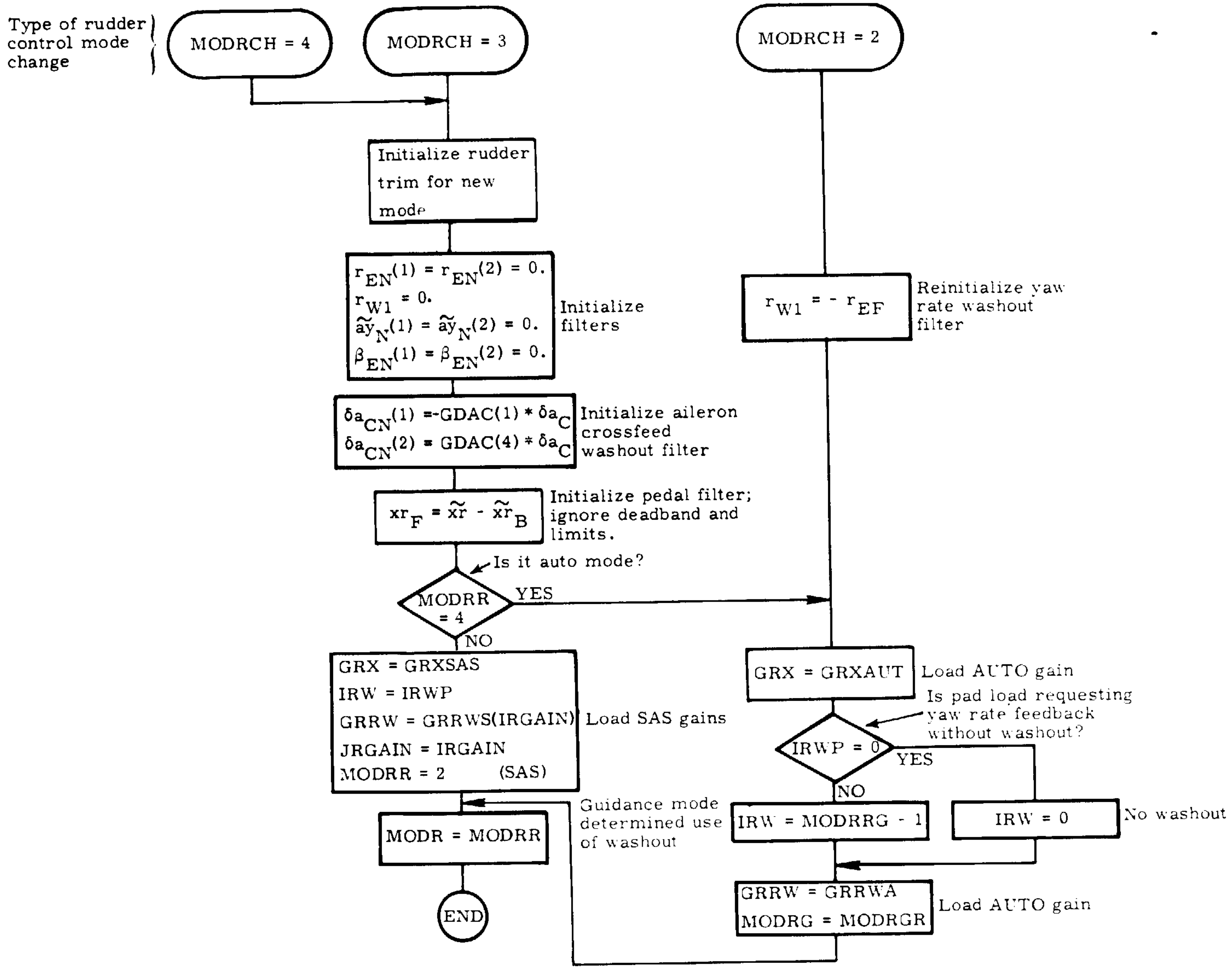
Type of rudder control mode change
MODRCH = 4
MODRCH = 3
MODRCH = 2
Initialize rudder trim for new mode
$r_{EN}(1) = r_{EN}(2) = 0.$
$r_{W1} = 0.$
$\tilde{ay}_N(1) = \tilde{ay}_N(2) = 0.$
$\beta_{EN}(1) = \beta_{EN}(2) = 0.$
Initialize filters
$r_{W1} = - r_{EF}$
Reinitialize yaw rate washout filter
$\delta a_{CN}(1) = -GDAC(1) * \delta a_C$
$\delta a_{CN}(2) = GDAC(4) * \delta a_C$
Initialize aileron crossfeed washout filter
$xr_F = \tilde{xr} - \tilde{xr}_B$
Initialize pedal filter; ignore deadband and limits.
Is it auto mode?
MODRR = 4
YES
NO
GRX = GRXSAS
IRW = IRWP
GRRW = GRRWS(IRGAIN)
JRGAIN = IRGAIN
MODRR = 2 (SAS)
Load SAS gains
GRX = GRXAUT
Load AUTO gain
Is pad load requesting yaw rate feedback without washout?
IRWP = 0
YES
NO
IRW = MODRRG - 1
IRW = 0
No washout
GRRW = GRRWA
MODRG = MODRGR
Load AUTO gain
Guidance mode determined use of washout
MODR = MODRR
END

Fig. 4-28 Functional Flow Diagram, Rudder Initialization Routine

APPENDIX 4A

DETAILED FLOWCHARTS FOR CRUISE PHASE DFCS

Detailed specifications for the cruise phase DFCS, in terms of FORTRAN flow charts of an operating version of the DFCS, are presented in Figs. 4A-1 through 4A-20. Minute functional details are covered, but unfortunately they are often overwhelmed by implementational aspects (e.g., higher-order-language syntax), and are thus less-than-ideal for specification purposes.

Figure 4A-1 depicts the cruise phase preflight (or first-pass) load manipulation operations. Figure 4A-2 presents the skeletal structure into which the remaining figures fit. In particular, there are five basic subroutines. These subroutines interface directly with the DFCS executive as shown in Section 1.2. Their functions for cruise phase are as follows:

Initialization Subroutine (Fig. 4A-3 through Fig. 4A-6)
handles all first-pass (preflight turn-on or inflight phase-change) and mode change initialization activity.

Filter Part 1 Subroutine (Fig. 4A-7 through Fig. 4A-10)
handles all preparatory calculations for the Control Output Subroutine, including pilot input signal processing, filter output node computations, control stick steering override detection, etc.

Control Law Subroutine (Fig. 4A-11 through Fig. 4A-13)
handles all control output calculations in preparation for the Control Output Subroutine (Subsection 2.2).

Filter Part 2 Subroutine (Fig. 4A-14 through Fig. 4A-18)
handles all filter wrapup processing and miscellaneous activity, such as body flap command calculations, bank-angle filter calculations, and reengaging semiautomatic operation following a control stick steering override.

BCS Subroutine (Fig. 4A-19 through Fig. 4A-20)
handles sequentially, the Filter Part 1, Control Law, Control Output, and Filter Part 2 calculations for a 4-axis BCS mode of operation.

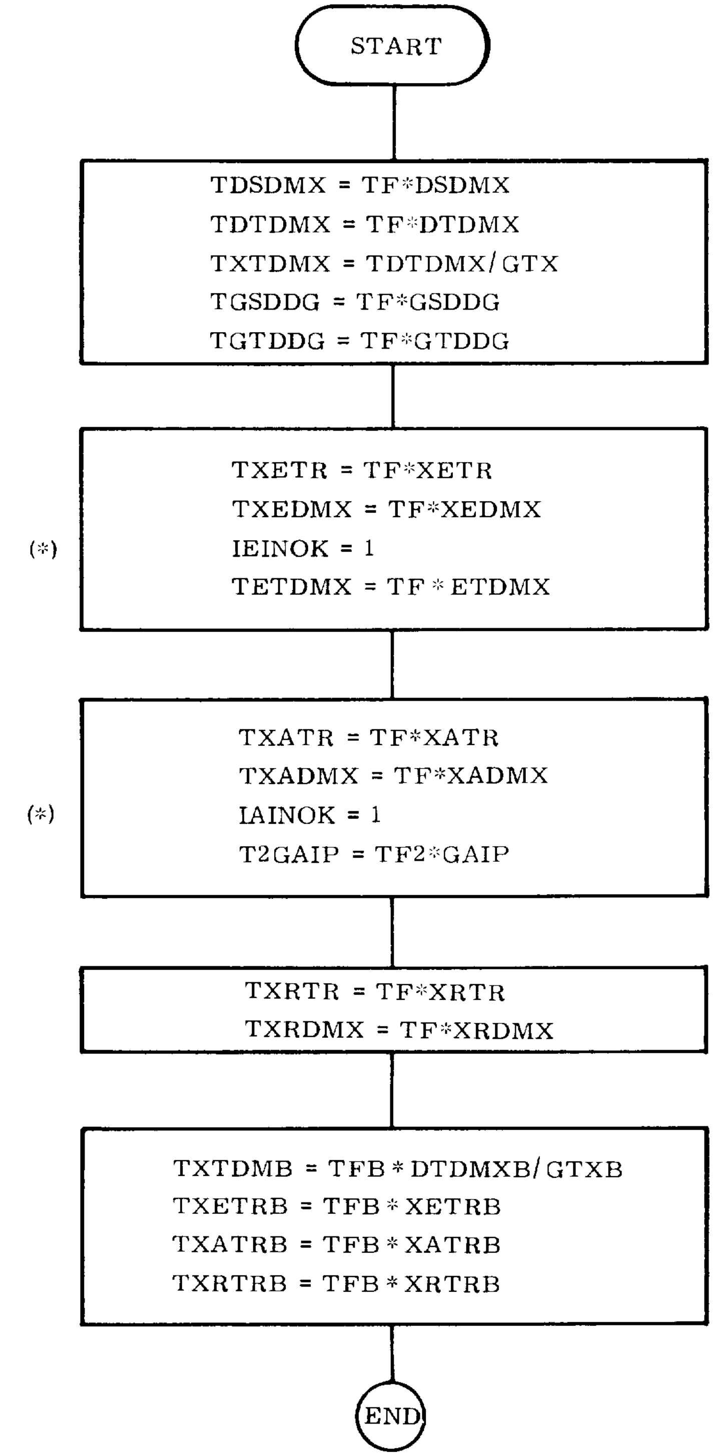

(*) For automatic integrator-activation at gear-retract; for manual reactivation load IEINOK = IAINOK = 0.

Fig. 4A-1 Load Manipulator Routine Cruise Section

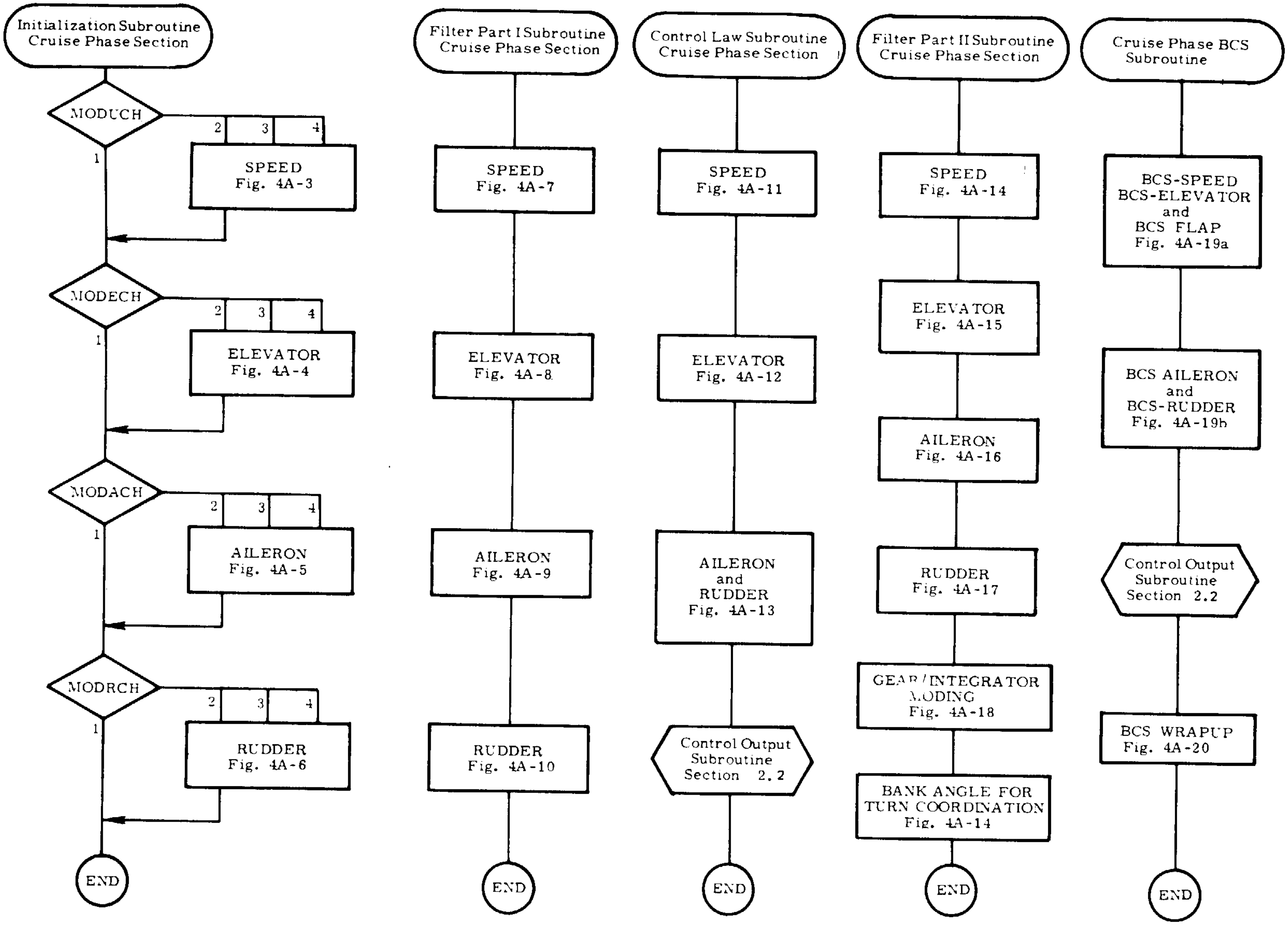
Initialization Subroutine Cruise Phase Section
MODUCH
1
2
3
4
SPEED Fig. 4A-3
MODECH
1
2
3
4
ELEVATOR Fig. 4A-4
MODACH
1
2
3
4
AILERON Fig. 4A-5
MODRCH
1
2
3
4
RUDDER Fig. 4A-6
END
Filter Part I Subroutine Cruise Phase Section
SPEED Fig. 4A-7
ELEVATOR Fig. 4A-8
AILERON Fig. 4A-9
RUDDER Fig. 4A-10
END
Control Law Subroutine Cruise Phase Section
SPEED Fig. 4A-11
ELEVATOR Fig. 4A-12
AILERON and RUDDER Fig. 4A-13
Control Output Subroutine Section 2.2
END
Filter Part II Subroutine Cruise Phase Section
SPEED Fig. 4A-14
ELEVATOR Fig. 4A-15
AILERON Fig. 4A-16
RUDDER Fig. 4A-17
GEAR/INTEGRATOR MODING Fig. 4A-18
BANK ANGLE FOR TURN COORDINATION Fig. 4A-14
END
Cruise Phase BCS Subroutine
BCS-SPEED BCS-ELEVATOR and BCS FLAP Fig. 4A-19a
BCS AILERON and BCS-RUDDER Fig. 4A-19b
Control Output Subroutine Section 2.2
BCS WRAPUP Fig. 4A-20
END

Fig. 4A-2 Overview of Cruise Section Fortran Flow Charts

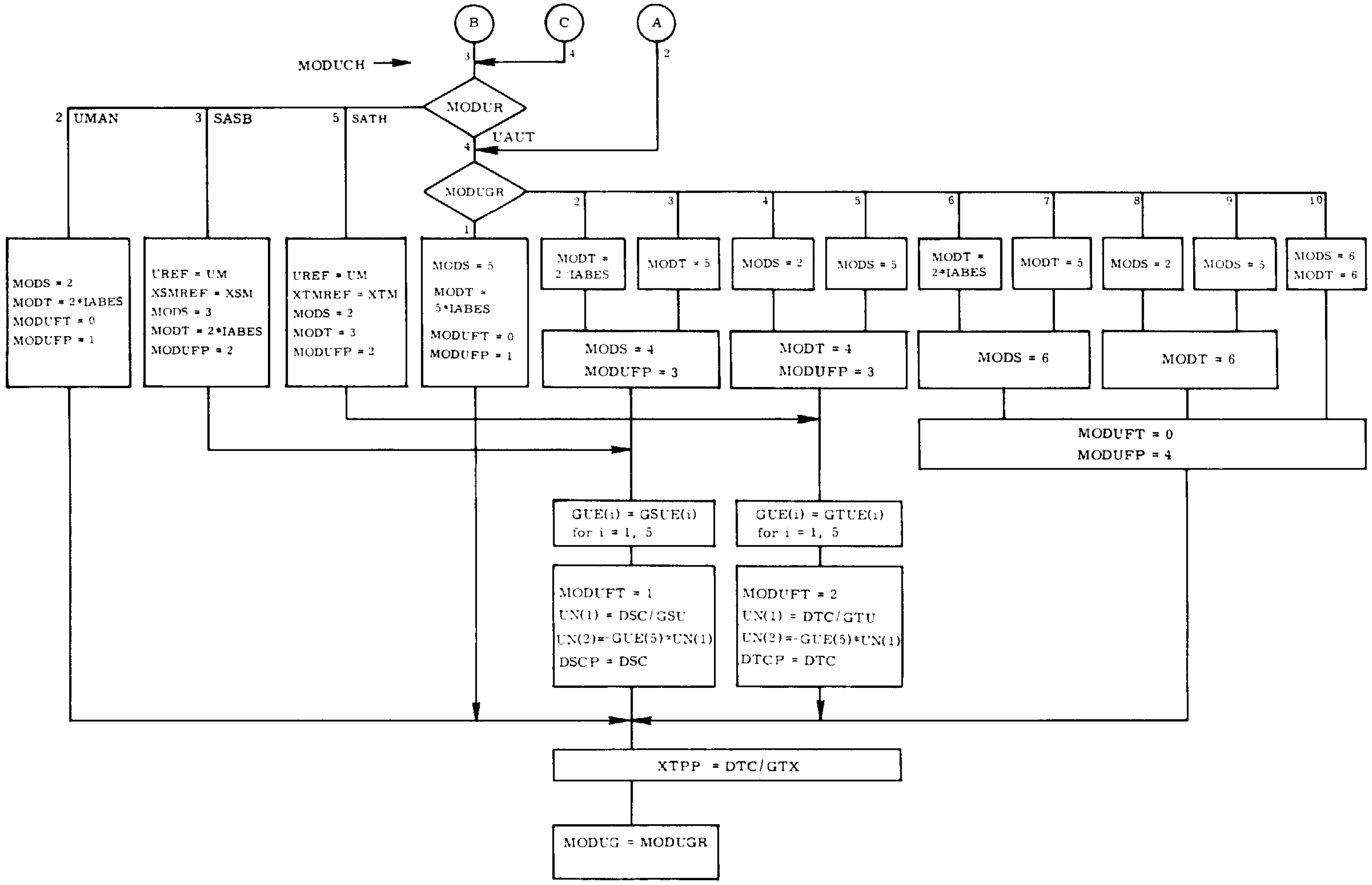

Fig. 4A-3 Initialization Subroutine, Cruise Phase Section, Speed Subsection

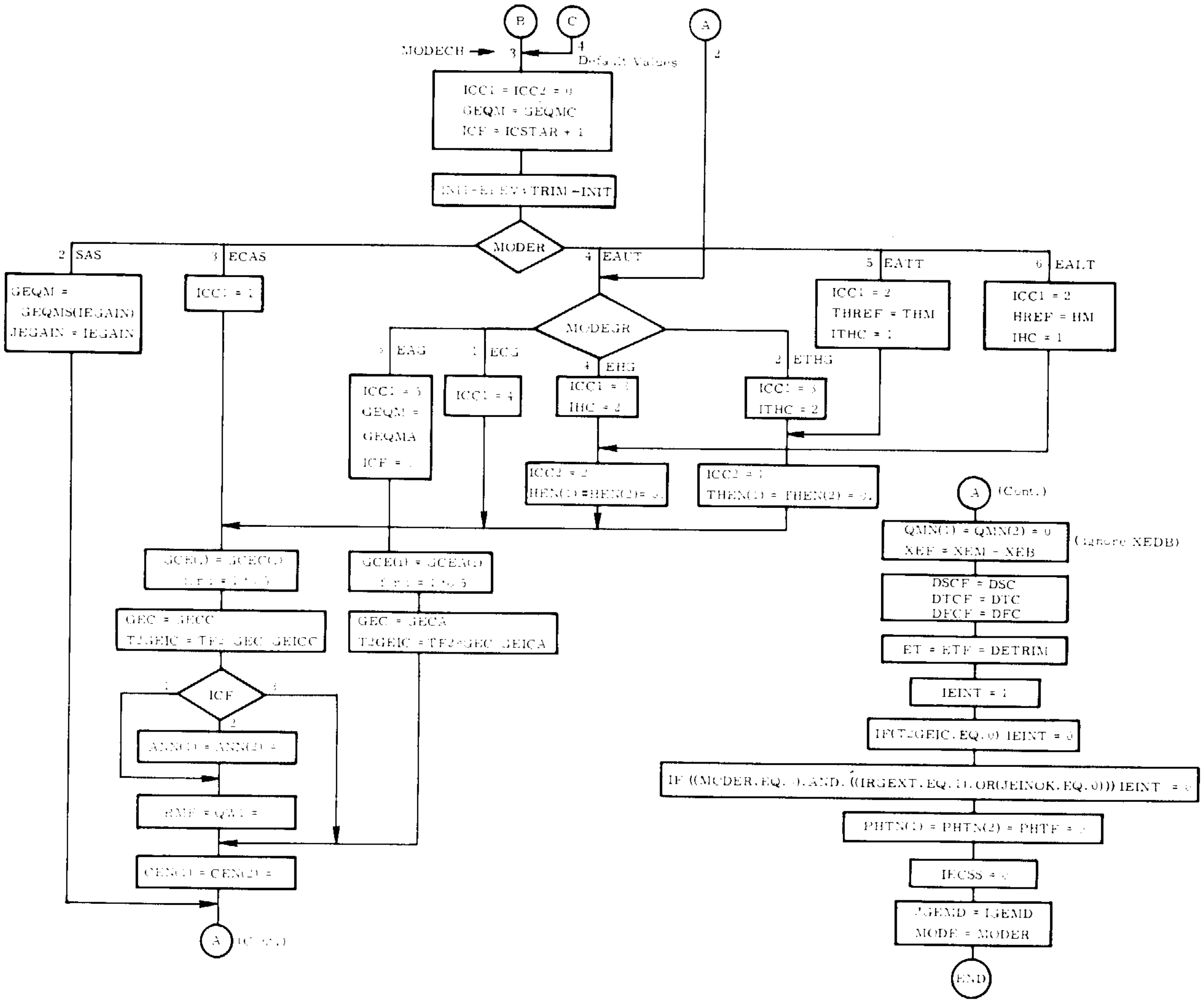

Fig. 4A-4a Initialization Subroutine, Cruise Phase Section, Elevator Subsection

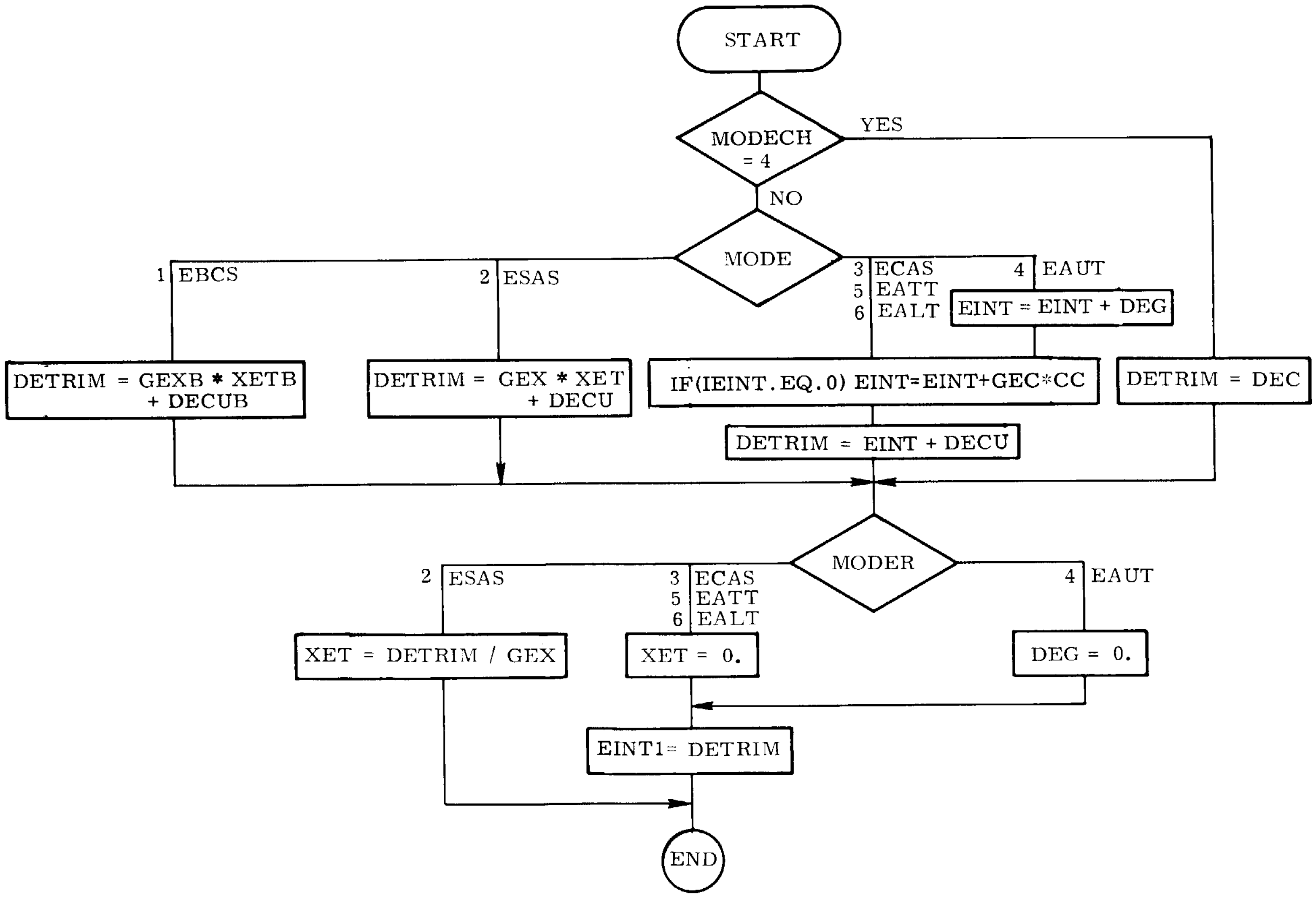

Fig. 4A-4b Initialization Subroutine, Cruise Phase Section, Elevator Trim Subsection

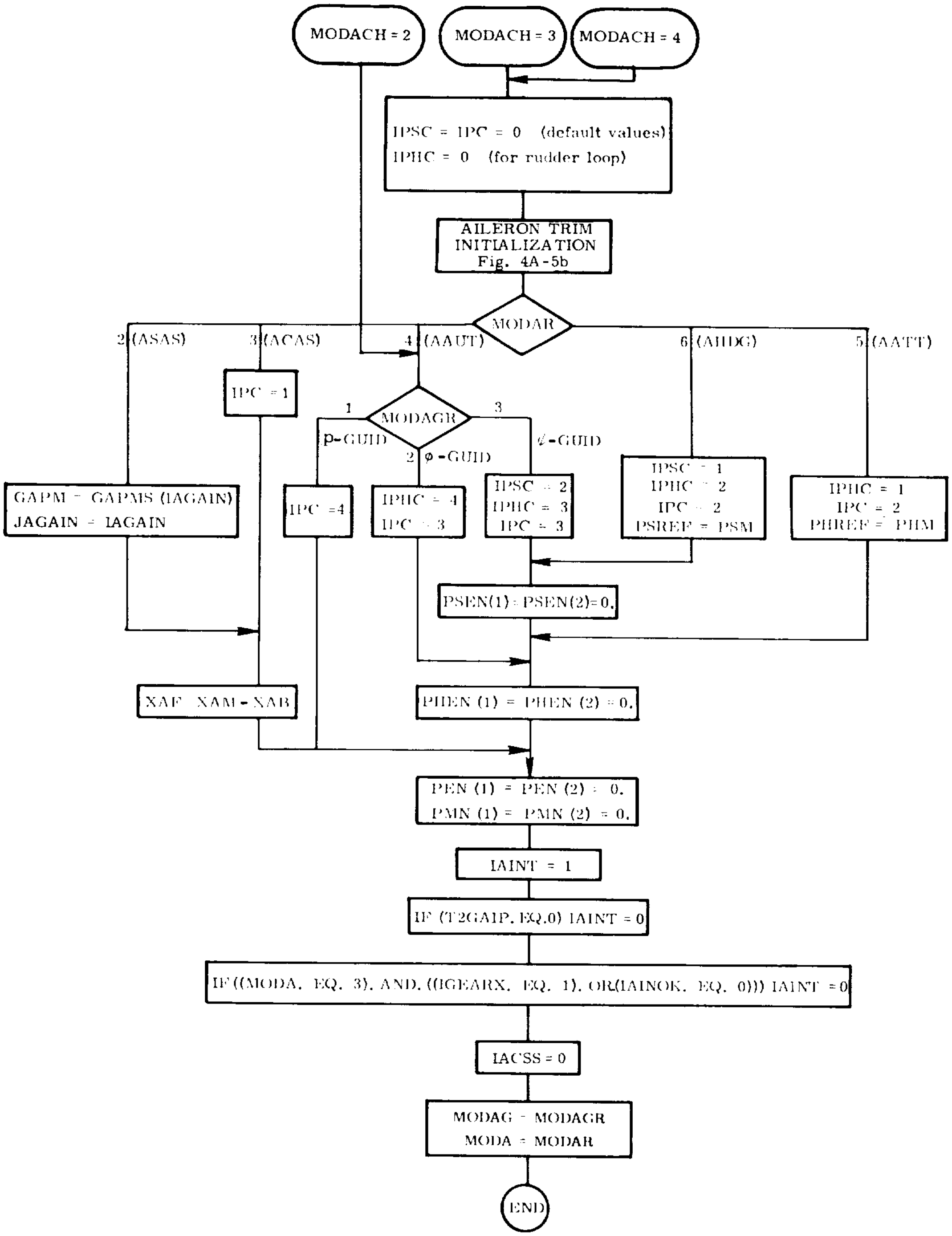

Fig. 4A-5a Initialization Subroutine, Cruise Phase Section, Aileron Subsection

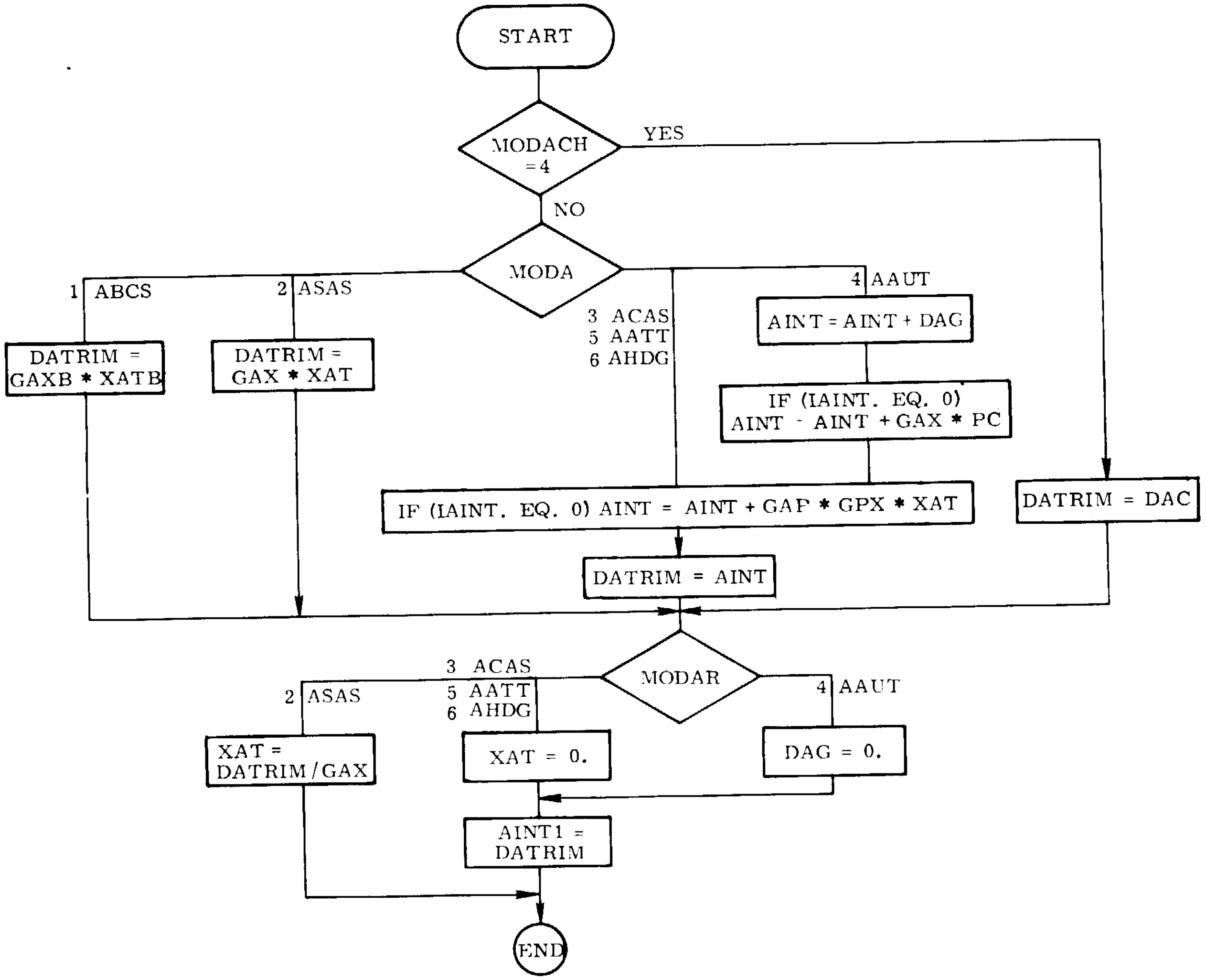

Fig. 4A-5b Initialization Subroutine, Cruise Phase Section, Aileron Trim Subsection

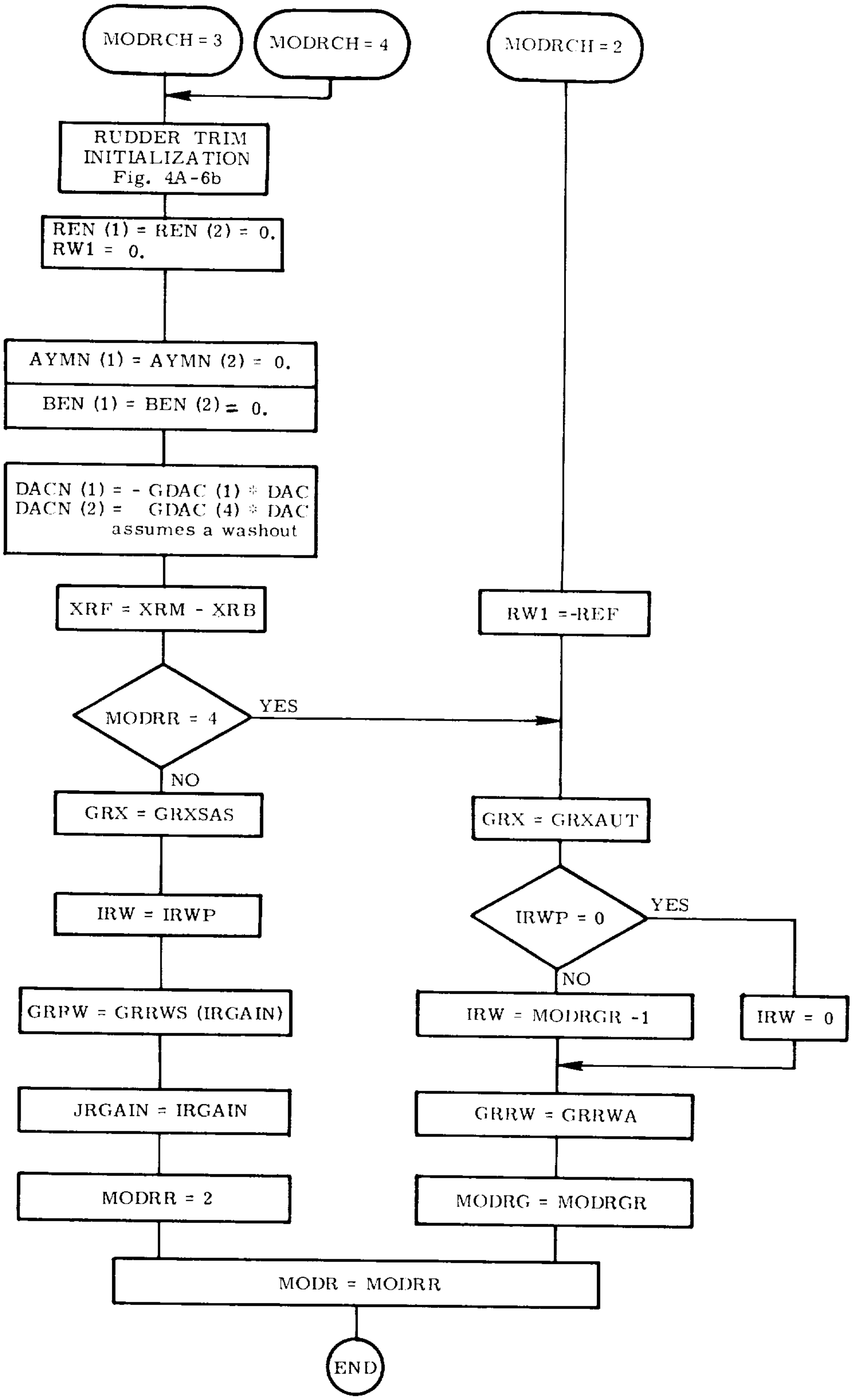

Fig. 4A-6a Initialization Subroutine, Cruise Phase Section, Rudder Subsection

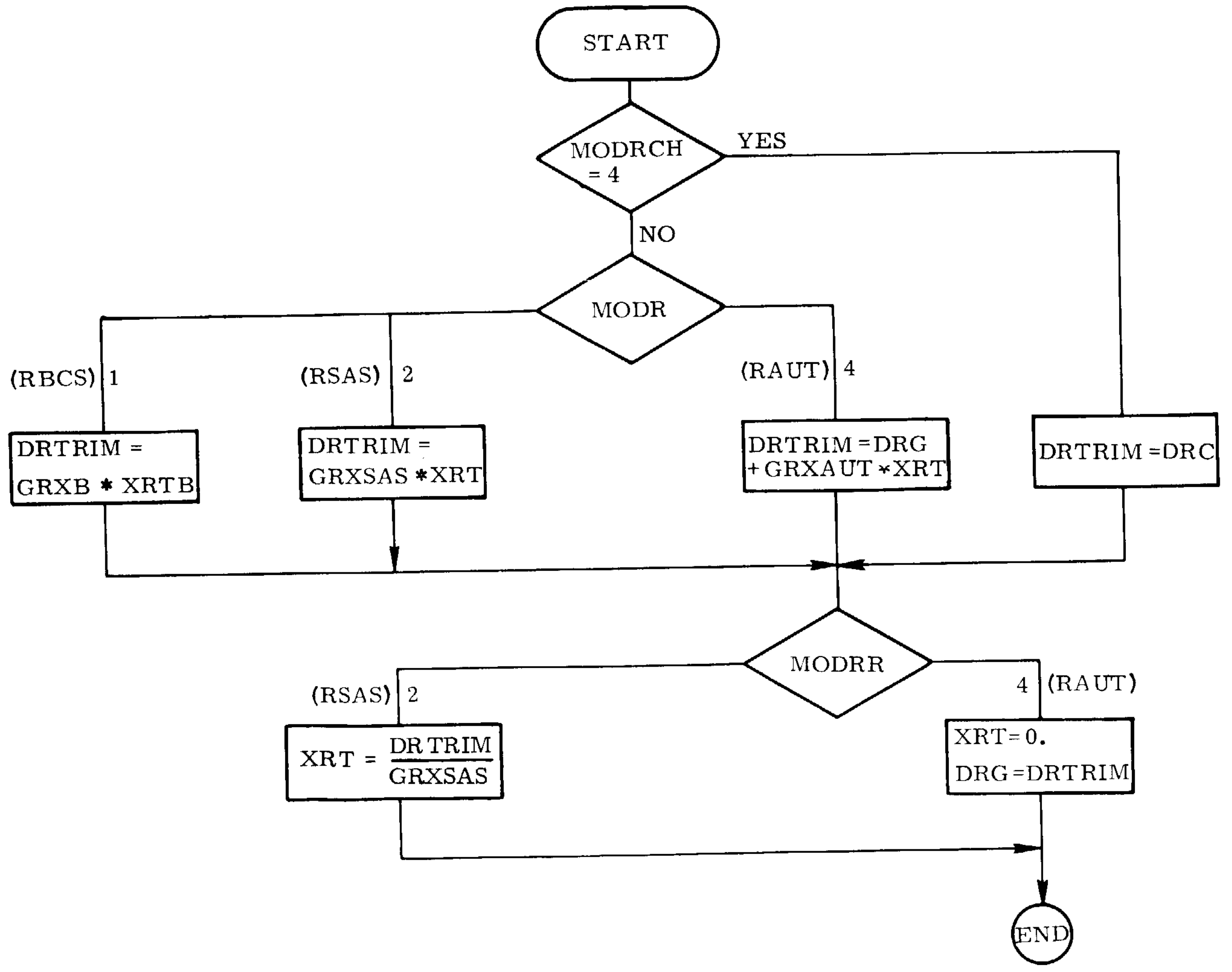

Fig. 4A-6b Initialization Subroutine, Cruise Phase Section, Rudder Trim Subsection

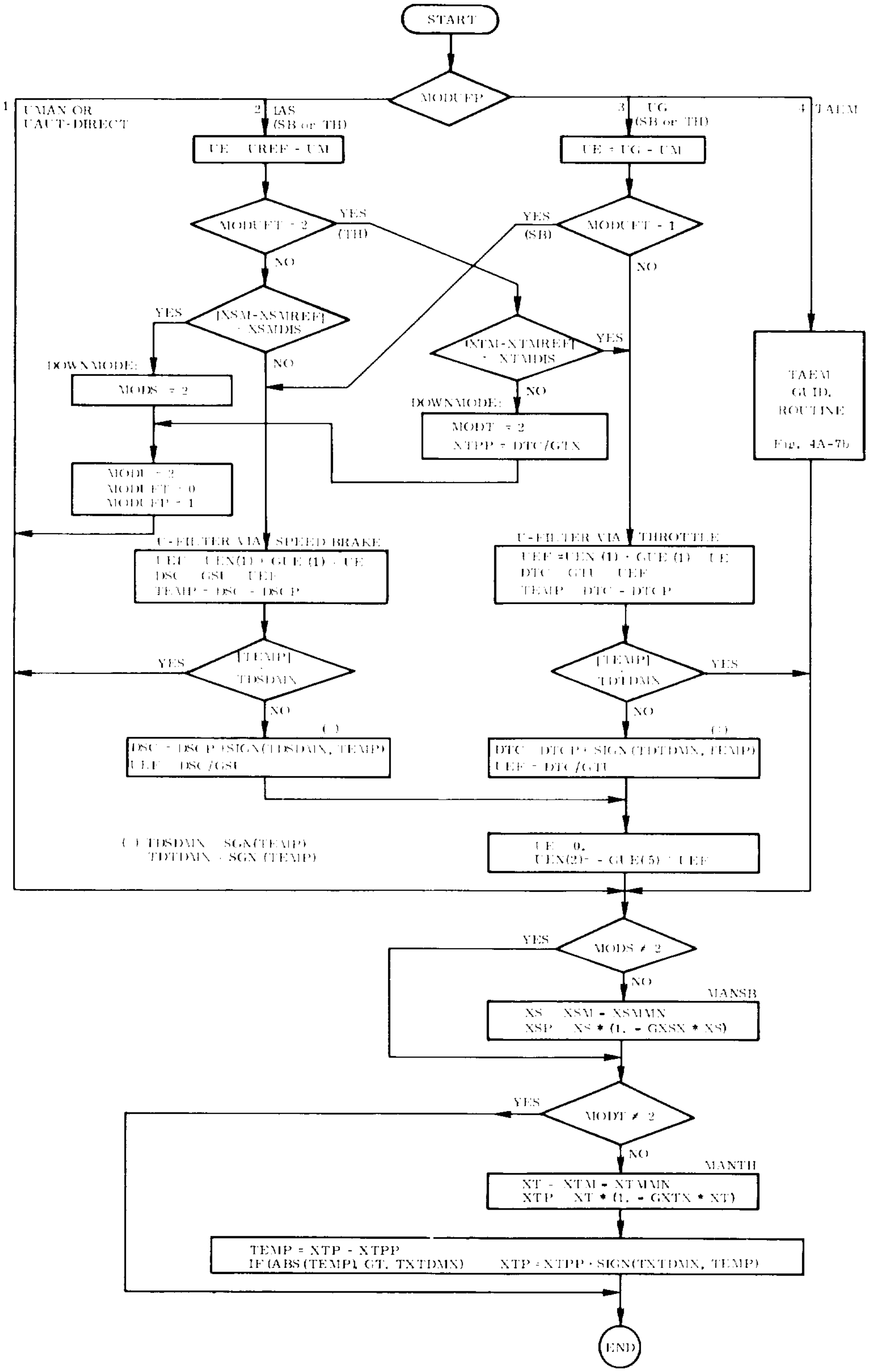

Fig. 4A-7a Filter Part I Subroutine, Cruise Phase Section Speed Subsection

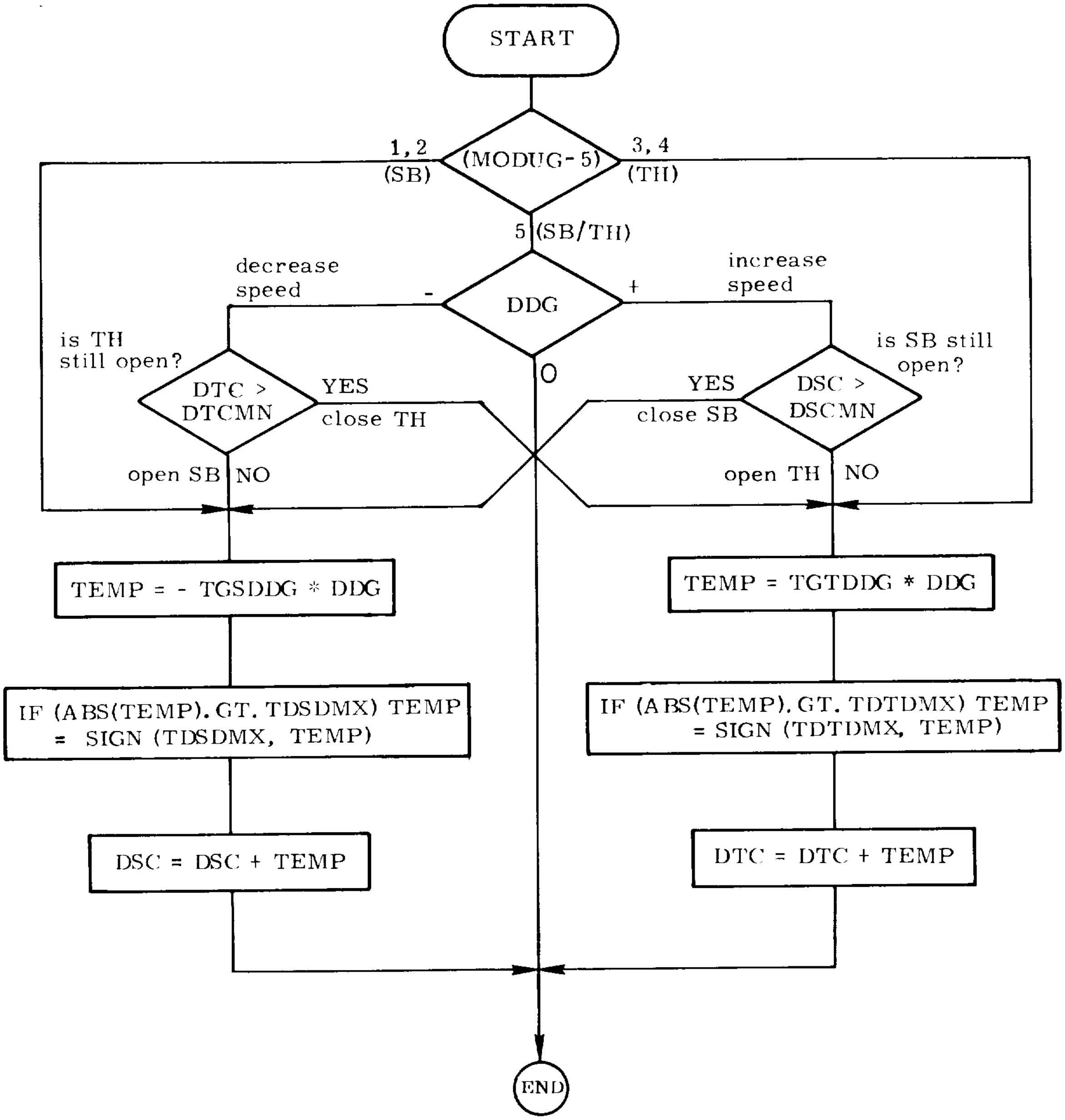

Fig. 4A-7b Filter Part I Subroutine, Cruise Phase Section Speed Subsection, (TAEM Guidance Routine)

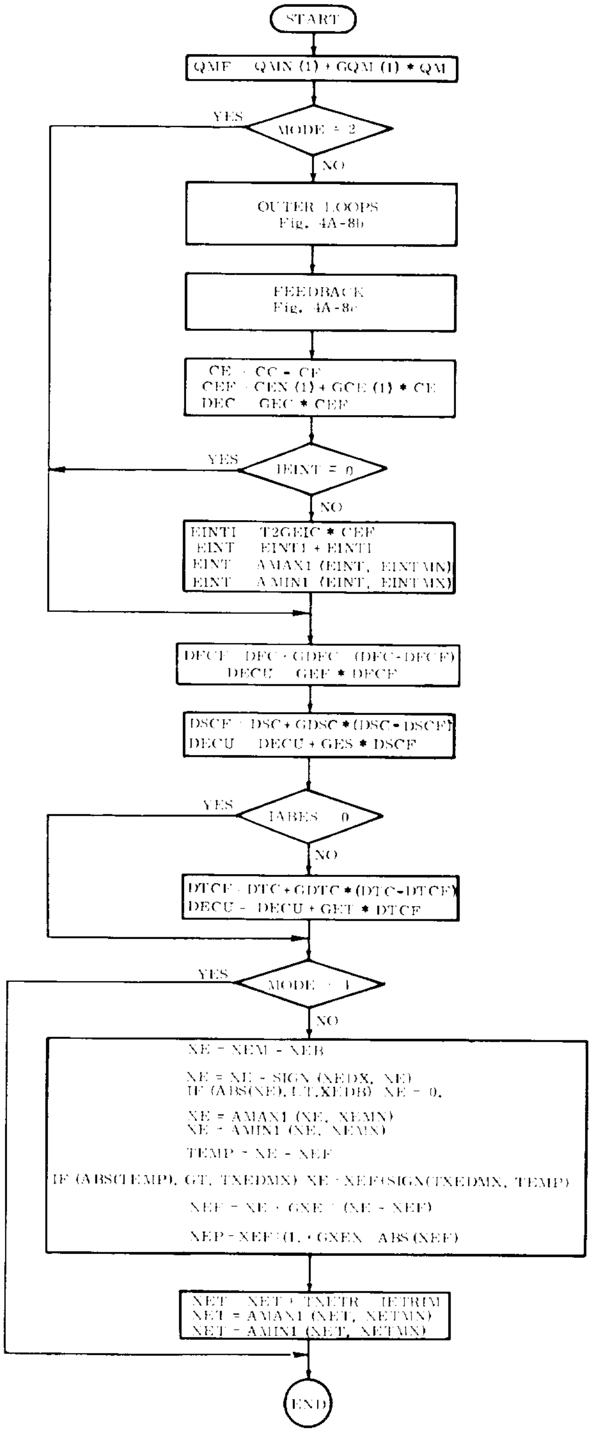

Fig. 4A-8a Filter Part I Subroutine, Cruise Phase Section, Elevator Subsection,

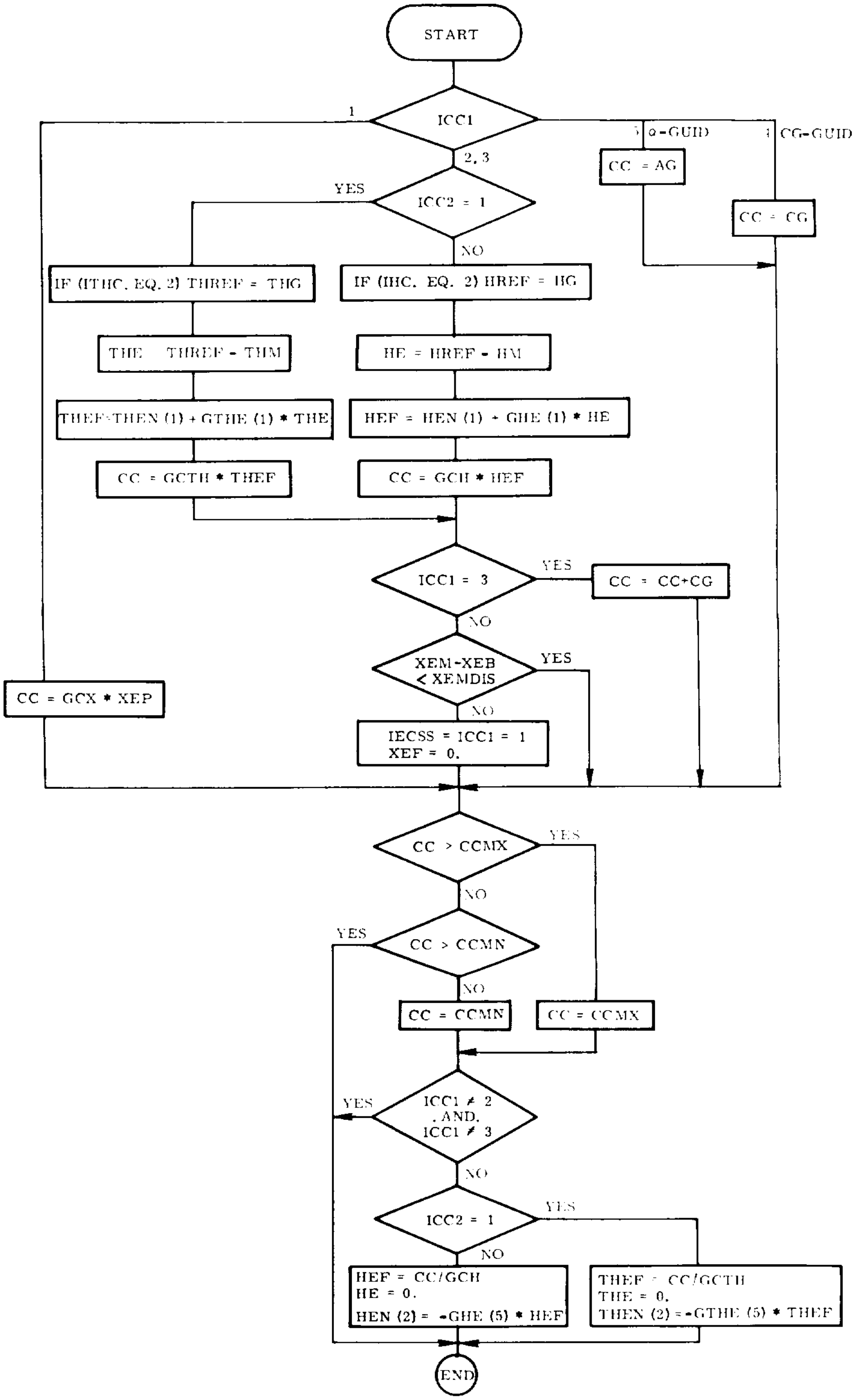

Fig. 4A-8b Filter Part I Subroutine, Cruise Phase, Elevator Subsection, Outer Loops

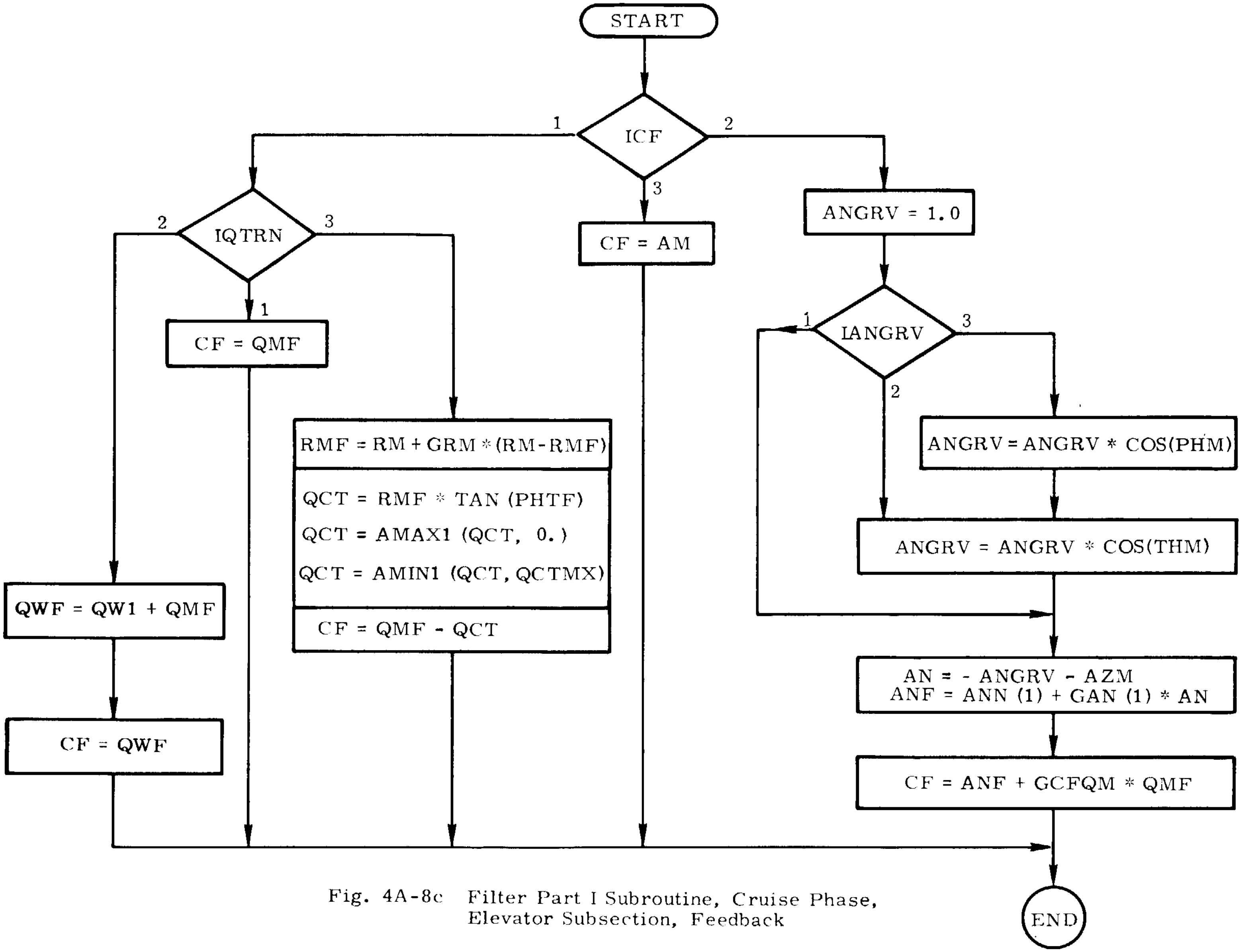

Fig. 4A-8c Filter Part I Subroutine, Cruise Phase, Elevator Subsection, Feedback

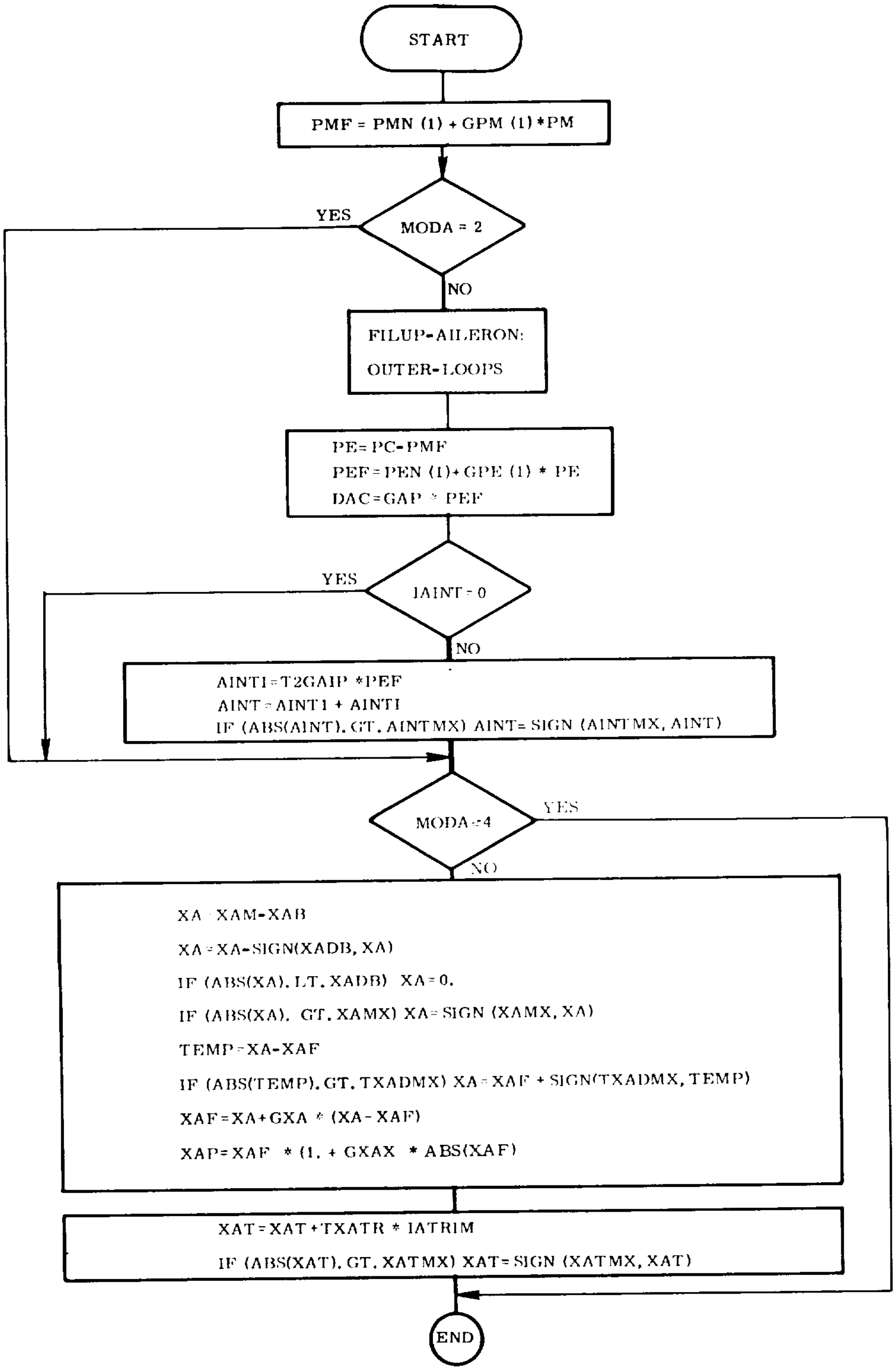
START
PMF = PMN (1) + GPM (1)*PM
YES
MODA = 2
NO
FILUP-AILERON:
OUTER-LOOPS
PE= PC-PMF
PEF=PEN (1)+GPE (1) * PE
DAC=GAP * PEF
YES
IAINT=0
NO
AINTI=T2GAIP *PEF
AINT=AINT1 + AINTI
IF (ABS(AINT).GT.AINTMX) AINT= SIGN (AINTMX, AINT)
MODA=4
YES
NO
XA=XAM-XAB
XA=XA-SIGN(XADB, XA)
IF (ABS(XA).LT.XADB) XA=0.
IF (ABS(XA). GT.XAMX) XA=SIGN (XAMX, XA)
TEMP=XA-XAF
IF (ABS(TEMP).GT.TXADMX) XA=XAF + SIGN(TXADMX, TEMP)
XAF=XA+GXA * (XA-XAF)
XAP=XAF * (1. + GXAX * ABS(XAF)
XAT=XAT+TXATR * IATRIM
IF (ABS(XAT).GT.XATMX) XAT=SIGN (XATMX, XAT)
END

Fig. 4A-9a Filter Part I Subroutine, Cruise Phase Section, Aileron Subsection

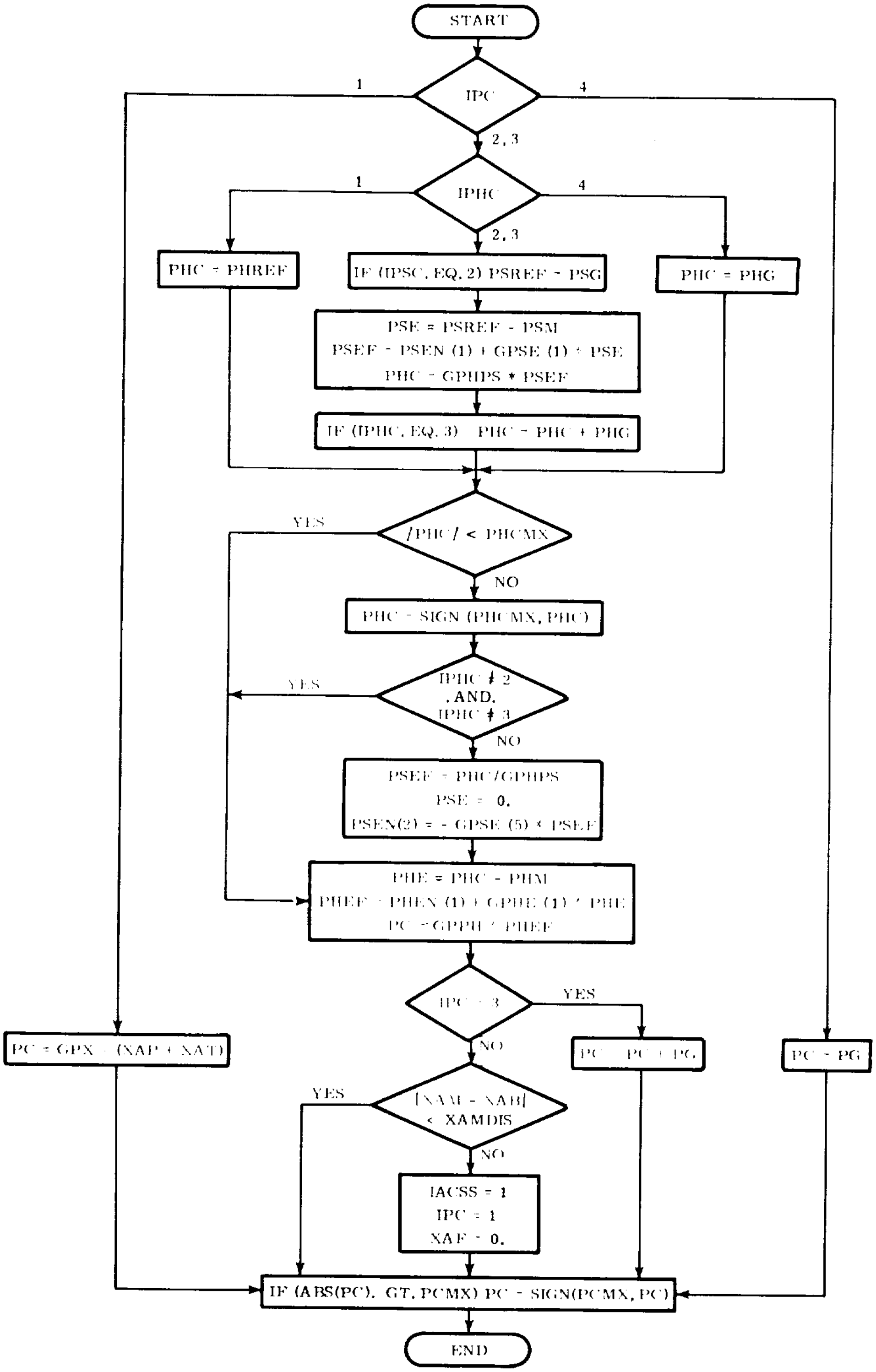

Fig. 4A-9b Filter Part I Subroutine, Cruise Phase Section, Aileron Subsection, Outer Loops

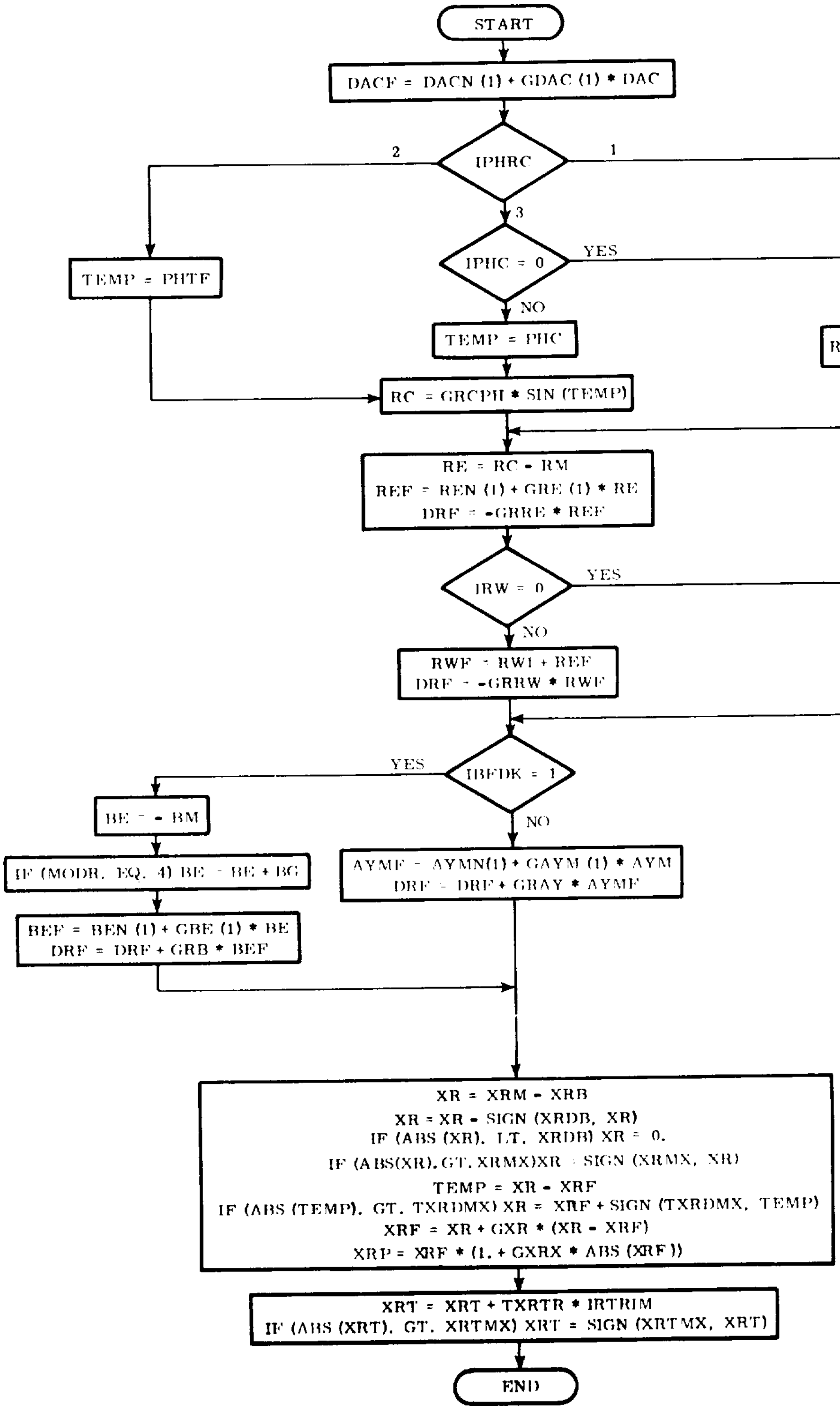
START
DACF = DACN (1) + GDAC (1) * DAC
IPHRC
2
1
3
IPHC = 0
YES
NO
TEMP = PHTF
TEMP = PHC
RC = 0.
RC = GRCPH * SIN (TEMP)
RE = RC - RM
REF = REN (1) + GRE (1) * RE
DRF = -GRRE * REF
IRW = 0
YES
NO
RWF = RW1 + REF
DRF = -GRRW * RWF
IBFDK = 1
YES
NO
BE = - BM
IF (MODR. EQ. 4) BE = BE + BG
BEF = BEN (1) + GBE (1) * BE
DRF = DRF + GRB * BEF
AYMF = AYMN(1) + GAYM (1) * AYM
DRF = DRF + GRAY * AYMF
XR = XRM - XRB
XR = XR - SIGN (XRDB, XR)
IF (ABS (XR). LT. XRDB) XR = 0.
IF (ABS(XR). GT. XRMX)XR = SIGN (XRMX, XR)
TEMP = XR - XRF
IF (ABS (TEMP). GT. TXRDMX) XR = XRF + SIGN (TXRDMX, TEMP)
XRF = XR + GXR * (XR - XRF)
XRP = XRF * (1. + GXRX * ABS (XRF))
XRT = XRT + TXRTR * IRTRIM
IF (ABS (XRT). GT. XRTMX) XRT = SIGN (XRTMX, XRT)
END

Fig. 4A-10 Filter Part I Subroutine, Cruise Phase Section, Rudder Subsection

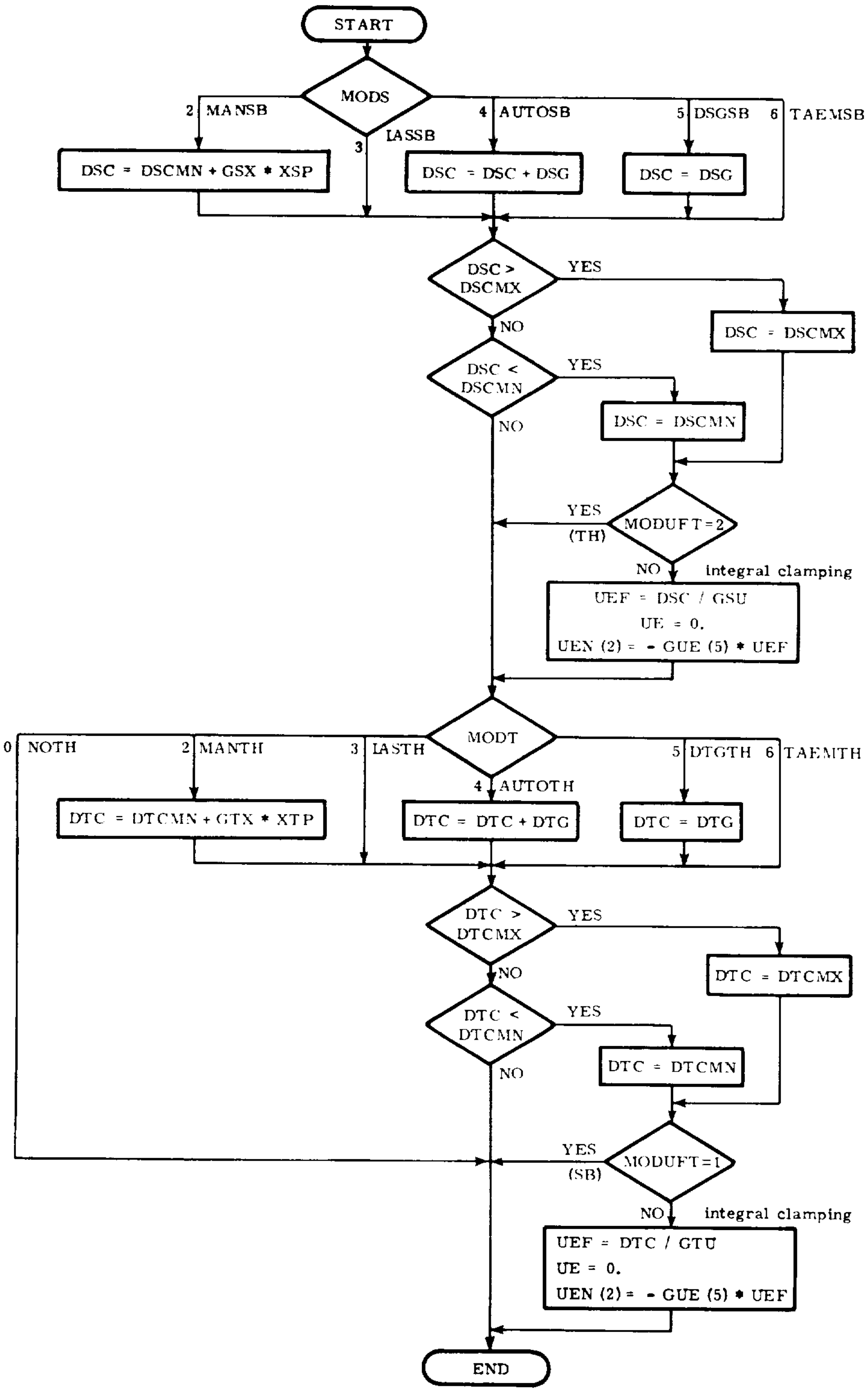

Fig. 4A-11 Control Law Subroutine, Cruise Phase Section, Speed Subsection

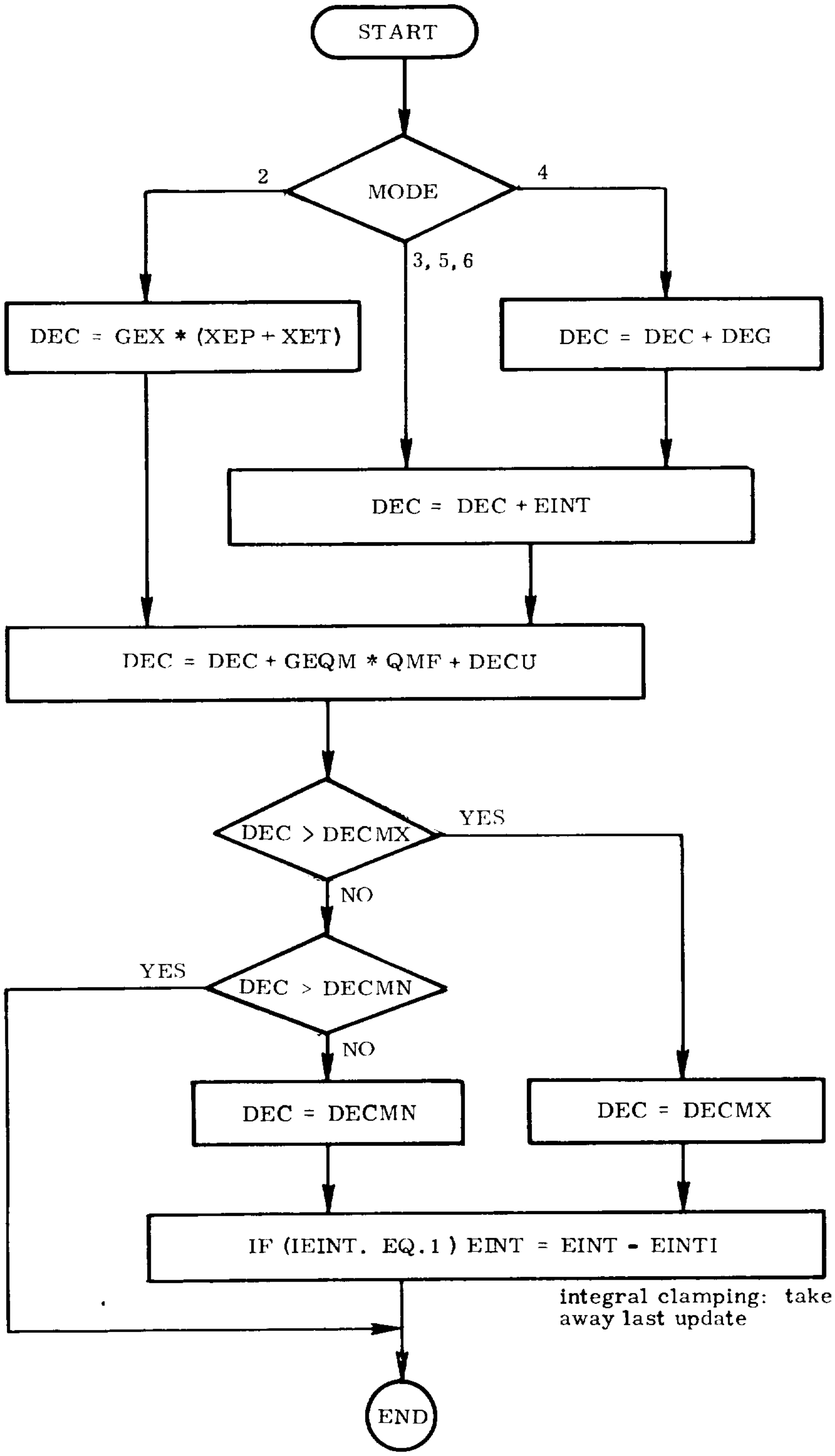

integral clamping: take away last update

Fig. 4A-12 Control Law Subroutine, Cruise Phase Section, Elevator Subsection

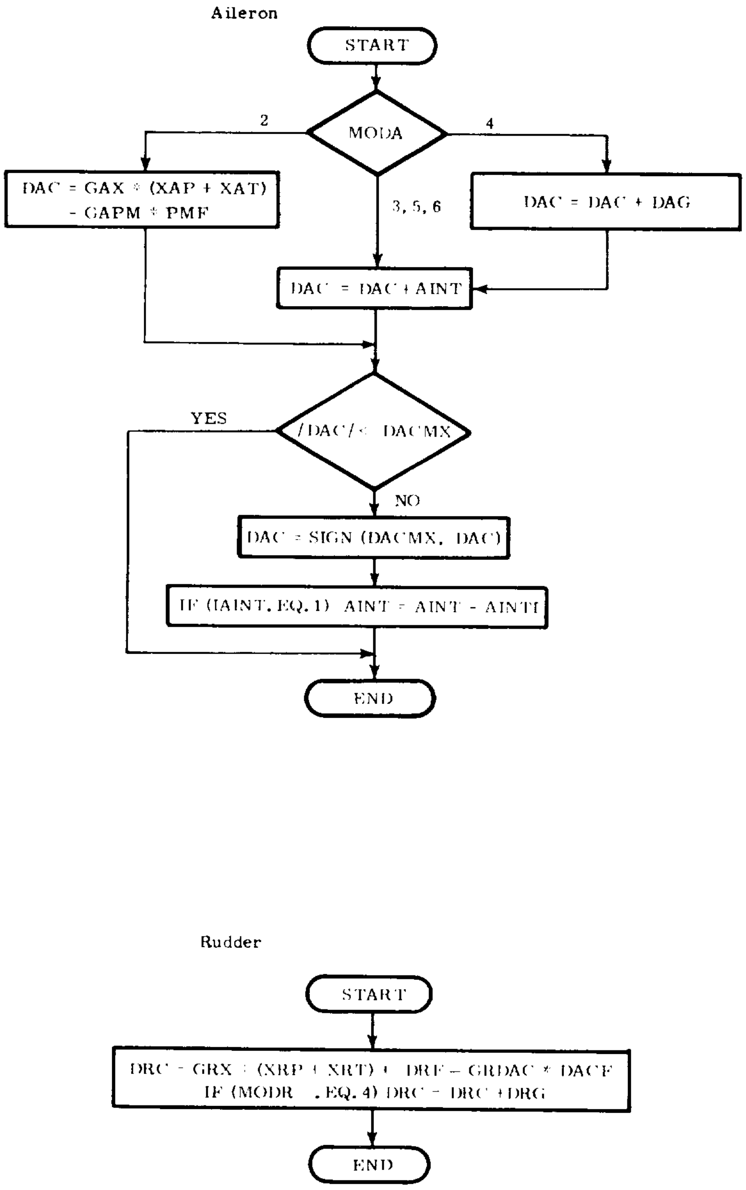

Fig. 4A-13 Control Law Subroutine, Cruise Phase Section, Aileron and Rudder Subsections

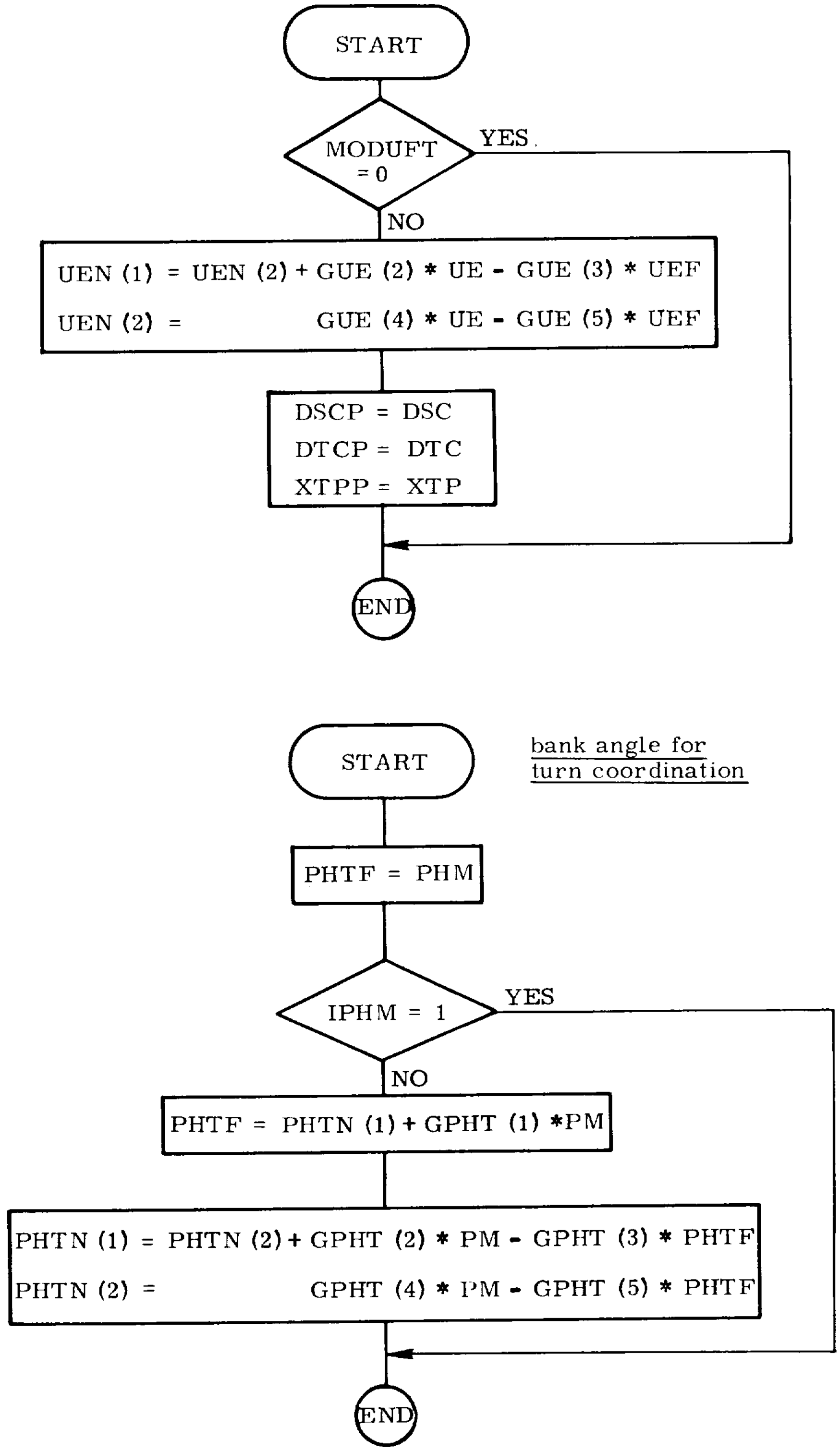
START
MODUFT = 0
YES
NO
UEN (1) = UEN (2) + GUE (2) * UE - GUE (3) * UEF
UEN (2) = GUE (4) * UE - GUE (5) * UEF
DSCP = DSC
DTCP = DTC
XTPP = XTP
END
START
bank angle for turn coordination
PHTF = PHM
IPHM = 1
YES
NO
PHTF = PHTN (1) + GPHT (1) *PM
PHTN (1) = PHTN (2) + GPHT (2) * PM - GPHT (3) * PHTF
PHTN (2) = GPHT (4) * PM - GPHT (5) * PHTF
END

Fig. 4A-14 Filter Part II Subroutine, Cruise Phase Section, Speed Subsection

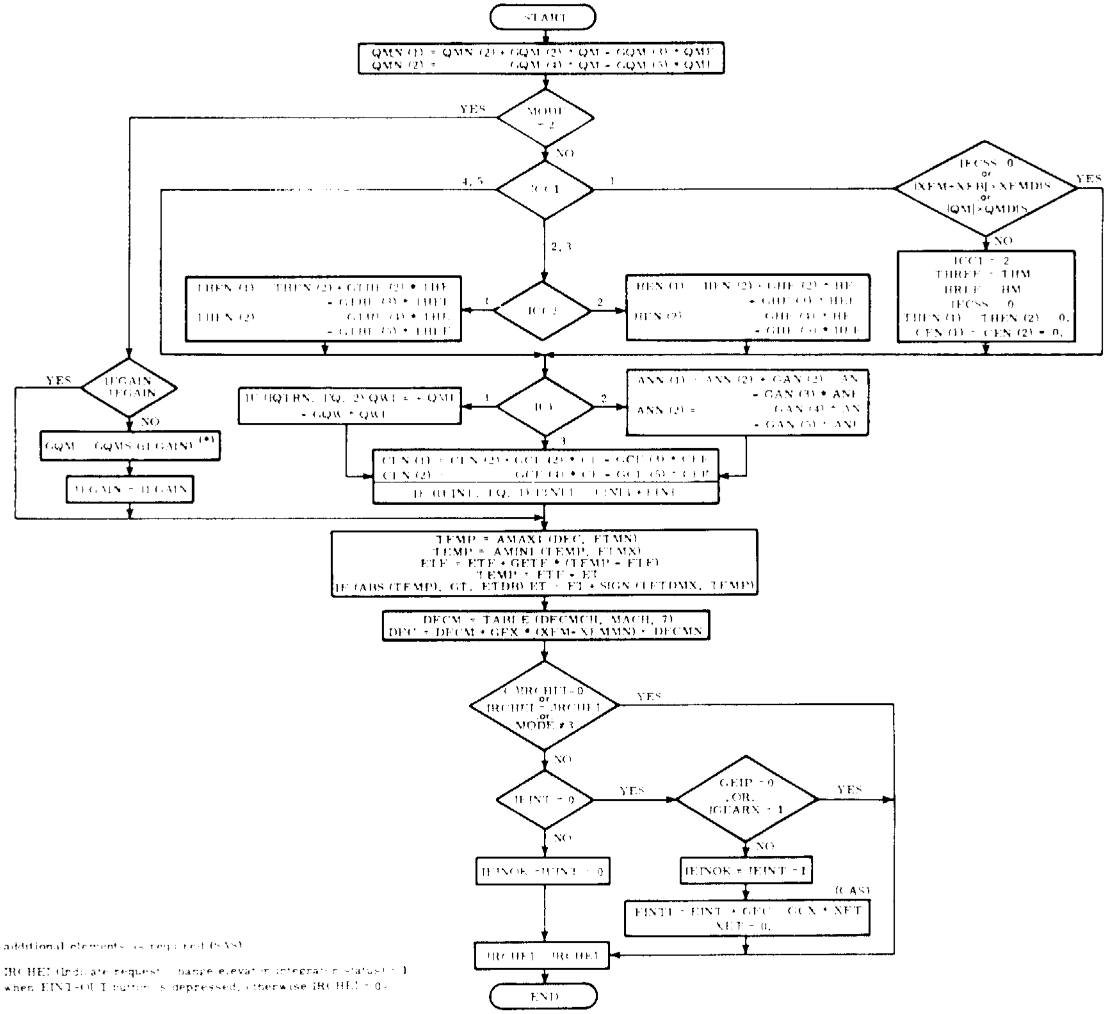
START
QMN (1) = QMN (2) + GQM (2) * QM - GQM (3) * QMF
QMN (2) = GQM (4) * QM - GQM (5) * QMF
MODE = 2
YES
NO
ICC 1
4, 5
1
2, 3
IFCSS 0 or |XEM+XEB|>XEMDIS or |QM|>QMDIS
YES
NO
ICCI = 2
THREF = THM
HREF HM
IFCSS 0
THEN (1) THEN (2) 0.
CEN (1) = CEN (2) = 0.
ICC 2
1
2
THEN (1) THEN (2) + GTHE (2) * THE
- GTHE (3) * THEF
THEN (2) GTHE (4) * THE
- GTHE (5) * THEF
HEN (1) HEN (2) + GHE (2) * HE
- GHE (3) * HEF
HEN (2) GHE (4) * HE
- GHE (5) * HEF
IFGAIN IEGAIN
YES
NO
GQM GQMS (IEGAIN) (*)
IEGMN = IEGAIN
ICC
1
2
3
IF (IQTRN. EQ. 2) QWE = - QMF
- GQW * QWE
ANN (1) = ANN (2) + GAN (2) AN
- GAN (3) * ANF
ANN (2) = GAN (4) * AN
- GAN (5) * ANF
CEN (1) = CEN (2) + GCE (2) * CE - GCE (3) * CEF
CEN (2) = GCE (4) * CE - GCE (5) * CEF
IF (IEINT. EQ. 1) EINTI EINTI + EINT
TEMP = AMAXI (DEC, ETMN)
TEMP = AMINI (TEMP, ETMX)
ETF = ETF + GETF * (TEMP - ETF)
TEMP = ETF - ET
IF (ABS (TEMP). GT. ETDB) ET = ET + SIGN (ETDMX, TEMP)
DECM = TABLE (DECMCH, MACH, 7)
DEC = DECM + GFX * (XEM- XEMMN) + DECMN
IRCHEI=0 or IRCHEI = IRCHEI or MODE ≠ 3
YES
NO
IEINT = 0
YES
NO
GEIP = 0 .OR. IGEARX = 1
YES
NO
IEINOK =IEINT = 0
IEINOK = IEINT = 1
(CAS)
EINTI = EINT + GEC GCX * NET
NET = 0.
IRCHEI IRCHEI
END

(*) additional elements as required (SAS)

(•) IRCHEI (Indicate request change elevator integration status) = 1 when EINT-OUT button is depressed, otherwise IRCHEI = 0.

Fig. 4A-15 Filter Part II Subroutine, Cruise Phase Section, Elevator Subsection

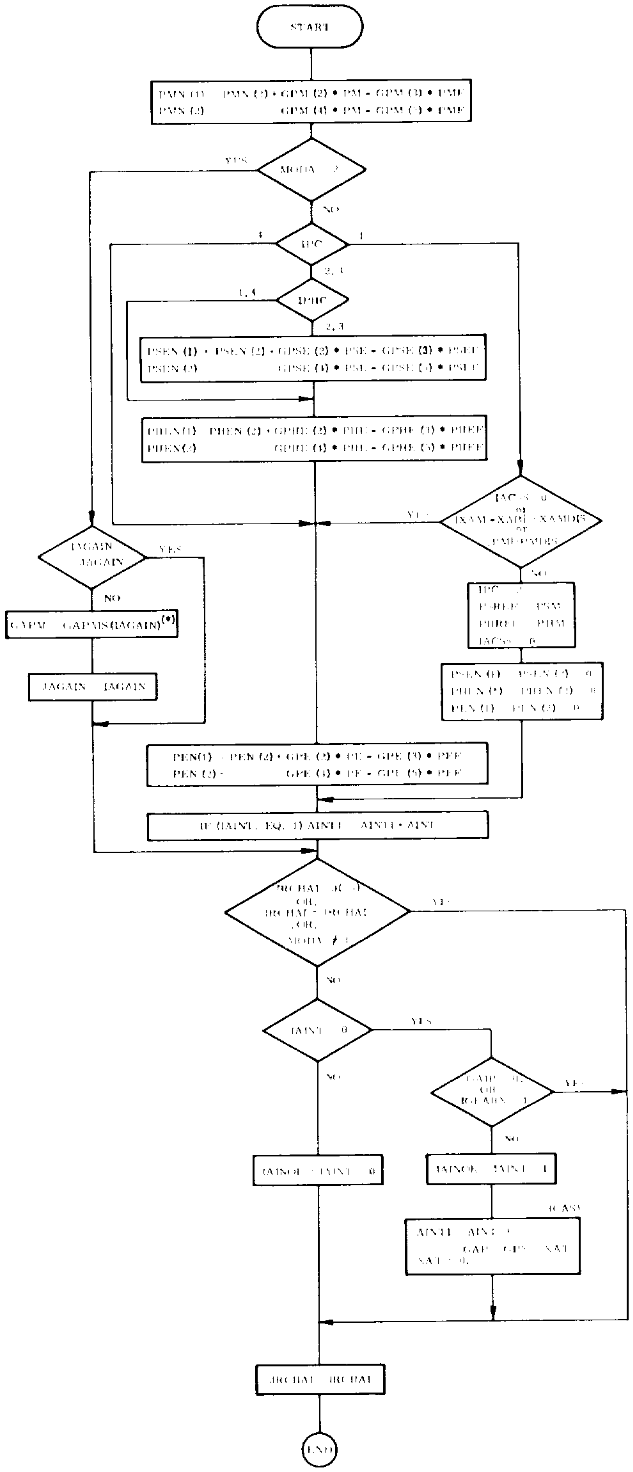
START
PMN (1)   PMN (2) + GPM (2) • PM - GPM (3) • PMF
PMN (2)   GPM (4) • PM - GPM (5) • PMF
YES
MODA 2
NO
4
IPC
1
2, 3
1, 4
IPHC
2, 3
PSEN (1) + PSEN (2) + GPSE (2) • PSE - GPSE (3) • PSEF
PSEN (2)   GPSE (4) • PSE - GPSE (5) • PSEF
PHEN (1)   PHEN (2) + GPHE (2) • PHE - GPHE (3) • PHEF
PHEN (2)   GPHE (4) • PHE - GPHE (5) • PHEF
IACS 0
or
IXAM • XAPE XAMDIS
or
PME PMDIS
YES
NO
IPC 2
PSREF PSM
PHREF PHM
IACS 0
PSEN (1) PSEN (2) 0
PHEN (1) PHEN (2) 0
PEN (1) PEN (2) 0
IYGAIN
JAGAIN
YES
NO
GAPM GAPMS(IAGAIN)(*)
JAGAIN IAGAIN
PEN(1) PEN (2) + GPE (2) • PE - GPE (3) • PEF
PEN (2) GPE (4) • PE - GPE (5) • PEF
IF (IAINT. EQ. 1) AINTI AINTI + AINT
IRCHAT JC
.OR.
IRCHAT IRCHAT
.OR.
MODA ≠ 3
YES
NO
IAINT 0
YES
NO
GAIP 0
OR
IGEAIN 1
YES
NO
IAINOL IAINT 0
IAINOL IAINT 1
(CAS)
AINTI AINT 0
GAP GPS SAT
SAT 0.
JRCHAT IRCHAT
END

(*) additional elements as required (SAS)

(+) IRCHAT tivate request change aileron integrator status:
1 when AINT-OUT button is depressed; otherwise IRCHAT 0

Fig. 4A-16 Filter Part II Subroutine, Cruise Phase Section, Aileron Subsection

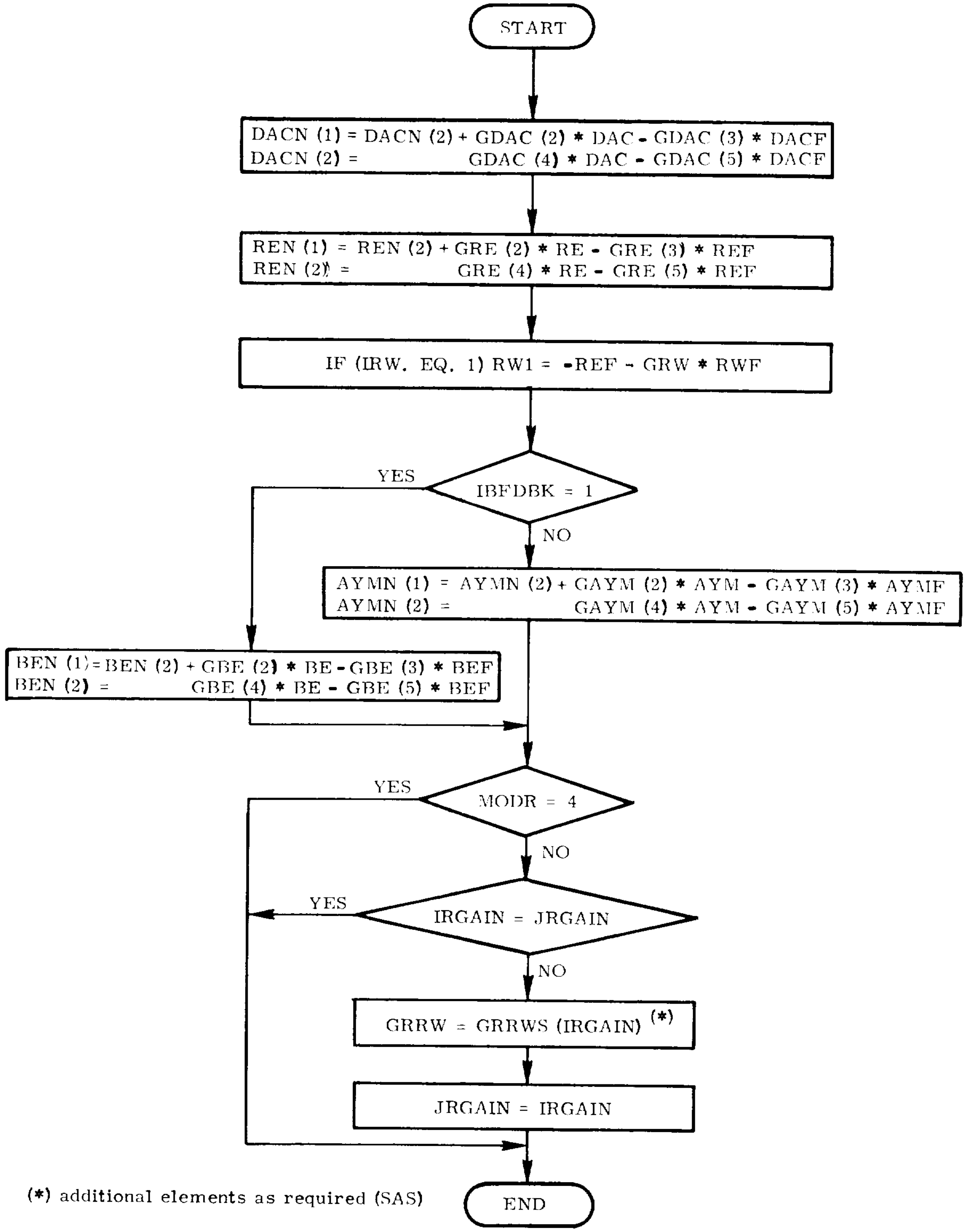
START
DACN (1) = DACN (2) + GDAC (2) * DAC - GDAC (3) * DACF
DACN (2) = GDAC (4) * DAC - GDAC (5) * DACF
REN (1) = REN (2) + GRE (2) * RE - GRE (3) * REF
REN (2) = GRE (4) * RE - GRE (5) * REF
IF (IRW. EQ. 1) RW1 = -REF - GRW * RWF
IBFDBK = 1
YES
NO
AYMN (1) = AYMN (2) + GAYM (2) * AYM - GAYM (3) * AYMF
AYMN (2) = GAYM (4) * AYM - GAYM (5) * AYMF
BEN (1) = BEN (2) + GBE (2) * BE - GBE (3) * BEF
BEN (2) = GBE (4) * BE - GBE (5) * BEF
MODR = 4
YES
NO
IRGAIN = JRGAIN
YES
NO
GRRW = GRRWS (IRGAIN) (*)
JRGAIN = IRGAIN
END

(*) additional elements as required (SAS)

Fig. 4A-17 Filter Part II Subroutine, Cruise Phase Section, Rudder Subsection

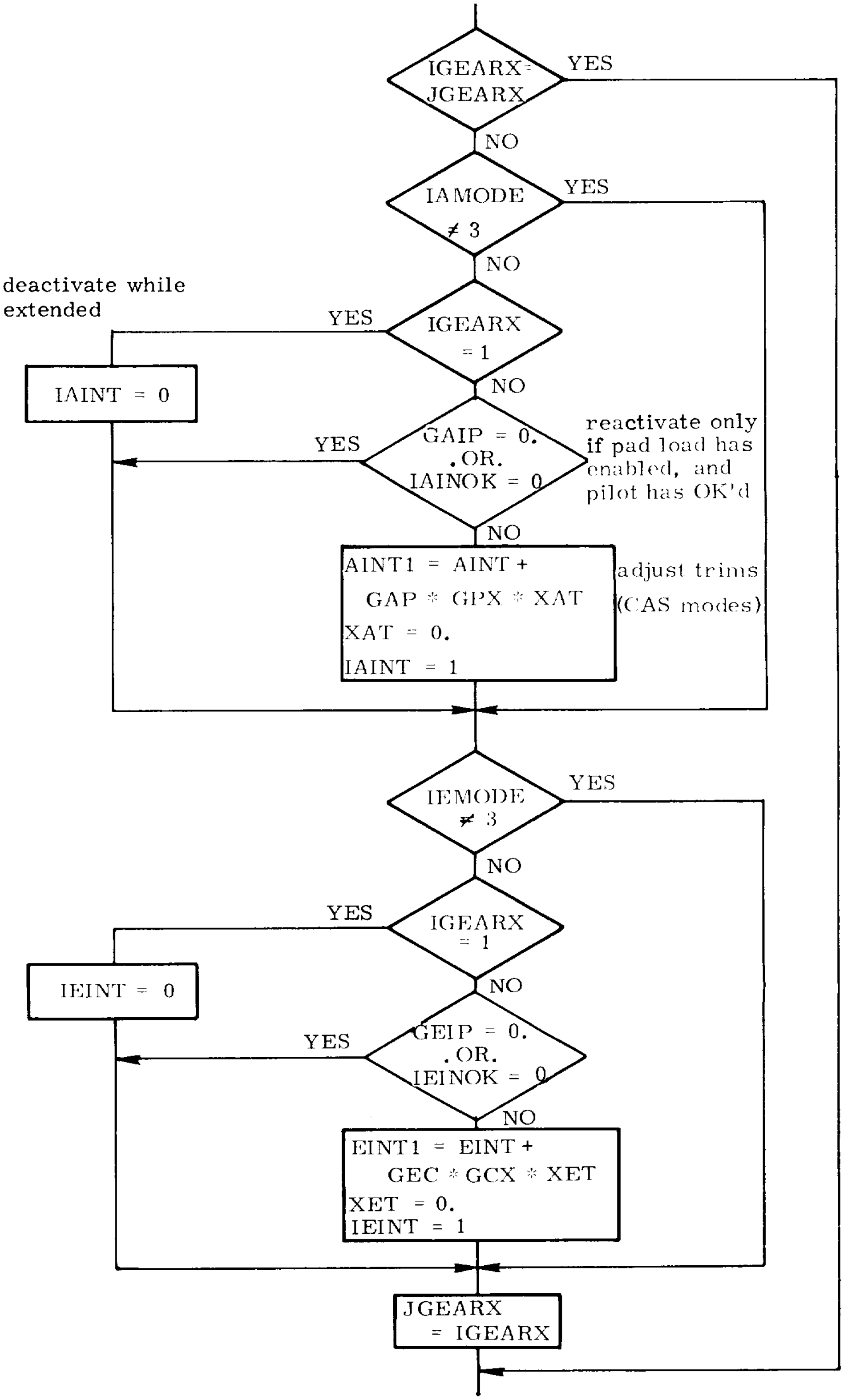

IGEARX= JGEARX
YES
NO
IAMODE ≠ 3
YES
NO
deactivate while extended
YES
IGEARX = 1
IAINT = 0
NO
YES
GAIP = 0. .OR. IAINOK = 0
reactivate only if pad load has enabled, and pilot has OK'd
NO
AINT1 = AINT + GAP * GPX * XAT
XAT = 0.
IAINT = 1
adjust trims (CAS modes)
IEMODE ≠ 3
YES
NO
YES
IGEARX = 1
IEINT = 0
NO
YES
GEIP = 0. .OR. IEINOK = 0
NO
EINT1 = EINT + GEC * GCX * XET
XET = 0.
IEINT = 1
JGEARX = IGEARX

Fig. 4A-18 Filter Part II Subroutine, Cruise Phase Section, Gear/Integrating Moding

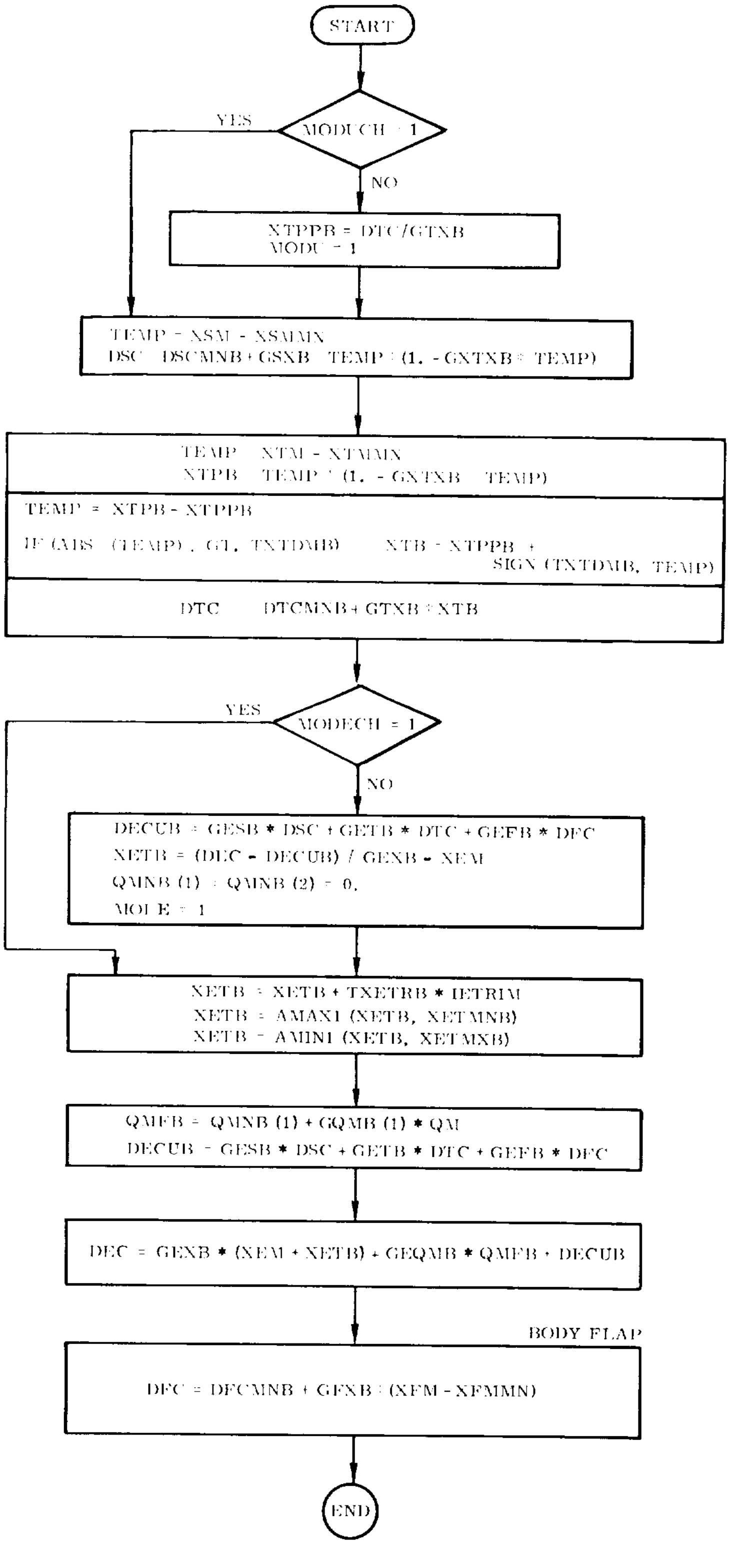
START
YES
MODUCH = 1
NO
XTPPB = DTC/GTXB
MODU = 1
TEMP = XSM - XSMMN
DSC DSCMNB+GSXB TEMP * (1. - GXTXB * TEMP)
TEMP XTM - XTMMN
XTPB TEMP * (1. - GXTXB TEMP)
TEMP = XTPB - XTPPB
IF (ABS (TEMP) . GT. TXTDMB) XTB = XTPPB + SIGN (TXTDMB, TEMP)
DTC DTCMNB+ GTXB * XTB
YES
MODECH = 1
NO
DECUB = GESB * DSC + GETB * DTC + GEFB * DFC
XETB = (DEC - DECUB) / GEXB - XEM
QMNB (1) = QMNB (2) = 0.
MOLE = 1
XETB = XETB + TXETRB * IETRIM
XETB = AMAX1 (XETB, XETMNB)
XETB = AMIN1 (XETB, XETMXB)
QMFB = QMNB (1) + GQMB (1) * QM
DECUB = GESB * DSC + GETB * DTC + GEFB * DFC
DEC = GEXB * (XEM + XETB) + GEQMB * QMFB + DECUB
BODY FLAP
DFC = DFCMNB + GFXB * (XFM - XFMMN)
END

Fig. 4A-19a Cruise Phase BCS Subroutine, Speed, Elevator, and Flap Subsection

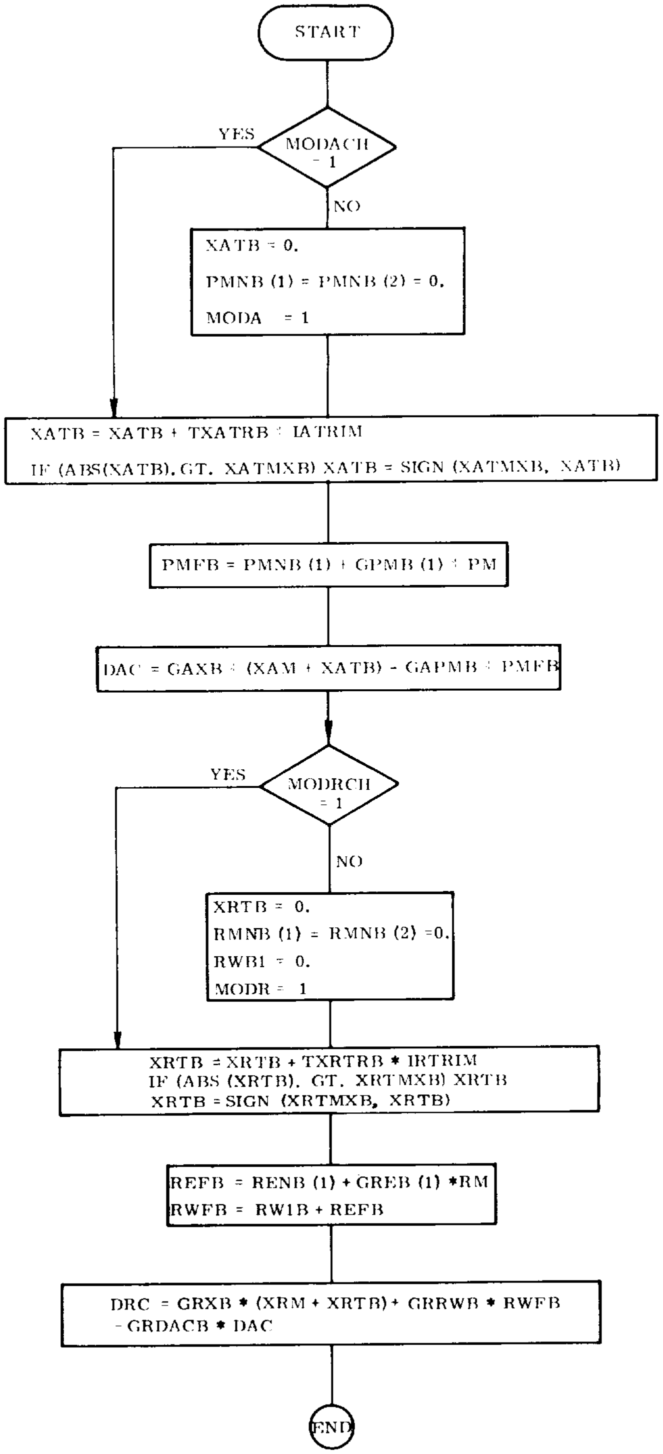
START
MODACH
= 1
YES
NO
XATB = 0.
PMNB (1) = PMNB (2) = 0.
MODA = 1
XATB = XATB + TXATRB * IATRIM
IF (ABS(XATB).GT. XATMXB) XATB = SIGN (XATMXB, XATB)
PMFB = PMNB (1) + GPMB (1) * PM
DAC = GAXB * (XAM + XATB) - GAPMB * PMFB
MODRCH
= 1
YES
NO
XRTB = 0.
RMNB (1) = RMNB (2) =0.
RWB1 = 0.
MODR = 1
XRTB = XRTB + TXRTRB * IRTRIM
IF (ABS (XRTB). GT. XRTMXB) XRTB
XRTB = SIGN (XRTMXB, XRTB)
REFB = RENB (1) + GREB (1) *RM
RWFB = RW1B + REFB
DRC = GRXB * (XRM + XRTB) + GRRWB * RWFB
- GRDACB * DAC
END

Fig. 4A-19b Cruise Phase BCS Subroutine, Aileron and Rudder Subsection

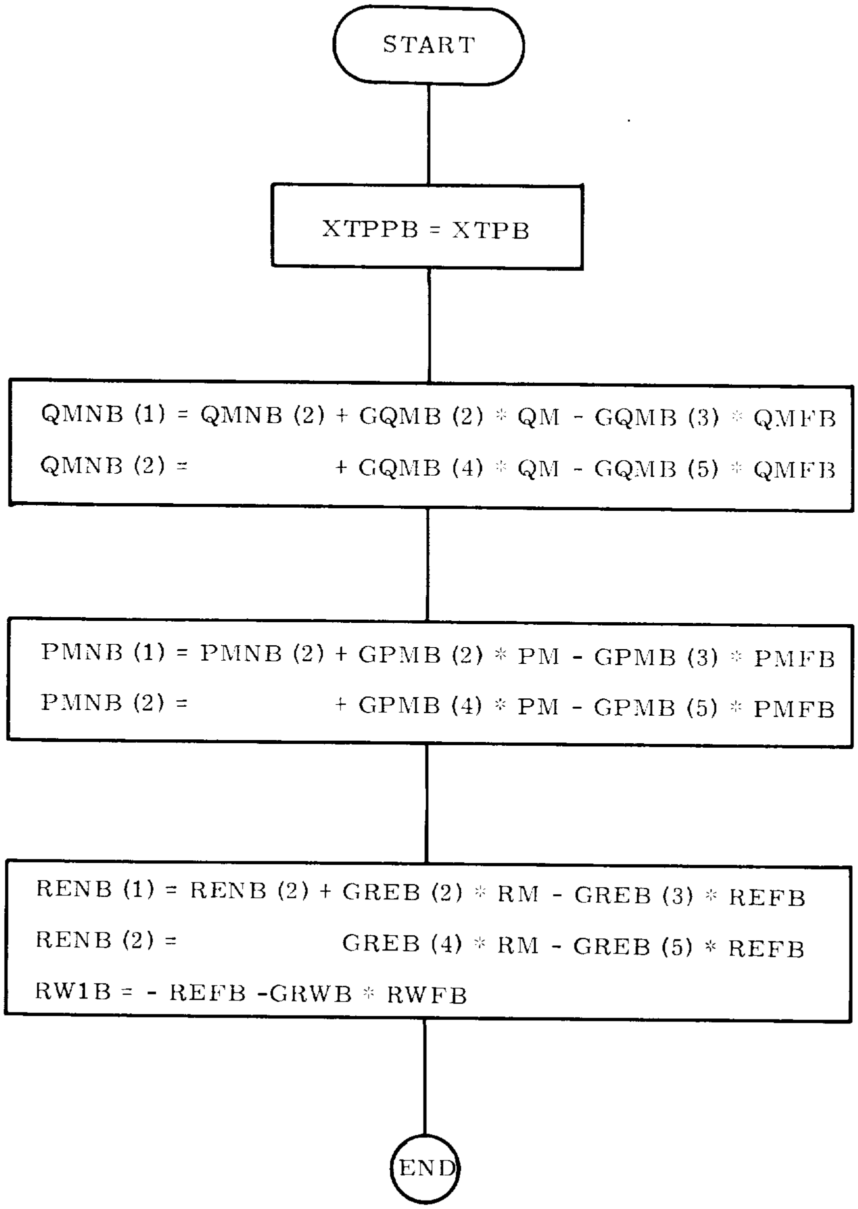
START
XTPPB = XTPB
QMNB (1) = QMNB (2) + GQMB (2) * QM - GQMB (3) * QMFB
QMNB (2) = + GQMB (4) * QM - GQMB (5) * QMFB
PMNB (1) = PMNB (2) + GPMB (2) * PM - GPMB (3) * PMFB
PMNB (2) = + GPMB (4) * PM - GPMB (5) * PMFB
RENB (1) = RENB (2) + GREB (2) * RM - GREB (3) * REFB
RENB (2) = GREB (4) * RM - GREB (5) * REFB
RW1B = - REFB -GRWB * RWFB
END

Fig. 4A-20 Cruise Phase BCS Subroutine, Wrap up Subsection

SECTION 5

ENTRY PHASE

5.1 Introduction

The DFCS design presented in this section is intended to provide stability-axis attitude control for the vehicle during entry, where this mission phase begins outside the sensible atmosphere (e.g., at approximately 400,000 ft altitude) and ends in the high subsonic flight regime. The control logic makes use of both the ACPS and the aerodynamic control surface torques, blended together in such a manner as to minimize ACPS jet activity, while providing capability for simultaneous parallel use when necessary.

The basic design features include gain scheduling and control submode switching (both as functions of selected trajectory parameters) to account for variations in the vehicle dynamics and to allow for reasonably constant closed-loop transient response characteristics. In addition, except for very low dynamic pressure operation, maximum use is made of the aerodynamic control surfaces to minimize ACPS fuel. Finally, the controller synthesis, and thus the design presented here, makes advantageous use of the vehicle's aerodynamic torques resulting from trim attitude deviations, allowing the vehicle's rigid body aerodynamics to aid in attitude maneuvers.

This section is organized into three subsections. Subsection 5.2 provides an overview of the entry DFCS organization and operational characteristics, while Subsection 5.3 is a detailed description of the entry DFCS, both functionally and as implemented in the present FORTRAN simulator. Finally, Subsection 5.4 is a brief summary of simulation experience to date.

5.2 Overview

Figure 5-1 provides an overview of the entry phase control logic structure. The interface, state estimation, and air data routines are described in Section 2 (Subsection 2.1), Section 3, and Section 2 (Subsection 2.2), respectively. The purpose of the first two is to provide estimates of the stability axis angles and rates, along with the guidance commands, while the purpose of the latter is to provide

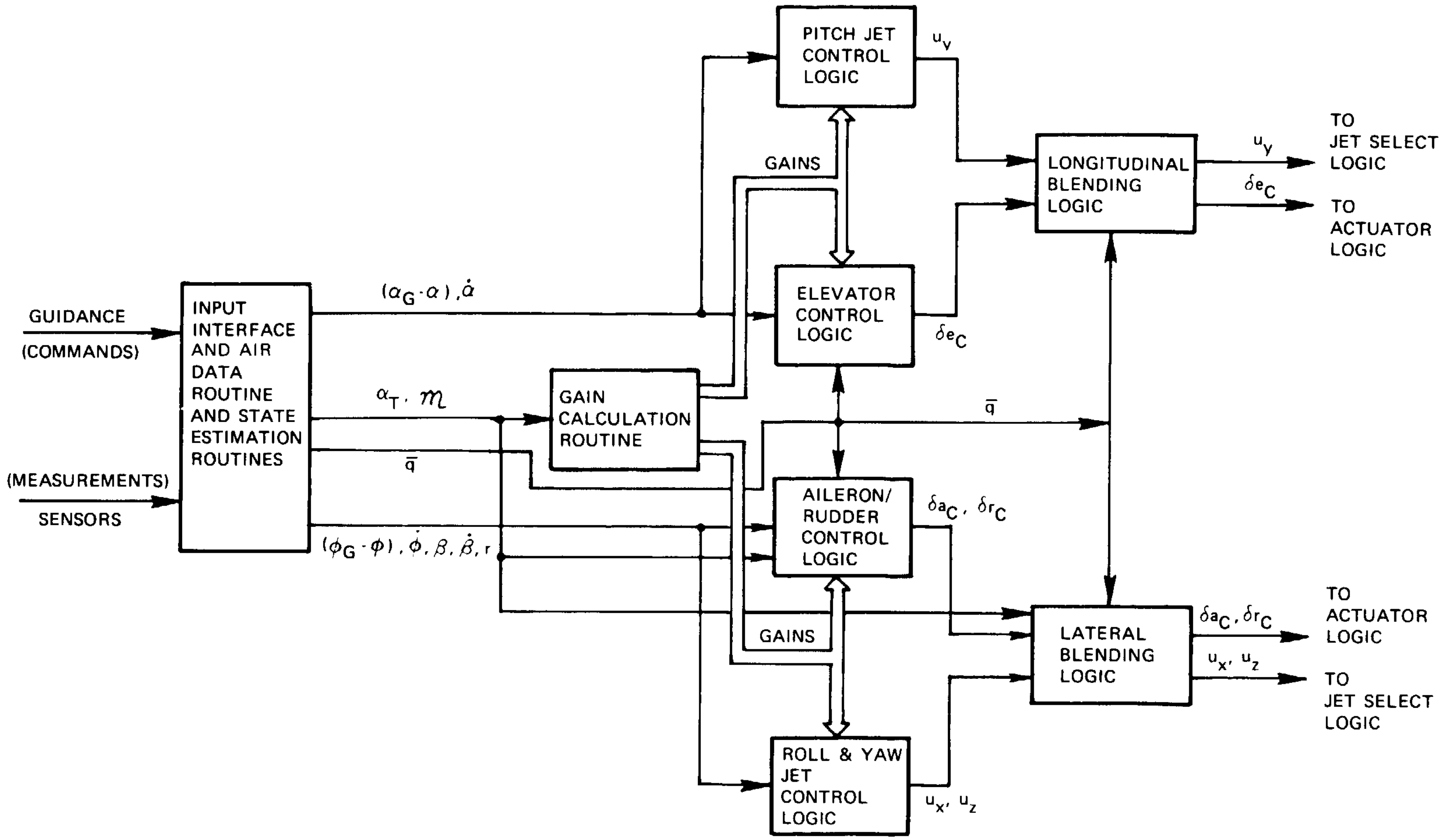

Fig. 5-1 Overview of Entry Control

estimates of the trajectory parameters (trim angle-of-attack, Mach number, and dynamic pressure).

Longitudinal control of angle-of-attack and pitch rate is provided by elevator (tandem elevon) deflections and pitch ACPS jet firings. The elevator logic uses conventional rate and position feedback (with feedforward trim integration) through scheduled gains to maintain relatively constant closed-loop pitch dynamics, while the ACPS logic uses phase-plane control to maintain a desired limit-cycle operation.

Lateral control of sideslip and bank angle is provided by aileron (differential elevon) and rudder deflections, and roll and yaw ACPS jet firings. The aileron/ rudder logic uses rate and position feedback of the lateral variables (with feed-forward trim integration for center-of-gravity offset compensation) to provide attitude and rate control of both sideslip and bank. The ACPS logic uses phase-plane control to maintain a desired limit-cycle operation when there is low dynamic pressure, and sideslip rate damping to maintain lateral stability when there is high dynamic pressure.

In both the lateral and longitudinal channels, blending of control by the surfaces and the ACPS is provided through a logic which determines ACPS inhibition on the basis of the magnitude of the current surface command, and on the basis of the vehicle's Mach number and angle-of-attack.

5.3 Description of Control Laws

This section presents the control system block diagrams, equations, system parameters, and detailed flow charts defining the entry DFCS design. For convenient reference, this section is divided into four subsections. Subsection 5.3.1 and 5.3.2 describe the longitudinal and lateral control laws, while Subsection 5.3.3 specifies the fixed and scheduled parameters used in the present design.

5.3.1 Longitudinal Control

Longitudinal control uses both elevator (tandem elevon) and pitch ACPS jets to maintain the commanded angle-of-attack. As shown in Fig. 5-2, which illustrates a typical sequence of control activity during entry, there are two control submodes for the elevator and one for the pitch jets.

Early in the entry, when the dynamic pressure is low, the elevator is used strictly for trim, so as to minimize pitch disturbance torques and thus fuel usage. The trim control law operates in a closed-loop fashion by slowly driving the elevator in the direction which nulls the pitch disturbance. The estimate of the disturbance torque is obtained by observing the pitch ACPS firing history. During this flight

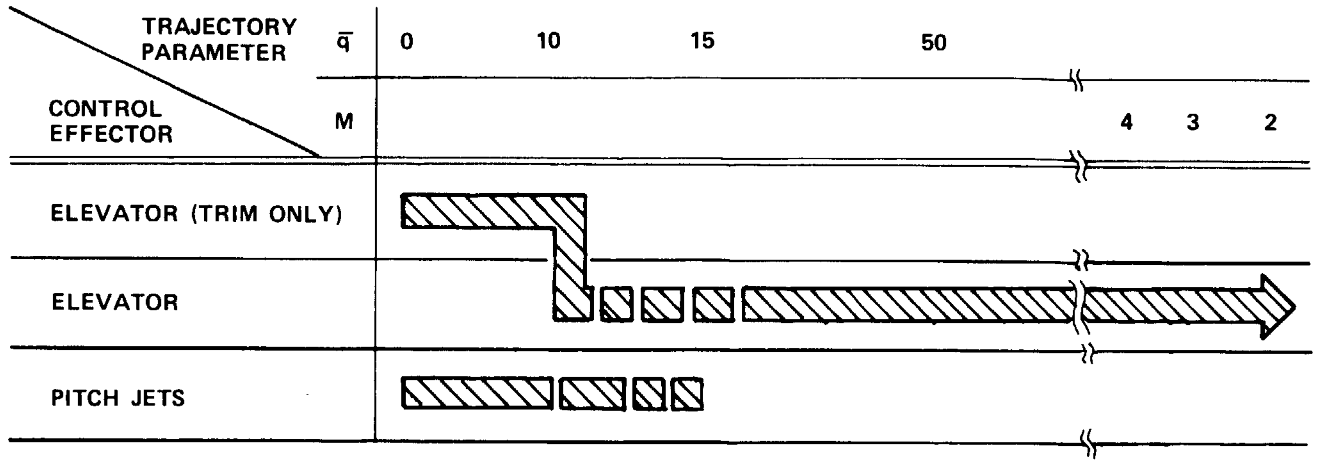

Fig. 5-2 Controller Activity during Entry (Longitudinal)

regime, the pitch ACPS jets, controlled by an angle-of-attack/pitch-rate phase-plane logic, provide attitude and rate control in response to guidance commands. There is no jet inhibition in this regime.

When the dynamic pressure gets high enough, $(\bar{q}_1)$, the elevator is used for both trim and transient control. Trim is initially maintained through the use of the trim logic of the previous submode. At a slightly higher dynamic pressure, $(\bar{q}_1^*)$, trim is maintained through the use of an integrator acting upon the angle-of-attack error; the initialization value of the integrator is obtained from the value generated by the previous trim logic. Elevator control of transient errors is maintained through feedback of angle-of-attack and pitch rate, with appropriate gains. During this flight regime, pitch jet control identical to that of the previous regime may be utilized together with the elevator, or control with the jets may be inhibited. This is done by the blending logic which is essentially a two-sided deadbanded relay with hysteresis. The commanded elevator deflection is compared with preset fractions of its maximum and minimum values; should the command be "small", it is assumed that the elevator has sufficient control authority, and thus the pitch jets are not required. Conversely, should the elevator command be "large", the pitch jet control is not inhibited, but is allowed to assist the elevator in controlling the vehicle. This blended control continues throughout the rest of the entry, so that the pitch jets are always available for control assistance.

The logic provides for a gradual turn-on of the elevator control so as to avoid a switching transient when the second control submode is entered.

The remainder of this section describes the longitudinal control laws, and their digital implementation, in detail. The block diagrams and equations defining the control logic for the elevator and pitch jets are given in Subsections 5.3.1.1 and 5.3.1.2. Subsection 5.3.1.3 consists of the controller coding summarized in flow chart form.

5.3.1.1 Elevator Control

Figure 5-3a is a block diagram of the elevator control loop, showing the two control submodes, with switching determined by $\bar{q}_1$[†].

When the dynamic pressure is less than $\bar{q}_1$, only an elevator trim setting is sent to the elevator actuator. This trim setting is determined by integrating the pitch ACPS commands (u_y), or, equivalently, by slowly driving the elevator so as to null the longitudinal disturbance torques.

When the dynamic pressure reaches $\bar{q}_1$, closed-loop control of the angle-of-

[†] See Subsection 5.3.3 for numerical values of the parameters

Note: $\bar{q}_1 < \bar{q}_1^*$

Nonlinearities: (1) Limiter; unity slope; $\delta e_C^{max} = (1 - K_e)\,\delta e_t + K_e\,\delta e^{max}$

$$\delta e_C^{min} = (1 - K_e)\,\delta e_t + K_e\,\delta e^{min}$$

(2) Clamped integrator; unity slope

(3) Limiter; unity slope

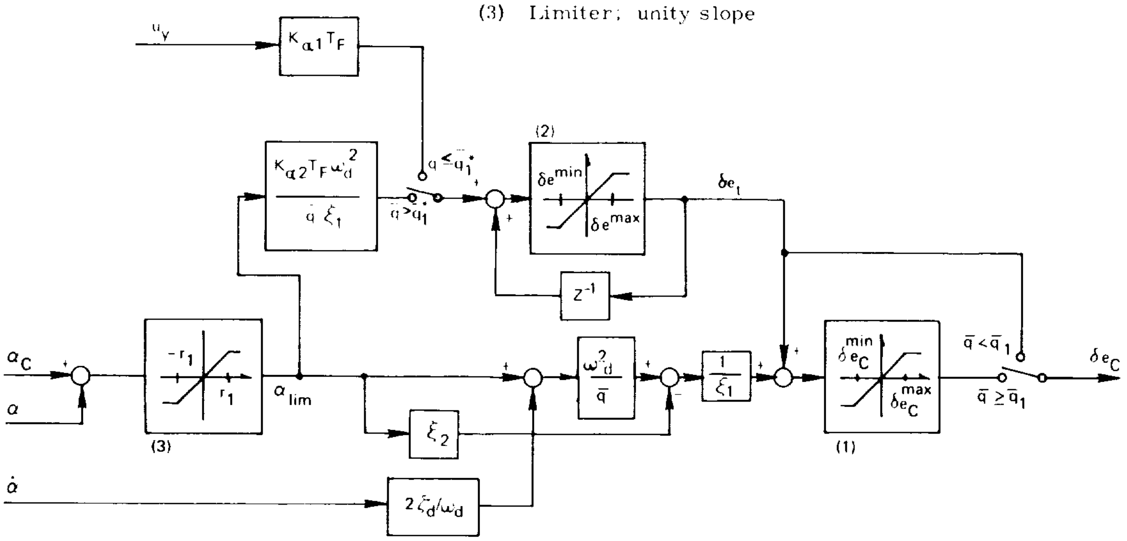

Fig. 5-3a Elevator Control Block Diagram

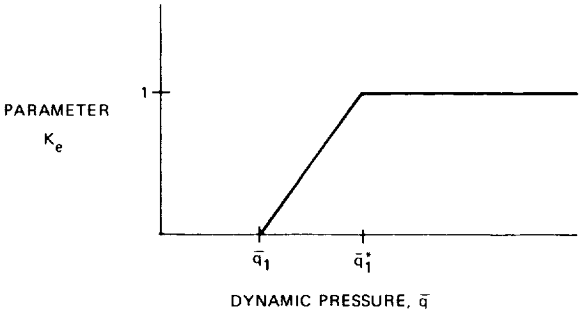

Fig. 5-3b Elevator Deflection Limit Parameter

attack is provided by conventional position (α) and rate ($\dot{\alpha}$) feedback through a network which attempts to maintain a constant transient response throughout the flight envelope. Specifically, the desired closed-loop transfer function is chosen to be a well-damped second-order system, or

$$\left[\frac{\alpha}{\alpha_G}\right]_{desired} = \frac{k_\alpha}{s^2 + 2\zeta_d\omega_d s + \omega_d^2} \qquad (5\text{-}1)$$

where (ζ_d, ω_d) are specified for acceptable performance (k_α is not explicitly specified). The gains shown in the diagram may be separated into one of three types: (1) prespecified by the desired closed-loop characteristics; (2) dynamic pressure dependent ($1/\bar{q}$); or (3) scheduled gains which are functions of the aerodynamic flight regime (e.g., ξ_1).[†] Trim control is accomplished in this submode either by the trim logic of the previous submode (if $\bar{q} \le \bar{q}_1^*$) or by a conventional clamped trim integrator acting on the angle-of-attack error, thus providing a steady-state trim elevator command in the absence of transient angle-of-attack errors.

As can be seen from Fig. 5-3a and 5-3b, in order to allow a gradual blending in of active elevator control, the elevator command limits are functions of dynamic pressure which gradually open up from the trim setting to the physical deflection limits.

5.3.1.2 Pitch ACPS Control

Shown in Fig. 5-4 is the ACPS phase-plane switch logic representation used for control of the pitch jets. For longitudinal control, the phase-plane coordinates are angle-of-attack error and angle-of-attack rate, or

$$(\epsilon_1, \epsilon_2) = (\alpha - \alpha_G, \dot{\alpha}) \qquad (5\text{-}2a)$$

The phase-plane is separated into three regions (by the switch curves), in which the commanded jet firing is either positive ($u = +1$), negative ($u = -1$), or zero ($u = 0$). Thus, for the particular application of pitch jet control

$$(u, U) = (u_y, U_y) \qquad (5\text{-}2b)$$

where u_y and U_y symbolize the jet command and the available acceleration level, respectively.

The equations for the switch curves themselves are based on the fuel-time optimal solution to the double integrator control problem and are modified by

[†] See Subsection 5.3.3 for numerical values of the parameters

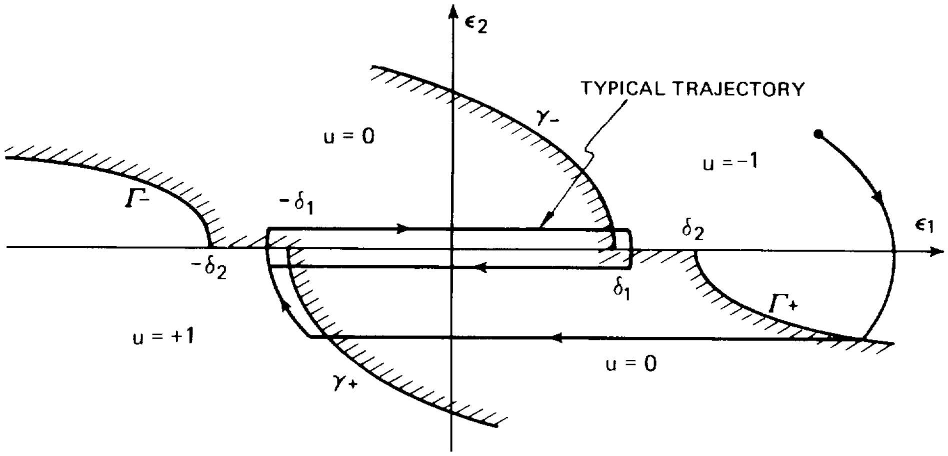

Fig. 5-4 ACPS Switch Logic

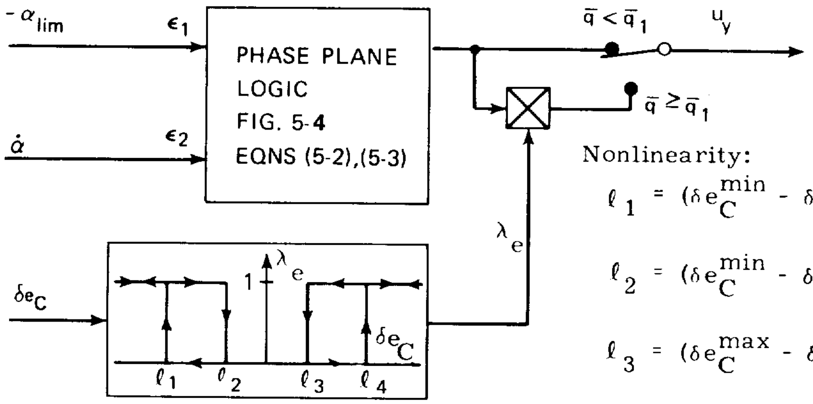

Nonlinearity:

$\ell_1 = (\delta e_C^{\min} - \delta e_t) f_1 + \delta e_t$

$\ell_2 = (\delta e_C^{\min} - \delta e_t) f_2 + \delta e_t$

$\ell_3 = (\delta e_C^{\max} - \delta e_t) f_2 + \delta e_t$

$\ell_4 = (\delta e_C^{\max} - \delta e_t) f_1 + \delta e_t$

[Note: α_{lim}, $\delta e_C^{\max}$, $\delta e_C^{\min}$ from Fig. 5-3a]

Output: λ_e = 1 or 0

Fig. 5-5 Pitch ACPS Control Block Diagram

deadband incorporation to ensure practical limit-cycle convergence (see typical trajectory of Fig. 5-4). The switch curves are defined by:

$$\gamma\pm: \quad \epsilon_1 = \mp(\delta_1 - \frac{1}{2U}\epsilon_2^2)$$

$$\Gamma\pm: \quad \epsilon_1 = \pm(\delta_2 + \frac{\sigma}{2U}\epsilon_2^2) \qquad (5\text{-}3a)$$

where, in this case, the deadbands are pitch attitude deadbands, or:

$$(\delta_1, \delta_2) = (\delta_{\alpha 1}, \delta_{\alpha 2}) \qquad (5\text{-}3b)$$

and σ is a fuel-time weighting constant greater than unity given for pitch control by:

$$\sigma = \sigma_\alpha \qquad (5\text{-}3c)$$

The interface (or blending) logic between commanded pitch jet firings and the commanded elevator deflections is shown in Fig. 5-5. The approach taken is to inhibit firing when there is "sufficient" pitch control acceleration from the elevator. This measure of sufficiency is obtained by comparing commanded elevator (δe_C shown in Fig. 5-3a) with threshold values to determine whether or not "excessive" elevator deflection is being called for. The hysteresis path included in the blending interface avoids chatter in elevator and ACPS activity due to cross-coupling effects. Note that this design includes an additional switch to preclude jet inhibition when the dynamic pressure is low and the elevator is used solely for trim.

5.3.1.3 Digital Implementation

Coding implementation for longitudinal control during the entry phase is summarized in flow-chart form in Fig. 5-6.

5.3.2 Lateral Control

Lateral control uses both aileron (differential elevons) and rudder, and roll and yaw ACPS jets to maintain small sideslip angles and follow commanded bank maneuvers. As shown in Fig. 5-7, which illustrates a typical sequence of control activity during entry, there are three control submodes for the aerodynamic control surfaces, one for the yaw jets, and three for the roll jets.

Early in the entry, when the dynamic pressure is low, the aileron and rudder commands are zero. During this regime, the yaw jets, controlled by a bank angle/yaw-rate phase-plane logic, provide attitude and rate control of the bank angle in response to guidance commands. The roll jets are controlled by one of two logics, depending on the yaw jet activity. When there are no yaw commands, the roll jets, controlled by a sideslip/sideslip-rate phase-plane logic, maintain small sideslip

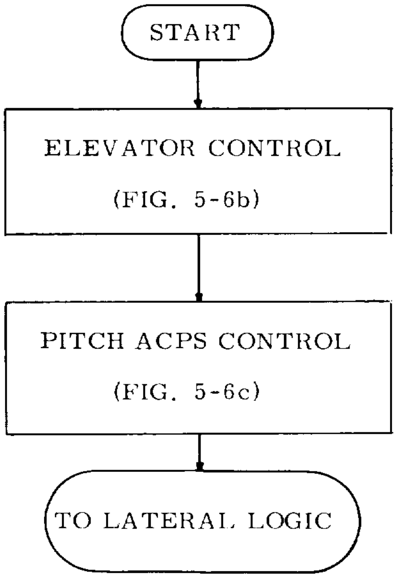

Fig. 5-6a Logic Flow for the Longitudinal Control Channel

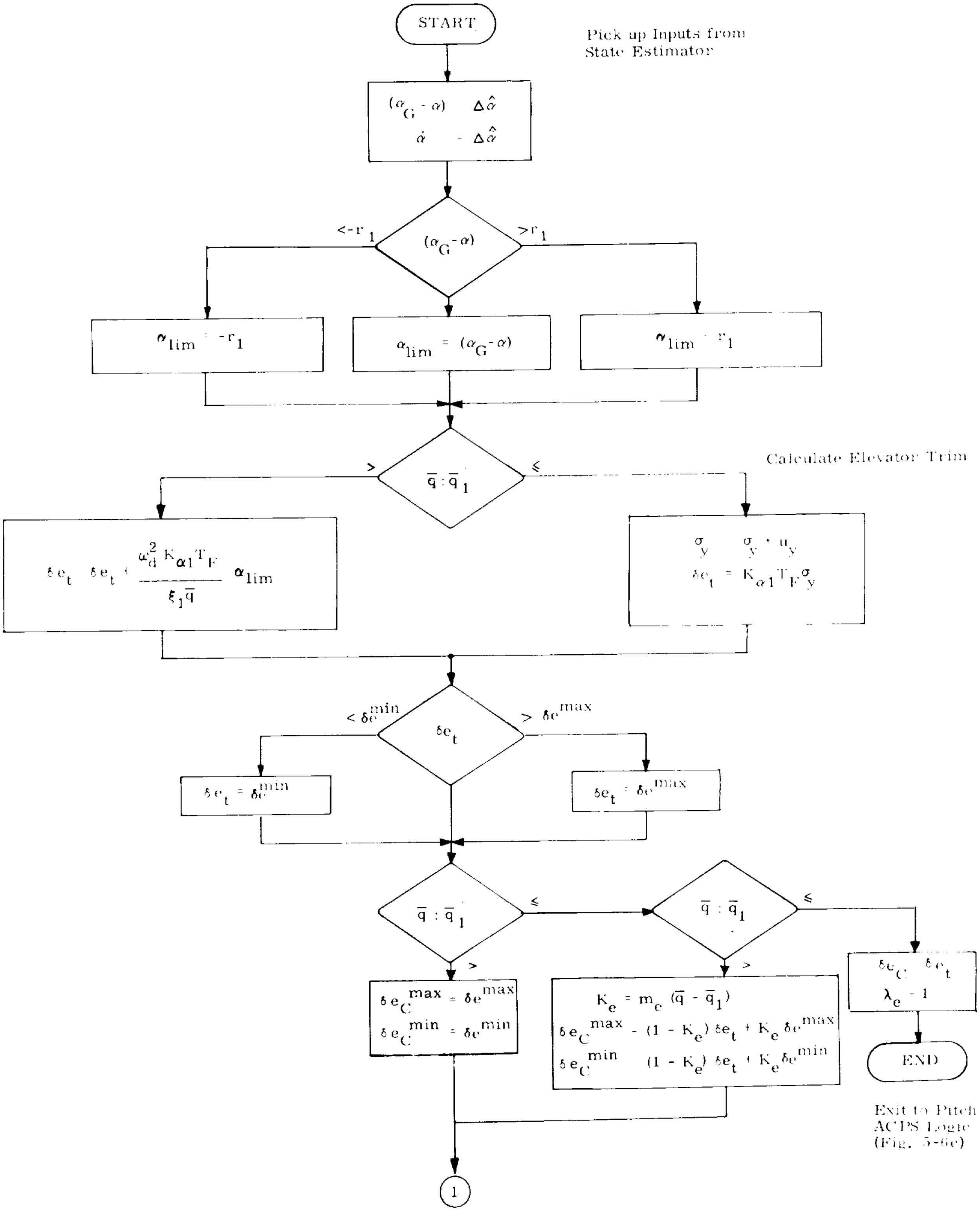
START
Pick up Inputs from State Estimator
$(\alpha_G - \alpha)$ $\Delta\hat{\alpha}$
$\dot{\alpha}$ $-\Delta\hat{\alpha}$
$<-r_1$
$(\alpha_G - \alpha)$
$>r_1$
$\alpha_{lim} = -r_1$
$\alpha_{lim} = (\alpha_G - \alpha)$
$\alpha_{lim} = r_1$
Calculate Elevator Trim
$>$
$\bar{q} : \bar{q}_1$
$\leq$
$\delta e_t = \delta e_t + \frac{\omega_d^2 K_{\alpha 1} T_F}{\xi_1 \bar{q}} \alpha_{lim}$
$\sigma_y = \sigma_y + u_y$
$\delta e_t = K_{\alpha 1} T_F \sigma_y$
$< \delta e^{min}$
δe_t
$> \delta e^{max}$
$\delta e_t = \delta e^{min}$
$\delta e_t = \delta e^{max}$
$\bar{q} : \bar{q}_1$
$\leq$
$\bar{q} : \bar{q}_1$
$\leq$
$>$
$>$
$\delta e_C^{max} = \delta e^{max}$
$\delta e_C^{min} = \delta e^{min}$
$K_e = m_e (\bar{q} - \bar{q}_1)$
$\delta e_C^{max} = (1 - K_e) \delta e_t + K_e \delta e^{max}$
$\delta e_C^{min} = (1 - K_e) \delta e_t + K_e \delta e^{min}$
$\delta e_C = \delta e_t$
$\lambda_e = 1$
END
Exit to Pitch ACPS Logic (Fig. 5-6e)
1

Fig. 5-6b Logic Flow for Elevator Control

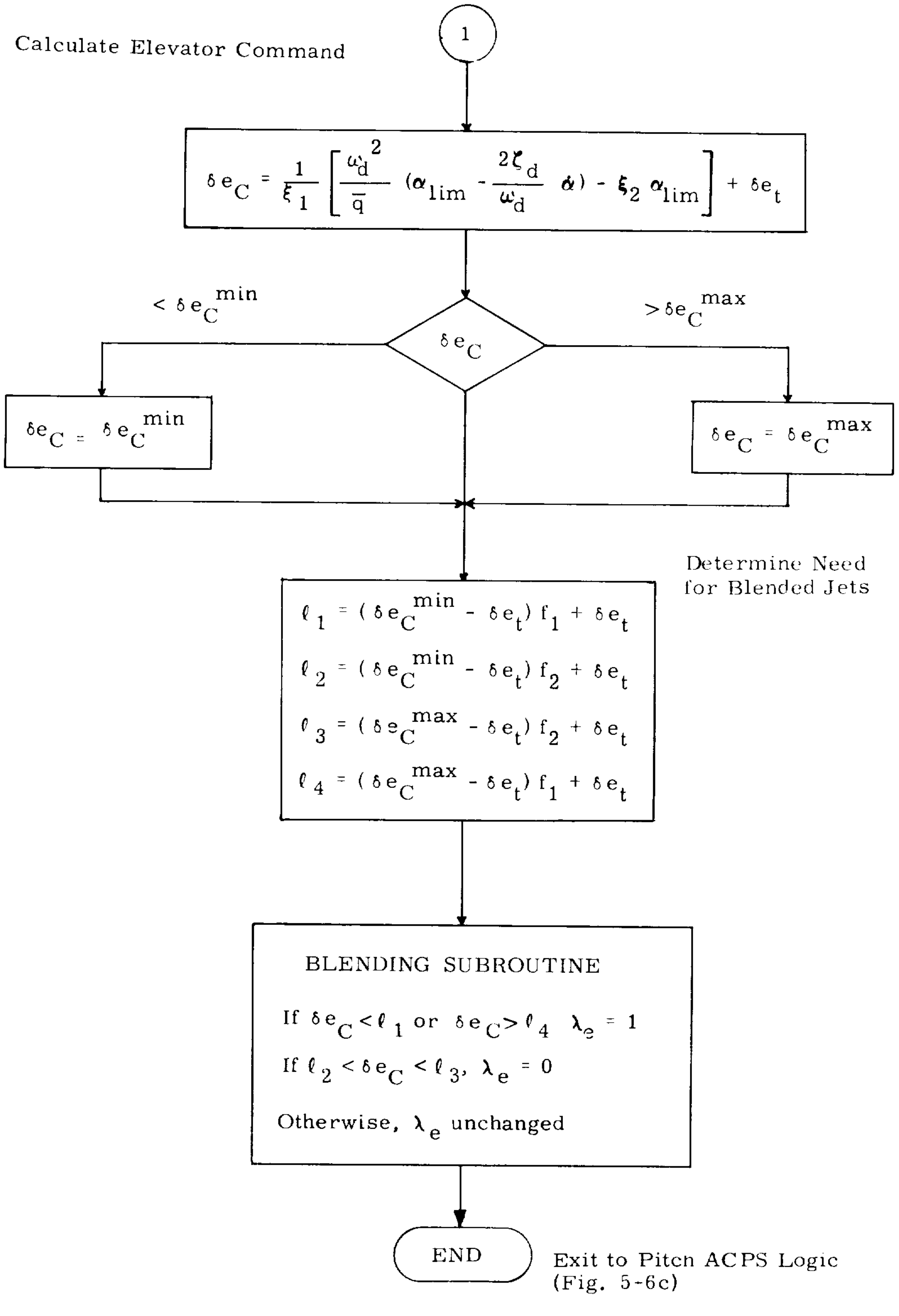
Calculate Elevator Command
1
$\delta e_C = \frac{1}{\xi_1}\left[\frac{\omega_d^2}{\bar{q}}\left(\alpha_{lim} - \frac{2\zeta_d}{\omega_d}\dot{\alpha}\right) - \xi_2\,\alpha_{lim}\right] + \delta e_t$
$< \delta e_C^{min}$
$> \delta e_C^{max}$
δe_C
$\delta e_C = \delta e_C^{min}$
$\delta e_C = \delta e_C^{max}$
Determine Need for Blended Jets
$\ell_1 = (\delta e_C^{min} - \delta e_t)\, f_1 + \delta e_t$
$\ell_2 = (\delta e_C^{min} - \delta e_t)\, f_2 + \delta e_t$
$\ell_3 = (\delta e_C^{max} - \delta e_t)\, f_2 + \delta e_t$
$\ell_4 = (\delta e_C^{max} - \delta e_t)\, f_1 + \delta e_t$
BLENDING SUBROUTINE
If $\delta e_C < \ell_1$ or $\delta e_C > \ell_4$ $\lambda_e = 1$
If $\ell_2 < \delta e_C < \ell_3$, $\lambda_e = 0$
Otherwise, λ_e unchanged
END
Exit to Pitch ACPS Logic (Fig. 5-6c)

Fig. 5-6b Logic Flow for Elevator Control (Cont)

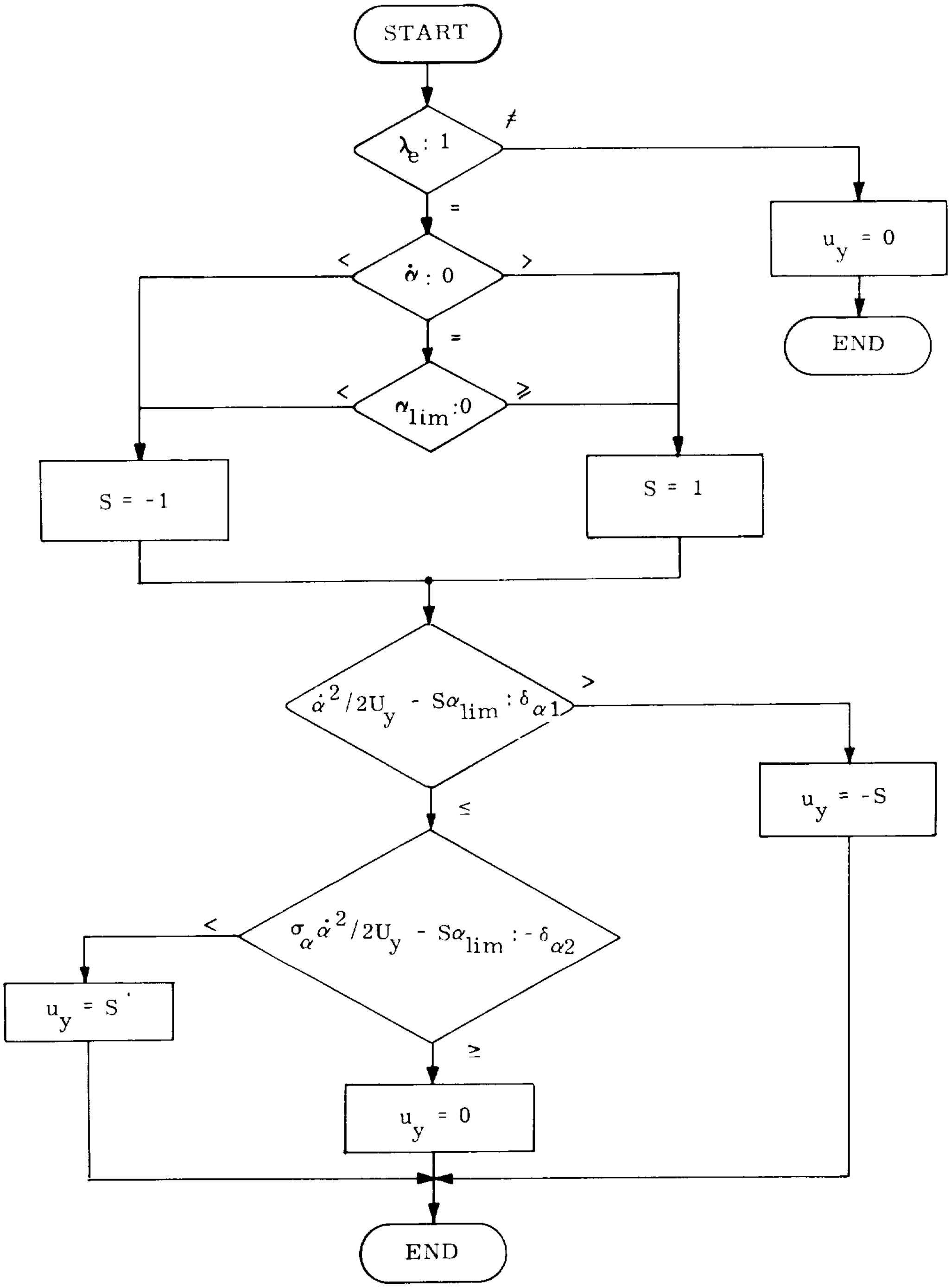
START
$\lambda_e : 1$
≠
$u_y = 0$
END
=
<
$\dot{\alpha} : 0$
>
=
<
$\alpha_{lim} : 0$
≥
S = -1
S = 1
$\dot{\alpha}^2 / 2U_y - S\alpha_{lim} : \delta_{\alpha 1}$
>
≤
$u_y = -S$
<
$\sigma_\alpha \dot{\alpha}^2 / 2U_y - S\alpha_{lim} : -\delta_{\alpha 2}$
$u_y = S$
≥
$u_y = 0$
END

Fig. 5-6c Logic Flow for Pitch ACPS Control

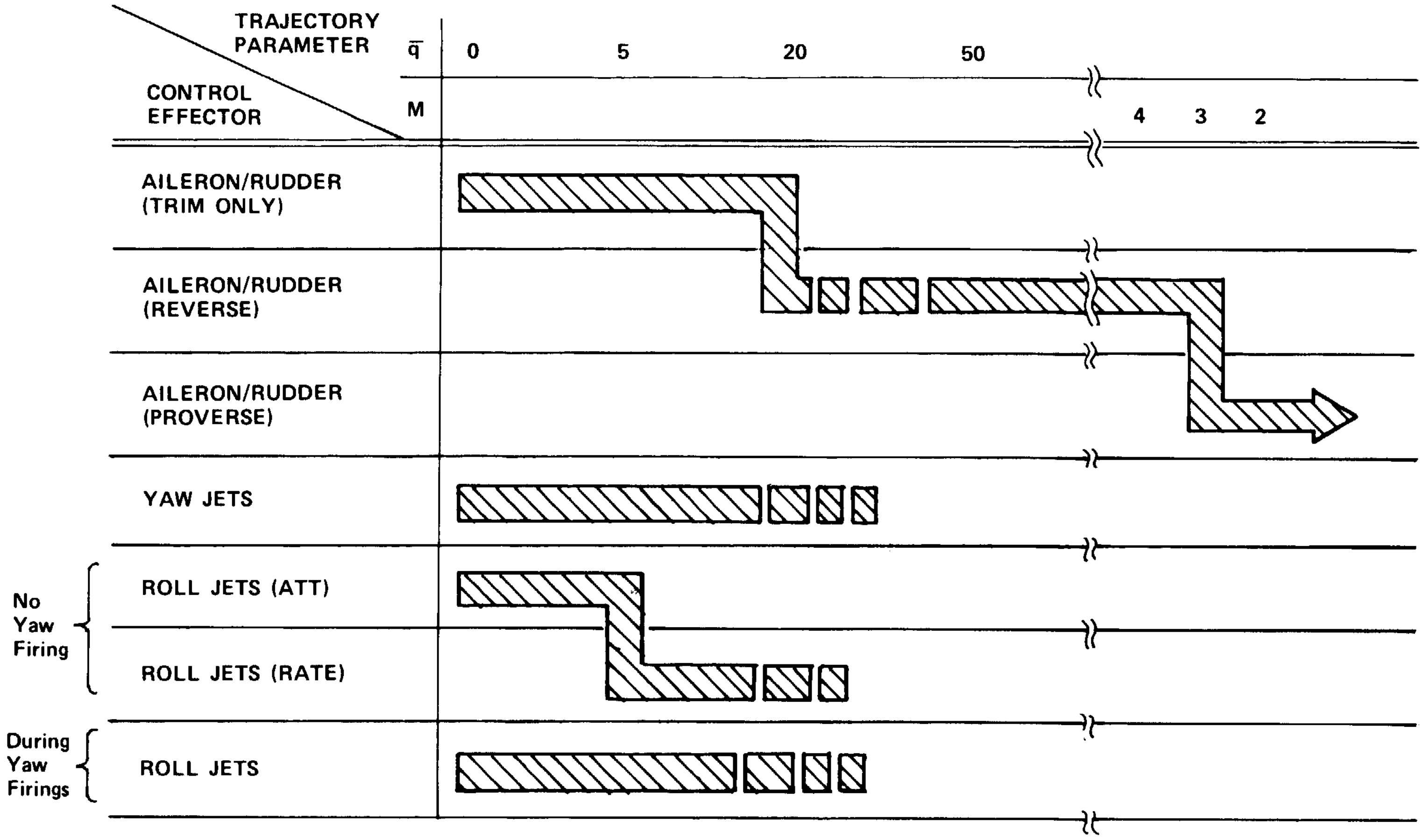

Fig. 5-7 Controller Activity during Entry (Lateral)

attitudes and rates. When the yaw jets are commanded to maneuver the vehicle, the roll jets are controlled by a sideslip/sideslip-rate phase-plane logic, which is similar to the first submode except that compensation for yaw jet torques is included. Again, the purpose of this logic is to maintain small sideslip attitudes and rates. There is no jet inhibition in this flight regime.

Later in the entry, when the dynamic pressure reaches a certain prespecified value ($\bar{q}_3$), the aileron and rudder commands are still zero. The yaw jets are controlled by the same logic as in the previous regime. The roll jets are controlled by one of two logics, again depending on yaw jet activity. When there are no yaw jet commands, the roll jets are commanded by a deadbanded relay logic which simply provides rate damping in sideslip. When the yaw jets are commanded to maneuver the vehicle, the roll jets are commanded by the same corresponding roll jet logic of the previous regime. There is no jet inhibition in this flight regime.

Still later in the entry, when the dynamic pressure is higher ($>\bar{q}_2$), the aileron is used for both trim and transient control. Trim is initially maintained at zero. At a slightly higher dynamic pressure ($\bar{q}_2^*$), trim is maintained through the use of an integrator acting upon the bank angle attitude error; the initialization value of the integrator is zero. Aileron control of transient errors (in a "reverse" sense, as it has come to be labeled) is maintained through feedback of bank and sideslip attitudes and rates with appropriate gains. During this regime, the rudder command is null until the Mach number reaches a certain level ($\mathcal{M}_1$), after which it is proportional to the commanded aileron deflection from trim. The proportionality variable is a constant. Also during this regime, roll and yaw jet control identical to that of the previous regime may be utilized together with the aileron and rudder, or control with the jets may be inhibited. This is done with the same type of blending logic used longitudinally; here, the commanded aileron deflection determines jet inhibition. Also as in the longitudinal case, there is a gradual turn-on of the allowed aerodynamic control authority.

Still later in the entry, when the vehicle has crossed a prespecified curve in the Mach-alpha plane, only the aileron and rudder are used for transient control, the jets being inhibited for the remainder of the entry. Aileron and rudder control (in a "proverse" sense to distinguish it from that of the previous submode) of transient errors is maintained through feedback of bank and sideslip attitudes and rates (to both surfaces), with appropriate gains. Lateral trim for this regime has not yet been implemented.

The remainder of this section describes the lateral control laws, and their digital implementation, in detail. The block diagrams and equations defining the control logic for the aileron and rudder are given in Subsection 5.3.2.1, while those for the yaw and roll jets are given in Subsection 5.3.2.2. Subsection 5.3.2.3 consists of the controller coding summarized in flow-chart form.

5.3.2.1 Aileron/Rudder Control

Figure 5-8 is an overview of the aileron/rudder control logic, illustrating the two control submodes, with switching determined by the flag I_{LAT}. This flag is specified by vehicle controllability considerations (see Subsection 5.4) and is defined by a curve in the Mach-alpha plane as shown in Fig. 5-9.

5.3.2.1.1 Early Aileron/Rudder Control

Figure 5-10a illustrates the "reverse" control submode. When the dynamic pressure is less than $\bar{q}_2$, aileron trim is set to zero, as are the aileron and rudder commands. When the dynamic pressure reaches $\bar{q}_2$, aileron trim and rudder command are still set to zero, but closed-loop control of bank and sideslip (by the aileron alone) is provided by position (β, ϕ) and rate ($\dot{\beta}$, $\dot{\phi}$) feedback of the lateral state variables, through a network which attempts to maintain a constant response throughout the trajectory. Specifically, the desired closed-loop transfer function for bank angle response is chosen to have four specified complex poles, or:

$$\left[\frac{\phi}{\phi_G}\right]_{\text{desired}} = \frac{k_\phi (s^2 - \omega_\phi{}^2)}{(s^2 + 2\zeta_1\omega_1 s + \omega_1{}^2)(s^2 + 2\zeta_2\omega_2 s + \omega_2{}^2)} \qquad (5\text{-}4)$$

where (ζ_i, ω_i) are chosen for acceptable transient response (k_ϕ is not explicitly specified and ω_ϕ is a function of the airframe dynamics.). This response is obtained, in the absence of rudder effectiveness, by making use of sideslip mistrims to bank the vehicle.

As with the longitudinal controller, the gains of Fig. 5-10a may be separated into one of three types: (1) prespecified by the desired closed-loop characteristics (e.g., a_1); (2) dynamic pressure dependent; or (3) scheduled gains which are functions of the aerodynamic flight regime (e.g., ξ_3). For convenient reference, the gains of the first category are defined in terms of desired response characteristics with the following equation set:

$$\begin{aligned} a_1 &= \omega_1{}^2\omega_2{}^2 \\ a_2 &= 2(\zeta_1\omega_2 + \zeta_2\omega_1)/(\omega_1\omega_2) \\ a_3 &= 2(\zeta_1\omega_1 + \zeta_2\omega_2) \\ a_4 &= \omega_1{}^2 + \omega_2{}^2 + 4\zeta_1\zeta_2\omega_1\omega_2 \end{aligned} \qquad (5\text{-}5)$$

where, as noted above, the (ζ_i, ω_i) are chosen for acceptable roll response.

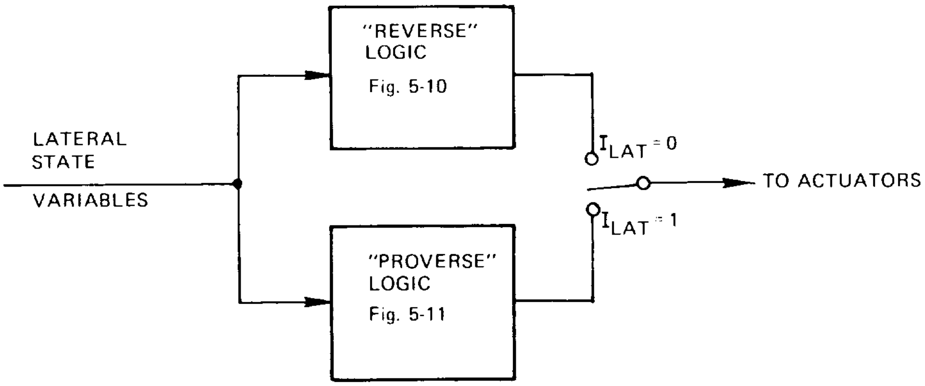

Fig. 5-8 Overview of Aileron/Rudder Control Logic

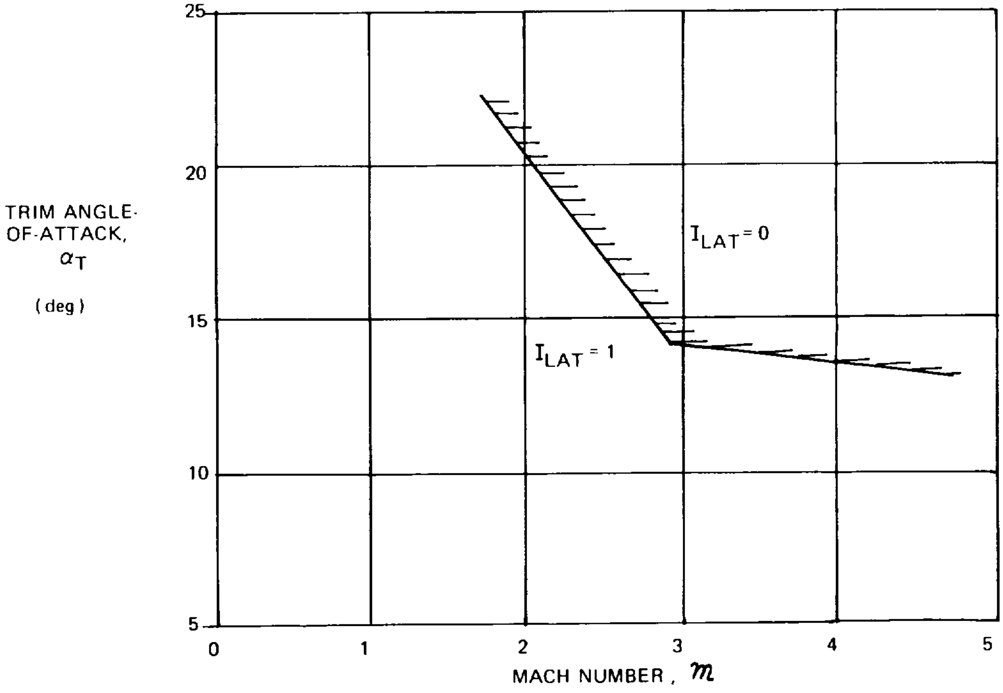

Fig. 5-9 Control Submode Switch Parameter Definition

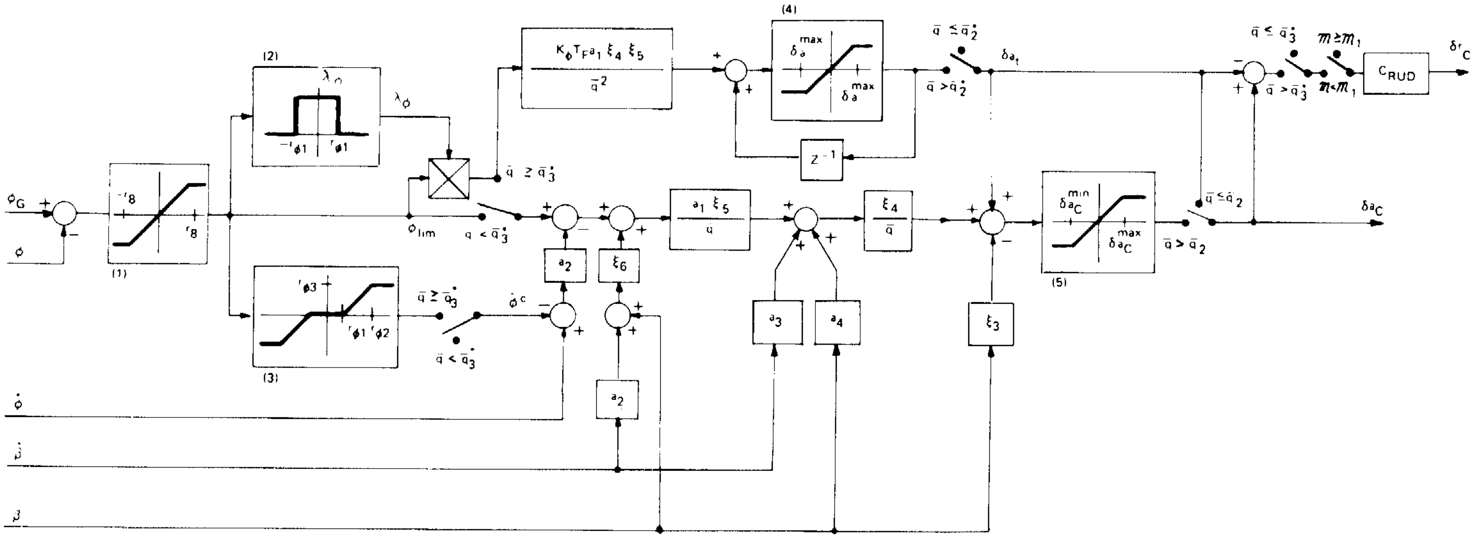

NON-LINEARITIES: (1) Limiter, unity slope

(2) Inverse deadband; $\lambda_\phi = 0$ or 1

(3) Limiter with deadband (symmetric)

(4) Limiter; unity slope

(5) Limiter; unity slope; $\delta_{a_C}^{max} = K_a \delta_a^{max}$, $\delta_{a_C}^{min} = -K_a \delta_a^{max}$

NOTE: $\bar{q}_2 < \bar{q}_2^* < \bar{q}_3^*$

Fig. 5-10a Aileron/Rudder Control Block Diagram (Reverse Mode, $I_{Lat} = 0$)

Aileron trim is commanded zero until the dynamic pressure reaches $\bar{q}_2^*$, and it is then determined through the use of a conventional clamped integrator in the bank angle error channel. This allows the vehicle to trim to a non-zero sideslip angle (by commanding a non-zero trim aileron deflection) in the presence of body-axis roll disturbance torques due to lateral displacements in the vehicle's center-of-gravity. To avoid interpreting large transients (such as occur during a bank reversal) as lateral cg-offset induced mistrims, integration of large magnitude errors is inhibited by the λ_ϕ switch. The gradual expansion of the aileron command limits during this submode as dynamic pressure increases is shown in Figs. 5-10a and 5-10b.

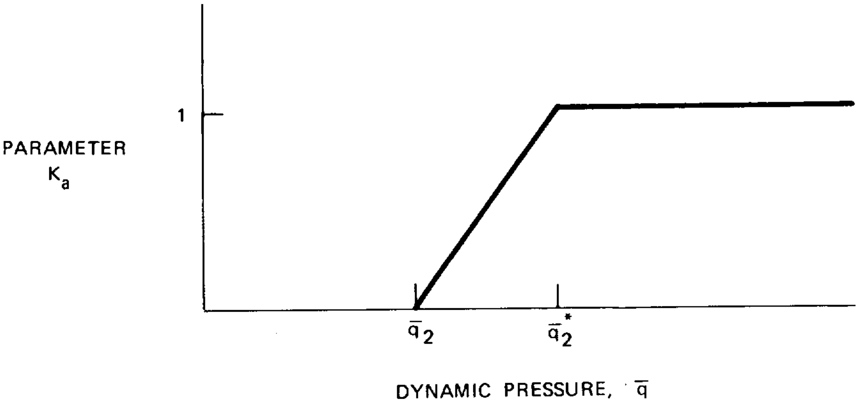

Fig. 5-10b Aileron/Deflection Limit Parameter

When the dynamic pressure reaches $\bar{q}_3^*$, later in this "reverse" submode, a rate command loop becomes effective when large attitude errors are detected (as in a bank reversal). As shown in Fig. 5-10a, when the attitude error is greater than $r_{\phi 1}$, the logic is no longer concerned with maintaining a bank attitude, but instead is configured to drive the vehicle to a desired bank rate. This allows the vehicle to complete the maneuver at higher rates than normally obtained with the attitude control loop providing the feedback.

Finally, when the Mach number drops below $\mathcal{M}_1$, the rudder is switched in to augment the aileron effectiveness. The aileron to rudder crossfeed gain is a constant.

5.3.2.1.2 Late Aileron/Rudder Control

Figure 5-11 illustrates the "proverse" control submode. Closed-loop control of bank and sideslip is provided by position (β, ϕ) and rate ($\dot{\beta}$, $\dot{\phi}$) feedback of the lateral state variables, through a network which attempts to maintain a constant response throughout the remainder of the trajectory. Specifically, the desired closed-loop transfer matrix describing bank and sideslip attitude response to a guidance commanded step is chosen to be:

$$\begin{bmatrix} (s^2 + a_{11}s + b_{11}) & (a_{12}s + b_{12}) \\ (a_{21}s + b_{21}) & (s^2 + a_{22}s + b_{22}) \end{bmatrix} \begin{bmatrix} \beta \\ \phi - \phi_G \end{bmatrix} = \begin{bmatrix} 0 \\ 0 \end{bmatrix} \tag{5-6}$$

where the a_{ij} and b_{ij} are chosen for acceptable transient response. It may be noted that in this "proverse" submode, the availability of the rudder allows for considerably more freedom in shaping the transient response, so that both sideslip and bank characteristics may be specified, in contradistinction to the previous submode (see Eq (5-4)).

As shown in the block diagram, there are eight gains (r_{ij} and p_{ij}) which are derived functions of both the desired closed-loop parameters (in Eq (5-6)) and of four selected scheduled gains. They are given by:

$$\begin{aligned} r_{11} &= a_{11}\gamma_{11} + a_{21}G_1\gamma_{12} & p_{11} &= b_{11}\gamma_{11} + b_{21}G_1\gamma_{12} \\ r_{12} &= a_{12}\gamma_{11} + a_{22}G_1\gamma_{12} & p_{12} &= b_{12}\gamma_{11} + b_{22}G_1\gamma_{12} \\ r_{21} &= a_{11}\gamma_{21} + a_{21}G_1\gamma_{22} & p_{21} &= b_{11}\gamma_{21} + b_{21}G_1\gamma_{22} \\ r_{22} &= a_{12}\gamma_{21} + a_{22}G_1\gamma_{22} & p_{22} &= b_{12}\gamma_{21} + b_{22}G_1\gamma_{22} \end{aligned} \tag{5-7a}$$

where G_1 is a constant and the γ_{ij} are scheduled gains. Also shown in the block diagram are a constant gain, G_1, two additional scheduled gains ν_1 and ν_2, and one additional derived gain, a function of the γ_{ij}:

$$\eta = \gamma_{11}\gamma_{22} - \gamma_{12}\gamma_{21} \tag{5-7b}$$

5.3.2.2 Yaw and Roll ACPS Control

Yaw and roll jet activity is completely inhibited while in the "proverse" aileron/rudder control submode ($I_{LAT} = 1$). This section describes the lateral ACPS control logic while in the "reverse" surface control submode.

Yaw jet ACPS control synthesis is based on double integrator modeling of the bank angle dynamics, so that the switch logic presented for pitch ACPS control may

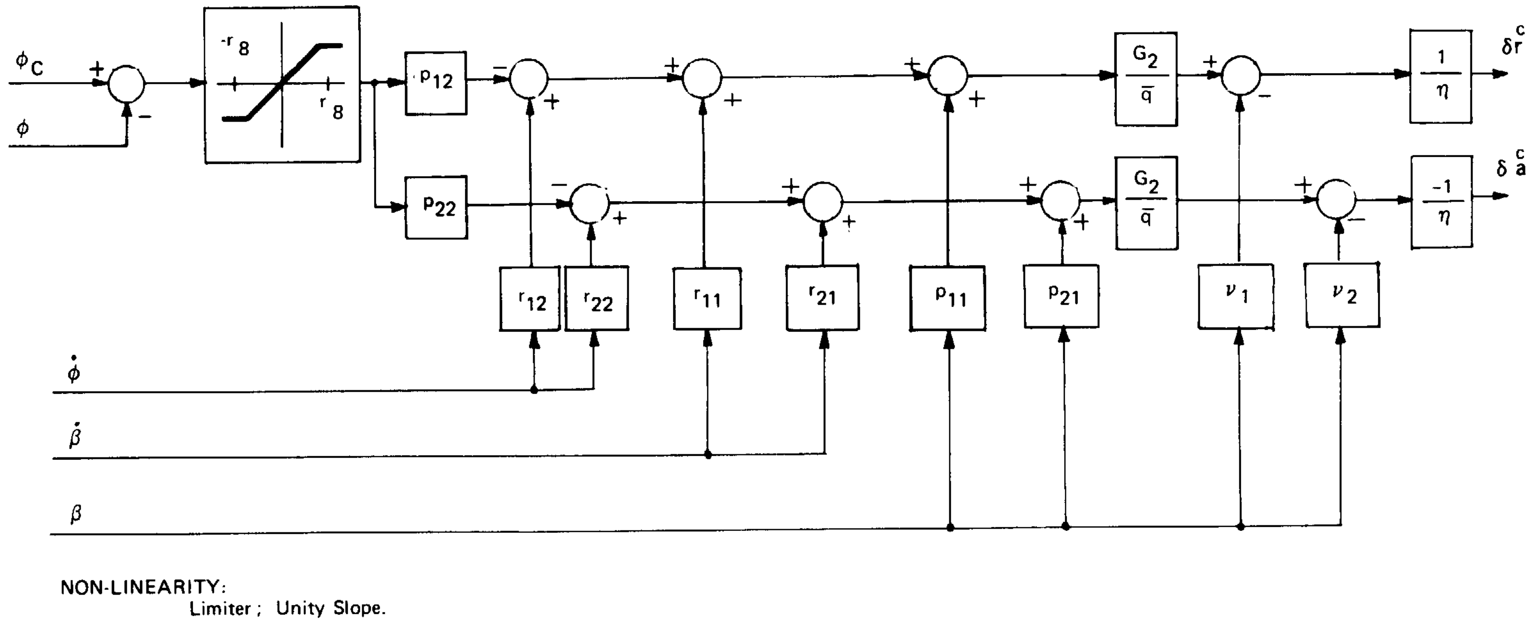

Fig. 5-11 Aileron/Rudder Control Block Diagram (Proverse Mode, $I_{Lat} = 1$)

be used. Roll jet logic consists of three models, one based on double integrator modeling of the sideslip dynamics, a second based on oscillator modeling, and a third which accounts for control axis cross-coupling.

5.3.2.2.1 Yaw Jet Control

A double integrator model of the bank angle dynamics, combined with the assumption of turn coordination provided by the roll jets, allows for the use of the ACPS pitch jet control logic, with the appropriate redefinition of control parameters. Specifically, yaw jet control is defined by the phase-plane switch logic of Fig. 5-4 and Eq (5-3a), where the coordinates are given by:

$$(\epsilon_1, \epsilon_2) = \left[-\phi_{lim} \sin \alpha_T, r \right] \qquad (5\text{-}8a)$$

and the switch curve parameters are given by:

$$(u, U) = (u_z, U_z) \qquad (5\text{-}8b)$$

$$(\delta_1, \delta_2) = (\delta_{\phi 1}, \delta_{\phi 2}) \qquad (5\text{-}8c)$$

$$\sigma = \sigma_\phi \qquad (5\text{-}8d)$$

The blending interface logic is discussed below.

5.3.2.2.2 Roll Jet Control

Roll jet control of vehicle sideslip is accomplished by the use of three control modes. Two of these use a double integrator model for sideslip; the remaining one uses an oscillator model.

The purpose of the first mode is to provide turn coordination when the yaw jets are firing ($u_z \neq 0$). This is accomplished by the phase-plane logic of Fig. 5-12, which is a generalized (β, $\dot{\beta}$) plane. The figure illustrates a typical state trajectory and the resultant limit cycle (with switch curve overshoots). The equations for the switch curve μ are:

$$\begin{aligned} \mu : \ S\beta &= \frac{1}{2U_1}\left[(\dot{\beta}^m)^2 - \dot{\beta}^2\right] \text{ if } S\dot{\beta} > \dot{\beta}^m \\ &= -\frac{1}{2U_2}\left[(\dot{\beta}^m)^2 - \dot{\beta}^2\right] \text{ if } S\dot{\beta} \leq \dot{\beta}^m \end{aligned} \qquad (5\text{-}9a)$$

where

$$\begin{aligned} U_1 &= U_z \cos \alpha_T \\ U_2 &= U_x \sin \alpha_T - U_z \cos \alpha_T \\ S &= \mathrm{sgn}\,(u_z) \\ \dot{\beta}^m &= \sqrt{2U_2 \delta_1} \end{aligned} \qquad (5\text{-}9b)$$

and where δ_1 is defined below in Eq (5-10).

The purpose of the second mode is to provide direct control over sideslip when the yaw jets are inactive ($u_z = 0$) and when the dynamic pressure is low. With double integrator modeling, the phase-plane logic of Fig. 5-4 and Eq (5-3a) may be used, where the coordinates are given by:

$$(\epsilon_1, \epsilon_2) = (\beta, \dot{\beta}) \qquad (5\text{-}10a)$$

and the switch curve parameters are given by:

$$(u, U) = (u_x, U_x \sin \alpha_T) \qquad (5\text{-}10b)$$

$$(\delta_1, \delta_2) = (\delta_{\beta 1}, \delta_{\beta 2}) \qquad (5\text{-}10c)$$

$$\sigma = \sigma_\beta \qquad (5\text{-}10d)$$

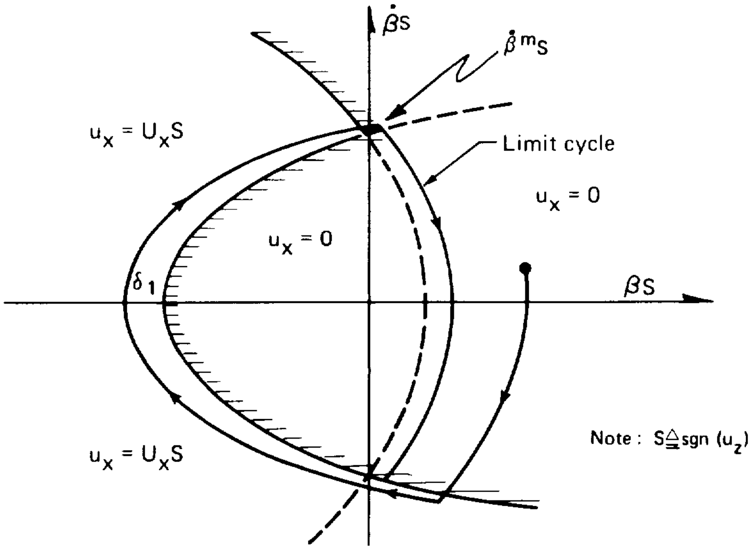

Fig. 5-12 Roll Jet Control when $u_z \neq 0$

It is convenient to label this control mode (used at low $\bar{q}$ and when $u_z = 0$) as attitude hold, since both rate and attitude error are driven toward zero.

The third control mode takes advantage of the vehicle's dynamic stability in sideslip, which becomes significant once the dynamic pressure becomes sufficiently high. What is required is simply rate damping of the sideslip angular velocity as shown below, where $\dot{\beta}^m$ is given by Eq (5-9b).

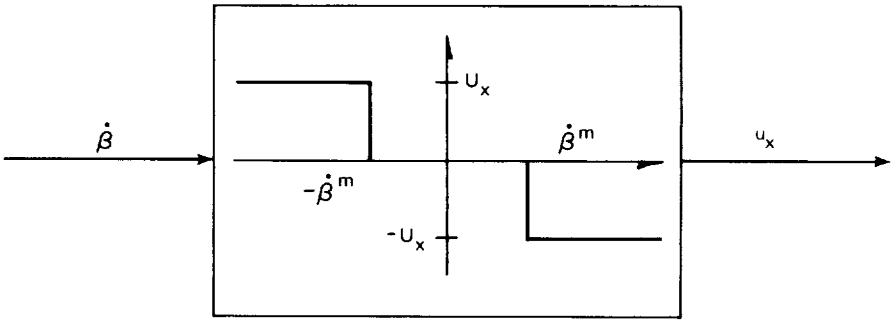

Fig. 5-13 Roll Jet Control when $u_z = 0$ ($\bar{q} \geq \bar{q}_3$)

The control modes described above, defining lateral control with yaw and roll jets, are summarized in block diagram form in Fig. 5-14. Several points should be noted. First, the mode select block which defines the roll jet control mode to be used is defined by:

$$\begin{array}{llll} \text{If} & u_z \neq 0 & \text{then Mode} = \text{I} & \\ & u_z = 0,\ \bar{q} < \bar{q}_3 & \quad\quad\quad\ \text{II} & (5\text{-}11) \\ & u_z = 0\ \ \bar{q} \geq \bar{q}_3 & \quad\quad\quad\ \text{III} & \end{array}$$

where the modes are coordination, attitude hold, and rate damping, respectively. The three roll control blocks correspond with the above modes. A second point to note is the gating by the blending parameter λ_a, which is defined by logic that is identical to that of the pitch channel. Finally, it may be noted that the logic disallows ACPS inhibition during aileron trim-only (null aileron command) operation.

5.3.2.3 Digital Implementation

Coding implementation for lateral control during the entry phase is summarized in flow-chart form in Fig. 5-15.

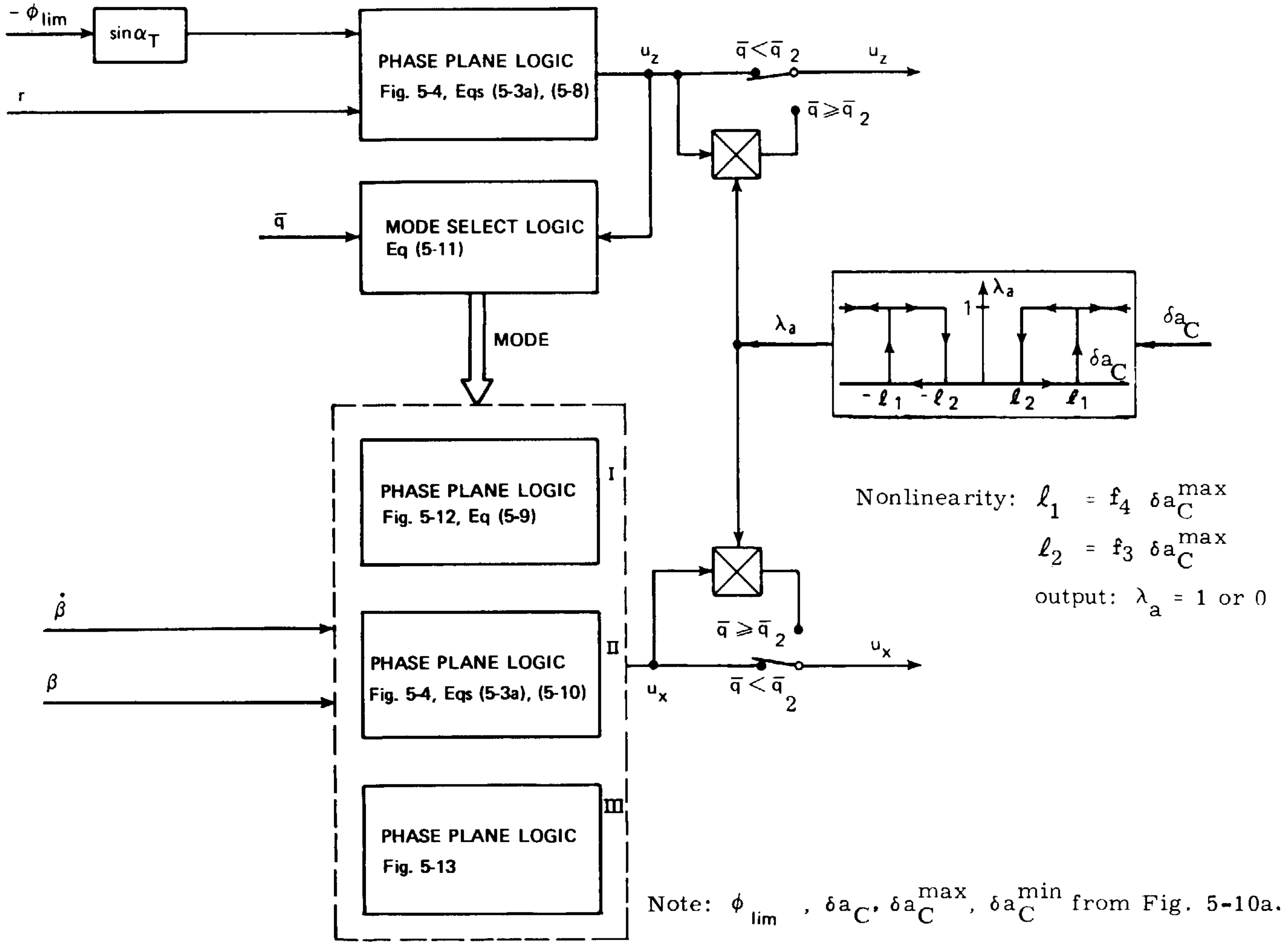

Nonlinearity: $\ell_1 = f_4 \ \delta a_C^{max}$

$\ell_2 = f_3 \ \delta a_C^{max}$

output: $\lambda_a = 1$ or 0

Note: ϕ_{lim} , δa_C, δa_C^{max}, δa_C^{min} from Fig. 5-10a.

Fig. 5-14 Yaw and Roll ACPS Control Block Diagram

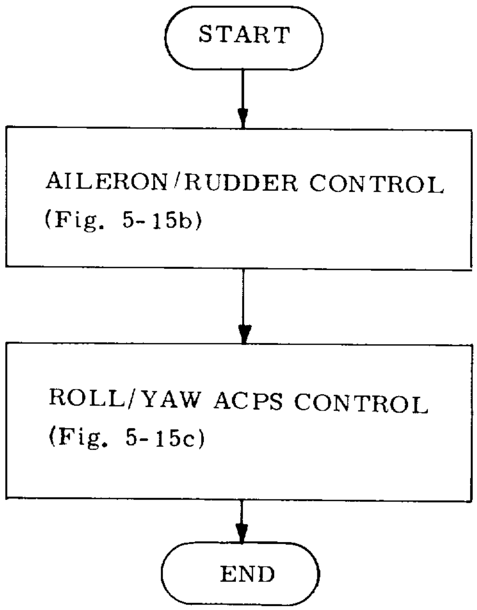

Fig. 5-15a Logic Flow for the Lateral Channel

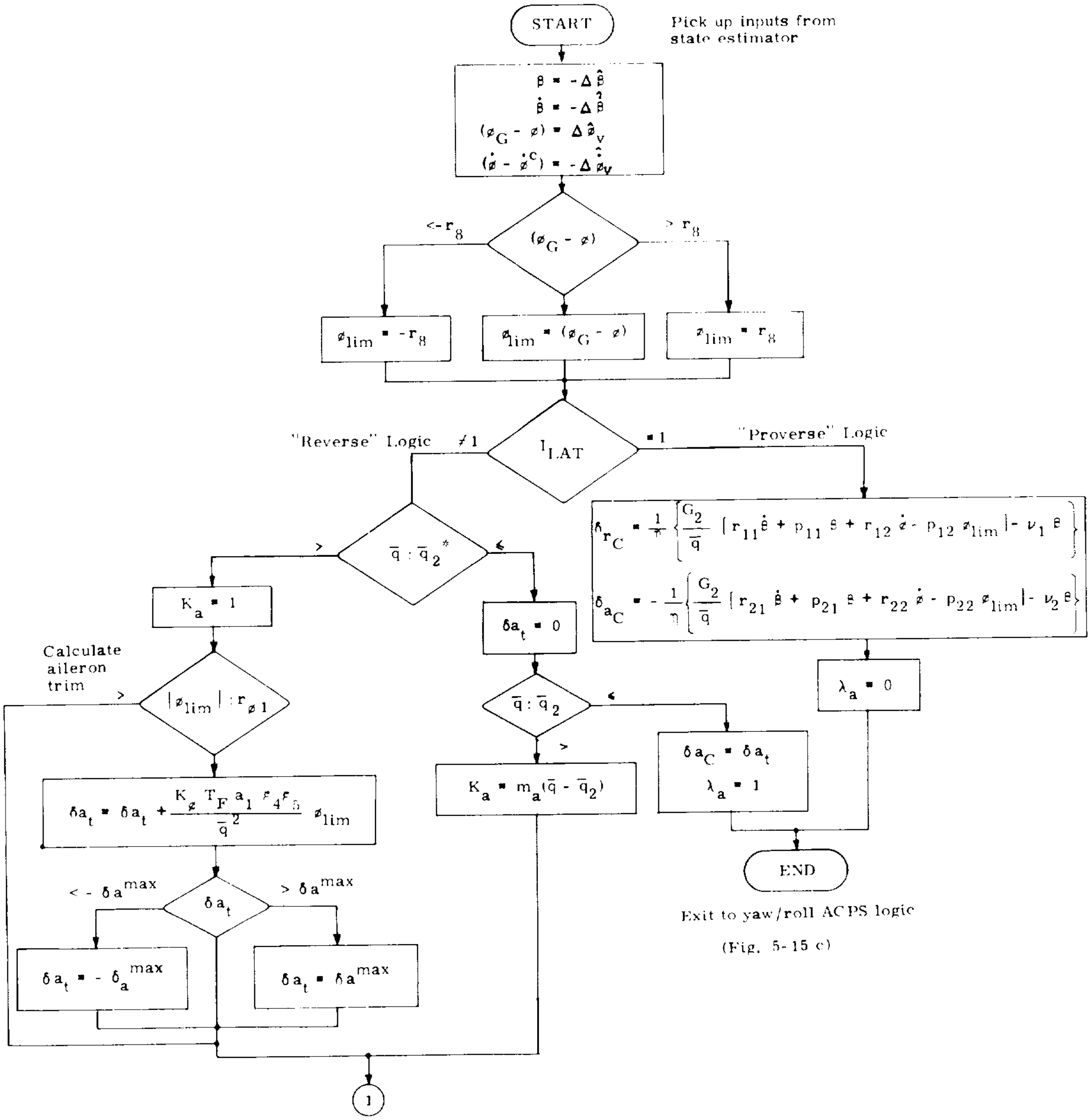
START
Pick up inputs from state estimator
$\beta = -\Delta\hat{\beta}$
$\dot{\beta} = -\Delta\hat{\dot{\beta}}$
$(\phi_G - \phi) = \Delta\hat{\phi}_v$
$(\dot{\phi} - \dot{\phi}^c) = -\Delta\hat{\dot{\phi}}_v$
$<-r_8$
$(\phi_G - \phi)$
$> r_8$
$\phi_{lim} = -r_8$
$\phi_{lim} = (\phi_G - \phi)$
$\phi_{lim} = r_8$
"Reverse" Logic
$\neq 1$
I_{LAT}
$= 1$
"Proverse" Logic
$\delta_{r_C} = \frac{1}{\eta}\left\{\frac{G_2}{\bar{q}}\left[r_{11}\dot{\beta} + p_{11}\beta + r_{12}\dot{\phi} - p_{12}\phi_{lim}\right] - \nu_1\beta\right\}$
$\delta_{a_C} = -\frac{1}{\eta}\left\{\frac{G_2}{\bar{q}}\left[r_{21}\dot{\beta} + p_{21}\beta + r_{22}\dot{\phi} - p_{22}\phi_{lim}\right] - \nu_2\beta\right\}$
$>$
$\bar{q} : \bar{q}_2{}^*$
$\leq$
$K_a = 1$
$\delta a_t = 0$
$\lambda_a = 0$
Calculate aileron trim
$>$
$|\phi_{lim}| : r_{\phi 1}$
$\bar{q} : \bar{q}_2$
$\leq$
$>$
$\delta a_C = \delta a_t$
$\lambda_a = 1$
$\delta a_t = \delta a_t + \frac{K_\phi T_F a_1 f_4 f_5}{\bar{q}^2}\phi_{lim}$
$K_a = m_a(\bar{q} - \bar{q}_2)$
END
Exit to yaw/roll ACPS logic (Fig. 5-15 c)
$< -\delta a^{max}$
δa_t
$> \delta a^{max}$
$\delta a_t = -\delta_a{}^{max}$
$\delta a_t = \delta a^{max}$
1

Fig. 5-15b Logic Flow for Aileron/Rudder Control

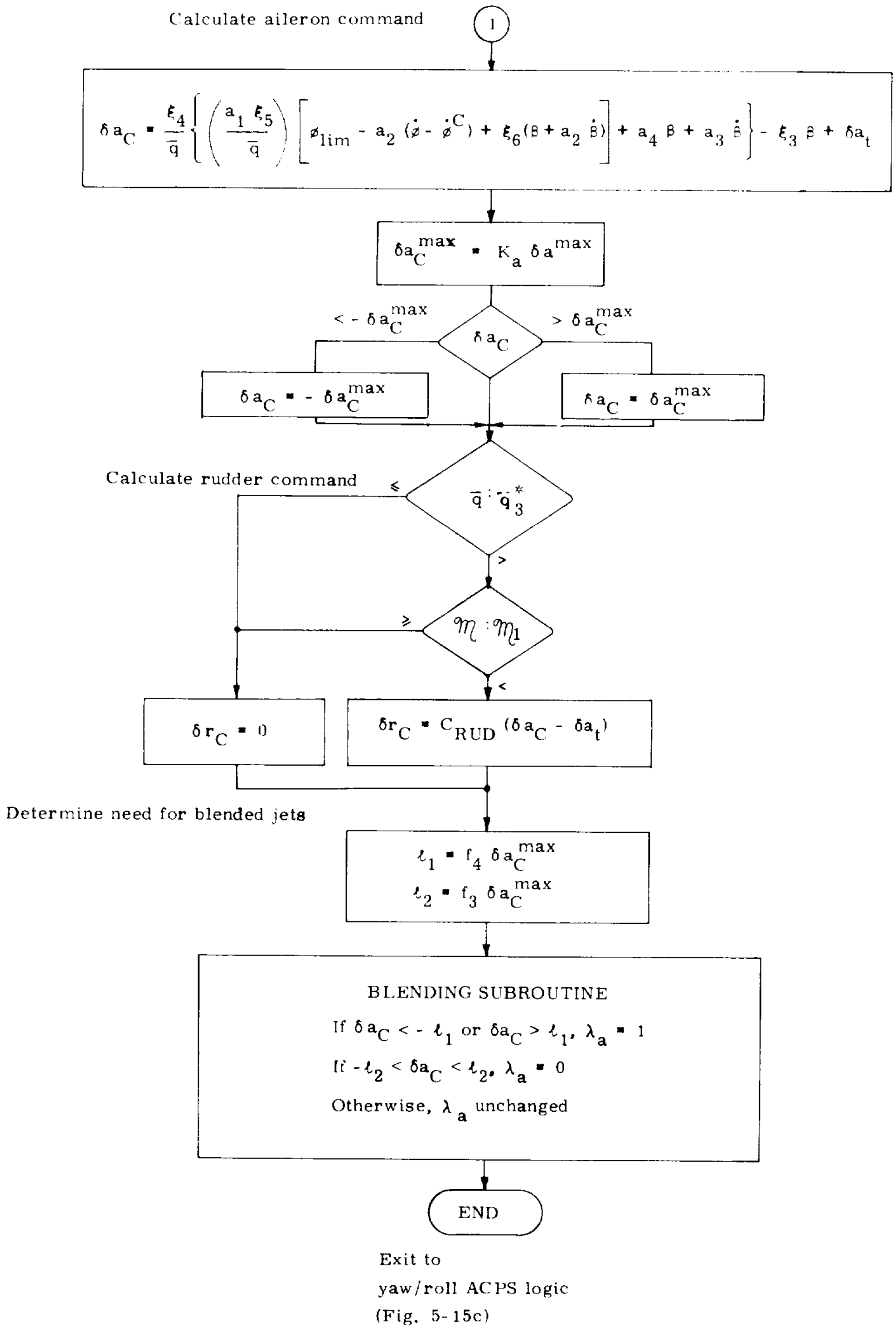
Calculate aileron command
1
$\delta a_C = \frac{\xi_4}{\bar{q}}\left\{\left(\frac{a_1\,\xi_5}{\bar{q}}\right)\left[\phi_{lim} - a_2\,(\dot{\phi} - \dot{\phi}^C) + \xi_6(\beta + a_2\,\dot{\beta})\right] + a_4\,\beta + a_3\,\dot{\beta}\right\} - \xi_3\,\beta + \delta a_t$
$\delta a_C^{max} = K_a\,\delta a^{max}$
$< -\delta a_C^{max}$
δa_C
$> \delta a_C^{max}$
$\delta a_C = -\delta a_C^{max}$
$\delta a_C = \delta a_C^{max}$
Calculate rudder command
$\leq$
$\bar{q} : \bar{q}_3^*$
$>$
$\geq$
$\mathcal{M} : \mathcal{M}_1$
$<$
$\delta r_C = 0$
$\delta r_C = C_{RUD}\,(\delta a_C - \delta a_t)$
Determine need for blended jets
$\ell_1 = f_4\,\delta a_C^{max}$
$\ell_2 = f_3\,\delta a_C^{max}$
BLENDING SUBROUTINE
If $\delta a_C < -\ell_1$ or $\delta a_C > \ell_1$, $\lambda_a = 1$
If $-\ell_2 < \delta a_C < \ell_2$, $\lambda_a = 0$
Otherwise, λ_a unchanged
END
Exit to
yaw/roll ACPS logic
(Fig. 5-15c)

Fig. 5-15b Logic Flow for Aileron/Rudder Control (Cont)

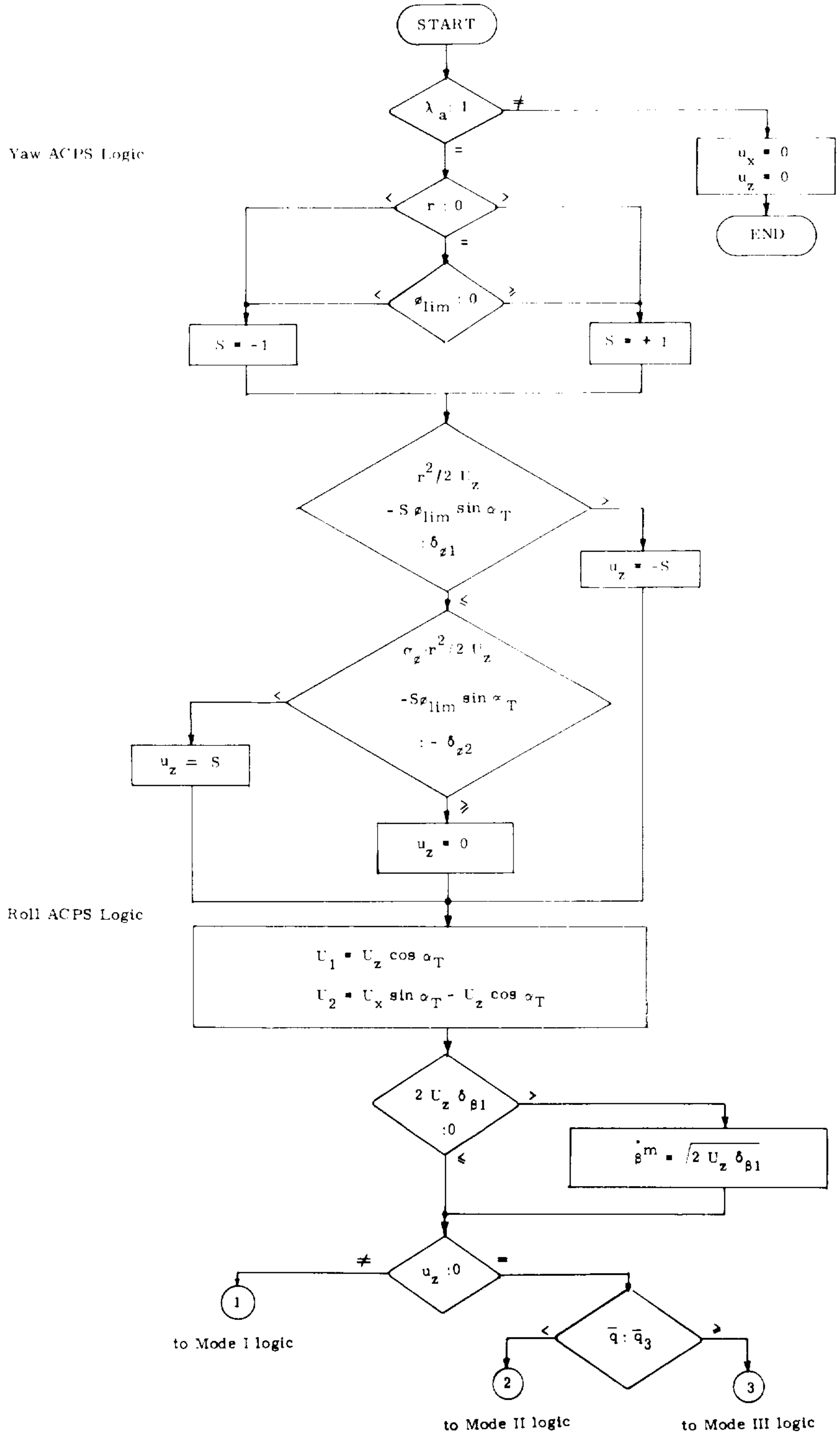

Fig. 5-15c Logic Flow for Yaw/Roll ACPS Control

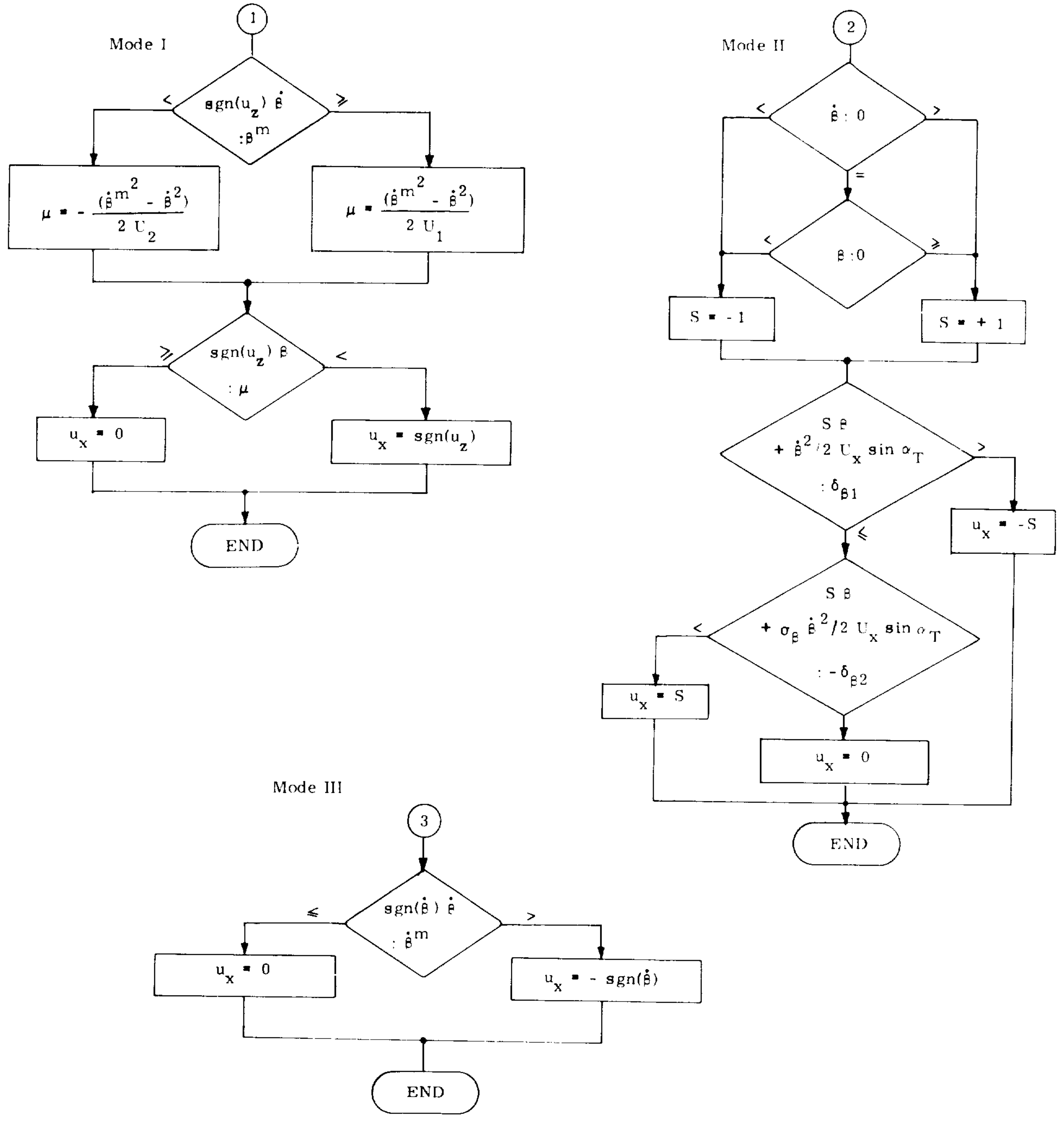

Fig. 5-15c Logic Flow for Yaw/Roll ACPS Control (Cont)

5.3.3 DFCS Parameter Specification

All parameters used in control computations for the entry phase are either fixed or are scheduled on the basis of Mach Number, $\mathcal{M}$. Table 5-1 tabulates all entry-phase fixed control parameters. The scheduled control gains ξ_1 through ξ_6 and ν_1 and ν_2 are plotted in Figs. 5-16 through 5-23. The scheduled control parameters γ_{11} through γ_{22} are plotted in Figs. 5-24 through 5-27. As noted in Subsection 5.3.2.1.1, the lateral gains r_{ij}, p_{ij}, and η are calculated as functions of the γ_{ij}, according to Eq (5-7).

In an initialization pass through the entry control logic, several parameters which are functions of pad-loaded values are calculated and stored for future use. The Load Manipulation Routine for the entry phase is shown in Fig. 5-28.

5.4 Performance Summary

Shown in Fig. 5-29 are three curves in the Mach-alpha plane which define regions of lateral controllability using differing control modes. Also shown is a typical late entry Mach-alpha profile. The curves were derived by conducting simulated maneuvers with the entry DFCS and the NR 00089B (Feb. version) vehicle at various Mach numbers and angles-of-attack. The curves separate desirable from undesirable simulated vehicle response.

Curve A indicates the lower boundary (in the Mach-alpha plane) to which the vehicle may be flown using ailerons alone for lateral control. By driving the rudder proportionally to the aileron command (with a crossfeed gain of 2), the region of "reverse" control may be considerably extended farther down the entry profile (curve B). Finally, the region of controllability using the "proverse" control mode is bounded (above) by curve C. The resultant overlapping region, defined by curves B and C, provides the motivation for the switch curve choice shown in Fig. 5-9.

It should be noted that an on-going effort in determining design sensitivity to aerodynamic coefficient uncertainties will reduce the area of the overlap region. However, the control design used in deriving the curves of Fig. 5-29 was not "tuned" so as to maximize the resultant overlap area. It is anticipated that future efforts in this direction will enlarge this region for the nominal aerodynamic coefficient values, while counteracting the shrinking effect of off-nominal aerodynamics.

Table 5-1: Fixed Parameters

Symbol	Value	Dimension
U_x	1.65	deg/sec^2
U_y	1.32	deg/sec^2
U_z	0.66	deg/sec^2
$\delta_{\alpha 1}$	0.75	deg
$\delta_{\alpha 2}$	1.0	deg
$\delta_{\beta 1}$	0.2	deg
$\delta_{\beta 2}$	0.4	deg
$\delta_{\phi 1}$	0.75	deg
$\delta_{\phi 2}$	1.5	deg
σ_{α}	5	-
σ_{β}	2	-
σ_{ϕ}	5	-
f_1	0.8	-
f_2	0.6	-
f_3	0.6	-
f_4	0.8	-
$\bar{q}_1$	10	lbf/ft^2
$\bar{q}_2$	20	lbf/ft^2
$\bar{q}_3$	5	lbf/ft^2
$\bar{q}_1^*$	20	lbf/ft^2
$\bar{q}_2^*$	30	lbf/ft^2
$\bar{q}_3^*$	80	lbf/ft^2

Table 5-1: Fixed Parameters (Cont)

Symbol	Value	Dimension
m_1	6	-
$K_{\alpha 1}$	-1.0	sec^{-1}
$K_{\alpha 2}$	0.2	sec^{-1}
K_{ϕ}	0.01	sec^{-1}
ω_d	0.7	sec^{-1}
ω_1	0.7	sec^{-1}
ω_2	0.7	sec^{-1}
ζ_d	0.7	-
ζ_1	1.4	-
ζ_2	0.7	-
r_1	5	deg
r_8	25	deg
$r_{\phi 1}$	5	deg
$r_{\phi 2}$	25	deg
$r_{\phi 3}$	8	deg/sec
C_{RUD}	2	-
a_{11}	1.0	sec^{-1}
a_{12}	0.0	sec^{-1}
a_{21}	0.0	sec^{-1}
a_{22}	1.3	sec^{-1}
b_{11}	1.0	sec^{-2}
b_{12}	0.0	sec^{-2}

Table 5-1: Fixed Parameters (Cont)

Symbol	Value	Dimension
b_{21}	1.0	sec^{-2}
b_{22}	0.8	sec^{-2}
G_1	0.133	-
G_2	29.0	$lbf\text{-}sec^2/ft^2$
δe^{min}, δe^{max}	see Subsection 2-2	
δa^{max}, δr^{max}		

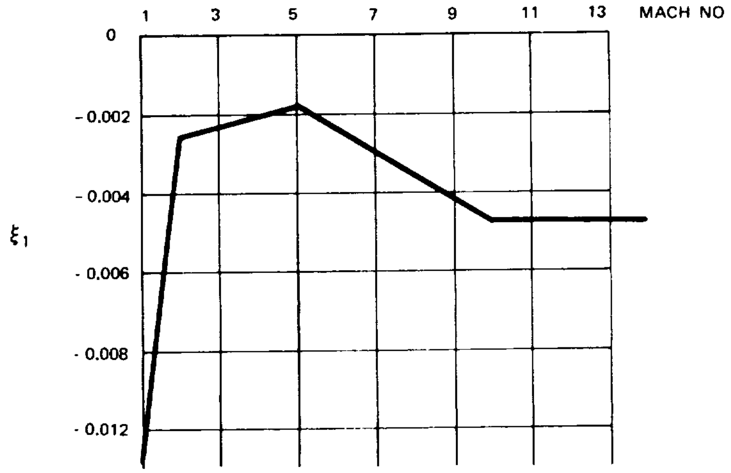

Fig. 5-16 Gain Schedule for ξ_1

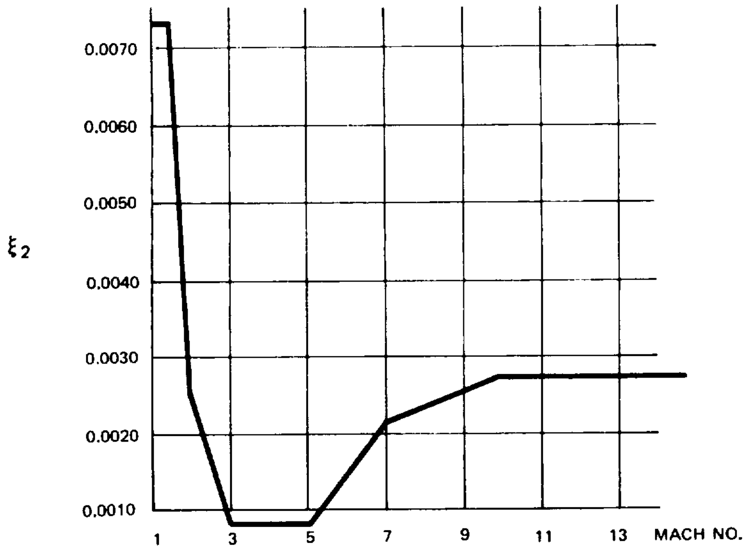

Fig. 5-17 Gain Schedule for ξ_2

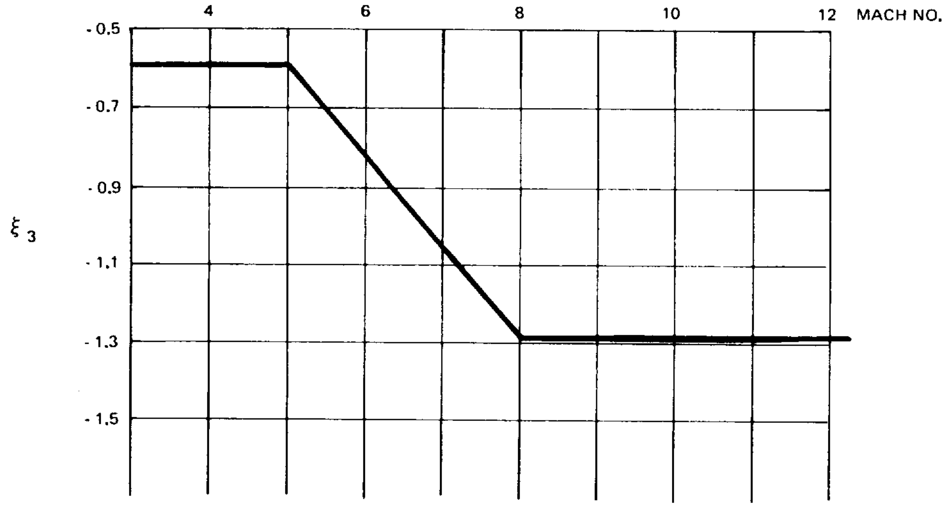

Fig. 5-18 Gain Schedule for ξ_3

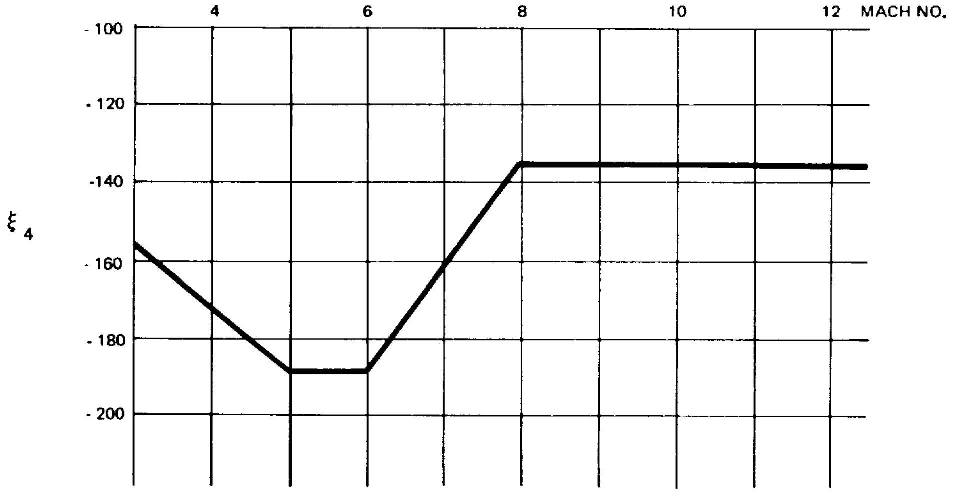

Fig. 5-19 Gain Schedule for ξ_4

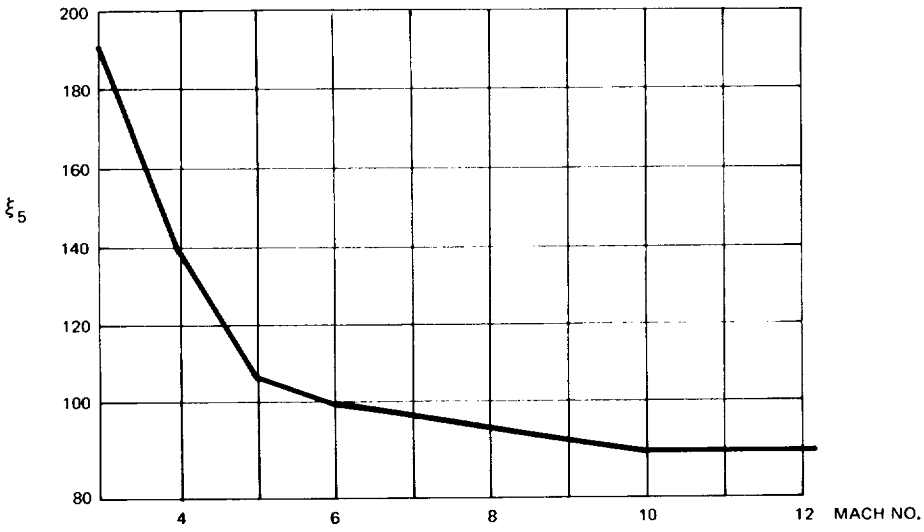

Fig. 5-20 Gain Schedule for ξ_5

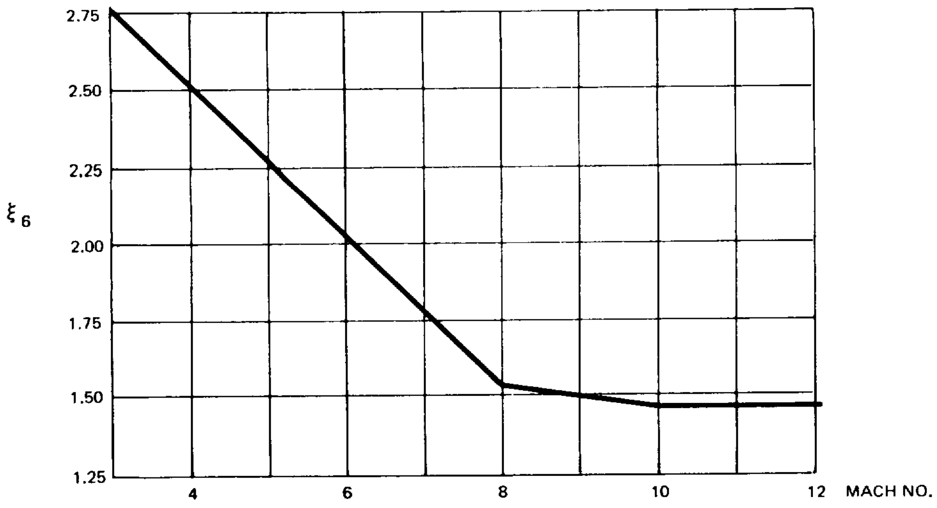

Fig. 5-21 Gain Schedule for ξ_6

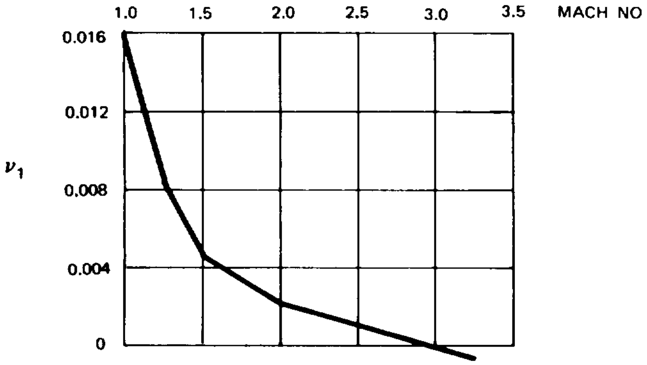

Fig. 5-22 Gain Schedule for ν_1

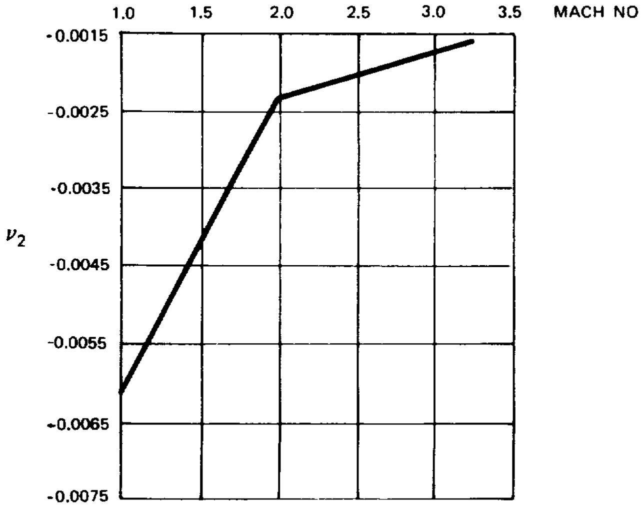

Fig. 5-23 Gain Schedule for ν_2

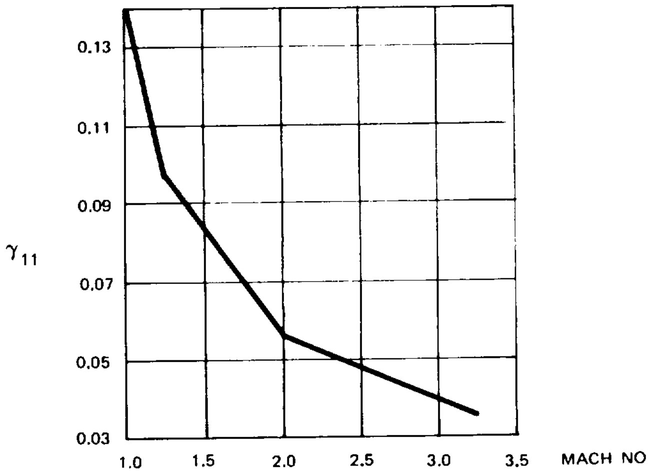

Fig. 5-24 Gain Schedule for λ_{11}

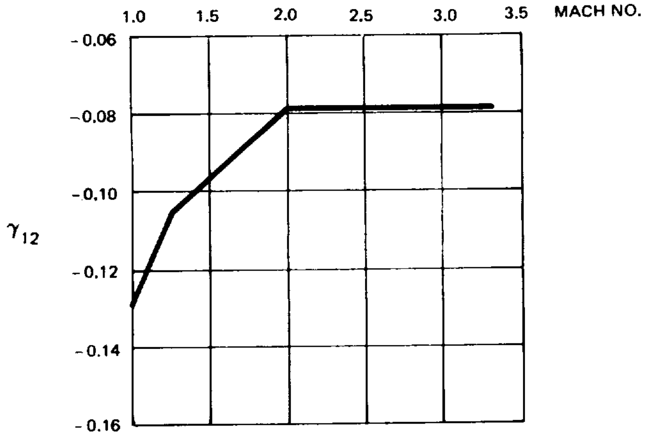

Fig. 5-25 Gain Schedule for λ_{12}

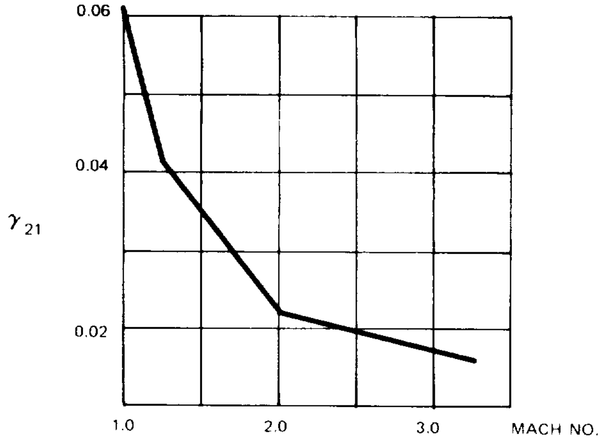

Fig. 5-26 Gain Schedule for γ_{21}

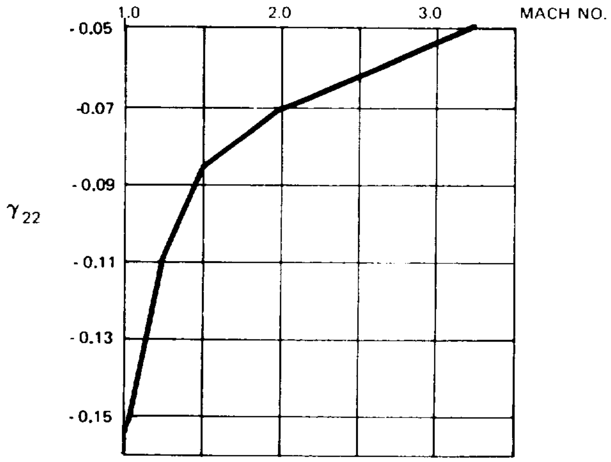

Fig. 5-27 Gain Schedule for γ_{22}

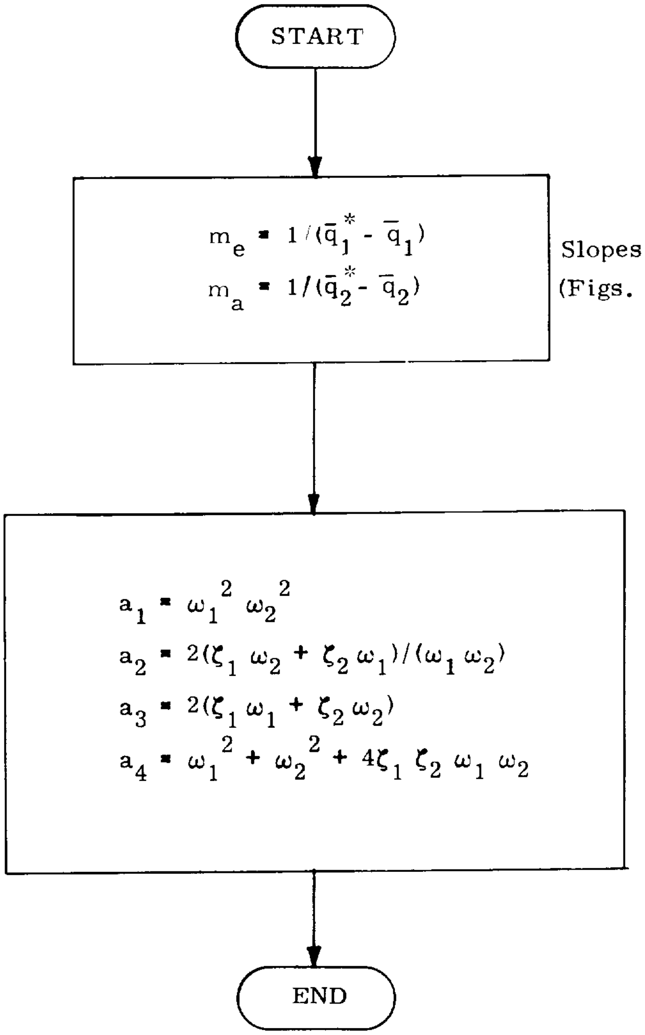
START
$m_e = 1/(\bar{q}_1^* - \bar{q}_1)$
$m_a = 1/(\bar{q}_2^* - \bar{q}_2)$
$a_1 = \omega_1^2 \omega_2^2$
$a_2 = 2(\zeta_1 \omega_2 + \zeta_2 \omega_1)/(\omega_1 \omega_2)$
$a_3 = 2(\zeta_1 \omega_1 + \zeta_2 \omega_2)$
$a_4 = \omega_1^2 + \omega_2^2 + 4\zeta_1 \zeta_2 \omega_1 \omega_2$
END

Slopes of deflection-limit curves (Figs. 5-3b, 5-10b)

Fixed lateral gains (Eq. (5-5))

Fig. 5-28 Entry Load Manipulation

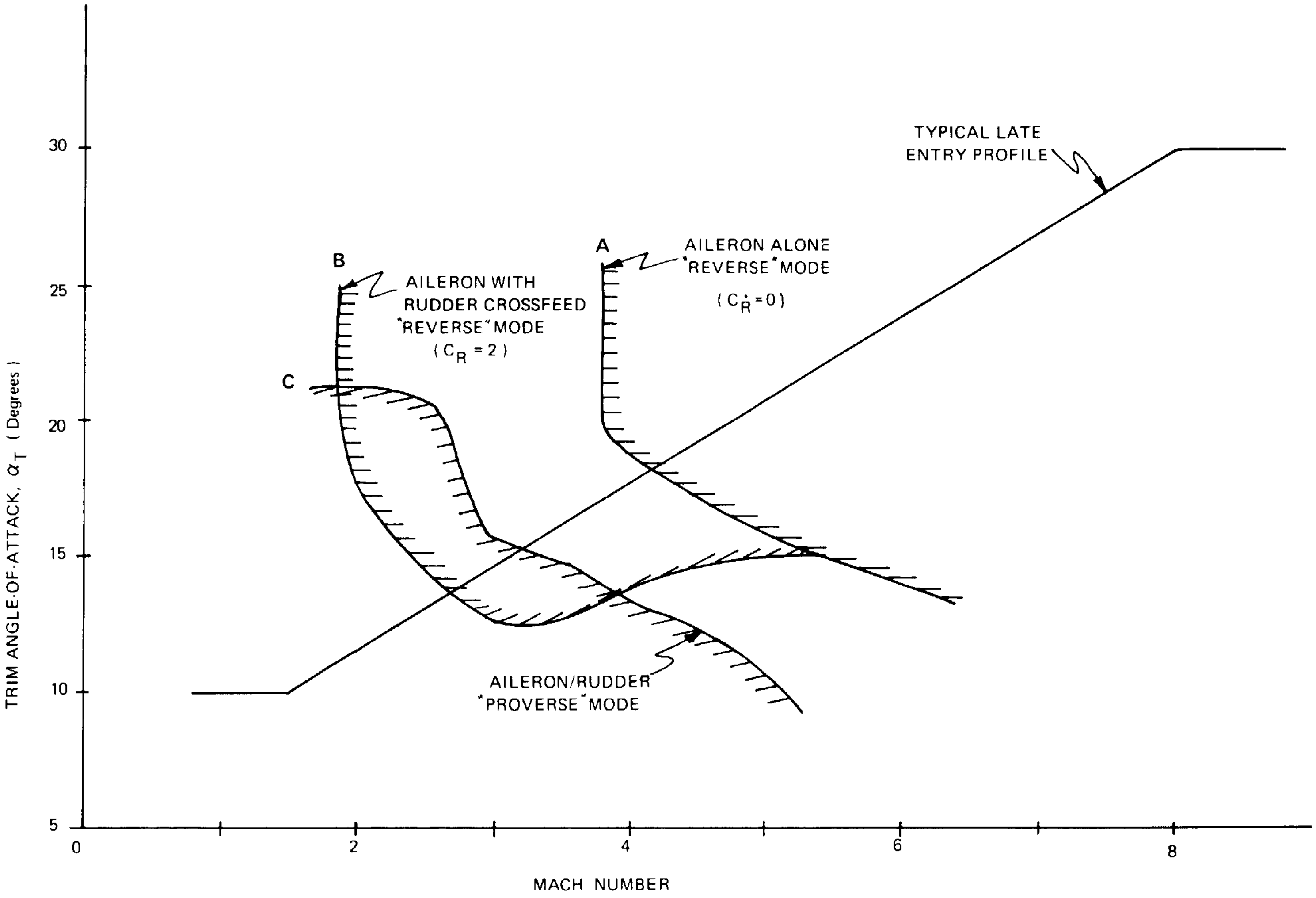

Fig. 5-29 Controllability Regimes

SECTION 6

ON-ORBIT PHASE

6.1 Introduction

The DFCS (Digital Flight Control System) will control the attitude and the translation of the Space Shuttle during the various orbital activities by using either the ACPS (Attitude Control Propulsion System) or the OMS (Orbital Maneuvering System). For the purpose of control, there are two orbital phases: the ACPS phase when the jets are the control effectors, and the TVC (Thrust Vector Control) phase when the gimbaled engines are used for control. The ACPS phase is presented first, in Subsection 6.2, followed by a preliminary description of the on-orbit TVC phase in Subsection 6.3. Digital implementation of the ACPS phase, presented in Subsection 6.4, and preliminary testing was accomplished using structured programming techniques in the HAL language. All symbols relevant to the on-orbit phase may be found in a separate glossary at the end of this section.

6.2 On-orbit ACPS Phase: Engineering Description

A block diagram of the DFCS during the on-orbit ACPS phase is illustrated in Fig. 6-1. The on-orbit attitude maneuver routine or another interface routine (see Part II) supplies to the DFCS:

1) a set of reference gimbal angles, $[\theta_d]$
2) a set of incremental reference gimbal angles, $[\Delta\theta_d]$
3) the desired angular velocity vector, $\underline{\omega}_d$
4) a set of bias gimbal angles, $[\beta_{BIAS}]$
5) a bias acceleration vector, $\underline{\alpha}_m$

Every t_{fast} seconds the DFCS adds $[\Delta\theta_d]$ to $[\theta_d]$ to give a new set of reference gimbal angles. The DFCS then compares these to the measured set of gimbal angles, $[\theta_{GA}]$, and computes the angular errors in control axes. The bias angles are added to these errors in control axes and fed to the phase plane switching logic. Also fed to the phase plane switching logic are the angular velocity error, $\underline{\omega}_e$, the net estimated disturbance acceleration, $\underline{\alpha}_{dm}$, the magnitudes of control accelerations, $[\alpha_C]$, and

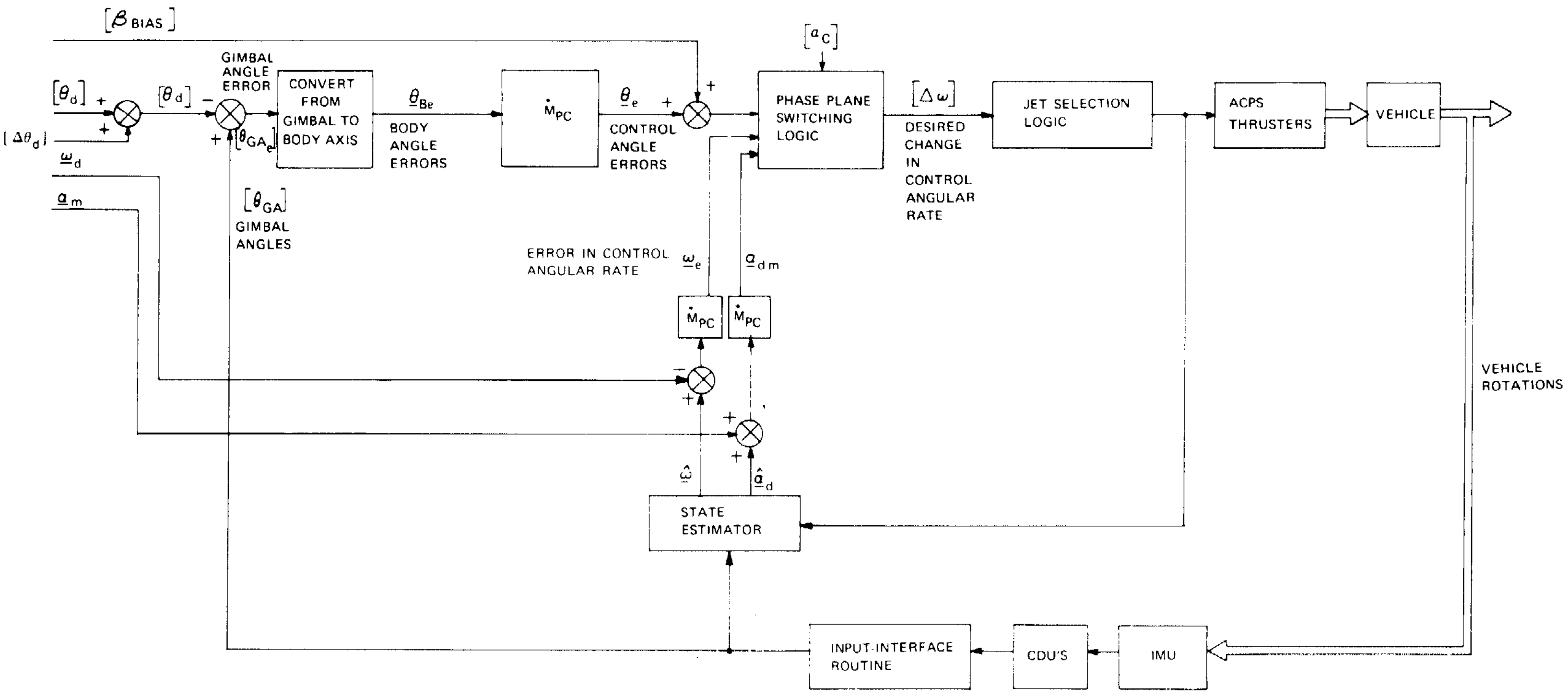

Fig. 6-1. On-Orbit ACPS

the last desired change in angular velocity. The angular velocity error, $\underline{\omega}_e$, is computed by subtracting the desired angular velocity, $\underline{\omega}_d$, from the estimated angular velocity, $\hat{\underline{\omega}}$, and transforming the result into control coordinates. The net estimated disturbance acceleration, $\underline{\alpha}_{dm}$, is computed by adding the bias acceleration, $\underline{\alpha}_m$, to the estimated disturbance acceleration, $\hat{\underline{\alpha}}_d$, and transforming the result into control coordinates. From these inputs the phase plane switching logic determines the desired angular rate changes,$[\Delta\omega]$, in control coordinates. From these desired rate changes the jet selection logic determines the appropriate jets to be fired, if any, and the corresponding firing times, and then turns the jets on and schedules their turn-off.

6.2.1 ACPS Control Axes

This subsection presents a technique for decoupling the ACPS control of the Shuttle Orbiter into three essentially independent axes. This technique permits one to treat the rigid body rotational dynamics of the vehicle, normally represented by a 6th order system, as three independent 2nd order systems, thus justifying the use of phase plane control logic. A similar technique was used in the design of the Lunar Module autopilot. The jet selection logic which has been implemented to utilize the decoupled axes is limited to specified jet pairs and provides only attitude control, not translation, in its present form. A more general scheme will be used in the future.

The ACPS thruster group locations for the NR ATP baseline configuration are given in Subsection 2.3. Define a +u thruster combination as one or more thrusters from group 2 and/or group 12: e.g., jet #14 and jet #31. Also define a -u thruster combination as one or more thrusters from groups 1 and 11: e.g., jets #10 and 25. The only restriction in selecting the jets is that the torque produced by the +u combination is opposite (or nearly opposite) in direction to that of the -u jets. Similarly, select a +v combination from groups 4 and 10, e.g., #9 and #26; and a -v combination from groups 3 and 9, e.g., #13 and #32. Finally, select a +w combination from groups 6 and 8, e.g., #5 and #18; and a -w combination from groups 5 and 7, e.g., #6 and #17. The suggested thruster combinations give moderate rotational control authority while minimizing the net translation.

The control axes are defined by the accelerations produced by the u, v and w jets. More specifically, let

$\underline{U}_{BASIS}$ = unit vector in the direction of the +u axis

$\underline{V}_{BASIS}$ = unit vector in the direction of the +v axis

$\underline{W}_{BASIS}$ = unit vector in the direction of the +w axis

$\overset{*}{J}$ = orbiter inertia matrix

$\underline{M}_{P2U}$, $\underline{M}_{M2U}$, $\underline{M}_{P2V}$, $\underline{M}_{M2V}$, $\underline{M}_{P2W}$, $\underline{M}_{M2W}$ = control torques produced by the ±u, ±v, ±w thruster combinations

then

$$\underline{U}_{BASIS} = \text{unit}\ (\overset{*}{J}^{-1}\ (\underline{M}_{P2U} - \underline{M}_{M2U})/2)$$

$$\underline{V}_{BASIS} = \text{unit}\ (\overset{*}{J}^{-1}\ (\underline{M}_{P2V} - \underline{M}_{M2V})/2)$$

$$\underline{W}_{BASIS} = \text{unit}\ (\overset{*}{J}^{-1}\ (\underline{M}_{P2W} - \underline{M}_{M2W})/2)$$

(The components are given in vehicle axes.)

The control axes orientations are shown in Fig. 6-2 for the thruster combinations given above. Note that the ±u accelerations are not exactly opposite. Neither are the ±v accelerations.

The transformation from control axes to vehicle (or pilot) axes is defined as:

$$\overset{*}{\underline{M}}_{CP} = (\underline{U}_{BASIS}, \underline{V}_{BASIS}, \underline{W}_{BASIS})$$

The transformation from vehicle (or pilot) axes to control axes is simply:

$$\overset{*}{M}_{PC} = (\overset{*}{M}_{CP})^{-1}$$

The attitude and rate errors for the autopilot are derived in vehicle axes. In order to utilize the decoupling technique these must be transformed from vehicle axes to control axes, i.e.,

$$\begin{pmatrix} \theta_{eu} \\ \theta_{ev} \\ \theta_{ew} \end{pmatrix} = \overset{*}{M}_{PC} \begin{pmatrix} \theta_{ex} \\ \theta_{ey} \\ \theta_{ez} \end{pmatrix}$$

$$\begin{pmatrix} \omega_{eu} \\ \omega_{ev} \\ \omega_{ew} \end{pmatrix} = \overset{*}{M}_{PC} \begin{pmatrix} \omega_{ex} \\ \omega_{ey} \\ \omega_{ez} \end{pmatrix}$$

6.2.2 State Estimator for the ACPS On-Orbit Phase

Control of the shuttle vehicle in orbit requires estimates of vehicle angular rate, ω, and vehicle angular disturbance acceleration, α_d. These quantities are

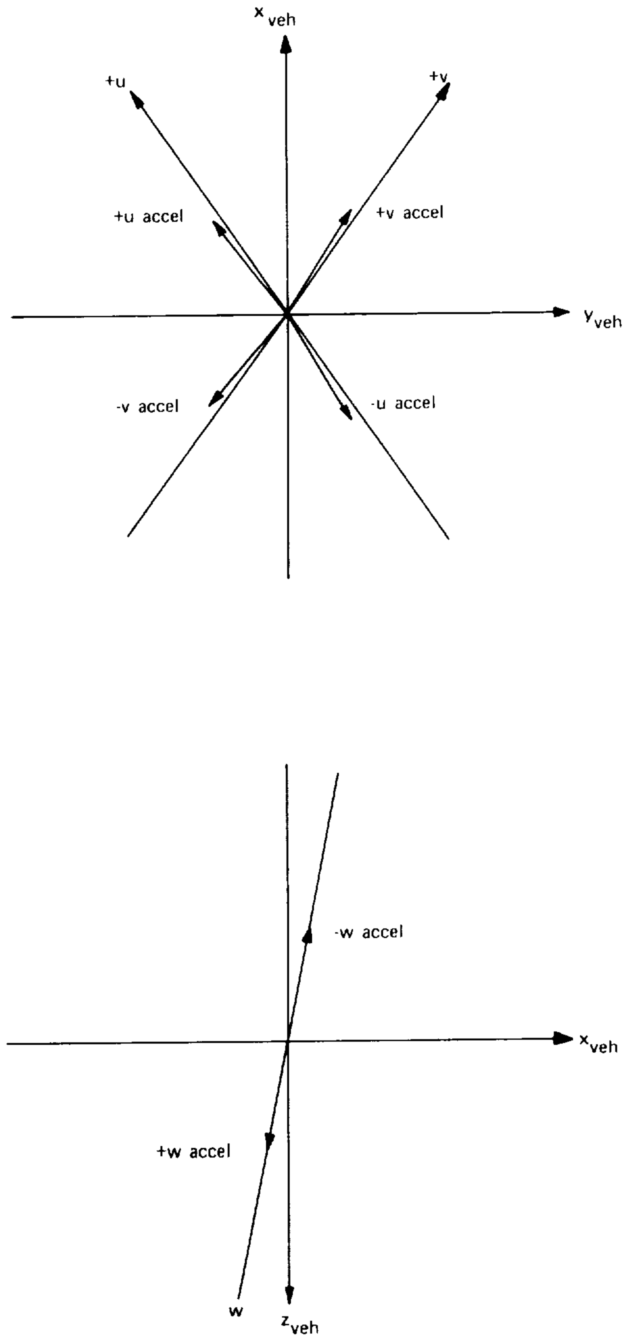

Fig. 6-2. u, v, w Control Axes

determined from measurements of the IMU gimbal angles. The procedure used is based on Kalman filter theory in which angular measurements are mixed with extrapolated state estimates to form a filtered estimate of the state. The process of extrapolation and measurement incorporation is described first in terms of a single axis. The complete three axis filter as implemented in the DFCS is discussed at the end of this subsection.

6.2.2.1 Vehicle Model

In estimation theory it is necessary to define a model of the process being observed. In the case of the shuttle vehicle, we will assume that it is a rigid body with the following equations of motion for one axis:

$$\begin{bmatrix} \dot{\theta}_B \\ \dot{\omega} \\ \dot{\alpha}_d \end{bmatrix} = \begin{bmatrix} 0 & 1 & 0 \\ 0 & 0 & 1 \\ 0 & 0 & 0 \end{bmatrix} \begin{bmatrix} \theta_B \\ \omega \\ \alpha_d \end{bmatrix} + \begin{bmatrix} 0 \\ \alpha_C \\ 0 \end{bmatrix} + \begin{bmatrix} 0 \\ \alpha_m \\ 0 \end{bmatrix} + \begin{bmatrix} 0 \\ n_\omega \\ n_\alpha \end{bmatrix} \qquad (6\text{-}1)$$

where

θ_B = vehicle altitude

ω = vehicle angular velocity

α_d = angular disturbance acceleration

α_C = control acceleration (produced by ACPS jets)

α_m = known bias acceleration

n_ω, n_α = driving noise terms

6.2.2.2 Extrapolation

The discrete filtering process can be divided into two parts: extrapolation and measurement incorporation. In the extrapolation process the estimate of the vehicle state, $\underline{\hat{x}}(t_0)$, given at some time, t_0, is integrated forward to the next measurement incorporation time, t_1. This integration includes the effect of any known biases or control inputs during the interval t_0, t_1. The result of the extrapolation process is a predicted estimate $\underline{\hat{x}}'(t_1)$. In our case $\underline{\hat{x}}'(t_1)$ is determined by integrating Eq.(6-1), i.e.,

$$\begin{aligned} \underline{\hat{x}}'(t_1) &= \overset{*}{\Phi}(t_1, t_0)\underline{\hat{x}}(t_0) + \int_{t_0}^{t_1} \overset{*}{\Phi}(t_1, \tau) \begin{bmatrix} 0 \\ \alpha_C(\tau) \\ 0 \end{bmatrix} d\tau \\ &\quad + \int_{t_0}^{t_1} \overset{*}{\Phi}(t_1, \tau) \begin{bmatrix} 0 \\ \alpha_m(\tau) \\ 0 \end{bmatrix} d\tau \end{aligned} \qquad (6\text{-}2)$$

where

$$\underline{\hat{x}}(t_0) = \begin{bmatrix} \hat{\theta}_B(t_0) \\ \hat{\omega}(t_0) \\ \hat{\alpha}_d(t_0) \end{bmatrix} = \text{state estimate at } t_0 \qquad (6\text{-}3)$$

and

$$\overset{*}{\Phi}(t_1, \tau) = \begin{bmatrix} 1 & (t_1 - \tau) & \dfrac{(t_1 - \tau)^2}{2} \\ 0 & 1 & (t_1 - \tau) \\ 0 & 0 & 1 \end{bmatrix} = \text{transition matrix} \qquad (6\text{-}4)$$

$\alpha_C(\tau)$ is the control acceleration applied by the ACPS jets. A typical plot of $\alpha_C(\tau)$ is shown in Fig. 6-3. It is assumed that the control acceleration can have one of three values $+|\alpha_C|$, 0, $-|\alpha_C|$. It is also assumed that if a jet goes on, it turns at the beginning of the interval, t_0. It is further assumed that when the jet goes off it remains off until the end of the interval. With this jet model we can now integrate the second term in Eq. (6-2).

$$\int_{t_0}^{t_1} \overset{*}{\Phi}(t_1, \tau) \begin{bmatrix} 0 \\ \alpha_C(\tau) \\ 0 \end{bmatrix} d\tau = \begin{bmatrix} |\alpha_C| \ \mathrm{SIGN}(\alpha_C) \ t_{JET} \left(\Delta T - \dfrac{t_{JET}}{2}\right) \\ |\alpha_C| \ \mathrm{SIGN}(\alpha_C) \ t_{JET} \\ 0 \end{bmatrix} \qquad (6\text{-}5)$$

where

$$\Delta T \overset{\Delta}{=} t_1 - t_0 = t_{fast}$$

$\alpha_m(\tau)$ is a known bias acceleration which is assumed to be constant over the over the integration interval:

$$\alpha_m(\tau) = \alpha_m(t_0)$$

The third term in Eq. (6-2) then reduces to

$$\int \overset{*}{\Phi}(t_1, \tau) \begin{bmatrix} 0 \\ \alpha_m^o(\tau) \\ 0 \end{bmatrix} d\tau = \begin{bmatrix} \alpha_m(t_0) \, \Delta T \left(\dfrac{\Delta T}{2}\right) \\ \alpha_m(t_0) \, \Delta T \\ 0 \end{bmatrix} \qquad (6\text{-}6)$$

Before grouping terms, define

$$\Delta\omega_{dm}(t_0) = [\hat{\alpha}_d(t_0) + \alpha_m(t_0)] \ \Delta T$$

$$\Delta\omega_C(t_0) = |\alpha_C| \ \mathrm{SIGN}(\alpha_C(t_0)) \ t_{JET}$$

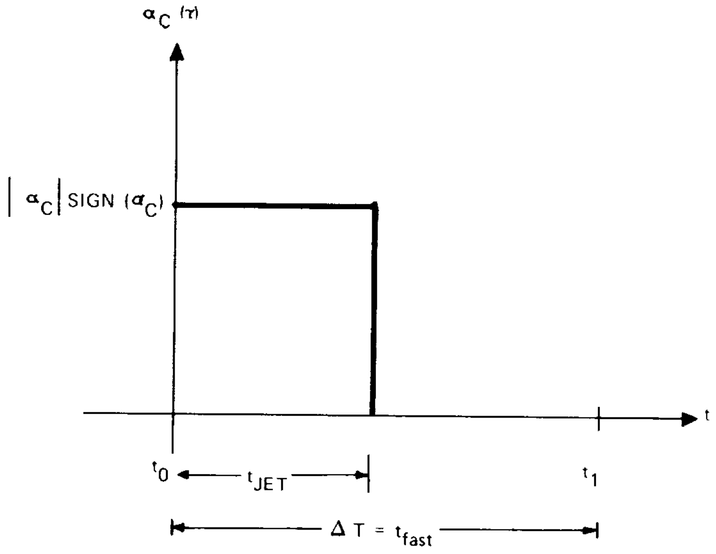

Fig. 6-3. ACPS Jet Control Acceleration Model

Combining results, we find

$$\hat{\theta}_B'(t_1) = \hat{\theta}_B(t_0) + \hat{\omega}(t_0)\Delta T + \Delta\omega_{dm}(t_0)\frac{\Delta T}{2} + \Delta\omega_C(t_0)\left(\Delta T - \frac{t_{JET}}{2}\right) \quad (6\text{-}7a)$$

$$\hat{\omega}'(t_1) = \hat{\omega}(t_0) + \Delta\omega_{dm}(t_0) + \Delta\omega_C(t_0) \quad (6\text{-}7b)$$

$$\hat{\alpha}_d'(t_1) = \hat{\alpha}_d(t_0) \quad (6\text{-}7c)$$

6.2.2.3 Measurement Incorporation

For the measurement incorporation process, the extrapolated state is combined with the measurement at time t_n in the following manner:

$$\hat{\theta}_B(t_n) = \hat{\theta}_B'(t_n) + K_\theta(\tilde{\theta}(t_n) - \hat{\theta}_B(t_n)) \quad (6\text{-}8a)$$

$$\hat{\omega}(t_n) = \hat{\omega}'(t_n) + K_\omega(\tilde{\theta}(t_n) - \hat{\theta}_B'(t_n)) / (t_n - t_\ell) \quad (6\text{-}8b)$$

$$\hat{\alpha}_d(t_n) = \hat{\alpha}_d'(t_n) + K_\alpha(\tilde{\theta}(t_n) - \hat{\theta}_B'(t_n)) / (t_n - t_\ell)^2 \quad (6\text{-}8c)$$

$$t_\ell \leftarrow t_n$$

where

K_θ = position gain (constant)

K_ω = velocity gain (constant)

K_α = acceleration gain (constant)

$\tilde{\theta}(t_n)$ = angle measurement at time t_n

t_ℓ = time of the last measurement incorporation

This measurement incorporation process is similar to the linear Kalman filter if the measurement interval, $t_n - t_\ell$, is fixed. However, for the Shuttle filter, measurements will be incorporated only if

$$|\tilde{\theta}(t_n) - \hat{\theta}_B'(t_n)| > \theta_{BT} \quad (6\text{-}9)$$

where

θ_{BT} = "trap" angle

If this condition is not true, then no measurement is processed and

$$\theta_B(t_n) = \theta_B'(t_n) \quad (6\text{-}10a)$$

$$\hat{\omega}(t_n) = \hat{\omega}'(t_n) \quad (6\text{-}10b)$$

$$\hat{\alpha}_d(t_n) = \hat{\alpha}_d'(t_n) \quad (6\text{-}10c)$$

This additional logic helps to reduce the effect of quantization of the gimbal angle measurements by "trapping" small-amplitude noise before it reaches the estimate.

6.2.2.4 The 3-Axis Filter as Implemented in the DFCS

The 3-axis state estimator is basically a simple extension of the single axis filter described above. Due to the kinematics of Euler rotations, however, the gimbal angle measurements are not simply related to the vehicle body rates. We can circumvent this problem by defining a set of "body angle" measurements. The body angles are defined as the integral of the body rates:

$$\theta_{B_1} = \int \omega_1 \, dt \qquad (6\text{-}11a)$$

$$\theta_{B_2} = \int \omega_2 \, dt \qquad (6\text{-}11b)$$

$$\theta_{B_3} = \int \omega_3 \, dt \qquad (6\text{-}11c)$$

To a good approximation we can calculate the body angles in recursive fashion as:

$$\begin{bmatrix} \tilde{\theta}_{B_1}(n) \\ \tilde{\theta}_{B_2}(n) \\ \tilde{\theta}_{B_3}(n) \end{bmatrix} = \begin{bmatrix} \tilde{\theta}_{B_1}(n-1) \\ \tilde{\theta}_{B_2}(n-1) \\ \tilde{\theta}_{B_3}(n-1) \end{bmatrix} \oplus \begin{bmatrix} 1 & \mathrm{SIN}(\theta_{GA_3}) & 0 \\ 0 & \mathrm{COS}(\theta_{GA_1})\mathrm{COS}(\theta_{GA_3}) & \mathrm{SIN}(\theta_{GA_1}) \\ 0 & -\mathrm{SIN}(\theta_{GA_1})\mathrm{COS}(\theta_{GA_3}) & \mathrm{COS}(\theta_{GA_1}) \end{bmatrix} \begin{bmatrix} \theta_{GA_1}(n) \ominus \theta_{GA_1}(n-1) \\ \theta_{GA_2}(n) \ominus \theta_{GA_2}(n-1) \\ \theta_{GA_3}(n) \ominus \theta_{GA_3}(n-1) \end{bmatrix} \qquad (6\text{-}12)$$

where

θ_{GA_1} = outer gimbal angle

θ_{GA_2} = inner gimbal angle

θ_{GA_3} = middle gimbal angle

and

$\oplus$ indicates modular addition

$\ominus$ indicates modular subtraction

(Modular addition and subtraction of two angles produces a result which lies in the range: $-180° < \theta \le 180°$.) Measurement incorporation is performed as before (Eq. (6-8)) except that the measurements are now the computed body angles (Eq.(6-12)). For the x axis,

if

$$\left| \tilde{\theta}_{B_x}(t_n) - \hat{\theta}'_{B_x}(t_n) \right| > \theta_{BT} \qquad (6\text{-}13)$$

then

$$\hat{\theta}_{B_x}(t_n) = \hat{\theta}'_{B_x}(t_n) \oplus K_\theta\left[\tilde{\theta}_{B_x}(t_n) \ominus \hat{\theta}'_{B_x}(t_n)\right] \tag{6-13a}$$

$$\hat{\omega}_x(t_n) = \hat{\omega}'_x(t_n) + K_\omega\left[\tilde{\theta}_{B_x}(t_n) \ominus \hat{\theta}'_{B_x}(t_n)\right]/(t_n - t_{\ell_x}) \tag{6-13b}$$

$$\hat{\alpha}_{dx}(t_n) = \hat{\alpha}_{dx}(t_n) + K_\alpha\left[\tilde{\theta}_{B_x}(t_n) \ominus \hat{\theta}_{B_x}(t_n)\right]/(t_n - t_{\ell_x})^2 \tag{6-13c}$$

$$t_{\ell_x} \leftarrow t_n \tag{6-13d}$$

otherwise,

$$\hat{\theta}_{B_x}(t_n) = \theta'_{B_x}(t_n) \tag{6-14a}$$

$$\hat{\omega}_x(t_n) = \omega'_x(t_n) \tag{6-14b}$$

$$\hat{\alpha}_{dx}(t_n) = \alpha'_{dx}(t_n) \tag{6-14c}$$

In the above equations

$\hat{\theta}_{B_x}$ = estimated value of the x body angle

$\hat{\theta}'_{B_x}$ = extrapolated value of the x body angle

$\tilde{\theta}_{B_x}$ = "measured" value of the x body angle

$\hat{\omega}_x$ = estimated x-axis body rate

$\hat{\omega}'_x$ = extrapolated x-axis body rate

$\hat{\alpha}_{dx}$ = estimated x-axis component of disturbing acceleration

$\hat{\alpha}'_{dx}$ = extrapolated x-axis component of disturbing acceleration

t_n = current time

t_{ℓ_x} = time of the last measurement incorporation for the x-axis

The y and z axis computations are similar. Note that a separate "trap" is required for each axis.

After the appropriate jet control is exercised the extrapolation of the vehicle state, which depends to a large extent on the ACPS jet selection and timing logic used in the Shuttle autopilot, is performed. It is currently assumed that the jet firings produce accelerations about the u, v and w axes defined in Subsection 6.2.1. That is, the angular acceleration produced about the vehicle axes by the jets is the sum of the three components:

$$\underline{\alpha}_{CU} = J^{-1} (\underline{M}_{P2U} - \underline{M}_{M2U})/2 \qquad (6\text{-}15a)$$

$$\underline{\alpha}_{CV} = J^{-1} (\underline{M}_{P2V} - \underline{M}_{M2V})/2 \qquad (6\text{-}15b)$$

$$\underline{\alpha}_{CW} = J^{-1} (\underline{M}_{P2W} - \underline{M}_{M2W})/2 \qquad (6\text{-}15c)$$

where J is the inertia matrix and the $\underline{M}$'s are the torque vectors defined in Subsection 6.2.1. It is also assumed that the restrictions on the timing of jet firings which were given for the single-axis filter apply. If we define

t_{JET_1} = time of firing of the u jets during the interval $t_0 < t < t_1$

t_{JET_2} = time of firing of the v jets during the interval $t_0 < t < t_1$

t_{JET_3} = time of firing of the w jets during the interval $t_0 < t < t_1$

and

$SGNC_1$ = sign of the desired u control acceleration

$SGNC_2$ = sign of the desired v control acceleration

$SGNC_3$ = sign of the desired w control acceleration

then by analogy with the results of the single axis filter:

$$\Delta \underline{\omega}_u(t_0) = |\underline{\alpha}_{CU}|\ SGNC_1\ t_{JET_1} \qquad (6\text{-}16a)$$

$$\Delta \underline{\omega}_v(t_0) = |\underline{\alpha}_{CV}|\ SGNC_2\ t_{JET_2} \qquad (6\text{-}16b)$$

$$\Delta \underline{\omega}_w(t_0) = |\underline{\alpha}_{CW}|\ SGNC_3\ t_{JET_3} \qquad (6\text{-}16c)$$

and

$$\Delta \underline{\omega}_{dm}(t_0) = (\hat{\underline{\alpha}}_d(t_0) + \underline{\alpha}_m(t_0))\Delta T \qquad (6\text{-}16d)$$

Note that these are vector quantities. The bias acceleration, $\underline{\alpha}_m$, is computed by the attitude maneuver routine as

$$\underline{\alpha}_m = -J^{-1}(\underline{\omega}_d x J \underline{\omega}_d) \qquad (6\text{-}17)$$

where $\underline{\omega}_d$ is the desired maneuver rate. With these definitions, the complete three axis extrapolation equations can be written as

$$\begin{aligned}\hat{\underline{\theta}}'_B(t_1) = \hat{\underline{\theta}}_B(t_0) \oplus \Big[& \hat{\underline{\omega}}(t_0)\Delta T + \Delta\underline{\omega}_{dm}(t_0)\frac{\Delta T}{2} \\ & + \Delta\underline{\omega}_u(t_0)\left(\Delta T - \frac{t_{JET_1}}{2}\right) + \Delta\underline{\omega}_v(t_0)\left(\Delta T - \frac{t_{JET_2}}{2}\right) \\ & + \Delta\underline{\omega}_w(t_0)\left(\Delta T - \frac{t_{JET_3}}{2}\right)\Big]\end{aligned} \qquad (6\text{-}18a)$$

$$\hat{\underline{\omega}}'(t_1) = \hat{\underline{\omega}}(t_0) + \Delta\, \underline{\omega}_{dm}(t_0) + \Delta\underline{\omega}_u(t_0) + \Delta\underline{\omega}_v(t_0) + \Delta\underline{\omega}_w(t_0) \tag{6-18b}$$

$$\hat{\underline{\alpha}}'_d(t_1) = \hat{\underline{\alpha}}_d(t_0) \tag{6-18c}$$

Note that these quantities are vectors with components in the x, y, z vehicle (body) axes.

The estimate of disturbance acceleration, $\hat{\underline{\alpha}}_d$, may be accurate enough for the powered flight phases, but it may be too noisy for use during drifting flight. If an estimate is needed during coasting flight to counteract such disturbances as gravity gradient and aerodynamic torques, then rate gyro measurements may be required. If not, the $\hat{\underline{\alpha}}_d$ estimation process may be disabled by using appropriate filter gains. Alternatively, the gain, K_{α}, simply can be reduced during coasting flight. In any event, the bias acceleration estimate, $\underline{\alpha}_m$, should be used during coasting flight maneuvers to reduce fuel consumption.

6.2.3 Control Laws for the On-Orbit ACPS Phase

The object of the phase plane switching logic is to compute changes in angular velocity so that by turning on or off the appropriate jets to achieve this velocity change the vehicle limit cycles about a desired attitude and attitude rate. The two dimensional phase plane is applied to the decoupled control axes described in Subsection 6.2.1. Limit cycling is desirable since it would be extremely costly to attempt to maintain the desired attitude and rate exactly. By designing appropriate switching lines into the phase plane, the vehicle can be driven into the desired limit cycle. Two separate logics are used depending on the size of the position and rate errors. For large errors, a switching logic has been designed to drive the state into the small-error control region. The small-error switching logic then drives the state into a limit cycle about the desired attitude and attitude rate. The distinction between large and small errors will be quantified later in this section.

The small-error switching logic has the following features:

1) The design is based upon the optimal switch curves for minimizing a weighted combination of fuel and response time. The optimal curves are separated by a deadband in order to allow for limit cycling.

2) The appropriate deadband can be chosen in order to
   a) fix the limit cycle period
   b) fix the limit cycle maximum rate
   c) fix the maximum attitude excursion while limit cycling

3) The average attitude error is minimized by biasing the placement of the switch curves.

4) Parabolic switch curves approximate the trajectories which the state follows. However, hysteresis logic prevents performance degradation due to errors in these approximations.

The design incorporating these features is described in the following subsections.

In Subsection 6.2.3.1 two idealized limit cycles are presented. One limit cycle is in the presence of positive disturbing accelerations while the other is in the presence of zero disturbing accelerations. For each limit cycle the average attitude error will be derived. In Subsection 6.2.3.2 the design of switching curves to drive the state into a limit cycle with zero average attitude error is described. This design is referred to as the small-error control logic. The large-error control logic is described in Subsection 6.2.3.3.

6.2.3.1 Idealized Limit Cycles

An idealized limit cycle for a positive disturbing acceleration is illustrated in Fig. 6-4. The coordinates θ_e and ω_e are chosen to be the state, where θ_e represents the angular position error and ω_e represents the angular rate error. X_{DB} is the attitude variation in the course of limit cycling. In the presence of a positive disturbance acceleration, U_D, the state is driven along the trajectory from A to B. At point B a negative control acceleration, $-U_C$, is applied to return the state to point A.

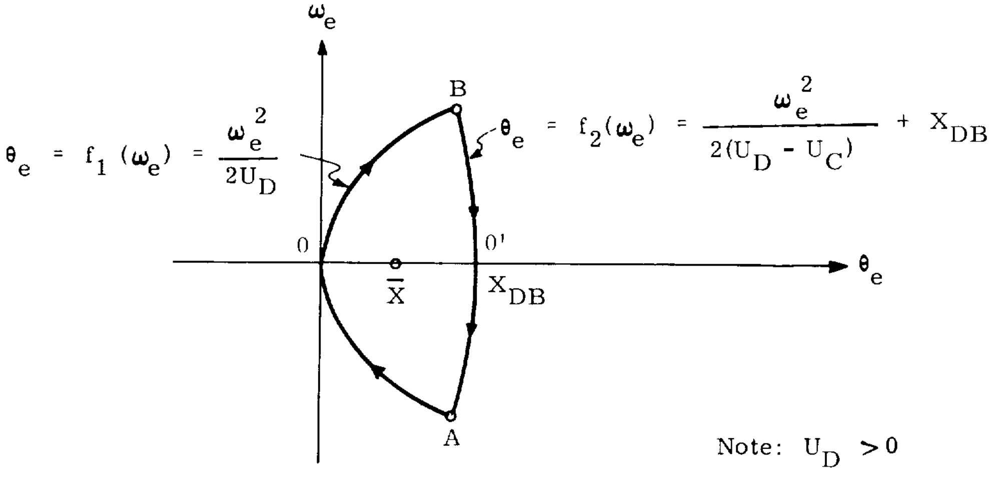
ω_e
B
$\theta_e = f_1(\omega_e) = \frac{\omega_e^2}{2U_D}$
$\theta_e = f_2(\omega_e) = \frac{\omega_e^2}{2(U_D - U_C)} + X_{DB}$
0
0'
$\bar{X}$
X_{DB}
θ_e
A
Note: $U_D > 0$

Fig. 6-4 Idealized Limit Cycle for a Positive Disturbing Acceleration

The average attitude error, $\overline{X}$, of the limit cycle in Fig. 6-4 is found by determining the average attitude error for each of the trajectories OB and BO$'$ (called $\overline{X}_1$ and $\overline{X}_2$) and then "weighting" them according to time to calculate the net average, $\overline{X}$.

Determination of $\overline{X}_1$:

$\overline{X}_1$ is, by definition,

$$\overline{X}_1 = \frac{1}{t_1} \int_0^{t_1} \frac{1}{2} U_D t^2 \, dt \qquad (6\text{-}19)$$

t_1, the time to travel from point O to point B, can be calculated from the value of the θ_e abscissa of point B, B_{θ_e}, since

$$B_{\theta_e} = \frac{1}{2} U_D t_1^2 \qquad (6\text{-}20)$$

B_{θ_e} is found by first rearranging $\theta_e = f_1(\omega_e)$ and $\theta_e = f_2(\omega_e)$ such that,

$$\omega_e = g_1(\theta_e), \quad \omega_e = g_2(\theta_e) \qquad (6\text{-}21)$$

Then, at point B, $g_1(\theta_e) = g_2(\theta_e)$, and,

$$B_{\theta_e} = X_{DB} \left(\frac{U_C - U_D}{U_C} \right) \qquad (6\text{-}22)$$

and from Eq(6-20)

$$t_1 = + \sqrt{\frac{2X_{DB} (U_C - U_D)}{U_C U_D}} \qquad (6\text{-}23)$$

Using t_1 in Eq(6-19)

$$\overline{X}_1 = \frac{1}{3} X_{DB} \left(\frac{U_C - U_D}{U_C} \right) \qquad (6\text{-}24)$$

Determination of $\overline{X}_2$:

The time average attitude error for the trajectory segment BO$'$ can be found by setting t = 0, at point B. Then,

$$\overline{X}_2 = \frac{1}{t_2} \int_0^{t_2} [X_o + \dot{X}_o t + \frac{1}{2} (U_D - U_C) t^2] \, dt$$

or,

$$\overline{X}_2 = X_o + \frac{\dot{X}_o t_2}{2} + \frac{1}{6} (U_D - U_C) t_2^2 \qquad (6\text{-}25)$$

X_o is defined in Eq (6-22) and $\dot{X}_o$ can be determined from,

$$\dot{X}_o = U_D t_1 = +\sqrt{\frac{2X_{DB}U_D(U_C - U_D)}{U_C}} \qquad (6\text{-}26)$$

To find t_2 one can use the following relation,

$$\dot{X}_o + (U_D - U_C)t_2 = 0$$

from which it follows,

$$t_2 = \sqrt{\frac{2X_{DB}U_D}{U_C(U_C - U_D)}} \qquad (6\text{-}27)$$

Substituting the results of Eq (6-22), (6-26) and (6-27) into Eq (6-25), yields:

$$\overline{X}_2 = X_{DB}\left(1 - \frac{U_D}{3U_C}\right) \qquad (6\text{-}28)$$

Determination of $\overline{X}$:

Finally, the total average attitude error, $\overline{X}$, can be found from:

$$\overline{X} = \frac{\overline{X}_1 t_1 + \overline{X}_2 t_2}{t_1 + t_2} \qquad (6\text{-}29)$$

Substituting the results of Eqs (6-23), (6-24), (6-27), (6-28) into Eq (6-29), yields:

$$\overline{X} = \frac{X_{DB}}{3}\left(1 + \frac{U_D}{U_C}\right) \qquad (6\text{-}30)$$

This is the average attitude error for the limit cycle in Fig. 6-4. Thus, the average attitude error would be zero if the intercept of the curve on the right, which is the trajectory along which the control is applied, were shifted from point O′ to have an abscissa of

$$DR = X_{DB} - \overline{X} \qquad (6\text{-}31)$$

A similar result can be obtained for the case of a negative disturbance acceleration. Equations (6-30) and (6-31) are used in the DFCS in order to minimize the average attitude error.

The attitude variation, X_{DB}, could be chosen as follows:

1) To achieve the cycle period, T:

$$\text{set } X_{DB} = \left[1 - \frac{|U_D|}{|U_C|}\right]\frac{|U_D|}{8}T^2 \qquad (6\text{-}32)$$

2) To achieve the limit cycle maximum rate, $\dot{X}_{max}$:

$$\text{set } X_{DB} = \frac{|U_C|\,(\dot{X}_{max})^2}{2|U_D|\,(|U_C| - |U_D|)} \qquad (6\text{-}33)$$

3) By simply setting X_{DB} to the allowable attitude variation.

Currently, the final option is employed in the DFCS.

An idealized limit cycle in the presence of no disturbing accelerations is illustrated in Fig. 6-5. From point A the state is allowed to drift to point B where a negative control acceleration, $-U_C$, (in the form of a minimum impulse jet firing) is applied to drive the state to point C. From point C the state is then allowed to drift to point D. At point D a positive control acceleration, $+U_C$, is applied to return the state to point A. By choosing DL = DR the state limit cycles with zero average attitude error. The generalized limit cycle for positive disturbing accelerations is made to reduce to the limit cycle for zero disturbing accelerations by selecting

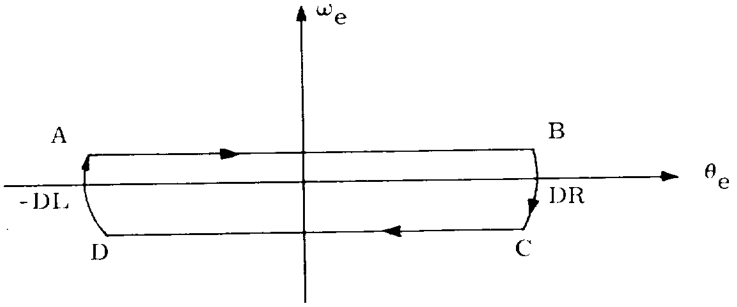

Fig. 6-5 Limit Cycle in Presence of No Disturbing Accelerations

$$DL = \overline{X} + \frac{1}{3} X_{DB} \tag{6-34}$$

6.2.3.2 Small-Error Control Law

Control regions for relatively small errors are illustrated in Fig. 6-6, definitions of curves are summarized in Table 6-1, and corresponding control actions are given in Table 6-2. All logic in this subsection is formulated in terms of positive disturbing accelerations. In the actual implementation, (see Subsection 6.4), negative disturbances are treated by inverting the signs of the state variables θ_e and ω_e. Biasing the right and left deadbands, DR and DL, to null the average attitude error in accordance with the equations derived in the preceeding subsection, defines the placement of the switching curves BOUNDARY_II_TO_COAST and BOUNDARY_III_TO_COAST. These curves approximate the trajectory of the state during a firing. When the state lies in Region II, control is applied to drive the state to the curve TARGET_DISTURB. The vehicle is then allowed to coast.

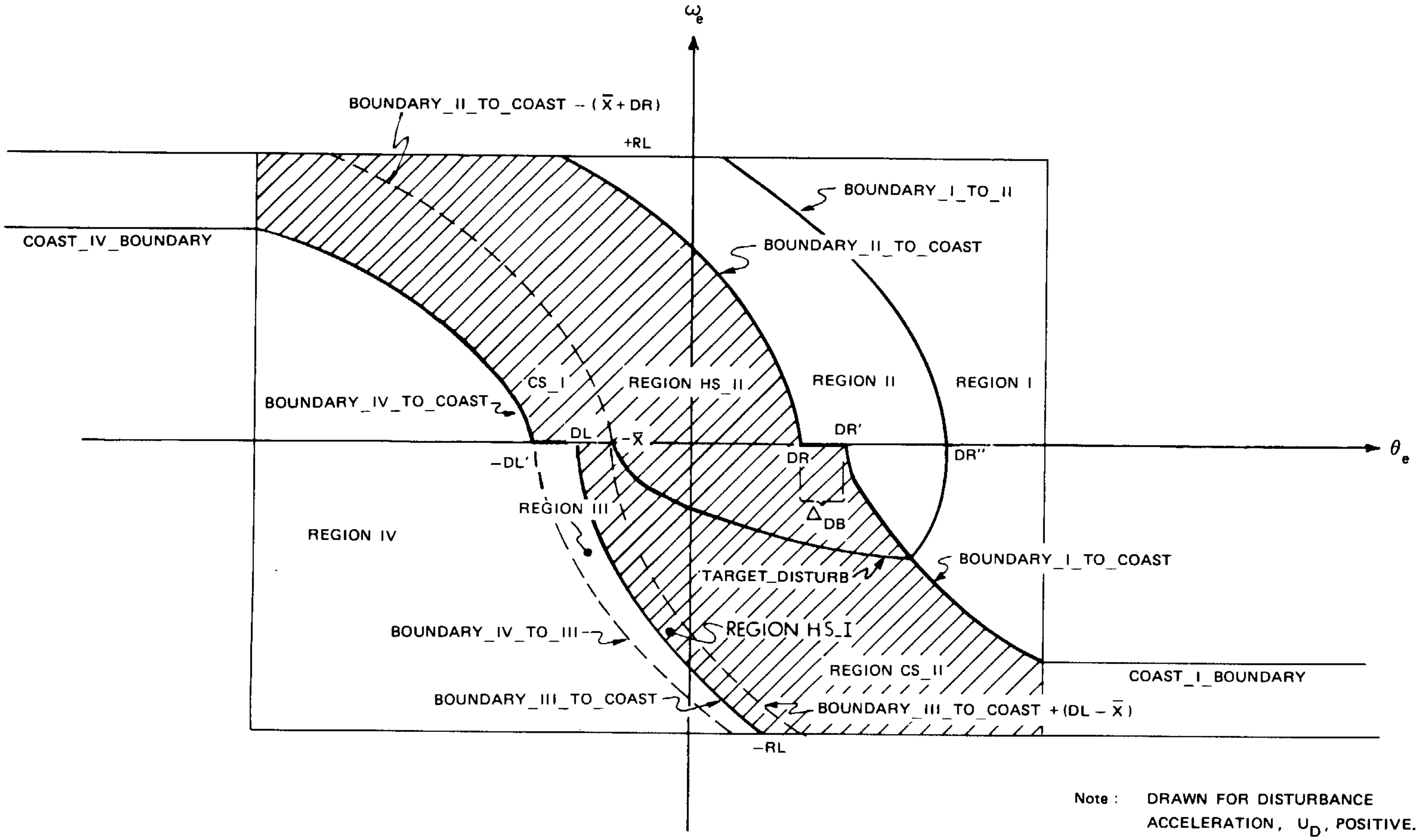

Note : DRAWN FOR DISTURBANCE ACCELERATION, U_D, POSITIVE.

Fig. 6-6. SMALL_ERROR_DISTURBANCE_LOGIC

Table 6-1: Definitions of Boundaries of Small-Error Control Regions

Boundary/Parameter	Definition
BOUNDARY_I_TO_II	$\theta_e = -\dfrac{\omega_e^2}{2(\lvert U_C\rvert - \lvert U_D\rvert)} + DR''$
BOUNDARY_II_TO_COAST	$\theta_e = -\dfrac{\omega_e^2}{2(\lvert U_C\rvert - \lvert U_D\rvert)} + DR$
BOUNDARY_I_TO_COAST	$\theta_e = +\dfrac{\omega_e^2}{2CD(\lvert U_C\rvert + \lvert U_D\rvert)} + DR'$
BOUNDARY_III_TO_COAST	$\theta_e = +\dfrac{\omega_e^2}{2(\lvert U_C\rvert + \lvert U_D\rvert)} - DL$
BOUNDARY_IV_TO_III	$\theta_e = +\dfrac{\omega_e^2}{2(\lvert U_C\rvert + \lvert U_D\rvert)} - DL'$
BOUNDARY_IV_TO_COAST	$\theta_e = -\dfrac{\omega_e^2}{2CD(\lvert U_C\rvert - \lvert U_D\rvert)} - DL'$
TARGET_DISTURB	$\theta_e = +\dfrac{\omega_e^2}{2\lvert U_D\rvert} - \overline{X}$

WHERE

$\Delta_{DB} = 0.2\ X_{DB}$

$DR = X_{DB} - \overline{X}$ $\qquad$ $DL = \overline{X} + \frac{1}{3} X_{DB}$

$DR' = DR + \Delta_{DB}$ $\qquad$ $DL' = DL + \Delta_{DB}$

$$DR'' = (\overline{X} + DR')(\lvert U_D\rvert)\left(\frac{(\lvert U_C\rvert - \lvert U_D\rvert) + CD(\lvert U_C\rvert - \lvert U_D\rvert)}{(CD(\lvert U_C\rvert + \lvert U_D\rvert) - \lvert U_D\rvert)(\lvert U_C\rvert - \lvert U_D\rvert}\right) + DR'$$

Table 6-2: Control Actions in Small-Error Control Regions

Region	Control Action
I	Drive state to BOUNDARY_I_TO_COAST
II	Drive state to TARGET_DISTURB
III	Drive state to zero rate
IV	Drive state to BOUNDARY_IV_TO_COAST
HS_I	If coming from LARGE ERROR CONTROL LOGIC or REGION III then drive state to zero rate, else coast
HS_II	If coming from LARGE ERROR CONTROL LOGIC or REGION II then drive state to TARGET_DISTURB, else coast
CS_I	coast
CS_II	coast

The deadband increment Δ_{DB} is added to prevent fuel-consuming overshoot when the disturbance acceleration is zero or very small. The points

$$DR' = DR + \Delta_{DB} \qquad (6\text{-}35)$$

$$DL' = DL + \Delta_{DB} \qquad (6\text{-}36)$$

define the placement of the curves BOUNDARY_I_TO_COAST and BOUNDARY_IV_TO_COAST.

The factor CD determines the weight given to response time as opposed to fuel consumption, by adjusting the steepness of the switch curves that are normally crossed when entering the coast region. To insure that BOUNDARY_IV_TO_COAST is always less than BOUNDARY_II_TO_COAST and BOUNDARY_I_TO_COAST is always greater than BOUNDARY_III_TO_COAST, CD must be between 0 and 1. Currently the value of CD is 0.8.

Hysteresis has been incorporated to make the most efficient use of disturbance accelerations, to prevent switching line chatter, and to prevent tight limit cycling about the point DR. The dashed curves within the shaded area and parallel to BOUNDARY_II_TO_COAST provide hysteresis in the regions HS_I and HS_II. If the state lies inside either Region HS_I or HS_II and the sign of the newly computed change in rate is not the same as the sign of the last computed change in rate, then no control is applied and the vehicle is allowed to coast. However if the signs are the same, then in

Region HS_I the state is driven to zero and in Region HS-II the state is driven to TARGET_DISTURB. Whenever the state lies inside either Region CS-I or CS_II the vehicle is simply allowed to coast.

When the state lies to the right of BOUNDARY_I_TO_II position error is reduced more quickly by driving the state to BOUNDARY_I_TO_COAST and then coasting instead of driving the state to TARGET_DISTURB and then coasting. This is particularly important as the disturbance acceleration approaches zero. The curve BOUNDARY_I_TO_II is defined by the intersection of TARGET_DISTURB and BOUNDARY_I_TO_COAST.

When in Region III the rate error is driven to zero, and when in Region IV the state is driven to BOUNDARY_IV_TO_COAST to more quickly reduce position and rate errors.

6.2.3.3 Large-Error Control Law

Control regions for relatively large errors are illustrated in Fig. 6-7, definitions of the boundaries are summarized in Table 6-3, and corresponding control actions are given in Table 6-4. As in the preceeding subsection, all logic is formulated in terms of positive disturbing accelerations. In the actual implementation (see Subsection 6.4), negative disturbances are treated by inverting the signs of the state variables, θ_e and ω_e.

The purpose of the large-error control logic essentially is to drive the state into the small-error control region. Bounds between the small-error and large-error regions are set by the values of the parameters RL and RL′ (currently 4.0 and 3.0 deg/sec respectively). The rate error bounds are equal to ± RL. The left position error limit, -PLL, is defined by the intersection of BOUNDARY_IV_TO_COAST and COAST_IV_BOUNDARY. Similarly, the right position error limit, +PLR, is defined by the intersection of BOUNDARY_I_TO_COAST and COAST_I_BOUNDARY. The boundaries COAST_IV_BOUNDARY and COAST_I_BOUNDARY are rate errors equal to ± RL′.

TARGET_ARL is the average of RL and RL′. TARGET_ARL and -(TARGET_ARL) are taken to be the target rate when the state is in Regions II and I respectively; i.e., when the firing is against the disturbance acceleration. When the state is in Regions III and IV the targets are the nearest boundary; i.e. COAST_IV_BOUNDARY and -RL respectively.

Hysteresis is incorporated into the large-error coast regions to prevent chatter about +RL and COAST_I_BOUNDARY. If the state is driven into Region HL-I from Region II, then it is further driven to TARGET_ARL. If the state otherwise appears in Region HL_I the vehicle is allowed to coast. Similarly, if the state is driven into Region HL_II from Region I then it is further driven to -(TARGET_ARL); otherwise the vehicle is allowed to coast. Should the state appear in either Region CL_I or Region CL_II the vehicle is simply allowed to coast.

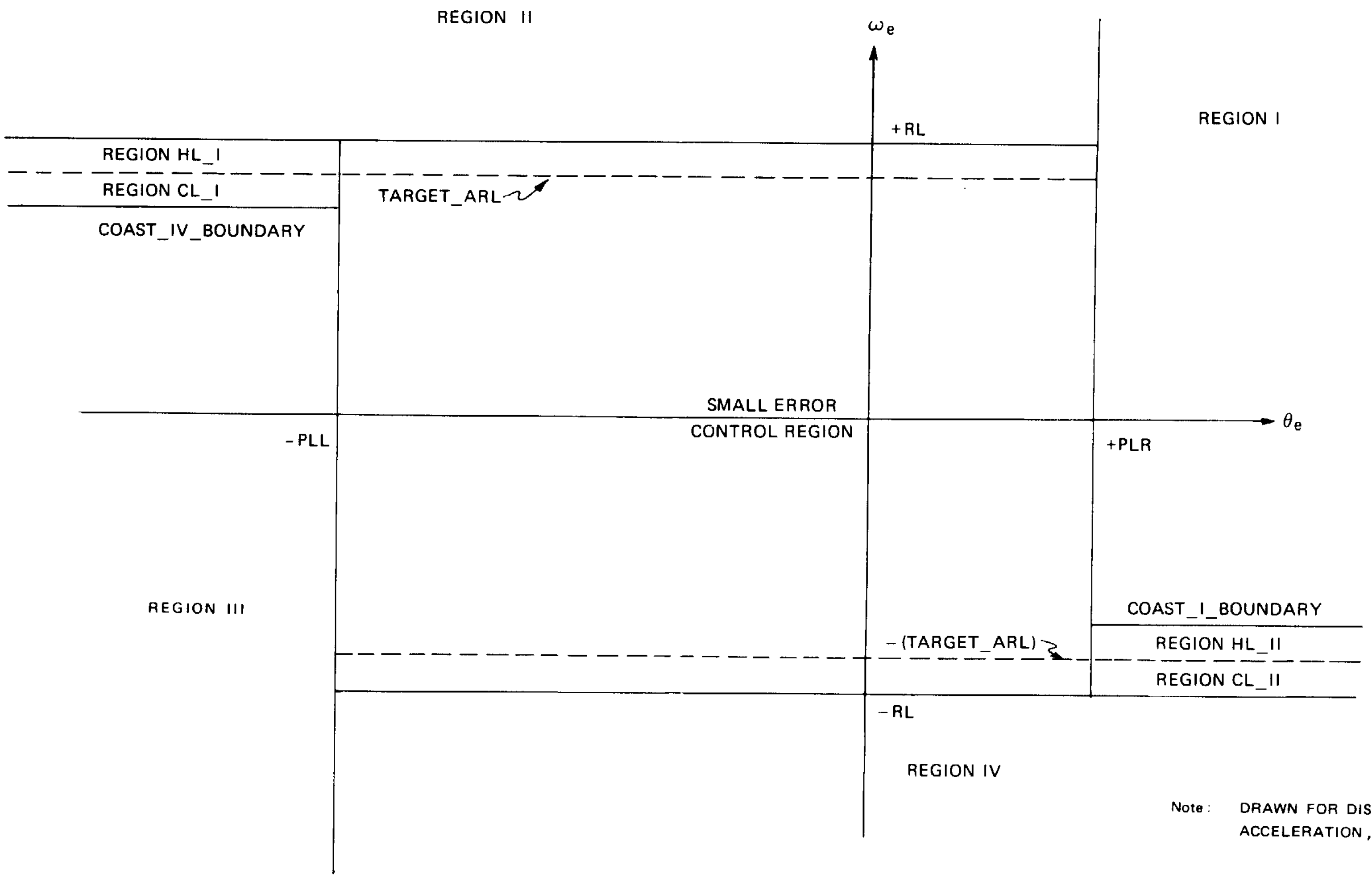

Note: DRAWN FOR DISTURBANCE ACCELERATION, U_D, POSITIVE.

Fig. 6-7. Large Error Control Region

Table 6-3: Definitions of Boundaries for the Large-Error Control Regions

Boundary/Parameter	Definition
COAST_IV_BOUNDARY	$\omega_e = RL'$
COAST_I_BOUNDARY	$\omega_e = -RL'$
TARGET_ARL	$\omega_e = (RL + RL')/2$
PLR	$\theta_e = + \dfrac{(RL')^2}{2CD(\lvert U_C\rvert + \lvert U_D\rvert)} + DR'$
PLL	$\theta_e = - \dfrac{(RL')^2}{2CD(\lvert U_C\rvert - \lvert U_D\rvert)} - DL'$

Table 6-4: Control Actions in Large-Error Control Regions

REGION	CONTROL ACTION
I	Drive state to -(TARGET_ARL)
II	Drive state to TARGET_ARL
III	Drive state to COAST_IV_BOUNDARY
IV	Drive state to -RL
HL_I	If coming from region II then drive state to TARGET_ARL, else coast
HL_II	If coming from region I then drive state to -(TARGET_ARL), else coast
CL_I	coast
CL_II	coast

A final feature of the small-error control logic can be described, now that TARGET_ARL has been introduced. If the disturbance acceleration is very large, part of the curve TARGET_DISTURB may lie below -(TARGET_ARL). In this situation a check is made to see if a rate change to drive the state to TARGET_DISTURB is greater than a rate change to drive the state to -(TARGET_ARL). If it is, the state is driven to -(TARGET_ARL), which means less fuel consumption with the result of finishing in a limit cycle about the origin.

6.3 On-Orbit TVC Phase: Preliminary Functional Summary

The Orbiter Maneuvering Subsystem (OMS) is used for major on-orbit maneuvers and to establish the deorbit entry trajectory. During powered flight the roll, pitch and yaw of the space-shuttle orbiter is achieved through deflection of the two gimbaled engines. Computation of gimbal servo commands in response to computed errors between commanded and measured attitudes is the function of the on-orbit TVC (Thrust Vector Control) "phase" of the DFCS. The following functional summary is an adaptation of the Apollo Command Module TVC control; it is illustrated in Fig. 6-8.

1) The steering-loop computations generate incremental attitude commands in inertial coordinates and transform them into body coordinates.

2) The DFCS back-differences the gimbal angles to obtain incremental variations over each sampling interval.

3) The gimbal increments over each sampling interval are then transformed into body coordinates and subtracted from the commanded increments which are generated by the steering program.

4) The respective attitude errors are fed to the roll, pitch and yaw compensation filters, whose outputs contribute to the commands to the engine gimbal servos. These signals bear the burden of controlling rapid transients, determining the system bandwidth and the stability of the vehicle slosh and bending modes.

5) As shown in Fig. 6-8b, the total command signal to each engine-gimbal servo is made up of the component from the associated compensation filter plus another component from a Thrust Misalignment Correction (TMC) loop. The latter component serves to bias the total command so that a zero output from the compensation filter will cause the thrust vector to pass exactly through the center of gravity (cg) when there is no cg motion and no motion of the thrust vector relative to the commanded angle.

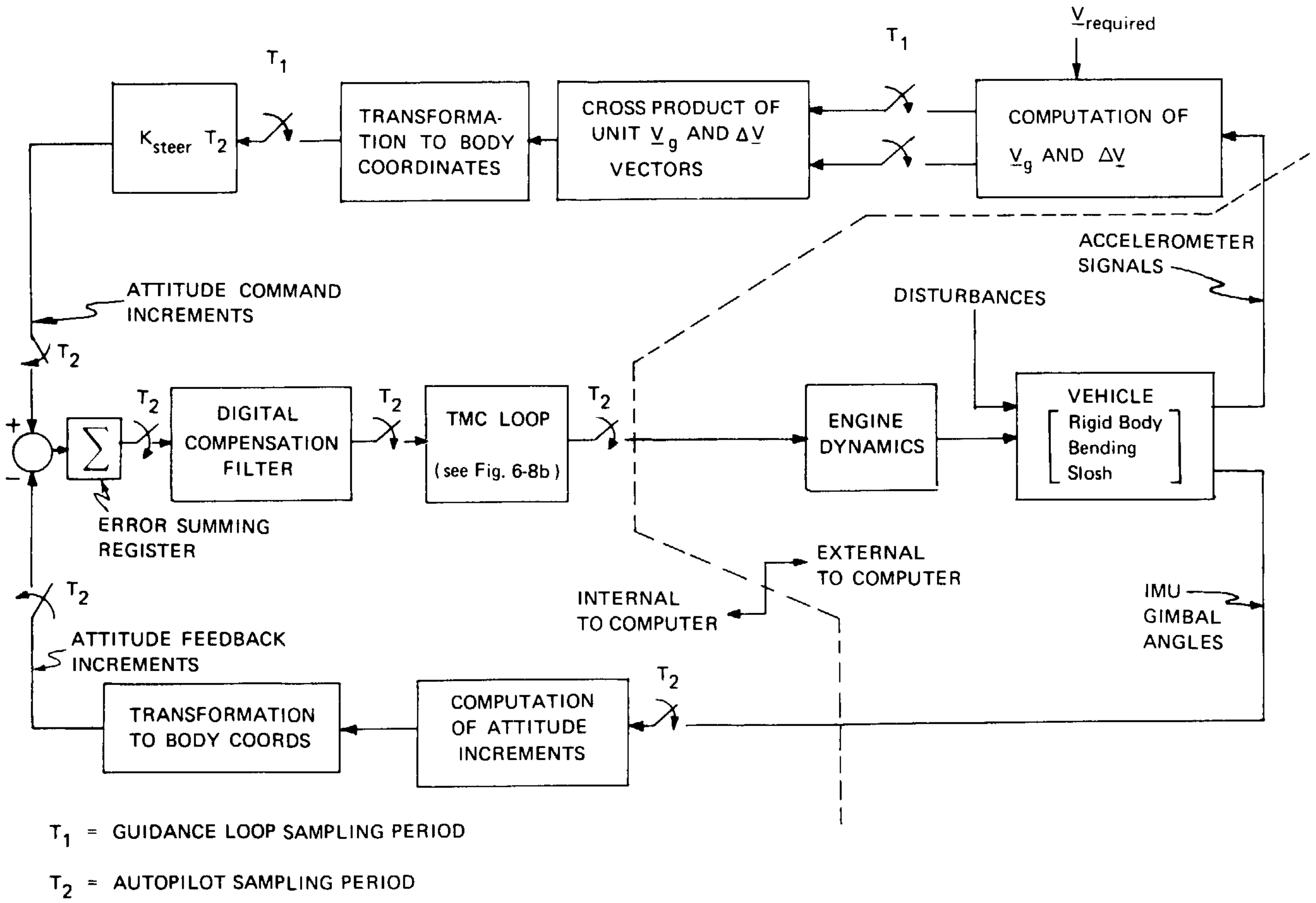
V required
T1
T1
COMPUTATION OF V g AND ΔV
CROSS PRODUCT OF UNIT V g AND ΔV VECTORS
TRANSFORMATION TO BODY COORDINATES
K steer T2
ACCELEROMETER SIGNALS
DISTURBANCES
ATTITUDE COMMAND INCREMENTS
T2
+
−
T2
T2
T2
DIGITAL COMPENSATION FILTER
TMC LOOP (see Fig. 6-8b)
ENGINE DYNAMICS
VEHICLE Rigid Body Bending Slosh
ERROR SUMMING REGISTER
EXTERNAL TO COMPUTER
INTERNAL TO COMPUTER
IMU GIMBAL ANGLES
T2
ATTITUDE FEEDBACK INCREMENTS
T2
TRANSFORMATION TO BODY COORDS
COMPUTATION OF ATTITUDE INCREMENTS
T1 = GUIDANCE LOOP SAMPLING PERIOD
T2 = AUTOPILOT SAMPLING PERIOD

Fig. 6-8a. Functional Block Diagram of the TVC DAP

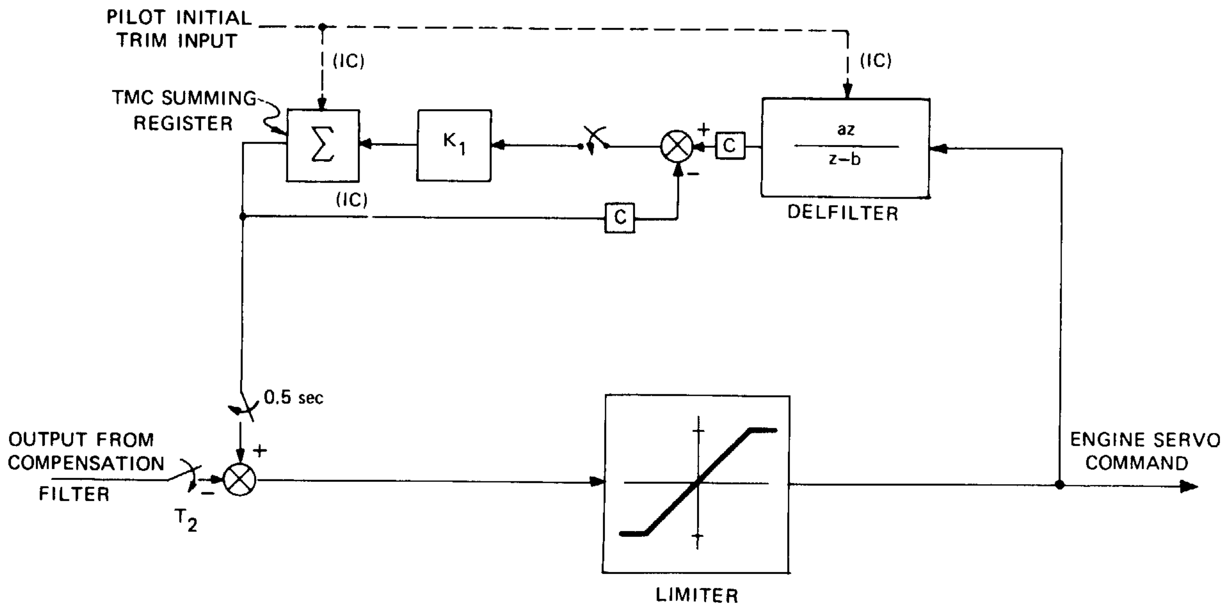

Fig. 6-8b. Block Diagram of the Thrust Misalignment Correction (TMC) Loop

6) The two major elements of the TMC loop are its summing register, which supplies the bias, and its low-pass filter, DELFILTER, which tracks the total command signal at autopilot sampling frequencies. The difference between the bias and the DELFILTER output is used to increment the summing register so as to slowly correct for the offset caused by thrust-to-cg misalignment. This slow reset action is roughly equivalent to inserting a proportional-plus-integral transfer function between the compensation filter and the total command signal. The TMC loop is designed so that its dynamics have no effect on the vehicle bending and slosh modes and very little effect on the rigid-body stability.

7) The operation of the TVC digital autopilot cannot be considered separately from that of the steering loop which interacts with the autopilot. The steering loop operations are shown in Fig. 6-8 for the case of "External ΔV" guidance. This form of guidance is based on achieving a desired accelerometer-measured velocity change, $\Delta \underline{V}_C$, which is inserted into the steering program as an initial value of the computed velocity-to-be-gained vector, $\underline{V}_g$. The $\underline{V}_g$ vector is periodically reduced during the course of the burn by subtracting the accelerometer-measured increments, $\Delta \underline{V}$.

8) The purpose of the steering loop is to align the vehicle thrust with the velocity-to-be-gained. This is achieved by commanding a vehicle turning-rate which is proportional to the normalized cross-product between these two vectors.

9) The pitch- and yaw-axis components of the vector cross-product are multiplied by the proportionality constant K_{steer} to obtain the commanded rates about these axes - and multiplied by the autopilot sampling period, T_2, to obtain attitude-command increments, which are supplied to the autopilot every T_2 seconds.

10) The roll control channel is designed to provide independent attitude and rate control about the roll axis by differential control of the OMS engines.

6.4 Digital Implementation (ACPS phase)

The overall composition of the DFCS as it applies to the on-orbit phase is reiterated in Fig. 6-9 in structured flow-chart form. The procedure MAJOR_TRANSIENT provides initial mode and flag information to be used by all mission phases. Currently, no initial mode or flag information unique to the on-orbit ACPS phase has been implemented in MAJOR_TRANSIENT. The procedure INPUT_INTERFACE contains, in general, information that is explicitly read by the DFCS from external sources. More specifically, when the on-orbit phase is selected, the gimbal angles are read and the time of their reading, t_n, is recorded. On the first pass of the DFCS for a given phase FILTER_AND_PARAM_INIT and PARAM are both called. FILTER_AND_PARAM_INIT currently does nothing in this phase. PARAM calls MASS_CALC (See Fig. 6-10)

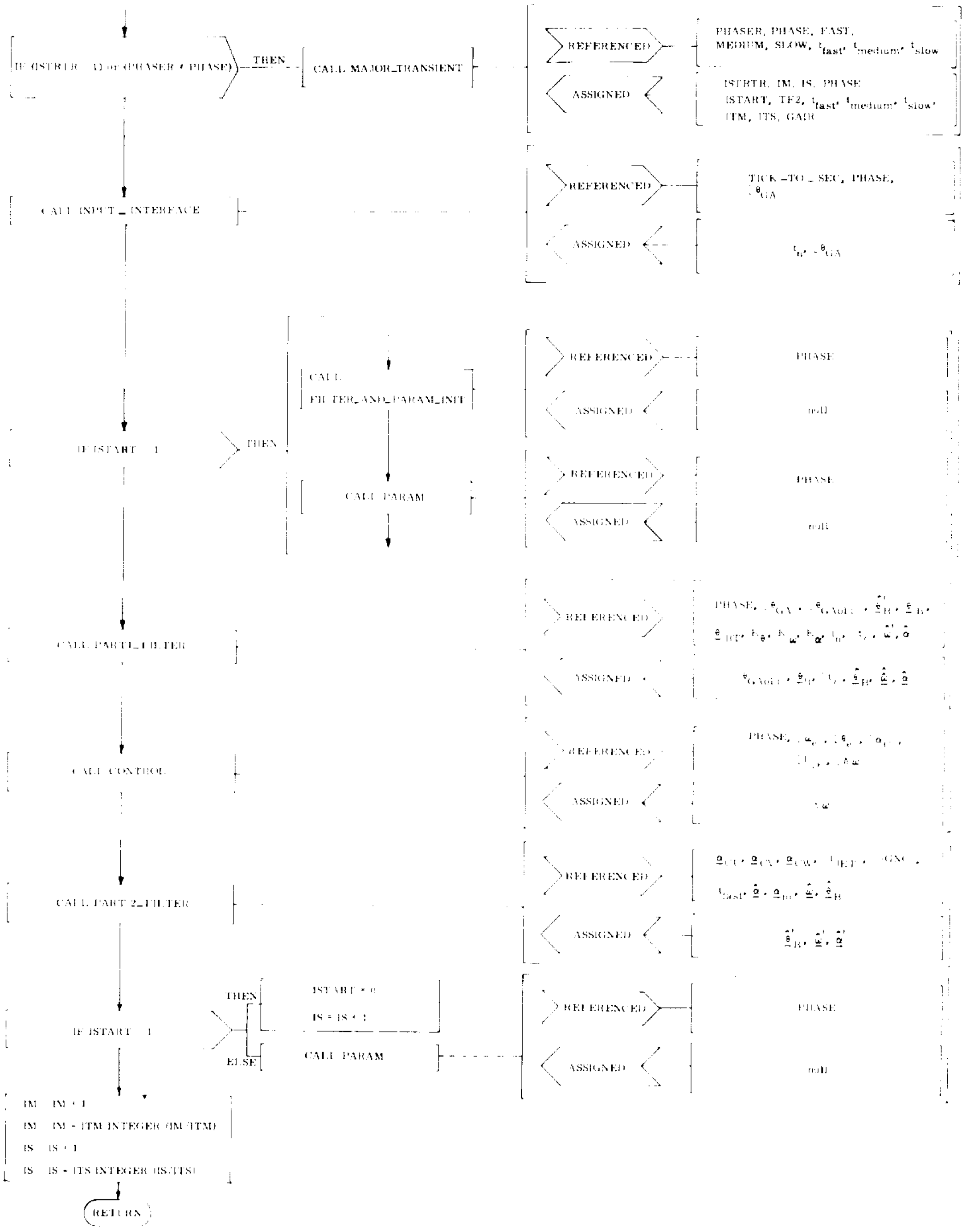

Fig. 6-9. Logic Flow of DFCS

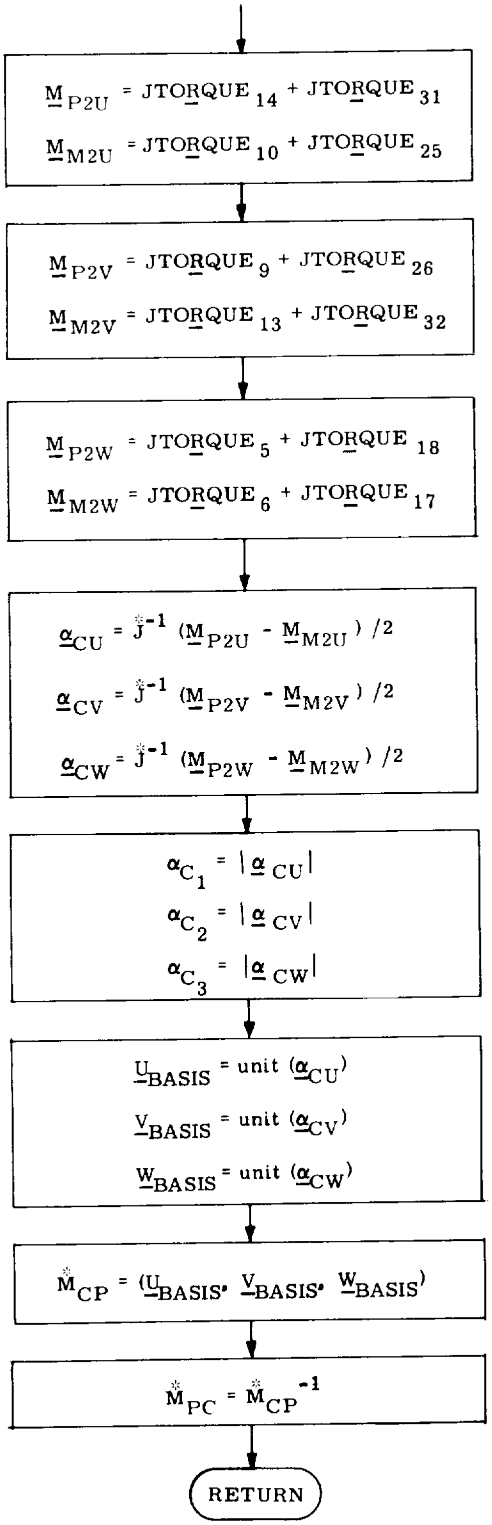
$\underline{M}_{P2U} = JTO\underline{R}QUE_{14} + JTO\underline{R}QUE_{31}$
$\underline{M}_{M2U} = JTO\underline{R}QUE_{10} + JTO\underline{R}QUE_{25}$
$\underline{M}_{P2V} = JTO\underline{R}QUE_{9} + JTO\underline{R}QUE_{26}$
$\underline{M}_{M2V} = JTO\underline{R}QUE_{13} + JTO\underline{R}QUE_{32}$
$\underline{M}_{P2W} = JTO\underline{R}QUE_{5} + JTO\underline{R}QUE_{18}$
$\underline{M}_{M2W} = JTO\underline{R}QUE_{6} + JTO\underline{R}QUE_{17}$
$\underline{\alpha}_{CU} = \overset{*}{J}^{-1} (\underline{M}_{P2U} - \underline{M}_{M2U}) /2$
$\underline{\alpha}_{CV} = \overset{*}{J}^{-1} (\underline{M}_{P2V} - \underline{M}_{M2V}) /2$
$\underline{\alpha}_{CW} = \overset{*}{J}^{-1} (\underline{M}_{P2W} - \underline{M}_{M2W}) /2$
$\alpha_{C_1} = |\underline{\alpha}_{CU}|$
$\alpha_{C_2} = |\underline{\alpha}_{CV}|$
$\alpha_{C_3} = |\underline{\alpha}_{CW}|$
$\underline{U}_{BASIS} = \text{unit } (\underline{\alpha}_{CU})$
$\underline{V}_{BASIS} = \text{unit } (\underline{\alpha}_{CV})$
$\underline{W}_{BASIS} = \text{unit } (\underline{\alpha}_{CW})$
$\overset{*}{M}_{CP} = (\underline{U}_{BASIS}, \underline{V}_{BASIS}, \underline{W}_{BASIS})$
$\overset{*}{M}_{PC} = \overset{*}{M}_{CP}^{-1}$
RETURN

Fig. 6-10. MASS_CALC

which then takes as an input the torques supplied by each ACPS thrust group and computes three more or less independent control axes and a pilot-to-control transformation matrix. The procedure PART1_FILTER shown in Fig. 6-11 is then entered which takes as an input the extrapolated estimates of angular position, rate, and disturbance acceleration for each axis and incorporates the measurement of gimbal angles taken at time t_n. From these updated estimates the procedure CONTROL (Fig. 6-12) calls upon:

1) ERRORS (Fig. 6-13) to compute the errors in attitude and angular rate from the desired
2) PHASE_PLANE (Fig. 6-14) to compute the desired change in angular rate to correct these errors
3) JET_CONTROL (Fig. 6-15) to select the appropriate jets and control their firings, according to provisional logic suggested in Subsection 6.2.1.

The digital implementation of the phase plane switching logic is composed of three principle routines:

PHASE_PLANE

The procedure PHASE_PLANE selects the appropriate sign to be attached to the computed change in angular rate, computes position error intercepts, and also computes the boundaries between the small error control logic and the large error control logic, as illustrated in the logic flow diagram in Fig. 6-14a. PHASE_PLANE then selects either the small-error control logic or the large-error control logic to compute the desired change in rate.

LARGE_ERROR_CONTROL_LOGIC

The procedure LARGE_ERROR_CONTROL_LOGIC computes the change in rate to drive the state into the small error control region. As illustrated in Fig. 6-14b, the region in which the state lies is singled out and then the appropriate control action is computed.

SMALL_ERROR_CONTROL_LOGIC

The procedure SMALL_ERROR_CONTROL_LOGIC computes the change in rate to drive the state into a limit cycle with specified deadband about the desired position and rate. Current testing has used deadbands of 0.5 and 5.0 degrees. As illustrated in Figs. 6-14c and 6-14d, the region in which the state lies is singled out and then the appropriate control action is computed.

The function BOUNDARY, illustrated in Fig. 6-14e, is implemented to compute the various switching curves.

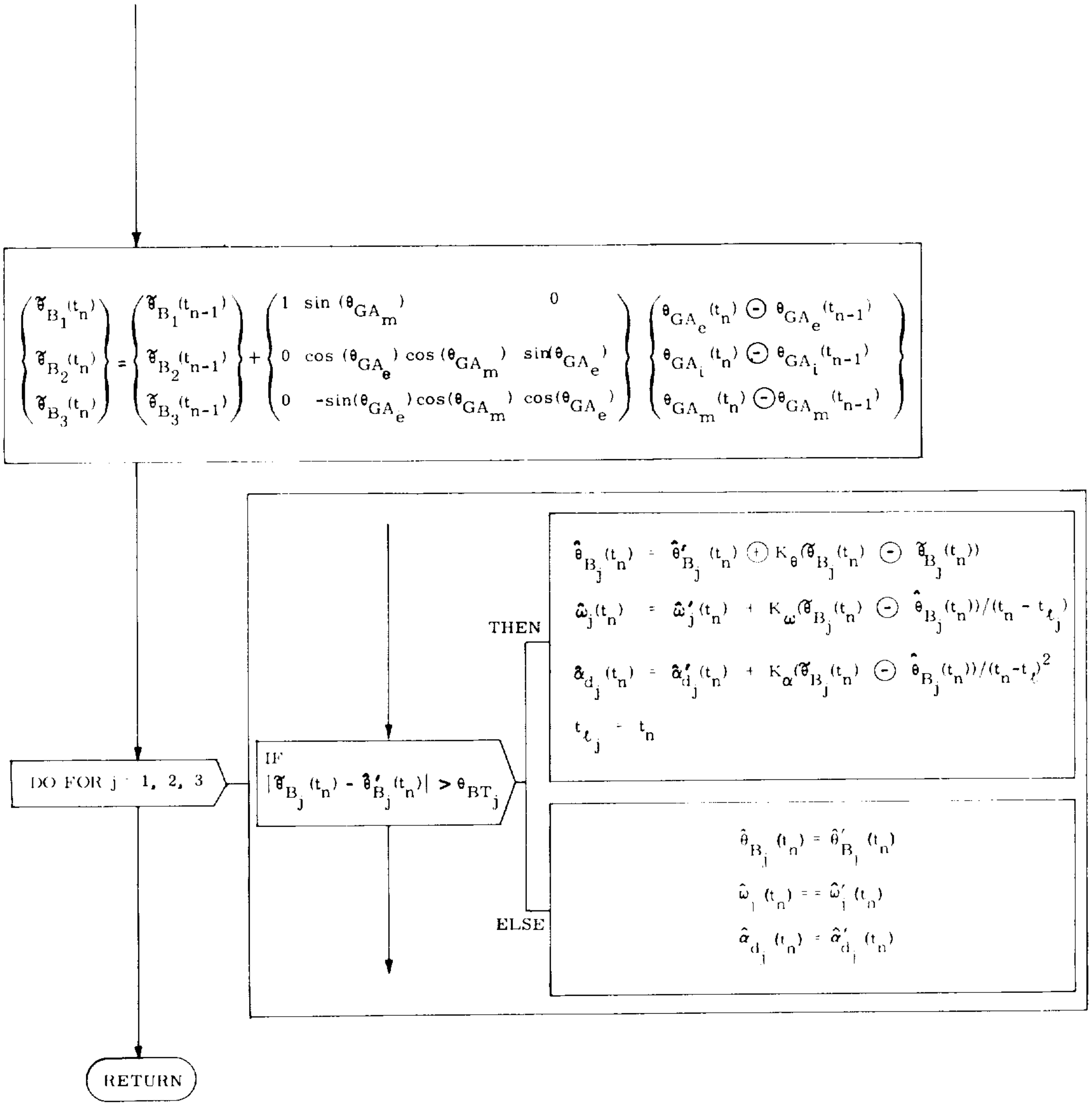
$\begin{pmatrix} \tilde{\theta}_{B_1}(t_n) \\ \tilde{\theta}_{B_2}(t_n) \\ \tilde{\theta}_{B_3}(t_n) \end{pmatrix} = \begin{pmatrix} \tilde{\theta}_{B_1}(t_{n-1}) \\ \tilde{\theta}_{B_2}(t_{n-1}) \\ \tilde{\theta}_{B_3}(t_{n-1}) \end{pmatrix} + \begin{pmatrix} 1 & \sin(\theta_{GA_m}) & 0 \\ 0 & \cos(\theta_{GA_e})\cos(\theta_{GA_m}) & \sin(\theta_{GA_e}) \\ 0 & -\sin(\theta_{GA_e})\cos(\theta_{GA_m}) & \cos(\theta_{GA_e}) \end{pmatrix} \begin{pmatrix} \theta_{GA_e}(t_n) \ominus \theta_{GA_e}(t_{n-1}) \\ \theta_{GA_i}(t_n) \ominus \theta_{GA_i}(t_{n-1}) \\ \theta_{GA_m}(t_n) \ominus \theta_{GA_m}(t_{n-1}) \end{pmatrix}$
DO FOR j = 1, 2, 3
IF
$|\tilde{\theta}_{B_j}(t_n) - \hat{\theta}'_{B_j}(t_n)| > \theta_{BT_j}$
THEN
$\hat{\theta}_{B_j}(t_n) = \hat{\theta}'_{B_j}(t_n) \oplus K_\theta(\tilde{\theta}_{B_j}(t_n) \ominus \tilde{\theta}_{B_j}(t_n))$
$\hat{\omega}_j(t_n) = \hat{\omega}'_j(t_n) + K_\omega(\tilde{\theta}_{B_j}(t_n) \ominus \hat{\theta}_{B_j}(t_n))/(t_n - t_{\ell_j})$
$\hat{\alpha}_{d_j}(t_n) = \hat{\alpha}'_{d_j}(t_n) + K_\alpha(\tilde{\theta}_{B_j}(t_n) \ominus \hat{\theta}_{B_j}(t_n))/(t_n - t_\ell)^2$
$t_{\ell_j} = t_n$
ELSE
$\hat{\theta}_{B_j}(t_n) = \hat{\theta}'_{B_j}(t_n)$
$\hat{\omega}_j(t_n) = = \hat{\omega}'_j(t_n)$
$\hat{\alpha}_{d_j}(t_n) = \hat{\alpha}'_{d_j}(t_n)$
RETURN

Fig. 6-11. On-orbit Segment of PART1_FILTER Procedure

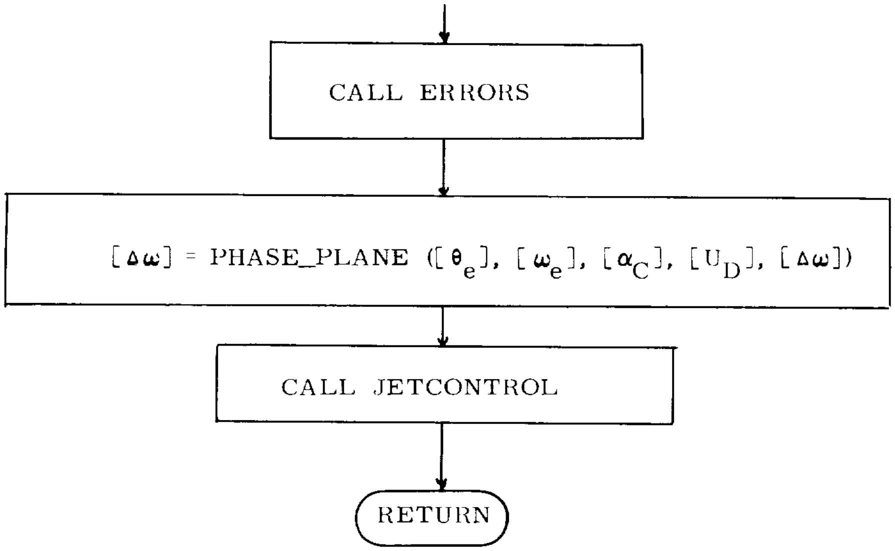

Fig. 6-12. On-orbit Segment of CONTROL Procedure

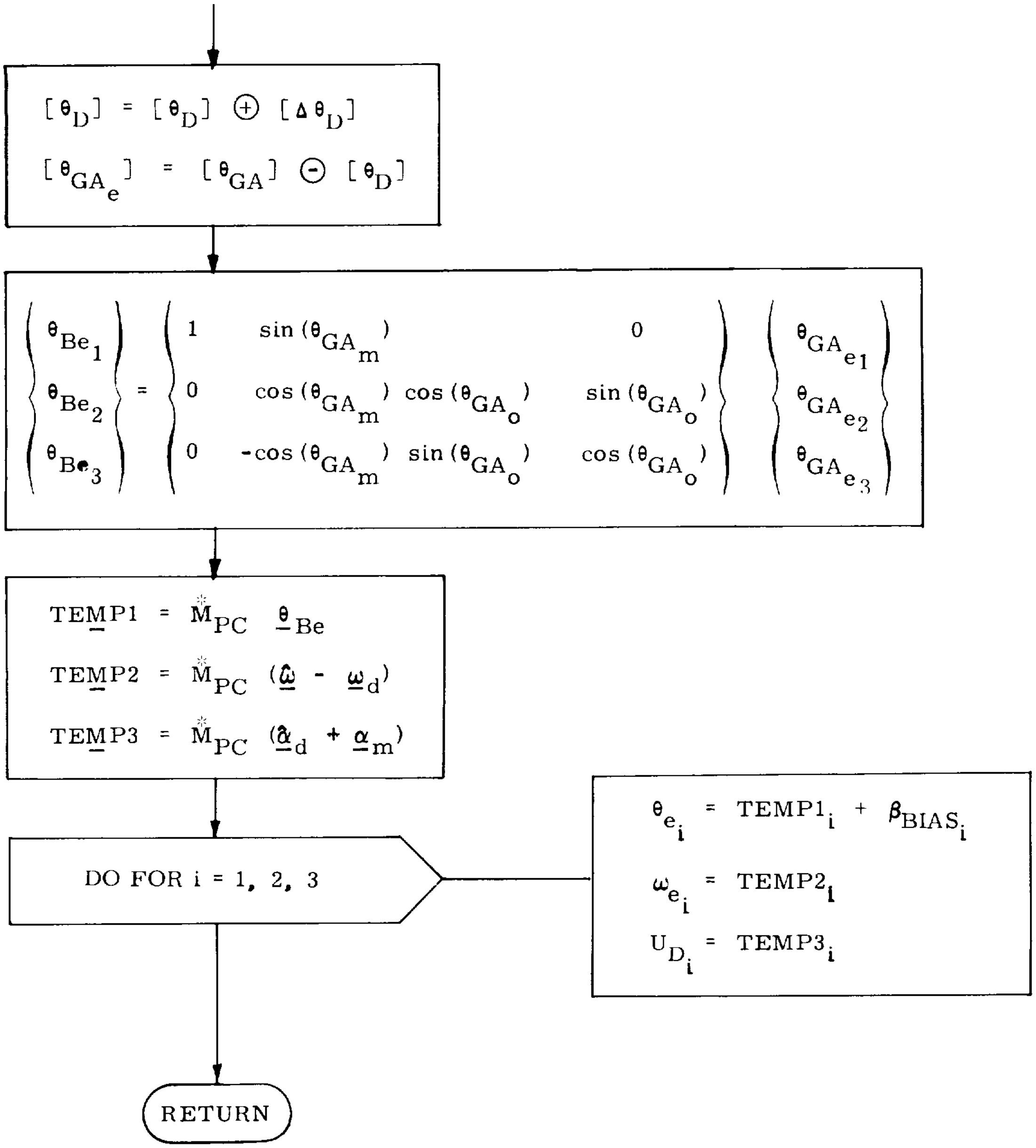
$[\theta_D] = [\theta_D] \oplus [\Delta\theta_D]$
$[\theta_{GA_e}] = [\theta_{GA}] \ominus [\theta_D]$
$\begin{Bmatrix} \theta_{Be_1} \\ \theta_{Be_2} \\ \theta_{Be_3} \end{Bmatrix} = \begin{pmatrix} 1 & \sin(\theta_{GA_m}) & 0 \\ 0 & \cos(\theta_{GA_m})\cos(\theta_{GA_o}) & \sin(\theta_{GA_o}) \\ 0 & -\cos(\theta_{GA_m})\sin(\theta_{GA_o}) & \cos(\theta_{GA_o}) \end{pmatrix} \begin{Bmatrix} \theta_{GA_{e1}} \\ \theta_{GA_{e2}} \\ \theta_{GA_{e3}} \end{Bmatrix}$
$\underline{TEMP1} = \overset{*}{M}_{PC}\ \underline{\theta}_{Be}$
$\underline{TEMP2} = \overset{*}{M}_{PC}\ (\hat{\underline{\omega}} - \underline{\omega}_d)$
$\underline{TEMP3} = \overset{*}{M}_{PC}\ (\hat{\underline{\alpha}}_d + \underline{\alpha}_m)$
DO FOR i = 1, 2, 3
$\theta_{e_i} = TEMP1_i + \beta_{BIAS_i}$
$\omega_{e_i} = TEMP2_i$
$U_{D_i} = TEMP3_i$
RETURN

Fig. 6-13. ERRORS

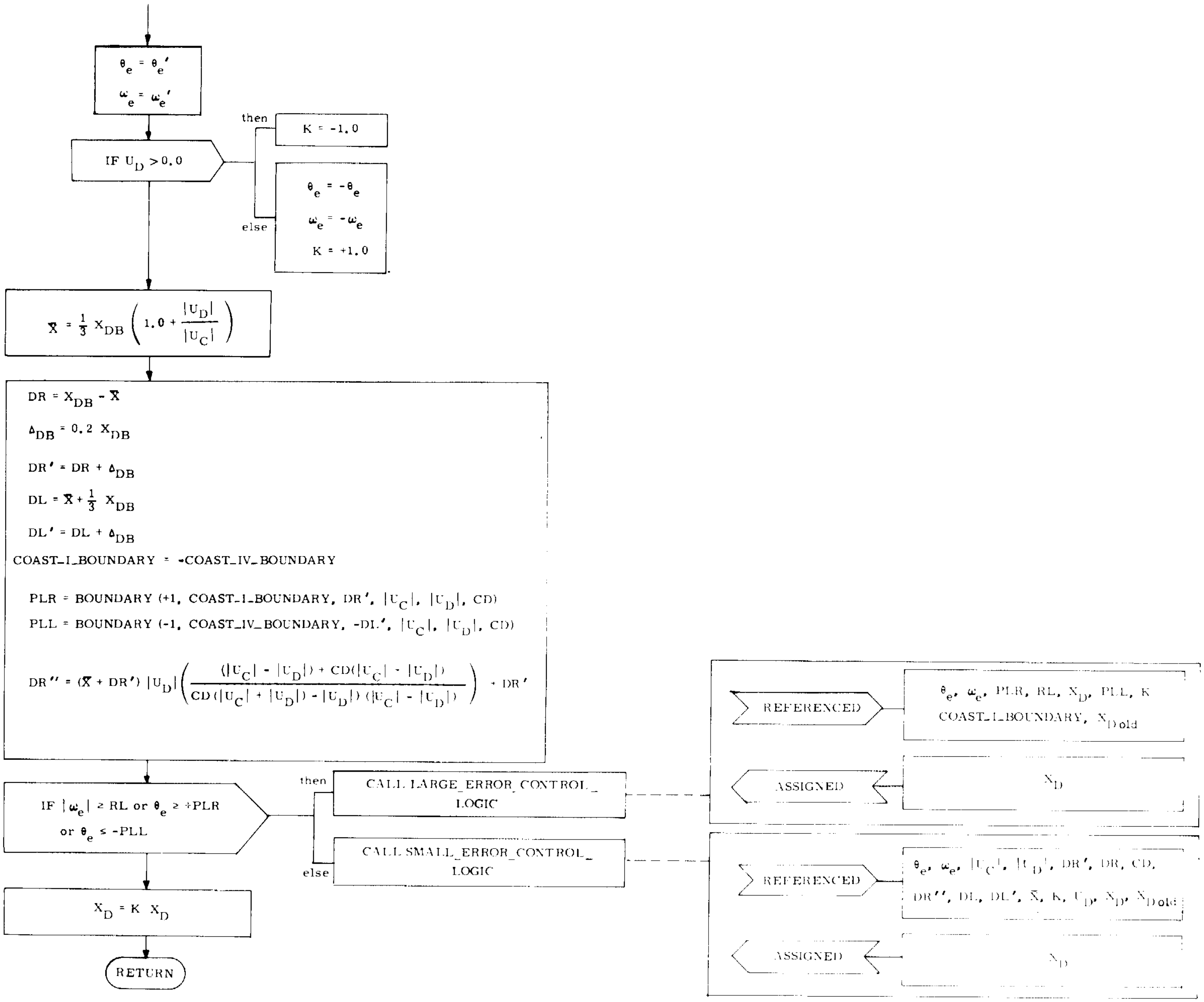
$\theta_e = \theta_e'$
$\omega_e = \omega_e'$
IF $U_D > 0.0$
then
$K = -1.0$
else
$\theta_e = -\theta_e$
$\omega_e = -\omega_e$
$K = +1.0$
$\bar{X} = \frac{1}{3} X_{DB} \left(1.0 + \frac{|U_D|}{|U_C|} \right)$
$DR = X_{DB} - \bar{X}$
$\Delta_{DB} = 0.2\ X_{DB}$
$DR' = DR + \Delta_{DB}$
$DL = \bar{X} + \frac{1}{3} X_{DB}$
$DL' = DL + \Delta_{DB}$
COAST_I_BOUNDARY = -COAST_IV_BOUNDARY
PLR = BOUNDARY (+1, COAST_I_BOUNDARY, DR', $|U_C|$, $|U_D|$, CD)
PLL = BOUNDARY (-1, COAST_IV_BOUNDARY, -DL', $|U_C|$, $|U_D|$, CD)
$DR'' = (\bar{X} + DR')\,|U_D| \left(\frac{(|U_C| - |U_D|) + CD(|U_C| - |U_D|)}{CD(|U_C| + |U_D|) - |U_D|)\,(|U_C| - |U_D|)} \right) + DR'$
IF $|\omega_e| \geq RL$ or $\theta_e \geq +PLR$ or $\theta_e \leq -PLL$
then
CALL LARGE_ERROR_CONTROL_ LOGIC
else
CALL SMALL_ERROR_CONTROL_ LOGIC
$X_D = K\ X_D$
RETURN
REFERENCED
θ_e, ω_e, PLR, RL, X_D, PLL, K COAST_I_BOUNDARY, $X_{D\,old}$
ASSIGNED
X_D
REFERENCED
θ_e, ω_e, $|U_C|$, $|U_D|$, DR', DR, CD, DR'', DL, DL', $\bar{X}$, K, U_D, X_D, $X_{D\,old}$
ASSIGNED
X_D

Fig. 6-14a. PHASE_PLANE: FUNCTION $(\theta_e', \omega_e', |U_C|, U_D, X_{D\,old})$

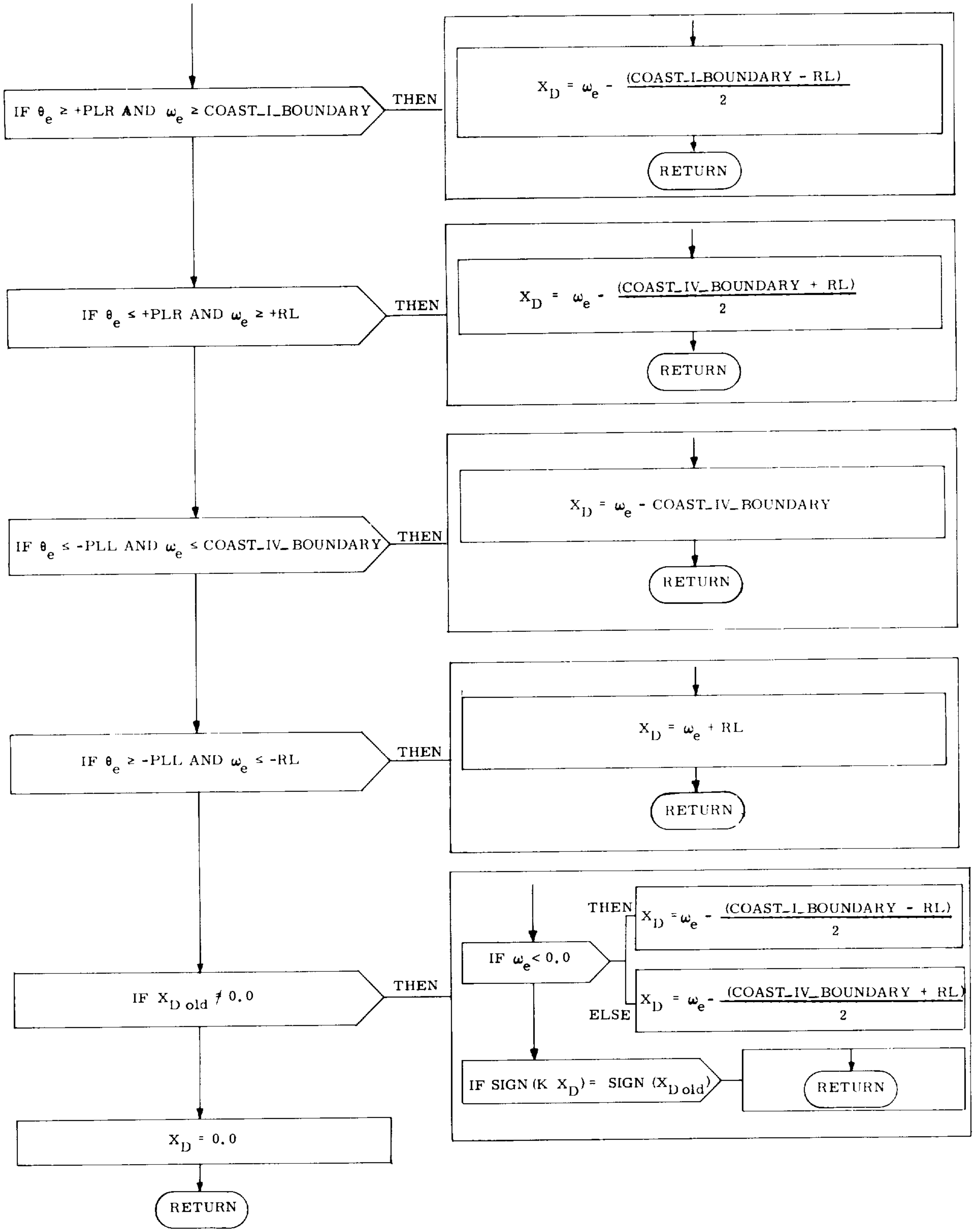
IF $\theta_e \geq$ +PLR AND $\omega_e \geq$ COAST_I_BOUNDARY
THEN
$X_D = \omega_e - \frac{(\text{COAST\_I\_BOUNDARY} - \text{RL})}{2}$
RETURN
IF $\theta_e \leq$ +PLR AND $\omega_e \geq$ +RL
THEN
$X_D = \omega_e - \frac{(\text{COAST\_IV\_BOUNDARY} + \text{RL})}{2}$
RETURN
IF $\theta_e \leq$ -PLL AND $\omega_e \leq$ COAST_IV_BOUNDARY
THEN
$X_D = \omega_e$ - COAST_IV_BOUNDARY
RETURN
IF $\theta_e \geq$ -PLL AND $\omega_e \leq$ -RL
THEN
$X_D = \omega_e$ + RL
RETURN
IF $X_{D\ old} \neq 0.0$
THEN
IF $\omega_e < 0.0$
THEN
$X_D = \omega_e - \frac{(\text{COAST\_I\_BOUNDARY} - \text{RL})}{2}$
ELSE
$X_D = \omega_e - \frac{(\text{COAST\_IV\_BOUNDARY} + \text{RL})}{2}$
IF SIGN (K X_D) = SIGN ($X_{D\ old}$)
RETURN
$X_D = 0.0$
RETURN

Fig. 6-14b LARGE_ERROR_CONTROL_LOGIC

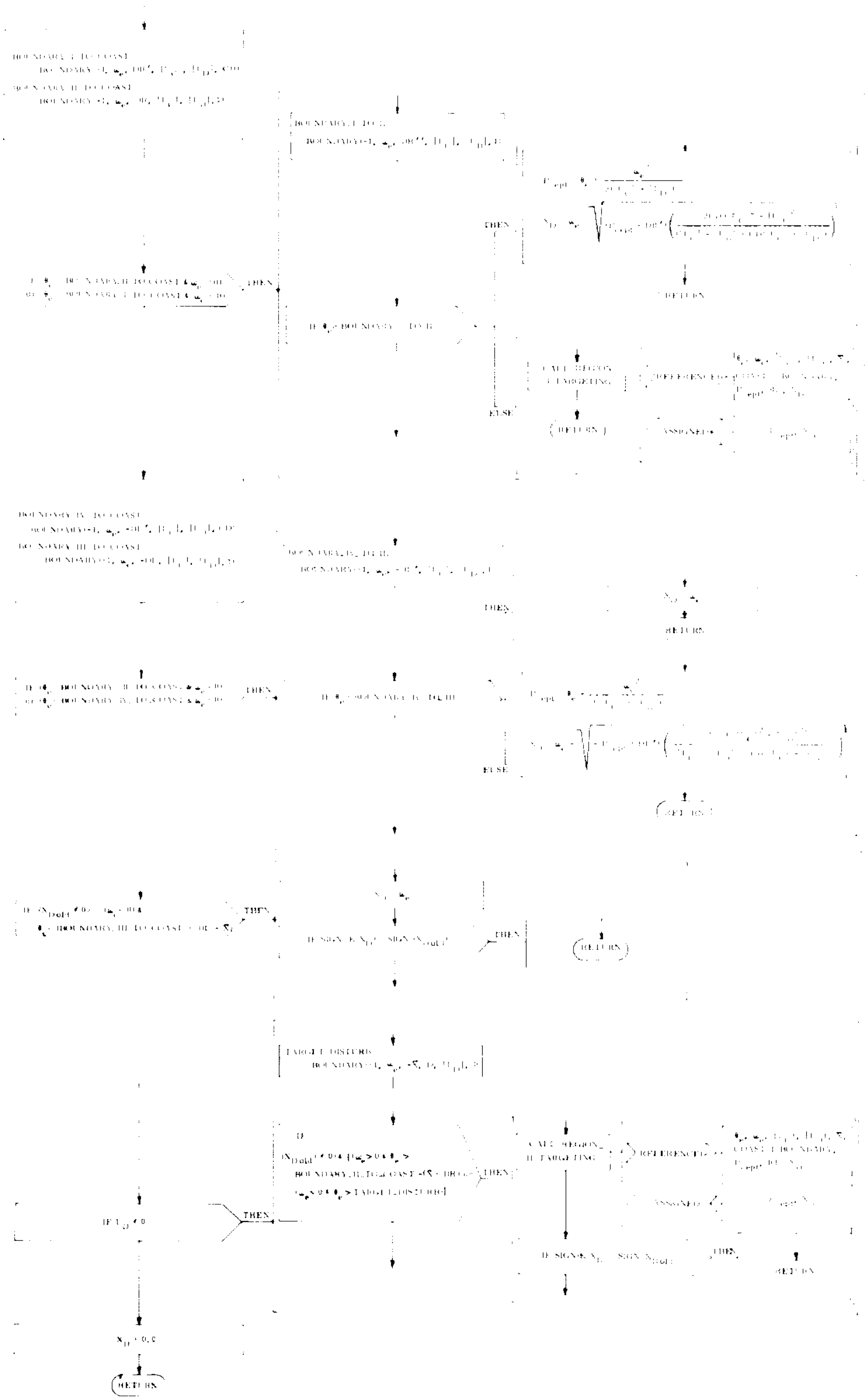

Fig. 6-14c SMALL_ERROR_CONTROL LOGIC

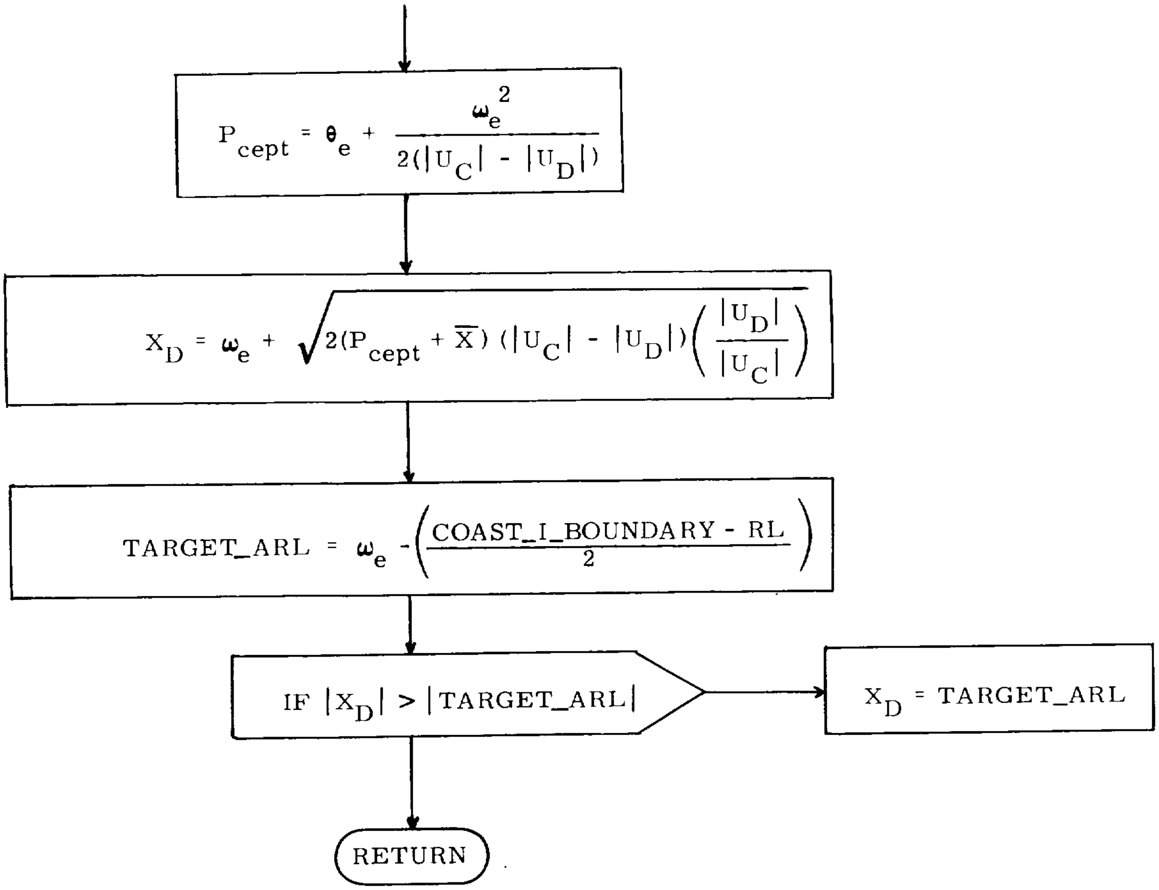
$P_{cept} = \theta_e + \frac{\omega_e^2}{2(|U_C| - |U_D|)}$
$X_D = \omega_e + \sqrt{2(P_{cept} + \overline{X})(|U_C| - |U_D|)\left(\frac{|U_D|}{|U_C|}\right)}$
$TARGET\_ARL = \omega_e - \left(\frac{COAST\_I\_BOUNDARY - RL}{2}\right)$
IF $|X_D| > |TARGET\_ARL|$
$X_D = TARGET\_ARL$
RETURN

Fig. 6-14d. REGION_II_TARGETTING

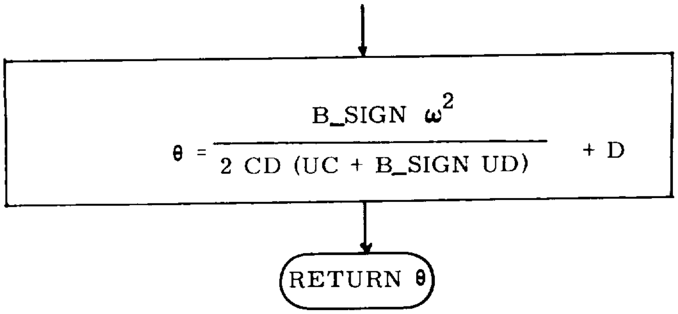
$\theta = \frac{B\_SIGN\ \omega^2}{2\ CD\ (UC + B\_SIGN\ UD)} + D$
RETURN θ

Fig. 6-14e BOUNDARY: FUNCTION (B_SIGN, ω, D, UC, UD, CD)

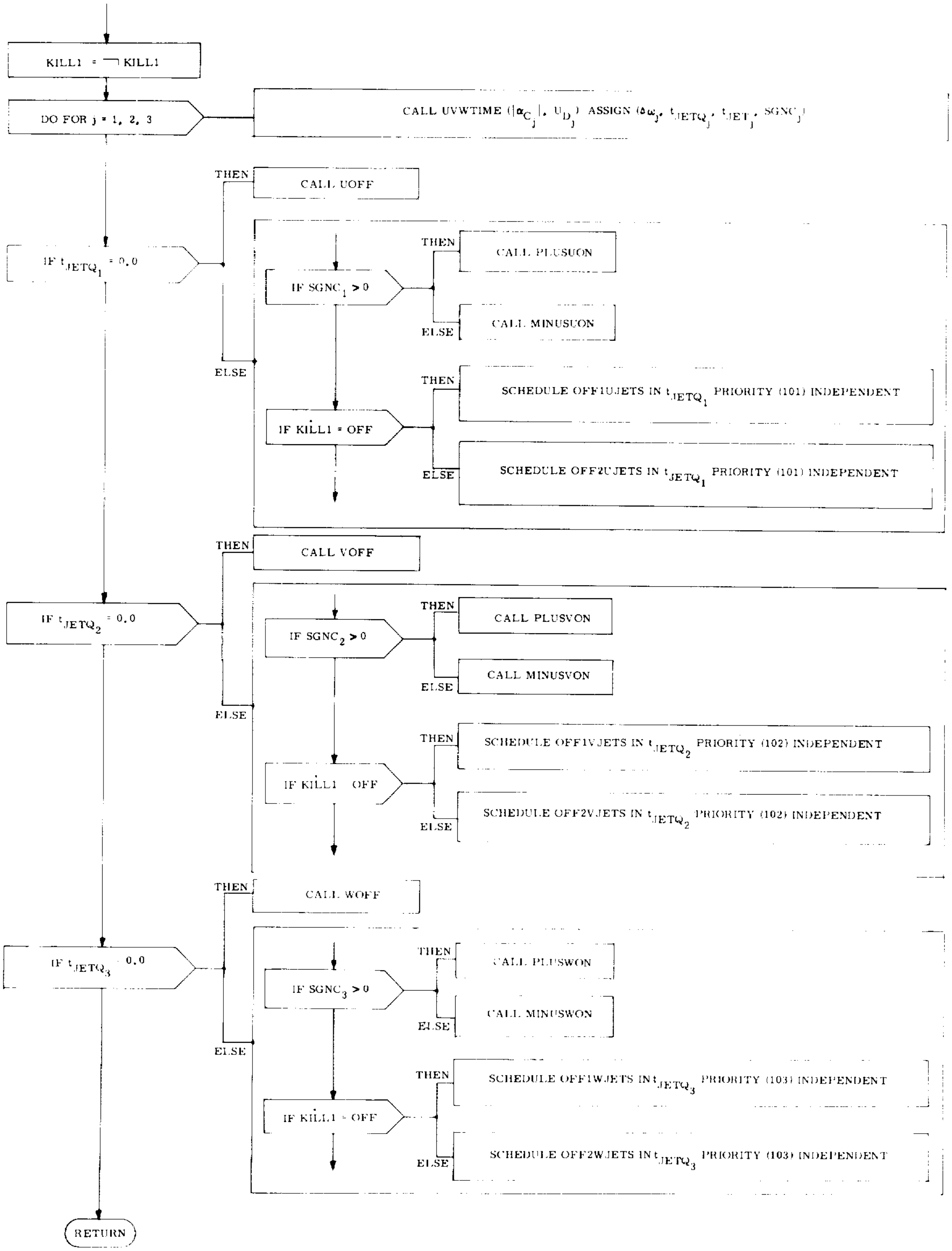
KILL1 = ¬ KILL1
DO FOR j = 1, 2, 3
CALL UVWTIME (|α_Cj|, U_Dj) ASSIGN (Δω_j, t_JETQj, t_JETj, SGNC_j)
THEN
CALL UOFF
IF t_JETQ1 = 0.0
ELSE
THEN
CALL PLUSUON
IF SGNC_1 > 0
ELSE
CALL MINUSUON
THEN
SCHEDULE OFF1UJETS IN t_JETQ1 PRIORITY (101) INDEPENDENT
IF KILL1 = OFF
ELSE
SCHEDULE OFF2UJETS IN t_JETQ1 PRIORITY (101) INDEPENDENT
THEN
CALL VOFF
IF t_JETQ2 = 0.0
ELSE
THEN
CALL PLUSVON
IF SGNC_2 > 0
ELSE
CALL MINUSVON
THEN
SCHEDULE OFF1VJETS IN t_JETQ2 PRIORITY (102) INDEPENDENT
IF KILL1 OFF
ELSE
SCHEDULE OFF2VJETS IN t_JETQ2 PRIORITY (102) INDEPENDENT
THEN
CALL WOFF
IF t_JETQ3 0.0
ELSE
THEN
CALL PLUSWON
IF SGNC_3 > 0
ELSE
CALL MINUSWON
THEN
SCHEDULE OFF1WJETS IN t_JETQ3 PRIORITY (103) INDEPENDENT
IF KILL1 = OFF
ELSE
SCHEDULE OFF2WJETS IN t_JETQ3 PRIORITY (103) INDEPENDENT
RETURN

Fig. 6-15a. JET_CONTROL Procedure

Inputs: α_C, U_D

Outputs: $\Delta\omega$, t_{JETQ}, t_{JET}, SGNC

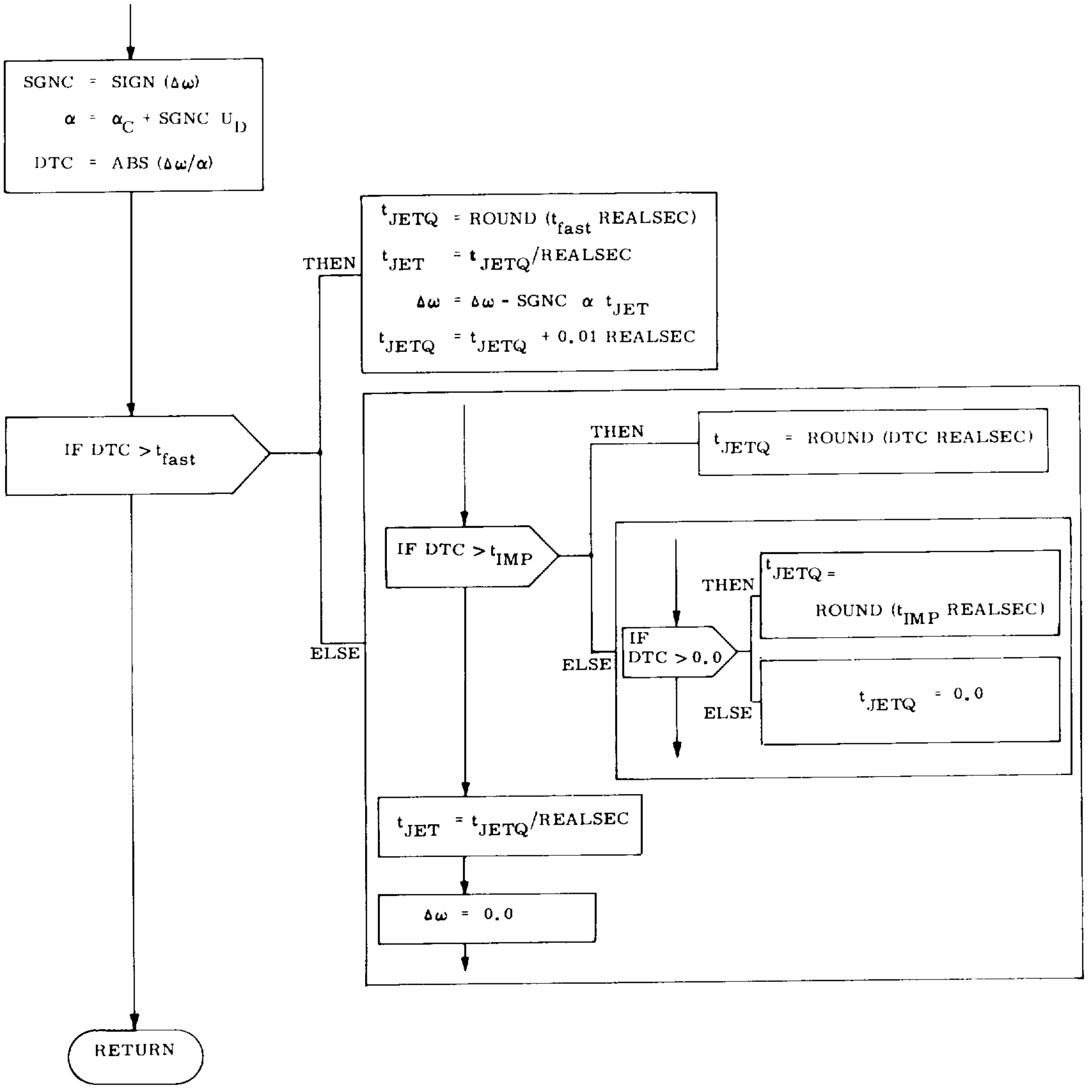

Fig. 6-15b. UVWTIME Procedure

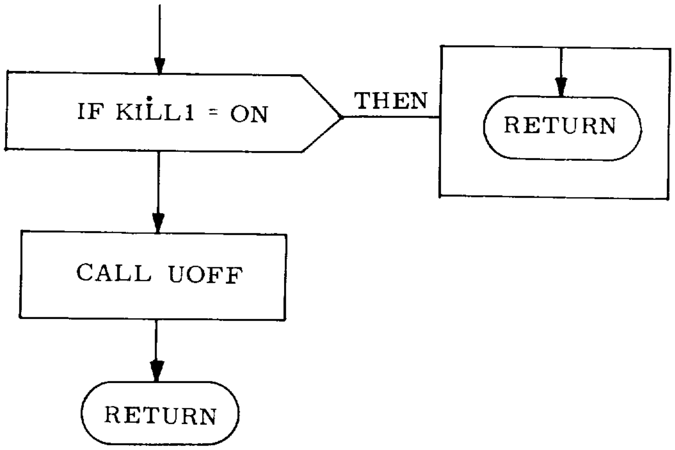

Fig. 6-15c. OFF1JETS Procedure

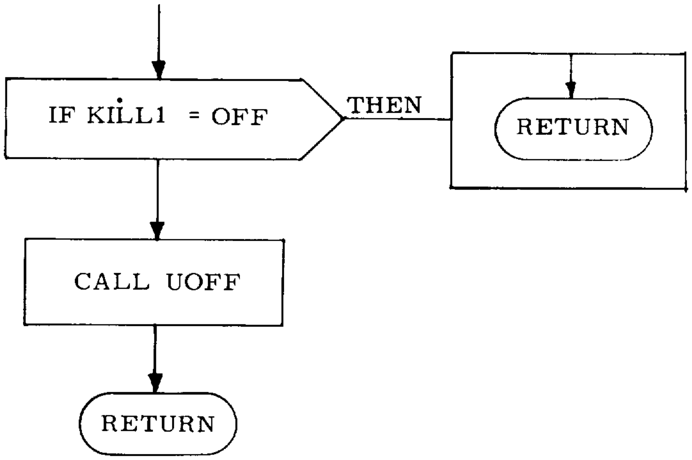

Fig. 6-15d. OFF2UJETS Procedure

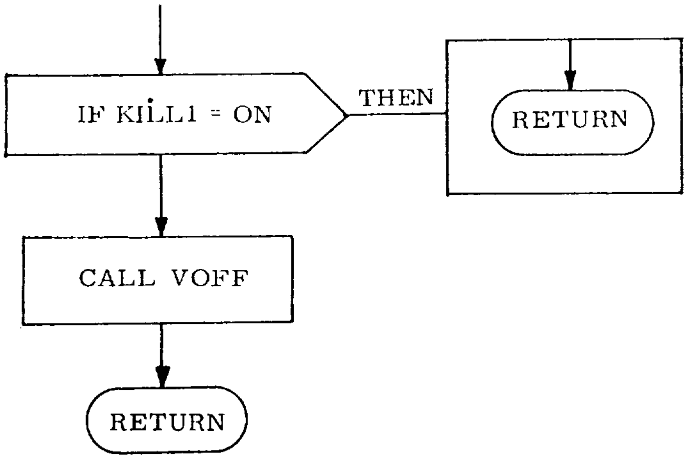

Fig. 6-15e. Off1VJETS Procedure

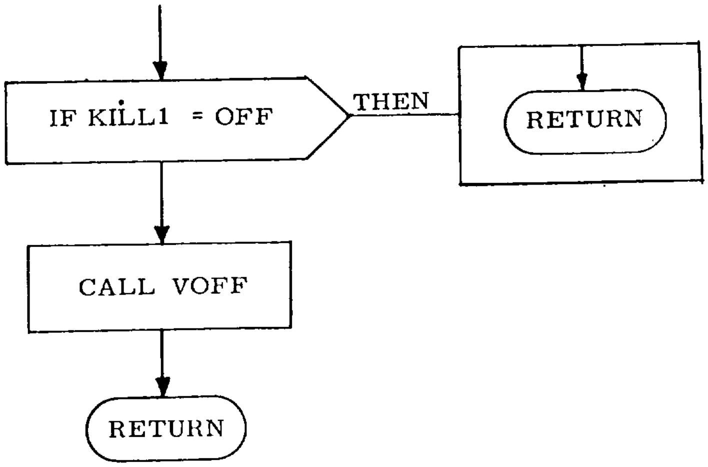

Fig. 6-15f. OFF2VJETS Procedure

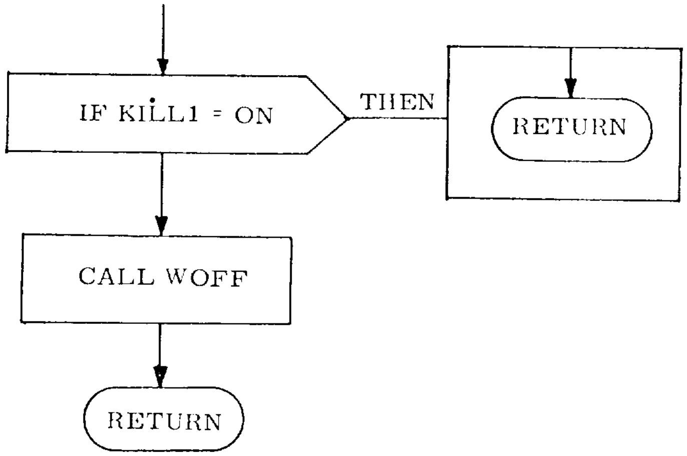

Fig. 6-15g. OFF1WJETS Procedure

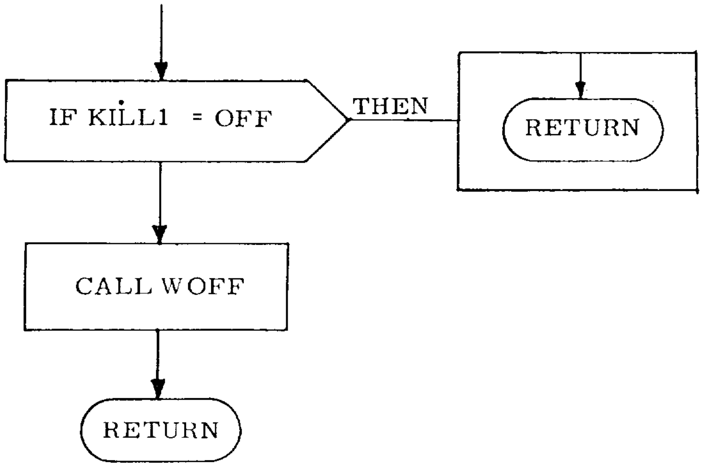

Fig. 6-15h. OFF2WJETS Procedure

After CONTROL has called JETCONTROL to implement the firing of various jets, the estimate of the state is extrapolated for the next pass of the DFCS by the procedure PART2_FILTER (see Fig. 6-16). Finally, PARAM is called on passes other than initialization passes, and the DFCS pass is terminated.

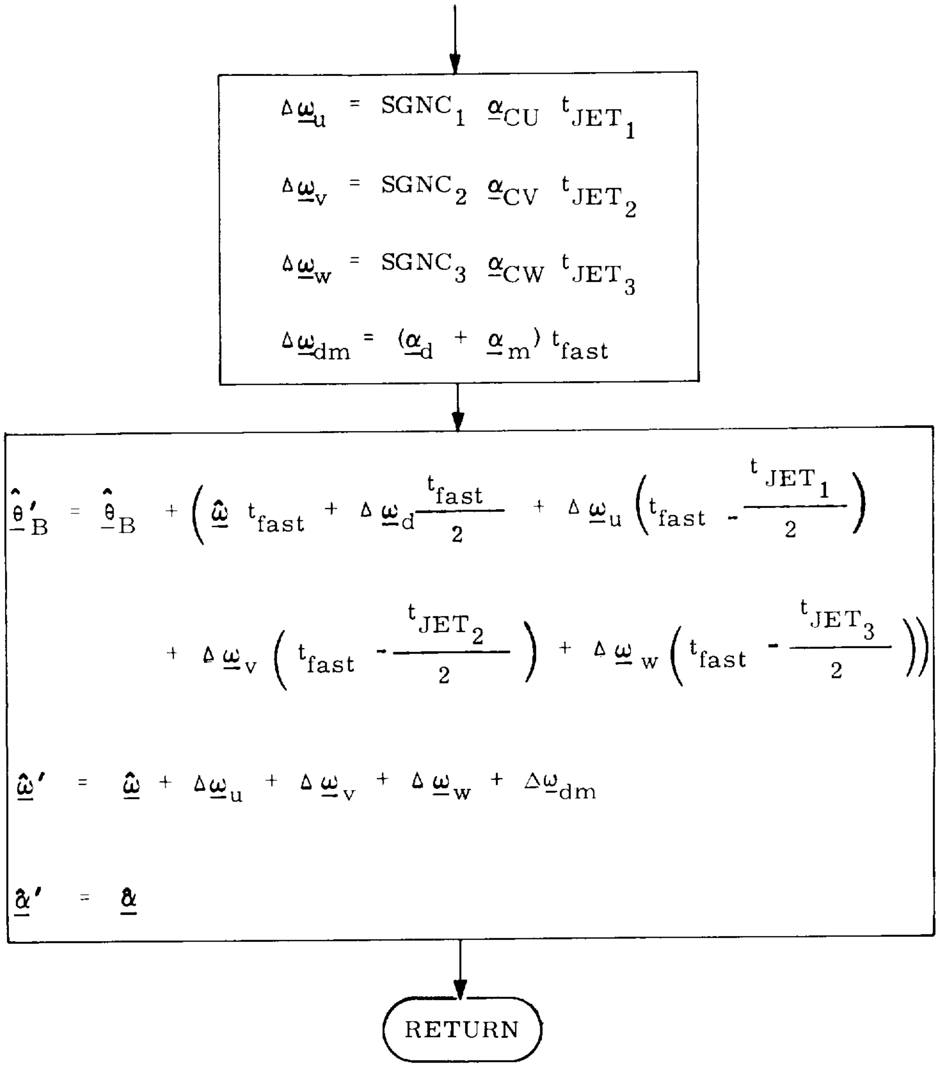

$$\Delta\underline{\omega}_u = SGNC_1\ \underline{\alpha}_{CU}\ t_{JET_1}$$

$$\Delta\underline{\omega}_v = SGNC_2\ \underline{\alpha}_{CV}\ t_{JET_2}$$

$$\Delta\underline{\omega}_w = SGNC_3\ \underline{\alpha}_{CW}\ t_{JET_3}$$

$$\Delta\underline{\omega}_{dm} = (\underline{\alpha}_d + \underline{\alpha}_m)\ t_{fast}$$

$$\hat{\underline{\theta}}'_B = \hat{\underline{\theta}}_B + \left(\hat{\underline{\omega}}\ t_{fast} + \Delta\underline{\omega}_d \frac{t_{fast}}{2} + \Delta\underline{\omega}_u\left(t_{fast} - \frac{t_{JET_1}}{2}\right) + \Delta\underline{\omega}_v\left(t_{fast} - \frac{t_{JET_2}}{2}\right) + \Delta\underline{\omega}_w\left(t_{fast} - \frac{t_{JET_3}}{2}\right)\right)$$

$$\hat{\underline{\omega}}' = \hat{\underline{\omega}} + \Delta\underline{\omega}_u + \Delta\underline{\omega}_v + \Delta\underline{\omega}_w + \Delta\underline{\omega}_{dm}$$

$$\hat{\underline{\alpha}}' = \hat{\underline{\alpha}}$$

Fig. 6-16. ORBIT_ACPS_FILTER2; On-orbit Segment of PART2_FILTER Procedure

Table 6-5: Glossary for On-Orbit Phase

MNEMONIC	ENGINEERING TERM	DEFINITION
ACC2U	$\underline{\alpha}_{CU}$	Angular acceleration about u-axis produced by $\underline{M}_{P2U}$ or $\underline{M}_{M2U}$
ACC2V	$\underline{\alpha}_{CV}$	Angular acceleration about v-axis produced by $\underline{M}_{P2V}$ or $\underline{M}_{M2V}$
ACC2W	$\underline{\alpha}_{CW}$	Angular acceleration about w-axis produced by $\underline{M}_{P2W}$ or $\underline{M}_{M2W}$
ALPHADBAR	$\hat{\underline{\alpha}}'_{d}$	Extrapolated disturbance acceleration
ALPHADHAT	$\hat{\underline{\alpha}}_{d}$	Estimated disturbance acceleration
ALPHAM	$\underline{\alpha}_{m}$	Bias acceleration
BASISU	$\underline{u}_{BASIS}$	Unit vectors along u, v, w control axes
BASISV	$\underline{v}_{BASIS}$	
BASISW	$\underline{w}_{BASIS}$	
[BIAS_BETA]	$[\beta_{BIAS}]$	Bias body angles
CD	CD	Scale factor used in phase plane switching logic
[CDU]	$[\theta_{GA}]$	Gimbal angles
[CDUERROR]	$[\theta_{GA_e}]$	Error in gimbal angles from the reference desired
DELTA	Δ_{DB}	Deadband factor
DELTA_POSITION	θ_e'	Angular position error (within PHASE_PLANE)
DELTA_RATE	ω_e'	Angular rate error (within PHASE_PLANE)
[DELTA_THETA_D]	$[\Delta\theta_D]$	Incremental desired reference gimbal angles
DELWDM	$\Delta\underline{\omega}_{dm}$	Change in angular velocity vector due to disturbance and bias accelerations
DELWU	$\Delta\underline{\omega}_{u}$	Change in angular rate due to u-control jets
DELWV	$\Delta\underline{\omega}_{v}$	Change in angular rate due to v-control jets
DELWW	$\Delta\underline{\omega}_{w}$	Change in angular rate due to w-control jets
DL, DL_PRIME1,	DL, DL'	Switching line angular position error intercepts
DR, DR_PRIME1,	DR, DR'	
DR_PRIME2	DR''	
[DRATE]	$[\Delta\omega]$	Components of changes of angular rates

Table 6-5: Glossary for On-Orbit Phase (cont)

MNEMONIC	ENGINEERING TERM	DEFINITION
DTC	DTC	Total firing time of an ACPS control jet for a maneuver
ISTRTR	ISTRTR	Restart required flag (external)
PHASER	PHASER	Mission phase flag (external)
[FAST]	[FAST]	Fast, medium, and slow sampling periods for each mission phase
[MEDIUM]	[MEDIUM]	
[SLOW]	[SLOW]	Slow sampling period for each mission phase
GAIR	G_{AIR}	Filter gain for air data
INERTIA	J	Inertia matrix
IM	IM	medium rate sampling index
IS	IS	Slow rate sampling index
ISTART	ISTART	Initial pass flag for mission phase
ITM	ITM	Ratio of medium to fast sampling periods
ITS	ITS	Ratio of slow to fast sampling periods
[JTORQUE]	[JTORQUE]	Array of ACPS jet torque vectors
K	K	Sign of rate change
KALPHA	K_{α}	Filter gains
KOMEGA	K_{ω}	
KTHETA	K_{θ}	
KILL1	KILL1	ACPS jet continuity indicator
[MAGACC]	$[\alpha_C]$	Array of magnitudes of control accelerations
MAG_U_D	$\vert U_D \vert$	Magnitude of disturbance acceleration
MAG_U_C	$\vert U_C \vert$	Magnitude of control acceleration
MP2U	$\underline{M}_{P2U}$	Torque in the +u direction by 2 u-jets
MM2U	$\underline{M}_{M2U}$	Torque in the -u direction by 2 u-jets
MP2V	$\underline{M}_{P2V}$	Torque in the +v direction by 2 v-jets
MM2V	$\underline{M}_{M2V}$	Torque in the -v direction by 2 v-jets

Table 6-5: Glossary for On-Orbit Phase (cont)

MNEMONIC	ENGINEERING TERM	DEFINITION
M$\overline{\text{P}}$2W	$\underline{M}_{P2W}$	Torque in the +w direction by 2 w-jets
M$\overline{\text{M}}$2W	$\underline{M}_{M2W}$	Torque in the -w direction by 2 w-jets
M$\overset{*}{\text{C}}$P	$\overset{*}{M}_{CP}$	Control to pilot transformation matrix
M$\overset{*}{\text{P}}$C	$\overset{*}{M}_{PC}$	Pilot to control transformation matrix
MINIMP	t_{IMP}	Time of a minimum impulse ACPS jet firing
NETACC	$[\alpha]$	Net acceleration
OME$\overline{\text{G}}$ABAR	$\hat{\underline{\omega}}'$	Extrapolated angular velocity
OME$\overline{\text{G}}$AHAT	$\hat{\underline{\omega}}$	Estimated angular velocity
-PLL	-PLL	Left angular position error limit
+PLR	+PLR	Right angular position error limit
P_CEPT	P_{cept}	Intermediate position error axis intercept
PHASE	PHASE	Phase of the mission
±RL	±RL	Upper and lower rate error limits
POS'TION_ERROR	$[\theta_e]$	Angular position error
RATE_ERROR	$[\omega_e]$	Angular rate error
REALSEC	REALSEC	Scale factor for scaling computer time $\left(= \frac{1}{\text{TICK\_TO\_SEC}}\right)$
RUNTIME	RUNTIME	Runtime of the computer in computer ticks
[SGNC]	[SGNC]	Signs of the angular rate components
TARGET_ARL	TARGET_ARL	Lower rate limit average
TF	t_{fast}	Fast sampling period
TM	t_{medium}	Medium sampling period
TS	t_{slow}	Slow sampling period
TE$\overline{\text{M}}$P1	T$\underline{\text{EMP}}$1	Temporary vector of body angle errors in control coordinates
TE$\overline{\text{M}}$P2	T$\underline{\text{EMP}}$2	Temporary vector of body rate errors in control coordinates
TE$\overline{\text{M}}$P3	T$\underline{\text{EMP}}$3	Temporary vector of acceleration in control coordinates
[TJET]	t_{JET}	Time of an ACPS jet firing in seconds

Table 6-5: Glossary for On-Orbit Phase (cont)

MNEMONIC	ENGINEERING TERM	DEFINITION
THETA̅BAR	$\hat{\underline{\theta}}'_B$	Extrapolated body angles
THETA̅HAT	$\hat{\underline{\theta}}_B$	Estimated body angles
TNOW	t_n	Time of present gimbal angle measurement
[TJETQ]	t_{JETQ}	Time of an ACPS jet firing scaled to the computer
RATE̅_INT	$\tilde{\underline{\theta}}_B$	"Measured" body angles
[TLAST]	t_{ℓ_j}	Time of the last gimbal angle measurement
[THETA_D]	$[\theta_D]$	Desired set of gimbal angles
TICK_TO_SEC	TICK_TO_SEC	Scale factor for scaling computer time
[U_D]	$[U_D]$	Array of disturbance accelerations
W̅_D	$\underline{\omega}_d$	Desired angular velocity
X_BAR	$\overline{X}$	Average angular position error
X_DB	X_{DB}	Deadband of limit cycle
X_D	X_D	One component of $\Delta\underline{\omega}$ the desired change in angular velocity
NO_CHANGE	$X_{D\,old}$	One component of the last desired change in angular velocity
XYZ̅E̅R̅ROR	$\underline{\theta}_{Be}$	Errors in x, y, z axis rotation angles

NOTATION CONVENTIONS

⊕	Modular addition
⊖	Modular subtraction
~	Measured quantity
^	Estimated quantity
'	Extrapolated quantity
_	Vector
*	Matrix
[ ]	Array

REFERENCES FOR SECTION 6

1. Keene, D., "Control Axes for the Shuttle On-Orbit Autopilot", SSV MEMO No. 73-23C-6, April 1973.

2. Keene, D., "State Estimator for the Shuttle On-Orbit Autopilot", SSV MEMO No. 73-23C-7, April 1973.

3. Keene, D. and Kubiac, E., Section 6, "On-Orbit Phase", Integrated Digital Flight Control System for the Space Shuttle Orbiter, E-2736, March 1973.

SECTION 7

BOOST PHASE

7.1 Introduction

The baseline launch configuration control system software described in this section satisfies the requirement to control the booster from lift-off through main engine cutoff at external tank separation. The system is adaptable to various control laws, including attitude control, drift minimum control (with and without accelerometer feedback) and/or load relief control through proper choice of gain schedules. It also contains the option of using rudder and thrust vector control combined in the roll channel.

The following paragraphs contain: A description of the control system with functional block diagrams of the pitch, yaw, and roll channels; an annotated flow diagram; and a discussion of the control gains.

7.2 Functional Description

The baseline launch control system is a digital autopilot receiving body attitude from an inertial reference system, body rates from three sets of body mounted rate gyros, and translational accelerations from two sets of body mounted accelerometers. The current baseline includes rate gyros at the aft end of each solid rocket booster and the orbiter. Normal and lateral accelerometers are located in the forward avionics bay and the aft end of the orbiter. The autopilot also utilizes prestored engine deflection commands and acceleration commands. The former are the nominal trim values for the expected center-of-gravity and aerodynamic histories, and the latter are the normal linear accelerations in the nominal trajectory.[7-1] The final inputs to the control loop are the attitude commands, which may either be prestored or come from a guidance system.

From the inputs, the control system determines and sends out deflection commands for the engines and the rudder. A general optimal mixing logic has been designed and may be installed at a later date. It has been designed to distribute the desired torques efficiently among the control actuators while accounting for failures and saturation.[7-2]

Table 7-1 summarizes the control system inputs and outputs.

Table 7-1 INPUT/OUTPUT SUMMARY

INPUTS

- Inertial attitude angles
- Body rotational rates
- Y & Z translational accelerations
- Prestored engine deflection commands
- Prestored accelerations commands
- Attitude commands from guidance system

OUTPUTS

- Deflection commands to orbiter engines
- Deflection commands to SRM engines
- Deflection commands to aerosurfaces (rudder)

Variable control gains have been calculated to satisfy the rigid body response requirements. They are stored as a function of time from lift-off; the numerical values are presented in Subsection 7.4. In the future, the design will be extended to include consideration of slosh and bending, and these prestored gains will be replaced by filters. All filters will be implemented as second order over second order. Filter inclusion in two places in each sensor loop recognizes common filtering requirements and reduces the order of the filter.

Some aspects of the design presented in this section are specific to the first stage of boost (prior to SRB separation). However, control of the orbiter during the second stage will utilize basically the same control law. The major differences are that the rudder will not be used and there will be no acceleration feedback in the second phase. Furthermore, there will only be one set of body mounted rate gyros available. These gyros will be located in the aft section of the orbiter. All filter coefficients and gains will be changed at separation and vary as the mass properties, flexible body and fuel slosh characteristics vary.

7.2.1 Roll Channel Description

Referring to Fig. 7-1, the block in the lower right hand corner labeled "Vehicle and Subsystem Dynamics" represents actuator and sensor dynamics, possible analog prefiltering of sensor outputs, input output voting, redundancy management, A/D and D/A converters. Inputs to the control system from "Vehicle and Subsystem Dynamics" are the inertial platform attitude angle and rate measurements from three sets of body mounted rate gyros. Outputs from the control system to the vehicle are engine deflection commands.

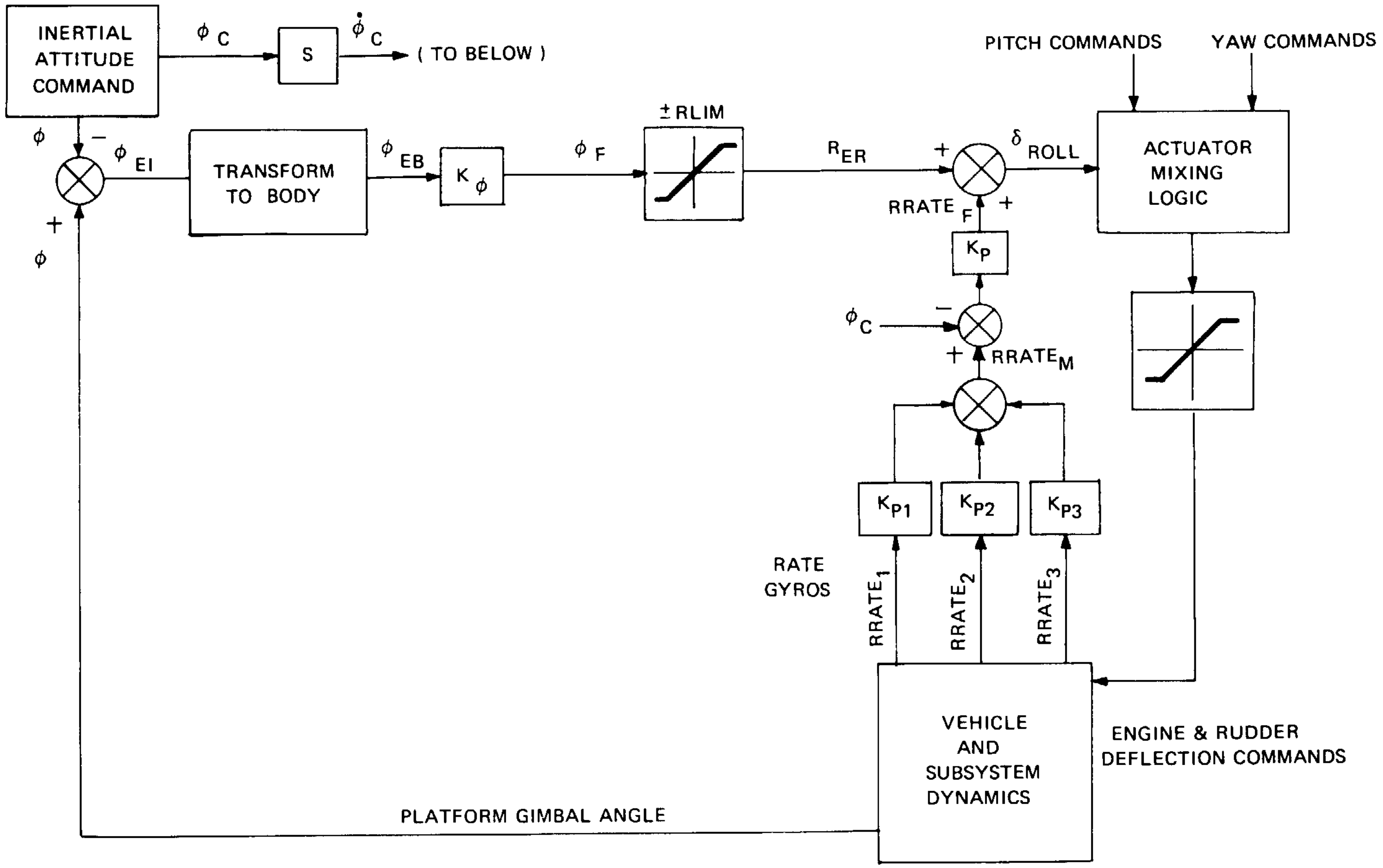

Fig. 7-1 Baseline Launch Configuration Control System Software Roll Channel

Following the attitude loop in Fig. 7-1, the platform gimbal angle, ϕ, is differenced with the inertial attitude command, ϕ_C , to produce the inertial attitude error', ϕ_{EI}. This inertial attitude error is transformed to a body roll error, ϕ_{EB}, by adding the inner gimbal error times the sine of the middle gimbal angle $(\phi_{EB} = \phi_{EI} + \phi_{EI} \sin \psi)$.

It should be noted that a limiter has been included in the attitude error loop. This limiter reserves some TVC authority for rate damping (even though the attitude error signal may be saturated) thus preventing oscillation and complete loss of control because of large signal instability. The limiter is set to a value less than 8-degrees.

Returning to the "Vehicle and Subsystem Dynamics" block in Fig. 7-1, three sets of roll rate gyro signals are filtered then blended and again scaled and filtered prior to being summed with the limited attitude error signals. The resulting signal is sent to the rudder and engine mixing logic for distribution to the individual engine and rudder actuators. Then each actuator command is limited to eight degrees to prevent the roll channel from usurping all pitch and yaw controllability. The rudder command is limited to 15 degrees.

7.2.2 Yaw Channel Description

The yaw channel block diagram in Fig. 7-2 is laid out in the same manner as the roll channel with the "Vehicle and Subsystem Dynamics" block in the lower right hand corner, the "Inertial Attitude Command" in the upper left hand corner and the "Actuator Mixing Logic" on the right. The rudder is not used for yaw control, because there is adequate engine control authority to handle yaw-plane torque.

Three features which were not included in the roll channel appear in the yaw channel. Two accelerometer inputs have been added to the attitude loop, a forward loop integrator follows the limiter, and a rate command signal is differenced with the input from the rate gyros.

The platform gimbal angle, ψ, is differenced with the inertial attitude command, ψ_C, transformed to body attitude error$(\psi_{EB} = \psi_{EI} \cos \phi - \theta_{EI} \sin \phi \cos \psi)$ and scaled. The attitude error signal is then modified by summing with an acceleration error signal and limiting. The acceleration error is obtained by blending appropriately filtered signals from two body mounted accelerometers and then applying gain and filtering compensation according to the control law or bending requirements. The accelerometer gain is varied with time to meet the drift minimum or load relief requirements. The forward loop integrator trims out steady state errors resulting from biases and thrust misalignments.

The rate command signal is introduced because the normal attitude command changes at a predictable rate. The rate command signal minimizes the tendency for vehicle attitude to lag behind the attitude command due to rate feedback. If the

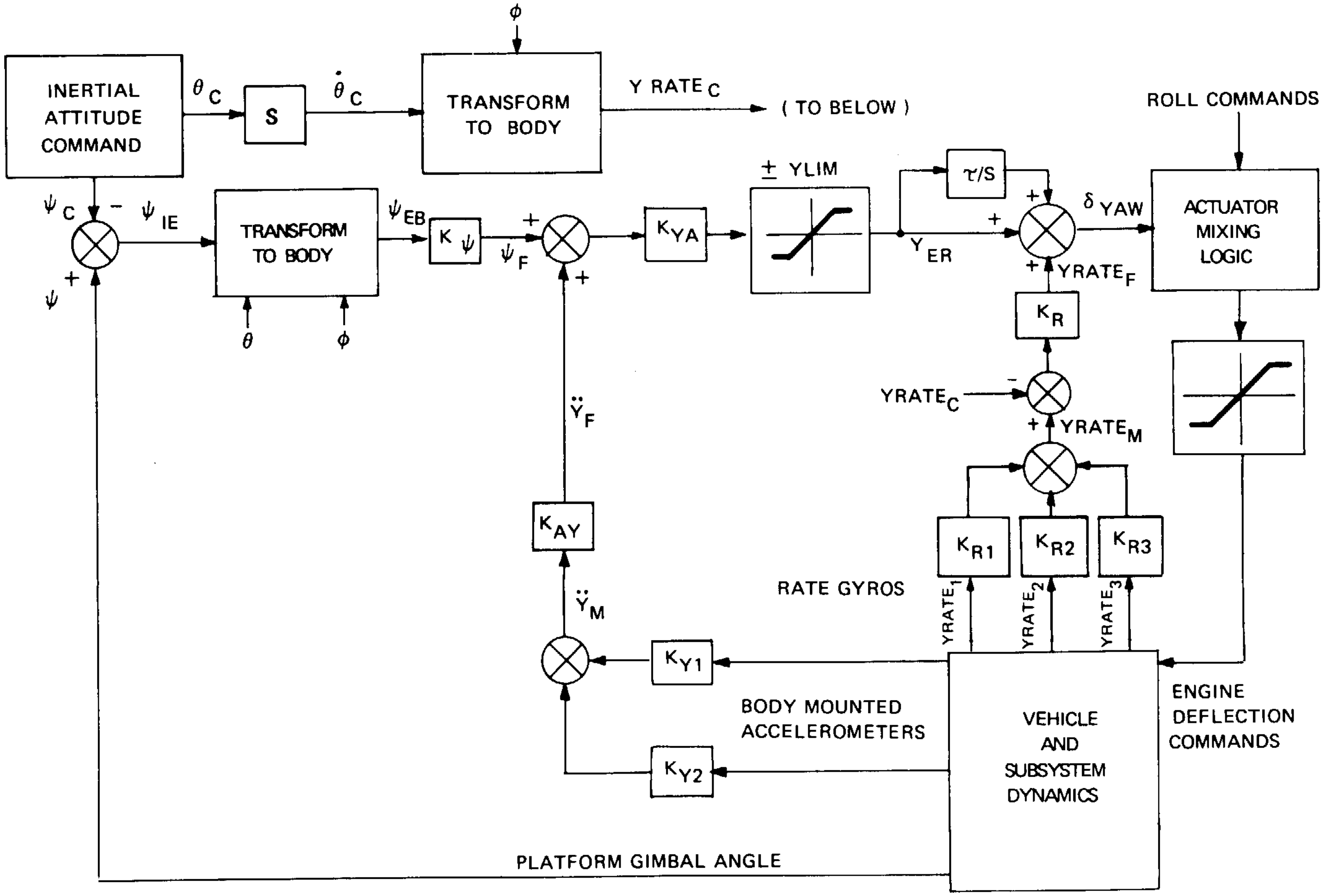

Fig. 7-2 Baseline Launch Configuration Control System Yaw Channel

vehicle rolls appreciably the rate command must be applied to the yaw channel. In operation, the attitude command is differentiated, multiplied by the sine of ϕ, and differenced with the rate feedback signal. The rate error signal is then added to the attitude error signal and sent to the actuator mixing logic routine. Actuator command limiting is performed for the same reason stated for roll control.

7.2.3 Pitch Channel Description

Comparison of Fig. 7-3, which is the pitch channel block diagram, with Fig. 7-2 (yaw channel) reveals that the only difference is the addition of prestored engine deflection and acceleration commands. Both of these command schedules are the nominal values from a reference trajectory.

The addition of the prestored acceleration command permits use of accelerometer feedback with any feasible trajectory to modify the attitude error signal to conform to the desired control law.

The prestored engine deflection command schedule provides coarse control of the engine gimbal trim in the pitch plane. Center of gravity travel alone could be handled by the integral compensation, but aerodynamic pitching moment increases sharply in the vicinity of Mach one and decreases again thereafter. A high integrator gain would be required to follow these rapidly changing deflection requirements. This is undesirable because it degrades the rigid body stability margin; therefore, the prestored commands are used to control the nominal part of this variation.

The rest of the pitch channel is the same as the yaw channel. All engine commands are sent to the actuator mixing logic routine.

7.3 Logic Flow Description

A flow chart showing the logic flow of the control system is presented in Fig. 7-4.

7.4 Values of Control Gains

The basic control system is independent of configuration, assuming that thrust vector control is primary for pitch and yaw, and that the principal guidance commands will be in the pitch plane. It includes no provision for use of elevons during boost.

The control gain and command schedules are, of course, configuration dependent . They will be affected by modifications to either the vehicle configuration or the reference trajectory. This will not impact the design, however, because all control gains and commands are continuously variable input functions of time. Some of them may subsequently be modified to dunctions of other trajectory variables, such as altitude and velocity, but this will involve only minor software modifications.

Table 7-2 presents the current numerical values of the control gains.

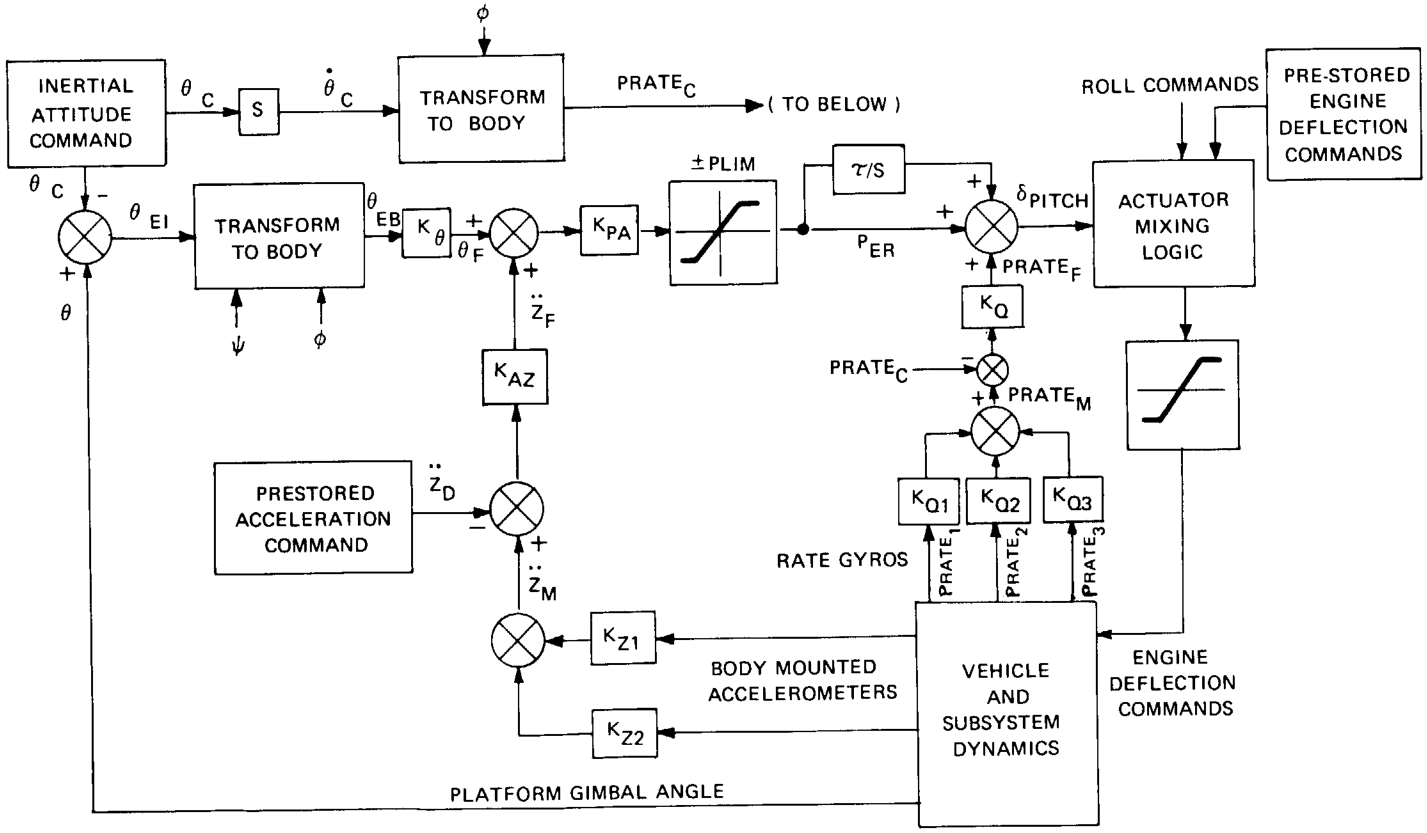

Fig. 7-3 Baseline Launch Configuration Control System Software Pitch Channel

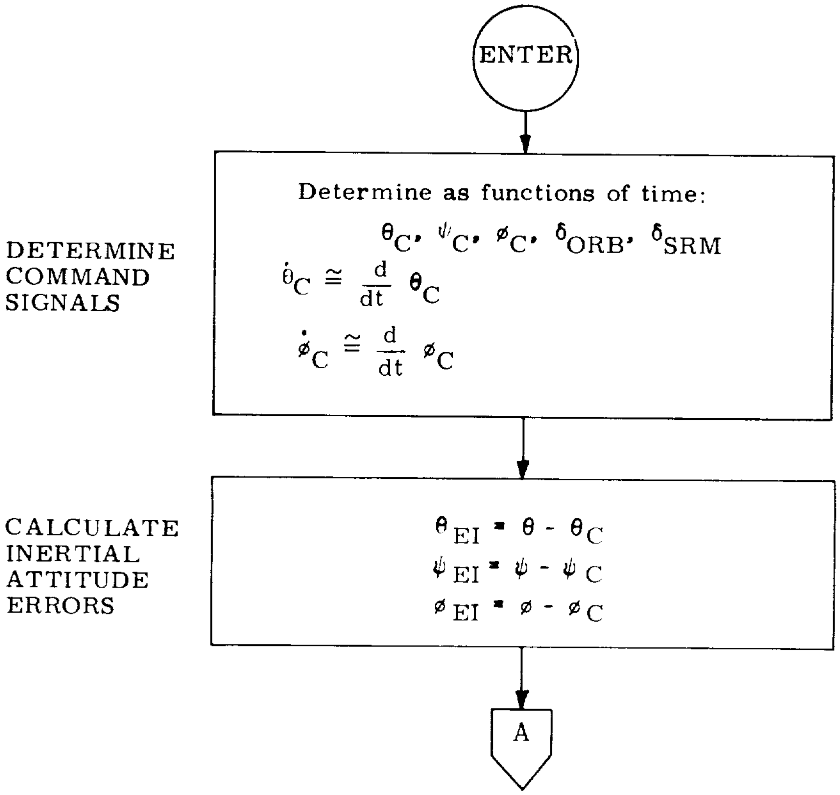
ENTER
DETERMINE COMMAND SIGNALS
Determine as functions of time:
θ_C, ψ_C, ϕ_C, δ_{ORB}, δ_{SRM}
$\dot{\theta}_C \cong \frac{d}{dt} \theta_C$
$\dot{\phi}_C \cong \frac{d}{dt} \phi_C$
CALCULATE INERTIAL ATTITUDE ERRORS
$\theta_{EI} = \theta - \theta_C$
$\psi_{EI} = \psi - \psi_C$
$\phi_{EI} = \phi - \phi_C$
A

Fig. 7-4 Logic Flow

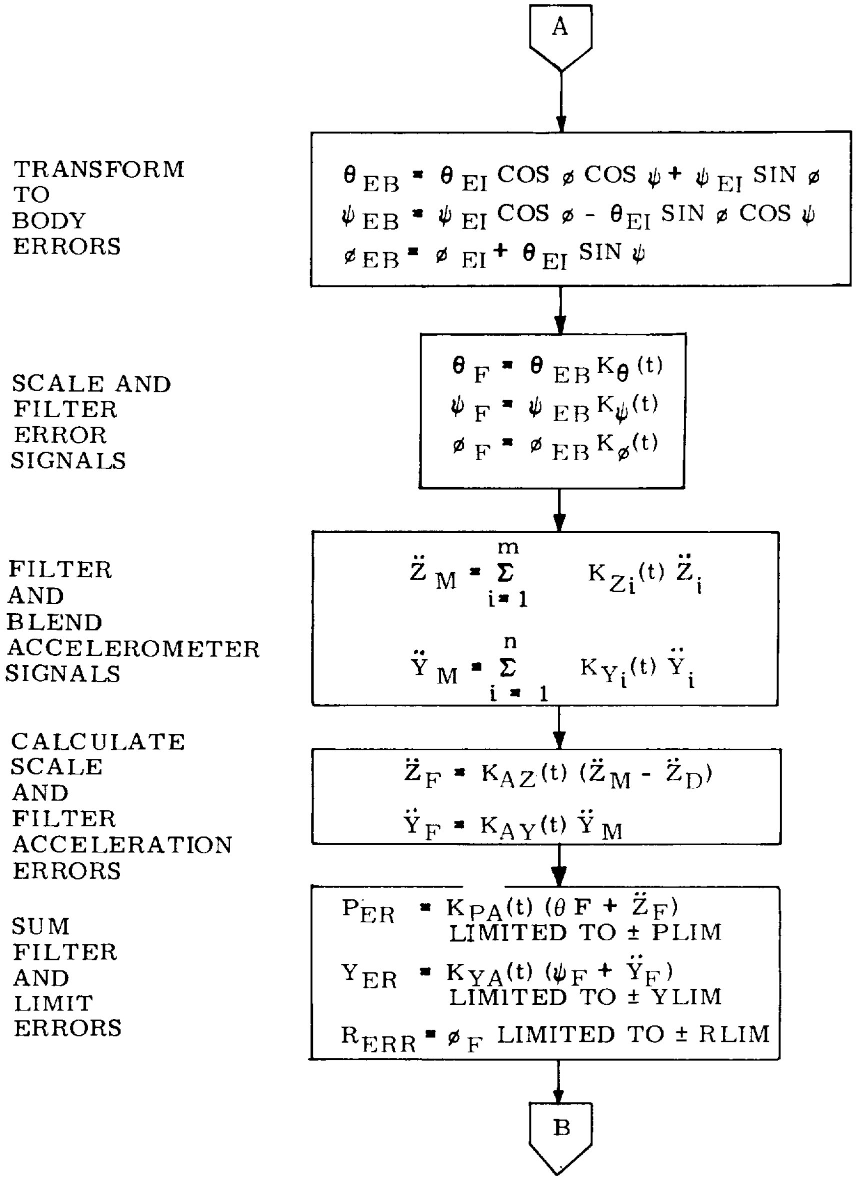
A
TRANSFORM TO BODY ERRORS
$\theta_{EB} = \theta_{EI} \text{ COS } \phi \text{ COS } \psi + \psi_{EI} \text{ SIN } \phi$
$\psi_{EB} = \psi_{EI} \text{ COS } \phi - \theta_{EI} \text{ SIN } \phi \text{ COS } \psi$
$\phi_{EB} = \phi_{EI} + \theta_{EI} \text{ SIN } \psi$
SCALE AND FILTER ERROR SIGNALS
$\theta_F = \theta_{EB} K_\theta(t)$
$\psi_F = \psi_{EB} K_\psi(t)$
$\phi_F = \phi_{EB} K_\phi(t)$
FILTER AND BLEND ACCELEROMETER SIGNALS
$\ddot{Z}_M = \sum_{i=1}^{m} K_{Zi}(t) \ddot{Z}_i$
$\ddot{Y}_M = \sum_{i=1}^{n} K_{Y_i}(t) \ddot{Y}_i$
CALCULATE SCALE AND FILTER ACCELERATION ERRORS
$\ddot{Z}_F = K_{AZ}(t) (\ddot{Z}_M - \ddot{Z}_D)$
$\ddot{Y}_F = K_{AY}(t) \ddot{Y}_M$
SUM FILTER AND LIMIT ERRORS
$P_{ER} = K_{PA}(t) (\theta F + \ddot{Z}_F)$ LIMITED TO ± PLIM
$Y_{ER} = K_{YA}(t) (\psi_F + \ddot{Y}_F)$ LIMITED TO ± YLIM
$R_{ERR} = \phi_F$ LIMITED TO ± RLIM
B

Fig. 7-4 Logic Flow (Cont)

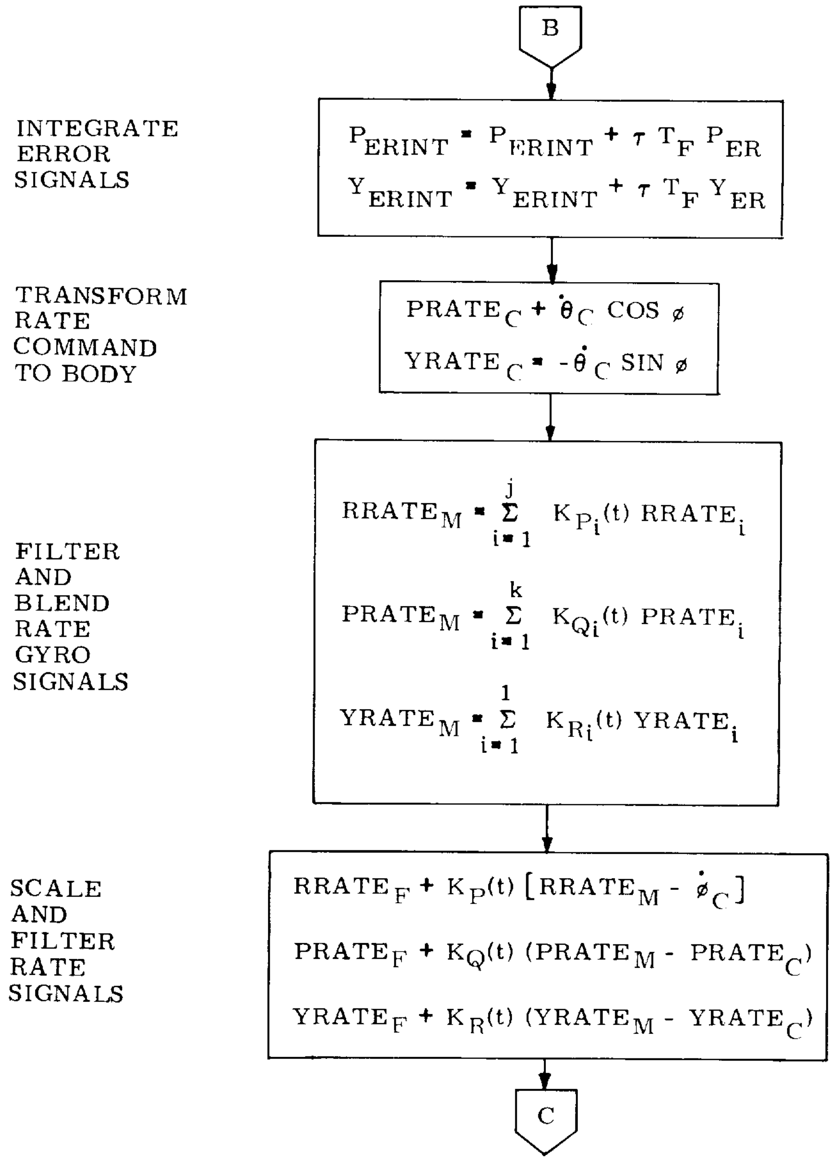
B
INTEGRATE ERROR SIGNALS
$P_{ERINT} = P_{ERINT} + \tau T_F P_{ER}$
$Y_{ERINT} = Y_{ERINT} + \tau T_F Y_{ER}$
TRANSFORM RATE COMMAND TO BODY
$PRATE_C + \dot{\theta}_C \cos \phi$
$YRATE_C = -\dot{\theta}_C \sin \phi$
FILTER AND BLEND RATE GYRO SIGNALS
$RRATE_M = \sum_{i=1}^{j} K_{P_i}(t)\, RRATE_i$
$PRATE_M = \sum_{i=1}^{k} K_{Q_i}(t)\, PRATE_i$
$YRATE_M = \sum_{i=1}^{1} K_{R_i}(t)\, YRATE_i$
SCALE AND FILTER RATE SIGNALS
$RRATE_F + K_P(t) [RRATE_M - \dot{\phi}_C]$
$PRATE_F + K_Q(t) (PRATE_M - PRATE_C)$
$YRATE_F + K_R(t) (YRATE_M - YRATE_C)$
C

Fig. 7-4 Logic Flow (Cont)

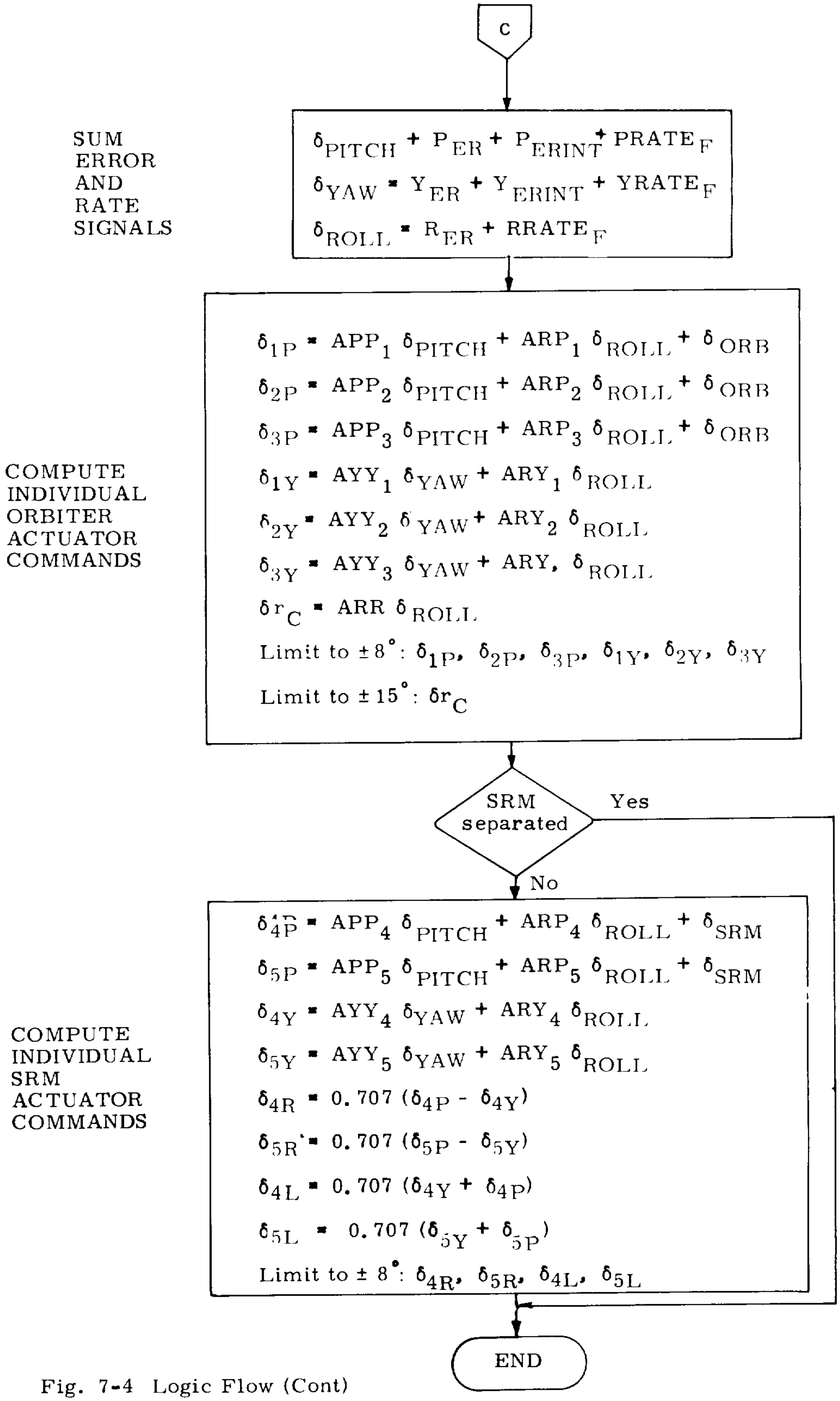
C
SUM ERROR AND RATE SIGNALS
$\delta_{PITCH} + P_{ER} + P_{ERINT} + PRATE_F$
$\delta_{YAW} = Y_{ER} + Y_{ERINT} + YRATE_F$
$\delta_{ROLL} = R_{ER} + RRATE_F$
COMPUTE INDIVIDUAL ORBITER ACTUATOR COMMANDS
$\delta_{1P} = APP_1\, \delta_{PITCH} + ARP_1\, \delta_{ROLL} + \delta_{ORB}$
$\delta_{2P} = APP_2\, \delta_{PITCH} + ARP_2\, \delta_{ROLL} + \delta_{ORB}$
$\delta_{3P} = APP_3\, \delta_{PITCH} + ARP_3\, \delta_{ROLL} + \delta_{ORB}$
$\delta_{1Y} = AYY_1\, \delta_{YAW} + ARY_1\, \delta_{ROLL}$
$\delta_{2Y} = AYY_2\, \delta_{YAW} + ARY_2\, \delta_{ROLL}$
$\delta_{3Y} = AYY_3\, \delta_{YAW} + ARY,\, \delta_{ROLL}$
$\delta r_C = ARR\, \delta_{ROLL}$
Limit to ±8°: $\delta_{1P}, \delta_{2P}, \delta_{3P}, \delta_{1Y}, \delta_{2Y}, \delta_{3Y}$
Limit to ± 15°: δr_C
SRM separated
Yes
No
COMPUTE INDIVIDUAL SRM ACTUATOR COMMANDS
$\delta_{4P} = APP_4\, \delta_{PITCH} + ARP_4\, \delta_{ROLL} + \delta_{SRM}$
$\delta_{5P} = APP_5\, \delta_{PITCH} + ARP_5\, \delta_{ROLL} + \delta_{SRM}$
$\delta_{4Y} = AYY_4\, \delta_{YAW} + ARY_4\, \delta_{ROLL}$
$\delta_{5Y} = AYY_5\, \delta_{YAW} + ARY_5\, \delta_{ROLL}$
$\delta_{4R} = 0.707\, (\delta_{4P} - \delta_{4Y})$
$\delta_{5R} = 0.707\, (\delta_{5P} - \delta_{5Y})$
$\delta_{4L} = 0.707\, (\delta_{4Y} + \delta_{4P})$
$\delta_{5L} = 0.707\, (\delta_{5Y} + \delta_{5P})$
Limit to ± 8°: $\delta_{4R}, \delta_{5R}, \delta_{4L}, \delta_{5L}$
END

Fig. 7-4 Logic Flow (Cont)

Table 7-2

Control Gains vs Time (sec)

	0.	25	30	75	95	120	150
K_θ	1.1	1.1	.88	.88	.66	.66	.66
K_ψ	1.4	1.4	.56	.56	1.4		1.4
K_ϕ	.707			.707	.424		.424
K_{AZ}	0	0	-.109	-.109	0		0
K_{AY}	0	0	.137	.137	0		0
K_P	.707			.707	.424		.424
K_Q	1.1			1.1	.66		.66
K_R	1.4			1.4	.84		.84

K_{P_i}, K_{Q_i}, K_{R_i}
K_{Y_i}, K_{Z_i}
K_{PA} K_{YA} } Currently unity for all values of time.

Mixing Logic Gains

Orbiter Engines	APP	AYY	ARP	ARY
1	1.4	0	0	-3.5
2	1.4	1.4	-3.5	1.8
3	1.4	1.4	3.5	1.8
SRM Engines				
4	1.4	1.4	-1.4	0
5	1.4	1.4	1.4	0

ARR = -7.0

Miscellaneous Fixed Gains

PLIM	7.00 degrees
YLIM	7.00 degrees
RLIM	5.00 degrees
τ	0.1

References

7-1 Space Division, Rockwell International (W. T. Schleich), Space Shuttle Guidance and Control Data Book, SD73-SH-0097, March 1973 (reference trajectory)

7-2 W. Peters, NASA/MSC/EG2, "Control Effector Mixing Logic for Parallel Burn Shuttle Ascent", 24 May 1972.

SECTION 8

DFCS GLOSSARY

Phase	Mnemonic	Symbol in Text	Definition
4	A 1,2,3,4	a_1, a_2, a_3, a_4	Gains for aileron control
4	A 11,12,21,22	$a_{11}, a_{12}, a_{21}, a_{22}$	Lateral fixed gains
8	ABC(1)	δ_{ROLL}	Total roll channel command
8	ABC(2)	δ_{PITCH}	Total pitch channel command
8	ABC(3)	δ_{YAW}	Total yaw channel command
8	ABE(1)	ϕ_{EB}	Body roll attitude error
8	ABE(2)	θ_{EB}	Body pitch attitude error
8	ABE(3)	ψ_{EB}	Body yaw attitude error
8	ABEF(1)	ϕ_F	Scaled roll error
8	ABEF(2)	θ_F	Scaled pitch error
8	ABEF(3)	ψ_F	Scaled yaw error
2,4	ACCBCD	$\underline{\tilde{a}}^b$	Linear accel measurement (body coord)
4	ACCG	g	Acceleration of gravity
4	ACCINT(1)	Δp^j	Roll integrated angular acceleration
4	ACCINT(2)	Δq^j	Pitch integrated angular acceleration
4	ACCINT(3)	Δr^j	Yaw integrated angular acceleration
4	ACCL	$\tilde{a}_L$	Measured lift acceleration
4	ACCLMN	a_{LM}	Mean lift acceleration
4	ADOT	$\dot{\alpha}$	Derivative of angle-of-attack wrt time
4	ADO(1)	$\Delta\hat{\dot{\alpha}}$	Angle-of-attack rate filter output
4	ADO(2)	$\Delta\hat{\dot{\alpha}}'$	Angle-of-attack rate filter extrapolated value
2,4	AG	α_G	Angle-of-attack guidance command
4	AGOLD	α_G^{old}	Previous-pass value of AG
4	AI(1)	$\Delta\tilde{\alpha}$	Angle-of-attack filter input
2	AINT	a_{INT}	Aileron integrator output

Phase	Mnemonic	Symbol in Text	Definition
2	AINTI		Aileron integrator input
2	AINT1		Aileron integrator node
2	AINTMX	a_{INT}^{max}	Aileron integrator output limits(+-max)
8	AIV(1)	ϕ	Platform outer gimbal angle
8	AIV(2)	θ	Platform inner gimbal angle
8	AIV(3)	ψ	Platform middle gimbal angle
8	AIVC(1)	ϕ_C	Platform outer gimbal angle command
8	AIVC(2)	θ_C	Platform inner gimbal angle command
8	AIVC(3)	ψ_C	Platform middle gimbal angle command
8	AIVE(1)	ϕ_{EI}	Platform outer gimbal angle error
8	AIVE(2)	θ_{EI}	Platform inner gimbal angle error
8	AIVE(3)	ψ_{EI}	Platform middle gimbal angle error
4	ALIM	α_{lim}	Limited value of angle-of-attack filter output
2	AM	$\tilde{\alpha}$	Measured angle-of-attack
4	AMEAN	α_T	Mean (trim) angle of attack
2	AN	an	Normal acceleration (-zbody, with gravity)
2	ANF	an_F	Normal acceleration filter output
2	ANGRV	an_{GRV}	Gravity corrections for AN
2	ANN(I)		Normal acceleration filter nodes
4	AO(1)	$\Delta\hat{\alpha}$	Angle-of-attack filter output
4	AO(2)	$\Delta\hat{\alpha}'$	Angle-of-attack filter extrapolated value
8	APP(I)	APP_i	Gains for scaling pitch input to the pitch actuators
8	ARP(I)	ARP_i	Gains for scaling roll input to the pitch actuators
8	ARR	ARR	Gain for scaling the roll input to the rudder
8	ARY(I)	ARY_i	Gains for scaling roll input to the yaw actuators

DFCS GLOSSARY (Cont)

Phase	Mnemonic	Symbol in Text	Definition
4	AX,AY,AZ	U_x, U_y, U_z	Jet acceleration in roll, pitch, yaw
2	AYM	$\tilde{ay}$	Measured lateral acceleration
2	AYMF	$\tilde{ay}_F$	Lateral acceleration filter output
2	AYMN(I)		Lateral acceleration filter nodes
8	AYY(I)	AYY_i	Gains for scaling yaw input to the yaw actuators
2	AZM	$\tilde{az}$	Measured normal acceleration (+zbody)
4	B	b	Fixed estimator parameter
4	B 11,12,21,22	$b_{11}, b_{12}, b_{21}, b22$	Lateral fixed gains
4	BANK	ϕ_V	Roll (bank) about air-relative velocity vector
4	BANKDO(1)	$\Delta\hat{\dot{\phi}}_V$	Bank rate filter output
4	3ANKDO(2)	$\Delta\hat{\dot{\phi}}_V'$	Bank rate filter extrapolated value
4	BANKG	ϕ_{VG}	Bank guidance command
4	BANKI(1)	$\Delta\tilde{\phi}_V$	Bank filter input
4	BANKM	ϕ_{VM}	Mean bank angle
4	BANKO(1)	$\Delta\hat{\phi}_V$	Bank filter output
4	BANKC(2)	$\Delta\hat{\phi}_V'$	Bank filter extrapolated value
4	BDOT	$\dot{\beta}$	Derivative of sideslip wrt time
4	BDO(1)	$\Delta\hat{\dot{\beta}}$	Sideslip rate filter output
4	3DO(2)	$\Delta\hat{\dot{\beta}}$	Sileslip rate filter extrapolated value
4	BDTM	$\dot{\beta}_M$	Rate limit in roll jet logic
2	BE	β_E	Sideslip error filter input
2	BEF	β_{EF}	Sideslip error filter output
2	BEN(I)		Sideslip error filter nodes
2	BG	β_G	Sideslip guidance command
4	BI(1)	$\Delta\tilde{\beta}$	Sideslip angle filter input

DFCS GLOSSARY (Cont)

Phase	Mnemonic	Symbol in Text	Definition
4	BKGOLD	ϕ_{VG}^{old}	Previous-pass value of BANKG
2	BM	$\tilde{\beta}$	Measured sideslip
4	BO(1)	$\Delta\hat{\beta}$	Sideslip angle filter output
4	BO(2)	$\Delta\hat{\beta}'$	Sideslip angle filter extrapolated value
4	BRGOLD	$\dot{\phi}_{VG}^{old}$	Previous-pass value of bank rate command
4	CAT	$\cos\alpha_T$	Cos (AMEAN)
2	CC	c_C	CAS command (QC, AC, or CSTARC)
2	CCAMN		Angle-of-attack values for CCMN
2	CCAMX		Angle-of-attack values for CCMX
2	CCCMN		CAS values (C* or q) for CCMN
2	CCCMX		CAS values (C* or q) for CCMX
2	CCMN	c_C^{min}	CAS command limit, min (working)
2	CCMX	c_C^{max}	CAS command limit, max (working)
2	CE	c_E	CAS error filter input
2	CEF	c_{EF}	CAS error filter output
2	CEN(I)		CAS error filter nodes
2	CF	c_F	CAS feedback (QF, AF, or CSTARF)
2	CG	c_G	CAS guidance command (QG or CSTARG)
4	CLBP	C'_{l_β}	Scheduled estimator parameter
4	CLDAP	$C'_{l_{\delta a}}$	Scheduled estimator parameter
4	CNBP	C'_{n_β}	Scheduled estimator parameter
4	CNDAP	$C'_{n_{\beta a}}$	Scheduled estimator parameter
2,4	CRTB	C_r^b	Reference-to-body direction cosine matrix
4	CRUD	C_{RUD}	Rudder crossfeed gain
2	CSTARG	c_G^*	CSTAR guidance command
4	DA1,DA2	$\delta_{\alpha 1}$, $\delta_{\alpha 2}$	Deadbands for pitch jet logic
-	DAC	δa_C	Aileron command

DFCS GLOSSARY (Cont)

Phase	Mnemonic	Symbol in Text	Definition
2	DACF	δa_{CF}	Aileron command filter output
2,4	DACMX	δa_C^{max}	Aileron command limit(+-max)
2	DACN(I)		Aileron command filter nodes
2	DAG	δa_G	Aileron guidance command
8	DAIVC	$\dot{\theta}_C$	Platform inner gimbal rate command
-	DAMAX	δa^{max}	Physical aileron limit (+-max)
4	DAT	δa_t	Aileron trim estimate
2	DATRIM		Effective aileron trim, for mode change
4	DB1,DB2	$\delta_{\beta 1}$, $\delta_{\beta 2}$	Deadbands for roll jet logic
2	DDG	$\dot{\delta}_G$	TAEM guidance interface variable
-	DEC	δe_C	Elevator command
2,4	DECMN	δe_C^{min}	Elevator command limit, min
2,4	DECMX	δe_C^{max}	Elevator command limit, max
2	DECU		Elevator command from speed loop crossfeeds
2	DECUB		BCS version of DECU
2	DEG	δe_G	Elevator guidance command
-	DELC	δEL_C	Left elevon command
8	DELL 4,5	δ_{4L}, δ_{5L}	Commands to SRM left gimbals
8	DELORB	δ_{ORB}	Prestored orbiter engine deflection command
8	DELP(I)	δ_{iP}	Commands to orbiter pitch gimbals (i=1,2,3)
8	DELP(I)	δ_{iP}	Commands to SRM pseudo pitch gimbals (i=4,5)
8	DELR 4,5	δ_{4R}, δ_{5R}	Commands to SRM right gimbals
8	DELSRM	δ_{SRM}	Prestored SRM engine deflection command
8	DELY(I)	δ_{iY}	Commands to orbiter yaw gimbals (i=1,2,3)
8	DELY(I)	δ_{iY}	Commands to SRM pseudo yaw gimbals (i=4,5)
-	DEMIN,DEMAX	δ_e^{min}, δ_e^{max}	Physical elevator lower (upper) limit
-	DERC	δER_C	Right elevon command

DFCS GLOSSARY (Cont)

Phase	Mnemonic	Symbol in Text	Definition
4	DET	δe_t	Elevator trim estimate
2	DETRIM		Effective elevator trim, for mode change
2	DFC	δf_C	Body-flap command
2	DFCF	δf_{CF}	Flap command filter output
2	DFCM	δf_{CM}	Flap command from Mach profile
2	DFCMCH(I,J)		2xN matrix of (DFCM,MACH) pairs
2	DFCMN	δf_C^{min}	Flap command limit, min
2	DFCMNB		BCS version of DFCMN
2	DFCMX	δf_C^{max}	Flap command limit, max
-	DFMIN,DFMAX	δf^{min}, δf^{max}	Physical flap lower (upper) limit
4	DP1STR	$\bar{q}_1^*$	Blending parameter for elevator use
4	DP2STR	$\bar{q}_2^*$	Blending parameter for aileron use
4	DP3STR	$\bar{q}_3^*$	Blending parameter for rudder use
4	DR1,DR2	$\delta_{\phi 1}$, $\delta_{\phi 2}$	Deadbands for yaw jet logic
-	DRC	δr_C	Rudder command
2	DRCMX	δr_C^{max}	Rudder command limit(+-max)
2	DRF	δr_F	Rudder loop feedback
2	DRG	δr_G	Rudder guidance command
-	DRMAX	δr^{max}	Rudder physical limit (+-max)
8	DRCLI	$\dot{\phi}_C$	Platform outer gimbal rate command
2	DRTRIM		Rudder effective trim, for mode change
-	DSC	δs_C	Speed brake command
2	DSCF	δs_{CF}	Speed brake command filter output
2	DSCMN	δs_C^{min}	Speed brake command limit, min
2	DSCMNB		BCS version of DSCMN
2	DSCMX	δs_C^{max}	Speed brake command limit, max
2	DSCP		Past value of DSC

Phase	Mnemonic	Symbol in Text	Definition
2	DSDMX	$\dot{\delta s}^{max}$	Speed brake (command) rate limit
2	DSG	δs_G	Speed brake guidance command
-	DSMIN,DSMAX	δs^{min}, δs^{max}	Speedbrake physical upper (lower) limit
2	DTC	δt_C	Throttle command
2	DTCF	δt_{CF}	Throttle command filter output
2	DTCMN	δt_C^{min}	Throttle command limit, min
2	DTCMNB		BCS version of DTCMN
2	DTCMX	δt_C^{max}	Throttle command limit, max
2	DTCP		Past value of DTC
2	DTDMX	$\dot{\delta t}^{max}$	Throttle (command) rate limit
2	DTDMXB		BCS version of DTDMX
2	DTG	δt_G	Throttle guidance command
-	DTMIN,DTMAX		Physical throttle lower (upper) limit
2,4	DYNP	$\bar{q}$	Dynamic pressure estimate
4	DYNP 1,2,3	$\bar{q}_1$, $\bar{q}_2$, $\bar{q}_3$	Dynamic pressure switch levels for elevator, aileron, roll jet mode III
2	EINT	e_{INT}	Elevator integrator output
2	EINTI		Elevator integrator input
2	EINTMN	e_{INT}^{min}	Elevator integrator output limit, min
2	EINTMX	e_{INT}^{max}	Elevator integrator output limit, max
2	EINT1		Elevator integrator node
4	EL 1,2,3,4	$\bar{\ell}_1$, $\bar{\ell}_2$, $\bar{\ell}_3$, $\bar{\ell}_4$	Temporary blending parameters
2	ET	e_T	Elevator trim tracker output
4	ETA	η	Lateral scheduled gain (late entry)
2	ETDB	e_{TDB}	Elevator trim tracker input deadband
2	ETDMX	$\dot{e}_T^{max}$	Elevator trim tracker rate limit
2	ETF	e_{TF}	Elevator trim tracker filter output

Phase	Mnemonic	Symbol in Text	Definition
2	ETMN	e_T^{min}	Elevator trim tracker input limit, min
2	ETMX	e_T^{max}	Elevator trim tracker input limit, max
4	F1,F2	f_1, f_2	Longitudinal blending parameters
4	F3,F4	f_3, f_4	Lateral blending parameters
4	FILTER	FILTER	State estimation flag: 0=no filter(use measured values of state) 1=filter
4	FKLAT	K_{lat}	Scheduled estimator gains: lateral channel
4	FKLON	K_{lon}	Scheduled estimator gains: longitudinal channel
4	G1,G2	G_1, G_2	Lateral fixed gains
2	GAINT		CAS aileron integral gain
2	GAIP		CAS aileron integrator gain (GAP*GAINT)
4	GAIR	G_A	Filter gain for air data (=TF/TS)
4	GAM11,12,21,2	$\gamma_{11}, \gamma_{12}, \gamma_{21}, \gamma_{22}$	Lateral scheduled gains (late entry)
4	GAMMA	γ	Flight path angle
2	GAN(I)		Normal acceleration filter coefficients
2	GAP		Roll rate to aileron CAS loop gain
2	GAPM		Roll rate to aileron SAS gain (working)
2	GAPMB		BCS version of GAPM
2	GAPMS(I)		Gain-switch-sensitive SAS values for GAPM
2	GAX		SAS roll stick gearing gain
2	GAXB		BCS version of GAX
2	GAYM(I)		Lateral acceleration filter coefficients
2	GBE(I)		Sideslip error filter coefficients
2	GCE(I)		CAS error filter coefficients (working)
2	GCEA(I)		Angle-of-attack values for GCE(I)
2	GCEC(I)		CAS values (C* or q) for GCE(I)

DFCS GLOSSARY (Cont)

Phase	Mnemonic	Symbol in Text	Definition
2	GCFQM		CSTAR q feedback gain
2	GCH		Altitude loop gain (H to C)
2	GCTH		Theta loop gain (TH to C)
2	GCX		CAS pitch stick gearing gain
2	GDAC(I)		Aileron cmnd filter coef. (A to R crossfeed)
2	GDFC		Flap command filter coefficient
2	GDSC		Speed brake to elevator crossfeed filter coef.
2	GDTC		Throttle to elevator crossfeed coefficient
2	GEC		CAS loop gain
2	GECA		Angle-of-attack value for GEC
2	GECC		CAS value (C* or q) for GEC
2	GEF		Flap to elevator crossfeed gain
2	GEFB		BCS version of GEF
2	GEIC		CAS elevator integration gain (GEC*GEINT)
2	GEICA		Angle-of-attack value for GEIC
2	GEICC		CAS value (C* or q) for GEIC
2	GEINT		CAS elevator integral gain (working)
2	GEINTA		Angle-of-attack value for GEINT
2	GEINTC		CAS value (C* or q) for GEINT
2	GEQM		Elevator damper loop gain (working)
2	GEQMA		Angle-of-attack value for GEQM
2	GEQMB		BCS version of GEQM
2	GEQMC		CAS value (C* or q) for GEQM
2	GEQMS(I)		Gain-switch-sensitive SAS values for GEQM
2	GES		Speed brake to elevator crossfeed gain
2	GESB		BCS version of GES
2	GET		Throttle to elevator crossfeed gain

Phase	Mnemonic	Symbol in Text	Definition
2	GETB		BCS version of GET
2	GETF		Elevator trim tracker filter coefficient
2	GEX		SAS pitch stick gearing gain
2	GEXB		BCS version of GEX
2	GFX		Flap controller gearing gain
2	GFXB		BCS version of GFX
2	GHE(I)		Altitude error filter coefficients
4	GNU1,GNU2		Lateral scheduled gains (late entry)
2	GPE(I)		Roll rate error filter coefficients
2	GPHE(I)		Bank angle error filter coefficients
2	GPHPS		Psi-loop gain (psi to phi)
2	GPHT(I)		Phi-turn filter coefficients
2	GPM(I)		Roll rate feedback filter coefficients
2	GPMB(I)		BCS version of GPM(I)
2	GPPH		Phi-loop gain (phi to p)
2	GPSE(I)		Psi error filter coefficients
2	GPX		CAS roll stick gearing gain
2	GQM(I)		Pitch rate feedback filter coefficients
2	GQMB(I)		BCS version of GQM(I)
2	GQW		Pitch rate washout filter coefficient
2	GPAY		Lateral acceleration feedback gain
2	GRB		Sideslip feedback gain
2	GRCPH		Phi to RC gain, turn coordination
2	GRDAC		Aileron to rudder crossfeed gain
2	GRDACB		BCS version of GRDAC
2	GRE(I)		Yaw rate error filter coefficients
2	GREB(I)		BCS version of GRE(I)

DFCS GLOSSARY (Cont)

Phase	Mnemonic	Symbol in Text	Definition
2	GRM		Yaw rate filter coef. (elevator loops)
2	GRRE		Yaw rate feedback gain
2	GRRW		Yaw rate washout feedback gain (working)
2	GRRWA		AUTO version of GRRW
2	GRRWB		BCS version of GRRW
2	GRRWS(I)		Gain-switch-sensitive SAS values for GRRW
2	GRW		Yaw rate washout filter coefficient
2	GRWB		BCS version of GRW
2	GRX		Pedal gearing gain (working)
2	GRXAUT		RAUT mode value for GRX
2	GRXB		BCS version of GRX
2	GRXSAS		RSAS mode value for GRX
2	GSDDG		TAEM guidance DDG to speed brake gain
2	GSU		Speed brake velocity loop gain
2	GSUE(I)		Speed brake values for GUE(I)
2	GSX		Speed brake manual controller gearing
2	GSXB		BCS version of GSX
2	GTDDG		TAEM guidance DDG to throttle loop gain
2	GTHE(I)		Theta error filter coefficients
2	GTU		Throttle velocity loop gain
2	GTUE(I)		Throttle values for GUE(I)
2	GTX		Throttle manual controller gearing
2	GTXB		BCS version of GTX
2	GUE(I)		Velocity error filter coefficents (working)
2	GXA		Roll stick filter coefficient
2	GXAX		Roll stick parabolic shaping gain
2	GXE		Pitch stick filter coefficient

DFCS GLOSSARY (Cont)

Phase	Mnemonic	Symbol in Text	Definition
2	GXEX		Pitch stick parabolic shaping gain
2	GXF		Pedal filter coefficient
2	GXRX		Pedal parabolic shaping gain
2	GXSX		Speedbrake controller parabolic shaping gain
2	GXSXB		BCS version of GXSX
2	GXTX		Throttle controller parabolic shaping gain
2	GXTXB		BCS version of GXTX
2	HE	H_E	Altitude error
2	HEF	H_{EF}	Altitude error filter output
2	HEN(I)		Altitude error filter nodes
2	HG	H_G	Altitude guidance command
2	HM	$\tilde{H}$	Measured altitude
2	HREF	H_{REF}	EALT mode reference altitude command
2	IABES		ABES present (1); ABES absent (0)
2	IAGAIN		AGAIN switch position (1 thru 4)
2	IAINT		Aileron integrator active (1); inactive (0)
2	IANGRV		Gravity corrections: UNITY(1), COSTH(2), COSTH * COSPH(3)
2	IAINCK		Pilot requested values for IAINT
2	IATRIM		Roll stick trim activity: 0,+1(rgt),-1(left)
2	IBFDBK		Beta feedback (1); lat. accel. feedback (0)
2	ICC1		CAS command switch #1 options (0=off): 1 = ECAS mode or control stick steering 2 = EATT or EALT mode 3 = THG or HG mode 4 = CG mode (QG or CSTARG) 5 = AG mode

Phase	Mnemonic	Symbol in Text	Definition
2	ICC2		CAS command switch #2 options (0=off): 1 = theta loop (THREF or THG) 2 = altitude loop (HREF or HG)
2	ICF		CAS feedback: Q(1), CSTAR(2), ALPHA(3)
2	ICSTAR		CAS mode options: CSTAR(1), FCAH(0)
2	IEGAIN		EGAIN switch position (1 thru 4)
2	IEINCK		Pilot-requested values for IEINT
2	IEINT		Elevator integrator active (1); inactive (0)
2	IETRIM		Pitch stick trim activity: 0,+1(fwd),-1(aft)
2	IGEARX		Extend gear (1), retract gear (0)
2	IHC		Altitude command: HREF (1), HG (2)
4	ILAT	I_{LAT}	Mode flag for entry phase lateral control 0 = early entry, "reverse" aileron 1 = late entry, "proverse" aileron
-	IM	IM	Medium-sampling-rate index: 0 = perform calculations this pass
-	INGUID	INGUID	Flag specifies guidance command set neg=commands not updated this pass +/- 1=BANKG,ALPHG specified +/- 2=ROLLG,QG specified
-	INSENS	INSENS	Flag specifies source of measurements 0=provided by simulator (hybrid sim.) 1=sensors or environment (SSFS) 2=G&N and sensors or environment (SSFS)
2	IPC		Roll rate command options (0=off): 1 = ACAS mode or control stick steering

DFCS GLOSSARY (Cont)

Phase	Mnemonic	Symbol in Text	Definition
			2 = AATT or AHDG mode
			3 = PHG or PSG mode
			4 = PG mode
2	IPHC		Bank angle command options (0=off):
			1 = AATT mode
			2 = AHDG mode
			3 = PSG mode
			4 = PHG mode
2	IPHM		PHM valid (1), invalid (0)
2	IPHRC		Phi source for yaw rate command options:
			1 = zero (beta/r-wash. fdbk)
			2 = PHM (measured)
			3 = PHC (commanded, if available)
2	IPSC		Psi command: PSREF(1), PSG(2)
2	IQTRN		Pitch rate turn coordination option:
			1 = off, use Q feedback
			2 = use Q washout feedback
			3 = use Q=R*TANPHI feedback
2	IRCHAI		Request change IAINT state (1), no request (0)
2	IRCHFI		Request change IFINT state (1), no request (0)
2	IRGAIN		RGAIN switch position (1 thru 4)
2	IRTRIM		Pedal trim activity: 0,+1(lft),-1(rgt)
2	IRW		Yaw rate washout active(1),inactive(0)
2	IRWP		Pad load indicator for IRW
-	IS	IS	Slow-sampling-rate index:
			0 = perform calculations this pass
-	ISTART	ISTART	Initialization pass(1), not initialization(0)

Phase	Mnemonic	Symbol in Text	Definition
-	ISTRTP	ISTRTR	Request initialization(1), no request(0)
2	ITHC		Theta command: THREF(1), THG(2)
-	ITM, ITS	ITM, ITS	Number of fast passes per medium (slow) pass
4	IXX	I_{xx}	Fixed estimator parameter
4	IZZ	I_{zz}	Fixed estimator parameter
2	JAGAIN		Local past-value copy of IAGAIN
2	JEGAIN		Local past-value copy of IEGAIN
2	JGEARX		Local copy of IGEARX
2	JRCHAI		Local copy of IRCHAI
2	JRCHEI		Local copy of IRCHEI
2	JRGAIN		Local past-value copy of IRGAIN
4	KA,KE	K_a, K_e	Aileron (elevator) deflection limit parameter
4	KALF1	$K_{\alpha 1}$	Elevator trim gain (early entry)
4	KALF2	$K_{\alpha 2}$	Elevator trim gain (late entry)
4	KC1,KC2	KC1, KC2	Low-dynamic-pressure constant filter gains
4	KPCLI	K_{ϕ}	Aileron trim gain
8	KY(I)	K_{Yi}	Individual y accelerometer gain
8	KZ(I)	K_{Zi}	Individual z accelerometer gain
4	LAMDAA,LAMDAE	λ_a, λ_e	Switch set to 1 if pitch (lateral) ACPS jets are needed
4	MA,ME	m_a, m_e	Slope of KA(KE) curve
2,4	MACH	$\mathcal{M}$	Mach number
2	MODA		Current aileron loop mode: 1 = ABCS 2 = ASAS 3 = ACAS 4 = AAUT 5 = AATT 6 = AHDG
2	MODACH		Indicate aileron loop mode change 1 = no change 2 = MODAGR change

Phase	Mnemonic	Symbol in Text	Definition
			3 = MODAR change 4 = first pass
2	MODAG		Current aileron guidance mode (MODA=4): 1 = PG 2 = PHG 3 = PSG
2	MODAGR		Requested values for MODAG
2	MODAR		Requested values for MODA
2	MODB		BCS mode (1), not BCS mode (0)
2	MODBR		Requested values for MODB
2	MODE		Current elevator loop mode: 1 = EBCS 2 = ESAS 3 = ECAS 4 = EAUT 5 = EATT 6 = EALT
2	MODECH		Indicate elevator loop mode change 1 = no change 2 = MODEGR change 3 = MODER change 4 = first pass
2	MODEG		Current elevator guidance mode (MODE=4): 1 = QG 2 = THG 3 = AG 4 = HG
2	MODEGR		Requested values for MODEG
2	MODER		Requested values for MODE
2	MODR		Current rudder loop mode: 1 = RBCS 2 = RSAS 3 = RCAS (=2=RSAS) 4 = RAUT
2	MODRCH		Indicate rudder loop mode change: 1 = no change 2 = MODRGR change 3 = MODRR change 4 = first pass
2	MODRG		Current rudder guidance mode (MODR=4): 1 = yaw rate feedback 2 = yaw rate washout feedback
2	MODRGR		Requested values for MODRG

Phase	Mnemonic	Symbol in Text	Definition
2	MODPP		Requested values for MODP
2	MODS		Current speed brake mode: 1 = BCSSB 2 = MANSB 3 = IASSB 4 = AUTOSB 5 = DSGSB 6 = TAEMS
2	MODT		Current throttle mode: 1 = BCSTH 2 = MANTH 3 = IASTH 4 = AUTOTH 5 = DTGTH 6 = TAEMTH
2	MODU		Current speed control mode: 1 = UBCS 2 = UMAN (IAS-man) 3 = UASB (IAS-sb) 4 = UAUT 5 = UATH (IAS-th)
2	MODUCH		Indicate speed control loop mode change: 1 = no change 2 = MODUGR change 3 = MODUR change 4 = first pass
2	MODUFP		Flag for FILUP subroutine speed control 1 = MANUAL or AUTO-dir 2 = IAS-hold 3 = AUTO(UG-guid) 4 = AUTO(TAEM-guid)
2	MODUFT		Flag for velocity filter moding: 0 = UFILT inactive 1 = SB-ufilt 2 = TH-ufilt
2	MODUG		Current guidance speed control mode: (1-10, see speed control flag table)
2	MODUGR		Requested values for MODUG
2	MODUR		Requested values for MODU
4	MU		Roll jet switch parameter
4	P 11,12,21,22	$P_{11}, P_{12}, P_{21}, P_{22}$	Lateral derived gains (late entry)
2	PC	P_C	Roll rate command

Phase	Mnemonic	Symbol in Text	Definition
8	PCEGK	K_{PA}	Pitch channel error gain
2	PCMX	p_C^{max}	Roll rate command limit, +-maximum
2	PE	p_E	Roll rate error / error filter input
2	PEF	p_{EF}	Roll rate error filter output
8	PEGK	K_θ	Pitch error gain
2	PEN(I)		Roll rate error filter nodes
8	PER	P_{ER}	Limited pitch channel error
8	PERINT	P_{ERINT}	Weighted integral of PER
2	PG	p_G	Roll rate guidance command
-	PHASE	PHASE	Flight phase flag (internal copy of PHASER)
-	PHASER	PHASER	Flight phase flag (external):1=rollout phase 2=cruising phase 4=entry phase 5=orbit TVC phase 6=orbit RCS phase 7=insertion TVC phase 8=booster TVC phase
2	PHC	ϕ_C	Bank angle command
2	PHCMX	ϕ_C^{max}	Bank angle command limit,+-maximum
2	PHE	ϕ_E	Bank angle error / error filter input
2	PHEF	ϕ_{EF}	Bank angle error filter output
2	PHEN(I)		Bank angle error filter nodes
2	PHG	ϕ_G	Bank angle guidance command
4	PHILAT	Φ_{lat}^{CL}	Estimator state transition matrix: lateral channel
4	PHILIM	ϕ_{lim}	Limited value of bank filter output
4	PHILON	Φ_{lon}^{CL}	Estimator state transition matrix: longitudinal channel

Phase	Mnemonic	Symbol in Text	Definition
2	PHM	$\tilde{\phi}$	Measured bank angle
2	PHREF	ϕ_{REF}	AATT mode reference bank angle command
2	PHSEL	ϕ_{SEL}	Pilot-selected values for PHREF
2	PHTF	ϕ_{TF}	Phi-turn filter output and/or bank angle for turn-coordination (a & r)
2	PHTN(I)		Phi-turn filter nodes
4	PI(1)	$\Delta\tilde{p}$	Roll rate filter input
8	PLIM	PLIM	Pitch error software limit
2,4	PM	$\tilde{p}$	Measured roll rate
2	PMDIS	$\tilde{p}_{DIS}$	Roll rate for AATT or AHDG reengage after ACSS
2	PMF	$\tilde{p}_F$	Roll rate filter output
2	PMFB		BCS version of PMF
2	PMNB(I)		BCS version of PMN(I)
2	PMN(I)		Roll rate filter nodes
4	PN	p_N	Nominal roll rate
8	PRATEC	$PRATE_C$	Pitch rate command
8	PRATEF	$PRATE_F$	Scaled pitch rate error
8	PRATEM	$PRATE_M$	Blended pitch rate
8	PRGG(I)	K_{Qi}	Individual pitch rate gyro gain
8	PRGK	K_Q	Pitch rate gain
2	PSE	Ψ_E	Heading error
2	PSEF	Ψ_{EF}	Heading error filter output
2	PSEN(I)		Heading error filter nodes
2	PSG	Ψ_G	Heading guidance command
2	PSM	$\tilde{\Psi}$	Measured heading
2	PSREF	Ψ_{REF}	AHDG mode reference heading command

DFCS GLOSSARY (Cont)

Phase	Mnemonic	Symbol in Text	Definition
2	PSSEL	Ψ_{SEL}	Pilot-selected values for PSREF
2	QCT	q_{CT}	Pitch turn coordination q-command
2	QCTMX	q_{CT}^{max}	QCT maximum (0. = min)
2	QG	q_G	Pitch rate guidance command
4	QI(1)	$\Delta\tilde{q}$	Pitch rate filter input
2,4	QM	$\tilde{q}$	Measured pitch rate
2	QMDIS	$\tilde{q}_{DIS}$	Pitch rate for EATT or EALT reengage after ECSS
2	QMF	$\tilde{q}_F$	Pitch rate filter output
2	QMFB		BCS version of QMF
2	QMN(I)		Pitch rate filter nodes
2	QMNB(I)		BCS version of QMN(I)
4	QN	q_N	Nominal pitch rate
2	QWF	q_{WF}	Pitch rate washout filter output
2	QW1		Pitch rate washout filter node
4	R1	r_1	Angle-of-attack error limits
4	R8	r_8	Roll angle error limits
4	R 11,12,21,22	$r_{11}, r_{12}, r_{21}, r_{22}$	Lateral derived gains (late entry)
8	RAGTVK	K_ϕ	Roll error gain
2	RC	r_C	Yaw rate command
4			Derivative of bank angle
4	RDOTC	$\dot{\phi}_C(\dot{\phi}^C)$	Bank rate command
2	RE	r_E	Yaw rate error
2	REF	r_{EF}	Yaw rate error filter output
2	REN(I)		Yaw rate error filter nodes
2	RENB(I)		BCS version of REN(2)
8	RER	R_{ER}	Limited roll error for TVC

DFCS GLOSSARY (Cont)

Phase	Mnemonic	Symbol in Text	Definition
2	RG	r_G	Yaw rate guidance command
2,4	RHO		Reference air density
4	RI(1)	$\Delta\tilde{r}$	Yaw rate filter input
8	RLIM	RLIM	Roll error software limit
2,4	RM	$\tilde{r}$	Measured yaw rate
2	RMF	$\tilde{r}_F$	Yaw rate filter output (elevator loops)
4	RN	r_N	Nominal yaw rate
2,4	ROLL	ϕ	Computed roll angle
2	ROLLG	ϕ_G	Guidance commanded roll angle
4	RPHI 1,2,3	$r_{\phi 1}, r_{\phi 2}, r_{\phi 3}$	Parameters for maneuver rate calculation
4	RR	$\underset{\sim}{R}_{rel}$	Position vector in reference coordinates
8	RRATEF	$RRATE_F$	Scaled roll rate for TVC
8	RRATEM	$RRATE_M$	Blended roll rate signals
8	RRCG(I)	K_{Pi}	Individual roll rate gyro gain
8	RRGTVK	K_P	TVC roll rate gain
2	RWFB		BCS version of RWF
2	RW1B		BCS version of RW1
2	RWF	r_{WF}	Yaw rate washout filter output
2	RW1		Yaw rate washout filter node
4	S	S	Fixed estimator parameter
4	SAT	$\sin\alpha_T$	Sin (AMEAN)
4	SIGMA A,B,P	$\sigma_\alpha, \sigma_\beta, \sigma_\varphi$	Gains for jet logic - pitch, roll, yaw
8	TAUINT	τ	Integrator gain
2	TDSDMX		TF * speed brake rate limit
2	TDTDMX		TF * throttle rate limit
2	TEMP		Temporary local variable(s)
2,4	TEMPFR	T_A	Air temperature, deg F and dimensionless
2,4	TEMPFK	TK_A	Input air temperature in deg. Kelvin

Phase	Mnemonic	Symbol in Text	Definition
2	TFTDMX		TF * elevator trim tracker rate limit
-	TF	T_F	Fast sampling interval
2	TF2		TF / 2.
2	TFB		BCS version of TF2
2	TGSDDG		TF * TAEM/SB loop gain
2	TGTDDG		TF * TAEM/TH loop gain
2	THE	θ_E	Theta error
2	THEF	θ_{EF}	Theta error filter output
2	THEN(I)		Theta error filter nodes
2	THG	θ_G	Theta guidance command
2	THM	$\tilde{\theta}$	Measured theta
2	THREF	θ_{REF}	EATT mode reference pitch attitude command
2	THSEL	θ_{SEL}	Pilot-selected values for THREF
-	TM	T_M	Medium sampling interval
-	TNEXT	TNEXT	Next DFCS entry time
-	TS	T_S	Slow sampling interval
2	TXADMX		TF * roll stick rate limit
2	TXATR		TF * roll stick trim rate
2	TXATRB		BCS version of TXATR
2	TXEDMX		TF * pitch stick rate limit
2	TXETR		TF * pitch stick trim rate
2	TXETRB		BCS version of TXETR
2	TXRDMX		TF * pedal rate limit
2	TXPTR		TF * pedal trim rate
2	TXPTRB		BCS version of TXPTR
2	TXTDMX		TF * throttle controller rate limit
2	T2GAIP		TF2 * roll integrator gain

DFCS GLOSSARY (Cont)

Phase	Mnemonic	Symbol in Text	Definition
2	T2GEIC		TF2 * pitch integrator gain
4	U1,U2	U_1, U_2	Roll jet logic gains
2	UE	u_E	Velocity error
2	UEF	u_{EF}	Velocity error filter output
2	UEF(I)		Velocity error filter nodes
2	UG	u_G	Velocity guidance command
4	UJ (1),(2),(3)	u_x, u_y, u_z	ACPS torque commands
4	UL(I)	$\underline{u}_L$	Vector in longitudinal plane normal to velocity
2	UM	$\tilde{u}$	Measured velocity
2	UREF	u_{REF}	IAS-hold mode reference velocity command
2	USEL	u_{SEL}	Pilot-selected values for UREF
2,4	UXV,UYV,UZV	$\underline{UV}_x, \underline{UV}_y, \underline{UV}_z$	Unit vectors along the velocity coordinate system, in reference coordinates
4	VBODY	$\underline{V}_{body}$	Air-relative velocity in body coordinates
4	VMACH1	M_1	Lateral switch parameter
4	VR	$\underline{V}_{rel}$	Air-relative velocity in reference coordinates
4	W1,W2	ω_1, ω_2	Gains for aileron control logic
8	WB(1,I)	$RRATE_i$	Individual roll rate gyro signal
8	WB(2,I)	$PRATE_i$	Individual pitch rate gyro signal
8	WB(3,I)	$YRATE_i$	Individual yaw rate gyro signal
4	WD	ω_d	Gain for elevator control
2	XA	xa	Local variable for XAM processing
2	XAB	xa_B	Roll stick detent bias
2	XADB	xa_{DB}	Roll stick deadband
2	XADMX	$\dot{xa}^{max}$	Roll stick rate limit
2	XAF	xa_F	XA filter output
2	XAM	$\tilde{xa}$	Measured roll stick deflection

Phase	Mnemonic	Symbol in Text	Definition
2	XAMDIS	$\tilde{xa}_{DIS}$	Roll stick disengage level for ACSS
2	XAMX	xa^{max}	Roll stick limits (+-max)
2	XAP	xa_P	Processed roll stick
2	XAT	xa_T	Roll stick trim
2	XATB		BCS version of XAT
2	XATMX	xa_T^{max}	Roll stick trim limit (+-max)
2	XATMXB		BCS version of XATMX
2	XATR	$\dot{xa}_T$	Roll stick trim rate
2	XATRB		BCS version of XATR
2	XE	xe	Local variable for XEM processing
2	XEB	xe_B	Pitch stick detent bias
2	XEDB	xe_{DB}	Pitch stick deadband
2	XEDMX	xe^{max}	Pitch stick rate limit
2	XEF	xe_F	XE filter output
2	XEM	$\tilde{xe}$	Measured pitch stick deflection
2	XEMDIS	$\tilde{xe}_{DIS}$	Pitch stick disengage level for ECSS
2	XEMN	xe^{min}	Pitch stick minimum (aft)
2	XEMX	xe^{max}	Pitch stick maximum (fwd)
2	XEP	xe_P	Processed pitch stick
2	XET	xe_T	Pitch stick trim
2	XETB		BCS version of XET
2	XETMN	xe_T^{min}	Pitch stick trim minimum (aft)
2	XETMNB		BCS version of XETMN
2	XETMX	xe_T^{max}	Pitch stick trim maximum (fwd)
2	XETMXB		BCS version of XETMX
2	XETR	xe_T	Pitch stick trim rate
2	XETRB		BCS version of XETR

Phase	Mnemonic	Symbol in Text	Definition
2	XFB		Flap controller bias
2	XFM	$\widetilde{xf}$	Measured flap controller deflection
2	XFMMN	$\widetilde{xf}^{min}$	Flap controller minimum
4	XI 1	ξ_1	Scheduled control gain: longitudinal
4	XT 2,3,4,5,6	$\xi_2, \xi_3, \xi_4, \xi_5, \xi_6$	Scheduled control gains:lateral, early entry
2	XR	xr	Local pedal variable
2	XRB	xr_b	Pedal detent bias
2	XRDB	xr_{DB}	Pedal deadband
2	XRDMX	$\dot{x}r^{max}$	Pedal rate limit
2	XRF	xr_F	XR filter output
2	XRM	$\widetilde{xr}$	Measured pedal deflection
2	XRMX	xr^{max}	Pedal limits (+-max)
2	XRP	xr_P	Processed pedal
2	XRT	xr_T	Pedal trim
2	XRTB		BCS version of XRT
2	XRTMX	xr_T^{max}	Pedal trim limits (+-max)
2	XRTMXB		BCS version of XRTMX
2	XRTR	$\dot{x}r_T$	Pedal trim rate
2	XRTRB		BCS version of XRTR
2	XS	xs	Local variable for XSM processing
2	XSM	$\widetilde{xs}$	Measured speed brake controller deflection
2	XSMDIS	$\widetilde{xs}_{DIS}$	XSM disengage level for IAS-sb
2	XSMMN	$\widetilde{xs}^{min}$	XSM minimum (retract)
2	XSMREF	$\widetilde{xs}_{REF}$	XSM reference for IAS-sb disengage
2	XSP	xs_P	Processed XSM
2	XT	xt	Local variable for XTM processing
2	XTM	$\widetilde{xt}$	Measured throttle controller deflection

DFCS GLOSSARY (Cont)

Phase	Mnemonic	Symbol in Text	Definition
2	XTMDIS	$\widetilde{xt}_{DIS}$	XTM disengage level for IAS-th
2	XTMMN	$\widetilde{xt}^{min}$	XTM minimum (idle)
2	XTMREF	$\widehat{xt}_{REF}$	XTM reference for IAS-th disengage
2	XTP	xt_P	Processed XTM
2	XTPB		BCS version of XTP
2	XTPP		Past value of XTP
2	XTPPB		BCS version of XTPP
8	YACCER	$\ddot{Y}_F$	Scaled y acceleration error
8	YACIN(I)	$\ddot{Y}_i$	Individual y accelerometer signal
8	YACSIG	$\ddot{Y}_M$	Blended y accelerometer signals
8	YAGK	K_{AY}	Y acceleration gain
8	YCEGK	K_{YA}	Yaw channel error gain
8	YEGK	K_{Ψ}	Yaw error gain
8	YER	Y_{ER}	Limited yaw channel error
8	YERINT	Y_{ERINT}	Weighted integral of YER
8	YLIM	YLIM	Yaw error software limit
8	YRATEC	$YRATE_C$	Yaw rate command
8	YRATEF	$YRATE_F$	Scaled yaw rate error
8	YRATEM	$YRATE_M$	Blended rate gyro signals
8	YRGG(I)	K_{Ri}	Individual vaw rate gyro gain
8	YRGK	K_R	Yaw rate gain
8	ZACCER	$\ddot{Z}_F$	Scaled z acceleration error
8	ZACD	$\ddot{Z}_D$	Z acceleration command
8	ZACIN(I)	$\ddot{Z}_i$	Individual z accelerometer signal
8	ZACSIG	$\ddot{Z}_M$	Blended z accelerometer signals
8	ZAGK	K_{AZ}	Z acceleration gain
4	ZETAD	ξ_d	Gain for elevator control
4	ZETA 1,2	ξ_1, ξ_2	Gains for aileron control logic

PERIPHERAL ROUTINES

The routines presented in this section were part of the Apollo / Skylab flight programs. They are a baseline for the Space Shuttle pointing and maneuvering routines.

SECTION 1

AUTOMATIC TRACKING

The automatic tracking function applies to any mission situation requiring the orbiter to track a designated body (or target vehicle) by pointing a specified body fixed vector at the target or to any mission situation requiring the orbiter to rotate at a constant rate around a specified axis. Typically, automatic tracking can be utilized for rendezvous navigation, local vertical tracking, landmark tracking, and passive thermal control. In this mode of operation, the autopilot (DAP) is utilized as a rate command system. Attitude control, if required, is maintained by the Tracking Attitude Routine (R61) with attitude feedback from the navigation functions. R61 operates at a variable computation period, Δt_c, which is generally much longer than the autopilot sampling period of 0.1 seconds. Initial alignment of the vehicle to the tracking attitude is generally performed by R61 using the automatic maneuver routine (R60). In the following TV denotes the target vehicle and ORB denotes the orbiter vehicle.

1.1 Tracking Options

There are five automatic tracking options as defined below:

Option	Purpose
0	Point a specified spacecraft vector at the TV. Do not constrain rotational attitude about this pointing vector. (Use VECPOINT)
1	Point a specified spacecraft vector at a celestial body. Do not constrain attitude about this vector (Use VECPOINT)
2	Rotate at a specified rate about a specified spacecraft vector.
4	Same as Option 0, but constraining attitude about the pointing vector to a specified value (OMICRON).
5	Same as Option 1, but constraining attitude about pointing vector to a specified value (OMICRON).

1.2 Option 0: Orient the Spacecraft Such that a Specified Body-Fixed Pointing Vector Aligns with the Estimated Line of Sight to the TV.

The pointing vector (SCAXIS) is defined by two angles:

1) A specified positive angle (γ) from the spacecraft X axis about the spacecraft Z axis ($0 \leq \gamma < 360$ deg)

2) A specified positive angle (ρ) about the Y'-axis produced in the XY plane as a result of γ($-90 \leq \rho \leq 90$ deg).

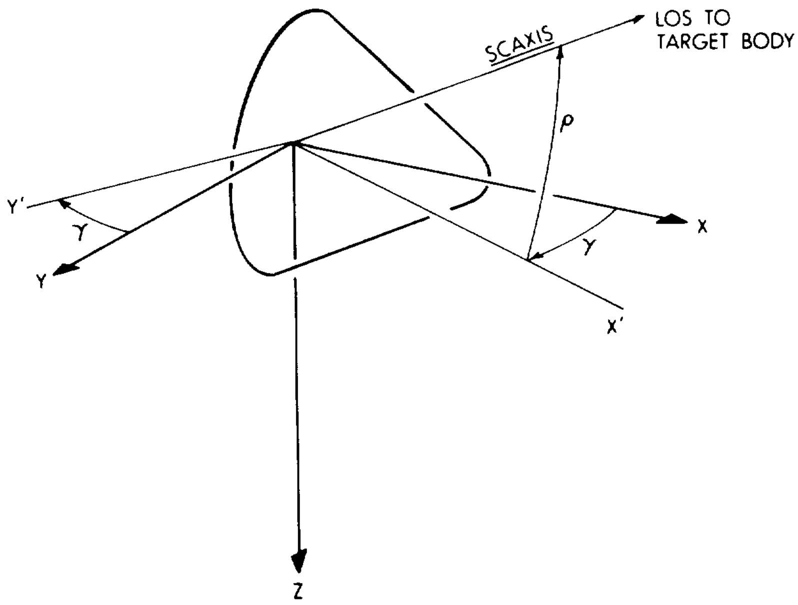

The LOS is determined by advancing the estimated ORB and TV state vectors to the current time. Once the coincidence of SCAXIS and LOS has been established, R61 establishes a spacecraft angular rate to maintain the coincidence. For Option 0, R61 provides the RCS DAP with the following quantities:

1) $\underline{\omega}_{CA}$.....desired LOS rate plus LOS correction rate in control-axis coordinates

2) IGA_D, MGA_D, OGA_D.....DAP reference angles, i.e., center of the deadband.

3) $\Delta\underline{G}A$.....a vector defining the desired incremental changes in the IMU gimbal angles every 0.1 second.

The desired LOS rate ($\underline{\omega}_{CA}$) is computed as follows:

$$\underline{u}_{LOS} = \underline{r}_W - \underline{r}_C$$

$$\underline{\omega}_{correction} = ([NBSM]\ \underline{SCAXIS} \times [REFSMMAT]\ \text{UNIT}\ (\underline{u}_{LOS}))/\Delta t_C$$

where NBSM uses the DAP reference angles THETADX, Y, and Z for the transformation from navigation-base to stable-member coordinates.

If $|\underline{\omega}_{correction}|$ exceeds MAXRATE, distribute as follows:

$$\underline{\omega}_{correction} = \text{MAXRATE}\ [\text{UNIT}\ (\underline{\omega}_{correction})]$$

$$\underline{\omega}_{LOS} = [REFSMMAT] \left\{ \frac{\text{UNIT}\ (\underline{u}_{LOS}) \times (\underline{v}_W - \underline{v}_C)}{|\underline{u}_{LOS}|} \right\} + \underline{\omega}_{correction}$$

$$\underline{\omega}_{CA} = [NBCA]\ [SMNB]\ \underline{\omega}_{LOS},$$

where $\underline{\omega}_{LOS}$ is the LOS rate in stable member coordinates. [SMNB] is the transformation from stable member axes to navigation base coordinates. [NBSM] is the transformation from navigation base coordinates to stable member coordinates. [REFSMMAT] is the transformation from reference inertial coordinates to stable member axes. [NBCA] is the matrix for transforming a vector from navigation base to control-axis coordinates. $\underline{r}_W$, $\underline{v}_W$, $\underline{r}_C$, and $\underline{v}_C$ are the position and velocity vectors of the TV and ORB in basic-reference coordinates. SCAXIS is the specified axis (γ, ρ). MAXRATE is the maximum correction rate and Δt_C is a conservative estimate of the R61 computation interval (thus preventing overshoot in vehicle attitude by the time of the next pass).

The vector $\Delta \underline{GA}$ is computed as follows:

$$\Delta \underline{GA} = \begin{bmatrix} \cos IGA \sec MGA & 0 & -\sin IGA \sec MGA \\ -\cos IGA \tan MGA & 1 & \sin IGA \tan MGA \\ \sin IGA & 0 & \cos IGA \end{bmatrix} (0.1\ \underline{\omega}_{LOS}$$

where

IGA = inner gimbal angle

MGA = middle gimbal angle

OGA = outer gimbal angle

where $\underline{\omega}_{LOS}$ is the LOS rate in stable-member coordinates computed previously.

1.3 Option 1: Orient the Spacecraft Such that SCAXIS Aligns with the LOS to a Specified Celestial Body.

For Option 1, the LOS is determined by advancing the estimated ORB state vector to the current time. Once the coincidence to SCAXIS and LOS has been established, R61 establishes a spacecraft angular rate to maintain the coincidence. R61 quantities provided to the RCS DAP under tracking-option 1 are as described for Option 0 with the following exceptions:

$\underline{u}_{LOS}$ = line of sight direction, including aberration correction

and,

if the target is a star or planet,

$\underline{\omega}_{LOS} = \underline{\omega}_{correction}$;

if the target is the center of the earth,

$$\underline{\omega}_{LOS} = [REFSMMAT] \left\{ \frac{UNIT\ (\underline{r}_C) \times (\underline{v}_C)}{|\underline{r}_C|} \right\} + \underline{\omega}_{correction}$$

1.4 Option 2: Rotate the Spacecraft About SCAXIS

Option 2 is effected by a special routine known as the Automatic Rotation Routine (R67). SCAXIS is as defined in Option 0. R67 initializes COF, BRATE, [DEL], [MIS], and ADB in KALCMANU and then executes the KALCMANU coding to issue the following quantities to the RCS DAP:

1) $\underline{\omega}_{CA}$ .... desired rotation rate

2) IGA_D, MGA_D, OGA_D, ... DAP reference angles, i.e., center of deadband.

3) $\underline{\Delta}GA$ .... a vector defining the desired incremental changes in the IMU gimbal every 0.1 seconds.

These calculations are repeated once per second.

1.5 Option 4: Orient the Spacecraft as in Option 0, but Further Specify an Angle (OMICRON) of Rotation About SCAXIS

SCAXIS is as defined in Option 0; OMICRON is the positive-sense angle between planes A and B - where plane A is defined by the negative orbital angular momentum vector (-H) and the LOS, and plane B is defined by the spacecraft +Y-axis and the LOS.

Alignment of the LOS with either the spacecraft Y axis or the momentum vector is proscribed since the necessary two-plane condition for specifying OMICRON would not exist.

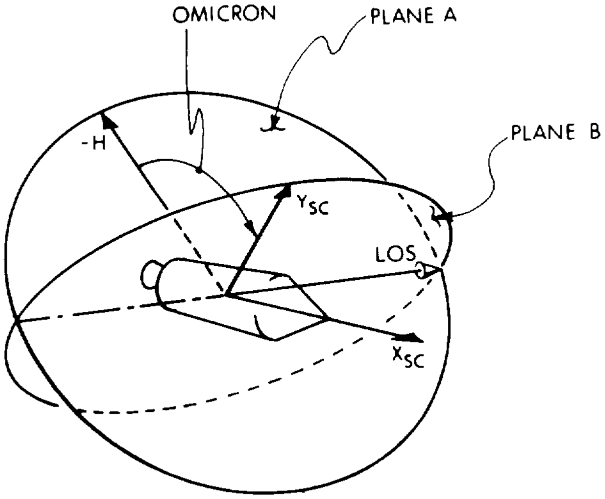

For Option 4, R61 provides the following quantities to the RCS DAP:

1) $\underline{\omega}_{CA}$ .... desired LOS rate in control-axis coordinates

2) IGA_D, MGA_D, OGA_D, ... DAP reference angles, i.e., center of the deadband.

3) $\Delta\underline{G}A$ .... a vector defining the desired incremental changes in the IMU gimbal angles every 0.1 second.

The desired LOS rate $\left(\underline{\omega}_{CA}\right)$ in control-axis coordinates is obtained as follows:

$$\underline{u}_{LOS} = \underline{r}_W - \underline{r}_C$$

$$\underline{\omega}_{LOS} = [REFSMMAT] \left\{ \frac{UNIT\ (\underline{u}_{LOS}) \times (\underline{v}_W - \underline{v}_C)}{|\underline{u}_{LOS}|} \right\}$$

$$\underline{\omega}_{CA} = [NBCA]\ [SMNB]\ \omega_{LOS},$$

Where $\underline{\omega}_{LOS}$ is the LOS rate in stable member cooridnates; $\underline{r}_W$, $\underline{v}_W$, $\underline{r}_C$, and $\underline{v}_C$ are the position and velocity vectors of the TV and ORB in basic reference coordinates.

The vector $(\Delta\underline{G}A)$ is computed as follows:

$$\Delta\underline{G}A = \begin{bmatrix} \cos IGA \sec MGA & 0 & -\sin IGA \sec MGA \\ -\cos IGA \tan MGA & 1 & \sin IGA \tan MGA \\ \sin IGA & 0 & \cos IGA \end{bmatrix} (0.1)\ \underline{\omega}_{LOS}$$

$$+\ \underline{\omega}_{correction},$$

where

$$\underline{\omega}_{correction} = \begin{bmatrix} \theta_{DX} - OGA_D \\ \theta_{DY} - IGA_D \\ \theta_{DZ} - MGA_D \end{bmatrix} \frac{0.1}{\Delta t_C}$$

θ_{DX}, θ_{DY}, θ_{DZ} desired gimbal angles :s

Δt_C = conservative estimate of R61 computation interval

The desired gimbal angles θ_{DX}, θ_{DY}, θ_{DZ} are computed as follows: First, four unit vectors are computed:

$$\underline{s}_A = \cos\ (OMICRON)\ unit\ (\underline{u}_{LOS} \times [\underline{v}_C \times \underline{r}_C])$$

$$+ \sin\ (OMICRON)\ unit \left[\underline{u}_{LOS} \times \left(\underline{u}_{LOS} \times (\underline{v}_C \times \underline{r}_C)\right)\right]$$

$$\underline{s}'_A = unit\ (\underline{SCAXIS} \times \underline{v}_{SC})$$

$$\underline{s}_B = \underline{u}_{LOS}$$

$$\underline{s}'_B = \underline{\text{SCAXIS}}$$

Given these unit vectors, the unit vectors $\underline{x}$, $\underline{y}$, and $\underline{z}$ are calculated defining the desired directions of the x, y, and z axes of the navigation base with respect to the Basic Reference Coordinate System. The unit vectors $\underline{x}$, $\underline{y}$, and $\underline{z}$ and the vectors $\underline{x}_{SM}$, $\underline{y}_{SM}$, $\underline{z}_{SM}$ from the matrix REFSMMAT are then used to compute the desired gimbal angles θ_{DX}, θ_{DY}, θ_{DZ}.

1.6 Option 5: Orient the Spacecraft as in Option 1, but Further Specify an Angle (OMICRON) of Rotation About SCAXIS.

SCAXIS is as defined in Option 0;

OMICRON is as defined in Option 4.

For Option 5, R6 quantities provided to the RCS DAP are as in Option 4, except as follows:

$\underline{u}_{LOS}$ = line of sight direction including aberration correction

and,

if the target is a star or planet

$\underline{\omega}_{LOS} = 0;$

if the target is the center of the earth,

$$\underline{\omega}_{LOS} = [\text{REFSMMAT}] \left\{ \frac{\text{UNIT } (\underline{r}_C) \times (\underline{v}_C)}{|r_C|} \right\}$$

SECTION 2

ON-ORBIT ATTITUDE MANEUVER ROUTINE

2.1 Introduction

The purpose of the attitude maneuver routine (ATTITUDE_MANEUVER) is to automatically reorient the spacecraft during coasting flight. ATTITUDE_MANEUVER is an adaptation of the R60 routine from the Apollo(5) flight programs to the Space Shuttle with the assumption that a 3-gimbal IMU is used. This implementation is coded in HAL and described in accordance with preliminary structured programming techniques. The general scope of variables and structure of ATTITUDE_MANEUVER is illustrated in Fig. 2-1. Each of the modules and variables used in the routine are defined in Tables 2-1 and 2-2 respectively (Subsection 2.7).

The desired attitude to which the spacecraft is to be aligned can be specified in one of two ways:

1) By a set of terminal desired gimbal angles, $\left[\theta_c\right]$.
2) By two unit vectors, $\underline{u}_{DSM}$ and $\underline{u}_{ANB}$.

where $\left[\theta_c\right]$ is the set of desired (or commanded) gimbal angles defined by

$$\left[\theta_c\right] = \begin{bmatrix} \theta_{c_o} \\ \theta_{c_i} \\ \theta_{c_m} \end{bmatrix} = \begin{bmatrix} \text{desired outer gimbal angle} \\ \text{desired inner gimbal angle} \\ \text{desired middle gimbal angle} \end{bmatrix}$$

$\underline{u}_{ANB}$ is a body-fixed axis vector, $\underline{u}_A$, with components in navigation-base-coordinates, $\underline{u}_{DSM}$ is a desired direction vector, $\underline{u}_D$, with components in stable-member coordinates and $\underline{u}_{DSM}$ specifies the direction in inertial space to which $\underline{u}_{ANB}$ is to be aligned. A flag switch, FLAG_3AXIS is provided to specify which of the two types of inputs is to be used.

If the vector type of input is chosen, the routine known as VECPOINT is used to compute a set of desired terminal gimbal angles, $\left[\theta_c\right]$, based on the values of $\underline{u}_{DSM}$, and $\underline{u}_{ANB}$, and the current gimbal angles, $\left[\theta\right]$. Regardless of the type of

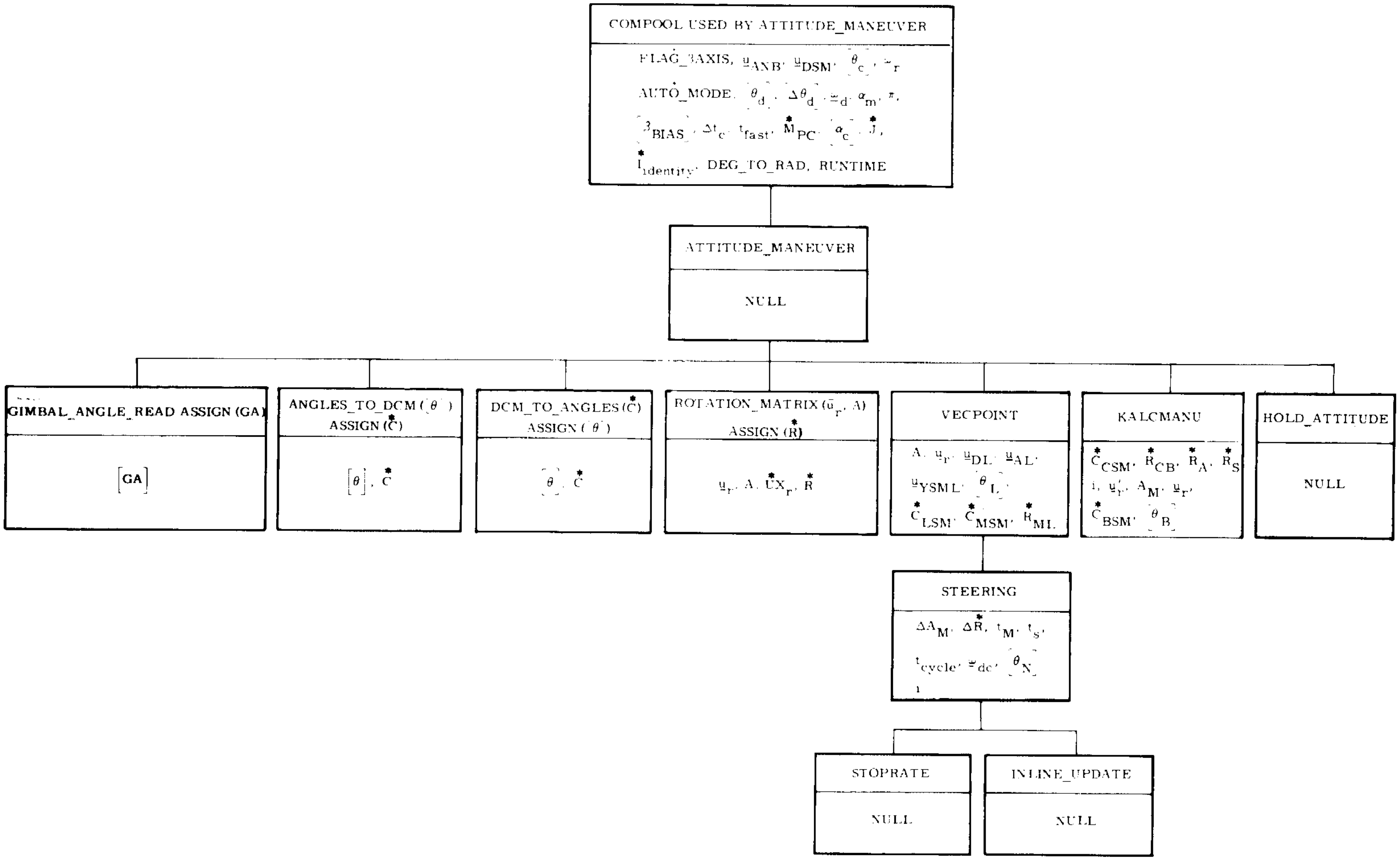
COMPOOL USED BY ATTITUDE_MANEUVER
FLAG_3AXIS, $\underline{u}_{ANB}$, $\underline{u}_{DSM}$, $[\theta_c]$, $\underline{\omega}_r$
AUTO_MODE, $[\theta_d]$, $[\Delta\theta_d]$, $\underline{\omega}_d$, α_m, π,
$[\beta_{BIAS}]$, Δt_c, t_{fast}, $\overset{*}{M}_{PC}$, $[\alpha_c]$, $\overset{*}{J}$,
$\overset{*}{I}_{identity}$, DEG_TO_RAD, RUNTIME
ATTITUDE_MANEUVER
NULL
GIMBAL_ANGLE_READ ASSIGN (GA)
[GA]
ANGLES_TO_DCM (θ) ASSIGN ($\overset{*}{C}$)
$[\theta]$, $\overset{*}{C}$
DCM_TO_ANGLES($\overset{*}{C}$) ASSIGN (θ)
$[\theta]$, $\overset{*}{C}$
ROTATION_MATRIX ($\underline{u}_r$, A) ASSIGN ($\overset{*}{R}$)
$\underline{u}_r$, A, $\overset{*}{UX}_r$, $\overset{*}{R}$
VECPOINT
A, $\underline{u}_r$, $\underline{u}_{DL}$, $\underline{u}_{AL}$,
$\underline{u}_{YSML}$, $[\theta_L]$,
$\overset{*}{C}_{LSM}$, $\overset{*}{C}_{MSM}$, $\overset{*}{R}_{ML}$
KALCMANU
$\overset{*}{C}_{CSM}$, $\overset{*}{R}_{CB}$, $\overset{*}{R}_A$, $\overset{*}{R}_S$
i, $\underline{u}'_r$, A_M, $\underline{u}_r$,
$\overset{*}{C}_{BSM}$, $[\theta_B]$
HOLD_ATTITUDE
NULL
STEERING
ΔA_M, $\Delta\overset{*}{R}$, t_M, t_s,
t_{cycle}, $\underline{\omega}_{dc}$, $[\theta_N]$
i
STOPRATE
NULL
INLINE_UPDATE
NULL

Fig. 2-1 ATTITUDE_MANEUVER Structure

input, KALCMANU is called if the automatic option is selected. Otherwise control returns to the executive system. KALCMANU computes a set of parameters ($\underline{u}_r$, A) that determine how the reorientation is to be performed. The maneuver is performed by rotating the spacecraft about the axis of single equivalent rotation, $\underline{u}_r$, by the angle A_M. The vector $\underline{u}_r$ and the angle A_M are completely determined by the initial orientation, $[\theta]$, and the desired terminal orientation, $[\theta_c]$. Once $\underline{u}_r$ and A_M are computed, KALCMANU calls the procedure STEERING.

The procedure, STEERING, cycles every Δt_c seconds and computes, on each pass, five sets of quantities to be used by the digital autopilot in following the angular path defined by $\underline{u}_r$, A. The first of these quantities is a set of autopilot reference angles, $[\theta_d]$(or intermediate desired CDU angles), which is updated regularly during the maneuver. To achieve a smoother sequence of commands between successive updates, the program generates a set of incremental CDU angles, $[\Delta\theta_d]$,to be added to $[\theta_d]$ by the digital autopilot. The steering routine also computes the component maneuver rates, $\underline{\omega}_d$ (in spacecraft coordinates), a set of bias accelerations, $\underline{\alpha}_m$, and a set of bias angles,$[\beta_{BIAS}]$. The bias angles,$[\beta_{BIAS}]$, are to be used by the autopilot to prevent fuel-consuming overshoot when starting and stopping an automatic maneuver.

The preceding method allows the autopilot to establish and maintain a spacecraft rotation about the vector $\underline{u}_r$ at a fixed rotation rate $\underline{\omega}_d$. The maneuvers are timed in open-loop fashion so that after a predetermined interval $[\Delta\theta_d]$, $\underline{\omega}_d$, $\underline{\alpha}_m$ and $[\beta_{BIAS}]$are set to zero and the autopilot reference angles, $[\theta_d]$, are set equal to the terminal angles, $[\theta_c]$. Thus, upon completion of the maneuver, the spacecraft will finish up in a limit cycle about $[\theta_c]$.

2.2 ATTITUDE_MANEUVER

A logic flow diagram of ATTITUDE_MANEUVER is illustrated in Fig. 2-2. If the vector option is selected by the calling program, the routine VECPOINT is used to compute the terminal desired gimbal angles $[\theta_c]$from $\underline{u}_{ANB}$ and $\underline{u}_{DSM}$. If the automatic maneuver is to proceed the automatic mode switch, AUTO_MODE, must be set "ON". If it is "ON", KALCMANU is called to calculate the rotation vector, $\underline{u}_r$, and the angle of rotation, A_M, and to initiate the cycling of STEERING.

2.3 VECPOINT

The desired gimbal angles, $[\theta_c]$, computed by VECPOINT are determined on the basis of minimizing the rotation angle required to align $\underline{u}_{ANB}$ with $\underline{u}_{DSM}$. In general, this procedure will reduce the fuel required for the maneuver by not constraining the orientation of the spacecraft about the pointing axis, defined by

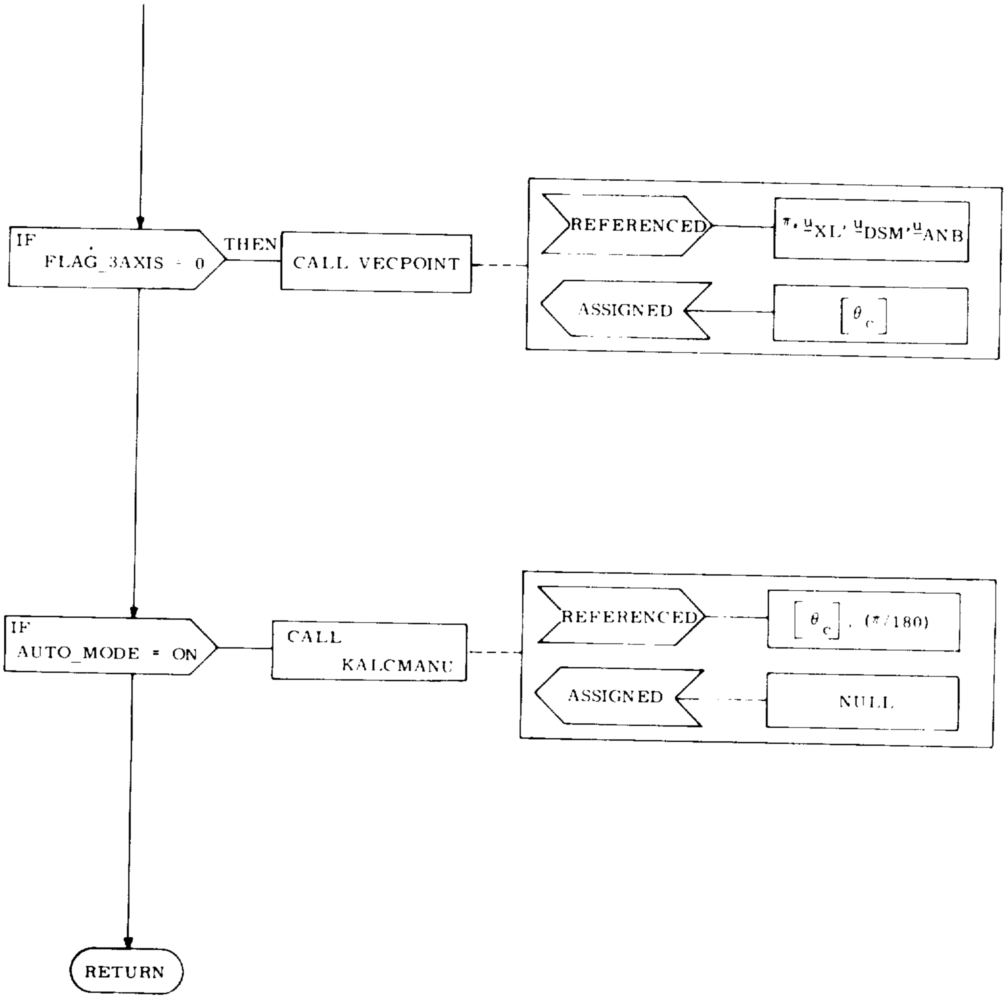

Fig. 2-2 ATTITUDE_MANEUVER : Program

$\underline{u}_{DSM}$. Additionally, the attitude about $\underline{u}_{DSM}$ will be left unchanged. Consequently, the crew may specify the attitude about the pointing axis to satisfy additional communication, visibility, or thermal constraints, if desired. This is done by manually reorienting the spacecraft about the pointing axis either prior to or after the maneuver. If this procedure is done after the automatic maneuver, a final trim will usually be required to assure that $\underline{u}_{ANB}$ is aligned with $\underline{u}_{DSM}$.

To compute the desired gimbal angles, $[\theta_c]$, from $\underline{u}_{DSM}$, $\underline{u}_{ANB}$, and the current gimbal angles, $[\theta]$, several service routines are required. These routines are described below.

2.3.1 ANGLES_TO_DCM

This procedure converts three gimbal angles, $[\theta]$, to a direction-cosine matrix, $\overset{*}{C}$, that relates the corresponding spacecraft navigation-base orientation to the stable-member frame. The formulas for this conversion are:

$$\overset{*}{C} = \begin{bmatrix} C_{1,1} & C_{1,2} & C_{1,3} \\ C_{2,1} & C_{2,2} & C_{2,3} \\ C_{3,1} & C_{3,2} & C_{3,3} \end{bmatrix}$$

$$\begin{array}{lcl}
C_{1,1} & = & \cos\theta_i \cos\theta_m \\
C_{1,2} & = & -\cos\theta_i \sin\theta_m \cos\theta_o + \sin\theta_i \sin\theta_o \\
C_{1,3} & = & \cos\theta_i \sin\theta_m \sin\theta_o + \sin\theta_i \cos\theta_o \\
C_{2,1} & = & \sin\theta_m \\
C2, 2 & = & \cos\theta_m \cos\theta_o \\
C_{2,3} & = & -\cos\theta_m \sin\theta_o \\
C_{3,1} & = & -\sin\theta_i \cos\theta_m \\
C_{3,2} & = & \sin\theta_i \sin\theta_m \cos\theta_o + \cos\theta_i \sin\theta_o \\
C_{3,3} & = & -\sin\theta_i \sin\theta_m \sin\theta_o + \cos\theta_i \cos\theta_o
\end{array}$$

where

$$\theta_o = \text{outer gimbal angle}$$

$$\theta_i = \text{inner gimbal angle}$$

$$\theta_m = \text{middle gimbal angle}$$

Also see Fig. 2-3 for the logic flow diagram of ANGLES_TO_DCM.

The interpretation of this matrix is as follows: If a_x, a_y, a_z represent the components of a vector in navigation-base axes, then the components of the same vector in stable-member axes (b_x, b_y, b_z) are

$$\begin{Bmatrix} b_x \\ b_y \\ b_y \end{Bmatrix} = \overset{*}{C}(\theta) \begin{Bmatrix} a_x \\ a_y \\ a_z \end{Bmatrix}$$

2.3.2 DCM_TO_CDU ANGLES

This procedure extracts the CDU angles from a direction-cosine matrix, $\overset{*}{C}$, that relates the navigation-base coordinates to the stable-member coordinates. The formulas for this conversion are

$$\theta_m = \arcsin C_{2,1}$$

$$\theta_i = \arcsin (-C_{3,1}/\cos \theta_m)$$

$$\left[\text{If } C_{1,1} \text{ is negative, } \theta_i \text{ is replaced by } \pi \text{ SGN}(\theta_i) - \theta_i\right]$$

$$\theta_o = \arcsin (-C_{2,3}/\cos \theta_m)$$

$$\left[\text{If } C_{2,2} \text{ is negative, } \theta_o \text{ is replaced by } \pi \text{ SGN}(\theta_o) - \theta_o\right]$$

The logic flow diagram is illustrated in Fig. 2-4.

2.3.3 ROTATION_MATRIX

This procedure computes the direction-cosine matrix, $\overset{*}{R}$, that relates one coordinate frame to another that is rotated with respect to the first by an angle A about a unit vector $\underline{u}_r$. The formula for this matrix is

$$\overset{*}{R}(\underline{u}_r, A) = \overset{*}{I} \cos A + \underline{u}_r \underline{u}_r^T (1 - \cos A) + \overset{*}{UX}_r \sin A$$

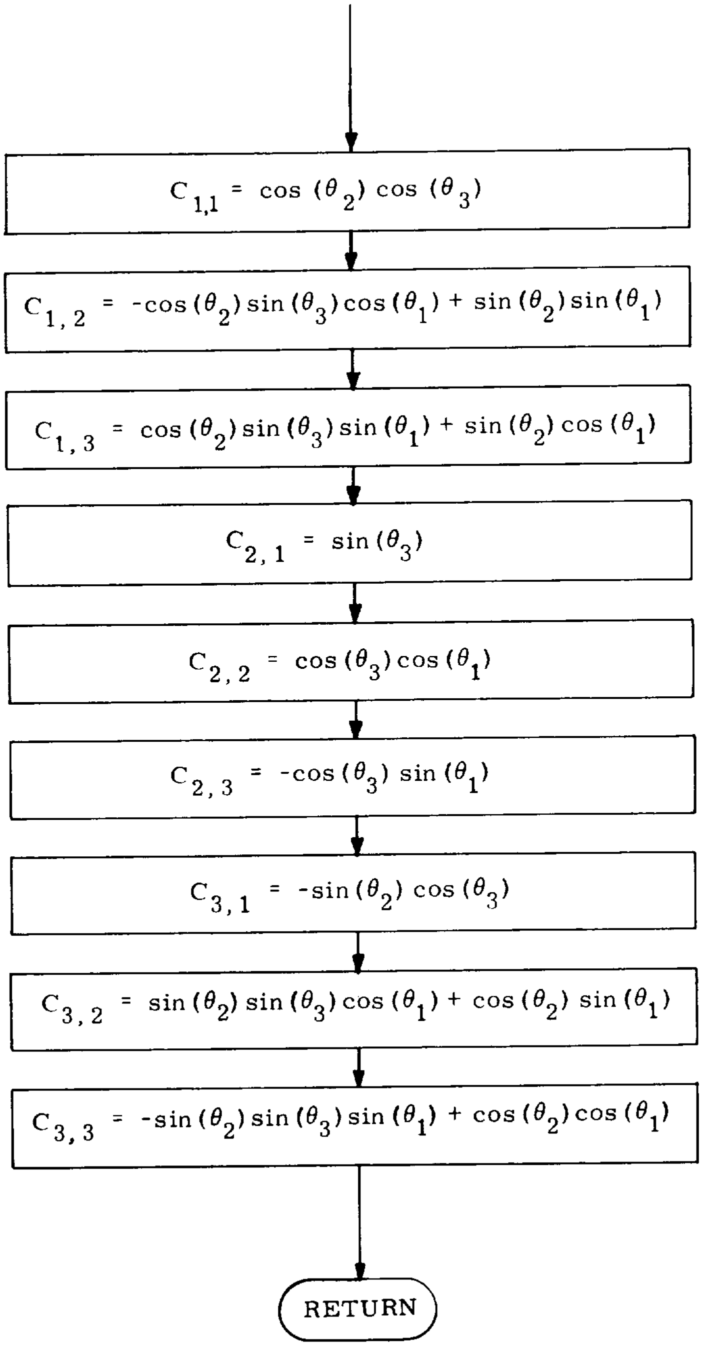
$C_{1,1} = \cos(\theta_2)\cos(\theta_3)$
$C_{1,2} = -\cos(\theta_2)\sin(\theta_3)\cos(\theta_1) + \sin(\theta_2)\sin(\theta_1)$
$C_{1,3} = \cos(\theta_2)\sin(\theta_3)\sin(\theta_1) + \sin(\theta_2)\cos(\theta_1)$
$C_{2,1} = \sin(\theta_3)$
$C_{2,2} = \cos(\theta_3)\cos(\theta_1)$
$C_{2,3} = -\cos(\theta_3)\sin(\theta_1)$
$C_{3,1} = -\sin(\theta_2)\cos(\theta_3)$
$C_{3,2} = \sin(\theta_2)\sin(\theta_3)\cos(\theta_1) + \cos(\theta_2)\sin(\theta_1)$
$C_{3,3} = -\sin(\theta_2)\sin(\theta_3)\sin(\theta_1) + \cos(\theta_2)\cos(\theta_1)$
RETURN

Fig. 2-3 ANGLES_TO_DCM : Procedure ($[\theta]$) Assign ($\overset{*}{C}$)

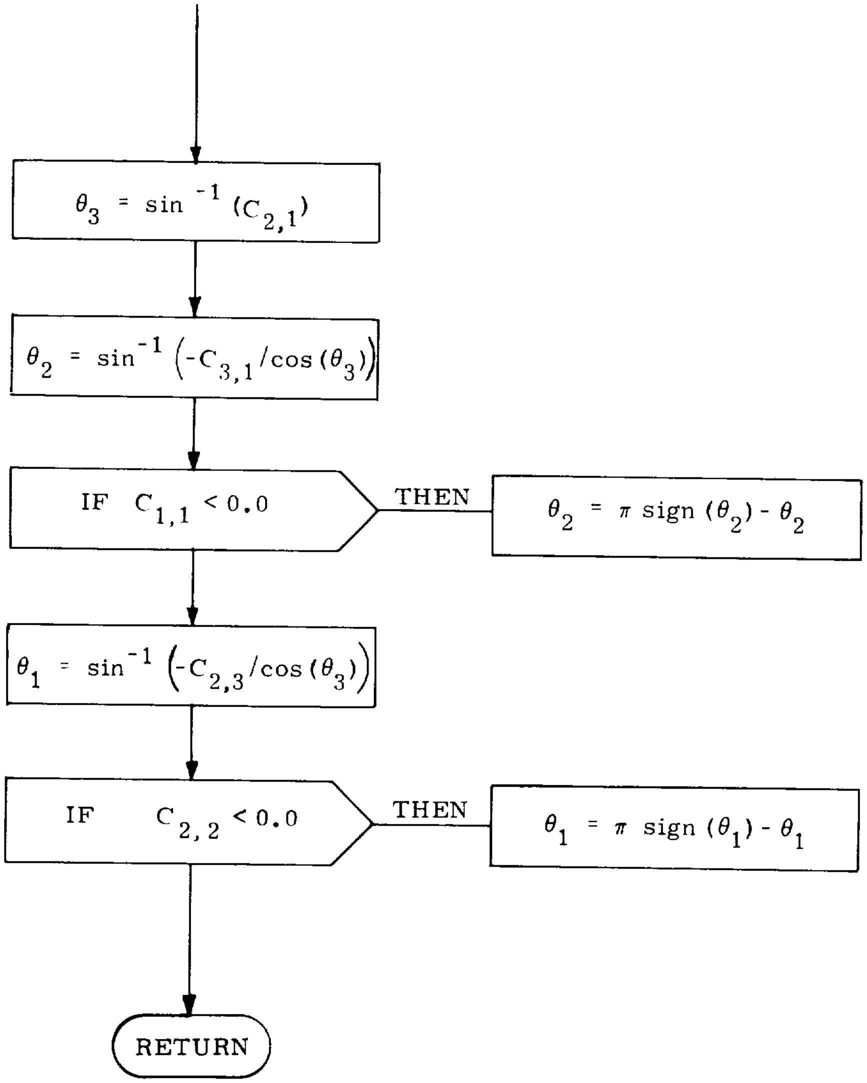
$\theta_3 = \sin^{-1}(C_{2,1})$
$\theta_2 = \sin^{-1}\left(-C_{3,1}/\cos(\theta_3)\right)$
IF $C_{1,1} < 0.0$
THEN
$\theta_2 = \pi \operatorname{sign}(\theta_2) - \theta_2$
$\theta_1 = \sin^{-1}\left(-C_{2,3}/\cos(\theta_3)\right)$
IF $C_{2,2} < 0.0$
THEN
$\theta_1 = \pi \operatorname{sign}(\theta_1) - \theta_1$
RETURN

Fig. 2-4 DCM_TO_ANGLES : Procedure ($\overset{*}{C}$) Assign ($[\theta]$)

where

$$\overset{*}{I} = \begin{bmatrix} 1 & 0 & 0 \\ 0 & 1 & 0 \\ 0 & 0 & 1 \end{bmatrix}$$

$$\underline{u}_r \underline{u}_r^T = \begin{bmatrix} u_{rx}^2 & u_{rx} u_{ry} & u_{rx} u_{rz} \\ u_{ry} u_{rx} & u_{ry}^2 & u_{ry} u_{rz} \\ u_{rz} u_{rx} & u_{rz} u_{ry} & u_{rz}^2 \end{bmatrix}$$

$$\overset{*}{UX}_r = \begin{bmatrix} 0 & -u_{rx} & u_{ry} \\ u_{rz} & 0 & -u_{rx} \\ -u_{ry} & u_{rx} & 0 \end{bmatrix}$$

$\underline{u}_r$ = unit rotation vector resolved into spacecraft axes

A = rotation angle

The logic flow diagram is illustrated in Fig. 2-5.

The interpretation of $\overset{*}{R}$ is as follows: If a_x, a_y, a_z represent the components of a vector in the rotated frame, then the components of the same vector in the original frame (b_x, b_y, b_z) are

$$\begin{Bmatrix} b_x \\ b_y \\ b_z \end{Bmatrix} = \overset{*}{R} (\underline{u}_r, A) \begin{Bmatrix} a_x \\ a_y \\ a_z \end{Bmatrix}$$

The process used by VECPOINT in determining the terminal desired angles, $[\theta_c]$, is illustrated schematically in Fig. 2-6 and in logic flow form in Fig. 2-7. VECPOINT uses two frames of reference: the L frame and the M frame - as well as the stable-member (SM) frame. The L frame is simply a base frame used as the starting point for subsequent rotations. In VECPOINT computations, the L frame is the initial navigation-base frame computed from the initial gimbal angles, $[\theta]$. The vector $\underline{u}_D$ is resolved from the stable-member frame into this frame as $\underline{u}_{DL}$ using the transformation $\overset{*}{C}{}^T_{LSM}$. The L frame is then rotated so that $\underline{u}_{AL}$ and $\underline{u}_{DL}$ are coincident. The rotation vector, $\underline{u}_r$, is defined by the cross product

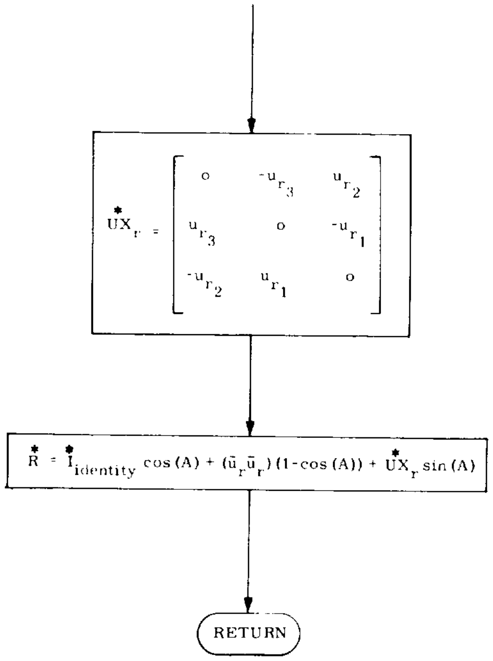

$\overset{*}{UX}_r = \begin{bmatrix} o & -u_{r_3} & u_{r_2} \\ u_{r_3} & o & -u_{r_1} \\ -u_{r_2} & u_{r_1} & o \end{bmatrix}$
$\overset{*}{R} = \overset{*}{I}_{identity} \cos(A) + (\bar{u}_r \bar{u}_r)(1-\cos(A)) + \overset{*}{UX}_r \sin(A)$
RETURN

Fig. 2-5 ROTATION_MATRIX:
Procedure ($\underline{u}_r$,A) Assign ($\overset{*}{R}$)

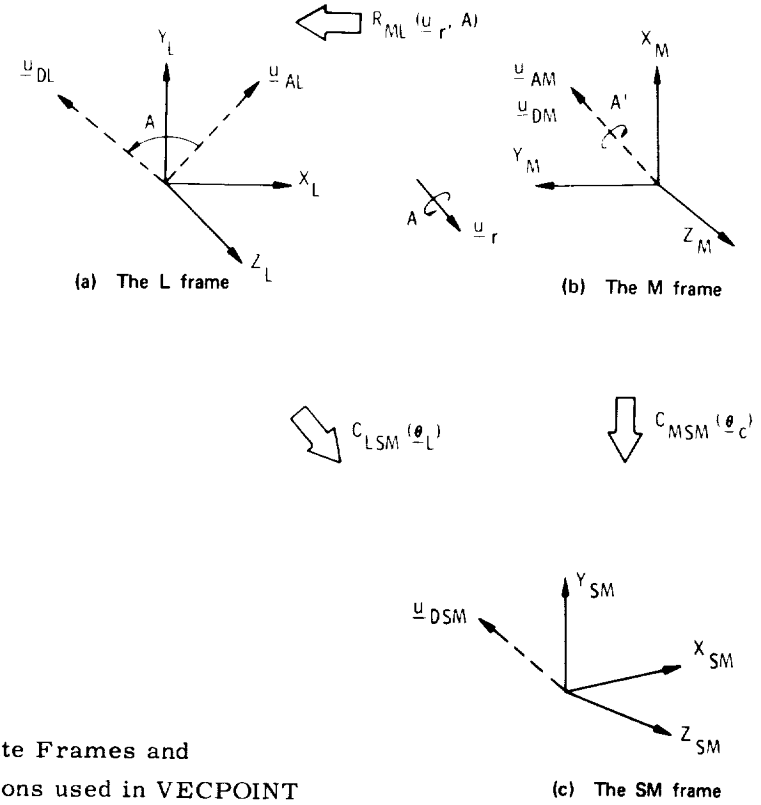

Fig. 2-6 The Coordinate Frames and
Transformations used in VECPOINT

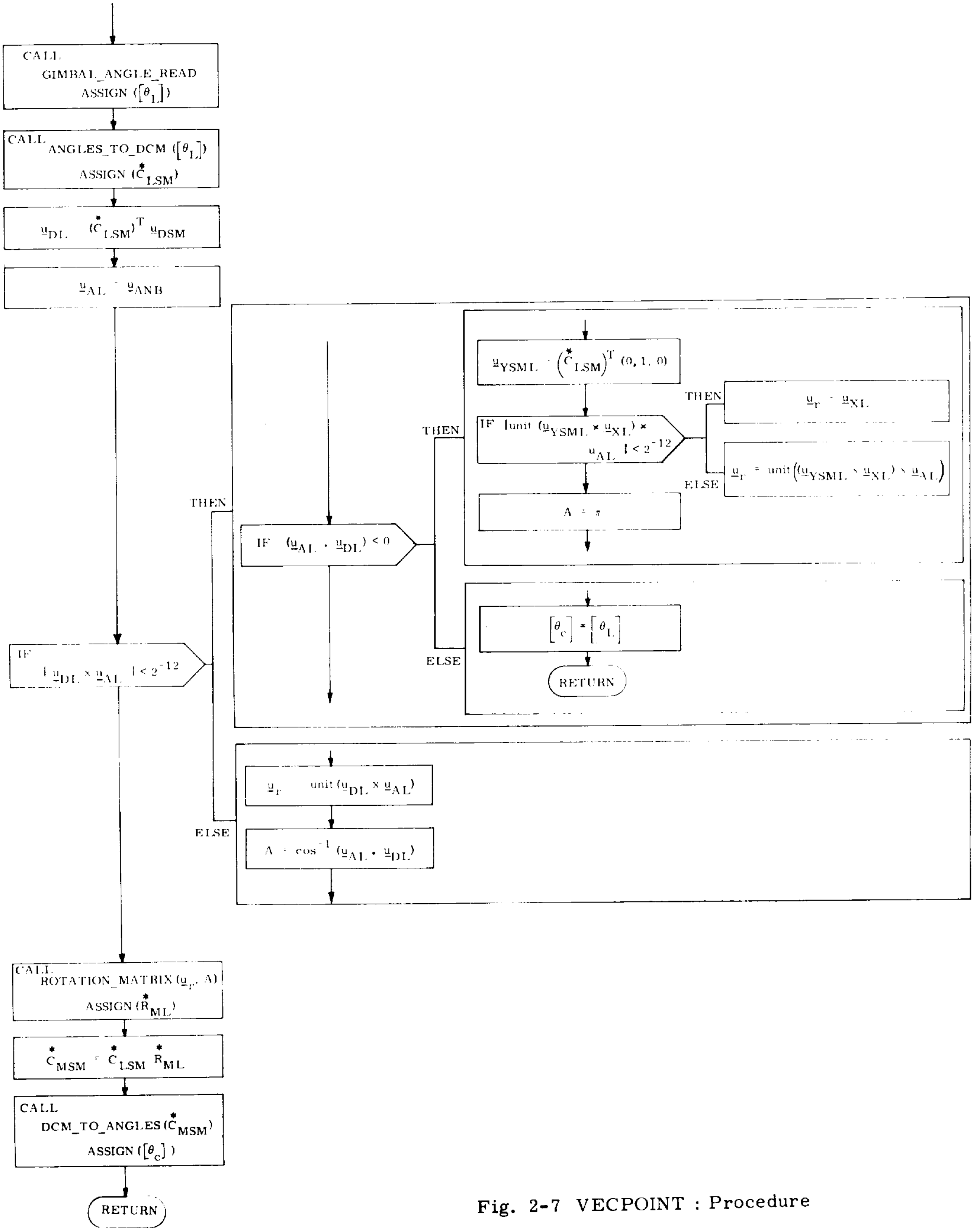
CALL
GIMBAL_ANGLE_READ
ASSIGN ($[\theta_L]$)
CALL ANGLES_TO_DCM ($[\theta_L]$)
ASSIGN ($\overset{*}{C}_{LSM}$)
$\underline{u}_{DL} = (\overset{*}{C}_{LSM})^T \underline{u}_{DSM}$
$\underline{u}_{AL} = \underline{u}_{ANB}$
IF
$|\underline{u}_{DL} \times \underline{u}_{AL}| < 2^{-12}$
THEN
IF $(\underline{u}_{AL} \cdot \underline{u}_{DL}) < 0$
THEN
$\underline{u}_{YSML} = (\overset{*}{C}_{LSM})^T (0, 1, 0)$
IF $|\text{unit}(\underline{u}_{YSML} \times \underline{u}_{XL}) \times \underline{u}_{AL}| < 2^{-12}$
THEN
$\underline{u}_r = \underline{u}_{XL}$
ELSE
$\underline{u}_r = \text{unit}((\underline{u}_{YSML} \times \underline{u}_{XL}) \times \underline{u}_{AL})$
$A = \pi$
ELSE
$[\theta_c] = [\theta_L]$
RETURN
ELSE
$\underline{u}_r = \text{unit}(\underline{u}_{DL} \times \underline{u}_{AL})$
$A = \cos^{-1}(\underline{u}_{AL} \cdot \underline{u}_{DL})$
CALL
ROTATION_MATRIX ($\underline{u}_r$, A)
ASSIGN ($\overset{*}{R}_{ML}$)
$\overset{*}{C}_{MSM} = \overset{*}{C}_{LSM} \overset{*}{R}_{ML}$
CALL
DCM_TO_ANGLES ($\overset{*}{C}_{MSM}$)
ASSIGN ($[\theta_c]$)
RETURN

Fig. 2-7 VECPOINT : Procedure

between $\underline{u}_{AL}$ and $\underline{u}_{DL}$. Rotation about the cross-product vector will assure that spacecraft maneuvering will be minimized and that the rotation vector will have no component in the $\underline{u}_{AL}$ or $\underline{u}_{DL}$ direction.

If the two vectors, $\underline{u}_{AL}$ and $\underline{u}_{DL}$, are either parallel or antiparallel, a special computation of $\underline{u}_r$ is performed. When $\underline{u}_{AL}$ and $\underline{u}_{DL}$ are almost parallel then $[\theta_c]$ is set equal to $[\theta_L]$. If the two vectors are almost antiparallel, then a 180° rotation is required for alignment. In this case, the rotation vector is chosen so that $\underline{u}_r$ is perpendicular to $\underline{u}_{AL}$ and lies in the plane that contains $\underline{u}_{YSM(L)}$ and $\underline{u}_{XL}$. If, however, $\underline{u}_{AL}$ happens to be perpendicular to the plane, then any vector in the plane may be used for $\underline{u}_r$. In this event the x-axis is chosen. From $\underline{u}_r$ and A the rotation matrix, $\overset{*}{R}_{ML}$, between the M- and L- frames is computed. Multiplying $\overset{*}{R}_{ML}$ by $\overset{*}{C}_{LSM}$ determines the direction - cosine matrix $\overset{*}{C}_{MSM}$ from which the terminal desired gimbal angles, $[\theta_C]$, are extracted.

2.4 KALCMANU Maneuver-Parameters Calculation

The procedure KALCMANU is designed to generate commands for the autopilot to reorient the spacecraft from an initial attitude to some desired attitude specified by $[\theta_c]$. Although a number of authors have discussed optimal solutions to this problem, the task is a formidable one because of the nonlinear nature of rigid-body dynamics and the kinematics of rotational motion. Optimal solutions for a particular class of spacecraft configurations are treated in Reference 1. In this reference, the criterion for optimality is based upon the product of maneuver duration and fuel expenditure. Using the same criterion, previous design studies based upon a number of suboptimal approaches$^{(2)}$ have shown that a reasonable design compromise is to rotate the spacecraft about a single inertially fixed axis. This technique is employed in KALCMANU.

The process used by KALCMANU in computing the rotation axis, $\underline{u}_r$, and the rotation angle, A_M, is illustrated in Fig. 2-8. From the current gimbal angles KALCMANU computes the transformation matrix between the initial spacecraft axes and the stable-member axes, $\overset{*}{C}_{BSM}$. This procedure also computes the matrix relating the desired terminal spacecraft attitude and the stable-member axes, $\overset{*}{C}_{CSM}$. The transformation between the desired and the initial attitude is $\overset{*}{R}_{CB}$, where where

$$\overset{*}{R}_{CB} = \overset{*}{C}{}_{BSM}^{T} \overset{*}{C}_{CSM}$$

$\overset{*}{R}_{CB}$ can be partitioned into its symmetric and antisymmetric components as follows. For the symmetric part,

$$\overset{*}{R}_S = \frac{1}{2} (\overset{*}{R}_{CB} + \overset{*}{R}{}_{CB}^{T})$$

By comparing this with the equations described in ROTATION_MATRIX it can be seen that

$$\overset{*}{R}_S = \overset{*}{I} \cos A_M + \underline{u}_r \underline{u}_r^T (1-\cos A_M)$$

For the antisymmetric part,

$$\overset{*}{R}_A = (\tfrac{1}{2})(\overset{*}{R}_{CB} - \overset{*}{R}_{CB}^T)$$

or

$$\overset{*}{R}_A = \begin{bmatrix} 0 & -u_{rz} & u_{ry} \\ u_{rz} & 0 & -u_{rx} \\ -u_{ry} & u_{rx} & 0 \end{bmatrix} \sin A_M$$

The maneuver angle can easily be obtained from $\overset{*}{R}_{CB}$ as

$$A_M = \cos^{-1}\left(\frac{\text{Trace}(\overset{*}{R}_{CB}) - 1}{2}\right)$$

The rotation vector, $\underline{u}_r$, is normally extracted from the antisymmetric part of $\overset{*}{R}_{CB}$; that is,

$$\underline{u}_r = \text{unit}\,(-R_{A_{3,3}}, R_{A_{1,3}}, -R_{A_{1,2}})$$

As sin A_M approaches zero, however, the unit operation becomes indeterminate and an alternative calculation must be performed. If the maneuver angle is less than 0.25 deg, then no complicated automatic maneuvering is necessary and therefore one can simply set the autopilot reference angle, $[\theta_d]$, equal to the terminal desired angles $[\theta_c]$ and exit. This is done by calling HOLD_ATTITUDE. If $A_M > 170$ deg, a method employing the symmetric part of $\overset{*}{R}_{CB}$ is used to determine $\underline{u}_r$, as illustrated in Fig. 2-8. The magnitudes of the components of $\underline{u}_r$ are easily determined as

$$|u_{rx}| = \sqrt{\frac{R_{S1,1} - \cos A_M}{1 - \cos A_M}}$$

$$|u_{ry}| = \sqrt{\frac{R_{S2,2} - \cos A_M}{1 - \cos A_M}}$$

$$|u_{rz}| = \sqrt{\frac{R_{S3,3} - \cos A_M}{1 - \cos A_M}}$$

To obtain the signs of each component, it is first necessary to determine the sign of the largest component by referring to the values of $\overset{*}{R}_A$. This is done to avoid the problem caused by truncation as sin A_M approaches zero. If A_M is equal to 180 deg, then the sign of the largest component may be arbitrarily chosen. The signs of the remaining components may be determined by examining the off-diagonal terms in $\overset{*}{R}_S$.

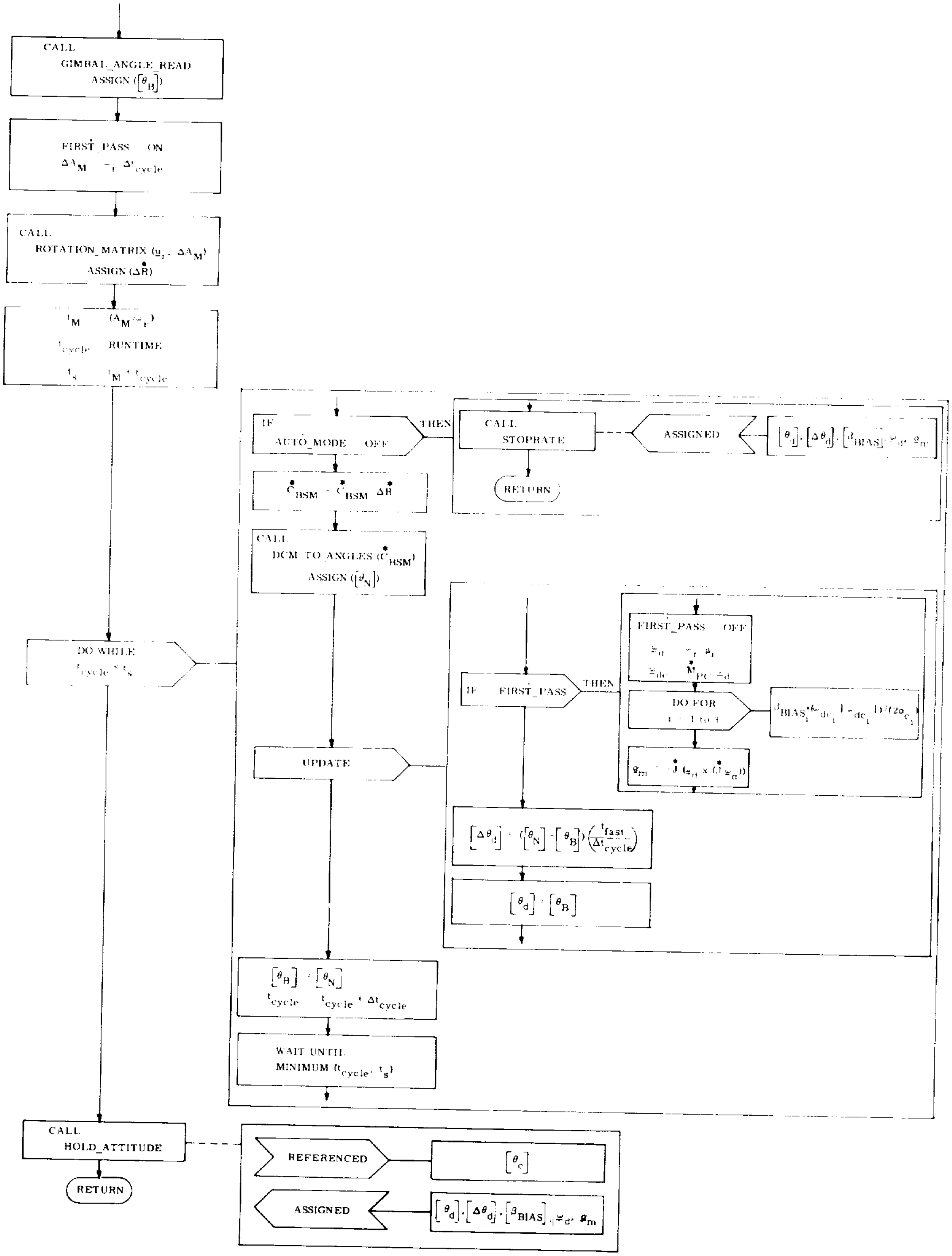

Fig. 2-8 KALCMANU : Procedure

2.5 Steering Through a Maneuver

The KALCMANU parameter calculations described in the preceding subsection solve the problem of what angular path to take in order to reorient the spacecraft without excessive fuel expenditure. However, the problem of how to steer the spacecraft along this path must now be considered. One solution is to iteratively solve for $\underline{u}_r$ and A_M explicitly as a function of the current spacecraft attitude and to control the spacecraft angular velocity, $\underline{\omega}$, by firing the RCS jets so that $\underline{\omega}$ is parallel to $\underline{u}_r$. This approach, however, leads to several problems. First of all, because of the deadband requirements of the autopilot, and control inaccuracies, explicit guidance can lead to excessive changes in control commands as the spacecraft approaches the terminal attitude. This problem of terminal guidance is characteristic of explicit guidance schemes unless special consideration is given to the terminal-control problem. Secondly, there is a timing problem since the computation of $\underline{u}_r$ and A_M is somewhat lengthy and would require an excessive amount of computer time. Instead, it is better to formulate the problem in terms of perturbations from a smooth reference trajectory that satisfies the end-point constraints. The method employed is to solve the global problem once via KALCMANU in order to establish a reference trajectory (defined by $\underline{u}_r$, A_M) and then have the autopilot solve the micro-problem of controlling the spacecraft deviations from this reference trajectory, using small-angle approximations. This approach not only avoids the terminal-guidance problem and the timing problem but also provides "tighter" path control for satisfying other boundary conditions that may be placed upon the selection of the reference trajectory.

In order to determine the required steering interface between KALCMANU and the autopilot, it is first necessary to define the nature of the autopilot control variables. To simplify the discussion, the problem of rotation about a single axis is considered first. There are two state variables of interest; namely, the attitude error, θ_e, defined by

$$\theta_e = \theta - \theta_d$$

where

θ = actual vehicle attitude

θ_d = desired vehicle attitude (constant)

and the angular velocity of the vehicle, ω. The "state" equations are

$$\dot{\theta}_e(t) = \omega(t)$$

and

$$\dot{\omega}(t) = f(\theta_e, \omega)$$

where f (θ_e, ω) is the control acceleration (applied by the jets) as determined by nonlinear phase-plane switching logic. The control law is defined so that θ_e and ω will be nulled to within the control-law deadbands so as to maintain attitude hold about the reference attitude, θ_d.

New state variables can be defined as follows:

$$\phi_e(t) = \theta(t) - \phi_d(t) + \beta_{BIAS}$$

and

$$\omega_e(t) = \omega(t) - \omega_d$$

where

$$\begin{aligned} \phi_d(t) &= \phi_d(t_o) + (\omega_d)(t - t_o) \\ \omega_d &= \text{a constant} \\ \beta_{BIAS} &= \text{a constant} \\ \phi_d(t_o) = \theta(t_o) &= \text{constant} \end{aligned}$$

The state equations for the new variables are

$$\begin{aligned} \phi_e &= \omega_e \\ \omega_e &= f(\phi_e, \omega_e) \end{aligned}$$

With these control variables, the autopilot will attempt to null the rate error, ω_e, thus forcing the spacecraft to rotate at a constant rate. Note that at the beginning of the maneuver the desired angle $\phi_d(t_o)$ is set equal to the initial angle $\theta(t_o)$. The constant, β_{BIAS}, is added to the attitude error to prevent overshoot when starting and stopping the maneuver, β_{BIAS} is computed as

$$\beta_{BIAS} = \frac{\omega_d \, |\omega_d|}{2 \, |\alpha_c|}$$

where

$$\alpha_c = \text{the control acceleration}$$

To interpret the effect of β_{BIAS}, refer to Fig. 2-9a. This figure shows a simplified phase-plane logic and a typical phase-point trajectory. The maneuver starts at point A with $\theta_e = 0$ and $\omega = 0$. With the application of steering commands, the phase-point instantaneously jumps to a biased condition at B where $\phi_e = \beta_{BIAS}$ and $\omega_e = -\omega_d$ (ω_d is negative for the case illustrated). The phase-point drifts to point C, where the control jets are turned on to reduce the rate error toward zero at point D. The trajectory then traverses a limit cycle DEFG until the maneuver finishes at point H, where the biases β_{BIAS} and ω_d are removed. At this point, the trajectory jumps to an unbiased condition at point I. Note that the actual rate is approximately equal to the desired rate and the phase-point drifts to point J, where the jets decelerate the vehicle back into a limit cycle around the desired attitude. The situation without angular bias, β_{BIAS}, is illustrated in Fig. 2-9b. Note the fuel-consuming overshoot in this case. The inclusion of the bias term is based on the assumption that the initial rates are small and that the desired rates are achievable during the maneuver. For the three-dimensional problem, it must also be assumed that β_{BIAS} is small enough so that the small-angle assumptions are not violated.

A bias acceleration, $\underline{\alpha}_m$, is also computed and sent to the autopilot to better approximate the switching curves in the phase-plane design. In the formulation of the phase-plane design a simplification is made to the equation of motion

$$\dot{\underline{\omega}}(t) = \overset{*}{J}^{-1} \underline{M} - \overset{*}{J}^{-1} (\underline{\omega} \times \overset{*}{J}\underline{\omega})$$

where

$\underline{M}$ = the torque supplied by the jets

$J^{-1}\underline{M}$ = $\underline{\alpha}_c$, the control acceleration

$-\overset{*}{J}^{-1} (\underline{\omega} \times \overset{*}{J}\underline{\omega})$ = $\underline{\alpha}_m$, the acceleration due to the non-diagonal moment of inertia $\overset{*}{J}$.

The bias acceleration, $\underline{\alpha}_m$, is assumed small and neglected to arrive at the state equations

$$\begin{bmatrix} \dot{\theta}(t) - \dot{\theta}_d(t) \\ \dot{\omega}(t) - \dot{\omega}_d(t) \end{bmatrix} = \begin{bmatrix} \theta_e \\ \omega_e \end{bmatrix} = \begin{bmatrix} 0 & 1 \\ 0 & 0 \end{bmatrix} \begin{bmatrix} \underline{\theta}_e \\ \underline{\omega}_e \end{bmatrix} + \begin{bmatrix} 0 \\ \underline{\alpha}_c \end{bmatrix}$$

and allow the design of three independent phase-planes. To refine the determination of the switching curves, $\underline{\alpha}_m$ is sent to the autopilot and is used in estimating the net acceleration.

The above steering logic has been implemented in the procedure STEERING which is described below.

2.6 STEERING

The procedure STEERING computes five sets of steering parameters to be sent to the autopilot. These parameters are

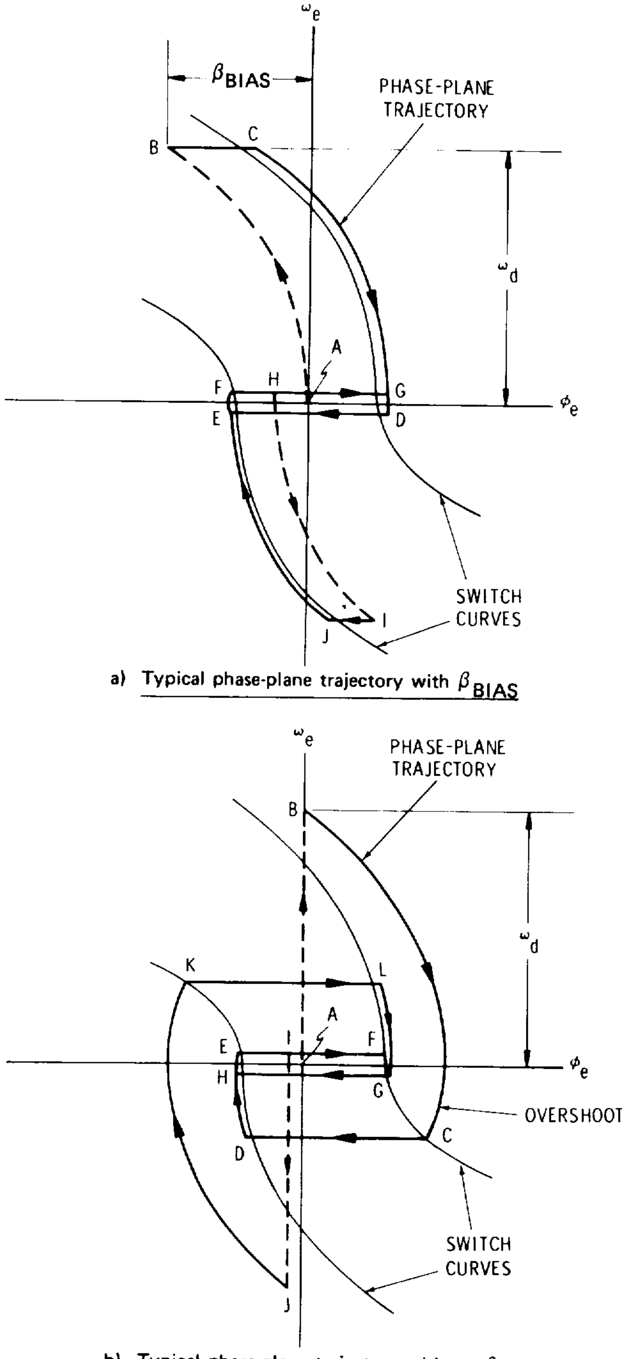

a) Typical phase-plane trajectory with β_{BIAS}

b) Typical phase-plane trajectory without β_{BIAS}

Fig. 2-9 Maneuver Phase-Plane Trajectories

1) $[\theta_d]$, a set of intermediate desired gimbal angles

2) $[\Delta\theta_d]$, a set of incremental desired gimbal angles

3) $[\beta_{BIAS}]$, a set of bias gimbal angles

4) $\underline{\omega}_d$, the desired angular velocity vector

5) $\underline{\alpha}_m$, a set of bias accelerations

STEERING operates on a cyclic basis with period Δt_c. The parameters$[\beta_{BIAS}]$, $\underline{\omega}_d$, and $\underline{\alpha}_m$ are computed once on the first pass whereas $[\theta_d]$and $[\Delta\theta_d]$are computed every Δt_c seconds until the maneuver is complete.

A logic flow diagram is illustrated in Fig. 2-10. The initial gimbal angles are read and the FIRST_PASS switch is set "ON". The incremental angle of rotation is computed from the requested magnitude of angular velocity and the time increment Δt_c. From this incremental rotation angle and the rotation vector $\underline{u}_r$, an incremental rotation matrix $\overset{*}{\Delta R}$ is determined by calling ROTATION_MATRIX. Two timing parameters are computed. These are the duration of the maneuver, t_M,

$$t_M = A_M/\omega_r$$

and the time at which to stop the maneuver, t_s,

$$t_s = t_M + t_{cycle}$$

where t_{cycle} has been set equal to the current time.

Cyclic computation of the steering parameters takes place in open-loop fashion until the computed time to stop the maneuver, t_s, is reached (Fig. 2-10). If the AUTO_MODE switch is "OFF" then STOPRATE is called which sets the desired reference gimbal angles $[\theta_d]$to the present gimbal angles and nulls the remaining four sets of parameters $[\Delta\theta_d]$, $[\beta_{BIAS}]$, $\underline{\omega}_d$, and $\underline{\alpha}_m$, as illustrated in Fig. 2-11. Control then returns to the executive system. However, if the AUTO_MODE switch is "ON" the direction-cosine matrix between the navigation-base and stable-member coordinate systems is determined by

$$\overset{*}{C}_{BSM_{N+1}} = \overset{*}{C}_{BSM_N} \ \overset{*}{\Delta R}$$

From this matrix, the gimbal angles projected to the time of the next pass, $[\theta_N]$, are calculated.

On the first pass STEERING sets the FIRST_PASS flag to "OFF" and computes $\underline{\omega}_d$, $[\beta_{BIAS}]$, and $\underline{\alpha}_m$ as illustrated in Fig. 2-10. The desired angular velocity vector, $\underline{\omega}_d$, is computed from the requested magnitude of angular velocity, ω_r, and the rotation vector, $\underline{u}_r$, supplied by KALCMANU.

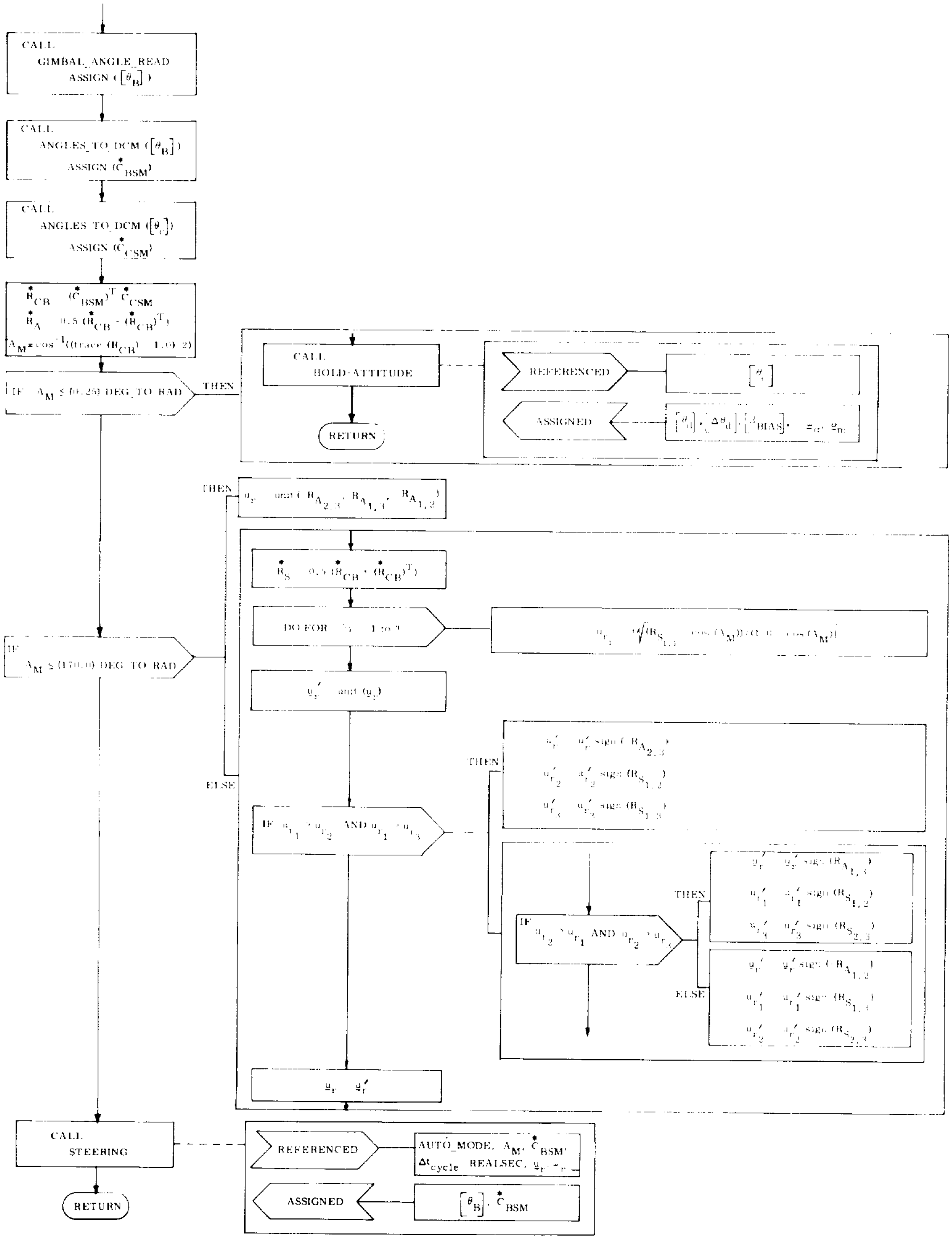

Fig. 2-10 STEERING : Procedure

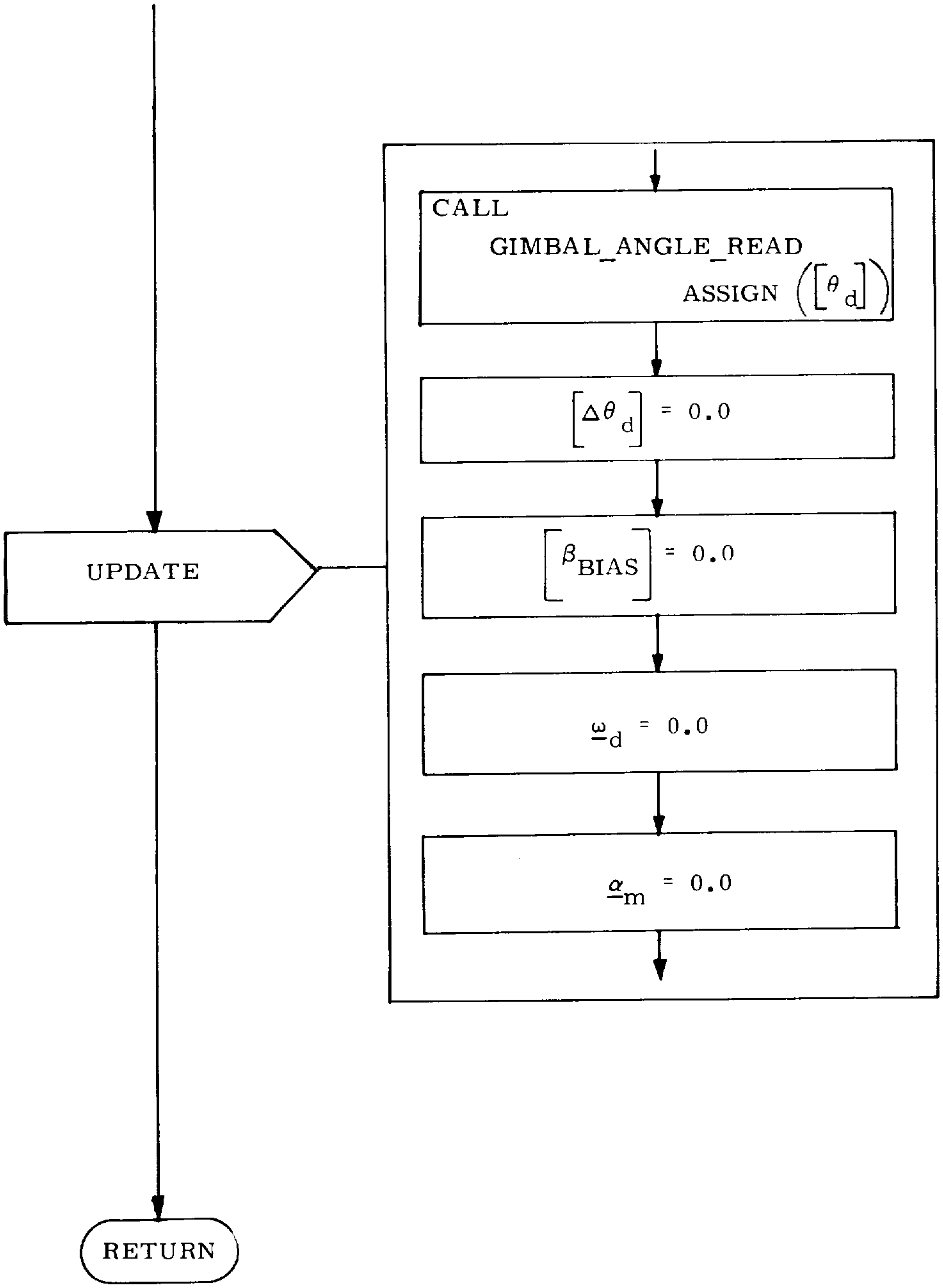

Fig. 2-11 STOPRATE : Procedure

$$\left[\beta_{BIAS}\right] = \begin{bmatrix} \beta_{BIAS(U)} \\ \beta_{BIAS(V)} \\ \beta_{BIAS(W)} \end{bmatrix} = \begin{bmatrix} \omega_{dc(U)} \mid \omega_{dc(U)} \mid / \ (2 \mid \alpha_{c(U)} \mid) \\ \omega_{dc(V)} \mid \omega_{dc(V)} \mid / \ (2 \mid \alpha_{c(V)} \mid) \\ \omega_{dc(W)} \mid \omega_{dc(W)} \mid / \ (2 \mid \alpha_{c}(W) \mid) \end{bmatrix}$$

where $\alpha_{c(U)}$, $\alpha_{c(V)}$, $\alpha_{c(W)}$ are the control accelerations as determined by the autopilot.

On every pass STEERING also updates the incremental desired gimbal angles, $[\Delta\theta_d]$, by

$$[\Delta\theta_d] = ([\theta_N] - [\theta_B]) (t_{fast}/\Delta t_c)$$

where $[\theta_N]$ = desired reference gimbal angles projected Δt_c seconds in advance

$[\theta_B]$ = present desired reference gimbal angles

Δt_c = period of the STEERING cycle

t_{fast} = sampling period of the autopilot

These incremental angles are subsequently added to $[\theta_d]$ by the autopilot at the start of each autopilot pass. $[\theta_d]$is then updated to $[\theta_B]$and $[\theta_B]$is replaced by $[\theta_N]$for use on the subsequent pass. The time of the next proposed pass, t_{cycle}, is computed by adding Δt_c to the present value of t_{cycle}. If t_{cycle} is less than the termination time of the maneuver, t_s, another pass is performed. Otherwise, HOLD_ATTITUDE is called to update the desired reference gimbal angles, $[\theta_d]$, to the commanded terminal set of gimbal angles $[\theta_c]$and nulls the remaining steering parameters $[\Delta\theta_d]$, $[\beta_{BIAS}]$, $\underline{\omega}_d$, and $\underline{\alpha}_m$. This updating is illustrated in Fig. 2-12. Control is then returned to ATTITUDE_MANEUVER which in turn transfers control to the executive system.

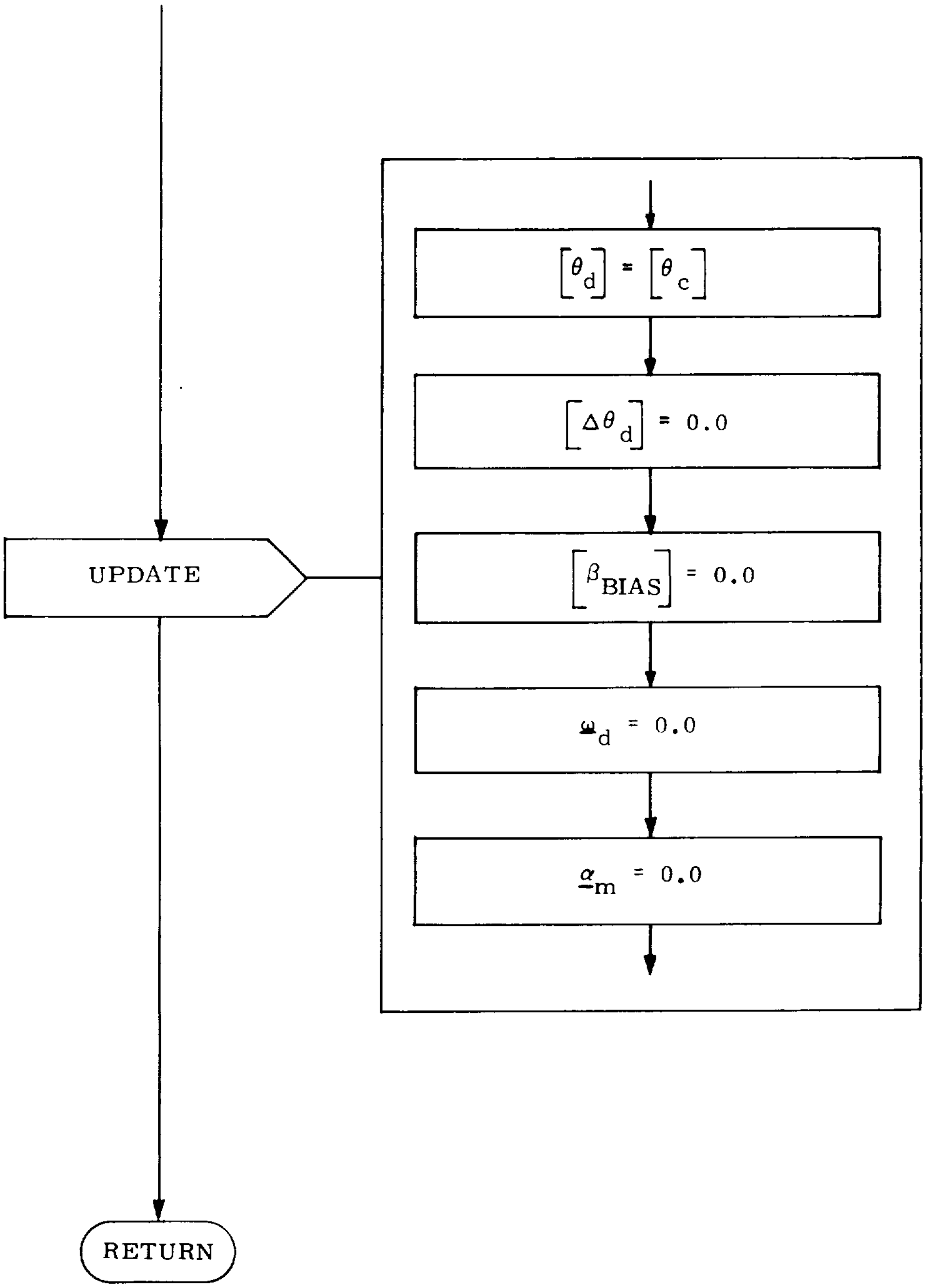
UPDATE
$[\theta_d] = [\theta_c]$
$[\Delta\theta_d] = 0.0$
$[\beta_{BIAS}] = 0.0$
$\underline{\omega}_d = 0.0$
$\underline{\alpha}_m = 0.0$
RETURN

Fig. 2-12 HOLD_ATTITUDE : Procedure

Table 2-1 ATTITUDE MANEUVER MODULE DICTIONARY

MNEMONIC	DEFINITION	CLASS	DECLARED IN	ENTRY FORMAT	INPUTS REFERENCED	OUTPUTS ASSIGNED	LEVEL
ANGLES_TO_DCM	Converts an array of angles to a direction-cosine matrix.	PROCEDURE	ATTITUDE_MANEUVER	ANGLES_TO_DCM: PROCEDURE ($[\theta]$) ASSIGN ($\overset{*}{C}$).	---	---	2
ATTITUDE_MANEUVER	Sequences an automatic reorientation during the ON-ORBIT phase.	PROGRAM	COMPOOL	ATTITUDE_MANEUVER: PROGRAM;	FLAG_3AXIS AUTO_MODE	---	1
DCM_TO_ANGLES	Converts direction-cosine matrix to an array of angles	PROCEDURE	ATTITUDE_MANEUVER	DCM_TO_ANGLES: PROCEDURE ($\overset{*}{C}$) ASSIGN ($[\theta]$);	-	--	2
GIMBAL_ANGLE_READ	Reads the gimbal angles	PROCEDURE	ATTITUDE_MANEUVER	GIMBAL_ANGLE_READ: PROCEDURE ASSIGN (GA),	---	---	2
HOLD_ATTITUDE	Sends steering parameters to the autopilot to hold attitude at commanded gimbal angles.	PROCEDURE	ATTITUDE_MANEUVER	HOLD_ATTITUDE: PROCEDURE;	$[\theta_c]$	θ_d, $[\Delta\theta_d]$, $[\beta_{BIAS}]$, $\underline{\omega}_d$, $\underline{\alpha}_m$	2
KALCMANU	Computes angle of rotation, A_M, and axis of single equivalent rotation, $\underline{u}_r$	PROCEDURE	ATTITUDE_MANEUVER	KALCMANU PROCEDURE;	$[\theta_c]$, DEG_TO_RAD	$\underline{u}_r$, A_M $[\theta_B]$, $\overset{*}{C}_{BSM}$	2
ROTATION_MATRIX	Computes rotation matrix $\overset{*}{R}$ from $\underline{u}_r$ and A_M.	PROCEDURE	ATTITUDE_MANEUVER	ROTATION_MATRIX: PROCEDURE ($\underline{u}_r$, A) ASSIGN ($\overset{*}{R}$);	$\overset{*}{I}_{identity}$	---	2
STEERING	Computes and sends to autopilot the steering parameters every Δt_c seconds	PROCEDURE	KALCMANU	STEERING: PROCEDURE;	A_M, $\underline{u}_r$, ω_r, $\overset{*}{M}_{PC}$, $\underline{\omega}_d$ $[\alpha_c]$, $\overset{*}{J}$, $[\theta_B]$, t_{fast}, Δt_c $\overset{*}{C}_{BSM}$, REALSEC, AUTO_MODE	$[\theta_d]$, $[\Delta\theta_d]$, $[\beta_{BIAS}]$ $\underline{\omega}_d$, $\underline{\alpha}_m$, $[\theta_B]$, $\overset{*}{C}_{BSM}$	3
STOPRATE	Sends steering parameters to the autopilot to hold attitude at present gimbal angles	PROCEDURE	ATTITUDE_MANEUVER	STOPRATE: PROCEDURE;	Present gimbal angles obtained from GIMBAL_ANGLE_READ	$[\theta_d]$, $[\Delta\theta_d]$, $[\beta_{BIAS}]$, $\underline{\omega}_d$, $\underline{\alpha}_m$	2
VECPOINT	Computes $[\theta_c]$ from $\underline{u}_{ANB}$ and $\underline{u}_{DSM}$	PROCEDURE	ATTITUDE_MANEUVER	VECPOINT: PROCEDURE;	$\underline{u}_{ANB}$, $\underline{u}_{DSM}$, $\underline{u}_{NL}$, π	$[\theta_c]$	2

*COMPOOL being on level 0

Table 2-2 ON-ORBIT ATTITUDE MANEUVER VARIABLE-CONSTANT DICTIONARY

MNEMONIC	ENGINEERING TERM, RANGE	UNITS	DEFINITION	DECLARED IN	ASSIGNED IN	REFERENCED IN	TYPE	ATTRIBUTES
A	$0 \leq \hat{A} < -$	rad	Formal parameter. Angle of rotation about $\underline{u}_r$.	VECPOINT	VECPOINT	VECPOINT	SCALAR	DOUBLE PRECISION, STATIC
A	$0 \leq \hat{A} \leq \pi$	rad	Formal parameter. Angle of rotation about $\underline{u}_r$.	ROTATION_MATRIX	ROTATION_MATRIX	ROTATION_MATRIX	SCALAR	DOUBLE PRECISION, STATIC
A_M	$0 \leq \hat{A}_M \leq \pi$	rad	Angle of rotation about $\underline{u}_r$	KALCMANU	KALCMANU	KALCMANU STEERING	SCALAR	DOUBLE PRECISION, STATIC
ALPHAM	$\underline{\alpha}_m$	rad/sec^2	Bias acceleration used by the autopilot	COMPOOL	STEERING STOPRATE HOLD_ATTITUDE	---	VECTOR (3)	DOUBLE PRECISION, STATIC, LOCKED
AUTȮ_MODE	AUTȮ_MODE	---	Automatic mode switch	COMPOOL	COMPOOL	ATTITUDE_ MANEUVER STEERING	BIT (1)	---
[BIAS_BETA]	$[\beta_{BIAS}]$	rad	Bias gimbal angles	COMPOOL	STEERING STOPRATE HOLD_ATTITUDE	---	ARRAY (3) SCALAR	DOUBLE PRECISION, STATIC, LOCKED
$\overset{*}{C}$	$\overset{*}{C}$	---	Formal parameter. Direction cosine matrix.	ANGLES_TO_DCM	ANGLES_TO_DCM	---	MATRIX (3, 3)	DOUBLE PRECISION, STATIC
$\overset{*}{C}$	$\overset{*}{C}$	---	Formal parameter. Direction cosine matrix.	DCM_TO_ANGLES	---	DCM_TO_ANGLES	MATRIX (3, 3)	DOUBLE PRECISION, STATIC
$\overset{*}{C}$_BSM	$\overset{*}{C}_{BSM}$	---	Direction cosine matrix between present vehicle axes and stable member axes.	KALCMANU	KALCMANU STEERING	KALCMANU STEERING	MATRIX (3, 3)	DOUBLE PRECISION, STATIC
$\overset{*}{C}$_CSM	$\overset{*}{C}_{CSM}$	---	Direction cosine matrix between commanded vehicle axes and stable member axes.	KALCMANU	KALCMANU	KALCMANU	MATRIX (3, 3)	DOUBLE PRECISION, STATIC
$\overset{*}{C}$_LSM	$\overset{*}{C}_{LSM}$	---	Direct cosine matrix between L-coordinate frame and stable member axes.	VECPOINT	VECPOINT	VECPOINT	MATRIX (3, 3)	DOUBLE PRECISION, STATIC

Table 2-2 ON-ORBIT ATTITUDE MANEUVER VARIABLE-CONSTANT DICTIONARY (Cont)

MNEMONIC	ENGINEERING TERM, RANGE	UNIT	DEFINITION	DECLARED IN	ASSIGNED IN	REFERENCED IN	TYPE	ATTRIBUTES
$\overset{*}{\mathrm{C}}$_MSM	$\overset{*}{C}_{MSM}$	---	Direction cosine matrix between M-coordinate frame and stable member axes.	VECPOINT	VECPOINT	VECPOINT	MATRIX (3, 3)	DOUBLE PRECISION, STATIC
DEG_TO_RAD	$\pi/180$	$\mathrm{rad}/_{\mathrm{deg}}$	Conversion factor	COMPOOL	COMPOOL	KALCMANU	SCALAR	DOUBLE PRECISION, STATIC CONSTANT
[DELTA_THETA_D]	$\left[\Delta\theta_d\right]$	rad	Incremental gimbal angles.	COMPOOL	STEERING STOPRATE HOLD_ATTITUDE	---	ARRAY (3) SCALAR	DOUBLE PRECISION, STATIC, LOCKED
DELTAA_M	ΔA_M	rad	Incremental rotation angle.	STEERING	STEERING	STEERING	SCALAR	DOUBLE PRECISION, STATIC, LOCKED
DEL$\overset{*}{\mathrm{T}}$AR	$\Delta\overset{*}{R}$	---	Incremental rotation matrix.	STEERING	STEERING	STEERING	MATRIX (3, 3)	DOUBLE PRECISION, STATIC, LOCKED
DELTAT_C	Δt_c	sec	Period of the cycle of STEERING	COMPOOL	COMPOOL	STEERING	SCALAR	DOUBLE PRECISION, STATIC, CONSTANT
FIRST_PASS	FIRST_PASS	---	First pass switch.	STEERING	STEERING	STEERING	BIT (1)	---
FLAG_3AXIS	FLAG_3AXIS	---	Type of input flag.	COMPOOL	calling program	ATTITUDE_ MANEUVER	BIT (1)	---
GA	θ	rad	Gimbal angles read from sensors	GIMBAL_ANGLE_ READ	GIMBAL_ANGLE_ READ	GIMBAL_ANGLE_ READ	ARRAY (3) SCALAR	DOUBLE PRECISION, STATIC
$\overset{*}{\mathrm{I}}$D_MATRIX	$\overset{*}{I}_{identity}$	---	Identity matrix	COMPOOL	COMPOOL	ROTATION_MATRIX	MATRIX (3, 3)	DOUBLE PRECISION, STATIC, CONSTANT
INE$\overset{*}{\mathrm{R}}$TIA	$\overset{*}{J}$	slug-ft^2	Inertia matrix of the vehicle	COMPOOL	COMPOOL	STEERING	MATRIX (3, 3)	DOUBLE PRECISION, STATIC
[MAGACC]	$[\alpha_c]$	$\mathrm{rad}/_{\mathrm{sec}^2}$	Magnitudes of the U, V, W control accelerations	COMPOOL	calling program	STEERING	ARRAY (3) SCALAR	DOUBLE PRECISION, STATIC
MAGNITUDE_W_D	ω_r	$\mathrm{rad}/_{\mathrm{sec}}$	Requested magnitude of angular velocity	COMPOOL	calling program	STEERING	SCALAR	DOUBLE PRECISION, STATIC
$\overset{*}{\mathrm{M}}$PC	$\overset{*}{M}_{PC}$	---	Transformation matrix from pilot to control axes	COMPOOL	calling program	STEERING	MATRIX (3, 3)	DOUBLE PRECISION, STATIC

Table 2-2 ON-ORBIT ATTITUDE MANEUVER VARIABLE-CONSTANT DICTIONARY (Cont)

MNEMONIC	ENGINEERING TERM, RANGE	UNITS	DEFINITION	DECLARED IN	ASSIGNED IN	REFERENCED IN	TYPE	ATTRIBUTES
PI	π	rad		COMPOOL	COMPOOL	VECPOINT DCM_TO_ANGLES	SCALAR	DOUBLE PRECISION, STATIC
$\overset{*}{R}$	$\overset{*}{R}$	---	Formal parameter. Rotation matrix.	ROTATION_MATRIX	ROTATION_MATRIX	ROTATION_MATRIX	MATRIX (3, 3)	DOUBLE PRECISION, STATIC
$\overset{*}{R}$_A	$\overset{*}{R}_A$	---	Antisymmetric component of $\overset{*}{R}_{CB}$.	KALCMANU	KALCMANU	KALCMANU	MATRIX (3, 3)	DOUBLE PRECISION, STATIC
$\overset{*}{R}$_CB	$\overset{*}{R}_{CB}$	---	Rotation matrix between commanded and initial attitudes.	KALCMANU	KALCMANU	KALCMANU	MATRIX (3, 3)	DOUBLE PRECISION, STATIC
$\overset{*}{R}$_ML	$\overset{*}{R}_{ML}$	---	Rotation matrix between the M and L coordinate frames.	KALCMANU	KALCMANU	KALCMANU	MATRIX (3, 3)	DOUBLE PRECISION, STATIC
$\overset{*}{R}$_S	$\overset{*}{R}_S$	---	Symmetric component of $\overset{*}{R}_{CB}$.	KALCMANU	KALCMANU	KALCMANU	MATRIX (3, 3)	DOUBLE PRECISION, STATIC
REALSEC	REALSEC	computer ticks/sec	Scale factor to synchronize with computer clock.	COMPOOL	COMPOOL	STEERING	SCALAR	DOUBLE PRECISION, STATIC, CONSTANT
T_CYCLE	t_{cycle}	sec	Time at which each new pass of STEERING begins.	STEERING	STEERING	STEERING	SCALAR	DOUBLE PRECISION, STATIC
T_M	t_M	sec	Time of maneuver duration.	STEERING	STEERING	STEERING	SCALAR	DOUBLE PRECISION, STATIC
T_S	t_s	sec	Time of maneuver completion.	STEERING	STEERING	STEERING	SCALAR	DOUBLE PRECISION, STATIC
TF	t_{fast}	sec	Period of the autopilot cycle.	COMPOOL	autopilot	STEERING	SCALAR	DOUBLE PRECISION, STATIC
[THETA]	$[\theta]$ $-\pi \leq \theta_i \leq \pi$	rad	Formal parameter. Gimbal angles.	ANGLES_TO_DCM	---	ANGLES_TO_DCM	ARRAY (3) SCALAR	DOUBLE PRECISION, STATIC

Table 2-2 ON-ORBIT ATTITUDE MANEUVER VARIABLE-CONSTANT DICTIONARY (Cont)

MNEMONIC	ENGINEERING TERM, RANGE	UNITS	DEFINITION	DECLARED IN	ASSIGNED IN	REFERENCED IN	TYPE	ATTRIBUTES
[THETA]	$[\theta]$ $-\pi \leq \theta_i \leq \pi$	rad	Formal parameter. Gimbal angles.	DCM_TO_ANGLES	DCM_TO_ANGLES	DCM_TO_ANGLES	ARRAY(3) SCALAR	DOUBLE PRECISION, STATIC
[THETA_B]	$[\theta_B]$ $-\pi \leq \theta_{B_i} \leq \pi$	rad	Gimbal angles at the start of KALCMANU	KALCMANU	KALCMANU STEERING	KALCMANU STEERING	ARRAY(3) SCALAR	DOUBLE PRECISION, STATIC
[THETA_C]	$[\theta_c]$ $-\pi \leq \theta_{c_i} \leq \pi$	rad	Commanded terminal gimbal angles.	COMPOOL	calling program or VECPOINT	HOLD-ATTITUDE	ARRAY(3) SCALAR	DOUBLE PRECISION, STATIC
[THETA_D]	$[\theta_d]$ $-\pi \leq \theta_{d_i} \leq \pi$	rad	Intermediate desired gimbal angles.	COMPOOL	STEERING STOPRATE HOLD_ATTITUDE	autopilot	ARRAY(3) SCALAR	DOUBLE PRECISION, STATIC, LOCKED
[THETA_L]	$[\theta_L]$ $-\pi \leq \theta_{L_i} \leq \pi$	rad	Gimbal angles at the start of VECPOINT	VECPOINT	VECPOINT	VECPOINT	ARRAY(3) SCALAR	DOUBLE PRECISION, STATIC
[THETA_N]	$[\theta_N]$ $-\pi < \theta_{N_i} < \pi$	rad	Gimbal angles predicted Δt_c in advance	STEERING	STEERING	STEERING	ARRAY(3) SCALAR	DOUBLE PRECISION, STATIC
$\overline{\text{U}}$_AL	$\underline{u}_{AL}$	ft	Prescribed unit vector $\underline{u}_A$ in the L-coordinate frame	VECPOINT	VECPOINT	VECPOINT	VECTOR(3)	DOUBLE PRECISION, STATIC
$\overline{\text{U}}$_ANB	$\underline{u}_{ANB}$	ft	Prescribed unit vector $\underline{u}_A$ in navigation-base coordinates.	COMPOOL	calling program	VECPOINT	VECTOR(3)	DOUBLE PRECISION, STATIC
$\overline{\text{U}}$_DL	$\underline{u}_{DL}$	ft	Desired unit vector in the L-coordinate frame	VECPOINT	VECPOINT	VECPOINT	VECTOR(3)	DOUBLE PRECISION, STATIC
$\overline{\text{U}}$_DSM	$\underline{u}_{DSM}$	ft	Desired unit vector in the stable-member coordinate frame.	COMPOOL	calling program	VECPOINT	VECTOR(3)	DOUBLE PRECISION, STATIC

Table 2-2 ON-ORBIT ATTITUDE MANEUVER VARIABLE-CONSTANT DICTIONARY (Cont)

MNEMONIC	ENGINEERING TERM. RANGE	UNITS	DEFINITION	DECLARED IN	ASSIGNED IN	REFERENCED IN	TYPE	ATTRIBUTES
$\overline{U}$_R	$\underline{u}_r$	ft	Single equivalent rotation vector. Rotation through the angle A.	VECPOINT	VECPOINT	VECPOINT	VECTOR(3)	DOUBLE PRECISION, STATIC
$\overline{U}$_R	$\underline{u}_r$	ft	Formal parameter. Single equivalent rotation vector.	ROTATION_MATRIX	ROTATION_MATRIX	ROTATION_MATRIX	VECTOR(3)	DOUBLE PRECISION, STATIC
$\overline{U}$_R	$\underline{u}_r$	ft	Single equivalent rotation vector. Rotation through the angle A_M.	KALCMANU	KALCMANU	KALCMANU STEERING	VECTOR(3)	DOUBLE PRECISION, STATIC
$\overline{U}$_RPRIME	$\underline{u}_r$	ft	Intermediate rotation vector used in determining proper signs of $\underline{u}_r$.	KALCMANU	KALCMANU	KALCMANU	VECTOR(3)	DOUBLE PRECISION, STATIC
$\overline{U}$_XL	$\underline{u}_{XL}$	ft	Unit vector along the navigation-based x-axis (1, 0, 0).	COMPOOL	COMPOOL	VECPOINT	VECTOR(3)	DOUBLE PRECISION, STATIC
$\overline{U}$_YSML	$\underline{u}_{YSML}$	ft	Unit vector along the y-axis of the stable-member frame projected into the L-frame.	VECPOINT	VECPOINT	VECPOINT	VECTOR(3)	DOUBLE PRECISION, STATIC, CONSTANT
$\overset{*}{U}$X_R	$\overset{*}{U}X_r$	ft	Antisymmetric matrix whose components are taken from $\underline{u}_r$.	ROTATION_MATRIX	ROTATION_MATRIX	ROTATION_MATRIX	MATRIX (3, 3)	DOUBLE PRECISION, STATIC
$\overline{W}$_D	$\underline{\omega}_d$	rad/sec	Desired angular velocity vector in navigation-based coordinate.	COMPOOL	STEERING STOPRATE HOLD_ATTITUDE	autopilot	VECTOR(3)	DOUBLE PRECISION, STATIC, LOCKED
$\overline{W}$_DC	$\underline{\omega}_{dc}$	rad/sec	Desired angular velocity vector in control coordinates	STEERING	STEERING	STEERING	VECTOR(3)	DOUBLE PRECISION, STATIC, LOCKED

REFERENCES

1. Dixon, M., "Fuel-Time Optimal Spacecraft Reorientation," Ph.D. Thesis T-502, Instrumentation Laboratory, M.I.T., May 1968.

2. Crisp, R. and Keene, D., "Attitude Maneuver Optimization to Conserve Reaction Control Propellants," Report E-1832, Instrumentation Laboratory, M.I.T., August 1965.

3. Crisp, R. and Keene, D., "Apollo Command and Service Module Reaction Control by the Digital Autopilot," Report E-1964, Instrumentation Laboratory, M.I.T., May 1966.

4. Keene, D., "Block II LGC Attitude Maneuver Routine: KALCMANU For Flight 206," Group 23 Internal Memo #8, Instrumentation Laboratory, M.I.T., November 1966.

5. Keene, D., "Coasting-Flight Attitude Maneuver Routine", Guidance Systems Operations Plan for Manned LM Earth Orbital and Lunar Missions Using Program Luminary 1E, Section 3 Digital Autopilot (Rev. 8), March 1972.

6. Gorman, S. and Kimball, G., Apollo Software Information Memo 5-68-9, "VECPOINT Automatic Maneuvers for Program SUNDISK," U.S. Government Memorandum, May 1968.